HARVARD OPEN OCEAN MODEL REPORTS

Reports in Meteorology and Oceanography

NUMBER 22

Gulfcasting: Dynamical Forecast Experiments for Gulf Stream Rings and Meanders November 1985 - June 1986

by N00014-84-C-0461 (ONR)
N00014-86-K-0602 (NRDA)

Allan R. Robinson, Michael A. Spall, Wayne G. Leslie

Leonard J. Walstad and Dennis J. McGillicuddy

HARVARD UNIVERSITY
Division of Applied Sciences
Cambridge, Mass.

August 1987

PREFACE

Gulf Stream rings and meanders are among the most energetic of all oceanic mesoscale eddy and frontal phenomena. The meander and ring field evolves, propagates and interacts. Periods of relatively smooth development are interrupted by dramatic and energetic synoptical dynamical events such as ring births or coalescences with the stream and ring mergers. Such events rupture and shift frontal gradients rapidly. Forecasting the evolution of the Gulf Stream meander and ring system is the counterpart within the ocean of weather forecasting in the atmosphere. Here we report on a series of seven real-time forecast experiments for the Gulf Stream (called GULFCASTS) carried out by the Harvard ocean dynamics and modelling group during the period November 1985 to June 1986. To our knowledge these represent the first systematic dynamically based real-time forecasting experiments for the Gulf Stream system.

The material of this report serves dual purposes: i) to record and document the selected forecast experiments, and ii) to present the components and techniques of the systematic forecasting methodology developed. Nowcasts and forecasts are carried out with the Harvard Open Ocean Model, a dynamical model with open boundary conditions developed with ONR support over several years for fundamental research in regional dynamical processes. The data employed is remotely sensed sea surface temperatures together with critically sited *in situ* temperature profiles obtained by airdropped AXBTs. A 'data assimilation' approach is adopted, melding observations via dynamical interpolations. The forecast scheme, as verified in these experiments is seen to be effective and useful in the Gulf Stream region for, at least, week-long forecasts in the thermocline.

The methodology as presented represents our state-of-the-art as of November 1986. At that time we initiated, on a routine and continuing basis, in the region 55-75 W Longitude, Gulfcasting involving a weekly dedicated AXBT flight. The basic methodology remains although several substantial technical developments have been made. The ability to predict

and transition energetic synoptical dynamical events has now been demonstrated on a regular basis.

The scientific basis for our Gulfcasting work is now available in the form of a submitted ms "Gulf Stream Simulations and the Dynamics of Ring and Meander Processes" by A.R. Robinson, M.A. Spall and N. Pinardi, available on request.

Accession For	
NTIS GRA&I	☑
DTIC TAB	☐
Unannounced	☐
Justification	
By per telecon	
Distribution/	
Availability Codes	
Dist	Avail and/or Special
A-1	

STATEMENT "A" per Dr. David Evans
ONR/Code 1122ML
TELECON 5/10/90 VG

ALL ATTACHED ENCLOSURES ARE PART OF BASIC TEXT per Dr. Alan Brandt
ONR/Code 1122SS
TELECON 5/25/90 VG

TABLE OF CONTENTS

2. SELECTED EXPERIMENTS

2.1) NOVEMBER 29 - DECEMBER 6, 1985

2.2) JANUARY 6 - 13, 1986

2.3) FEBRUARY 3 - 10, 1986

2.4) APRIL 2 - 23, 1986

2.5) MAY 19 - JUNE 6, 1986

2.5.1) Extended domain forecast

2.5.2) Sensitivity forecast

2.5.3) Operational forecast

1. INTRODUCTION

The forecasts presented in this report were done in real time between Nov 29, 1985 and June 6, 1986. Many of the techniques presented here as the Gulf Stream Operational Forecasting Methodology were developed during these experiments. As a result, not all of the experiments follow the complete procedure outlined here. These experiments have been selected because each was significant in the learning process.

1.1 Gulf Stream Operational Forecasting Methodology

Data Sets:

1) Satellite SST
2) Satellite SSH
3) AXBT flights
4) XBTs of opportunity
5) other

Purposes of Model Runs:

1) Nowcasts and forecasts
2) Dynamical interpolation
    a. vertical - to depth
    b. horizontal - to fill out sparse data
3) Sensitivity studies
4) Error estimates

Domains:

1) Large Domains - inclusive
2) Subdomains of special operational interest and associated "domains of influence"
3) Set of standard preselected subdomains

Procedure from startup:

– Start weli ahead of the time of interest (approximately 2-3 weeks).

1) Look at IR-SST to identify stream axis and rings (Fig. 1).

2) Identify features - definite and ambiguous.

3) Review old data sets to help remove ambiguities.

4) From historical data sets estimate propagation of crests, troughs and rings.

5) Make simplified feature maps by projecting propagation speeds into the future – i.e. "connect the dots" to get future boundary condition data (Fig. 2a, 2b).

6) Choose best initial conditions. Evaluate indices of feature models.

7) Choose appropriate model domain relative to features and region of interest.

8) Run a "central forecast" in both subdomain for 1-2 weeks (Run C1) (Fig. 8) and large supercomputer domain (Run L1) (Fig. 9) for 2-4 weeks.

9) Determine ambiguities in features (ring/no ring, size, speed, position, contact with stream, etc.).

10) Run "sensitivity matrix" in subdomain for various initial conditions (Runs S1A, S1B, S1C, etc.) (Fig. 8).

11) From central and sensitivity forecasts determine critical events such as ring and stream interactions that cause rapid evolution. Study the forecast sensitivity to critical events.

12) From (8), (9), (10), (11) determine which features require most accurate location.

13) Obtain *in situ* data from AXBT flights (Fig. 3-7). Design AXBT flights to:

    a) locate critical features accurately.

    b) locate and determine the deep structure of all major features (stream axis, crests, troughs, rings, etc.)

    Prioritize the track with respect to getting the most important information first.

    Locate XBT drops along the track non-uniformly, increasing coverage in critical areas.

14) Determine from the AXBT data the improved positions of features and remaining ambiguities (Fig. 10).

15) Obtain new IR SST data if available.

16) From (10), (14) and (15) and possibly new SST data, choose the best model run from the matrix of sensitivity studies.

17) Reinitialize the model from a composite analysis of (14), (15) and (16) and forecast ahead for approximately one week, starting typically 1 to 2 days prior to the AXBT flight. Perhaps use boundary conditions interpolated from large domain supercomputer run (Run C2). This is the operational nowcast and forecast (Run F1) (Fig. 11).

18) Send out AXBT verification flights. The evolution of critical flow indices (i.e. crests, troughs, ring-stream interactions, etc.) are a good measure of the accuracy of the numerical forecast and should be located with appropriate flight tracks. Verification data is very important and is obtained regularly even for well established weather forecasting systems. It is especially critical for a new system still undergoing development such as the Harvard ODPS.

19) Steps (9) through (18) may be iterated to further refine the fields for the final product. Forecast F1 will become C2 and the next level of sensitivity runs will become S2A, S2B, S2C, etc.

Maintaining nowcasts and forecasts:

1) The verification data (18) from the previous forecast F1 can be used to update the field analysis for the next set of sensitivity runs.

2) Steps (11) through (16) are carried out to produce the next operational forecast, F2. The large domain supercomputer run is also carried out from the best initial condition.

3) When maintaining the ODPS as a continuing nowcasting and forecasting system, procedural pairs from the above list are indistinguishable (e.g. (8) and (17); (13) and (18), etc.). All *in situ* and high quality remotely sensed data will play a dual role as updating and verification data.

1.2 Samples of data, data analysis, and model output

A sample figure for each of the steps in the forecasting procedure follows. Figure 1 is a sea surface temperature map for May 23, 1986 derived from satellite IR denoting the thermal fronts associated with the Gulf Stream and its rings (Step 1). Important points on the use of this product are also noted. Figure 2a contains the same IR data in Harvard feature model format. In Figure 2b the feature positions have been propagated to estimate their position one week into the future (May 30) for use as boundary conditions (Step 5). Figures 3, 4, 5, 6 and 7 show a sample AXBT flight track and the various types of output used to analyze the data (Step 13). Figures 8 and 9 are sample model forecasts for the sensitivity runs and the large supercomputer domain, respectively (Step 8). Figure 10 is a composite analysis locating the features for the best model initialization. Information from Figures 1-9 are included in this step (Step 14). The final operational forecast is shown in Figure 11 with derived analysis fields in Figures 12 and 13 (Step 17).

Fig. 1 – Oceanographic Analysis Product

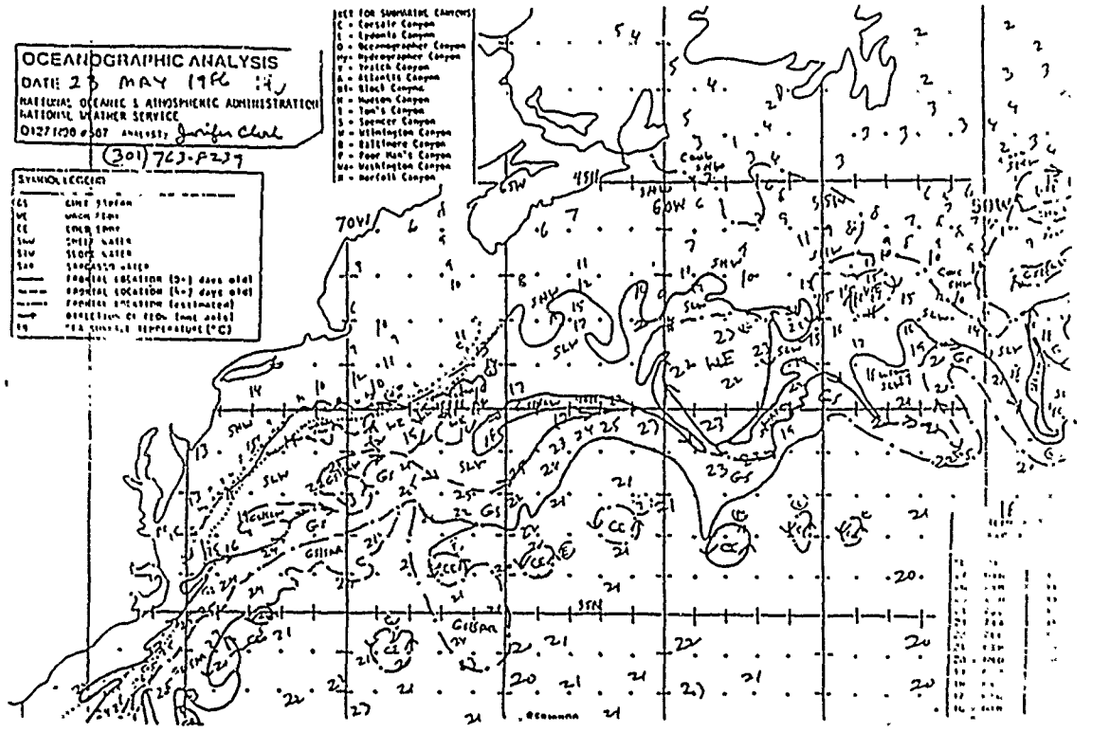

Notes on the use of this product:

Sea surface temp and contours of strong thermal fronts are given

Recent data (3 days old) is marked by a solid line.

Old data (4–7 days old) is marked by a dashed line.

Estimated data (7 days old) is marked by a dashed–dot line.

Remember – surface signature – may be misleading.

Rings not observed are persisted at last observation.

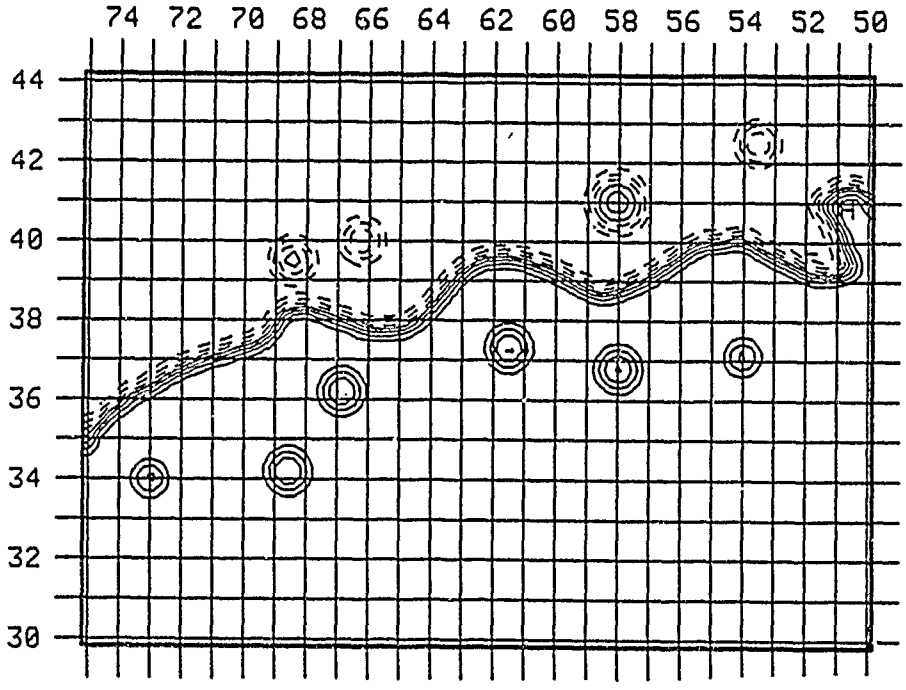

Fig. 2a — Initial conditions from NOAA IR — May 23, 1986

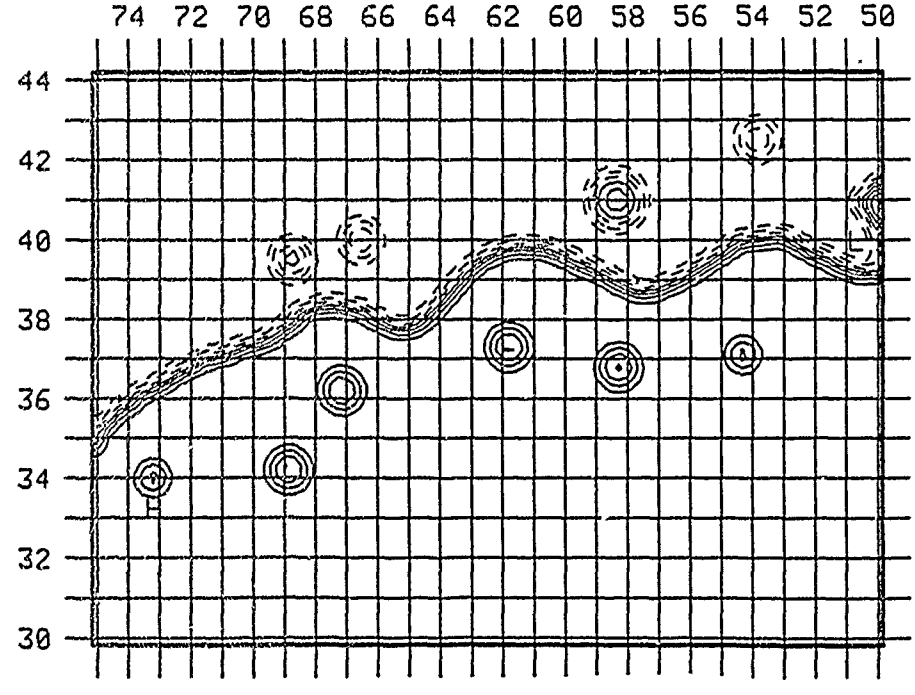

Fig. 2b — Boundary conditions; estimated for May 30, 1986

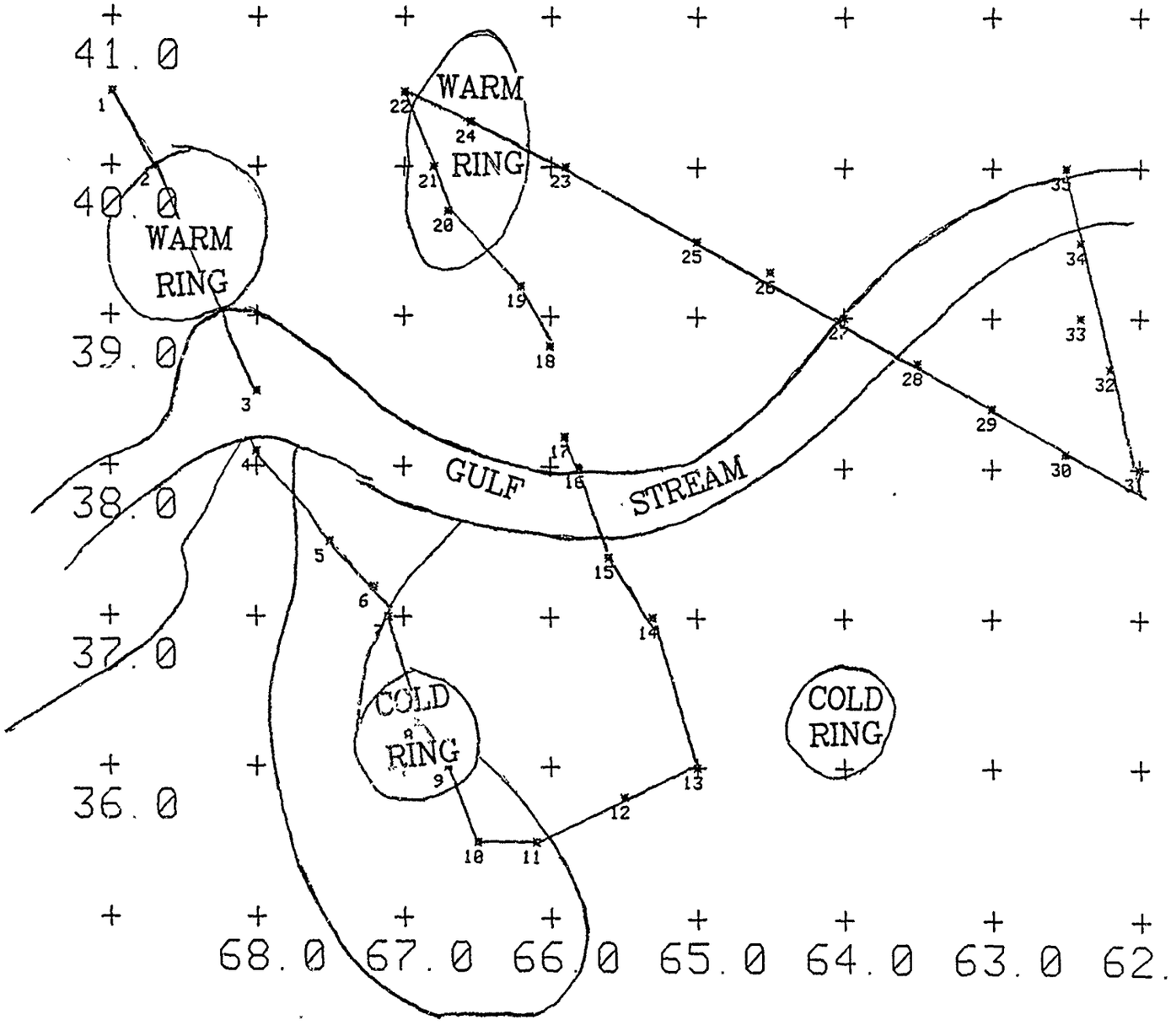

Fig. 3 — AXBT track with surface fronts

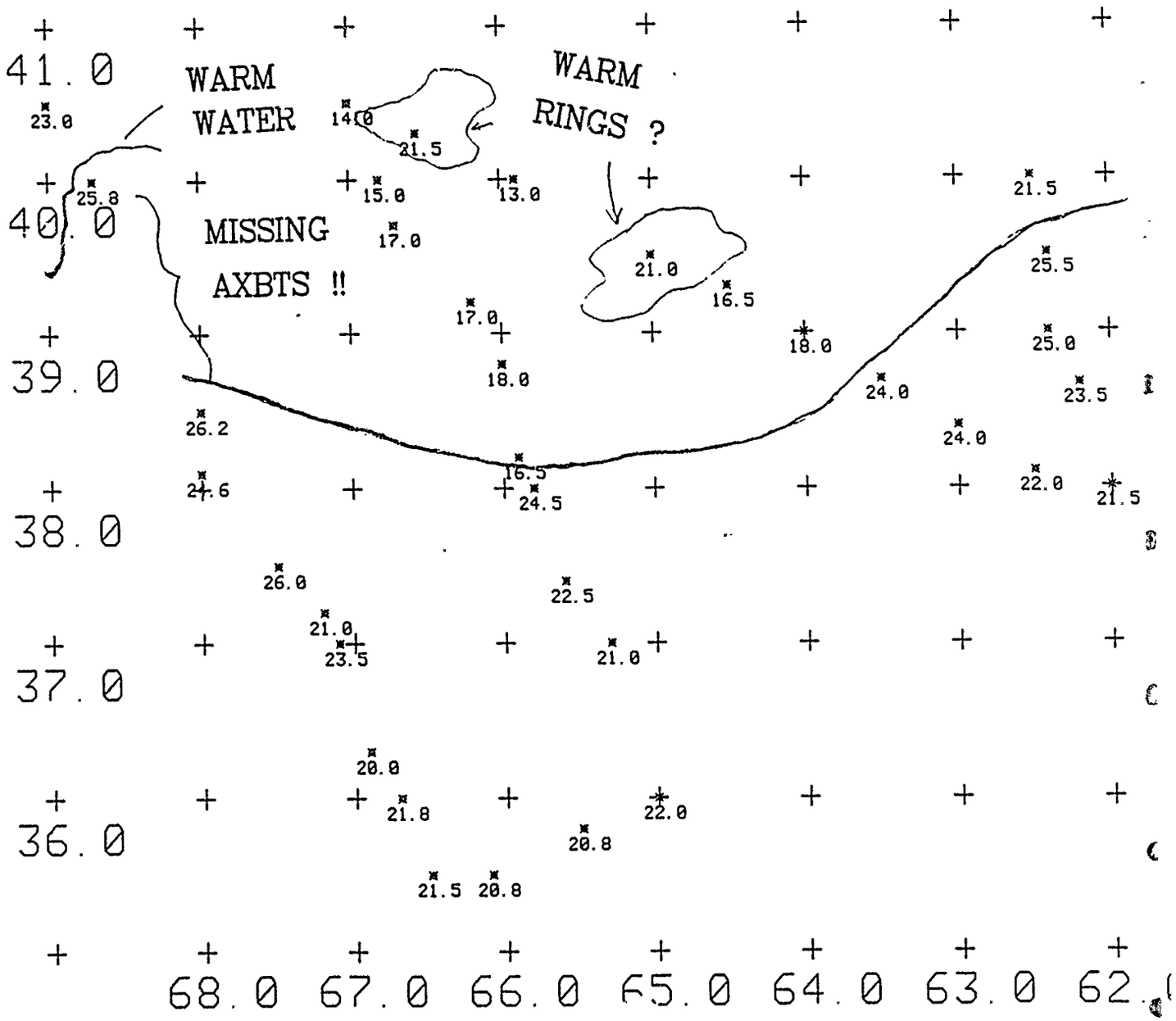

Fig. 4 — Surface temperature

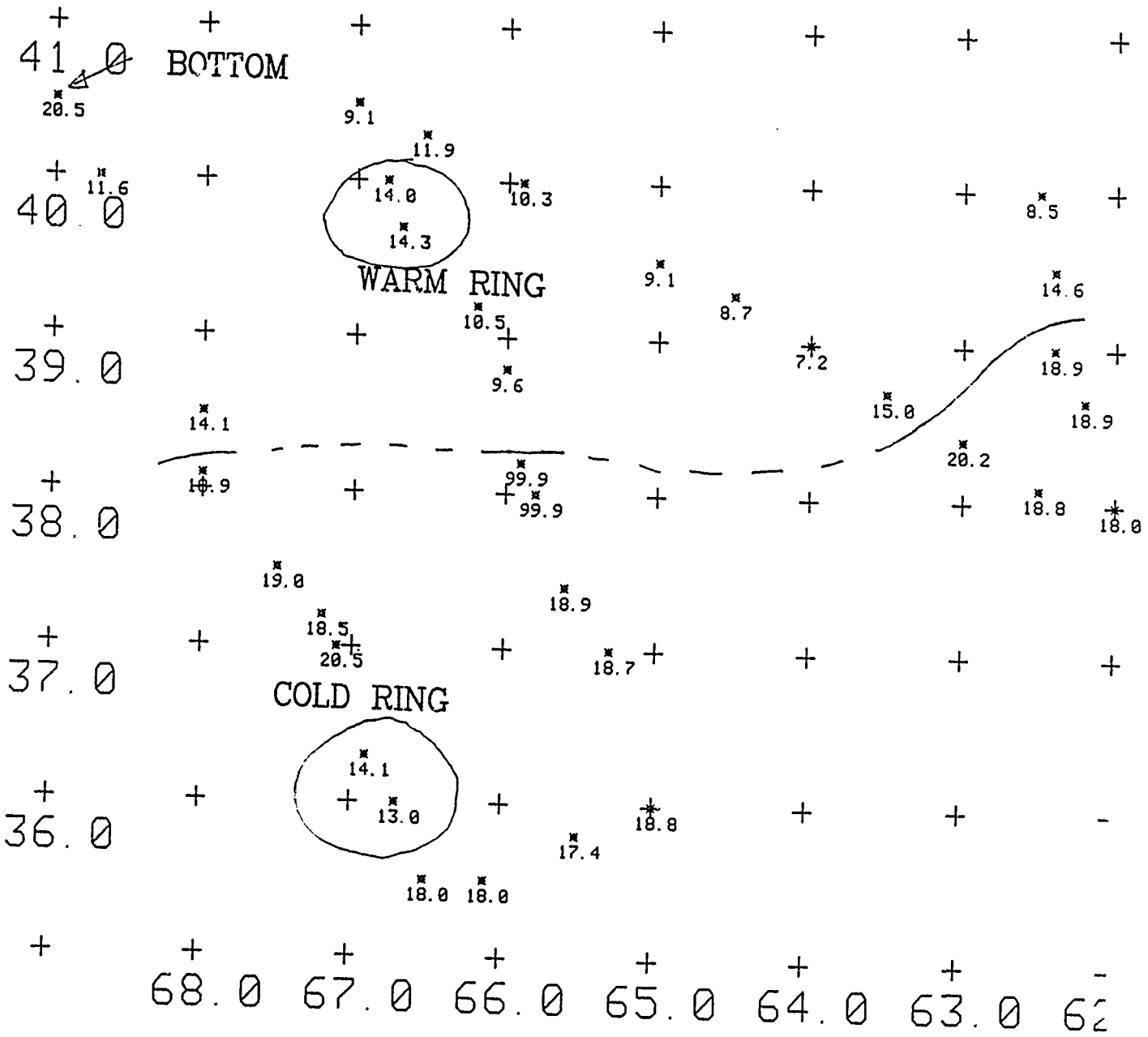

Fig. 5 — Temperature at 300m

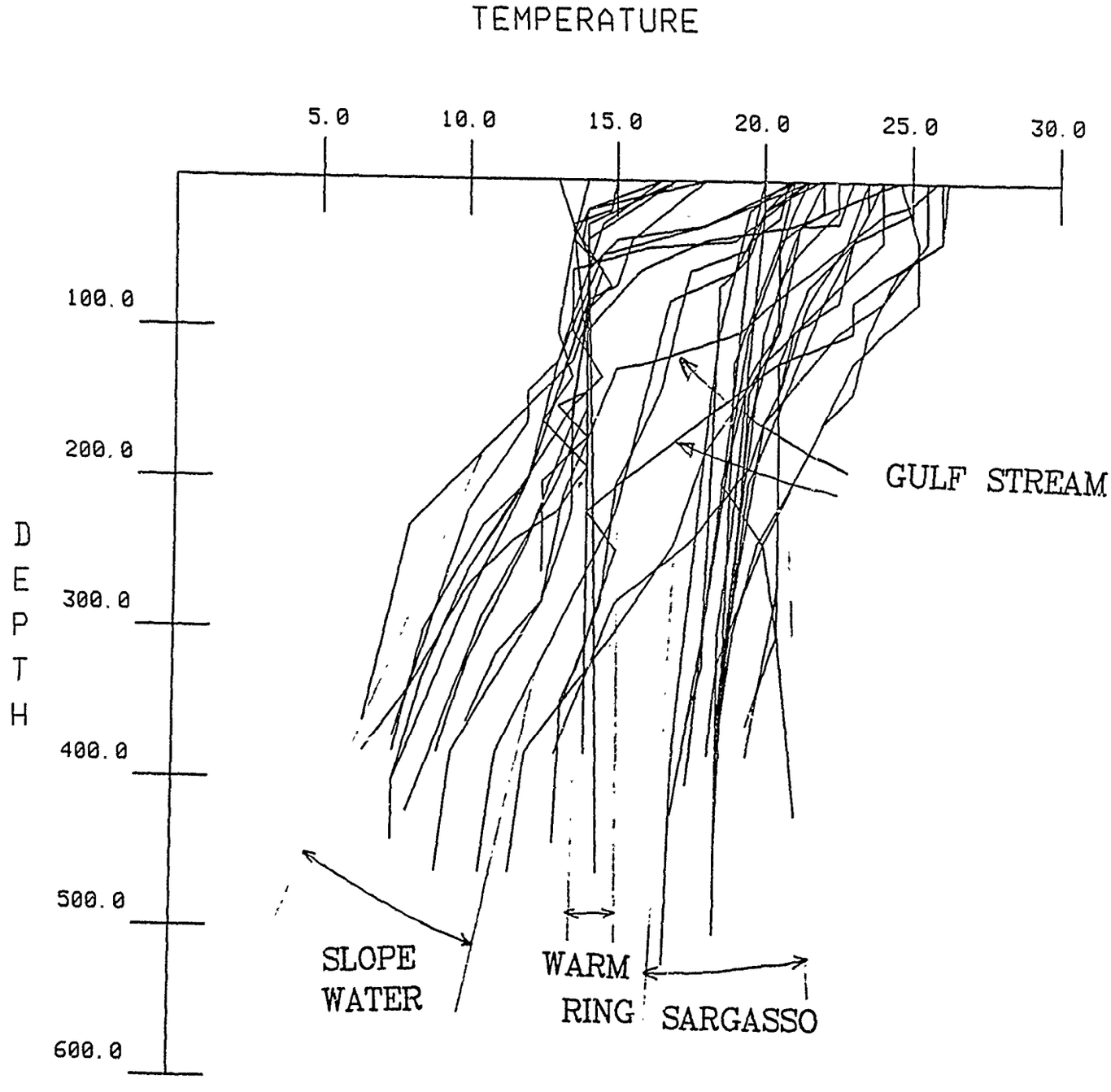

Fig. 6 — Composite vertical temperature profiles

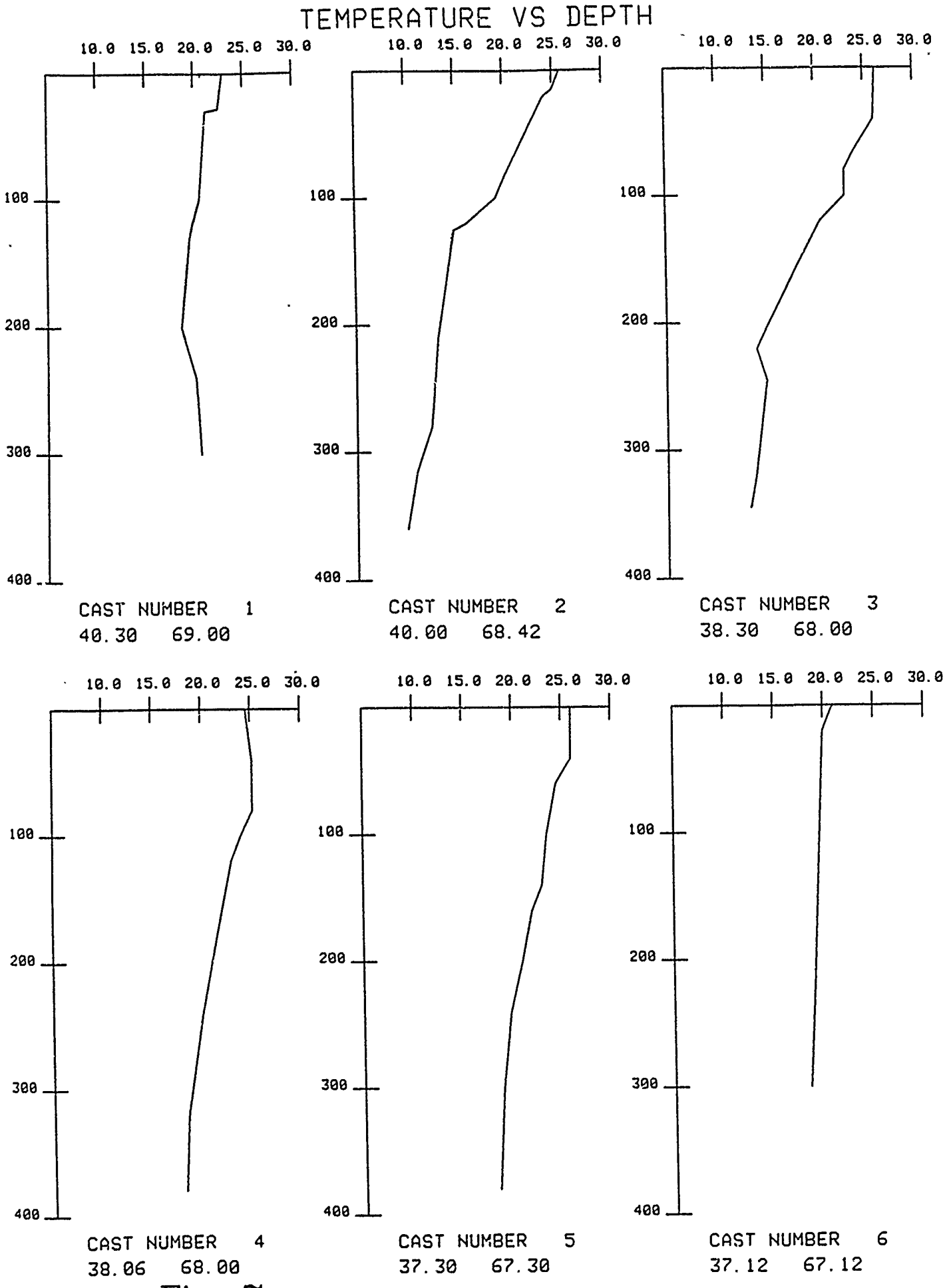

Fig. 7 — Sample individual AXBT profiles

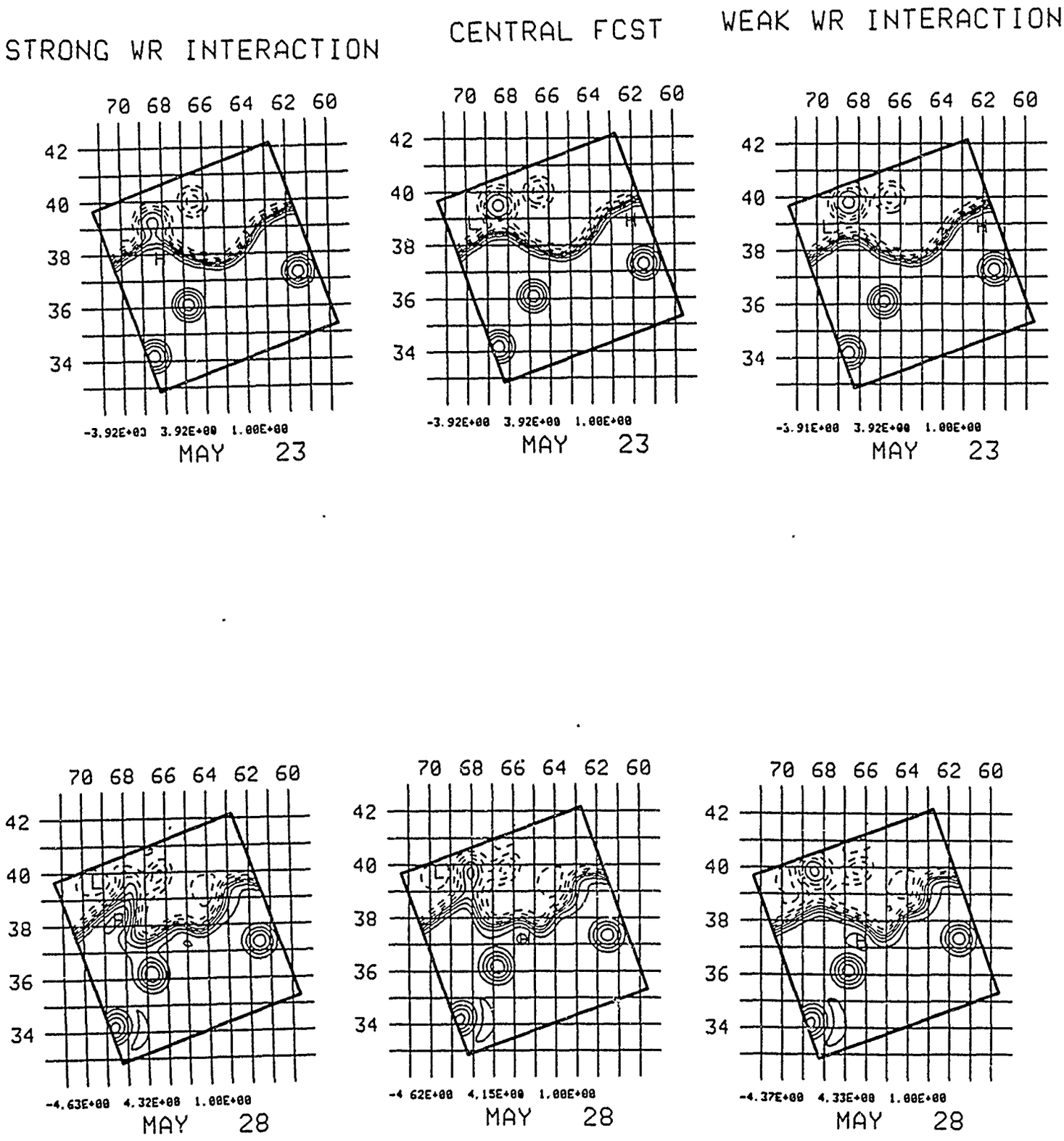

Fig. 8 — Warm ring interaction sensitivity study

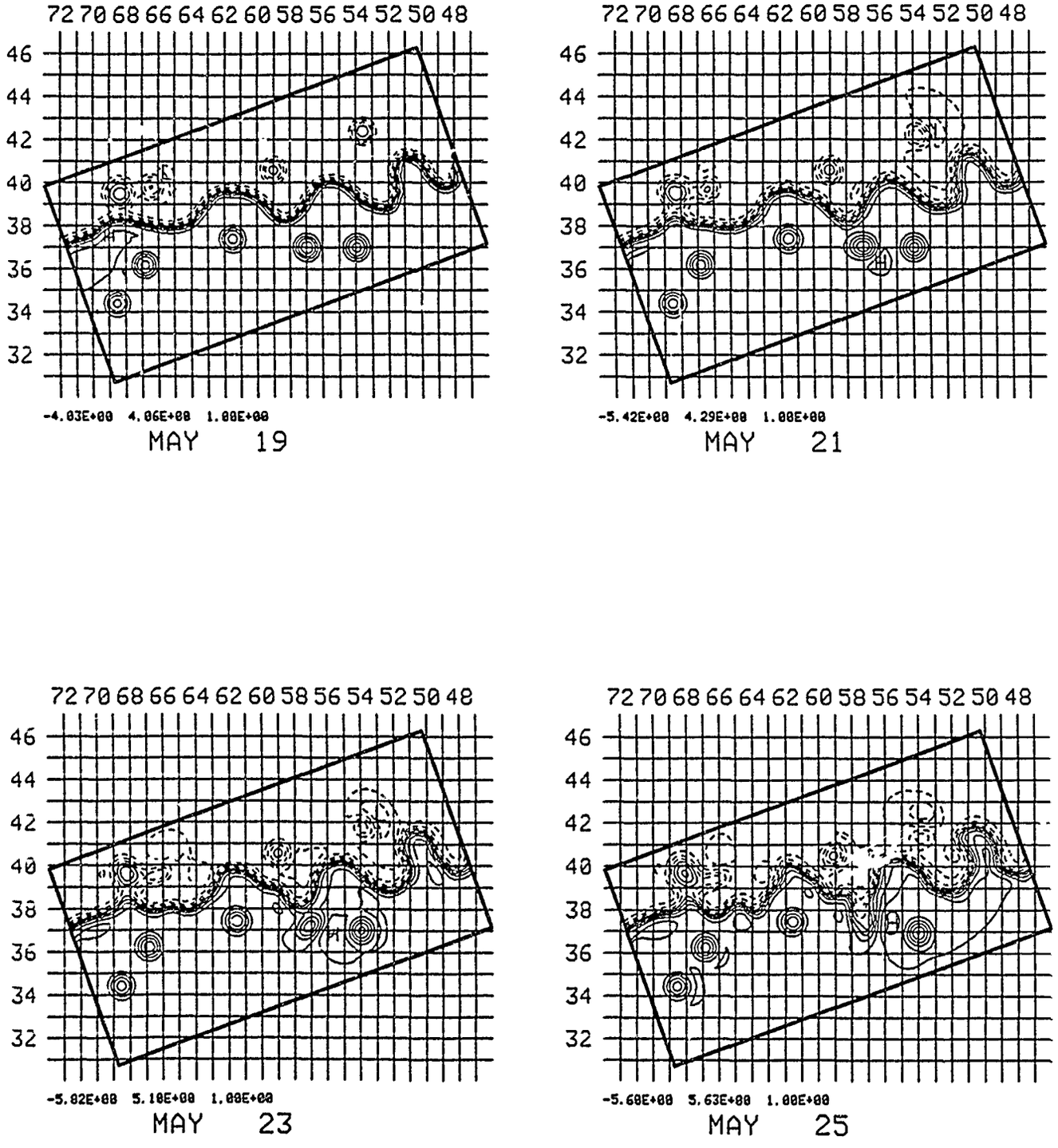

Fig. 9 — Large domain supercomputer forecast

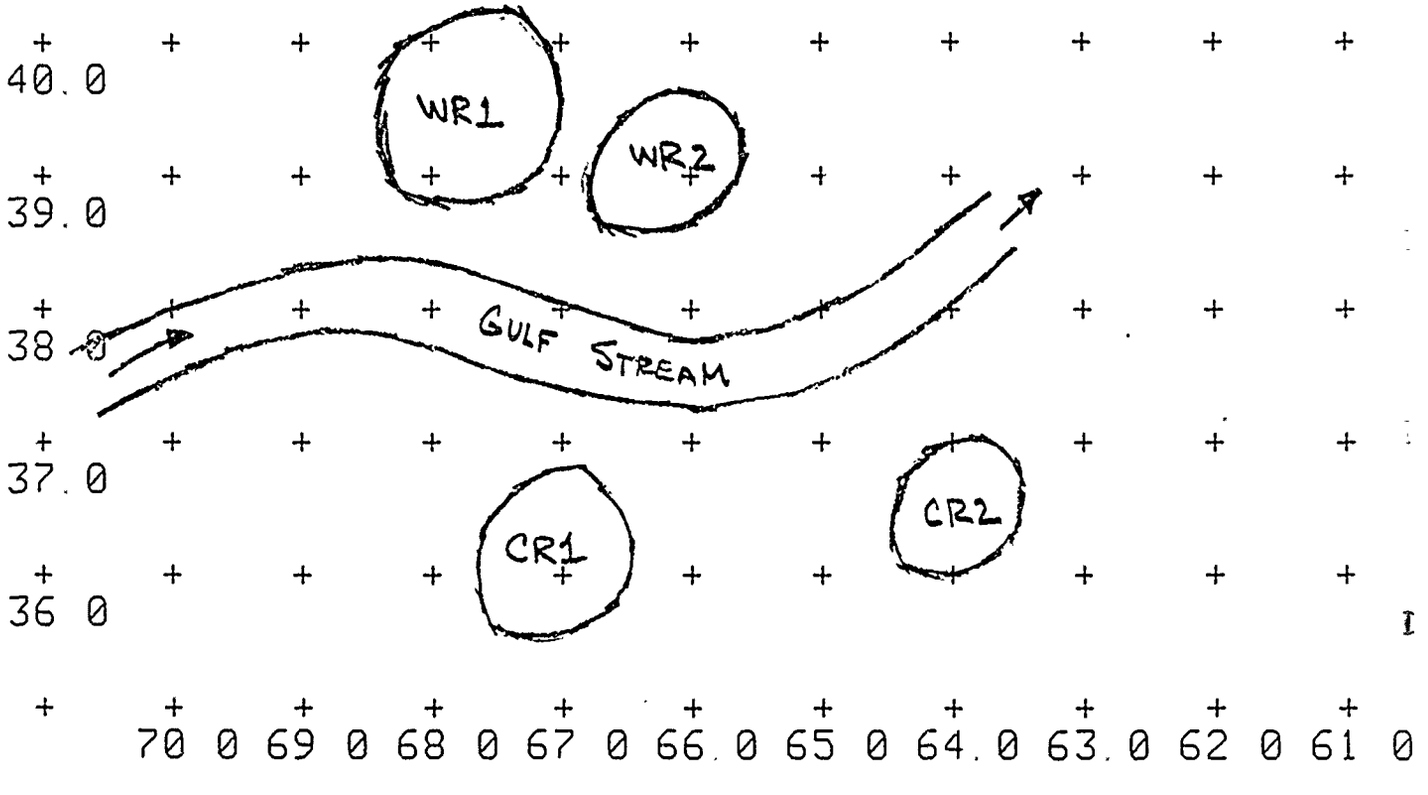

Data used for position:

GULF STREAM – IR, AXBT, Model

CR1 – AXBT

CR2 – IR

WR1 – AXBT, Model

WR2 – AXBT, Model

Fig. 10 – Composite analysis

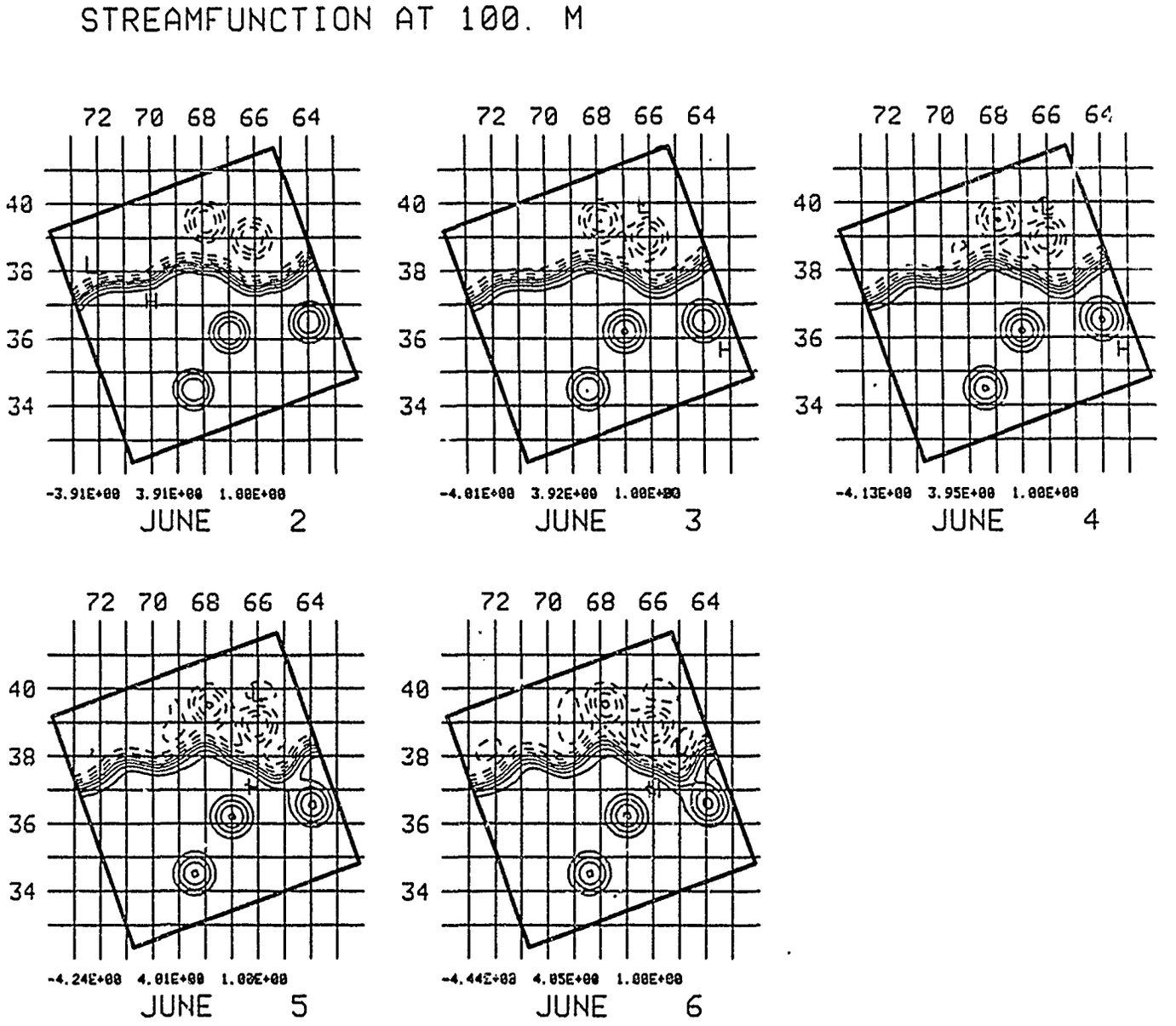

Fig. 11 — Final forecast for 2–6 June 1986

Fig. 12 — Horizontal analysis on 6 June 1986

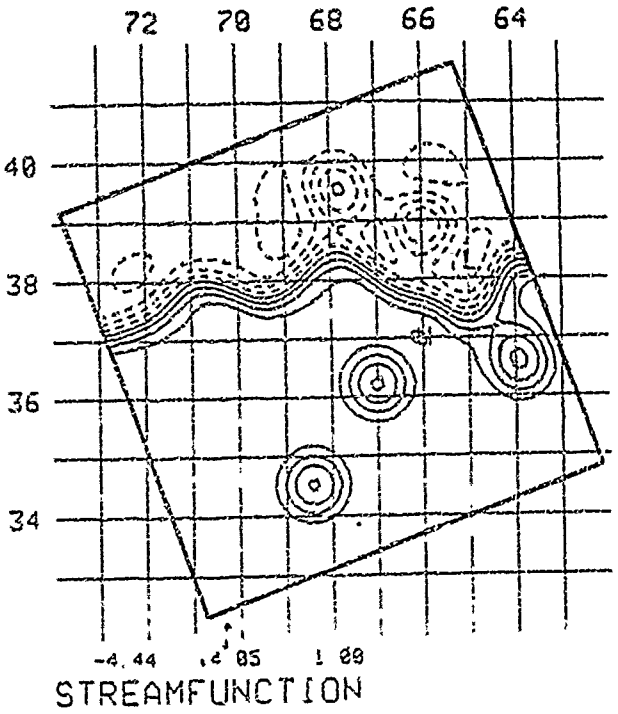

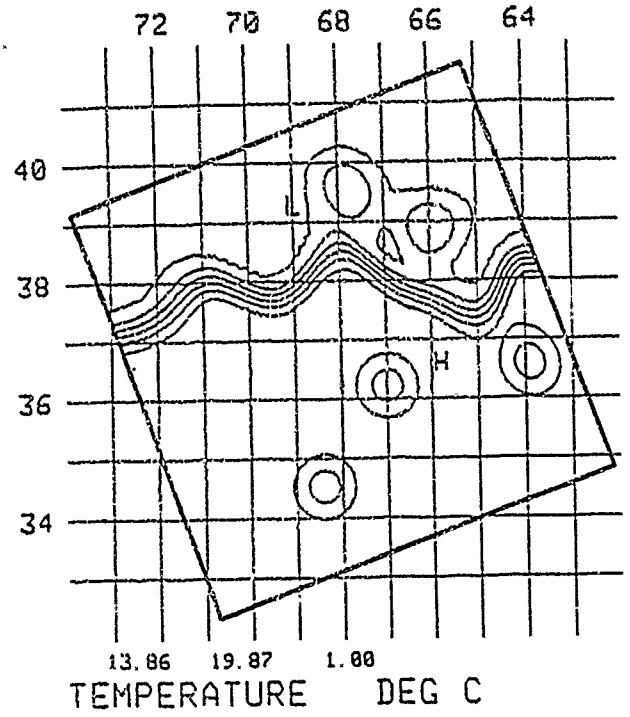

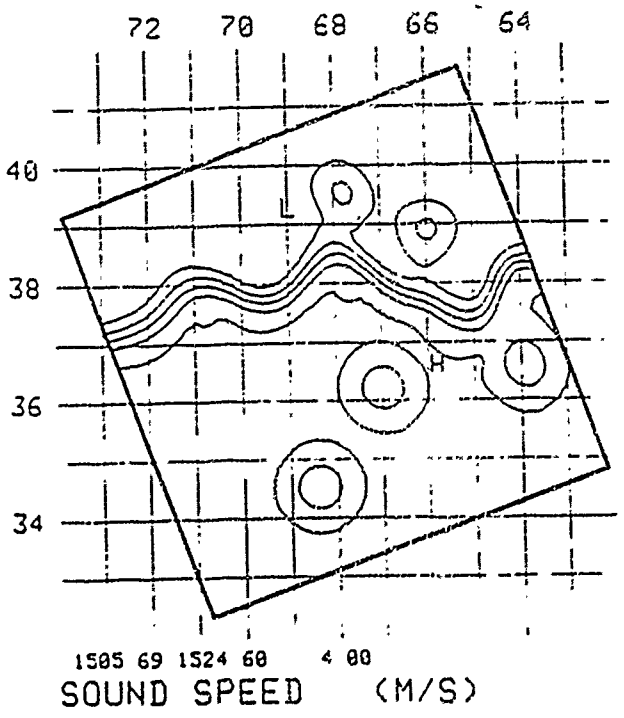

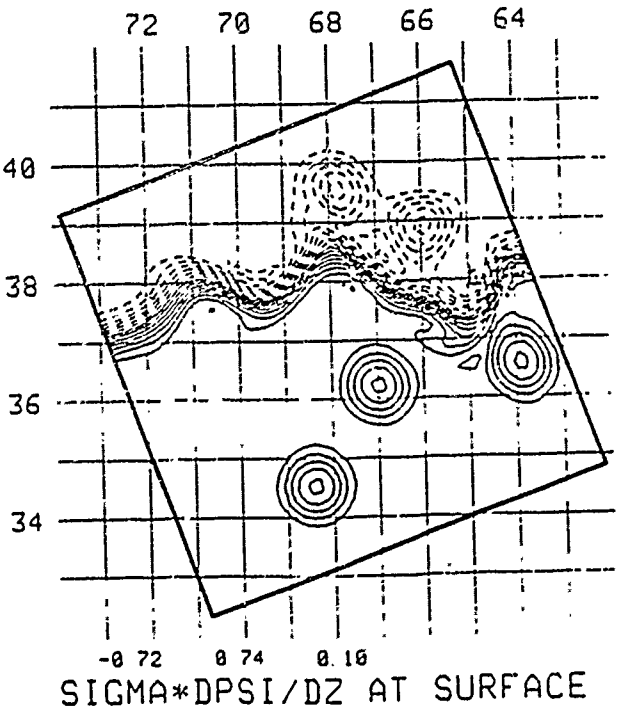

Fig. 13 — Vertical section on 5 June 1986

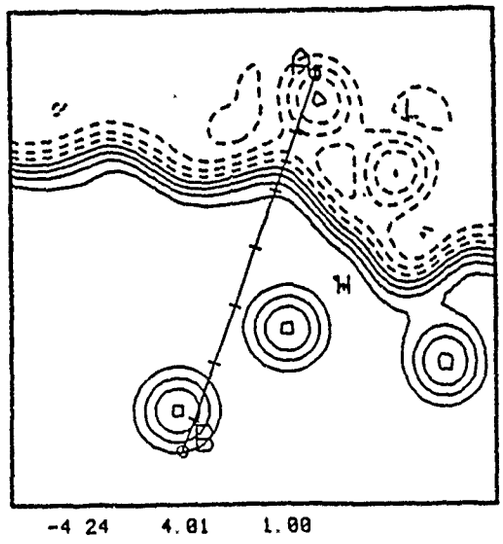

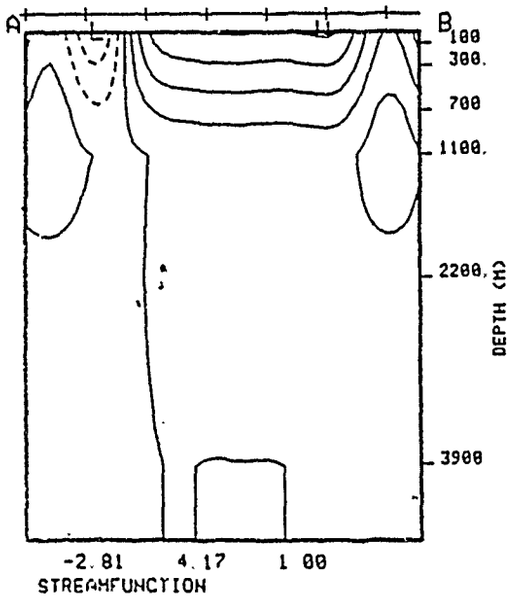

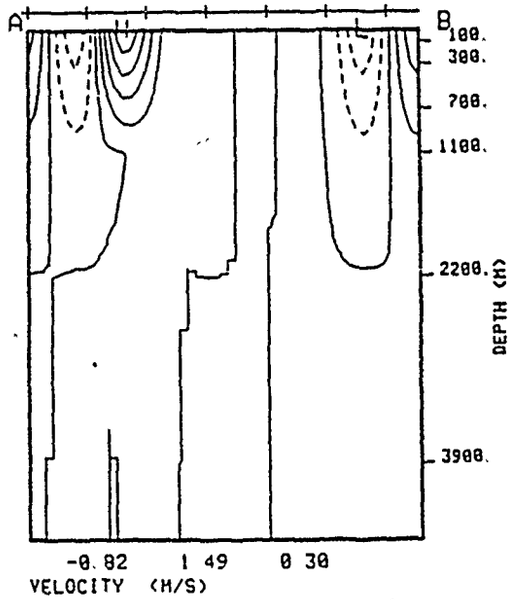

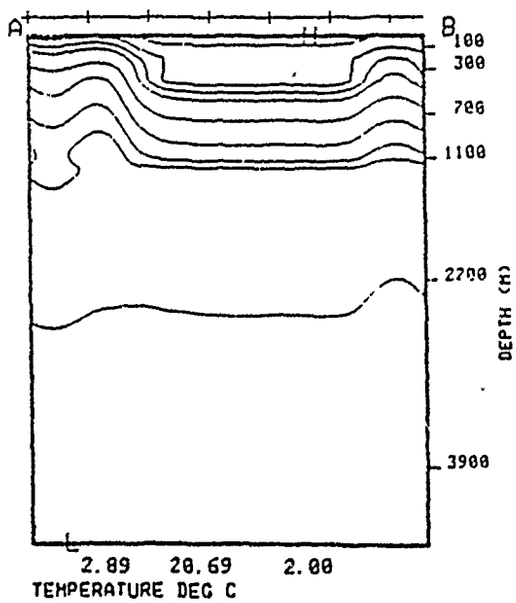

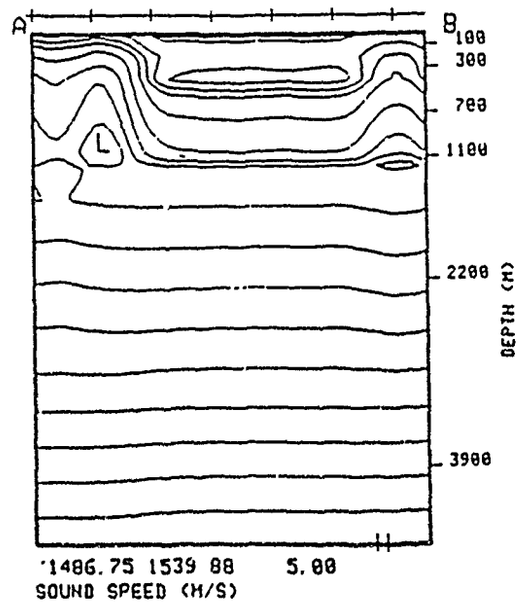

1.3 Initial and Boundary Conditions for Gulf Stream Forecasts

In order to do a forecast for a given domain of interest, initial and boundary conditions must be generated for the appropriate domain of influence. Model calculations are generally done simultaneously in both large extended regions and smaller subregions. The extended region forecast is run on a supercomputer in a standard domain that contains the entire Gulf Stream meander and ring formation region. Several considerations are involved in the choice of model domain for the subregion forecast, including the nature of the available data, the bottom topography, computational resources, and feature locations. The domain should include all known features which may influence evolution in the domain of interest. Features such as upstream meanders and ring-stream interactions may be important even though they may be several hundred kilometers from the region of interest. It is also important to choose the model domain so that the boundary conditions are simple and well observed. The inclusion of features in an influence domain larger than the region of interest can obviate the problem of "future" boundary conditions. The occurrence of large meanders or cloud covered sections near the boundaries should be avoided if at all possible. The primary concern regarding bottom topography is the continental shelf break. It is often convenient to place the northern edge of the model domain along the 1000m isobath of the shelf break for regions east of 70W. Transition regions where the bottom depth varies greatly or changes rapidly violate assumptions in the model and therefore should be avoided if possible, although this is often not the case. The New England Seamounts are both steep (0.15 m/m) and tall (O(1000m)) and are often contained within the domain of influence. They may be treated in several ways, namely (1) removing them completely, (2) shortening them by filtering, or (3) leaving them unchanged. The latter approach is most often used for operational forecasting purposes. Although this does violate some quasigeostrophic assumptions, sensitivity studies show that the effects are not important on time scales of 1-2 weeks. Such forecasts are of "short" duration on the inter-

nal synoptic/mesoscale time scale of the ocean. Thus the overall and long-time effects of the bottom topography interactions may be implicitly contained in the initialization and updating data.

Once the model domain is chosen, the initial and boundary conditions are generated using a feature model approach. Due to the large spacial extent of the phenomena of interest (hundreds of kilometers) it is not economically feasible to obtain the data necessary to produce frequent synoptic realizations through objective mapping of the field variables. The feature model approach takes advantage of the fact that the Gulf Stream and its associated warm and cold rings are the dominant features in the region. These features are large, energetic, and easily identifiable. Further, each one has characteristic properties regarding its size, shape, structure, and strength. In other words, the Gulf Stream looks the same (for the most part) in cross section anywhere along its path. Likewise, rings have similar velocity structures although their magnitudes may decay in time. Thus, historical data sets can be used to obtain approximate three dimensional flow fields for a given configuration in the Gulf Stream region. Individual representations of these feature models with flow parameters are shown in Figure 14. Figure 15 is a schematic sketch of a 6 level model initialization.

The initial condition is obtained through a composite analysis of all available data. This may include SST, SSH, AXBT information, float tracks, and previous model calculations. Either the axis or the north wall of the Gulf Stream must be located throughout the model domain as a set of discrete points. A smooth curve is then fit through these points using a cubic spline fit. There is some sensitivity to the digitization of the stream. Care must be taken to ensure that the digitized track represents the path accurately. Often times small changes to the discrete points are required to avoid unrealistic small scale bumps, perturbations, and artifacts of the curve fitting scheme. Having determined the stream position and its characteristics (strength, width and thermocline depth) the feature

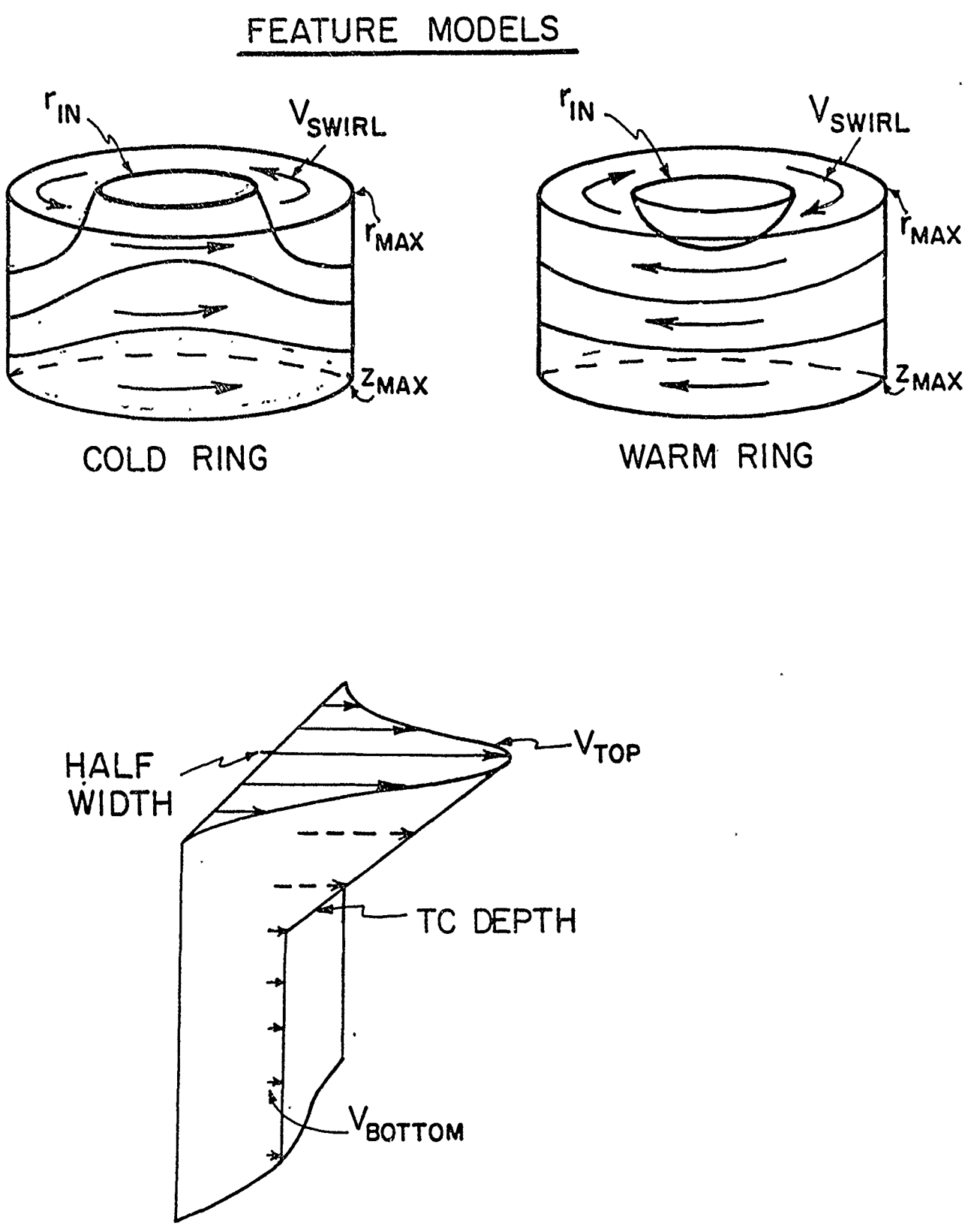

Fig. 14 — Gulf Stream feature models

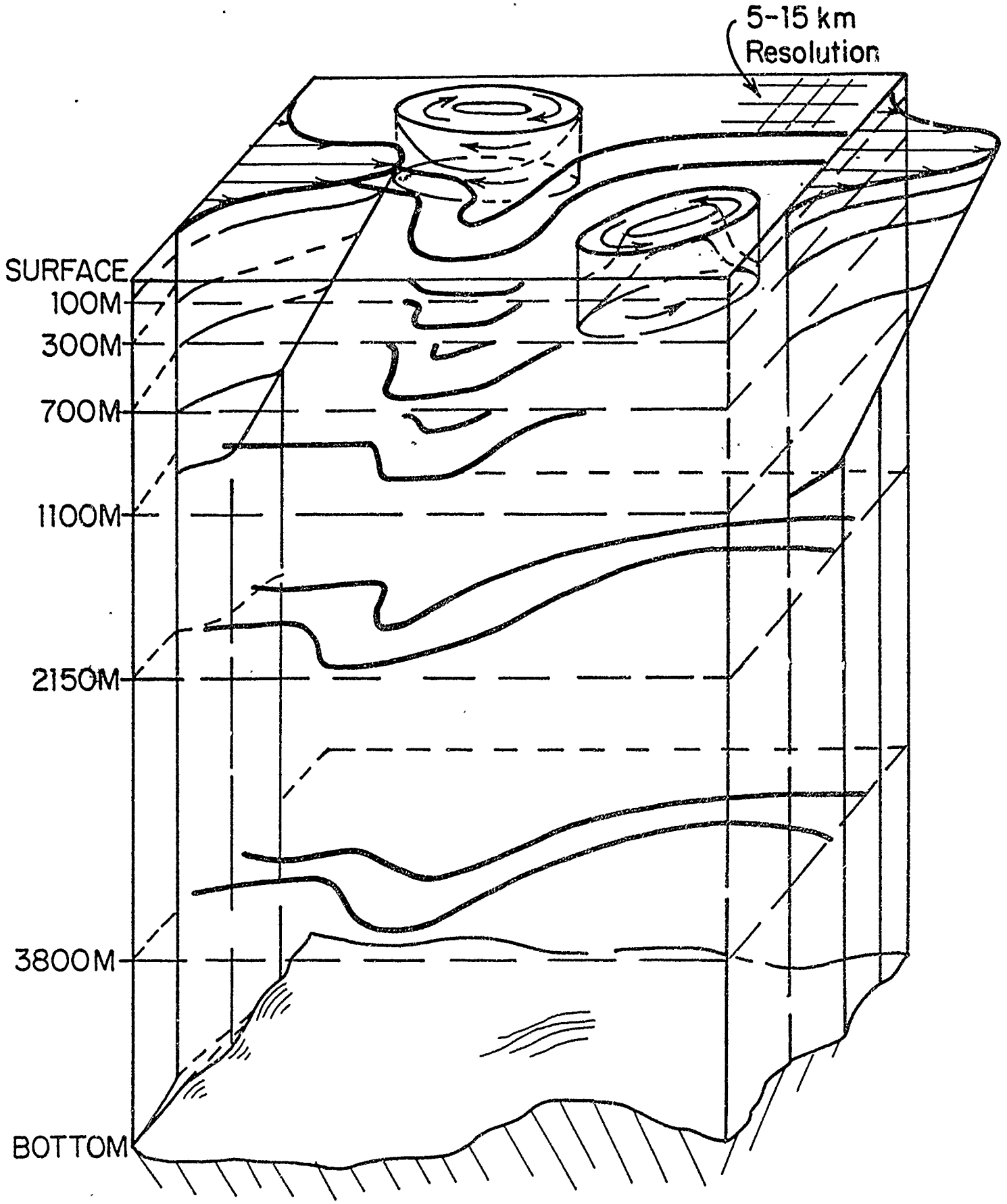

Fig. 15 — Schematic of feature model initialization

model is laid down in "still" water. Next the rings are added to the field. Ring parameters to be chosen include swirl speed, maximum radius, radius of maximum velocity, maximum depth, vertical shear and the type of ring (warm or cold). Again, these features are simply laid down into the model domain in the appropriate position. In the event that two features are interacting their fields are superimposed. The feature model initialization approach thus allows for the generation of three dimensional fields through limited data sets. These initial fields then evolve and fill in the near fields to produce realistic phenomena not included in the initial condition such as shingles, outbreaks, countercurrents, mesoscale eddies, and recirculations. As feature models for these additional flow components are developed they will be added to the initialization scheme.

The feature model initialization undergoes a three phase evolution during model integration: dynamical adjustment, dynamical interpolation, and dynamical evolution. Dynamical adjustment of the features takes place in the first couple of days of integration. The analytic fields make slight adjustments to come into balance with quasigeostrophic dynamics. Then dynamical interpolation takes place between the features as the motionless water spins up to the presence of the rings and the stream. These near field circulations begin to appear after a couple of days and continue to strengthen and develop. The dynamical evolution takes place on time scales of several days to weeks as the features interact and evolve in accordance with the QG equations. See the sample forecast in Figure 11.

In addition to initial flow fields, the QG model requires data at the boundaries throughout the forecast. Because the operational forecasts are done in real time, no actual data is available. Estimates must therefore be made for the future positions of inflow and outflow. Analog forecasting is used to propagate the feature positions ahead in time (see Figure 2). The propagation rate and direction may be estimated in two ways. First, typical propagation rates for the various features based on historical data sets may be used to predict future behavior. The second method estimates the propagation rates based on

recent behavior (in the past 2-3 weeks) of the features. Typically, meanders propagate eastward at about one degree per week and rings propagate 0.3 degrees per week to the southwest.

1.4 Model Domains

The correct choice of model domain is essential in producing accurate forecasts. Many factors must be considered including available data, purpose of the model run, bottom topography, and computational resources. The model is used for extended domain supercomputer runs, operational forecasting, and special subregion or geophysical fluid dynamical studies. Standard domains for each of these applications have been developed and are described in Table 1. Each of these domains is pictured in Figure 16. In general, one of these off-the-shelf domains will satisfy the requirements of a typical forecast.

Table 1 — Standard domains

DOMAIN	XBASIN	YBASIN	M	N	CLAT	CLONG	THETA	USAGE
H1	36000	28800	61	49	37.5	64.5	20	OP.FCASTING
H2	48000	36000	81	61	38	62.5	20	OP.FCASTING
H4	36000	28800	61	49	38.5	61	0	OP.FCASTING
I2	32400	28800	55	49	36	70	30	INLETREGION
I3	32400	28800	55	49	38	65	30	INLETREGION
L1	84000	43200	141	73	38.5	59.5	20	S.COMPUTER
R1	26800	9000	49	31	40	65	0	RING GFD STUDY
S_	32400	32400	55	55	37	68	20	OP FCAST SUBR.
S0	32400	32400	55	55	37.5	66.8	20	OP FCAST SUBR.
S1	32400	32400	55	55	37.5	65.5	20	OP FCAST SUBR.
S2	32400	32400	55	55	38.5	60	10	OP FCAST SUBR.
S3	32400	32400	55	55	39.8	55	0	OP FCAST SUBR.
T1	14400	14400	49	49	39	68	0	HIGH RES SUBR.

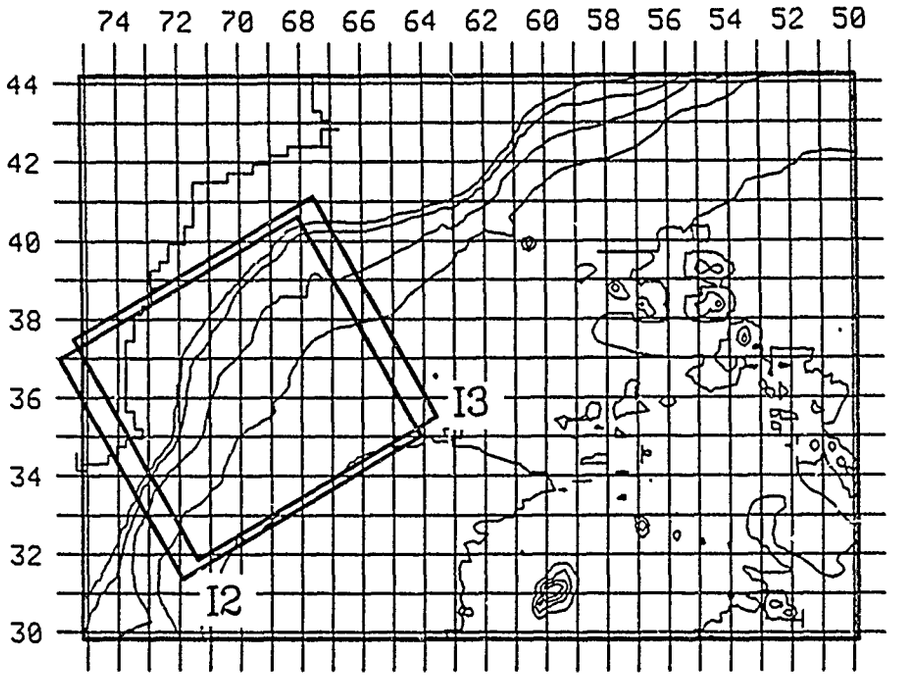

Fig. 16b — Inlet region domains

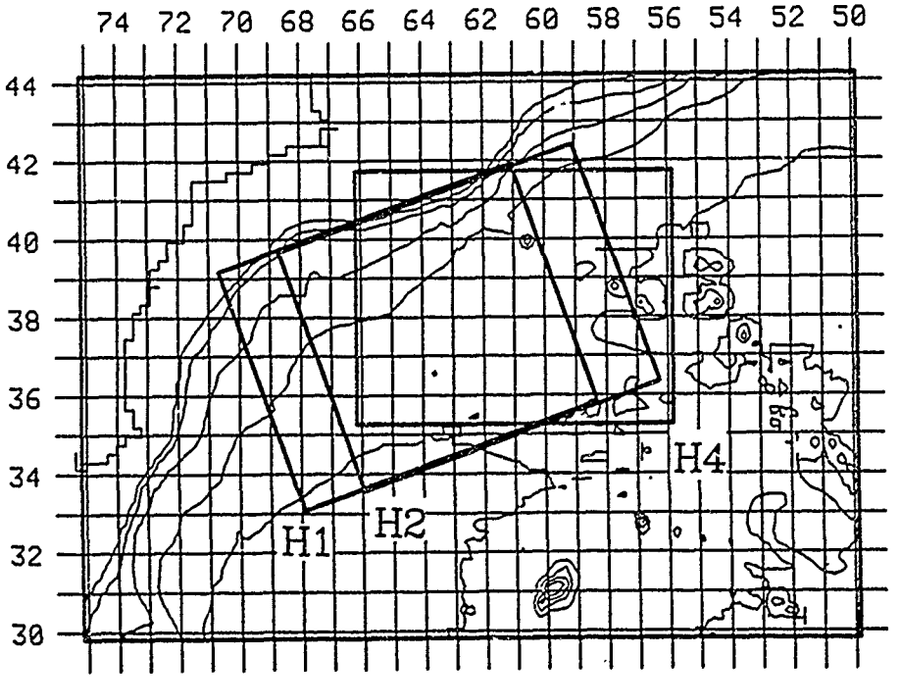

Fig. 16a — Operational domains

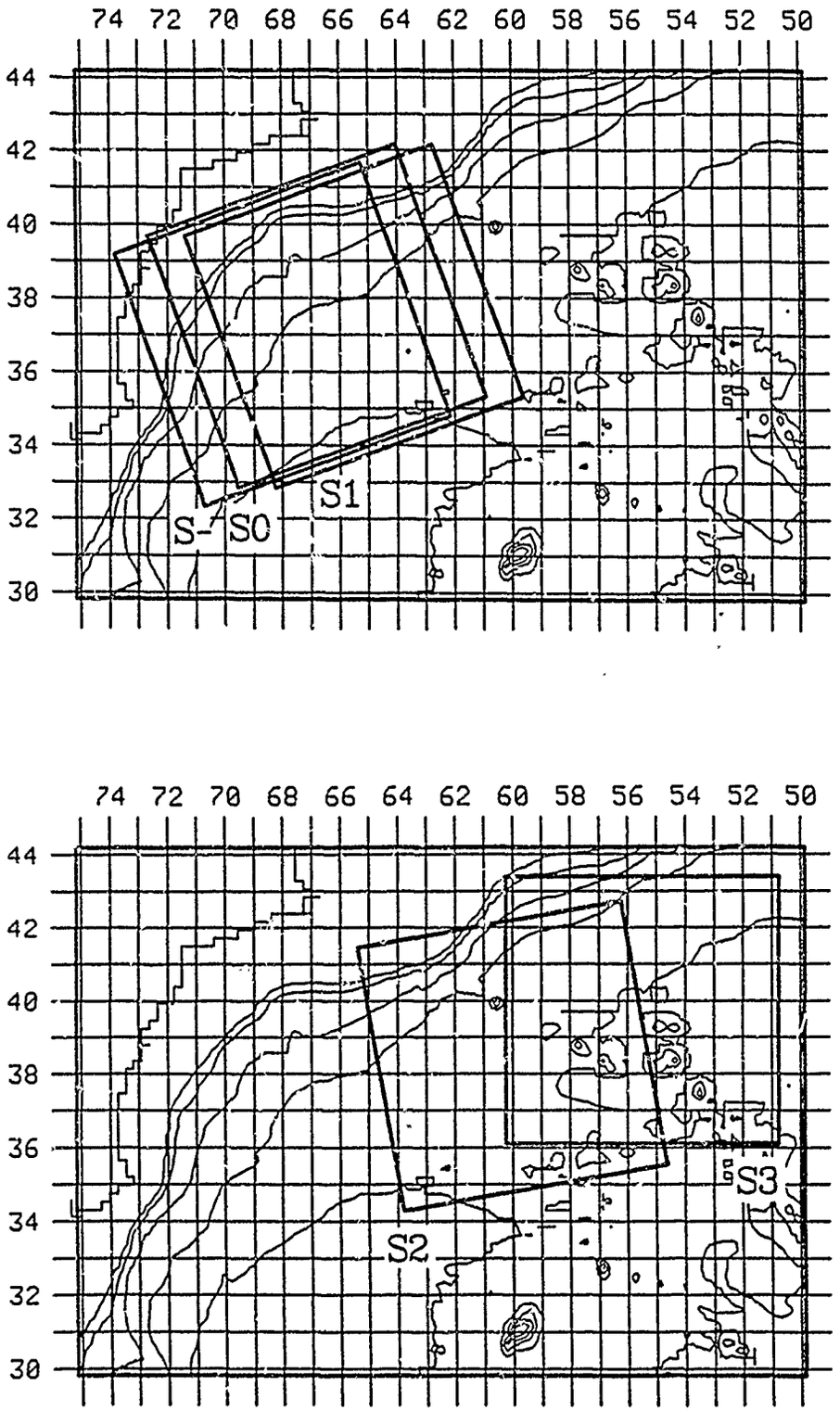

Fig. 16c — Subregion domains

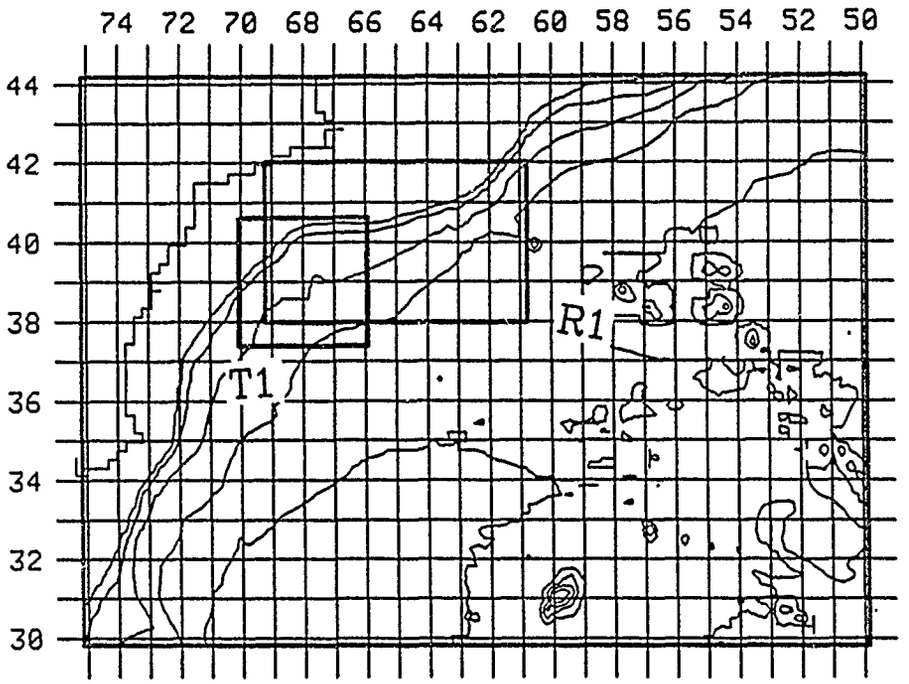

Fig. 16d — GFD study domains

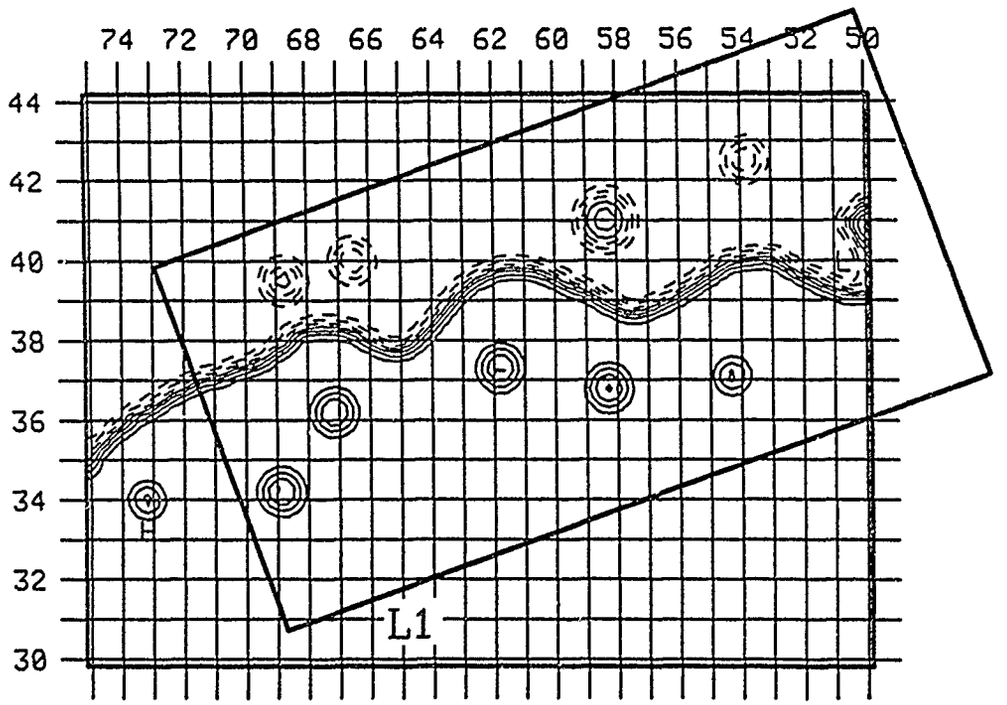

Fig. 16e — Extended domain; supercomputer applications

1.5 Timeline and run tables

Real time forecasting has been underway in the Gulf Stream region since November of 1985; since January 6, 1986 an attempt has been made to maintain nowcasts and forecasts within the capabilities of our academic research group. During that time there have been several joint experiments conducted with outside groups. The Harvard group has produced real time operational information in specified regions of interest while AXBT information has been provided for model initialization and verification. The number of forecasts produced between January 6 and June 2 is shown in Figure 17a, which shows clearly the three start-ups during this period. Figures 17b and 17c show the initial conditions and final forecast field for each of the experiments. Details of the model runs are provided in Table 2. Table 3 lists the subset of selected experiments presented in this report.

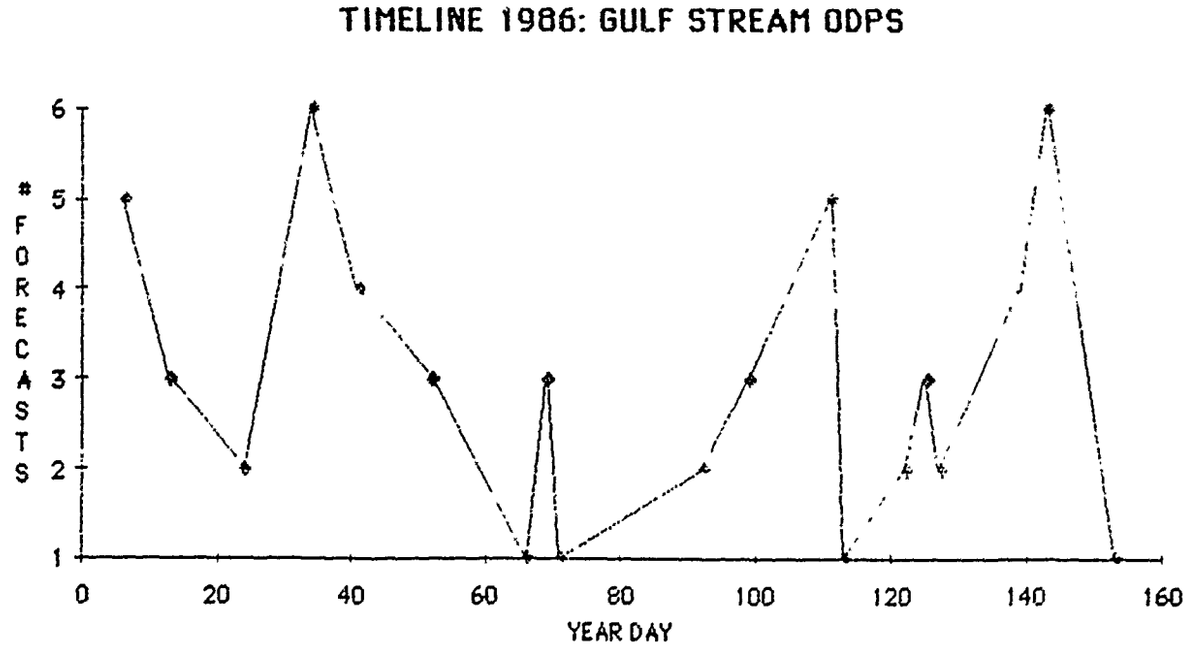

Fig. 17a — Forecasting frequency for 1 Jan – 6 Jun 1986

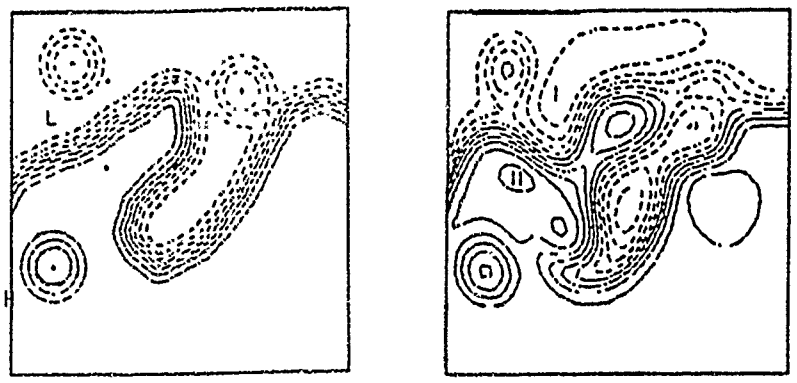

29 Nov – 4 Dec 1985

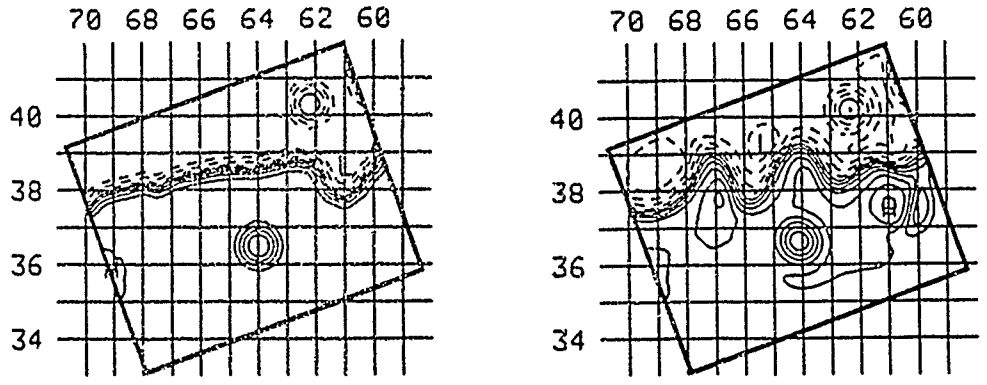

6–13 Jan 1986

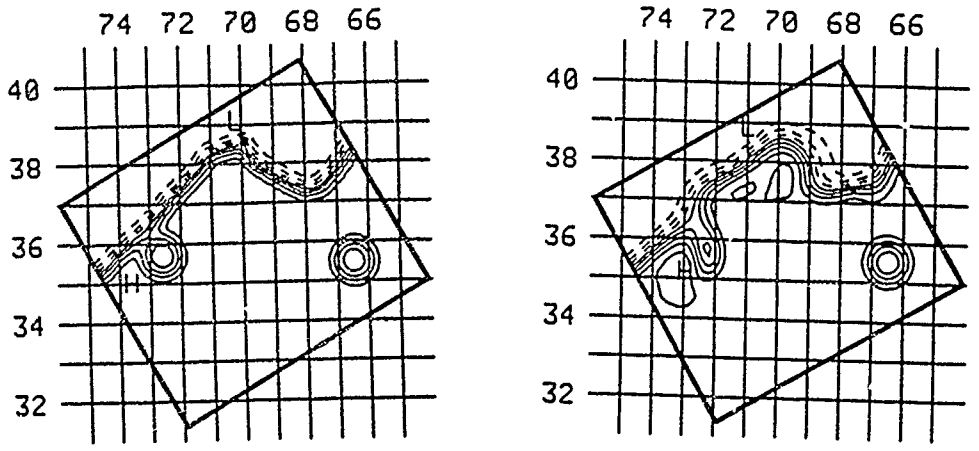

3–6 Feb 1986

Fig. 17b – Initial Condition and Final Forecast Field

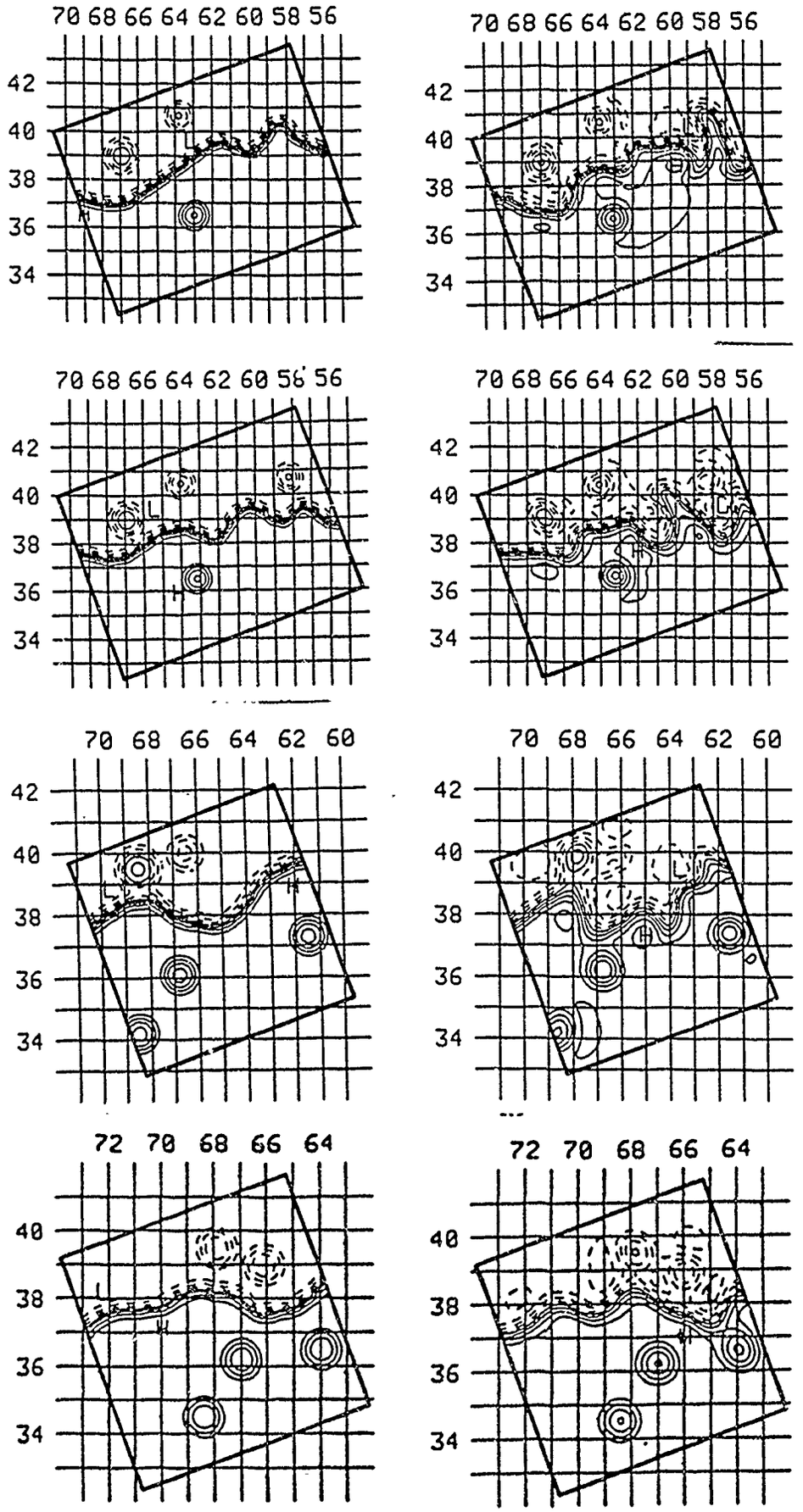

Fig. 17c — Initial Condition and Final Forecast Field

Table 2 — Forecasts performed 29 Nov 1985 – 6 June 1986

FCAST #	DATES	STARTYD	DURATION	DOMAIN	BC	AXBTs	DESCRIBED IN SECTION
1	NOV 29-DEC 5	332	7	1	E	YES	2.1
2	NOV 29-DEC 5	332	7	1	E	YES	
3	NOV 29-DEC 5	332	7	1	E	YES	
4	JAN 6-JAN 13	6	7	H1	I	YES	2.2
5	JAN 6-JAN 13	6	7	H1	P	YES	
6	JAN 6-JAN 13	6	7	I1	I	YES	
7	JAN 6-JAN 13	6	7	I1	P	YES	
8	JAN 6-JAN 13	6	7	I1	P	YES	
9	JAN 13-JAN 24	13	11	H1	I	NO	
10	JAN 13-JAN 24	13	11	H1	P	NO	
11	JAN 13-JAN 24	13	11	I1	P	NO	
12	JAN 24-FEB 3	24	10	H1	P	NO	
13	JAN 24-FEB 3	24	10	I1	P	NO	
14	FEB 3-FEB 10	34	7	I2	I	YES	2.3
15	FEB 3-FEB 10	34	7	I2	I	YES	
16	FEB 3-FEB 10	34	7	I2	I	YES	
17	FEB 3-FEB 10	34	7	I2	E	YES	
18	FEB 3-FEB 10	34	7	I2	E	YES	
19	FEB 3-FEB 10	34	7	I2	E	YES	
20	FEB 10-FEB 17	41	7	I2	P	NO	
21	FEB 10-FEB 17	41	7	I2	P	NO	
22	FEB 10-FEB 26	41	16	I2	E	NO	
23	FEB 10-FEB 26	41	16	I2	E	NO	
24	FEB 21-FEB 28	52	7	I2	E	NO	
25	FEB 21-FEB 28	52	8	I2	E	NO	
26	FEB 21-FEB 28	52	8	I2	E	NO	
27	MAR 7-MAR 15	66	8	H1	E	NO	
28	MAR 10-MAR 17	69	7	H1	E	NO	
29	MAR 10-MAR 17	69	7	H1	E	NO	
30	MAR 10-MAR 17	69	7	H1	E	NO	
31	MAR 12-MAR 17	71	5	H1	E	NO	
32	APR 2-APR 9	92	7	H2	I	NO	2.4
33	APR 2-APR 9	92	7	H2	I	NO	
34	APR 9-APR 16	99	7	H2	E	NO	
35	APR 9-APR 16	99	7	H2	E	NO	
36	APR 9-APR 16	99	7	H2	E	NO	
37	APR 21-APR 28	111	7	H2	E	YES	
38	APR 21-APR 28	111	7	S1	E	YES	
39	APR 21-APR 28	111	7	T1	E	YES	
40	APR 21-APR 28	111	7	T2	E	YES	
41	APR 21-APR 28	111	7	T3	E	YES	
42	APR 23-APR 30	113	7	T1	E	YES	
43	MAY 2-MAY 9	122	7	H2	E	YES	
44	MAY 2-MAY 9	122	7	S1	E	YES	
45	MAY 5-MAY 12	125	7	S1	E	YES	
46	MAY 5-MAY 12	125	7	S1	E	YES	
47	MAY 5-MAY 12	125	7	S1	E	YES	
48	MAY 7-MAY 14	127	7	L1	E	YES	
49	MAY 7-MAY 14	127	7	S1	E	YES	
50	MAY 19-MAY 26	139	7	L1	E	YES	2.5.1
51	MAY 19-MAY 26	139	7	S1	E	YES	
52	MAY 19-MAY 26	139	7	S2	E	YES	
53	MAY 19-MAY 26	139	7	S3	E	YES	

Table 2 — Forecasts performed 29 Nov 1985 – 6 June 1986

54	MAY 23-MAY 30	143	7	S1	E	YES	2.5.2
55	MAY 23-MAY 30	143	7	S1	E	YES	
56	MAY 23-MAY 30	143	7	S1	E	YES	
57	MAY 23-MAY 30	143	7	S1	E	YES	
58	MAY 23-MAY 30	143	7	S1	E	YES	
59	MAY 23-MAY 30	143	7	S1	E	YES	
60	JUN 2-JUN 7	153	5	S_	E	YES	2.5.3

Table 3 — Forecasts described in text

FCAST #	DATES	STARTYD	DURATION	DOMAIN	BC	AXBTs	DESCRIBED IN SECTION
1	NOV 29-DEC 5	332	7	1	E	YES	2.1
2	NOV 29-DEC 5	332	7	1	E	YES	
3	NOV 29-DEC 5	332	7	1	E	YES	
4	JAN 6-JAN 13	6	7	H1	I	YES	2.2
5	JAN 6-JAN 13	6	7	H1	P	YES	
14	FEB 3-FEB 10	34	7	I2	I	YES	2.3
15	FEB 3-FEB 10	34	7	I2	I	YES	
16	FEB 3-FEB 10	34	7	I2	I	YES	
17	FEB 3-FEB 10	34	7	I2	E	YES	
18	FEB 3-FEB 10	34	7	I2	E	YES	
32	APR 2-APR 9	92	7	H2	I	NO	2.4
33	APR 2-APR 9	92	7	H2	I	NO	
34	APR 9-APR 16	99	7	H2	E	NO	
35	APR 9-APR 16	99	7	H2	E	NO	
36	APR 9-APR 16	99	7	H2	E	NO	
50	MAY 19-MAY 26	139	7	L1	E	YES	2.5.1
54	MAY 23-MAY 30	143	7	S1	E	YES	2.5.2
55	MAY 23-MAY 30	143	7	S1	E	YES	
56	MAY 23-MAY 30	143	7	S1	E	YES	
57	MAY 23-MAY 30	143	7	S1	E	YES	
58	MAY 23-MAY 30	143	7	S1	E	YES	
59	MAY 23-MAY 30	143	7	S1	E	YES	
60	JUN 2-JUN 7	153	5	S_	E	YES	2.5.3

2. SELECTED EXPERIMENTS

2.1 November 29 - December 6, 1985

2.1.1 Precis

This forecast was the first real time application of the Gulf Stream ODPS. The region of interest was 37.0N-38.0N, 69.5W-71.5W. Domain 1 was chosen and used in a series of sensitivity runs. The results compared very well with AXBT verification data.

2.1.2 Data analysis

NOAA IR: (Figure 18)

Nov. 29: IR was clear in the region of interest. A strong warm ring-stream interaction is occurring at 38.0N 68.5W with a deep sock meander downstream. The stream is very convoluted. Status of interaction is not well known. A second warm ring exists near 39.0N 72.0W but is not presently observed. There is a surface signature of two cold rings at 35.0N 75.0W but it is believed to be a single cold ring near the stream.

Dec. 6: Very poor IR data. No new information was provided by the IR between Nov. 29 - Dec. 6. The stream is flat near 74.0W to about 71.0W and a section of the deep sock meander may also be observed from 39.0N 69.5W to 37.0N 68.0W but is not very clear.

AXBT DATA: (Figures 19-22)

Dec. 3: North wall located at 38.1N 70.7W and 38.2N 70.0W. No evidence of deep sock meander.

Dec. 4: North wall located at 38.1N 70.8W.

Dec. 5: North wall is to the north of 38.1N along 70.0W.

2.1.3 Model runs

The primary ambiguity in the initial condition was the status of the warm ring-stream interaction near 38.5N 69.0W. A series of forecasts was done to study the influence of this interaction on the flow evolution. These model runs are forecasts 1 through 3 in the selected run table. A brief description of the model runs follows.

Central forecast C1, Figure 24: This was the central forecast for the experiment. An intermediate strength interaction was used. The warm ring is absorbed and a new stronger ring appears to be reforming. The stream turns to the south near 72.0W and then flows into the deep sock meander.

Sensitivity run S1A, Figure 25: In this sensitivity run all of the warm and cold rings have been removed from the initial condition. The stream on Dec 3 is very similar to run C1. The rings do not appear to have a large effect on the forecast.

Sensitivity run S1B, Figure 26: The warm ring has been removed. The results are very similar to C1 except that the new warm ring formation appears to be a little slower. There is a small error in the boundary conditions of this run which may account for the differences.

2.1.4 Summary

The AXBT data located the stream and was in good agreement with the NOAA IR near 70.0W on Dec 3, 4 and 5. There was no evidence of the deep sock meander on Dec 3. There was no IR data available on that day. No AXBT data was available in the vicinity of the warm ring-stream interaction.

The model runs showed an insensitivity to the rings present in the initial condition. The tendency to form a strong large looping meander at 69.0W is evident in all runs. The deep sock meander changes shape and deepens slightly in each forecast.

The model results compared well with the AXBT data on Dec 3, 4 and 5 in locating the north wall along 70.0W. IR and additional AXBT data was not sufficient for a more complete verification.

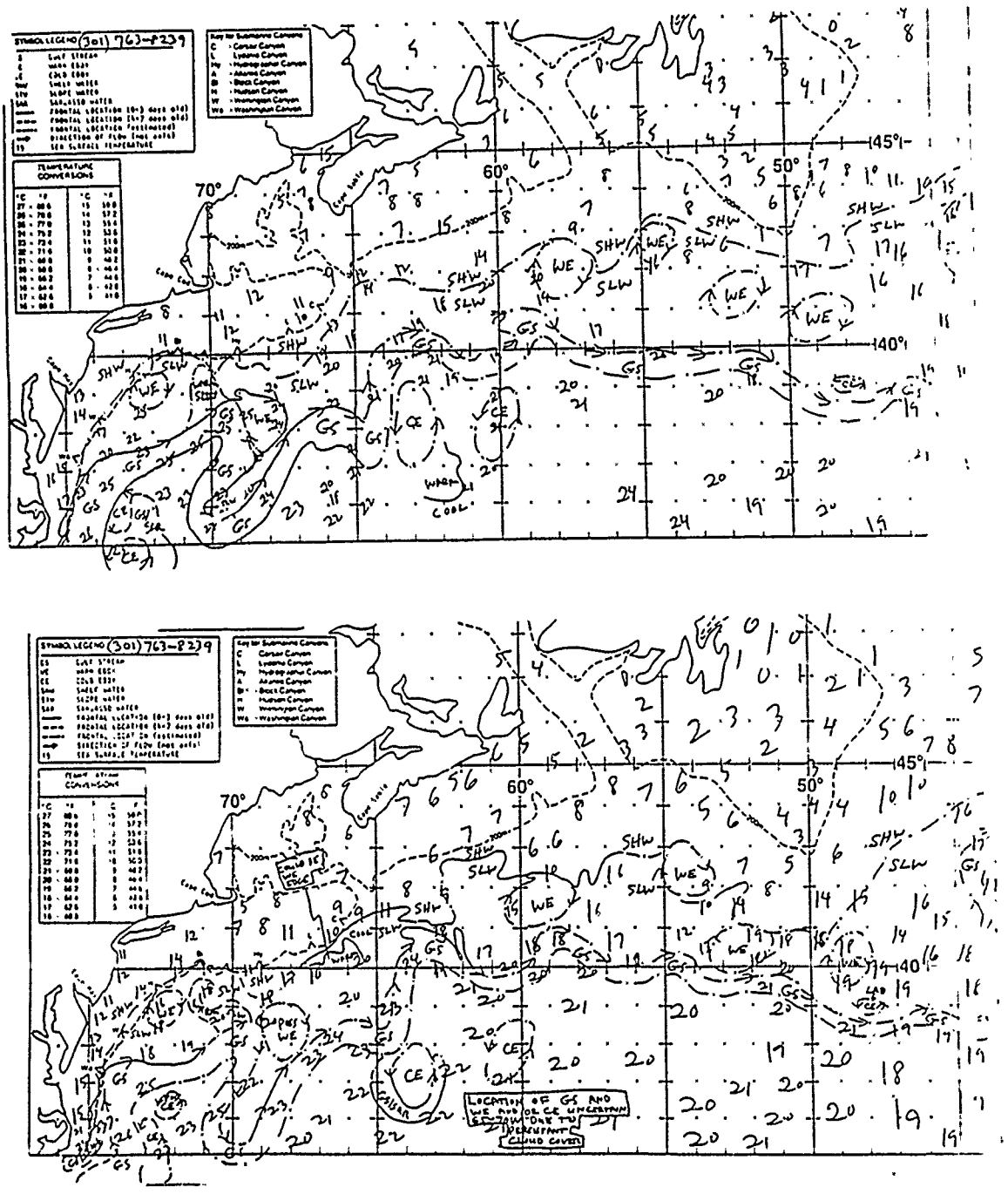

Fig. 18 — NOAA IR data for 29 November and 6 December 1985

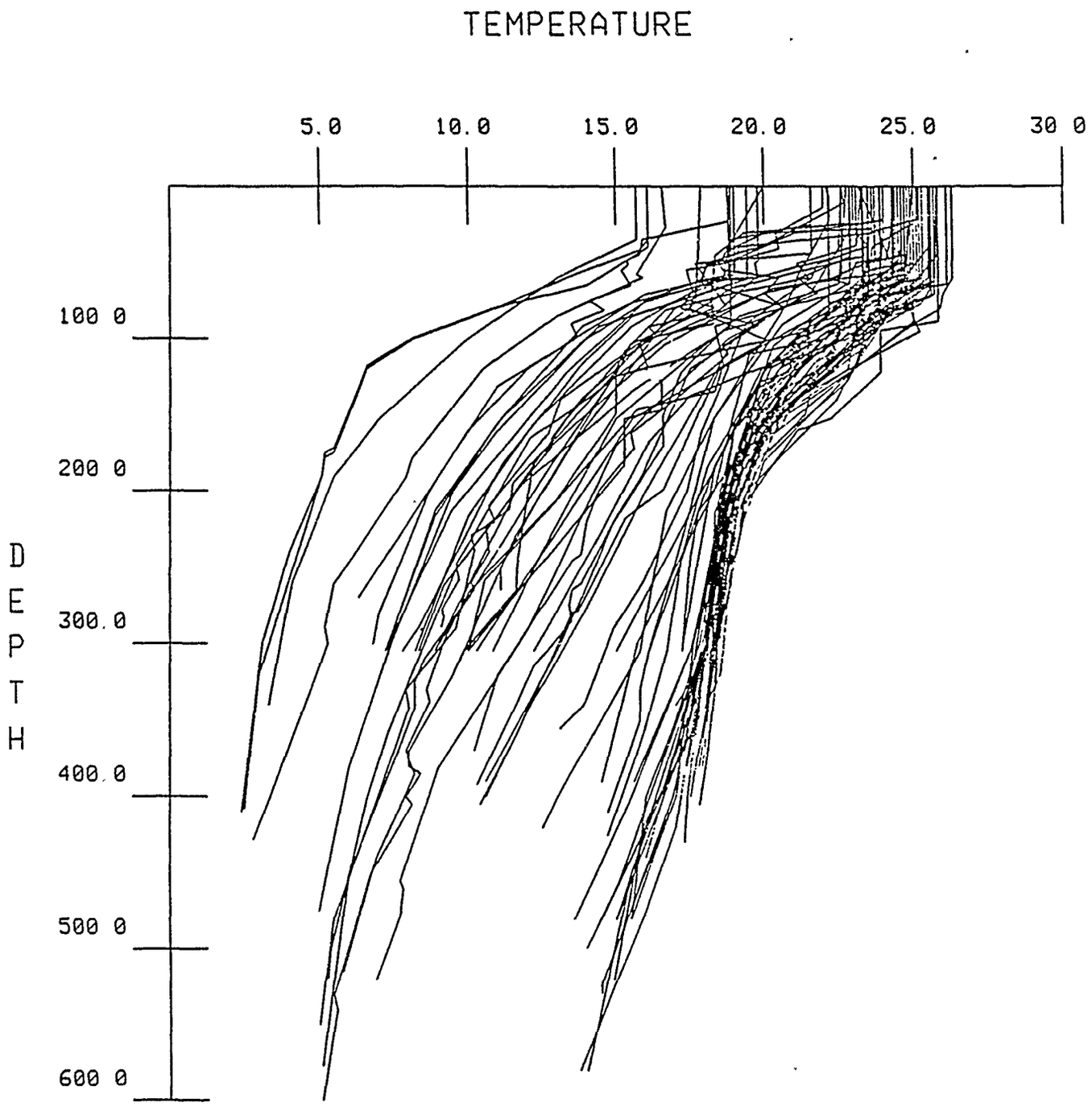

Fig. 19 — Composite of AXBT traces 3–5 December 1985

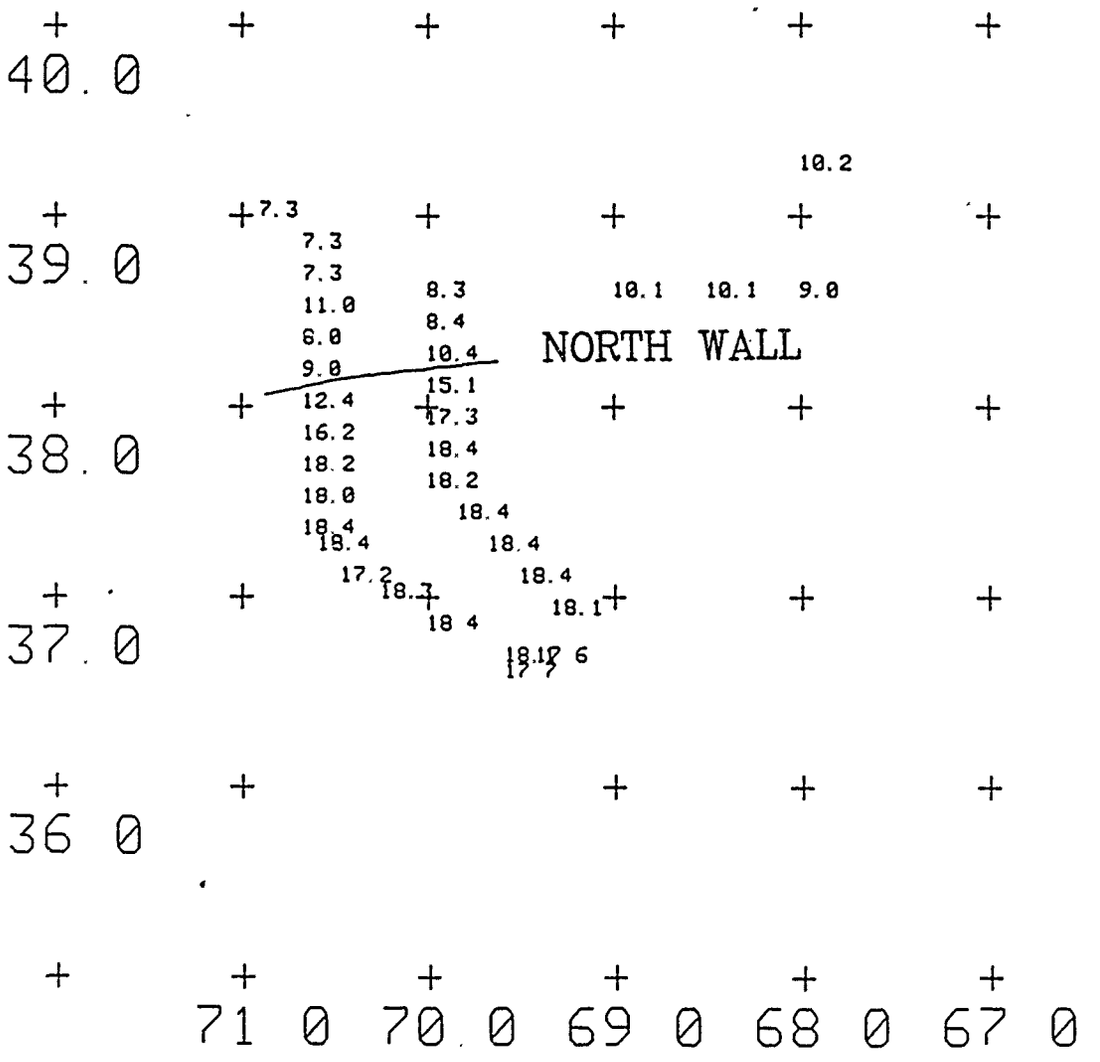

Fig. 20 — AXBT data 3 December 1985: 300m temperature

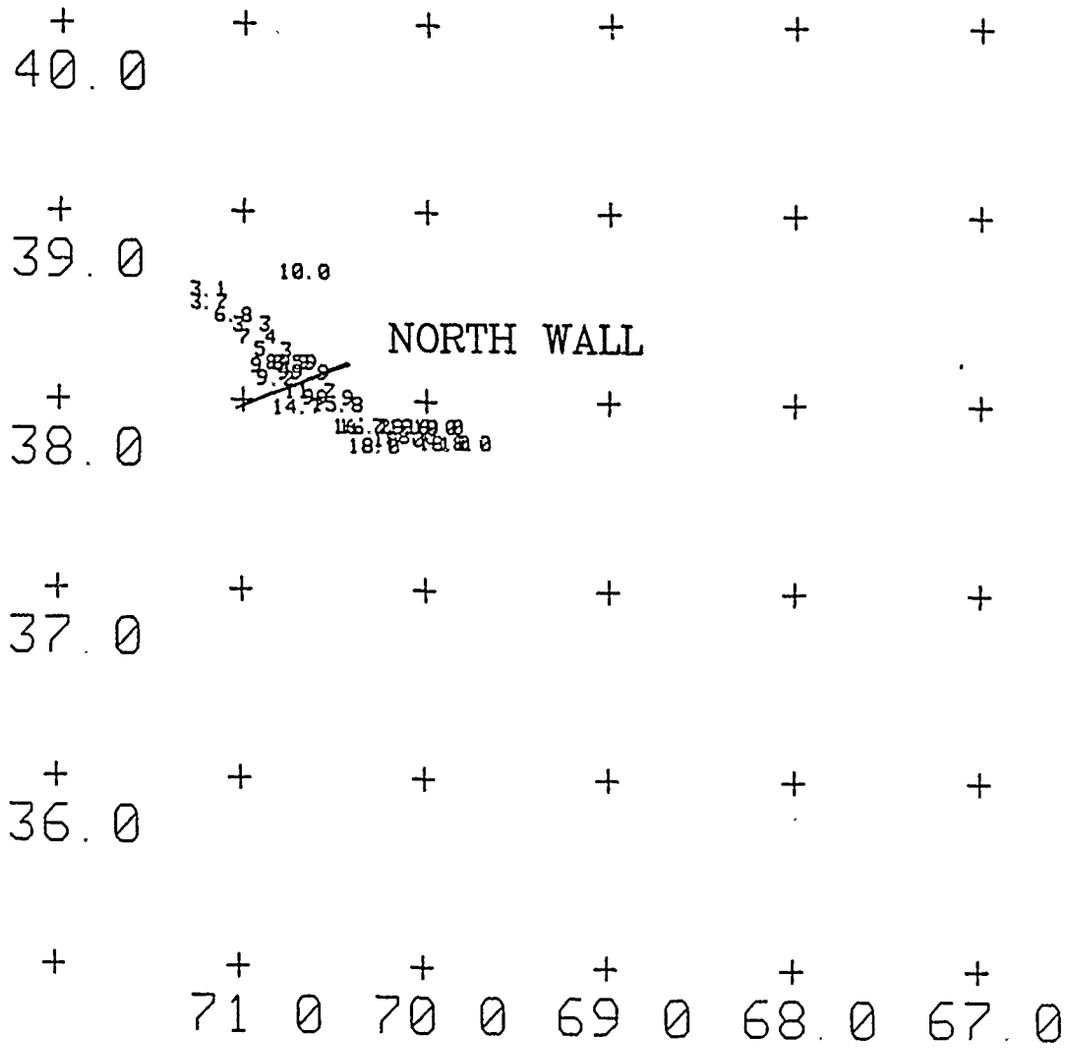

Fig. 21 — AXBT data 4 December 1985: 300m temperature

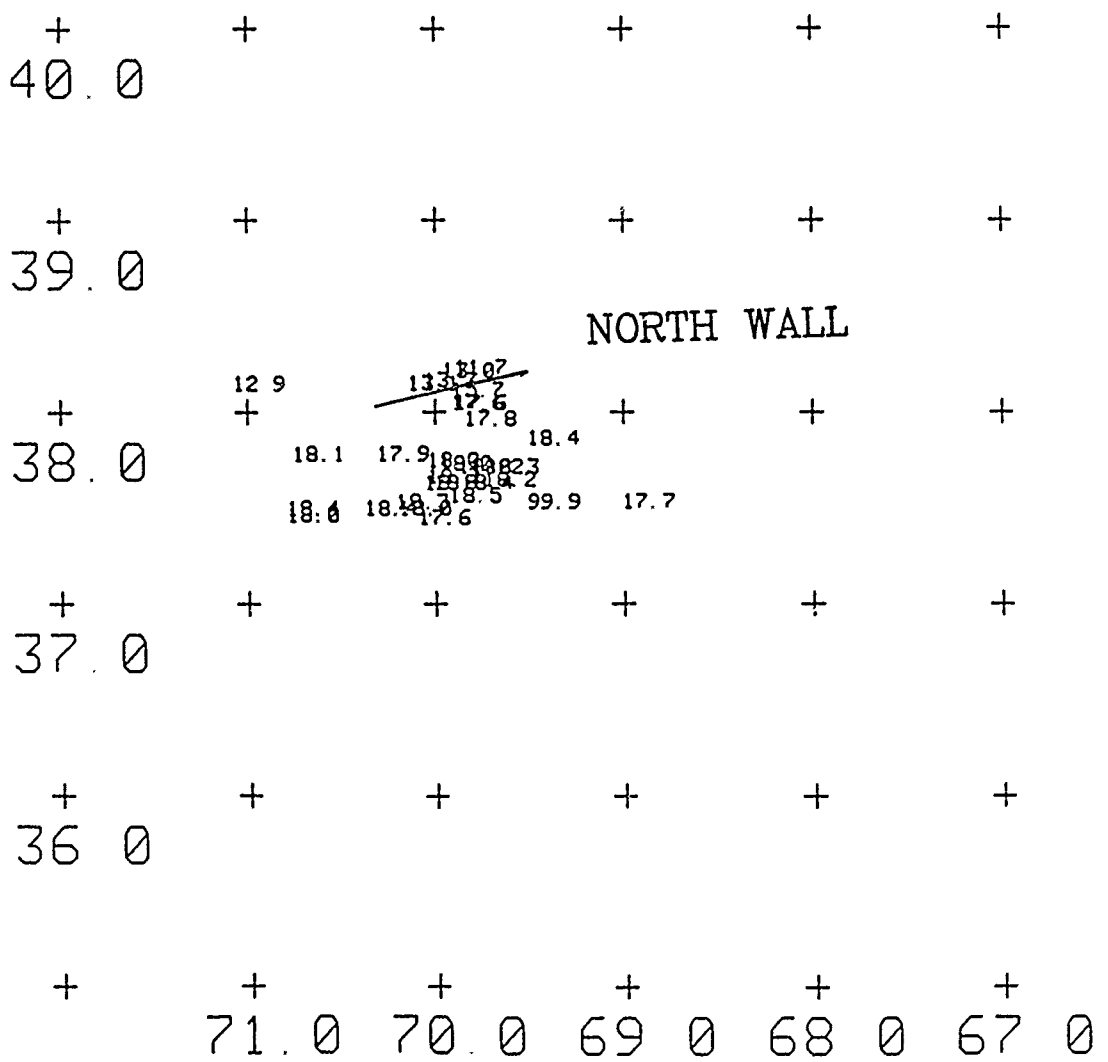

Fig. 22 — AXBT data 5 December 1985: 300m temperature

Weak ring–stream interaction

Central forecast C1

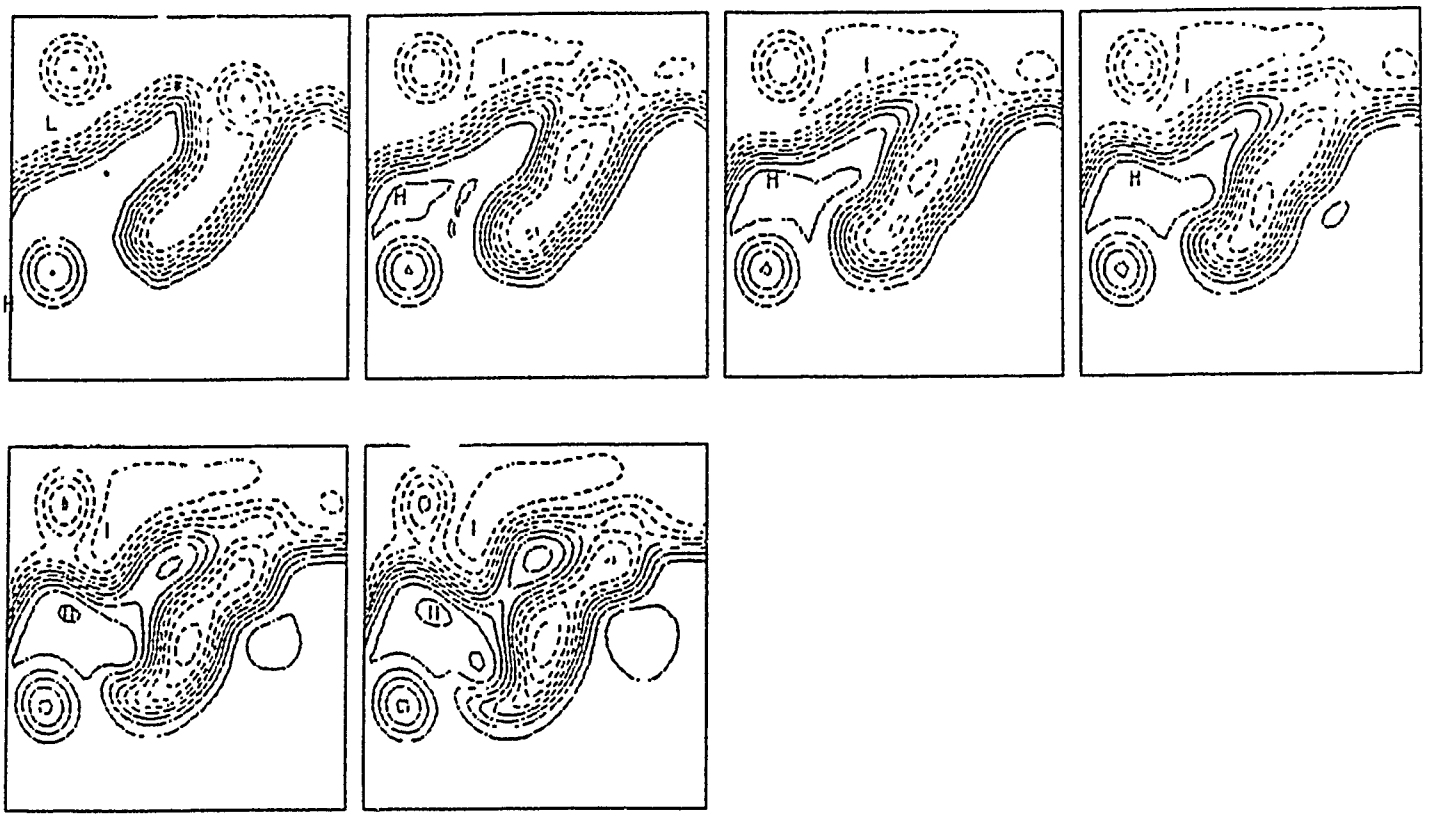

Fig. 24 – Gulf Stream forecast for 29 Nov – 4 Dec 1985

Initialized with no rings

Sensitivity forecast S1A

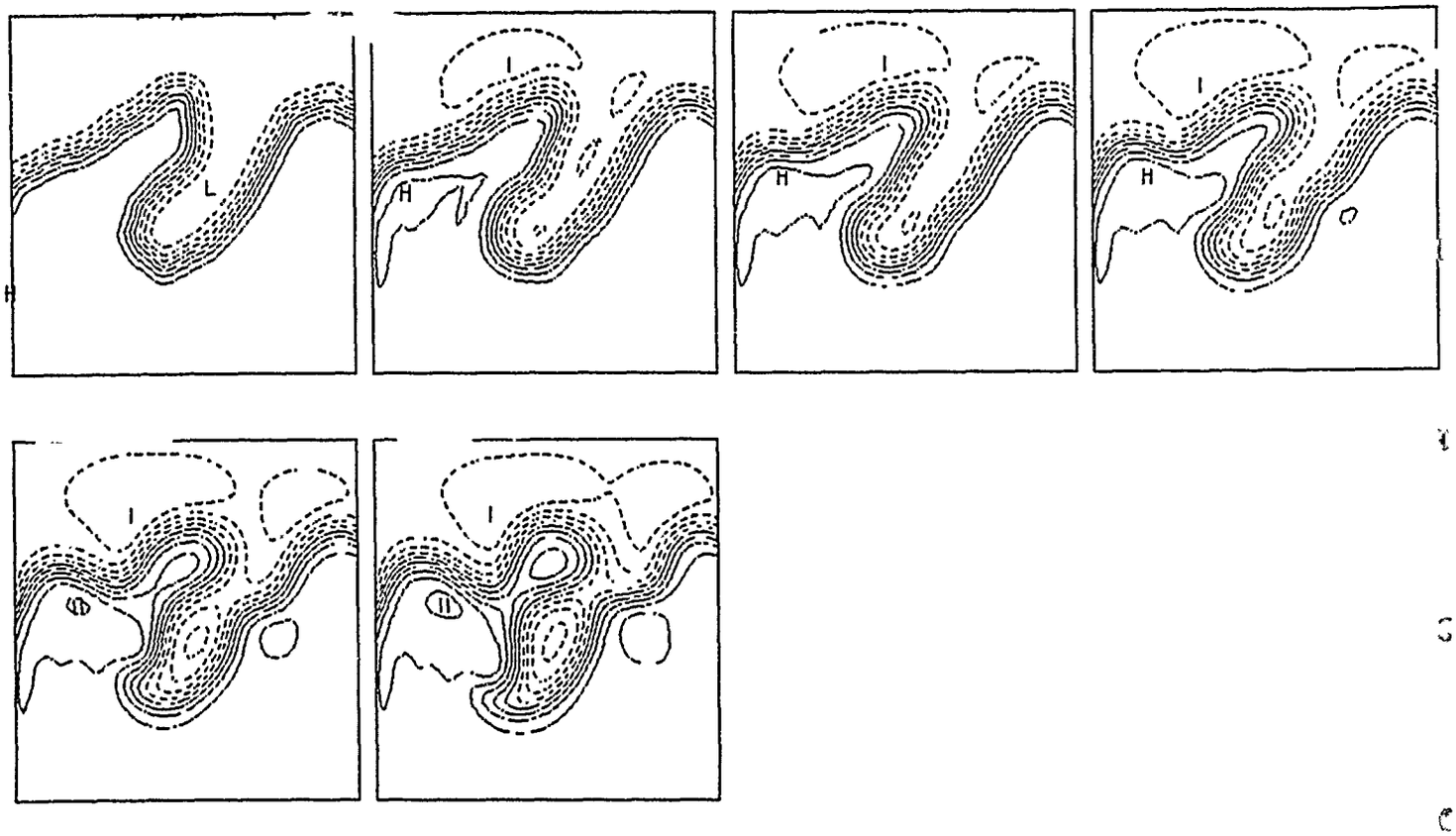

Fig. 25 — Gulf Stream forecast for 29 Nov – 4 Dec 1985

No ring–stream interaction

Sensitivity forecast S1B

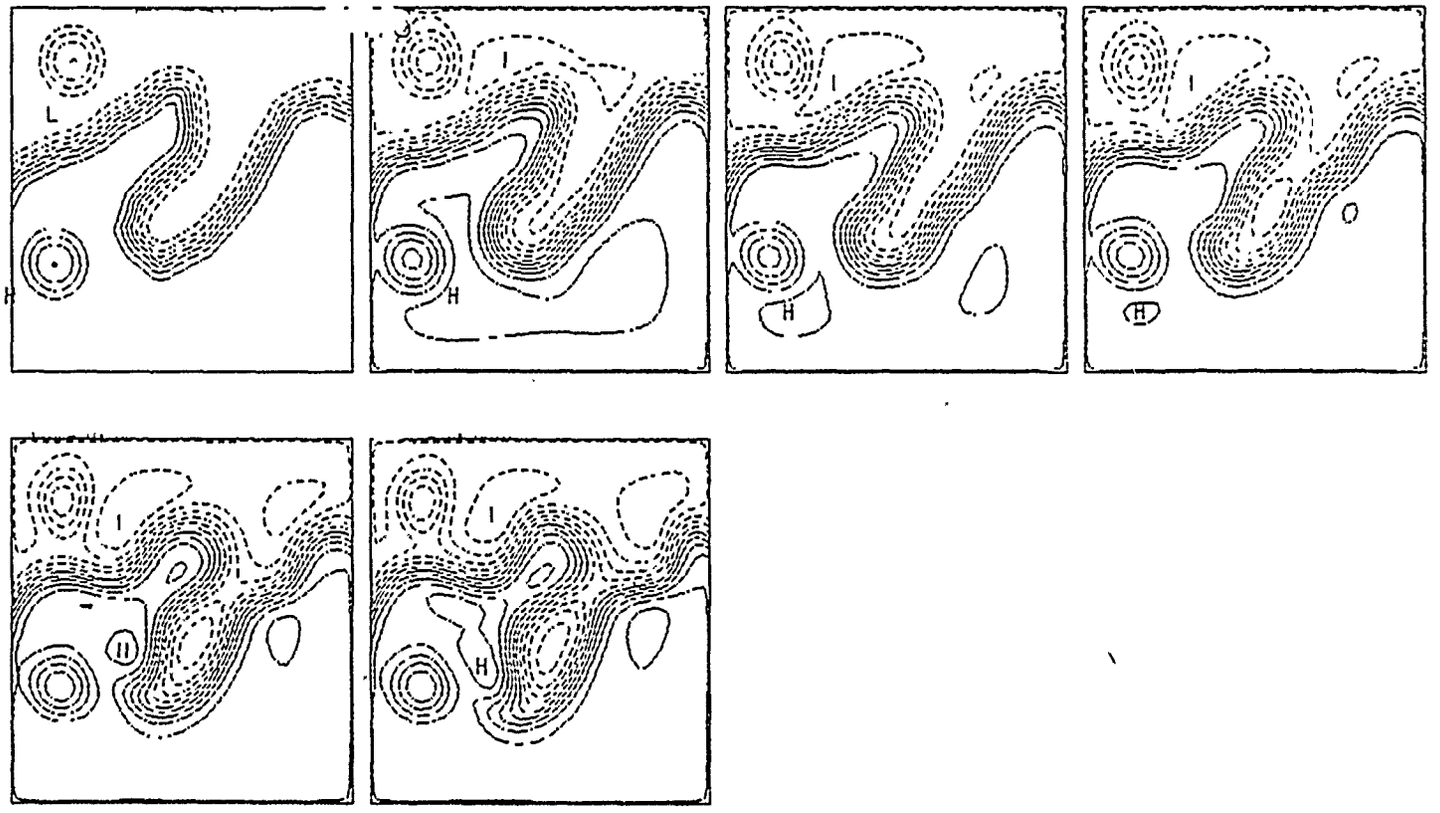

Fig. 26 – Gulf Stream forecast for 29 Nov – 4 Dec 1985

2.2 January 6-13, 1986: Startup of Continual Gulf Stream ODPS

2.2.1 Precis

This experiment was the beginning of the continual real time Gulf Stream ODPS. The region of interest was 36.0N-40.0N, 64.0W-68.0W. Domain H1 was run using both persisted and extrapolated boundary conditions. Prototype dynamic height fields were calculated from AXBTs and melded with the forecast results. There were very good comparisons with both IR and AXBT information.

2.2.2 Data analysis

NOAA IR: (Figure 27)

Jan 6: North wall well observed. South wall position estimated. WE 4 observed, CE C position estimated. The stream is fairly flat from 63.0W-70.0W with small meanders at 61.0W and 72.0W.

Jan 13: Large double meander develops between 64.0W and 71.0W. The small meander initially at 61.0W straightens out. No change in ring status.

AXBT DATA: (Figures 28-29)

Jan 10: North wall located 38.5N 67.0W, 38.6N 66.0W, 38.7N 65.3W, 40.0N 65.0W. Possible warm ring near 40.0N 65.0W. There is a deep upper mixed layer down to below 100m.

A prototype dynamic height calculation was done from the AXBT data set of Jan 10. The dynamic height at 100m relative to 300m was calculated using an average T-S relationship from the Northwest Atlantic. More accurate methods which will identify water types and use the appropriate T-S relationship are currently being investigated. See Figures 34-35 for the dynamic height fields.

2.2.3 Model Runs

Central forecast C1, Figure 30: There were no real ambiguities in the IR data. In this central forecast, the boundary conditions were persisted from January 6 to January 13.

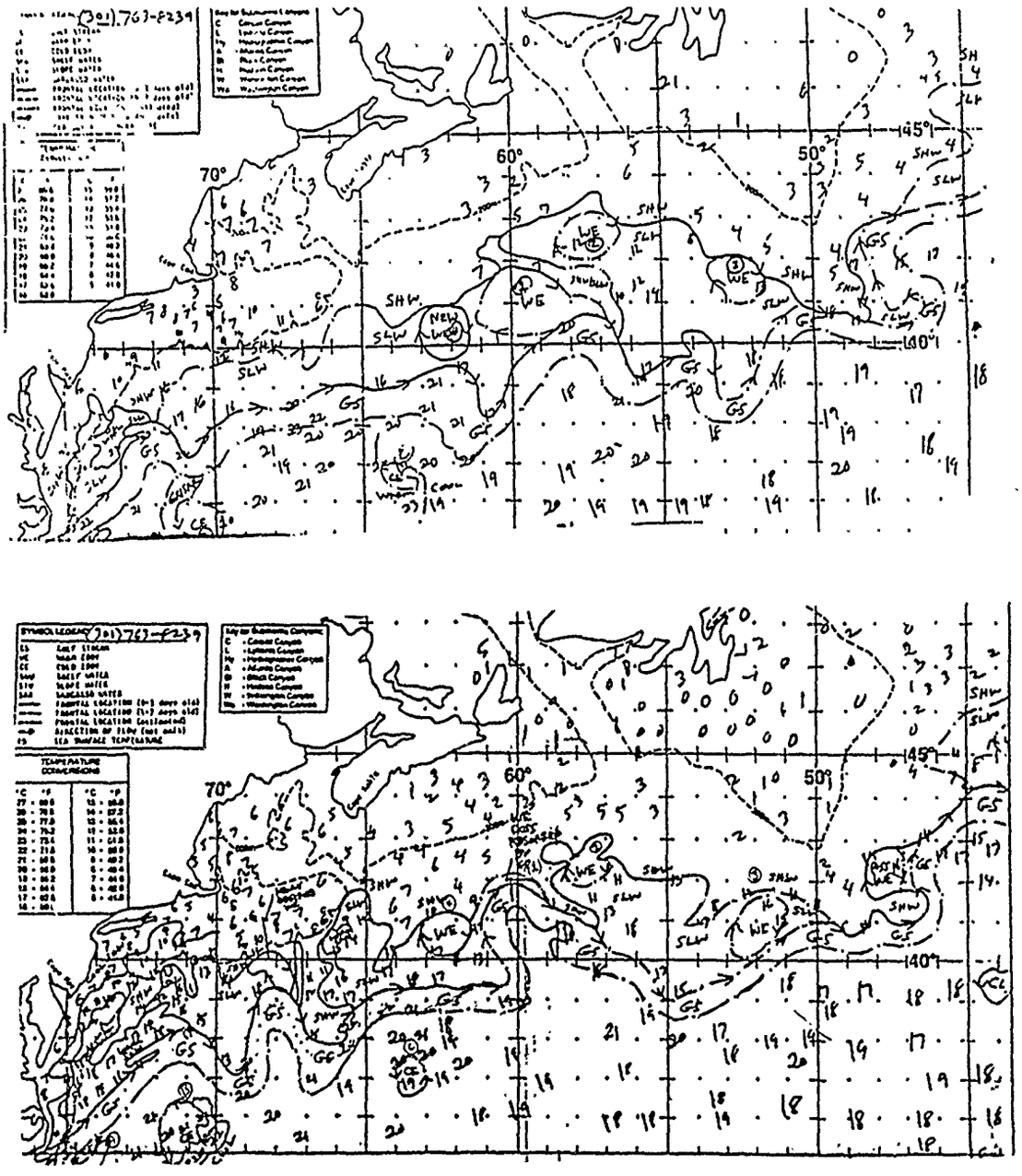

Fig. 27 – NOAA IR data for 6 and 13 January 1986

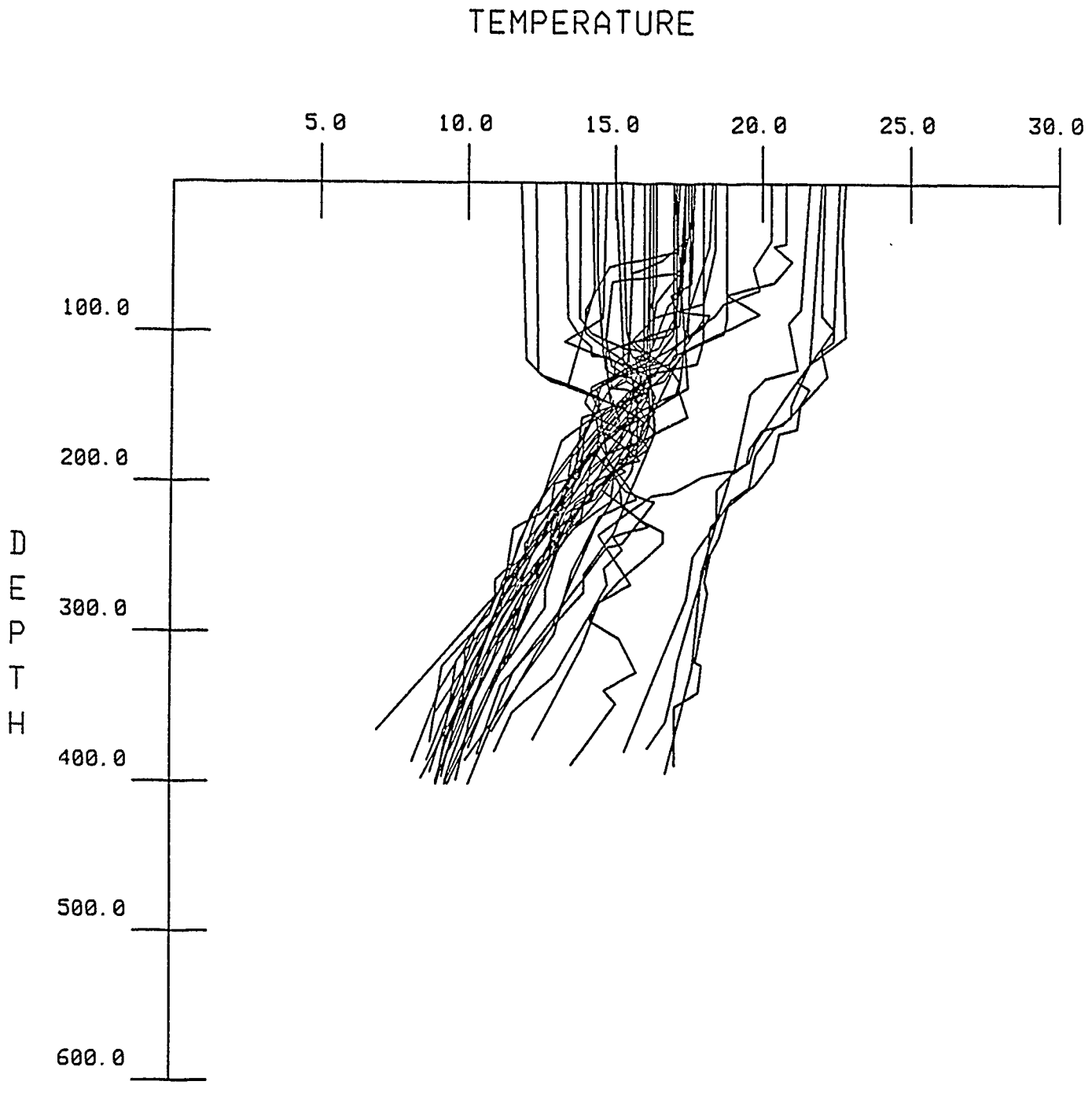

Fig. 28 — Composite of AXBT traces 10 January 1986

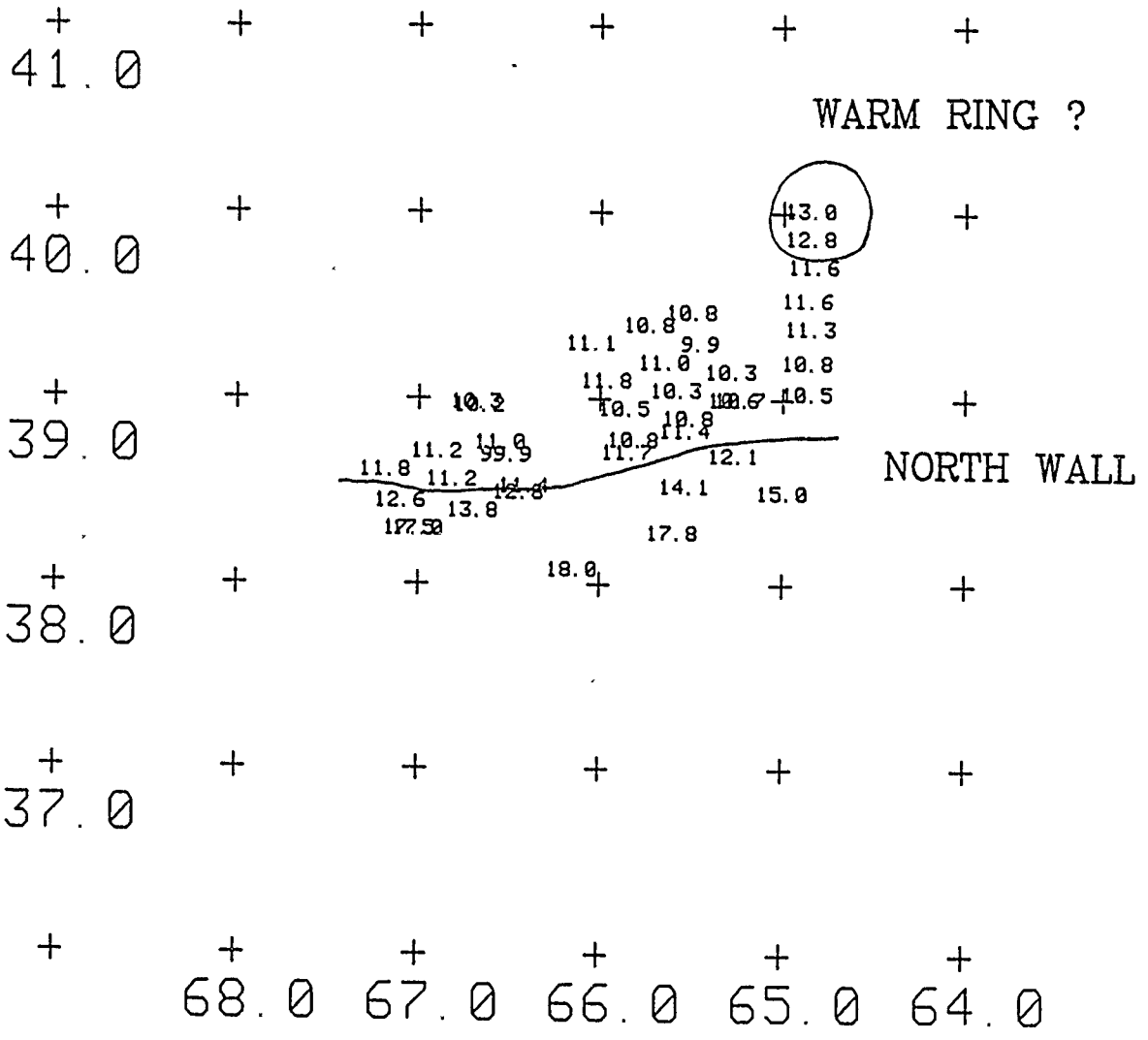

Fig. 29 — AXBT data 10 January 1986: 300m temperature

A large double meander develops from 64.0W-70.0W and the small dip at 61.0W flattens out.

Sensitivity run S1A, Figure 31: The sensitivity of the model prediction to the inflow/outflow boundary conditions was tested. In this run the boundary data was interpolated between observations on Jan 6 and 13. Therefore, this was not a forecast in the true sense of the word. The double meander observed in S1 again forms but it is slightly larger in amplitude and of different shape near the inflow boundary.

2.2.4 Summary

The large double meander which was seen to develop in the IR was reproduced well in both forecasts. The fact that C1 did so well indicates that the growth is largely due to internal dynamics and therefore not boundary driven. The forecast with updated boundary data compares better than C1 with both the shape and amplitude of the observed meander, indicating that the inflow vorticity was inhibiting the full evolution in C1. Horizontal and vertical analysis fields are included in Figures 32-33. They show very realistic velocity and temperature profiles.

The prototype dynamic height calculation is in good agreement with the model calculation. Because the calculation was done relative to only 300m, it basically reflects the shear in the stream from 100-300m. The combined field at 100m (model field at 300m + dynamic height calculated from 300m to 100m) has the same structure in the Gulf Stream although the near fields and transport of the jet have been reduced. See Figure 34 for the analysis and Figure 35 from the streamfunction fields in the model domain.

Fig. 30 — Fcst for 6–13 Jan 1986: Persisted BC

Central forecast C1

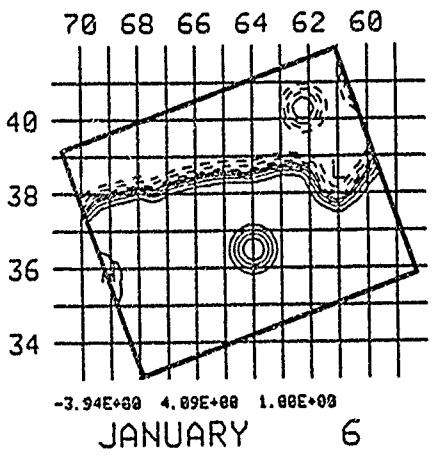

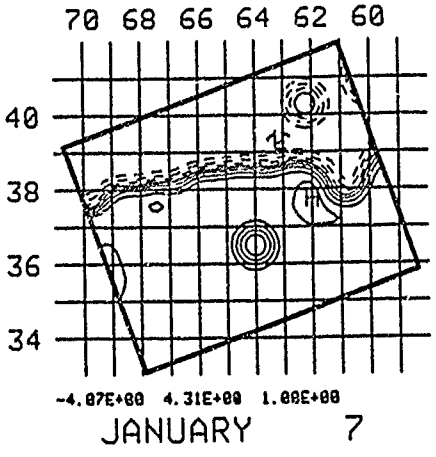

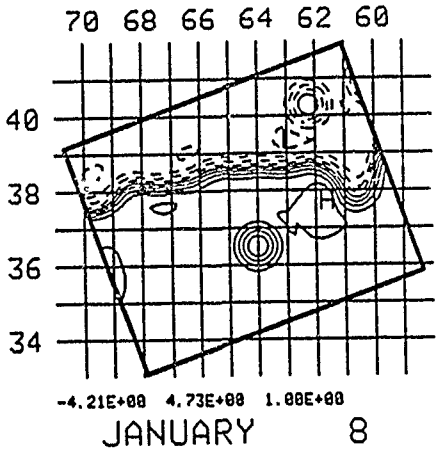

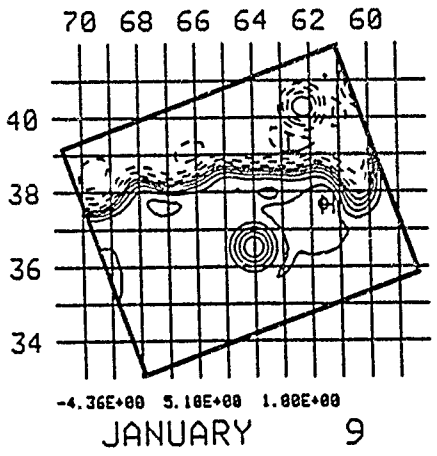

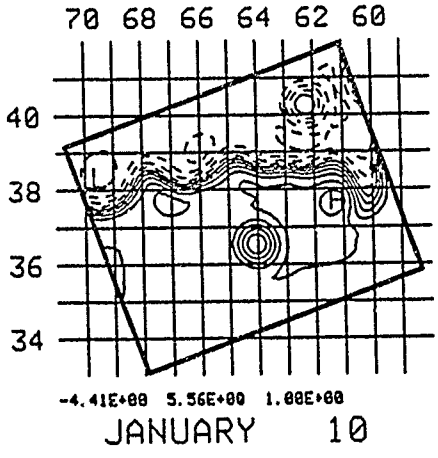

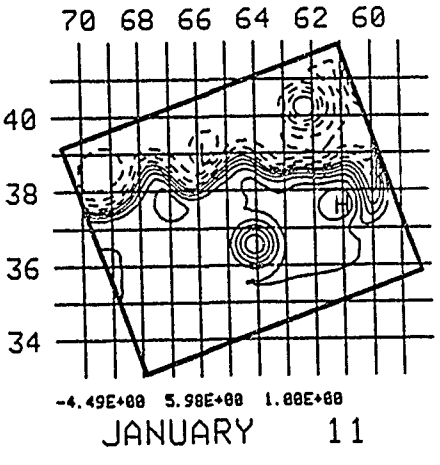

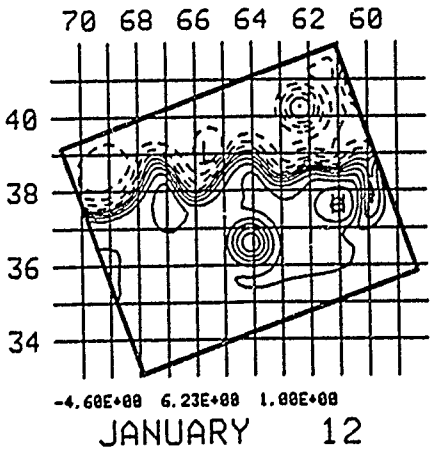

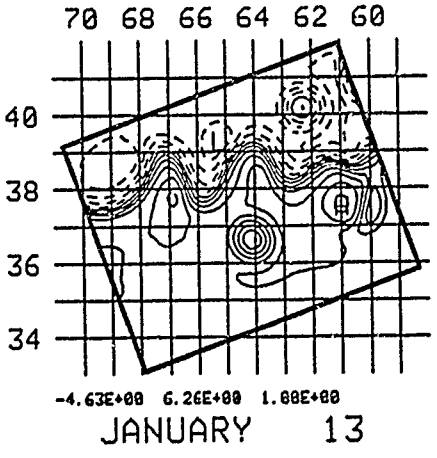

Fig. 31 — Fcst for 6–13 Jan 1986: Interpolated BC

Sensitivity forecast S1A

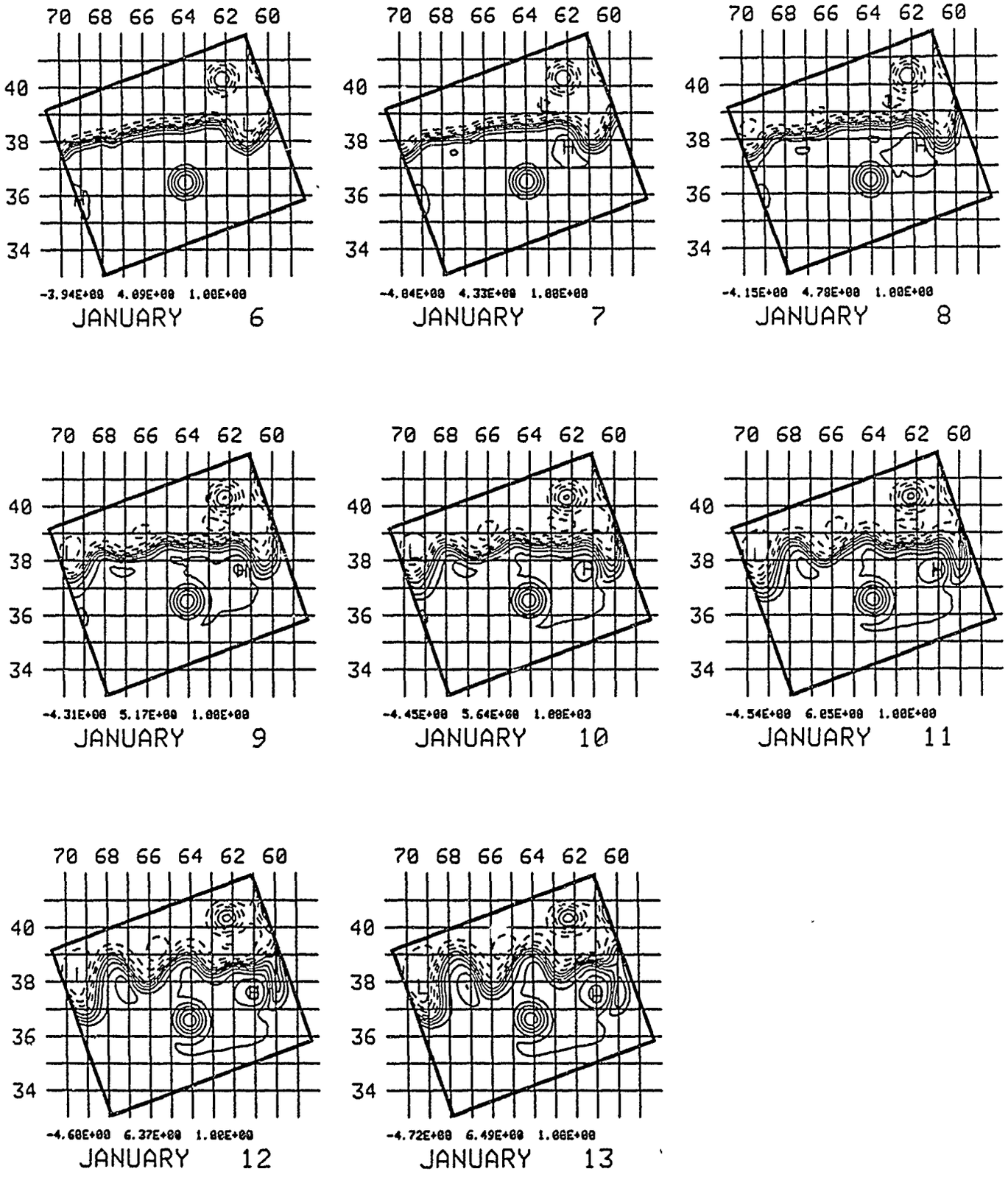

Fig. 32 — Vertical section on 13 Jan 1986

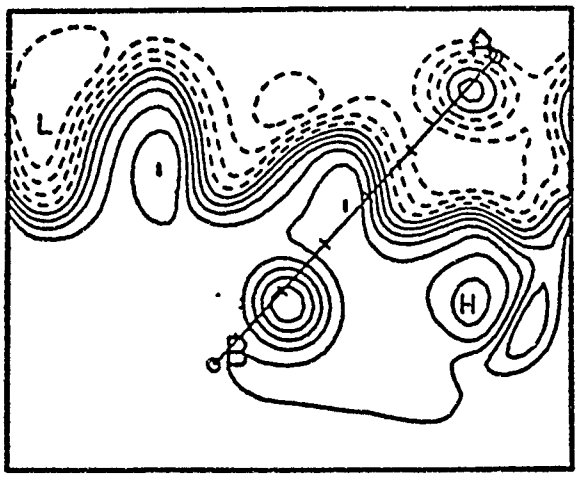

MIN=-4.73E+00 MAX= 6.49E+00 CI=1.00E+00

STREAMFUNCTION AT 100. M TIME= 7.0 DAYS

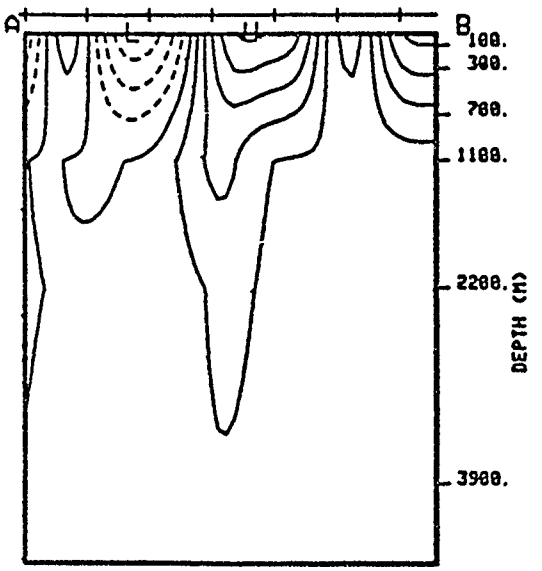

MIN=-3.91E+00 MAX= 5.25E+00 CI=1.00E+00

STREAMFUNCTION

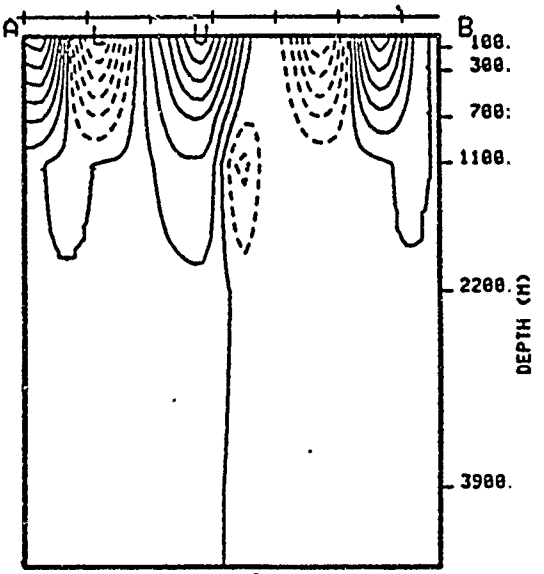

MIN=-1.29E+00 MAX= 1.58E+00 CI=2.00E-01

VELOCITY (M/S)

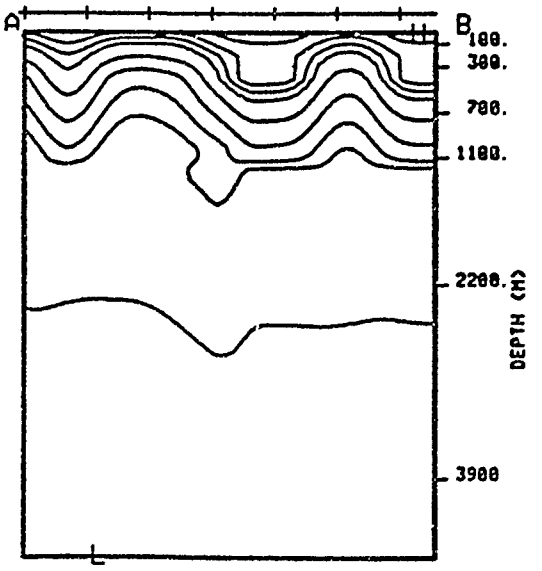

MIN= 2.09E+00 MAX= 2.87E+01 CI=2.00E+00

TEMPERATURE DEG C

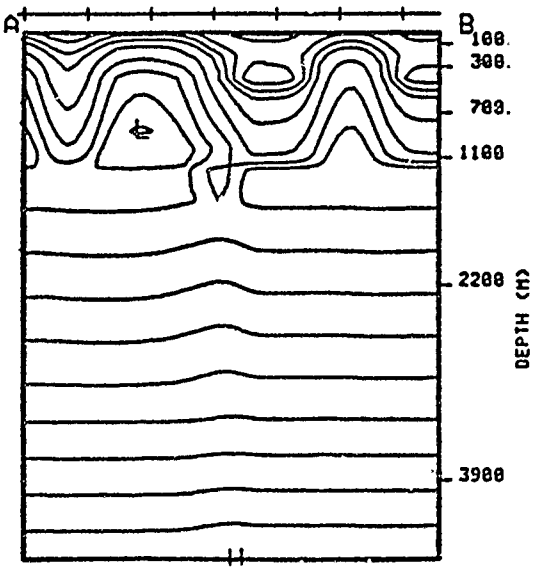

MIN= 1.48E+03 MAX= 1.54E+03 CI=5.00E+00

SOUND SPEED (M/S)

Fig. 33 — Horizontal analysis on 13 Jan 1986

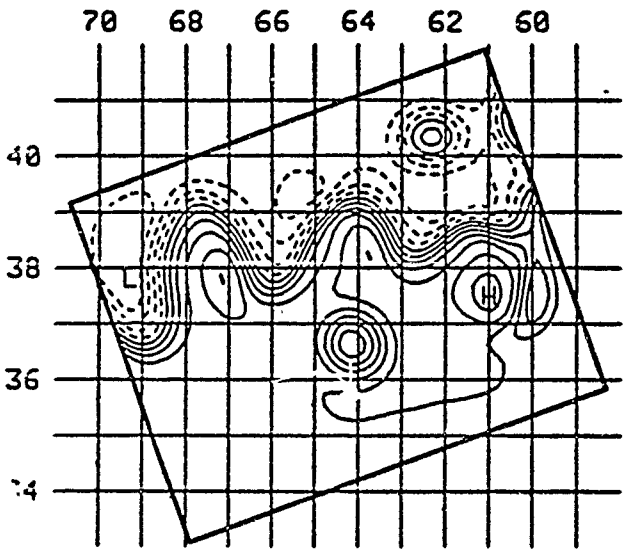

MIN=-4.73E+00 MAX= 6.49E+00 CI=1.00E+00
STREAMFUNCTION

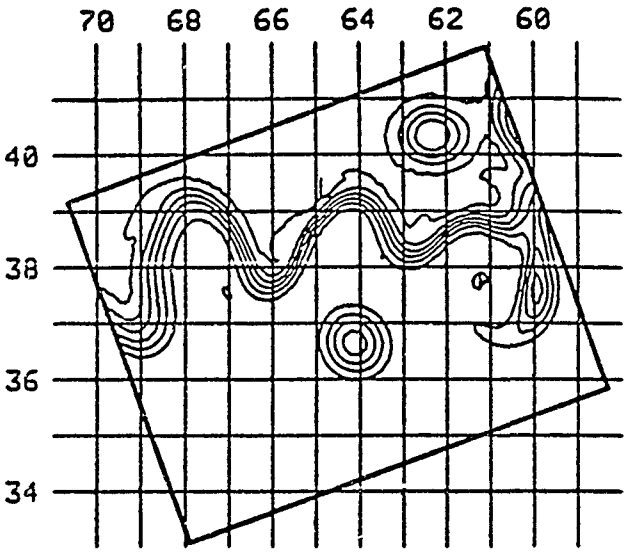

MIN= 1.37E+01 MAX= 2.81E+01 CI=1.00E+00
TEMPERATURE DEG C

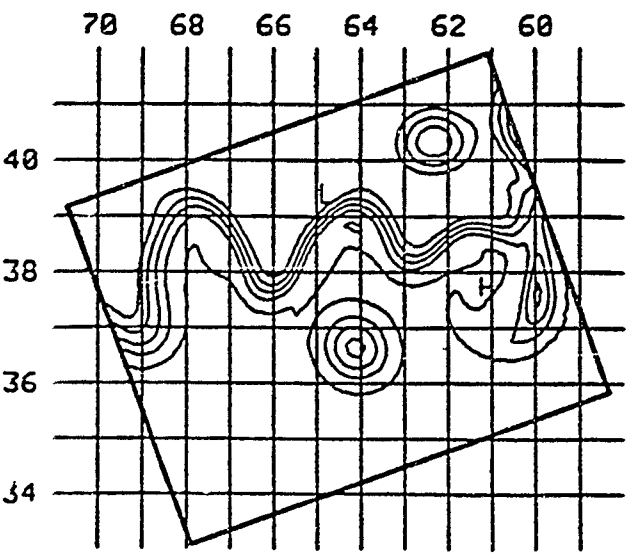

MIN= 1.51E+03 MAX= 1.53E+03 CI=4.00E+00
SOUND SPEED (M/S)

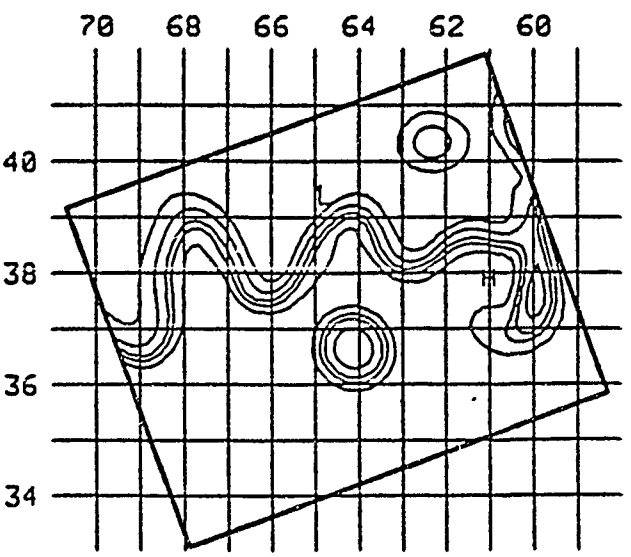

MIN= 3.50E+01 MAX= 5.00E+02 CI=1.00E+02
DEPTH OF 15 DEG ISOTHERM

Fig. 34 — 10 Jan 1986: Fields for optimal combination

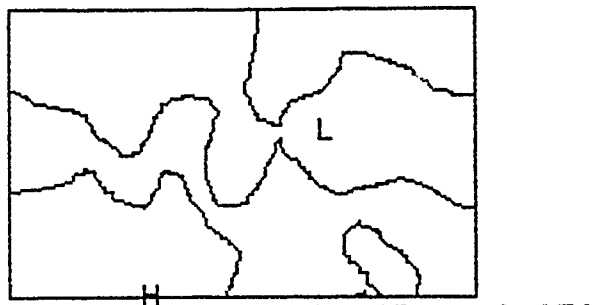

100 METER DH FROM OA

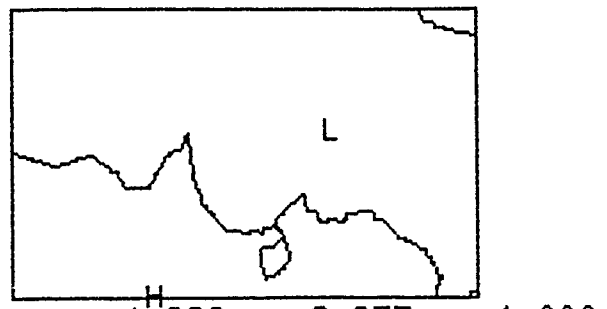

100 METER DH FROM OA (SCALED)

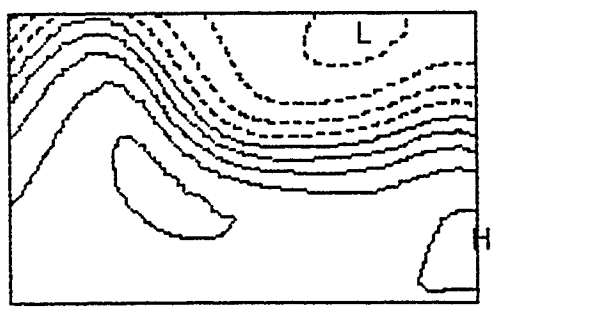

100 METER PSI FROM FCST

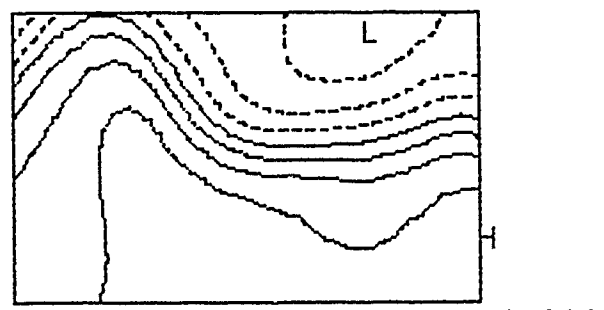

300 METER PSI FROM FCST

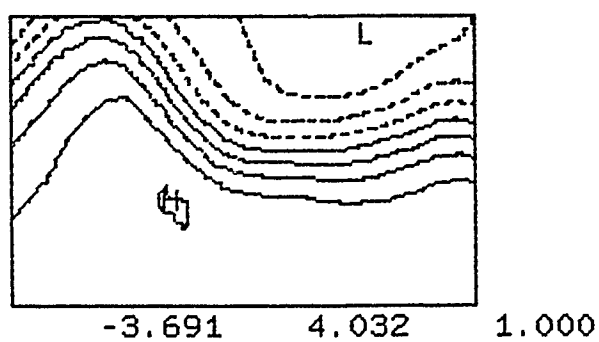

100 METER PSI FROM EST

Fig. 35 — 10 Jan 1986: Streamfunction field comparison

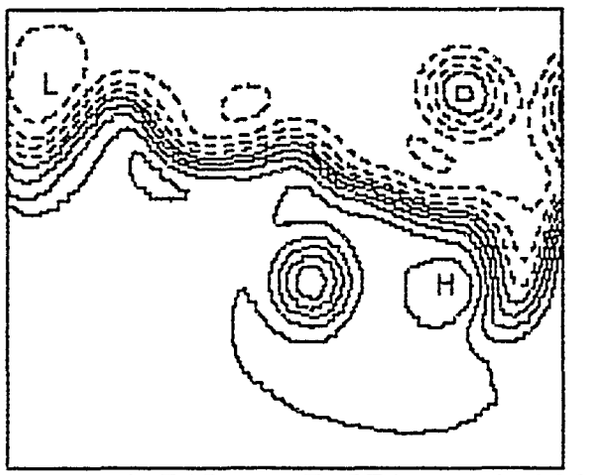

100 METER PSI FROM FCST

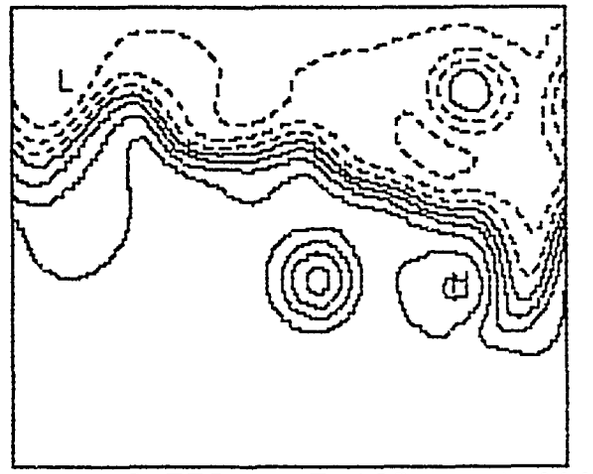

300 METER PSI FROM FCST

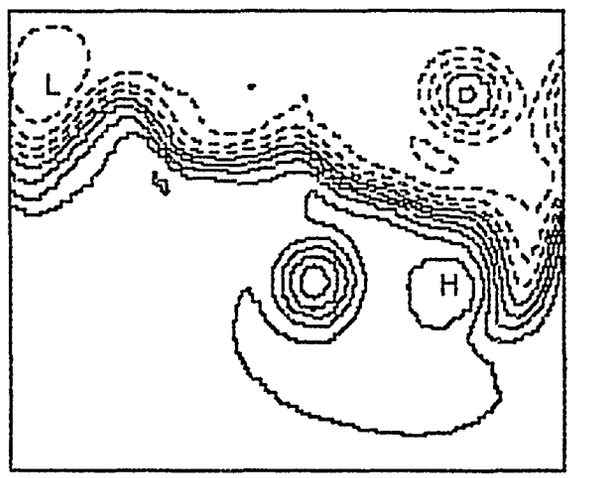

100 METER PSI FROM EST

2.3 February 3-10, 1986

2.3.1 Precis

This experiment demonstrated the mobility of the Harvard ODPS. All of the calculations were done at the airport from which the AXBT flights originated. The study was located at the inlet region of the Gulf Stream. A sensitivity study was done on the initial position of a cold ring near the stream. Good qualitative agreement is seen with the AXBT and IR verification data.

2.3.2 Data analysis

NOAA IR: (Figure 36)

Feb. 3: The north wall is observed throughout the model domain. Two cold ring positions are estimated. A trough exists just east of 70.0W.

Feb 10: Thermal fronts are observed at the north and south edges of the stream from 71.0W to 73.0W but the exact position of the stream axis is somewhat unclear due to shingling and warm outbreaks. A small trough develops at 70.0W. Previous trough east of 70.0W flattens out. Status of cold ring is uncertain (possibly absorbed by stream).

AXBT DATA: (Figures 37-41)

Feb. 4: North wall position located at the points 37.0N 72.5W, 38.5N 69.5W. No evidence of the cold ring near 35.5N 71.5W.

Feb. 6: North wall position not accurately located. Possible north wall at 36.3N 73.6W. Data coverage is sparse with no evidence of the cold ring.

Feb. 7: Data coverage to sparse to locate features.

Feb. 10: North wall is bracketed between 72.5W and 73.0W at 36.8N. Possible cold ring at 36.5N 71.0W.

2.3.3 Model runs

The position of the cold ring last observed at 36.5N 72.0W was not verified by the data. A series of sensitivity experiments was conducted to determine the role of this cold

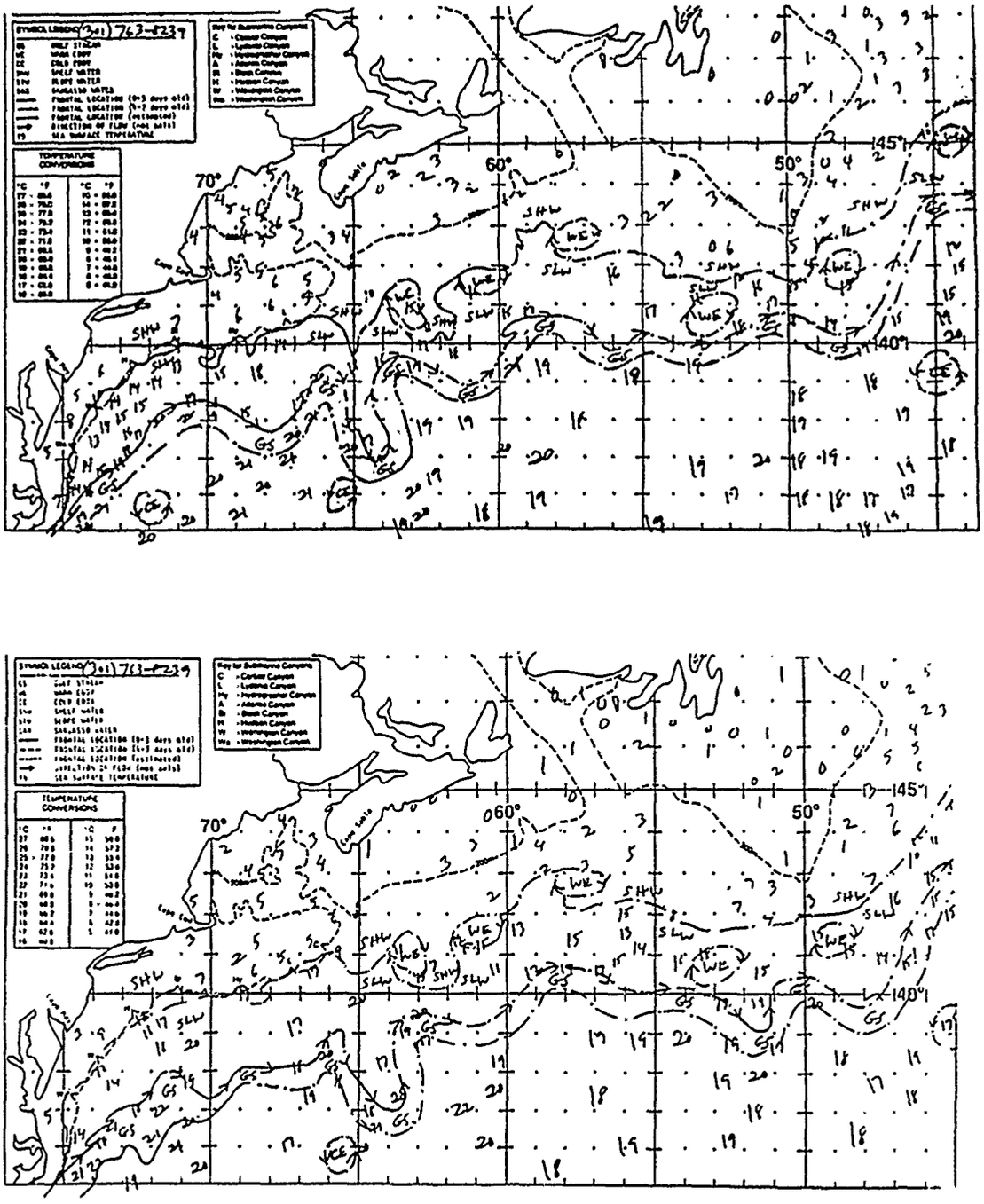

Fig. 36 — NOAA IR data for 3 and 10 February 1986

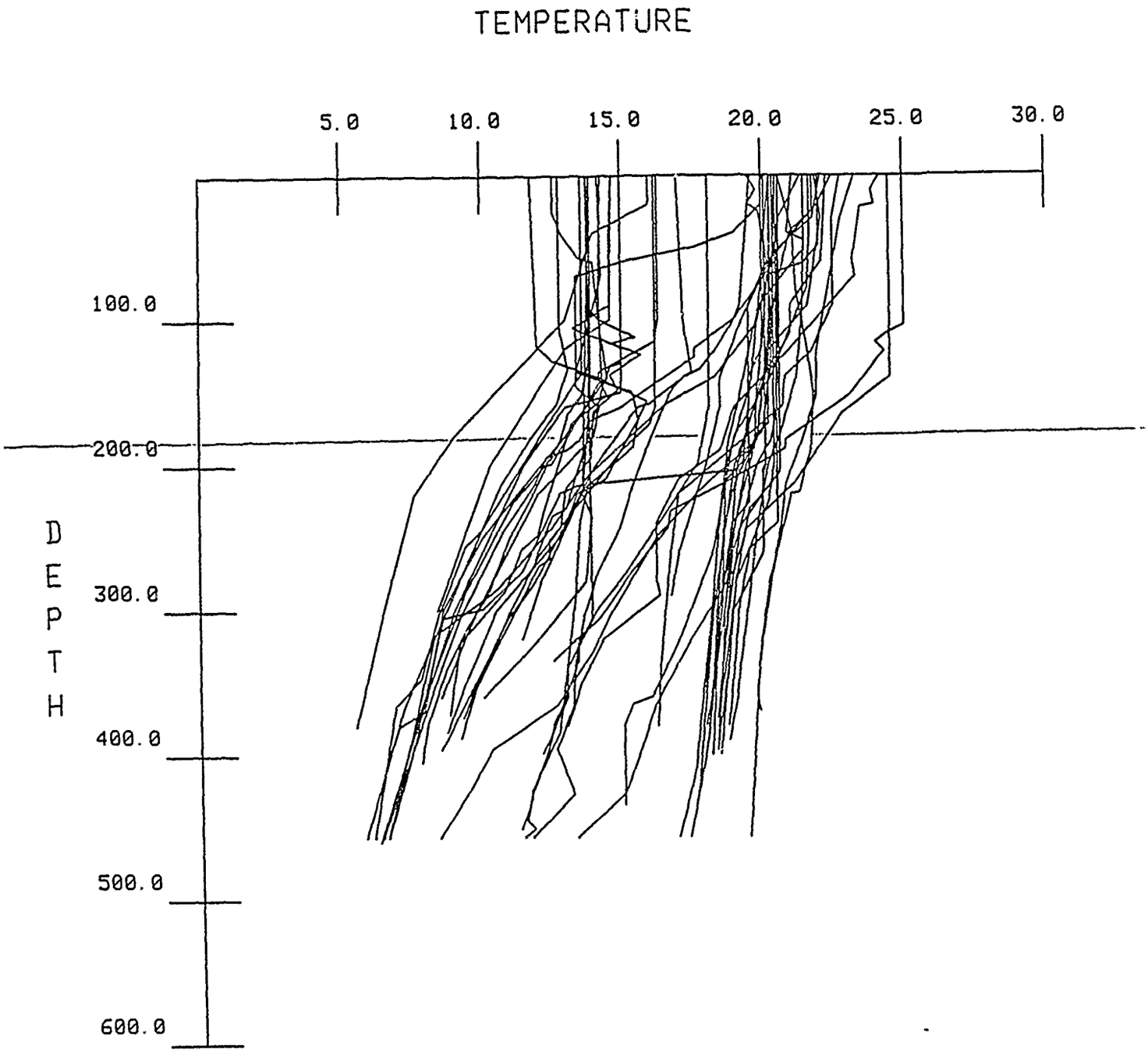

Fig. 37 — Composite of AXBT traces 4–10 February 1986

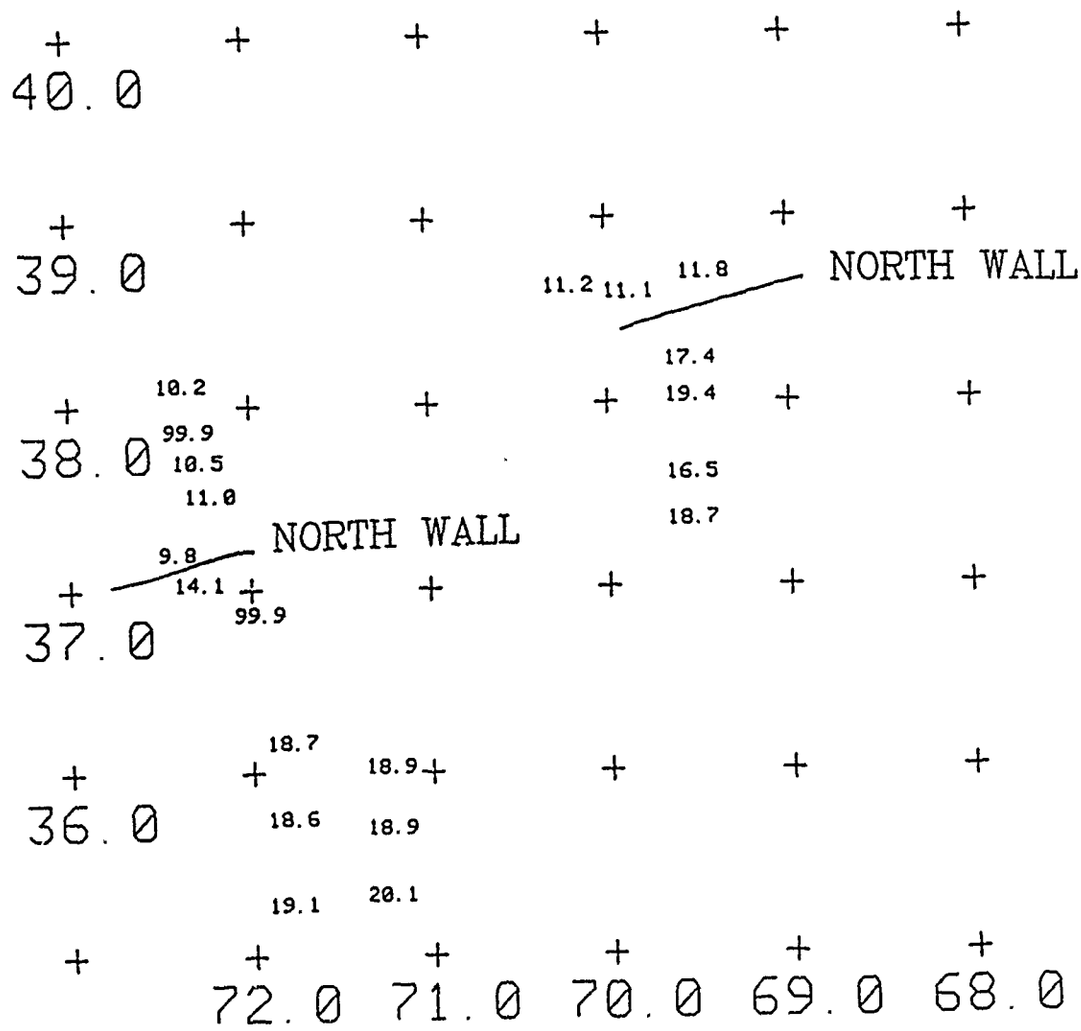

Fig. 38 — AXBT data 4 February 1986: 300m temperature

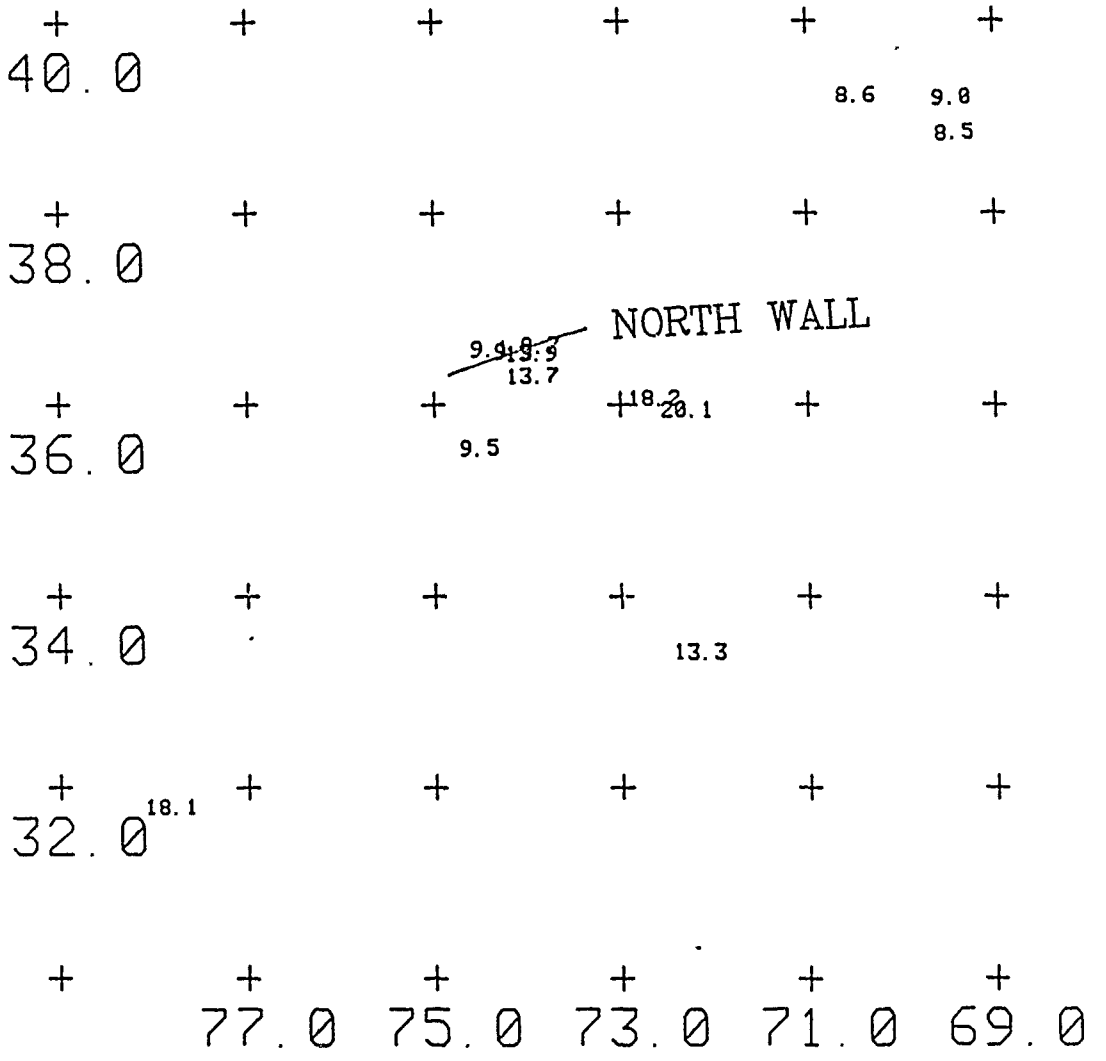

Fig. 39 — AXBT data 6 February 1986: 300m temperature

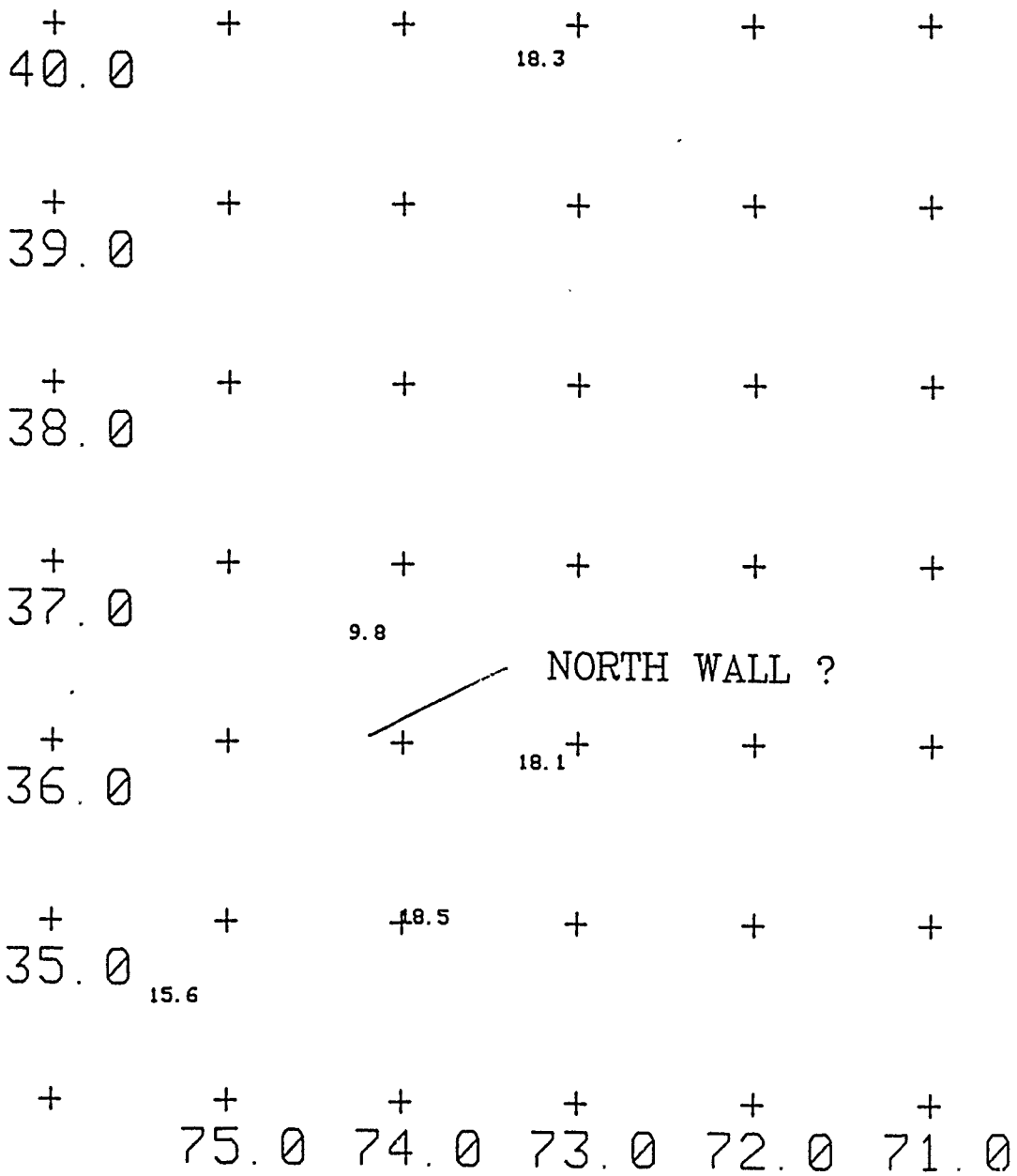

Fig. 40 — AXBT data 7 February 1986: 300m temperature

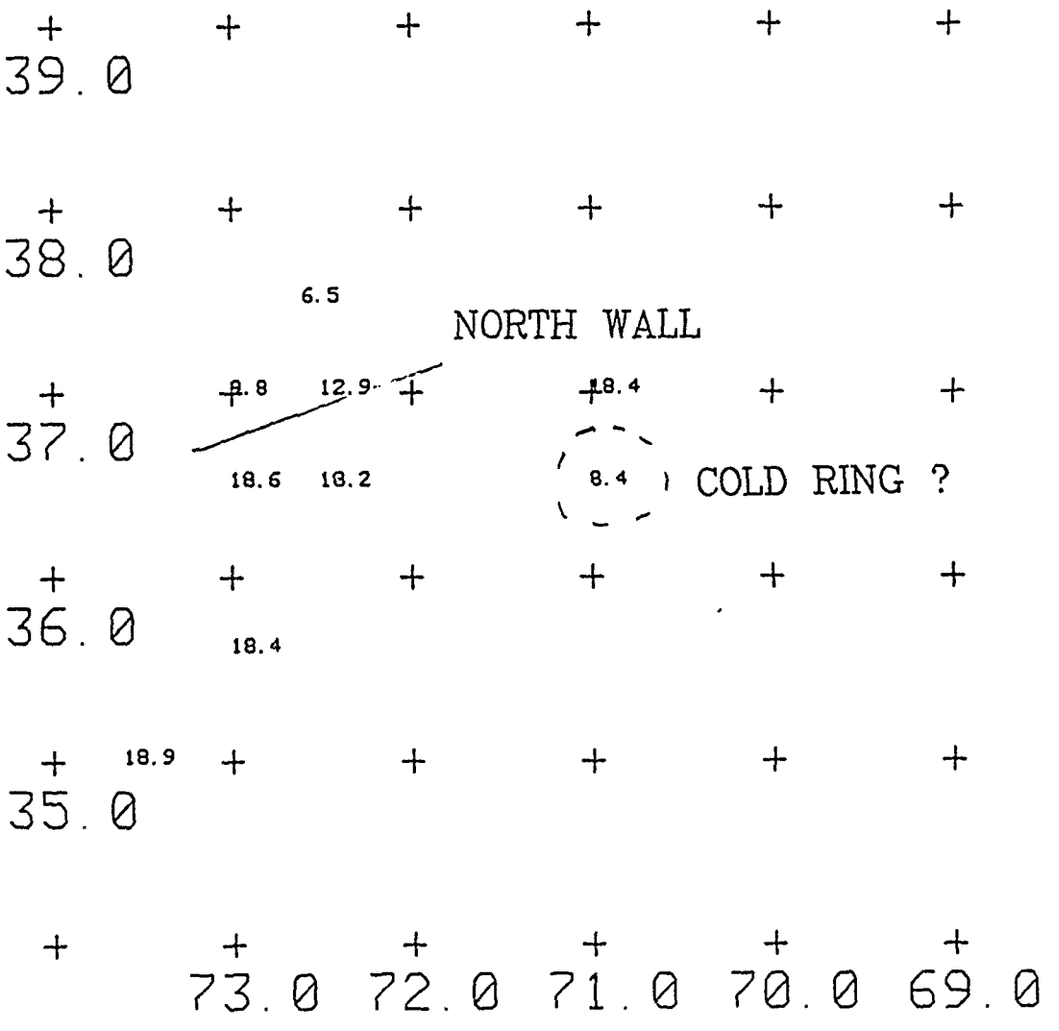

Fig. 41 — AXBT data 10 February 1986: 300m temperature

ring in the evolution of the stream. This cold ring will be referred to as CR1.

Central forecast C1, Figure 44: The cold ring was placed so that it was weakly interacting with the stream in the initial condition. The forecast was run for only three days. CR1 interacts with the stream and produces a slight perturbation. The large meander to the east flattens out from 67.0W-69.0W.

Sensitivity run S1A, Figure 42: CR1 was placed very far from the stream. It was possible that the ring had propagated that far to the southwest since it was last observed. For the duration of the forecast the stream remains fairly straight from 71.0W to 74.0W. East of 70.0W the trough sharpens and appears as though it may be straightening out.

Sensitivity run S1B, Figure 43: CR1 is adjacent to the stream in the initial condition. There is a very slight interaction with the stream which produces a minor perturbation near 72.5W on Feb 10. Otherwise it is very nearly the same as S1A.

Sensitivity run S1C, Figure 45: CR1 is interacting with the stream in the initial condition. The ring is nearly absorbed and produces a very large wavelike pattern in the stream from 69.0W-73.0W. East of 69.0W the pattern is the same as found in the previous runs.

Sensitivity run S1D, Figure 46: CR1 is placed strongly interacting with the stream in the initial condition. The ring is absorbed by the stream and its signature is advected downstream. On Feb 10 evidence of the cold ring is seen at 36.5N 71.5W. A large wavelike meander develops as a result of the ring-stream interaction.

2.3.4 Summary

The north wall of the stream was well observed with the NOAA IR and the AXBT flights. A cold ring was believed to be in the area but it had not been observed for a month and the AXBT flights failed to locate it until Feb. 10 (possibly). A series of sensitivity runs were done on the initial position of the ring. As the ring-stream interaction increased in the initial conditions, the stream was perturbed by a greater amount. Very strong

Fig. 42 — Gulf Stream forecast for 3–10 Feb 1986

Cold ring far from Gulf Stream

Sensitivity forecast S1A

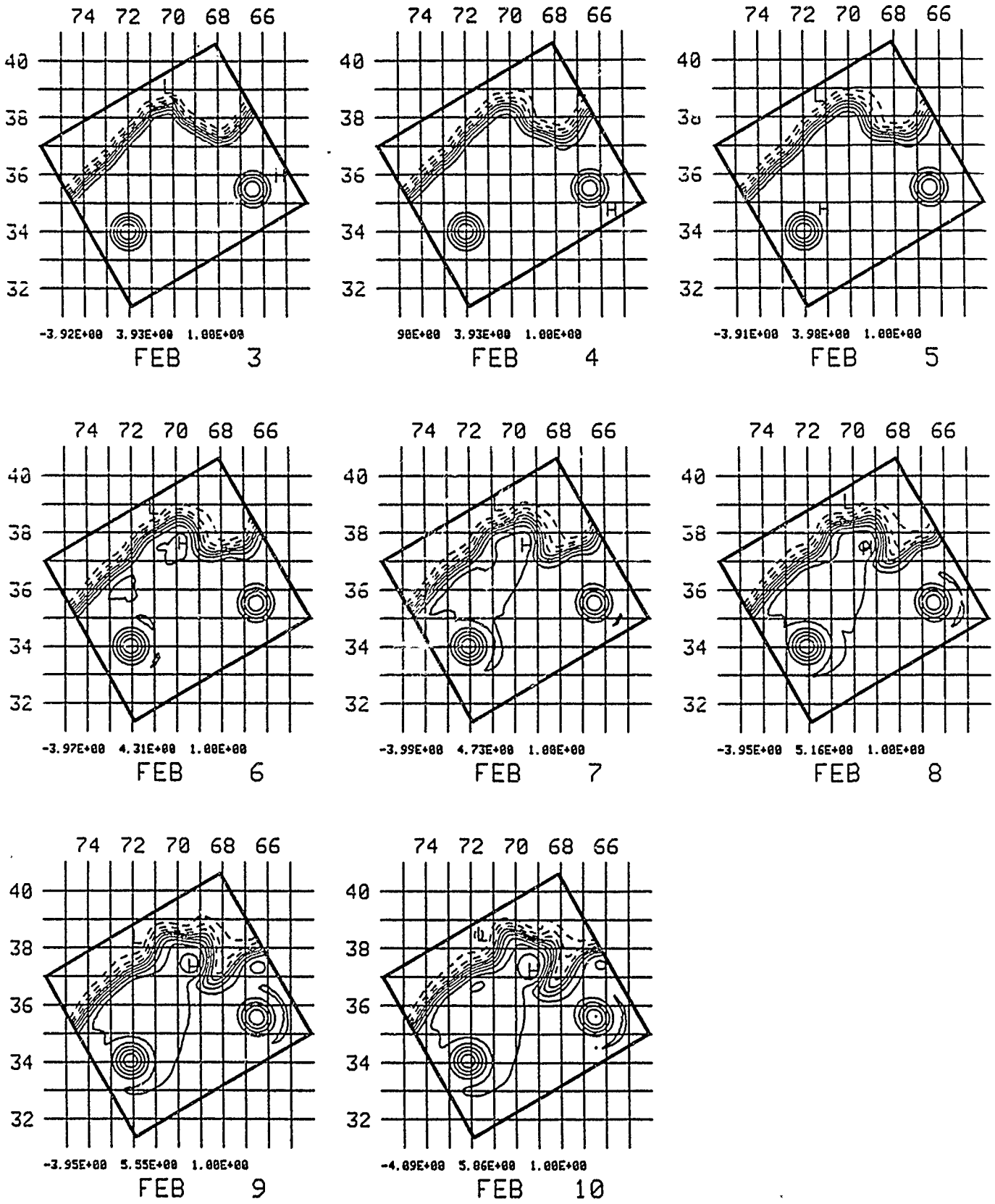

Fig. 45 — Gulf Stream forecast for 3–10 Feb 1986

Intermediate ring–stream interaction

Sensitivity forecast S1C

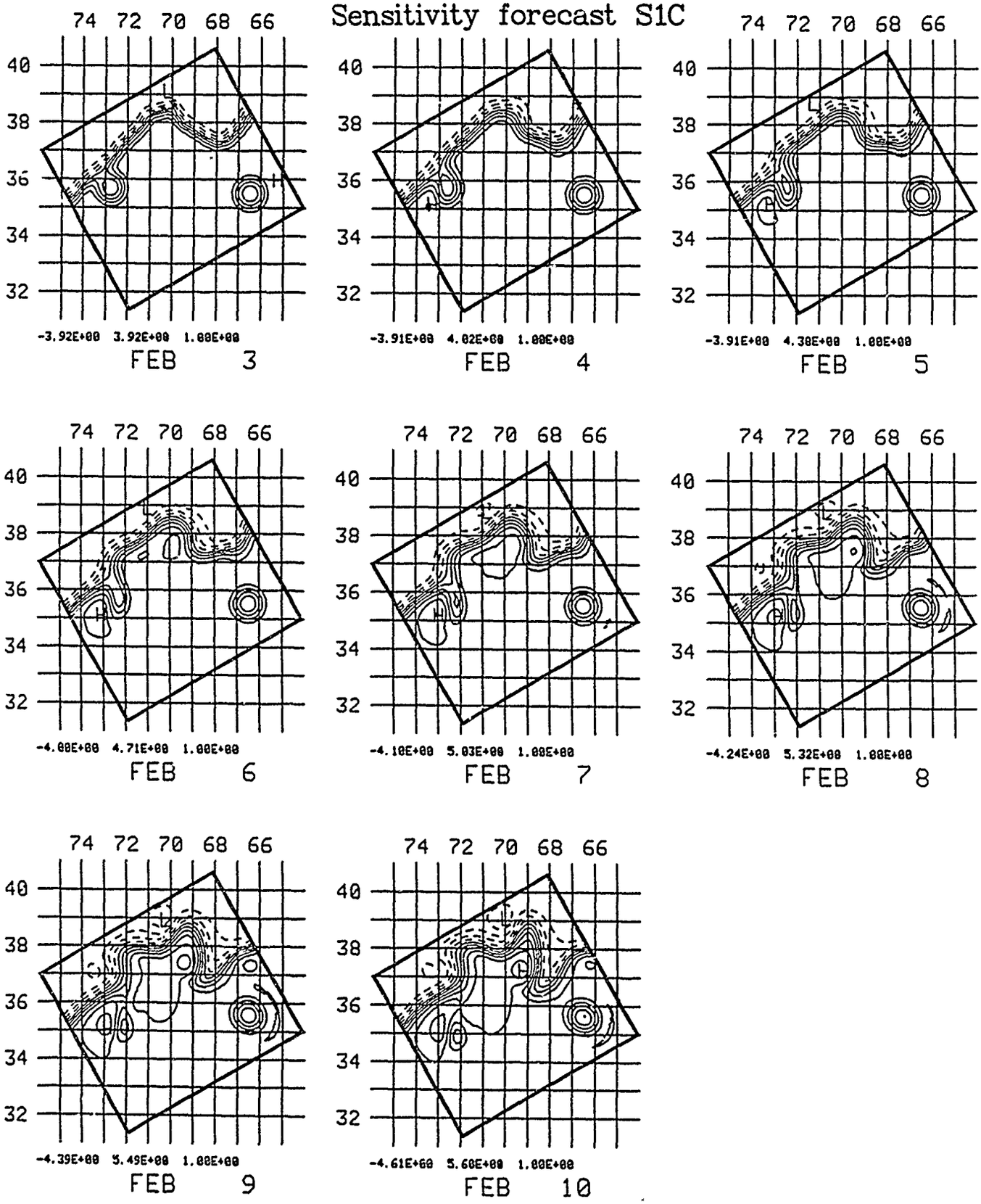

Fig. 46 — Gulf Stream forecast for 3–10 Feb 1986

Strong ring–stream interaction

Sensitivity forecast S1D

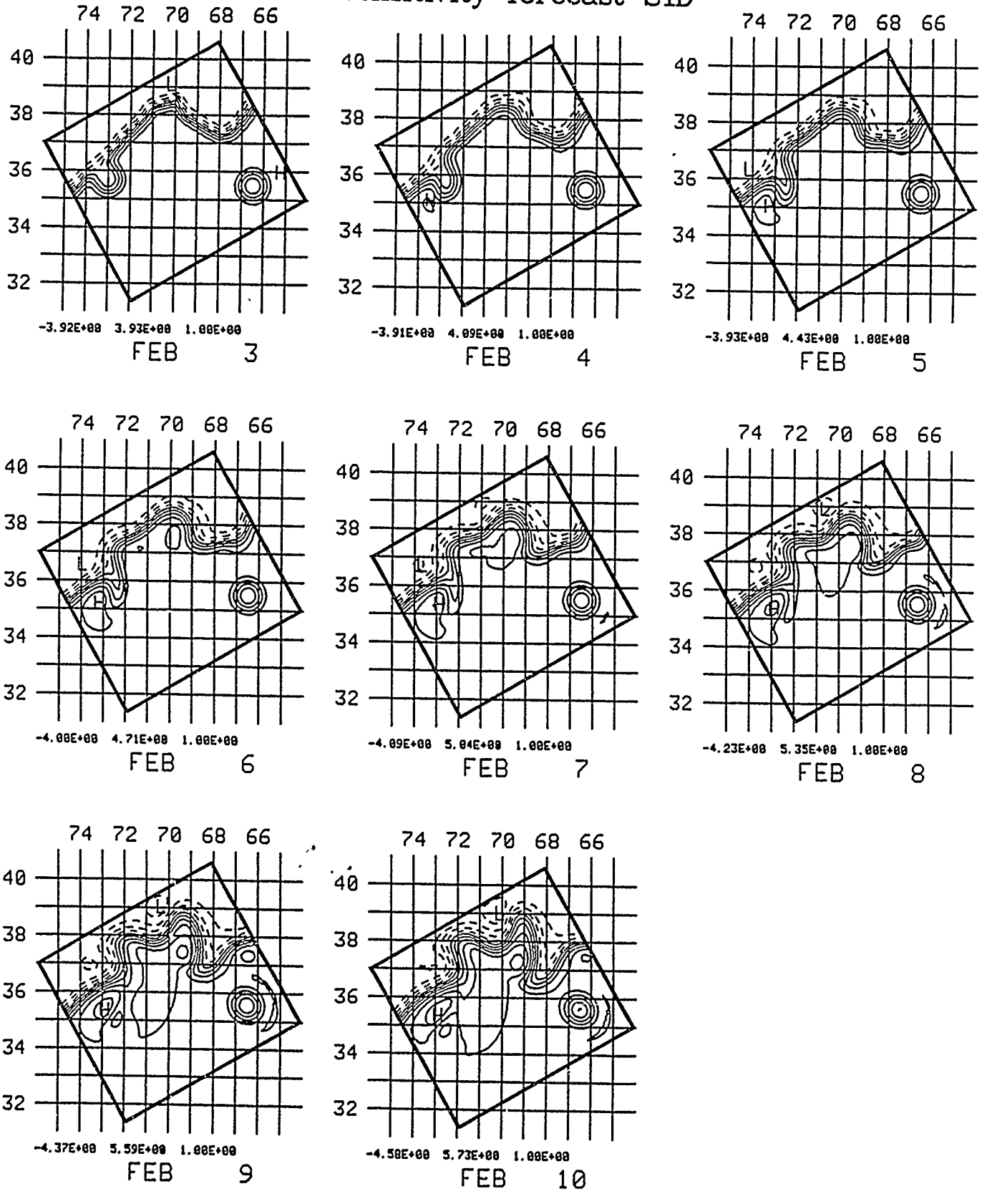

interactions caused the ring to be advected downstream and absorbed. Sensitivity run S1D showed a large trough devlop at 70.0W and showed the signature of the cold ring at 36.5N 71.5W. The stream shape is in qualitative agreement with the IR of Feb 10 and a cold ring signature was seen in the AXBT data at 36.5N 71.0W.

2.4 April 2-23, 1986

2.4.1 Precis

This experiment was done in real time; concurrent with the Ocean Prediction Workshop (OPW '86) held at Harvard University. A forecast was produced in the slightly larger domain H2 that agreed very well with NOAA IR images. Unfortunately no AXBT verification data was available.

April 2-9

2.4.2 Data analysis

NOAA IR: (Figure 47)

Apr. 2: North wall well observed to 57.0W. Considerable shingling exists from 65.0W to 72.0W. South wall and associated outbreaks observed to 59.0W. Position of CE E estimated by observed streamer. WEs 1 and 4 observed, 3 estimated as interacting with the stream.

Apr. 4: North wall observed to 59.0W. South wall observed to 65.0W. Stream shifts slightly northward from 65.0W to 70.0W. A small bump is developing at 66.0W. Same rings observed.

Apr. 9: North wall observed over the entire domain. Gaps in south wall observation at 62.0W and 56.5W. WE 4 has moved slightly southwest. WE 1 position estimated. Small trough forms at 62.0W as crest at 61.8W propagates eastward to 60.5W. New WE forming from meander at 58.0W. A large meander has developed from a previously straight section at 62.0W-66.0W.

2.4.3 Model runs

Central forecast C1, Figure 48: The boundary conditions were linearly interpolated between IR observations on April 2 and 9. The flat section of the stream from 62.0W-66.0W develops a large meander. The small trough at 60.0W flattens out as it propagates downstream. The crest at 58.5W grows and propagates to the east almost one full degree.

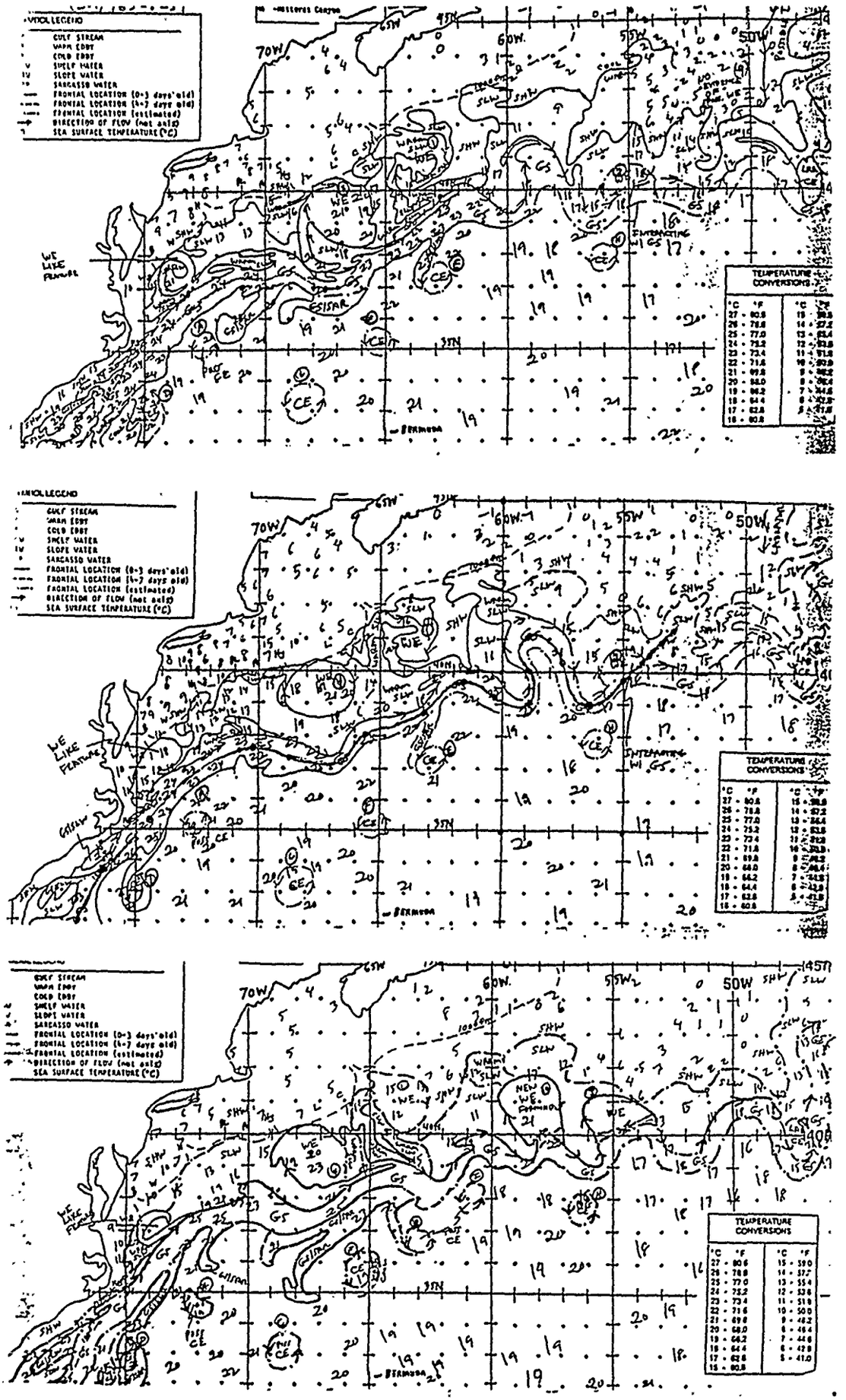

Fig. 47 — NOAA IR data for 2,4 and 9 April 1986

Fig. 48 — Gulf Stream forecast for 2–9 April 1986

Central forecast C1

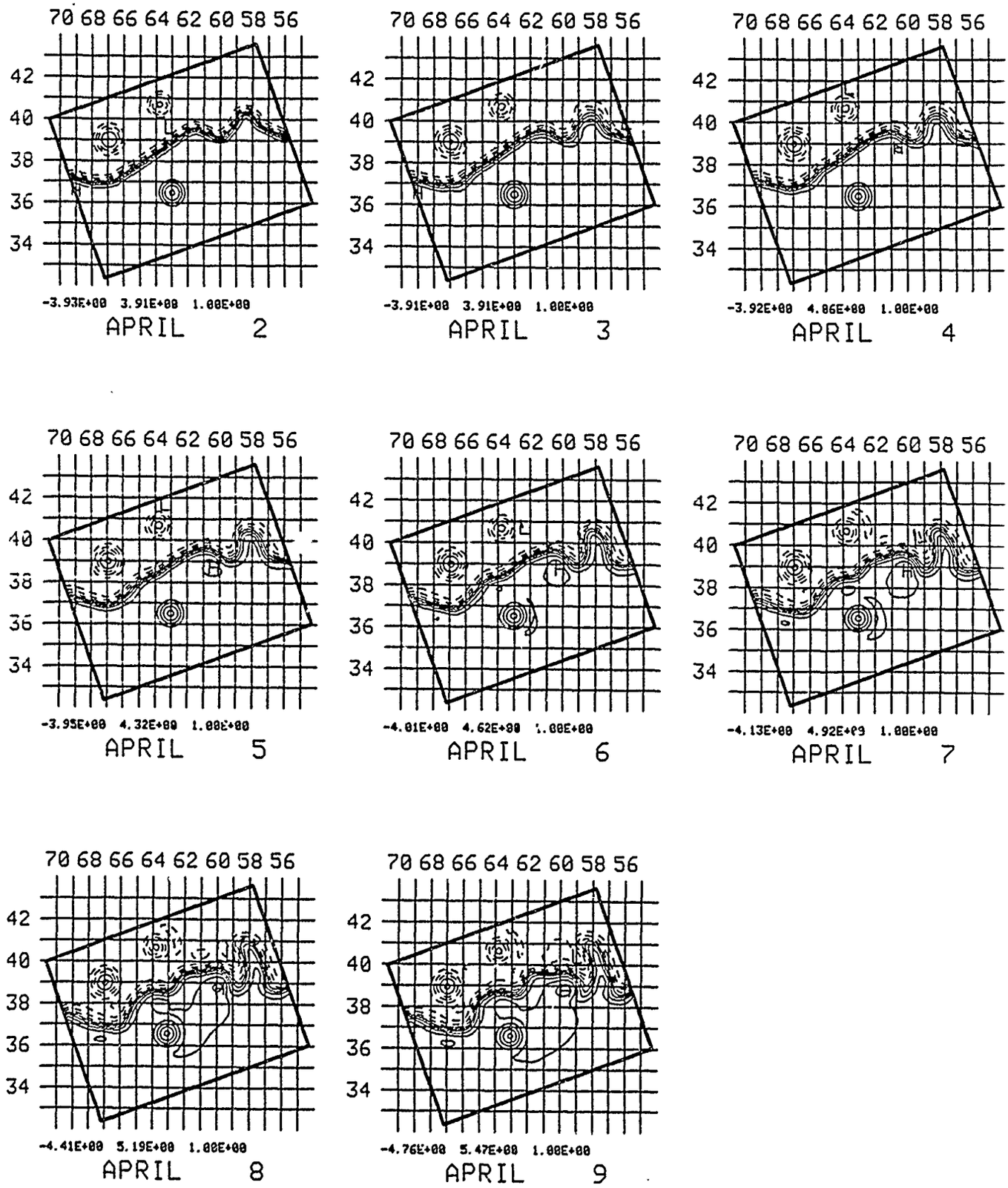

There were no sensitivity runs.

2.4.4 Summary

The model reproduces the tendencies seen in the IR quite well. The large meander that develops from 62.0W-66.0W compares very well. A vertical section through this meander and two rings is shown in Figure 49. The development of the crest at 58.5W does not disagree with the observed possible warm ring formation. A restart of this model run does indeed pinch off a warm ring a few days later.

The stream runs east-west where it should dip just west of the meander at 58.0W that will eventually form the WE. The high that develops just west of the trough at 59.0W appears to be responsible for the unrealistic flattening of the stream from 62.0W to 59.0W. This may be a result of the sharp bends in the linear fit of the digitized stream axis.

April 9-16

2.4.5 Data analysis

NOAA IR: (Figure 50)

Apr. 11: CEs observed at 36.5N 63.6W and 37.5N 60.8W. WE partially observed at 40.6N 64.0W. The Gulf Stream position is all old data.

Apr. 14: North wall well observed except for small break at 62.5W. South wall observed west of 66.5 W. WE shed at 58.0W, and the stream flattens to the south. CE pulls of a streamer at 56.5W. The broad trough from 66.0W to 69.0W appears to be sharpening at 66.5W.

Apr. 16: Stream observed west of 66.0W with warm outbreaks to the south. North wall observed from 65.0W to 62.0W. WEs 1 and 4 observed. The stream now runs nearly east-west from 70.0W to 66.0W at about 37.5N, and 65.0W to 61.8W at about 38.8N. A very sharp step has developed at 66.0W. There is no good data east of 61.0W.

2.4.6 Model runs

Fig. 49 — Vertical section on 9 April 1986

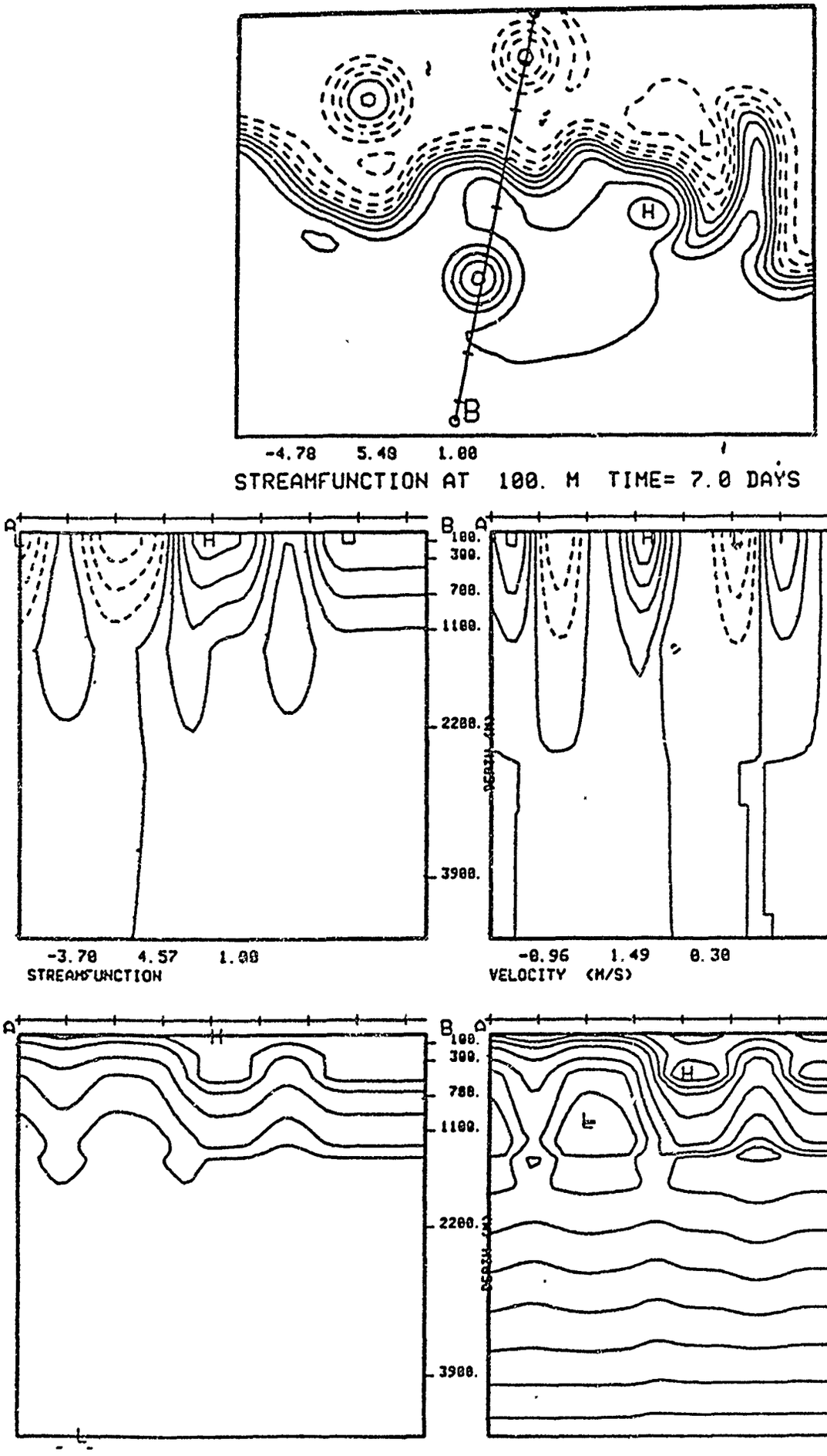

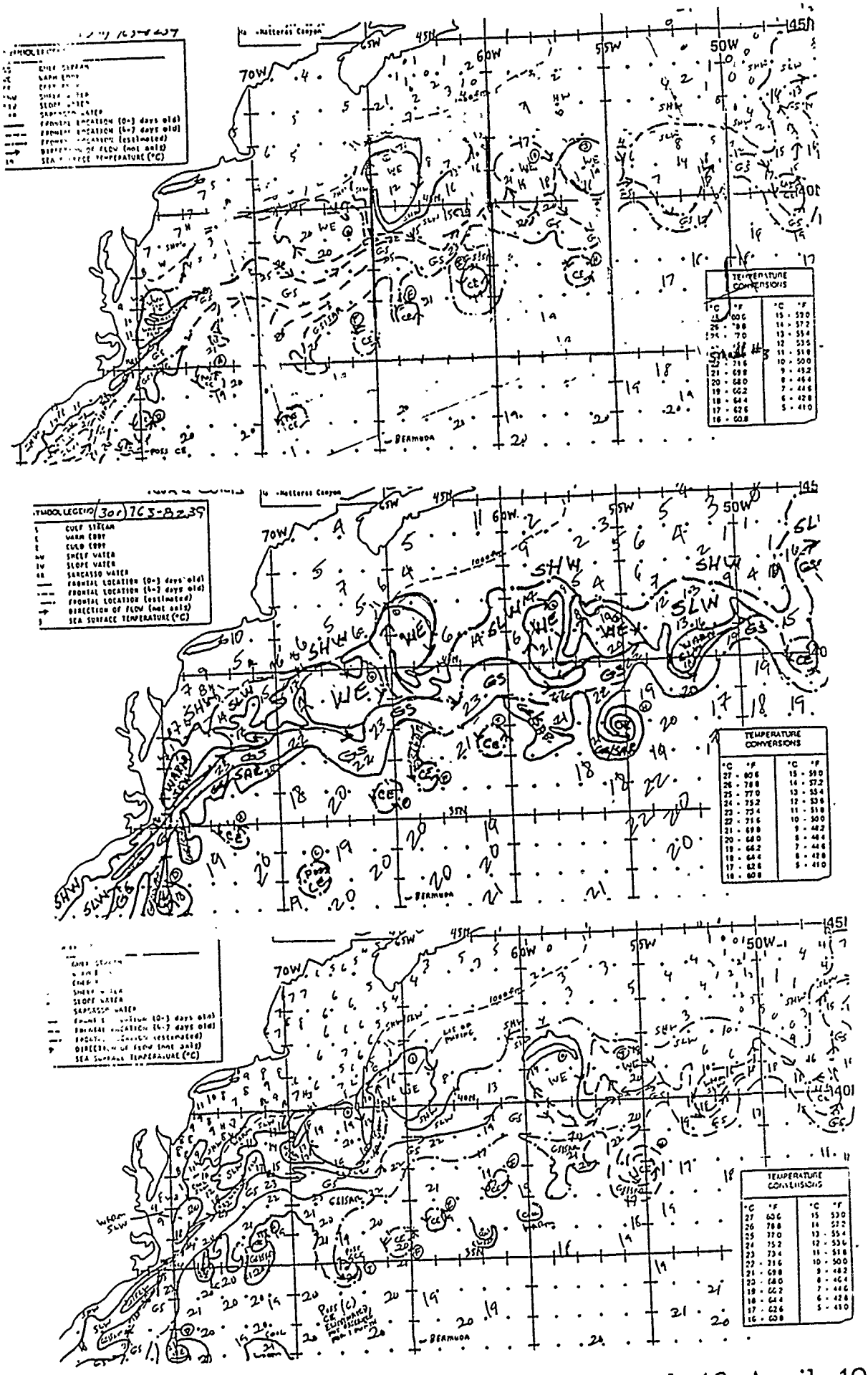

Fig. 50 — NOAA IR data for 11,14 and 16 April 1986

Central forecast C1, Figure 51: Digitized initial field with linearly interpolated boundary conditions. WE near 58.0W is assumed to be already formed and separated from the stream.

Sensitivity run S1A, Figure 52: Same as C1 except the warm ring is not quite formed yet and is still interacting with the stream.

Sensitivity run S1B, Figure 53: Restart from model output on April 9. Linearly interpolated boundary conditions.

2.4.7 Summary

The major changes seen in the IR are the flattening of the two meanders in the stream. The trough from 66.0W to 69.0W becomes very straight along 38.0N from 71.0W to 66.0W. There is a very sharp step up to about 39.0N where the stream has also flattened out, flowing straight to about 39.5N 61.5W. East of here there is no new data.

In the central forecast C1, the stream flattens from 70.0W to 66.0W and agrees very well with the IR data. Likewise, the model predicts the nearly east-west path of the stream from 65.0W to 62.5W. However, a large meander develops at 60.0W where IR data is not available due to cloud cover.

The two regions of flattening are represented just as well in the S1A forecast. The questionable meander near 60.0W develops in this run also. The WE forms by Apr. 13, and is stronger than its counterpart in the previous forecast.

Overall the S1B forecast does not match the IR data. The stream flattens some in the western part of the domain, but the flat region does not extend as far east as it should. The warm ring at 58.0W is pinched off in the same location as was observed in the IR but a little later. A trough develops at 65.5W that is not observed in the IR. A large instability occurs at 64.5W that appears to be forming a new WE. The region from 65.0W to 62.0W does not resemble the observed east-west stream path. The erroneous crest at 60.5W that also appears in the other two forecasts is accentuated here.

Fig. 51 – Gulf Stream forecast for 9–16 April 1986

Warm eddy already formed

Central forecast C1

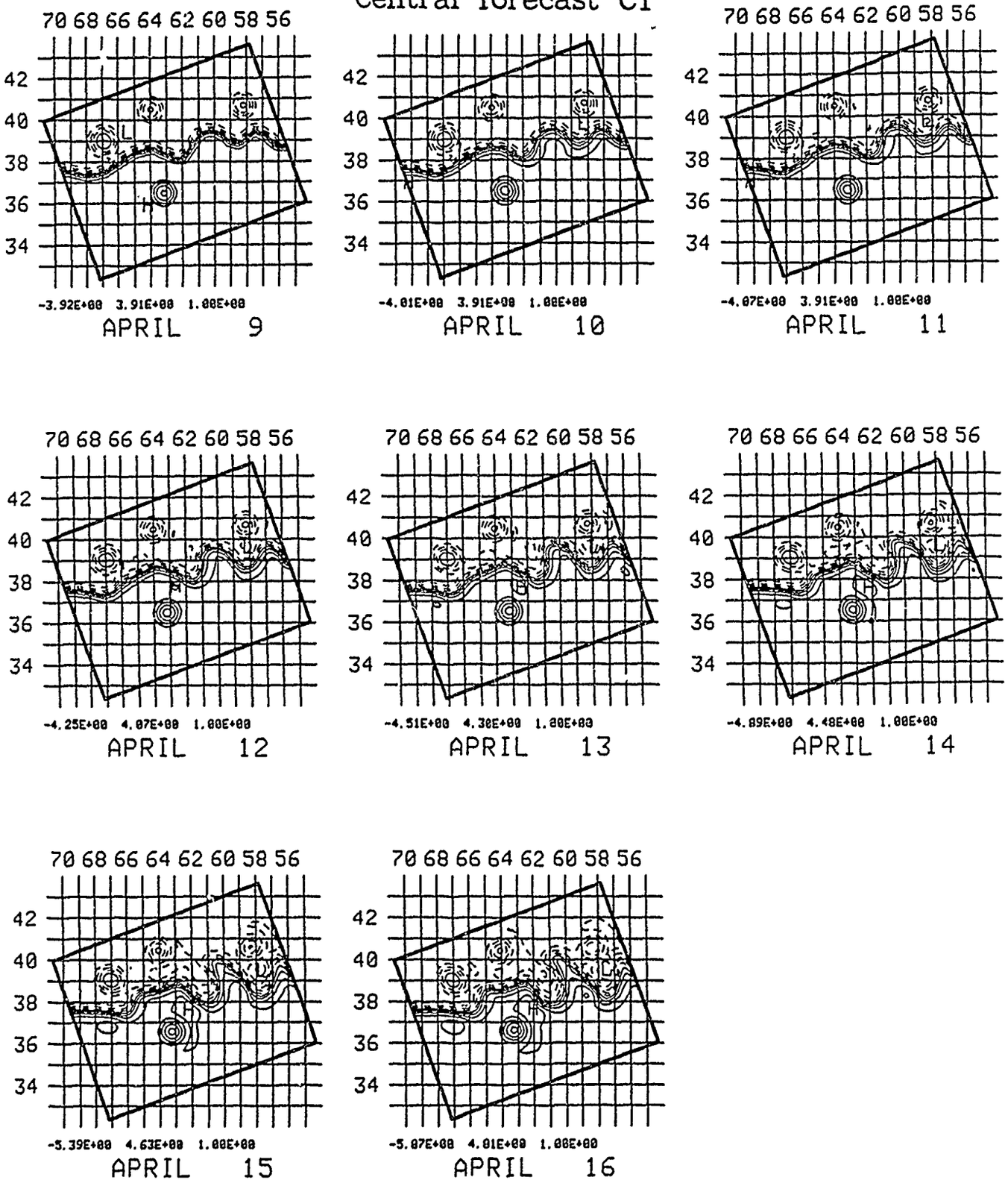

Fig. 52 — Gulf Stream forecast for 9–17 April 1986

Warm eddy interacting

Sensitivity forecast S1A

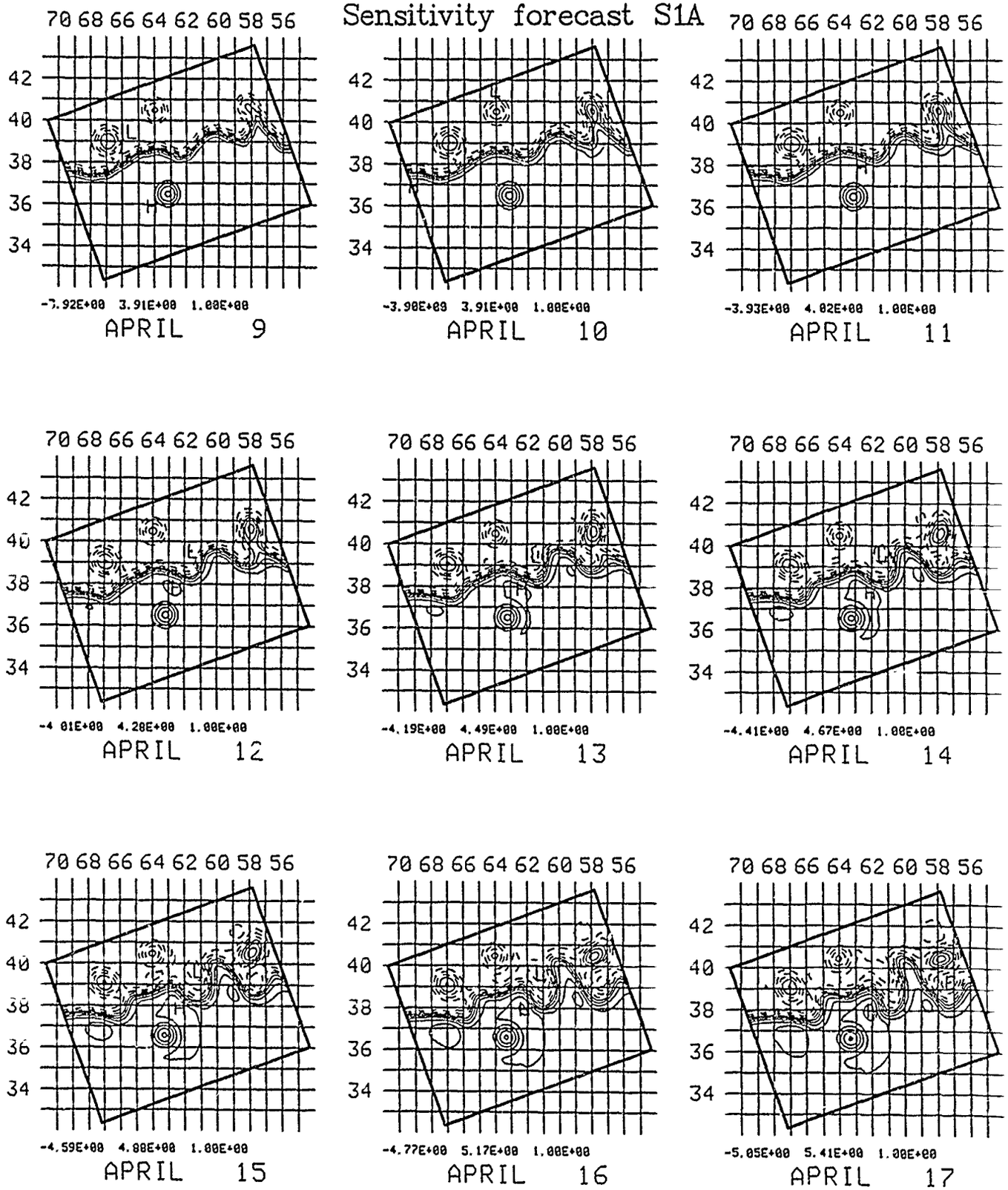

Fig. 53 — Gulf Stream forecast for 10–16 April 1986

Restart of previous fcst ending 9 April

Sensitivity forecast S1B

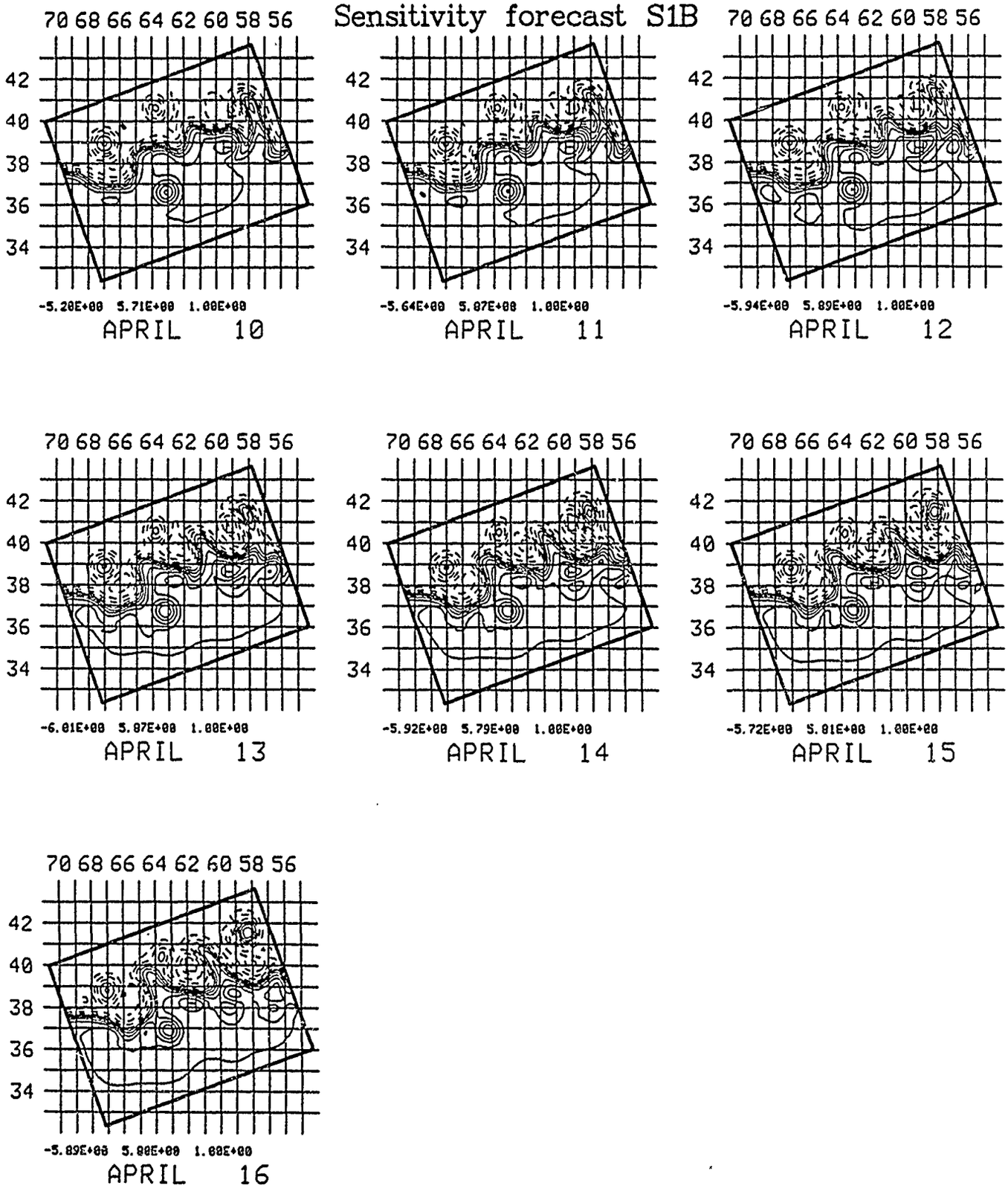

2.5 May 19 - June 6, 1986

This experiment took place between May 19 and June 6, 1986. The goal was to produce an accurate real time forecast at sea in a region of interest between 65.0W and 70.0W. All of the experience gained from the previous experiments was put to use in this example. The experiment has been broken down into three sections: (1) a supercomputer run, (2) sensitivity runs, and (3) the final operational product. The supercomputer run was done on May 19 in the extended domain prior to exact knowledge of the region of interest. As the region became more clearly defined, AXBT flight tracks and sensitivity runs were designed. Many of these model runs were done at sea and are contained in section 2. The final section uses a combined analysis from sections 1 and 2 to produce the operational forecast in real time while at sea. An operational product consisting of horizontal maps and vertical sections of temperature, velocity, and sound speed was provided by the forecast.

2.5.1 MAY 19-26, 1986: Extended Domain Forecast

2.5.1.1 Precis

This forecast was done in preparation for the at-sea experiment, run on the Cray XMP at the Naval Research Laboratory in domain L1. Output from this model run may be used as approximate boundary conditions for the next set of subregion forecasts.

2.5.1.2 Data analysis

NOAA IR: (Figure 54)

May 19: Stream well observed except for minor gaps at 58.0W and 53.0W. There are a great deal of outbreaks and ring-stream interactions, as well as some shingling. WEs 4, 10 and 3 well observed. WE 1 position estimated. CEs F, I, M and H well observed. CE J position estimated. CEs E and L not included.

May 21: Where there is new data available, there is little noticeable change except for the slight eastward propagation of the crests at 55.0W and 69.0W. A wavelike meander appears to be propagating downstream near 70.0W.

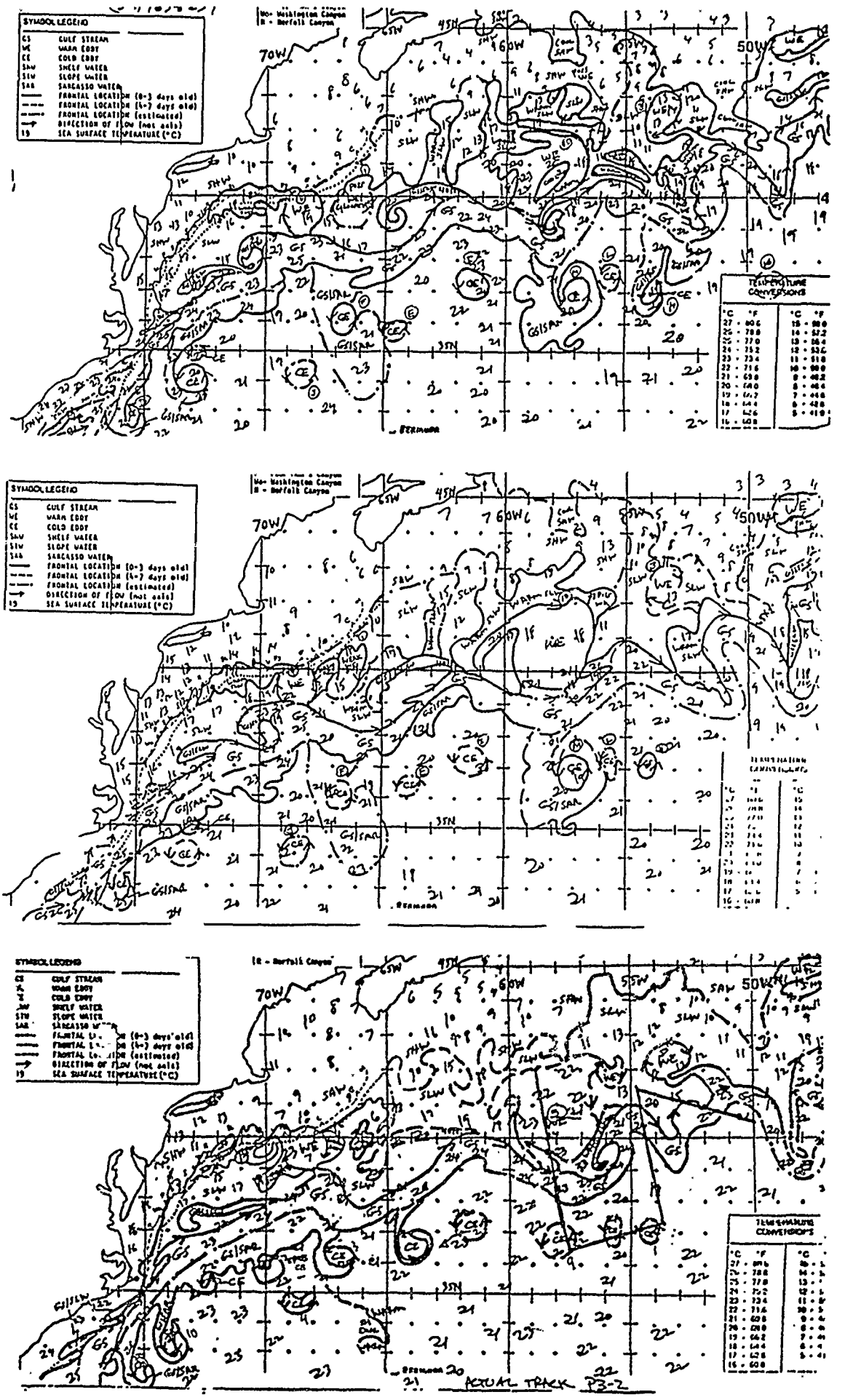

Fig. 54 — NOAA IR data for 19,21 and 28 May 1986

May 28: May 28 is shown here because the IR from May 26 was very poor. A small trough has developed at 66.0W, just downstream of the ring-stream interaction of WE 4. The meanders from 65.0W to 55.0W have propagated eastward, and a sharp trough has developed at 53.5W.

2.5.1.3 Model Run

Large domain forecast L1, Figure 55: The large domain supercomputer run was initialized on May 19 and run ahead for 1 week. The boundary conditions were estimated. The ring-stream interaction of WE 4 begins on May 21 as reflected in the IR image. The interaction continues to strengthen and a dip develops just downstream. By May 23 slight crests have developed at 65.5W and 59.5W. By May 26, the cold ring M has begun to be absorbed by the stream. The crest that formed at 65.5W on May 23 grows and propagates east to 64.5W on May 26. This may be a result of the interaction induced meander upstream.

2.5.1.4 Summary

Good IR data is available on May 19, 23 and 28. There is a lot of activity throughout the entire region including shingling, outbreaks, and ring-stream interactions. It appears as though a warm ring-stream interaction at 69.0W causes a slight dip to develop just downstream. This event has been reproduced very well in the model forecast. An additional crest develops at 64.5W that is not observed in the IR. It may be possible that the cold ring newly observed on May 28 interacting with the stream at 64.5W is important to this evolution. Further downstream at 57.5 the model run absorbs a cold ring into the stream where there is no signature of a cold ring in the IR. It is clear that there are many ambiguities which must be resolved with more model runs and AXBT flights.

Fig. 55a —Gulf Stream forecast for 19–26 May 1986

Supercomputer domain: 19–22 May

Large domain forecast L1

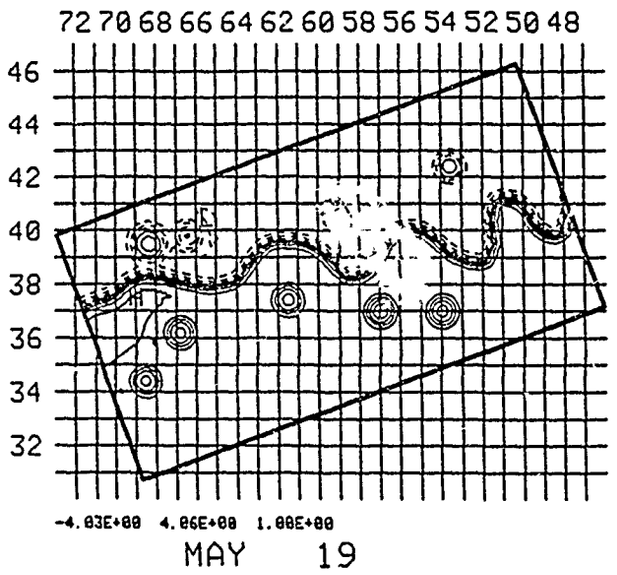

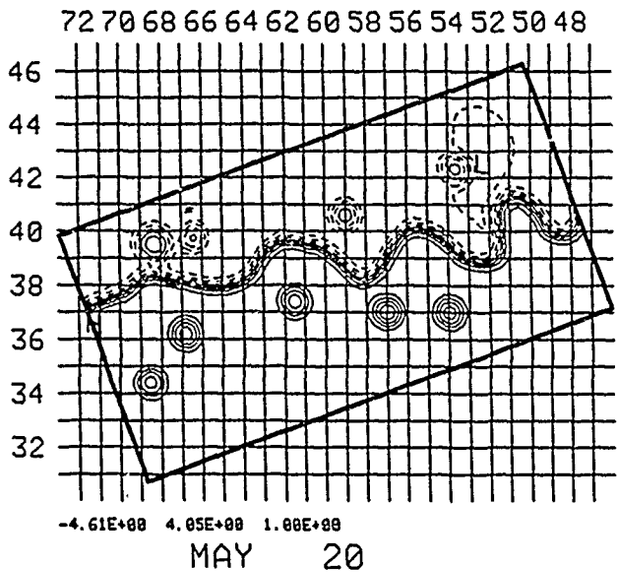

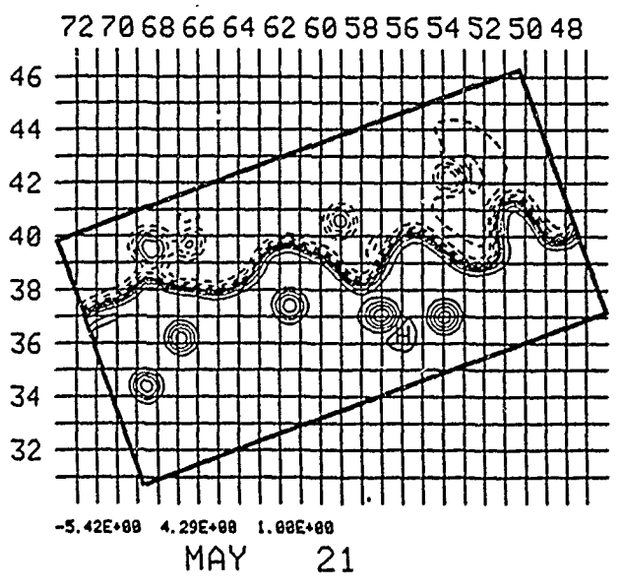

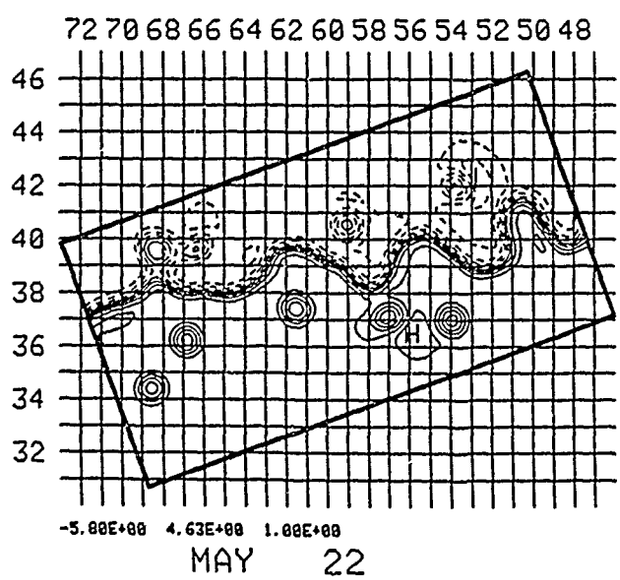

Fig. 55b —Gulf Stream forecast for 19–26 May 1986

Supercomputer domain: 23–26 May

Large domain forecast L1

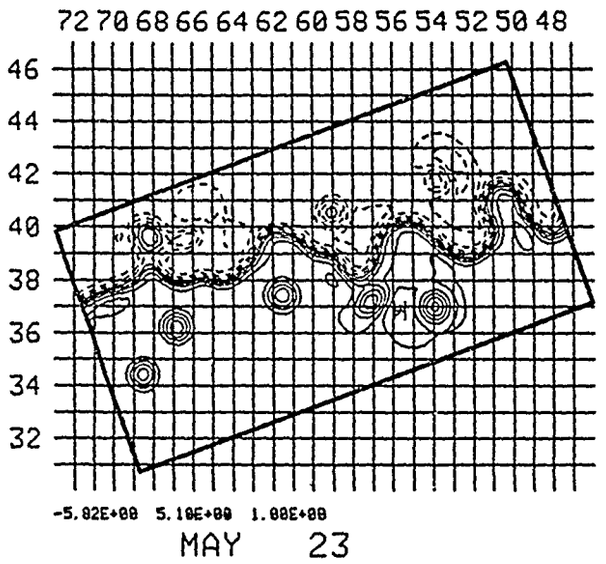

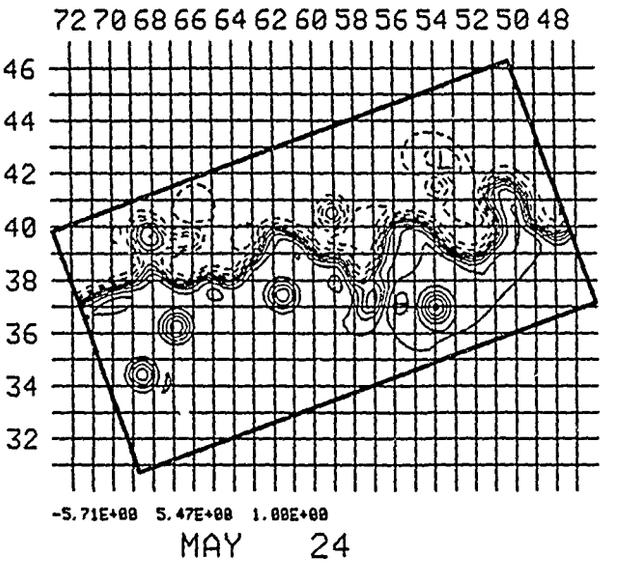

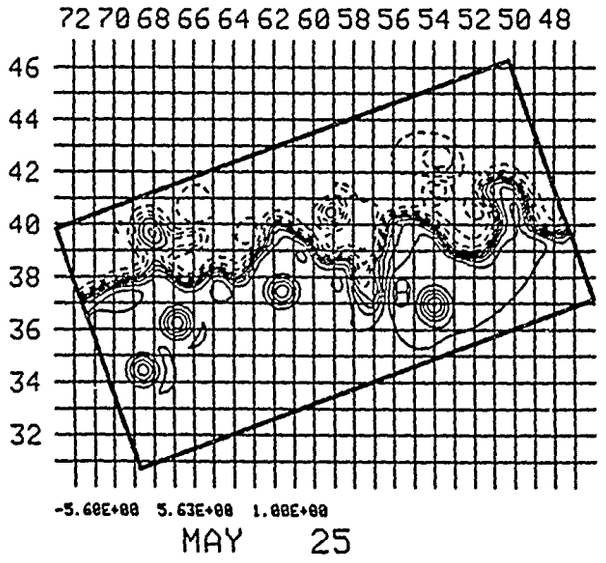

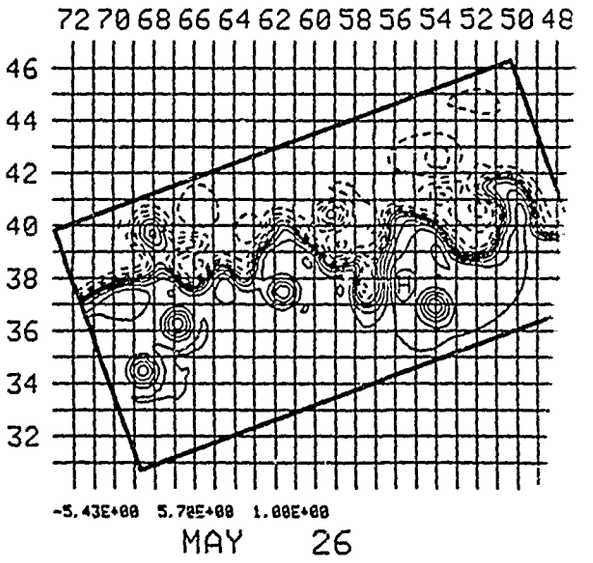

2.5.2 May 23-30, 1986: Sensitivity Forecasts

2.5.2.1 Precis

These forecasts were done in preparation for the at-sea experiment. A series of forecasts were run to determine the sensitivity to the initial position of a warm ring near the stream. The results agreed very well with the IR and all available AXBT information and were useful in understanding and interpreting the data as well. These forecasts were also used in a composite synthesis to obtain the best initial condition for the at-sea forecast. Several of these were run at-sea. A supercomputer run was initialized in the extended domain L1 prior to departure and run ahead through the duration of the experiment.

2.5.2.2 Data analysis

NOAA IR: (Figure 56)

May 23: Stream position observed only over the eastern half of the domain. Crest at 68.5W, trough at 65W. Crest at the boundary 62.0W. WE 4,1 positions estimated. CE J, F, I positions estimated. CE E not included.

May 28: Stream position observed over nearly the entire domain. All ring positions observed except for CE I. Trough develops at 66.0W and crest at 61.5 becomes sharper.

May 30: Trough at 66.0W extends south to 37.3N. WE positions observed, CE positions estimated.

AXBT DATA: (Figures 57-59)

May 23: North wall located by flight P3-1 at 38.8N 63.75W, 39.7N 62.5W. North wall bracketed by 37.4N and 38.7N along 66.0W and to the north of 38.5N along 68.0W. Warm ring located at 39.8N 66.7W and a possible WE near 40.0N 68.7W. Cold ring located at 36.2N 66.8W. Due to equipment failure, very important AXBTs were missed near 39.5N 68.5W at the location of the ring-stream interaction.

May 29: North wall located at 38.2N 69.0W, 38.2N 67.2W. North wall bracketed by 38.5N to the north along 65.0W. Warm rings located at 39.0N 67.8W, and 38.6N 66.1W.

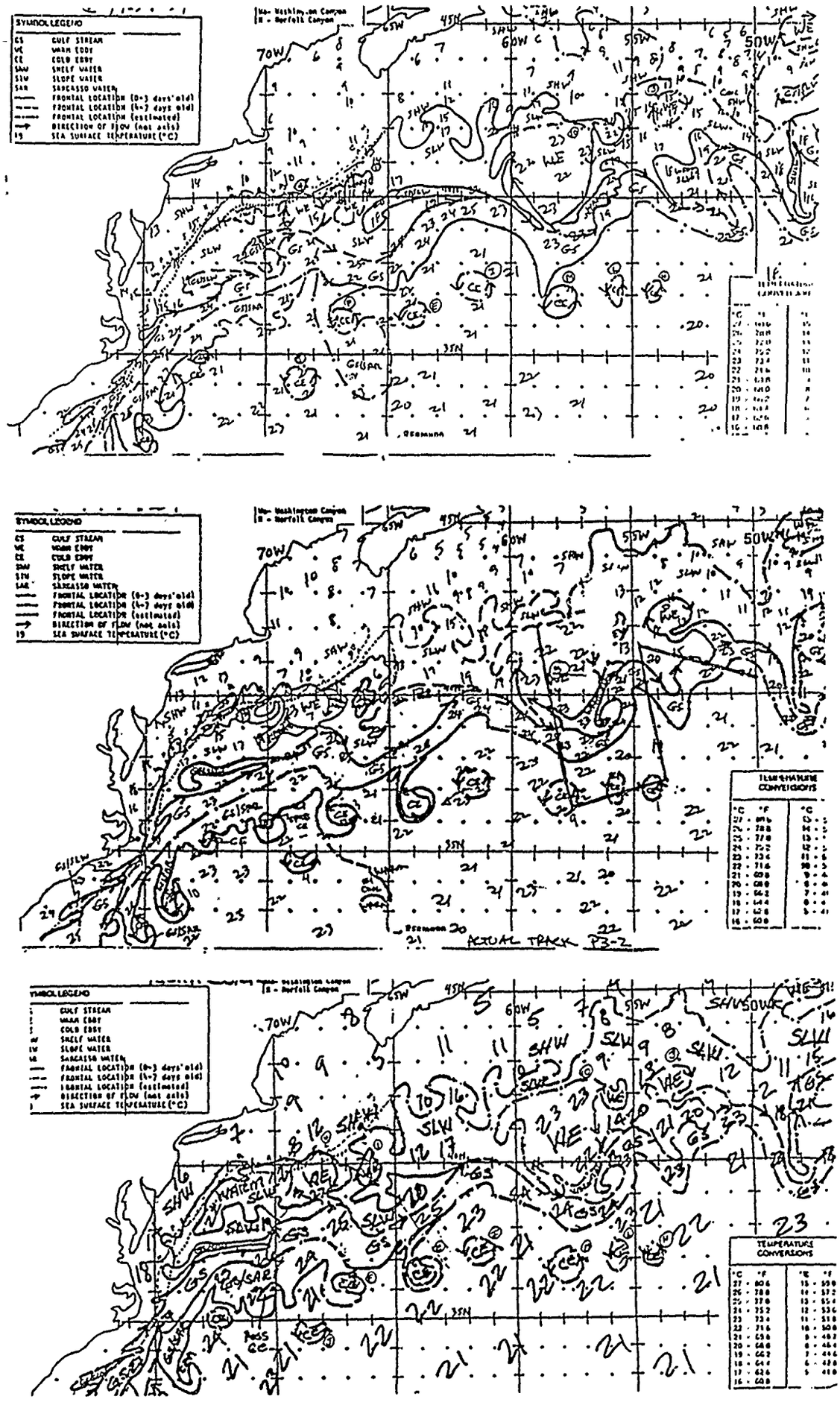

Fig. 56 — NOAA IR data for 23,28 and 30 May 1986

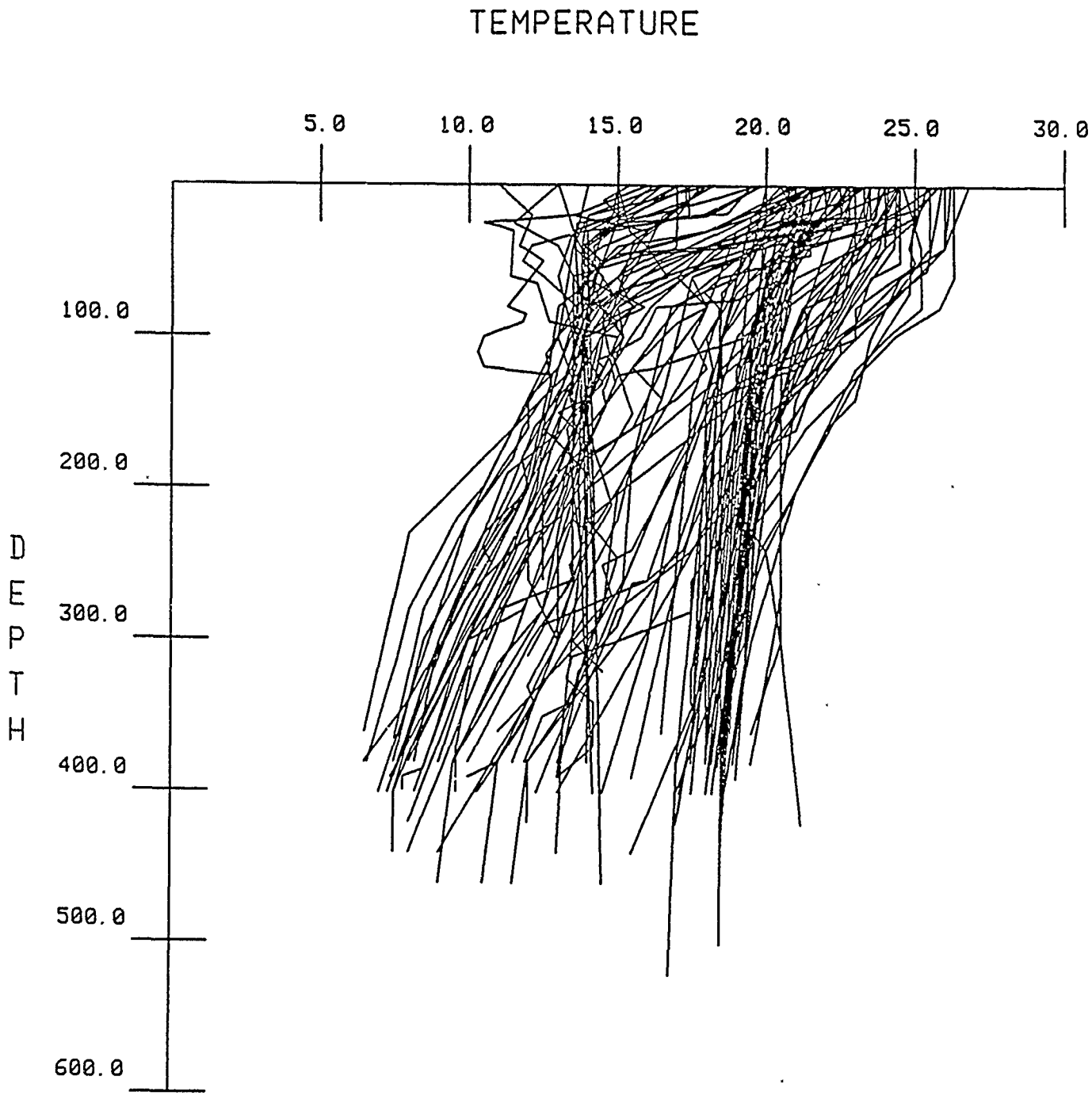

Fig. 57 — Composite of AXBT traces 23 May – 2 June 1986

Fig. 58 — AXBT data 23 May 1986: 300m temperature

Value of 7.0 °C removed from the observations

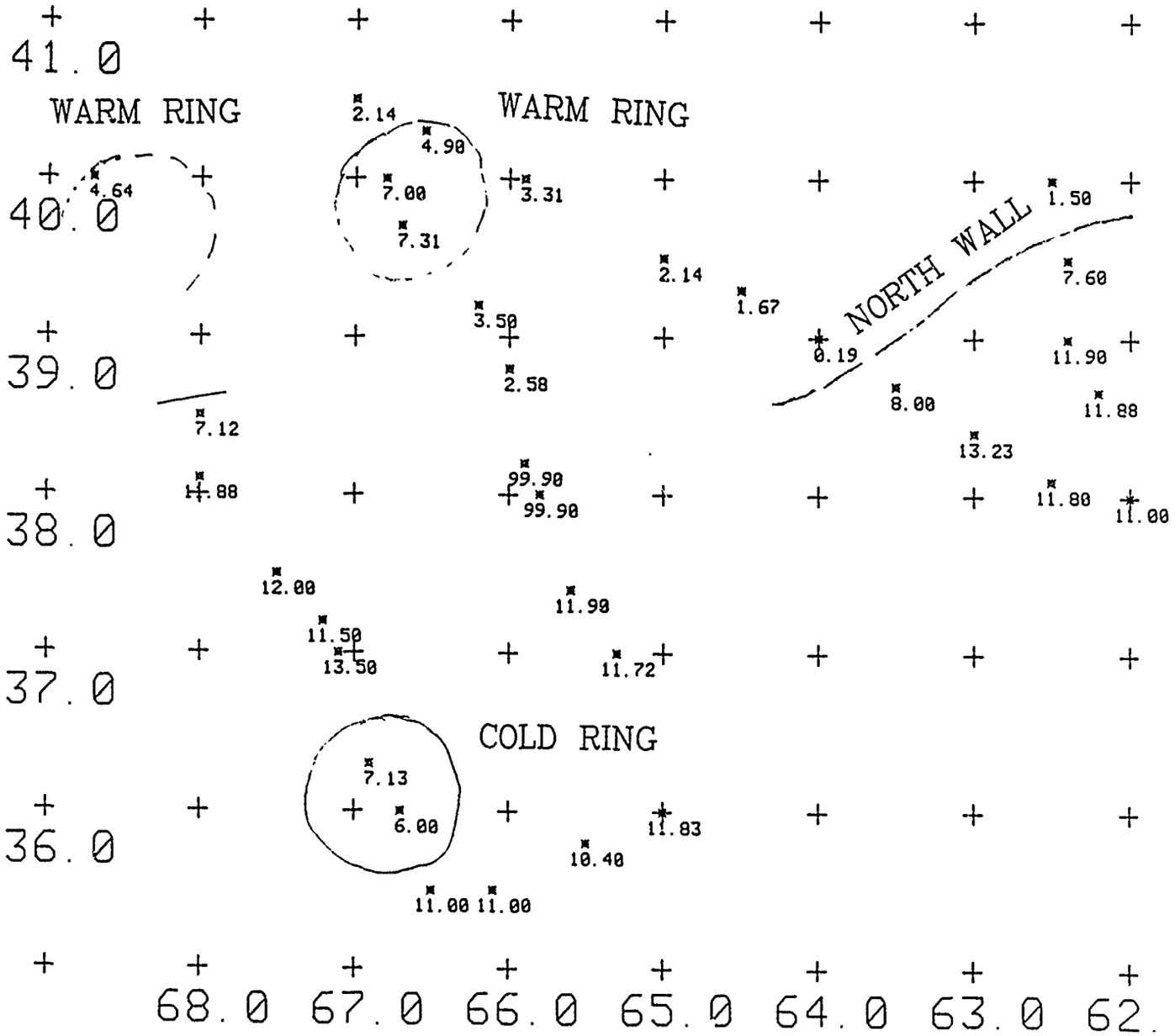

Fig. 59 — AXBT data 29 May 1986: 300m temperature

Value of 9.0 °C removed from the observations

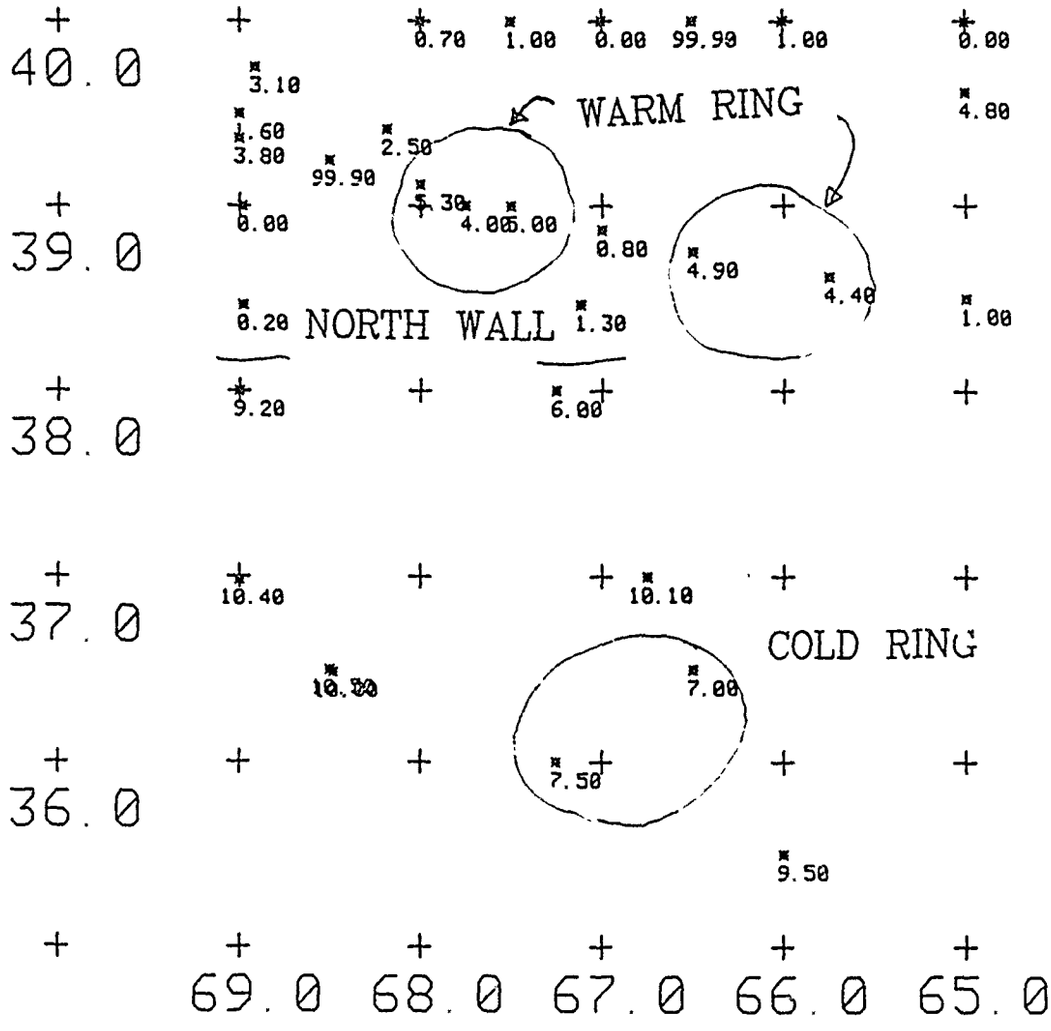

Cold ring located at 36.2N 66.8W.

2.5.2.3 Model runs

Large domain forecast L2, Figure 60: A forecast was initialized in the large domain from the IR data only on May 28 and run ahead for 12 days (through the duration of the experiment). This run was done prior to departure and the results were brought to sea. The information was available for use as boundary data for the refined subregion forecasts but was not used. Very strong ring-stream interactions occur near the region of interest (62.0W-70.0W). The initial positions of these rings was estimated from the IR data only and may not be correct. The inflow region remains fairly smooth but downstream many small scale waves develop and grow.

Central forecast C2, Figure 61: This central forecast was initialized on May 23 and run ahead for 1 week. A slight interaction between the warm ring at 68.5W and the stream is assumed. During the forecast, this interaction strengthens. The stream advects the ring 70km to the east and develops a large dip just downstream. A small wavelike pattern develops from 62.0W to 65.0W.

A series of sensitivity forecasts was designed to test different strengths of the ring-stream interaction at 68.5W.

Sensitivity run S2A, Figure 62: A slightly weaker ring-stream interaction is assumed. The stream continues to flow smoothly to the east for the next five days. A slight sharpening of the stream develops in the trough at 65.0W.

Sensitivity run S2B, Figure 63: This run was initialized with a strong ring-stream interaction. The stream reacts very strongly and the ring is completely absorbed by May 28. A very large meander develops downstream.

Sensitivity run S2C, Figure 64: In this run the strength of both the warm ring and the ring-stream interaction have been decreased. The result is very similar to run S2A. The stream remains smooth with a slight wavelike pattern for 62.0W to 65.0W.

Sensitivity run S2D, Figure 65: This forecast was initialized with the IR data only. The primary modification was the shape of the stream west of 68.0W. The IR placed the stream much further to the south, approximately 60km at 70.0W. The resulting ring-stream interaction is very slight. The crest at 68.0W propagates to the east about 1.5 degrees. As a result the trough at 65.5W sharpens slightly.

Sensitivity run S2E, Figure 66: The warm ring-stream interaction was changed again slightly in this run, between runs C2 and S2A. The interaction results in the development of a sharp trough at 66.5W. The ring is pulled to the east about 60km. Again, small wavelike patterns develop from 62.0 to 65.0W.

2.5.2.4 Summary

Evidence in the IR suggests a warm ring-stream interaction near 68.5W results in the development of a sharp trough at 66.0W on May 28-30. AXBT flights on May 23 and May 29 place the stream position slightly to the north of the IR data. A warm ring was located at 39.8N 66.7W and a cold ring at 36.0N 66.8W. Equipment failure caused the position of a very critical warm ring to be missed near 39.5N 68.5W. The second AXBT flight located the cold ring again and gives an interesting analysis of the warm rings. The IR locates 2 warm rings at 39.5N 68.5W and 40.0N 66.0W. Temperatures at 300m indicate that those rings have moved to 39.0N 67.8W and 38.8N 66.0W. The model sensitivity runs helped to clear up what we believe happened. Run S2E shows the ring-stream interaction cause the development of a sharp trough at 66.5W in good agreement with the IR. In addition, the warm ring was shifted to the east at 39.8N 67.9W and the second warm ring pulled to the south at 39.8N 66.2W. These positions are in qualitative agreement with the AXBT data of May 29.

Fig. 60 — Gulf Stream forecast for 28 May – 8 June 1986

Supercomputer domain: 28–31 May

Large domain forecast L2

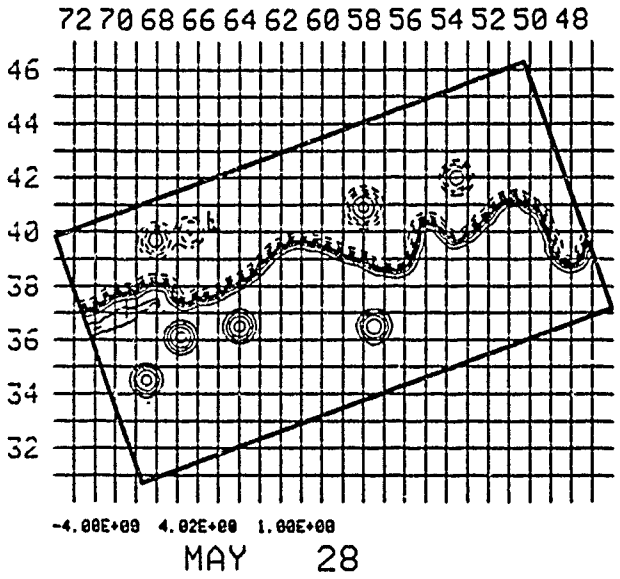

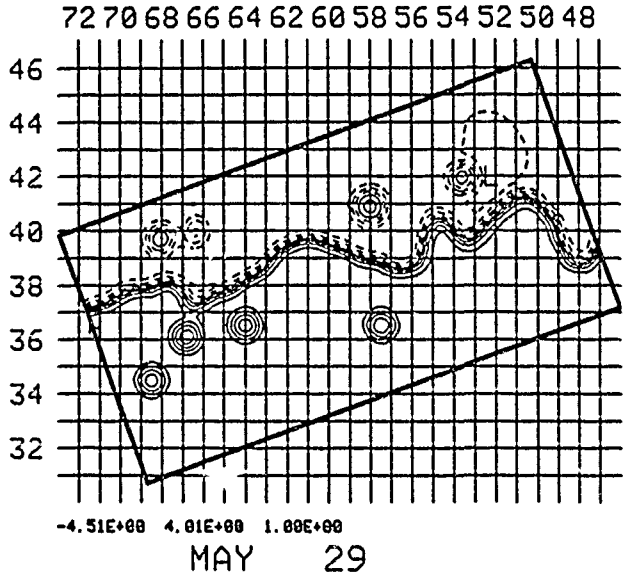

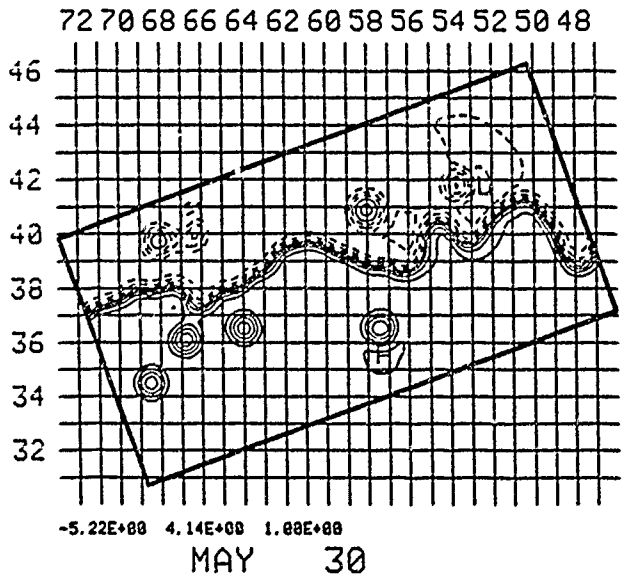

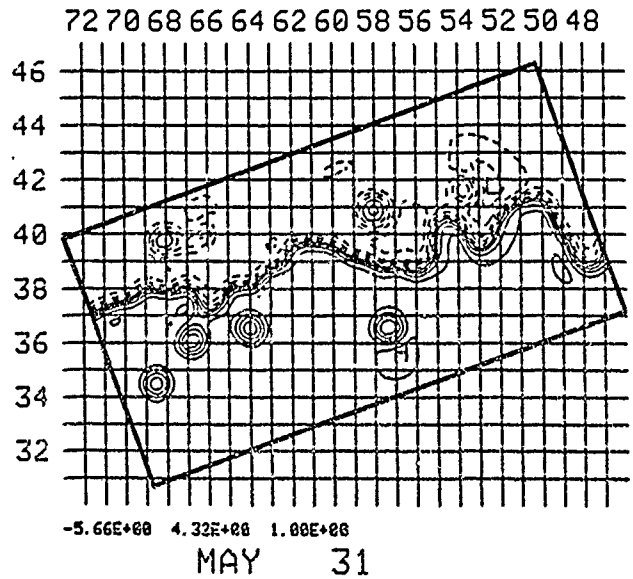

Fig. 60 — Gulf Stream forecast for 28 May – 8 June 1986

Supercomputer domain: 1–4 June

Large domain forecast L2

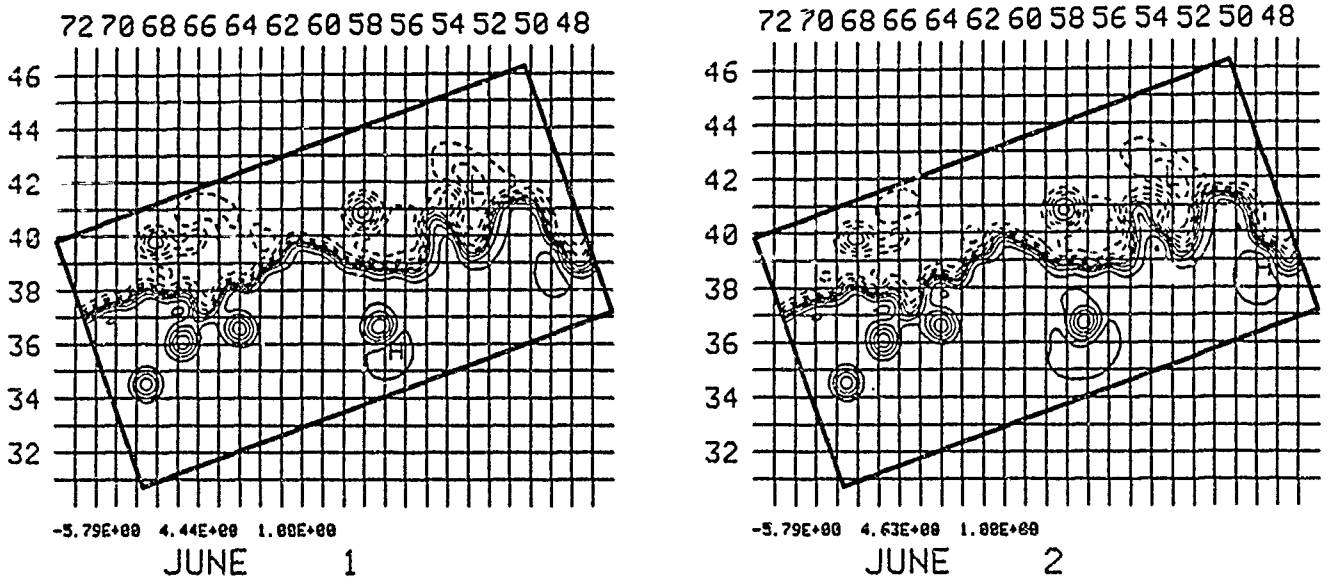

Fig. 60 — Gulf Stream forecast for 28 May – 8 June 1986

Supercomputer domain: 5–8 June

Large domain forecast L2

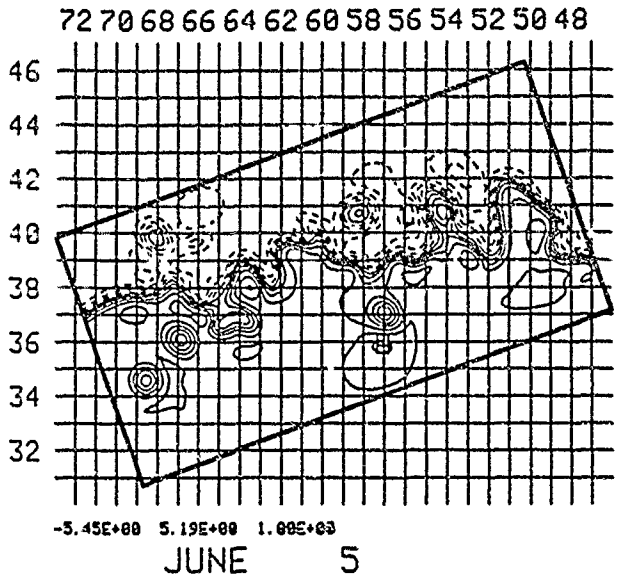

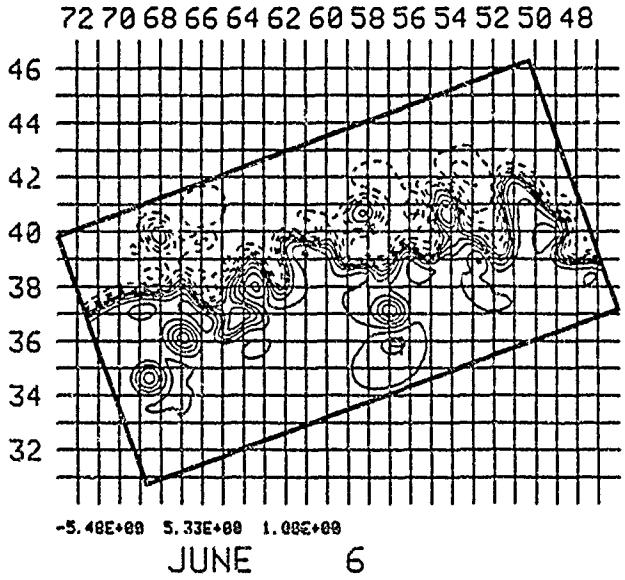

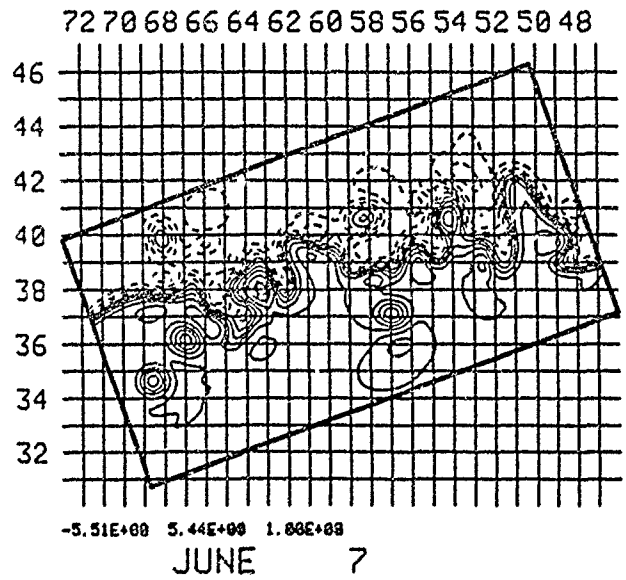

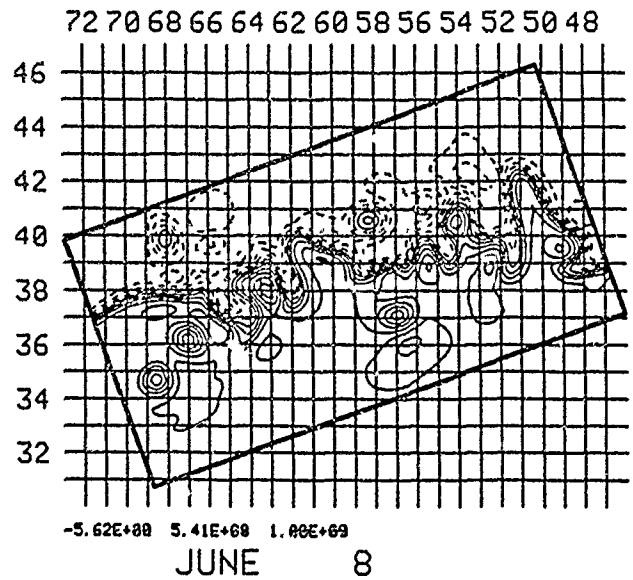

Fig. 61 — Gulf Stream forecast for 23–30 May 1986

Central forecast

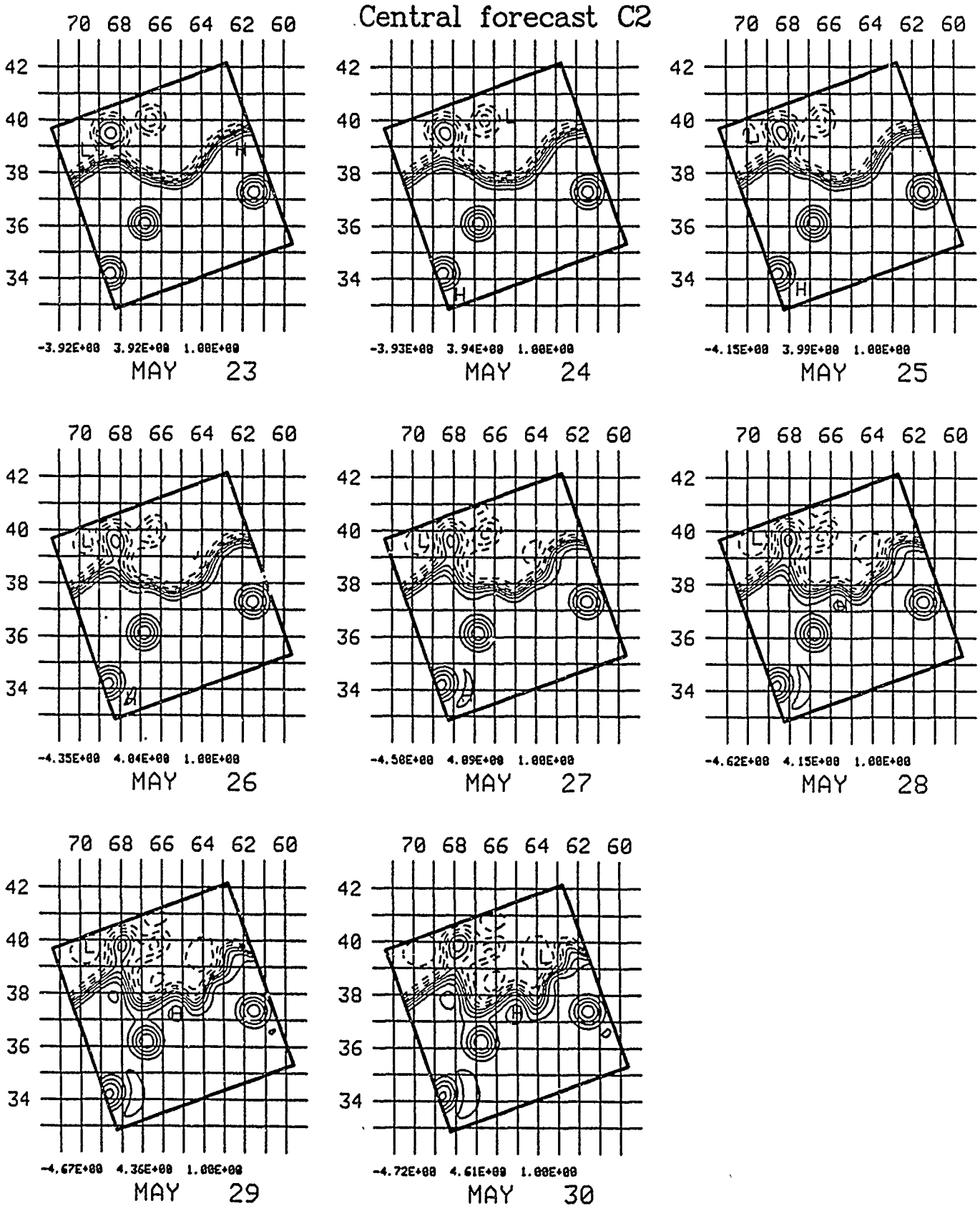

Fig. 62 — Gulf Stream forecast for 23–28 May 1986

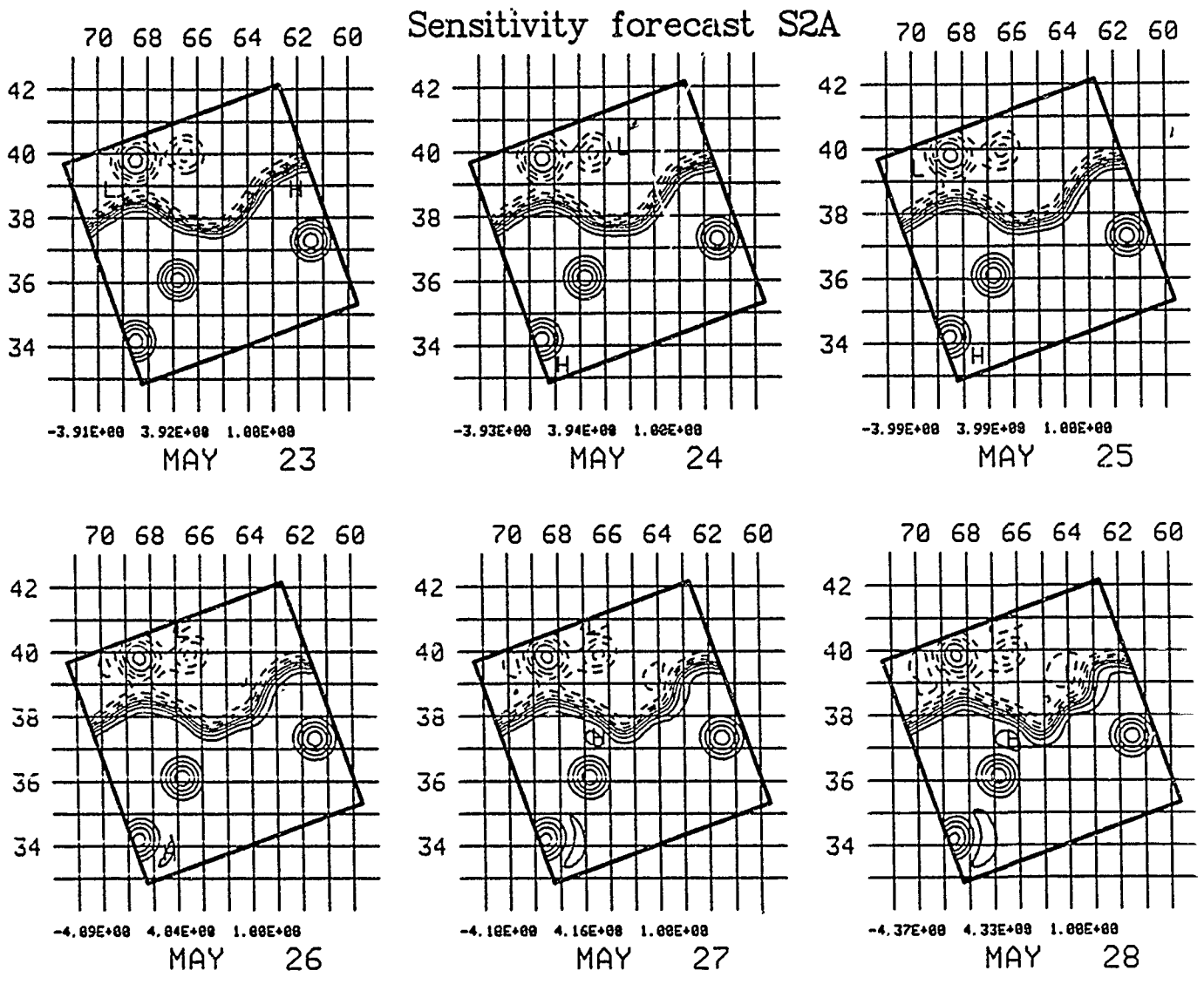

Fig. 63 – Gulf Stream forecast for 23–28 May 1986

Strong warm ring interaction

Sensitivity forecast S2B

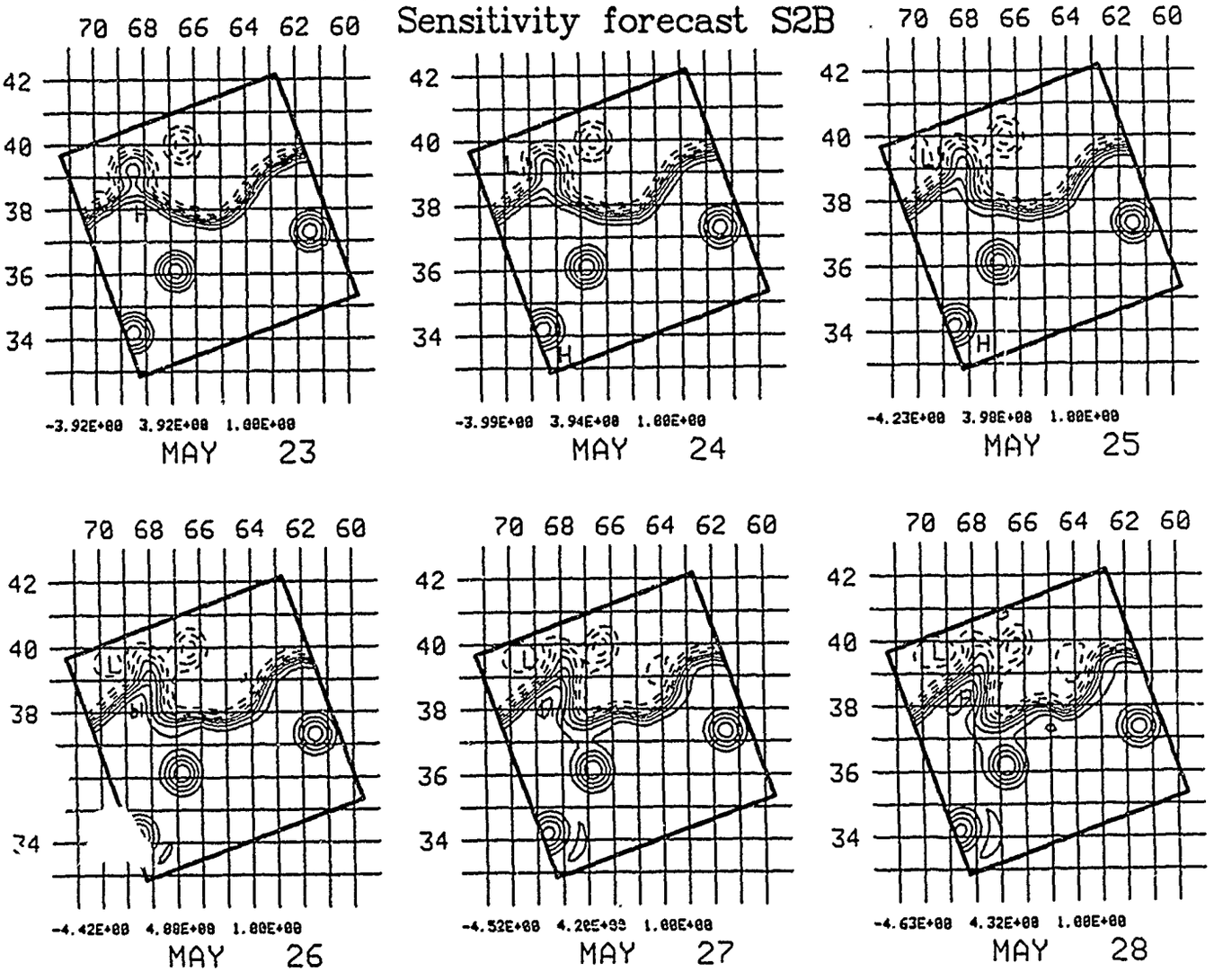

Fig. 64 — Gulf Stream forecast for 23–28 May 1986

Small warm ring, weak interaction

Sensitivity forecast S2C

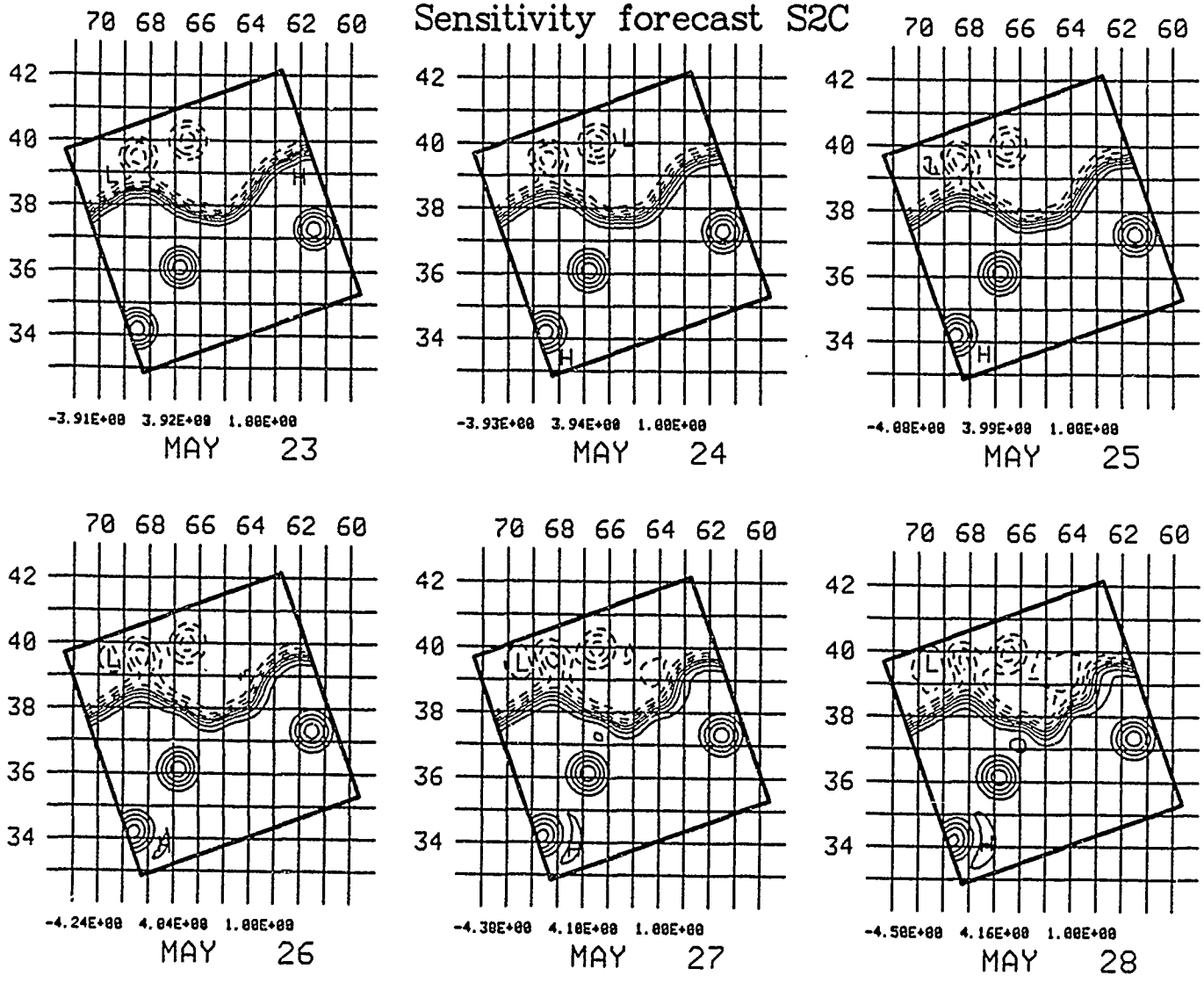

Fig. 65 — Gulf Stream forecast for 23–30 May 1986

Initialized without P3 data

Sensitivity forecast S2D

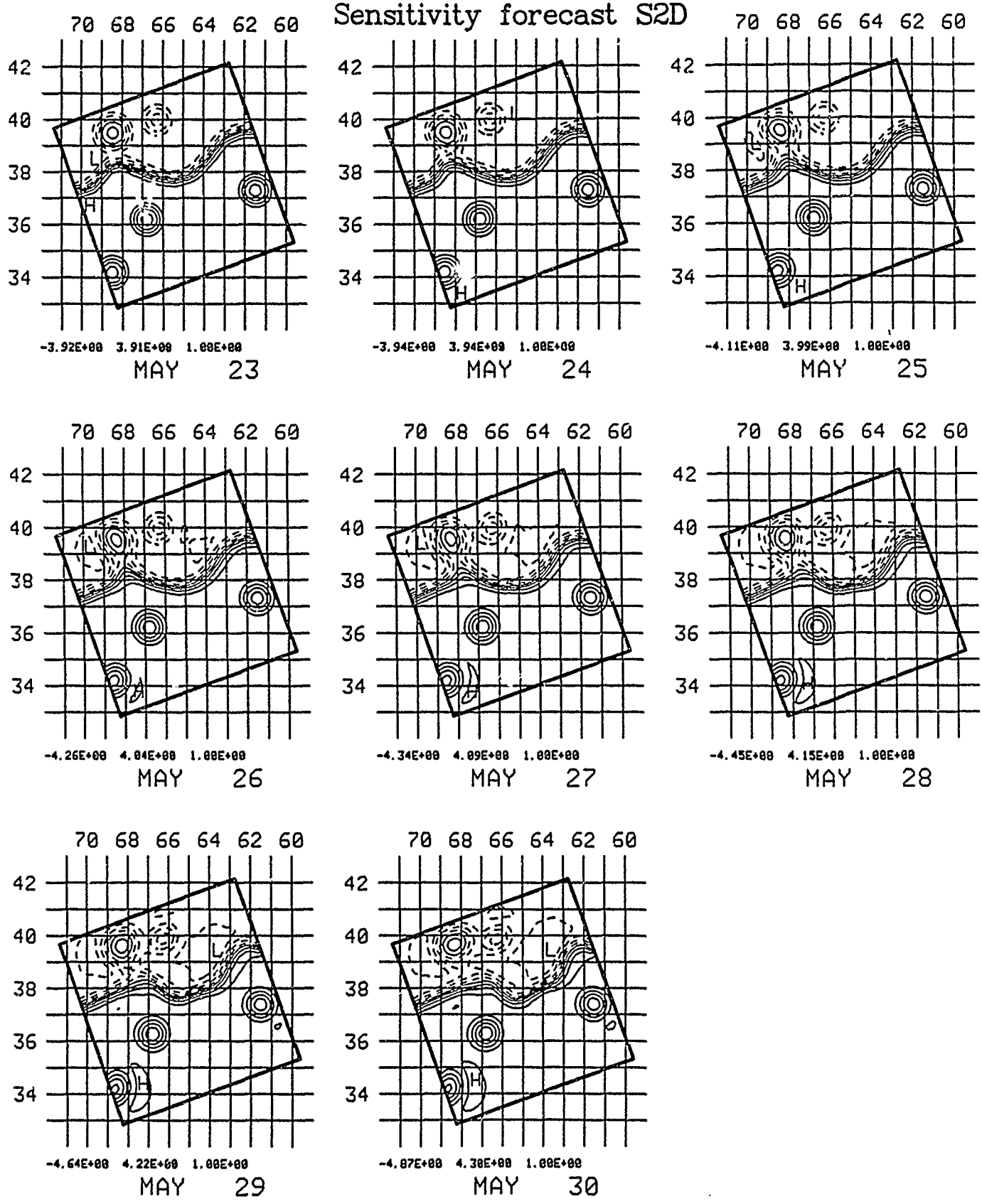

Fig. 66 — Gulf Stream forecast for 23–30 May 1986

Intermediate warm ring interaction

Sensitivity forecast S2E

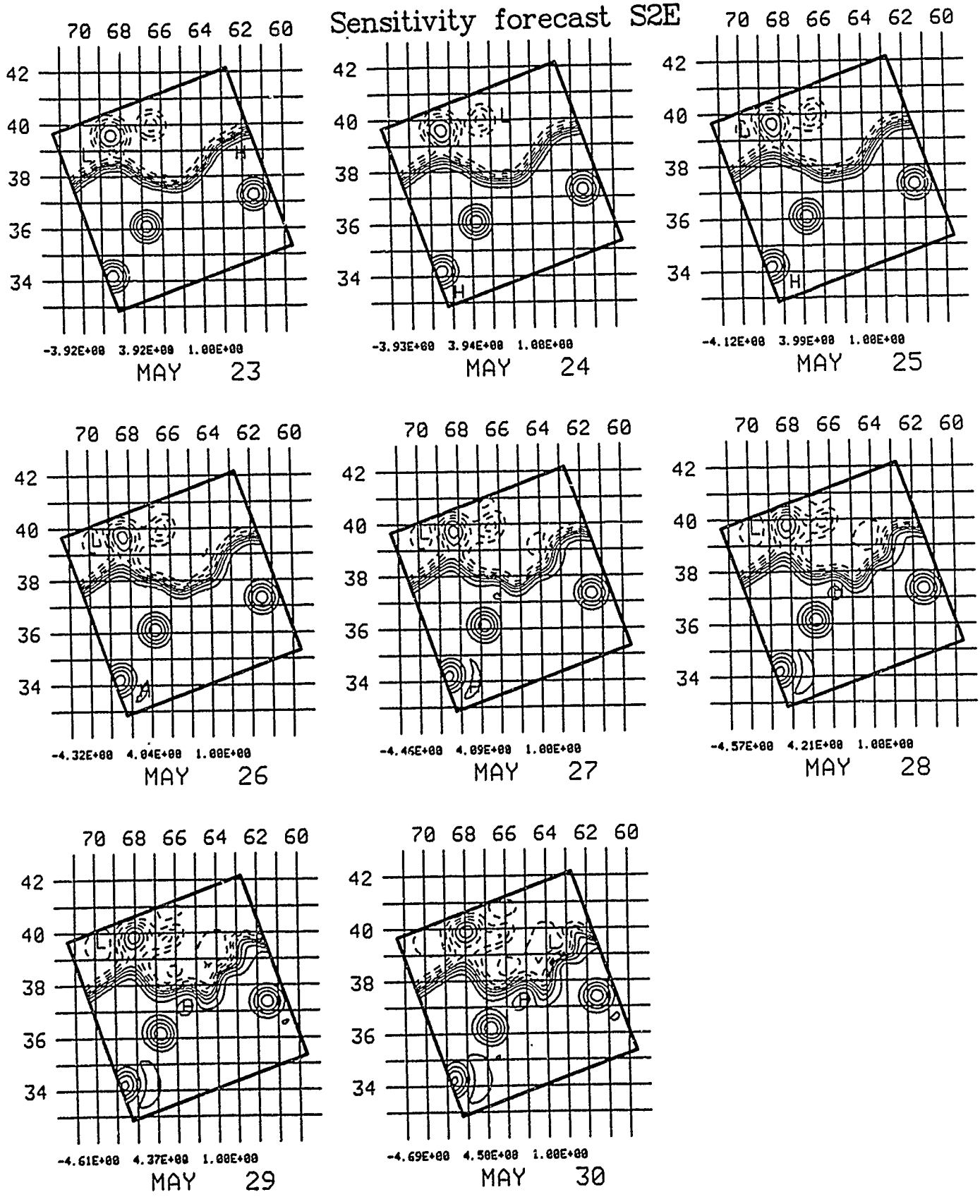

2.5.3 June 2-6, 1986: Operational Forecast

2.5.3.1 Precis

This is the final product for the at-sea experiment. The initial condition was obtained through an analysis using AXBTs, satellite data previous to June 1, and previous model forecasts. The forecast fields agreed very well with all available data.

2.5.3.2 Data analysis

NOAA IR: (Figure 67)

Note: None of the NOAA IR data was available for use in this experiment. It is shown here for comparison purposes only.

June 2: North wall observed over entire domain except for brief break at 71.0W. South wall observation lacking a large chunk from 68.0W to 66.0W. CE J, F, E position estimated. WE 1, 4 positions observed.

June 4: The stream axis is well observed. A small wavelike pattern develops from 68.0W to 71.0W. The trough at 65.0W propagates eastward. Existence of a streamer suggests slight ring-stream interaction with CE E. WE 1, 4 and CE E, F observed.

June 6: Very little new data. North wall observed 68.0W to 65.0W. Data outside model domain shows that the meander has propagated further east.

AXBT DATA: (Figure 68)

One stream crossing was completed that yielded a north wall position of 38.2N 69.0W on June 2. AXBTs show the stream bracketed by 37.0N and 39.0N at 72.0W. One questionable cold ring at 35.0N 72.5W was found to be nonexistent. Insufficient coverage due to air space problems and equipment failure made it impossible to determine the status of the possible cold ring at 35.5N 70.5W.

2.5.3.3 Model run

Central forecast C3, Figure 69: The best estimate of the field was used as an initial condition for a 4 day forecast from June 2-6 in domain S1. The forecast shows a slight

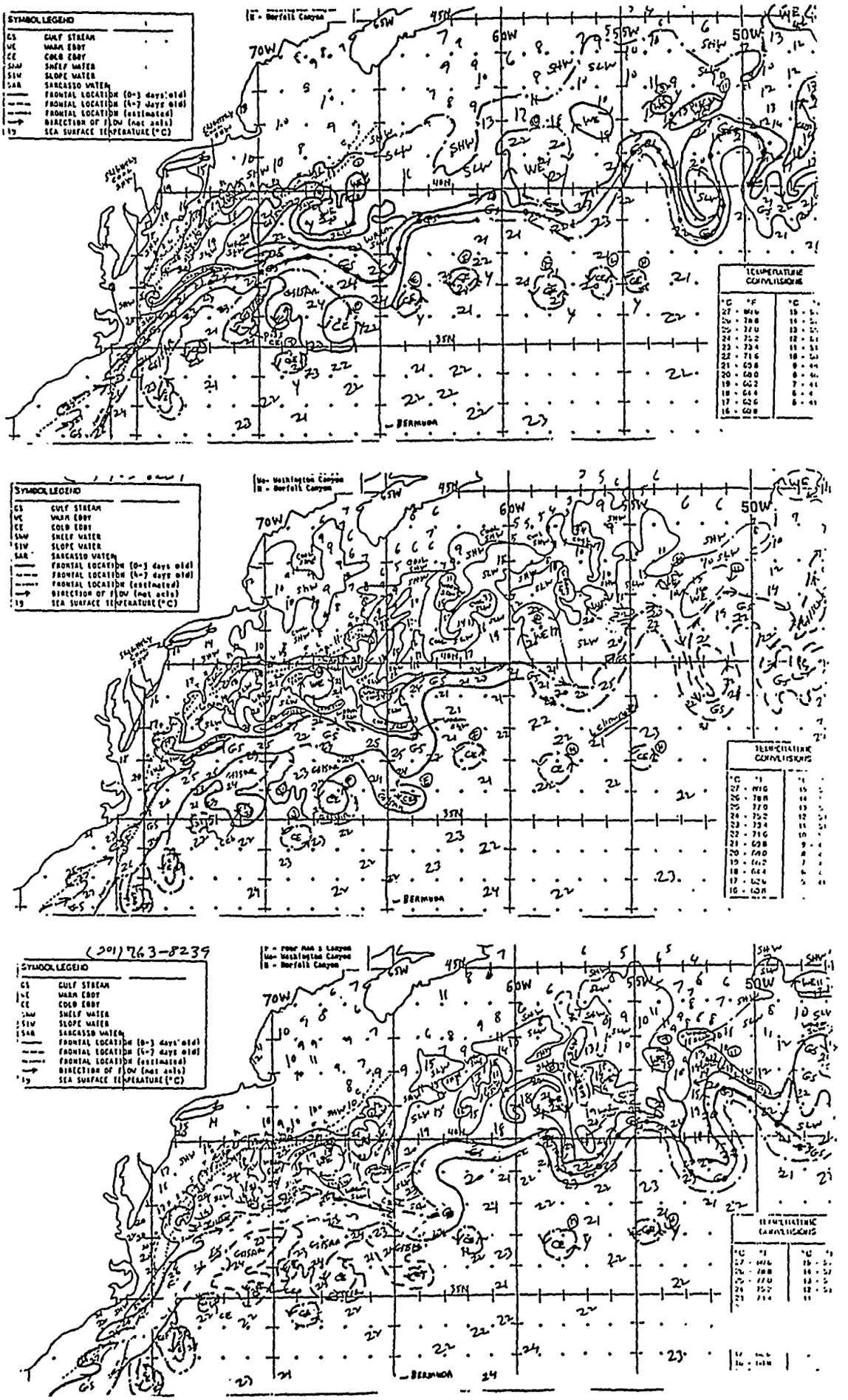

Fig. 67 — NOAA IR data for 2,4 and 6 June 1986

Fig. 68 — AXBT data 2 June 1986: 300m temperature

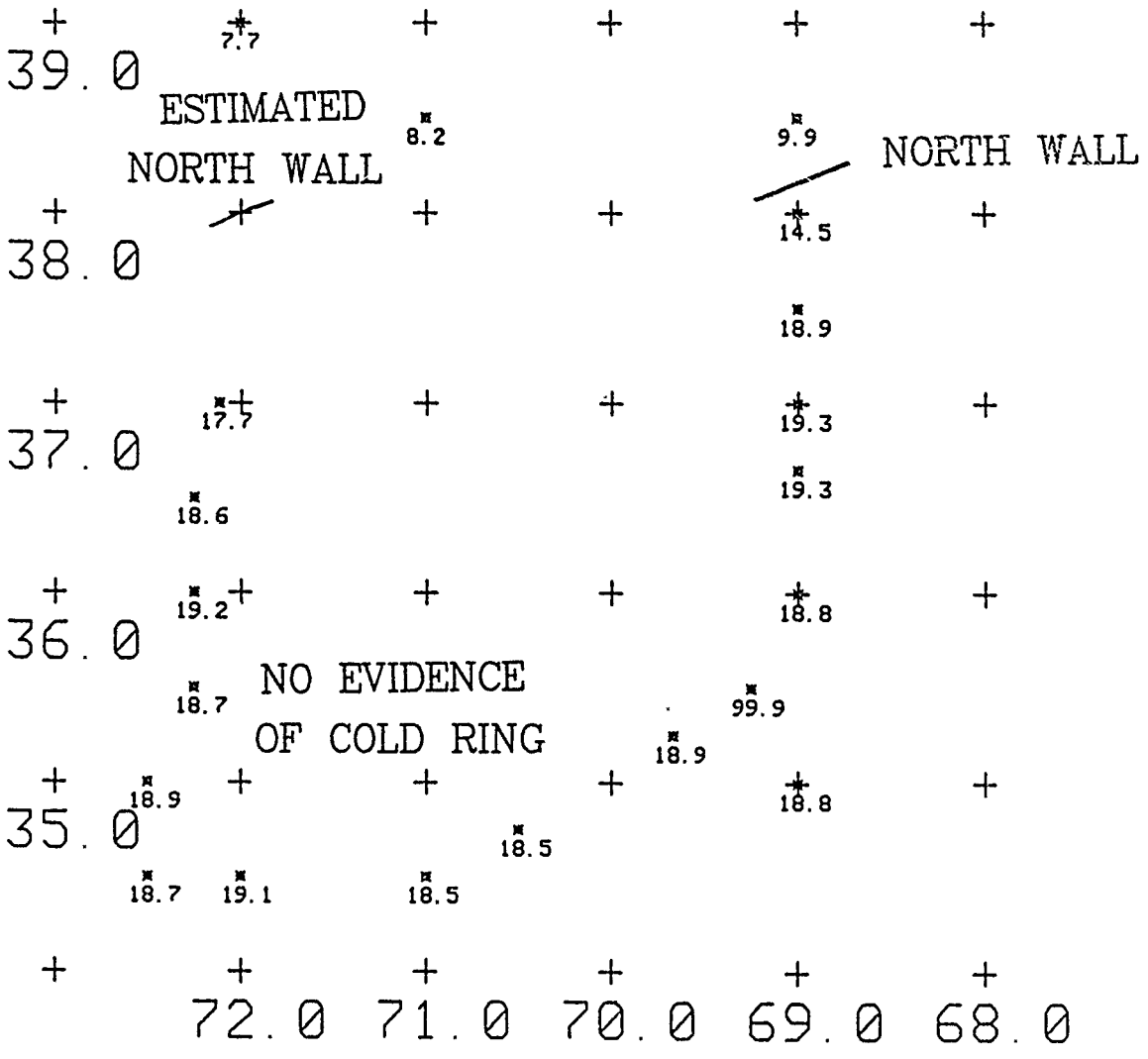

Fig. 69 — Gulf Stream forecast for 2–6 June 1986

Central forecast C3

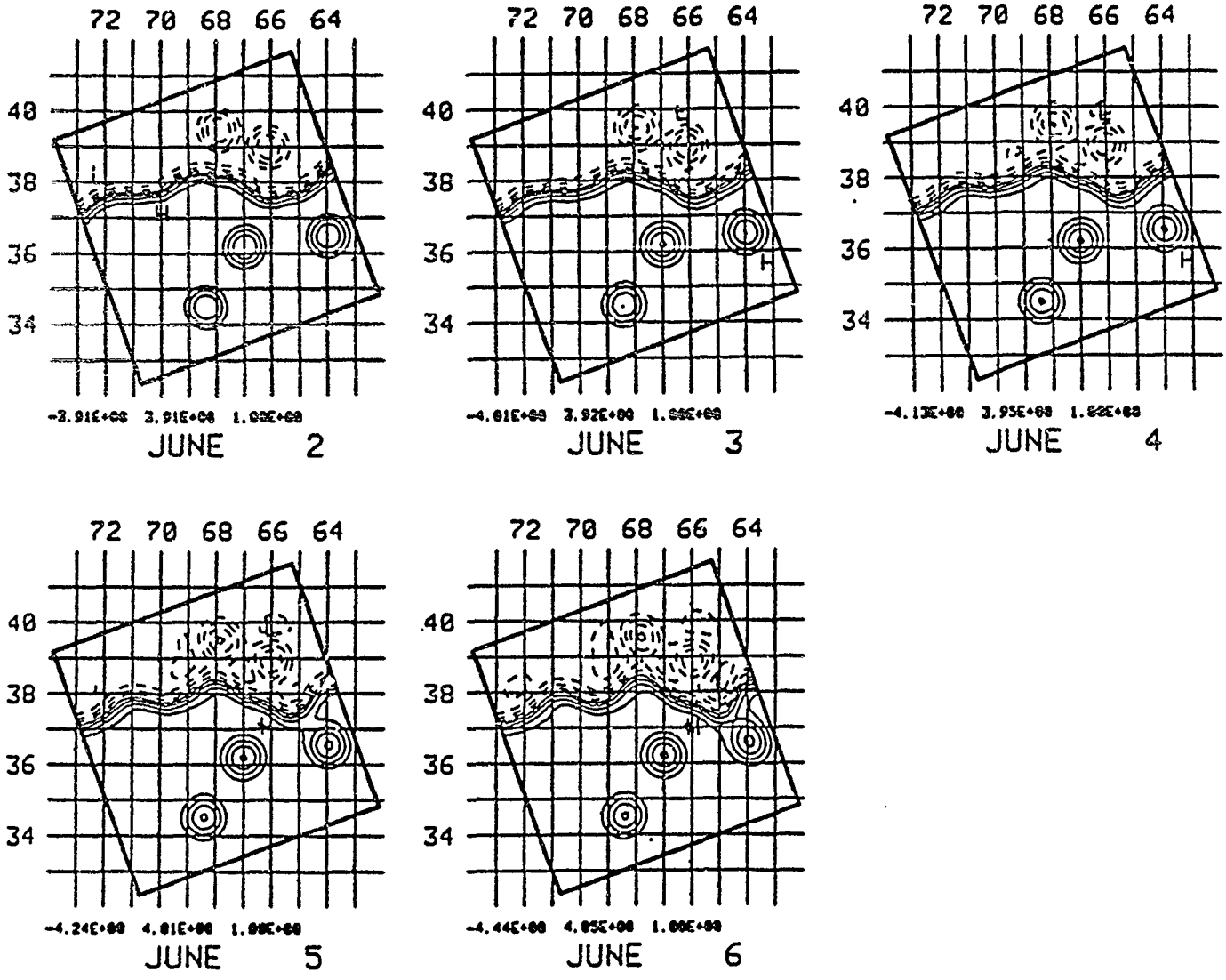

interaction between the two warm rings and a ring-stream interaction with WE 1. A small wavelike meander develops from 68.0W-72.0W, possibly coupled to the interaction. The trough at 66.0W deepens slightly and propagates downstream at approximately 25 km/day. On June 5 the trough begins to interact with CE E, becoming stronger on June 6. Only limited in situ data was available for verification. The north wall was located at 37.90N 70.40W and 38.15N 68.85W by AXBT data. A horizontal analysis of the fields on June 6 is shown in Figures 70 and 71. The model calculation agrees to within 10km in both places. In general, the model forecast places the stream to the north of the IR images by as much as 60km. A comparision of north wall positions from the Harvard forecast, the Norfolk operational nowcast and the *in situ* AXBT data is show in Figure 72.

ACKNOWLEDGEMENTS

We acknowledge the help of Dr. Arthur Mariano in providing selected relevant historical data for the region, and of Mr. Ralph Milliff for technical and logistical support. We thank Ms. Marsha Glass Cormier for essential arrangements. This research was supported by the Office of Naval Research under contract no. N00014-84-C-0461 for Ocean Dynamics and the report preparation was partially supported by NORDA's Naval Oceanography Program, contract no. N00014-86-K-6002.

Fig. 70 — Horizontal analysis on 6 June 1986

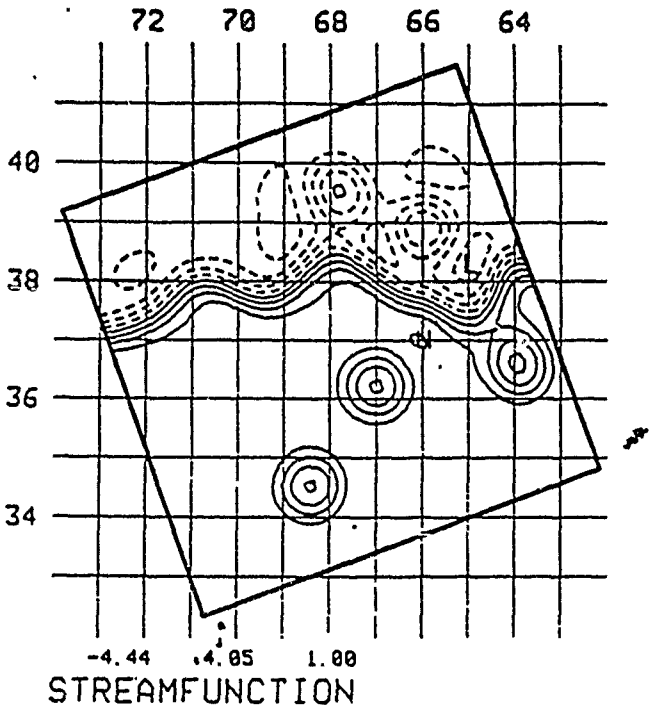

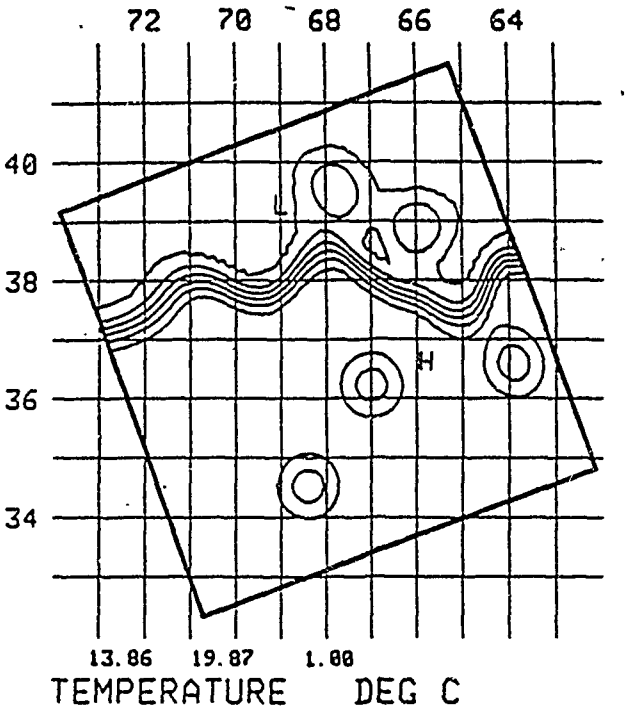

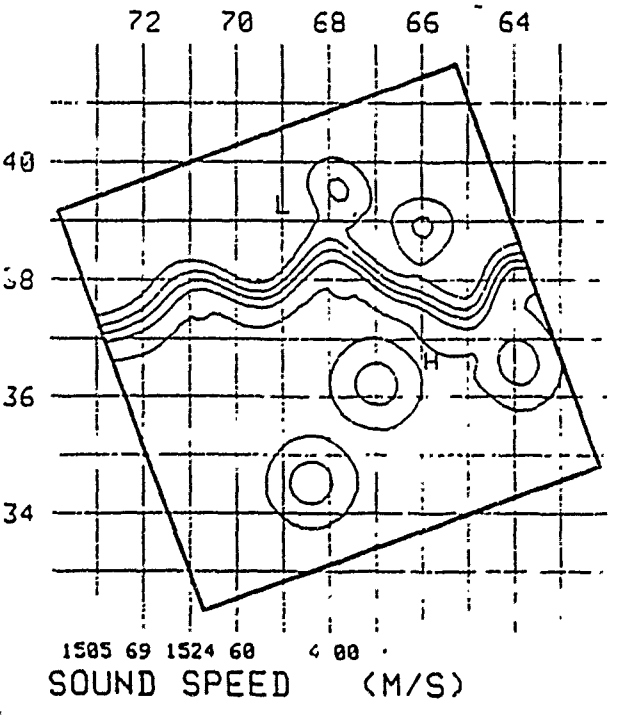

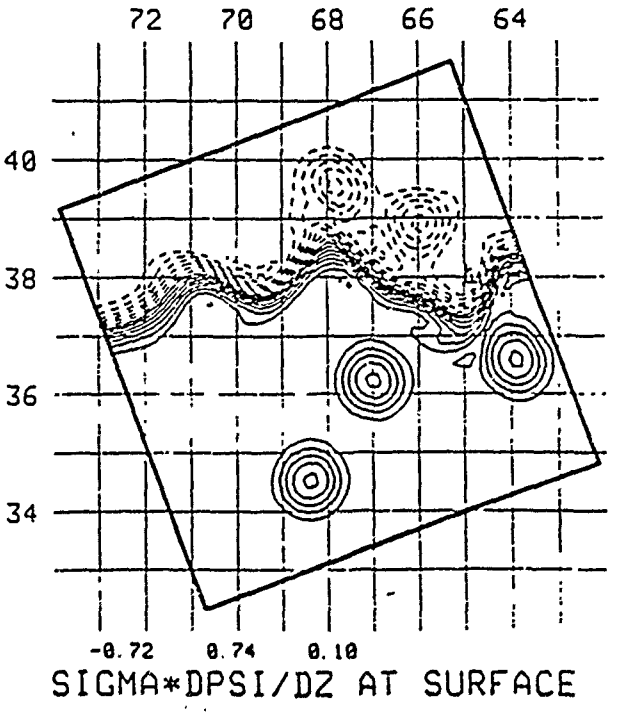

Fig. 71 — Composite analysis on 5 June 1986

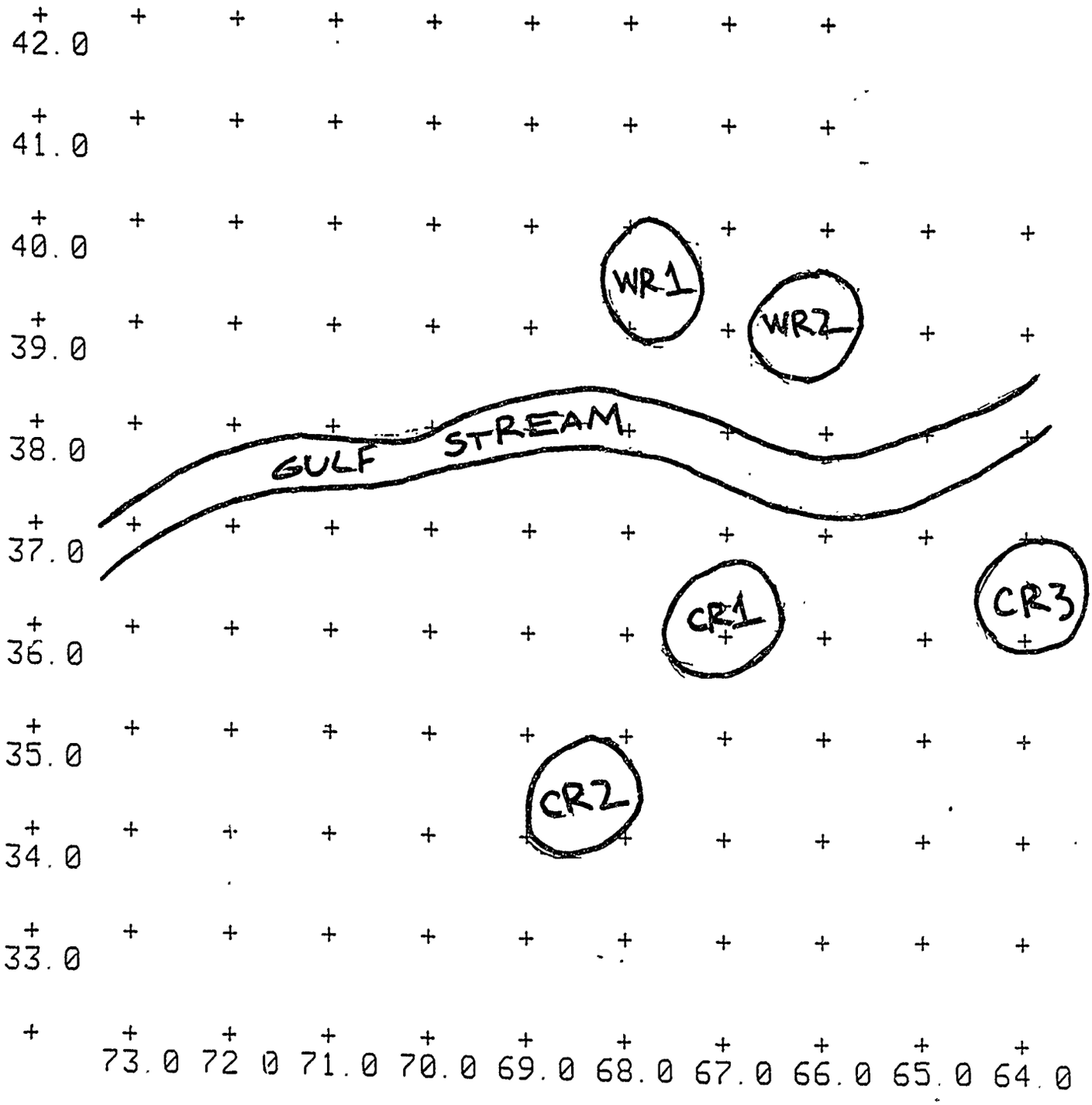

Fig. 72 — North Wall position comparison 6 June 1986

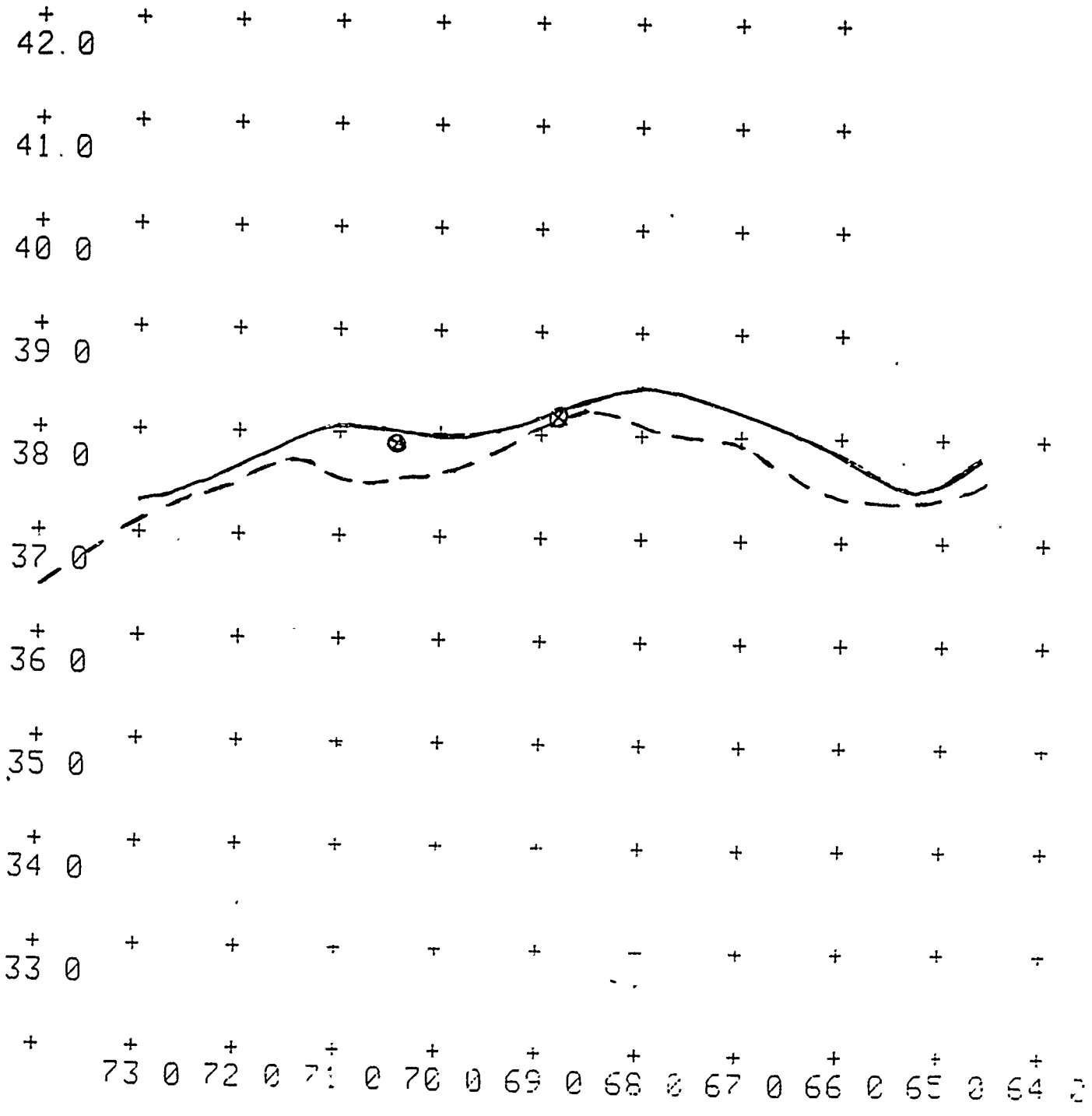

Harvard model forecast north wall

Norfolk satellite data north wall

North wall position from XBT data

Dynamics of Atmospheres and Oceans, 13 (1989) 301–316
Elsevier Science Publishers B.V., Amsterdam – Printed in The Netherlands

DATA ASSIMILATION AND DYNAMICAL INTERPOLATION IN GULFCAST EXPERIMENTS

ALLAN R. ROBINSON, MICHAEL A. SPALL, LEONARD J. WALSTAD and WAYNE G. LESLIE

Division of Applied Sciences, Harvard University, Cambridge, MA 01238 (U.S.A.)

(Received April 25, 1988; revised September 20, 1988; accepted October 4, 1988)

ABSTRACT

Robinson, A.R., Spall, M.A., Walstad, L.J. and Leslie, W.G., 1989. Data assimilation and dynamical interpolation in GULFCAST experiments. Dyn. Atmos. Oceans, 13: 301–316.

GULFCAST is a forecast system for the Gulf Stream meander and ring region consisting of a dynamical open-ocean model and an observational network comprised of remotely sensed sea-surface temperatures (and recently, sea-surface height) and critically located air-dropped expendable bathythermographs (AXBTs). We present here the case study of a real-time forecast system carried out for 2 weeks in the Spring of 1986 during the development of GULFCAST methodology. The AXBT data from successive flights were assimilated and a frontal location was 'nowcast' and forecast within the error bounds of navigation, AXBT sampling and model resolution during a multiple ring–stream interaction event.

INTRODUCTION

The Gulf Stream meander and ring (GSMR) region lies to the east of Cape Hatteras and to the south of the Grand Banks, extending to about 50°W longitude. Eastward the flow weakens, branches and breaks off filaments as it develops into the Gulf Stream extension and North Atlantic current systems. Within the GSMR region, the Gulf Stream is a powerful and well-formed free jet, which, with little change of axial profile, snakes along a well defined but contorted path that varies energetically with time. Meanders and waves grow and propagate, loops intensify and snap off into cold and warm core rings. Typically, the region is populated by several rings; warm cores trapped in the alley between the stream and the continental rise to the north and cold cores roaming more freely south of the stream and into the Sargasso Sea. Ring–stream and ring–ring interactions occur, reabsorption by coalescence is often the fate of a ring and multiple ring–stream interactions occur. The energetic GSMR region is interesting

0377-0265/89/$03.50

dynamically, important practically and accessible to remote sensing. The phenomena described above are, within the ocean, the counterpart of atmospheric weather phenomena. We have established a system for forecasting the internal weather of the sea in the GSMR region called GULFCAST.

Data assimilation is recognized by ocean scientists to be a general methodology of great potential for dynamical studies and essential for efficient and feasible ocean prediction (Mooers et al., 1987). Four-dimensional data assimilation in meteorology and numerical weather forecasting, and the theoretical basis of optimal field estimation procedures (Ghil, 1988) provide guidance to ocean dynamicists as they develop their dedicated methods. Data assimilation is essentially a systematic field estimation procedure where observational estimates are melded with dynamical model estimates via some weighting procedure. To us it seemed natural, initially, to adopt an engineering approach in order to bring to bear oceanographic experience to the complex real fields of interest, in the context of a new situation involving dynamical model initializations with real but limited data. The procedure involves subjective weights in the melding of dynamical model output and non-uniform surface and subsurface temperature observations in the estimation of the temperature fronts associated with the jet's axis and the ring currents. These frontal locations are then used to reinitialize the dynamical model via a 'feature-model' method, and thus to enable the advance of the forecast in time.

The GULFCAST system was set up (Robinson et al., 1987) during the period November 1985 to November 1986, and since that time has been providing weekly research forecasts on a regular basis (Glenn et al., 1987). As initially set up the system's components were a dynamical model consisting of the Harvard quasi-geostrophic open-ocean model, and an observational network consisting of satellite-observed infra-red (IR) sea-surface temperatures (SST) together with occasional dedicated and designed air-dropped expendable bathythermographs (AXBT) flights. During the period November 1985 to June 1986 we developed methodology, calibrated the model and established the validity of GULFCAST concepts through a series of five real-time forecast experiments in subregions of the GSMR region. This paper presents a case study of the most extensive of these experiments carried out from 19 May to 6 June 1986.

Considering the GSMR phenomena introduced in the first paragraph, it is reasonable to expect forecast verification, both qualitatively and quantitatively, to depend upon phenomenological regimes. A 'propagation regime' in which pre-existing features develop and translate is dynamically different and simpler than an 'interaction regime' (Robinson, 1987, Chapter 2) in which an energetic synoptical-dynamical event is taking place. We use the term synoptical–dynamical event for interactions between rings and/or

rings and the stream, which can drastically alter frontal locations rapidly. These include ring births and reabsorptions by the stream, ring mergers, etc. In both regimes, but especially the latter, it is data assimilation that can control phase error and yield frontal forecasts of the practical accuracy $O(10$ km) useful for operational forecasting. The experiments of the set-up period (Robinson et al., 1987) indicated the capability of the GULFCAST system to achieve this accuracy with adequate AXBT data. The case illustrated here involves a multiple ring–stream interaction.

2. CONTEXT AND METHODOLOGY

Because the phenomena of interest exist over large spatial scales in the Gulf Stream meander and ring region, it is not economically feasible to obtain the data necessary for the traditional approach of objectively mapping the fields from a grid of observations, as we have done previously for model initializations in the POLYMODE (Carter and Robinson, 1987) and California Current regions (Robinson et al., 1986). The dynamical model is baroclinic and quasi-geostrophic with open boundary conditions (Robinson and Walstad, 1987). However, the fact that the Gulf Stream region contains individual, identifiable energetic features may be exploited to initialize the model with only limited data sets, i.e., segments of the fronts associated with the stream and rings. The method, called 'feature-model initialization', is presented in Robinson et al. (1988), to which the reader is referred for details. When viewed in the stream coordinates, the Gulf Stream always looks more or less the same all along its meandering path. The Gulf Stream and its associated rings have characteristic properties regarding their shape, size, structure and strength. Feature models, analytic representations of these structures with tuning parameters, have been designed based on historical data. The parameters for the Gulf Stream are maximum velocity at the surface, base of the thermocline, and bottom, *e*-folding width of the stream, and depth of the base of the thermocline. The ring parameters are maximum velocity, maximum radius, radius of maximum velocity, maximum depth and vertical shear. The feature-model initialization undergoes a three-phase evolution during model integration. These phases are dynamical adjustment of the features, dynamical interpolation between the features, and dynamical evolution of the fields. The analytic features first make slight dynamical adjustments during the model integration but with the structures remaining largely unchanged. The motionless water between the features spins up through the process of dynamical interpolation and at the same time the vorticity interactions among the features begin. Near-field circulations are established after about a day of integration. Dynamical evolution then occurs as the features interact and evolve in accordance with the

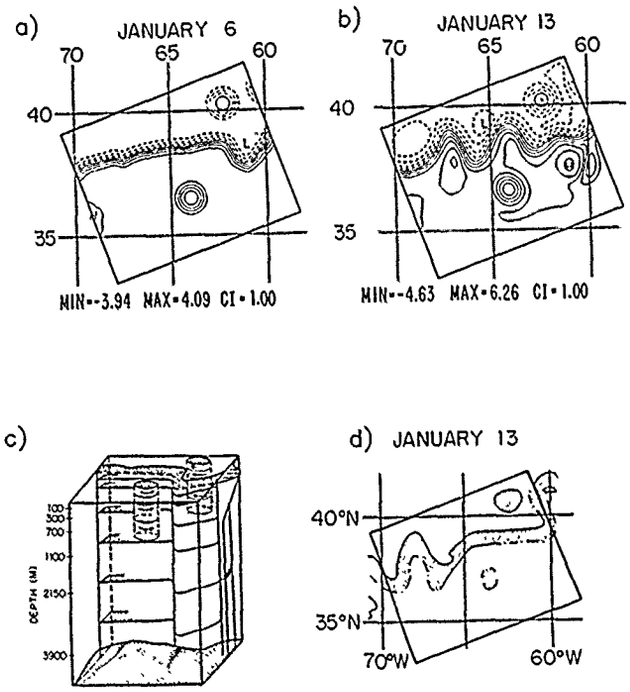

Fig. 1. (a) 100-m streamfunction field for quasi-geostrophic (QG) model initialization on January 6, 1986. (b) 100-m streamfunction forecasted for January 13, 1986. (c) Three-dimensional feature-model initialization. (d) January 13, 1986 Gulf Stream north wall and ring position from satellite IR.

dynamical model. The feature models represent initialization fields only, subsequent fields of course have the structure as determined by the quasi-geostrophic model and its computational grid.

An initial condition with the feature models hung beneath the IR images for January 6, 1986 is shown in Fig. 1a and c. The stream is flat over most of the region with a slight dip near 62° W. Figure 1 shows (b) the actual real-time 7-day model forecast with persisted boundary conditions, and (d) satellite IR for that day. A dramatic development of a large double meander has occurred and was predicted by the dynamical model 1 week prior to the actual event. Further experiments show that using the observed boundary conditions for the feature inflow/outflow gives even closer agreement with the IR. This real-time forecast provided a good example of the dynamical model's ability to deal with energetic and non-obvious developments. The capability of the model to make realistic rings is treated in detail in Robinson et al. (1988) and a real-time forecast of an unusual large ring is illustrated by Glenn et al. (1987).

Satellite sea-surface temperature images (IR) were available in each of the five forecast experiments to test and develop real-time forecasting capabilities in the GSMR region and AXBTs were available for four out of the five experiments. These two data sources complement each other well; the satellite IR gives surface thermal front information with large spatial coverage and the AXBTs give temperature profiles down to about 400 m at specific points. The IR is a very good tool to define large-scale structures of the Gulf Stream and rings from the strong thermal signature at the surface. However, satellite IR gives no data over clouded regions and may give misleading information in regions of surface warming or cooling. Cold rings often lose their surface signature because of atmospheric forcing, but still have very strong subsurface fields. Large patches of warm water are seen on the slope side of the stream, which hint at the presence of a warm ring but have no deep structure at all. Because the AXBTs can locate the subsurface thermal signature of the Gulf Stream and warm and cold rings, they have a dual role in model initialization and verification. They may be used to determine if questionable surface features seen in the IR have any deep structure and to locate very accurately the position and strength of critical features already known to exist, and to search for features, such as cold rings, that may have covered over and lost their surface signal. A great deal of information can be obtained from a limited number of AXBTs by using satellite IR and dynamical model calculations to plan efficient and effective flight tracks. Direct aerial mapping with a regular grid would require one or two orders of magnitude larger number of probes.

The GULFCAST system, consisting of the model together with IR and occasional dedicated AXBT observations, was tested under a wide range of circumstances. The phenomena that were predicted by the forecasting procedure included Gulf Stream meander growth and propagation, straightening out a previously meandering stream, ring formations, and ring–stream interactions and movements (Robinson et al., 1987). The model domains ranged from 720×720 km^2 to 1200×900 km^2 and were located from the inlet region near 70° W out to 58° W. A total of 23 model forecasts were conducted; ranging from 4 days to 1 week in duration. A total of 12 AXBT flights were flown during these exercises, of which 11 gave information useful for model verification. Fifteen north-wall positions were determined from the AXBT data sets. The difference between the predicted and measured location of the north wall was found to be < 10 km in 10 of the 15 comparisons. Three of the remaining five comparisons showed 10-km differences. The remaining two locations were off by 20 and 60 km; the latter being influenced by a poor inflow boundary condition. The tendencies observed in the IR images were reproduced in all regions where there was no cloud cover; very good agreement was seen three out of four times. Errors

associated with 'north wall' frontal location are due to possible navigation error 0 (1 km), AXBT interpretation (sampling interval about 20 km), or definition of the north wall in model forecasts (model grid usually 15 km). Satellite IR is not used for precise location of the north wall because atmospheric forcing can shift the surface signature by tens of kilometers, but it is useful to define the larger scale tendencies of the flow.

These experiments contributed to the development of our real-time forecasting methodology for the GSMR region, summarized here for the case of starting a new forecast. Ambiguities in the initial condition are removed through a combined analysis of dynamical model calculations, repeated AXBT flights and satellite IR. First, IR, AXBT data and previous model forecasts are used to define and position the feature models for initialization. This forecast is run in both a large domain, $O(2000 \times 1000\ \text{km}^2)$, on a supercomputer, and in a subregion, $O(1000 \times 1000\ \text{km}^2)$ or less, on a local microcomputer. The subregion run serves as a central forecast for a matrix of sensitivity runs in which the initial condition is varied to determine which features are most critical to the evolution of the flow field. The AXBT flight tracks are then designed to locate those features, taking into account trade-offs between horizontal resolution, spatial coverage, feature location and vulnerability to equipment failure. The dynamical model is reinitialized with a composite analysis of (1) AXBT data, (2) model runs and (3) satellite data. Boundary conditions for the real-time forecast are provided either by (i) estimating new feature positions using forward time extrapolation of meanders and rings by a simple propagation speed or by (ii) interpolating information from the large domain supercomputer run. With the uncertainties of the region now lessened and the features better defined, the model forecasts the flow fields ahead in time. New AXBT flights should be executed to locate critical flow indices (i.e., crests, troughs, ring–stream interactions) for both model verification and reinitialization of the next set of real-time forecasts.

The dynamical model has several uses in this scheme. It is first used to determine the most critical features that must be located with AXBT flights via the sensitivity runs. Secondly, the supercomputer run is used to get boundary conditions for subregion forecasts from the approximate forecast in the larger domain. Most importantly the model dynamically interpolates the data both horizontally between the features and vertically beneath the features as well as projecting its evolution ahead in time. Dynamical interpolation produces smooth three-dimensional dynamically consistent fields of the quantities of interest ('nowcast' and forecasts). Benchmark hindcasting (Robinson et al., 1988) indicates that the dynamical model can evolve fields forward in time for 2–4 weeks, passing through more than one synoptical–dynamical event.

3. THE GULFCAST EXPERIMENT 19 MAY TO 6 JUNE 1986

This experiment is presented in some detail, because, as the major effort during the developmental phase of GULFCASTing, it was of 3 weeks duration, had adequate associated AXBT resources and effectively utilized all elements of the methodology described above. An attempt was made to achieve an accurate forecast of the location of the Gulf Stream front, i.e., not only to represent correctly events and features, but to control phase error via the data assimilation approach. This was accomplished successfully for a section of the stream and in an interesting situation in which a multiple ring–stream interaction was occurring.

The experiment was a start-up situation that was initiated via the NOAA IR SST for 19 May, which is shown in Fig. 2a. Additional IR data were utilized for 28 May (Fig. 2b), but not after that time as the later stages of this GULFCAST were carried out at sea and the IR data were not available

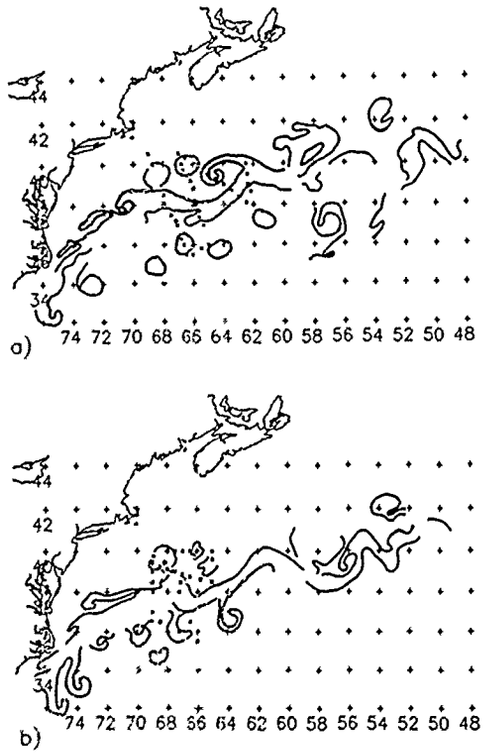

Fig. 2. (a) Gulf Stream fronts and ring positions for May 19, 1986 and AXBT positions for May 23, 1986. (b) Gulf Stream fronts and ring positions for May 28, 1986 and AXBT positions for May 29, 1986. Front and ring positions are determined from satellite IR.

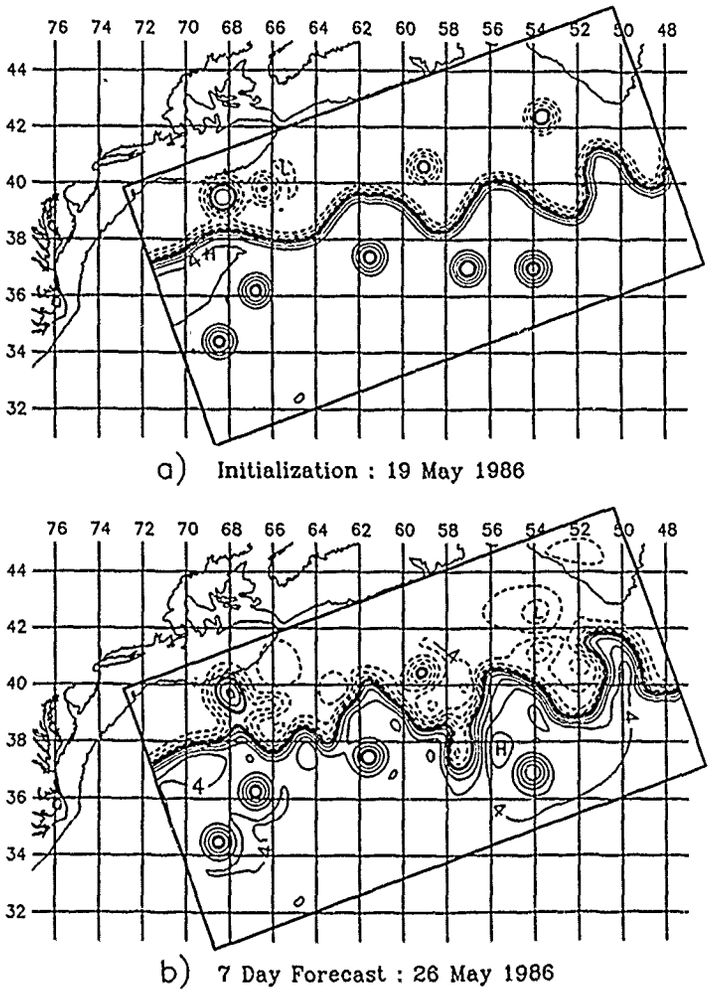

Fig. 3. (a) 100-m streamfunction field for supercomputer forecast. (b) 100-m streamfunction field after a 7-day forecast.

in real time. The starting GULFCAST region was large, extending from 48 to 72° W longitude (Fig. 3), but was reduced in size to 64–72° W for the final ac urate forecast attempt for 6 June. This latter, approximately 800-km^2 region, was also used for extensive sensitivity forecast experiments (see Fig. 5) and sampled by AXBTs. Dedicated AXBT flights were carried out on 23 and 29 May (Fig. 2) and four additional stream crossings were obtained by AXBTs, for updating and verification, two each on 2 and 6 June.

The jet and ring frontal information contained in the two IR maps of Fig. 2 is fortuitously good. Solid lines indicate observed surface frontal features,

and dotted lines indicate information from previous data for regions that were cloud covered or featureless (according to standard NOAA convention). On 19 May, to the east of 72° W longitude, there are four meander crests, six cold eddies, and five warm eddies indicated. As usual we are concerned with whether or not the surface eddies correspond to thermocline rings, the location of thermocline fronts relative to surface indicators and the usefulness of past information and subjective interpretations. These questions are especially demanding at start-up time. The new information revealed by the IR of 28 May are: the deepening of the meander trough at 67°, eastward propagation of some long-wave feature between 65° and 55°, the development of a sharp feature at 53°, and definite surface signals of the two cold eddies centered on 64° and 67° W longitude.

The large domain forecast carried out on the CRAY XMP at NRL was initialized with six levels and 15 km resolution via the interpretation of the 19 May data shown in Fig. 3a. There are four warm and five cold rings present. The cold ring at 64° W should of course have been included, but the omission of the warm eddy at 65° will be shown to be correct. The forecast 1 week ahead shows the evolution of features as displayed on Fig. 3b. The two warm rings in the west and the stream are mutually interacting. The smaller ring is being absorbed by the larger ring, which is in contact with the stream. The stream is distorting into a pattern that includes a deepening trough at 66° W and also one at 63° (in the vicinity of the missing ring). Further downstream, meanders steepen and propagate eastward and the cold ring at 57° has attached.

The interaction of the stream and the two warm rings can be identified as the critical synoptical–dynamical event controlling the frontal location and evolution in the western half of the domain, and a careful definition of the interaction was attempted. The first AXBT flight was designed on the basis of the first forecast, as seen on the nominal track of Fig. 4a, to locate the two warm rings relative to the stream, to investigate the possible existence of a third warm ring, to locate similarly one cold ring, and to position and determine the shape of the current by four crossings. The subsurface fields of velocity and temperature predicted by the model along the first section of the track are shown on Fig. 4b. Realistic fields have filled in by dynamical interpolation and evolved by 23 May from the feature-model initialization of 19 May. Typical signatures of features are shown on Fig. 4c from sample AXBTs; all profiles obtained for this experiment are reported in Robinson et al. (1987).

The AXBT flight, as actually carried out on 23 May, consisted of 34 drops with only two failures in the pattern shown on Fig. 2a. All the objectives of the flight were successfully accomplished except that technical difficulties occurred in the region between 38.5° N 68.0° W and 40.0° N 68.7° W, thus

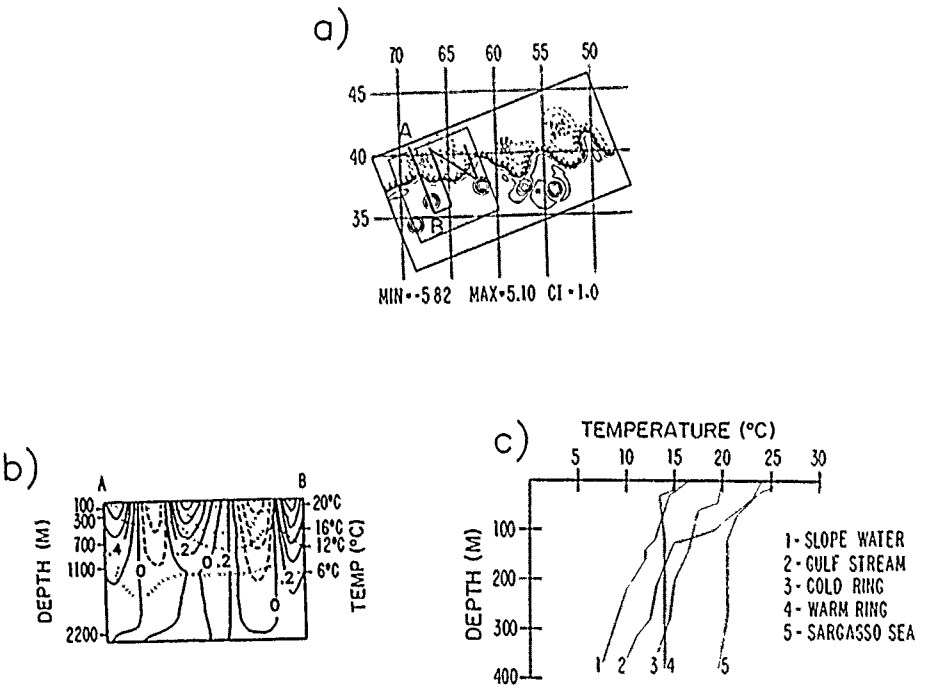

Fig. 4. (a) 100-m streamfunction field from supercomputer forecast for May 23, 1986; domain for subregion forecasts (light line); AXBT flight track (heavy line). (b) velocity and temperature section along line A–B of (a). Velocity contour interval is 0.2 m s^{-1}; temperature contour interval is 4° C. (c) Sample AXBT temperature profiles.

failing to quantify accurately the major stream–ring relationship or interaction in the most critical region. At the time of this flight and subsequently, the sensitivity experiments (Fig. 5) to be discussed below were being performed and analyzed. On the basis of those results, together with the new IR SST (Fig. 2b) and the results of the first flight, the second flight was designed and flown (Fig. 2b) with 27 drops and only one failure. The main objectives were to locate the positions of the two warm rings relative to each other and the stream and, additionally, to locate a nearby cold ring that could possibly enter into a mutual interaction. These were successfully accomplished. The information concerning features and frontal locations from all the flights is presented in Table I and on Fig. 6, which also summarizes the ring signals indicated by the IR.

The situation with respect to the cold rings in the region was ambiguous on 19 May, but was clarified by strong signals for all three rings on the 28 May. Additionally, ring C_1 was located on each of the first two AXBT flights. The two stream crossings indicated in Table I on June 2 were accomplished by a flight pattern down 69° W and up 72° W, which were

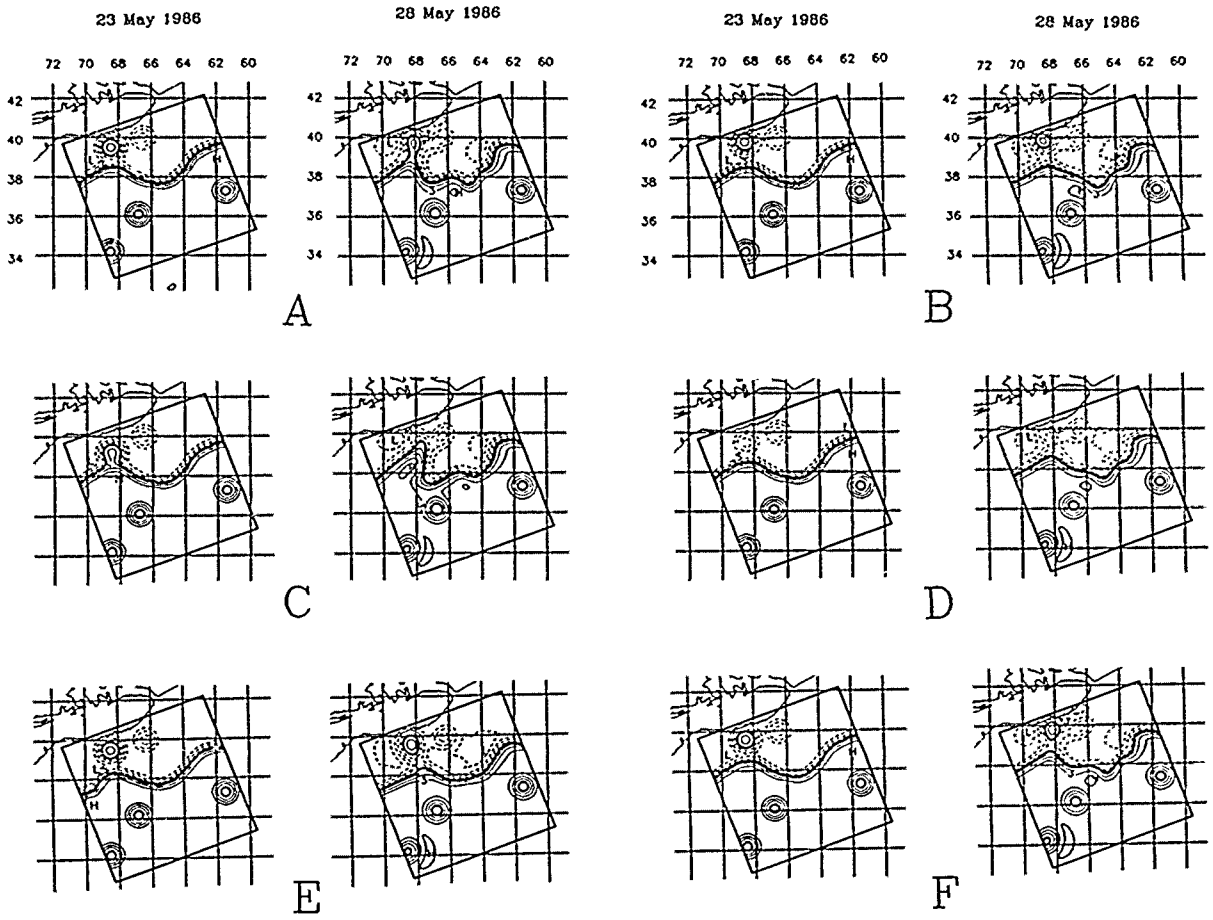

Fig. 5. Initialization and 7-day forecast 100-m streamfunction fields for six sensitivity forecasts performed in the subregion shown in Fig. 4a.

TABLE I

Gulf Stream Frontal Locations (North Wall) by AXBTs

Date	23-5-86	23-5	23-5	23-5	29-5	29-5
Latitude (°N)	38.8	39.7	> 37.4, < 38.7	> 38.5	38.2	38.2
Longitude (°W)	63.8	62.5	66.0	68.0	69.0	67.2

Date	29-5	2-6	2-6	6-6	6-6
Latitude (°N)	< 38.5	38.5	> 37.0, < 39.0	37.9	38.2
Longitude (°W)	65.0	69.0	72.0	70.4	68.9

The notation $\lesssim$ indicates a bound, e.g., on 23-5 at 68.0° W the Gulf Stream was determined to be located to the north of 38.5° N.

connected by a track along 34.5° N. This flight was seeking evidence of another cold ring, however none were found. The warm-ring picture was quite complicated and the interpretation presented schematically in Fig. 6 was evolved with some difficulty in real time, and involved interpretative input from the dynamical model runs. We believe the model initialization of 2 June for the final forecast to have been unambiguous and reasonably

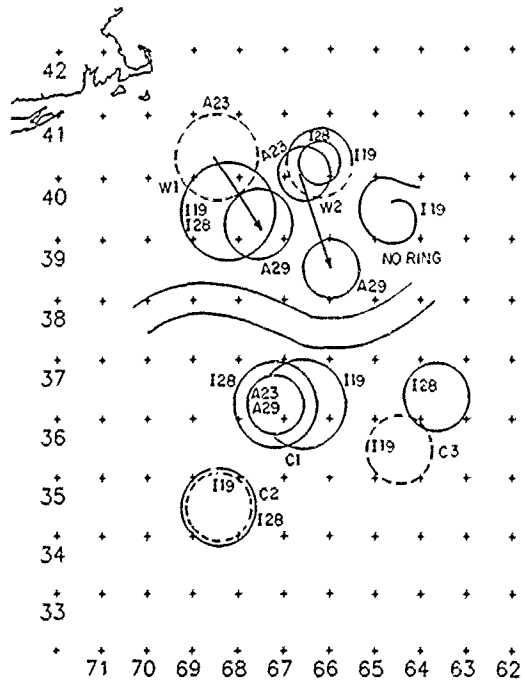

Fig. 6. Schematic interpretation of ring and stream positions as determined from satellite IR, AXBTs and dynamical forecasts.

accurate. The flight of 23 June gave some indication of a ring centered to the north of the surface IR signal of 19 June at 68.5° W, definitely located a ring in the vicinity of the partial IR surface signal near 66.5° W and showed that the feature at 65.0° W, which had a definite surface signal in AXBTs, did not extend to thermocline depth. Both W_1 and W_2 were well located on the flight of 29 June. W_2 moved to the south by southeast by just under 200 km in 6 days, indicating a speed of ~ 30 km day^{-1} (~ 35 cm s^{-1}). The data for W_1 are not as good, but it appeared to move to the eastsoutheast at perhaps a comparable but somewhat slower speed. Both speeds and directions are unusual and indicate an interaction event. The stream crossings in Table I are consistent with the interaction event and are useful in the interpretation of the sensitivity forecast and in the context of the IR frontal segment estimates.

The matrix of sensitivity forecasts was carried out for a set of model initializations designed on the basis of all information available following the immediate analysis of the May 23 AXBT data. The overall objectives were: to determine the range of stream–W_1–W_2 (hereafter referred to as S–W_1–W_2) interactions consistent with this information base, to anticipate the magnitude of frontal shifts that could be induced by the interaction in the next few days, and to assess possible critical data requirements for the next AXBT flight. The major parameter studied was the exact location of W_1 relative to the stream but the size of W_1 and the stream shape were also

TABLE II

Sensitivity forecasts for stream–W_1–W_2 interaction

Run	Initial condition	Ring evolution	Stream evolution
A	Central forecast.	$W_1 \rightarrow$ NE	Trough develops at 67° W
	W_1 partially attached	$W_2 \rightarrow$ S	crest at 68.5° W
		W_1 coalescing	
		W_1–W_2 begin merger	
B	Weak interaction.	W_1 stationary	straightens from 68 to 65° W
	W_1 separated to N	W_2 slightly → S	
C	Strong interaction.	W_1 rapidly → SE	sharp meander
	W_1 overlapping Stream	$W_1 \rightarrow$ S	N–S front along 68° W
		W_1 fully absorbed	deep trough at 67° W
		W_2 coalescing	
D	Weak interaction.	$W_1 \rightarrow$ E	stationary
	Small W_1, grazing	W_2 stationary	
E	Weak interaction.	W_1 slightly → E	straightens from 68 to 70° W
	Stream to S from 68 to 70° W	W_2 slightly → S	
F	Intermediate interaction.	$W_1 \rightarrow$ NE	small amplitude
	W_1 grazing	$W_2 \rightarrow$ S	waves from 68.5 to 65° W

varied. The runs are summarized in Table II and the initial (23 May) and final (28 May) states are shown in Fig. 5.

Examination of the results indicate that interaction of W_1 and the stream leads to an eastward advection of W_1, which can also have either a northward or a southward component, depending upon where the advection occurs or 'grabs hold' relative to the meander crest initially at 68.5° W. Strong interaction leads to complete coalescence or absorption of W_1 by the stream. Eastward movement of W_1 favors interaction with W_2, and since W_1 is considerably stronger than W_2, the initial stage is a southward advection of W_2 by W_1. The ultimate development of a strong interaction is not illustrated here but should be dependent upon phasing of the three-way $S-W_1-W_2$ interaction, i.e., either merger of W_1 and W_2 could occur (case D) followed by coalescence of the larger ring, or W_2 could coalesce with the stream following absorption of W_1 (case C). The flight pattern of Fig. 2b pinned down the ring–stream system on 29 May. The movements to the southeast schematized on Fig. 6 indicate an interaction intermediate between runs A and C, i.e., strong enough for southeast advection of W_1 but not for absorption.

The final forecast in this series was carried out from 2 to 4 June 1986 in a domain shifted slightly to the west, as shown in Fig. 7. The initialization (Fig. 7a) was the best estimate of the fields possible obtained by synthesizing the information available from the IR of the 28 May, and the AXBTs from 29 May and dynamical model results. The initialization was prepared via dynamical adjustment and interpolation from 29 May, which matched the

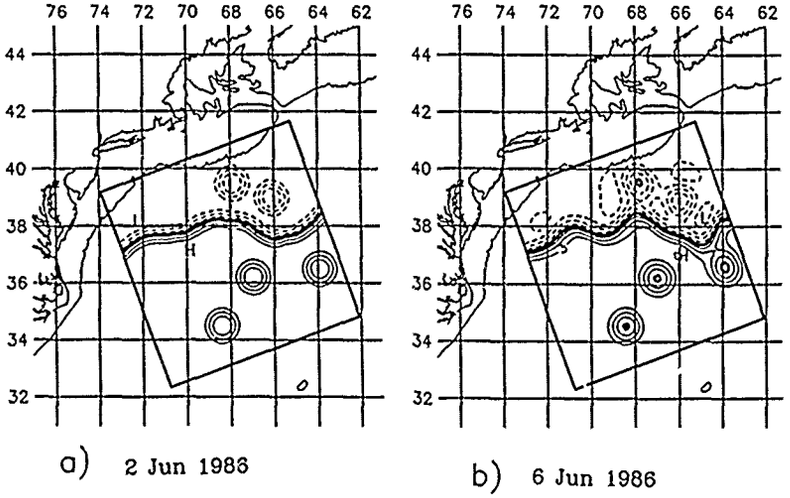

Fig. 7. (a) 100-m streamfunction field for initialization of final forecast beginning June 2, 1986. (b) 100-m streamfunction field forecasted for June 6, 1986.

stream crossings of 2 June and included cold ring C_3 first observed in the IR of 28 May. The forecast (Fig. 7b) is seen to involve a three-way type of grazing 'advective' interaction among $S-W_1-W_2-S$. This is accompanied by a deep looping distortion of the stream to the south (trough at 65° W), which initiates an additional interaction with C_3. There is also growth of a 300-km wave in the west of the domain. The distortion of the stream associated with the $S-W_1-W_2-S-C_3$ interaction event has shifted the Gulf Stream frontal position by almost 100 km in 4 day around 65° W and shifts of 30–50 km occur along the stream. These magnitudes are of considerable practical consequence. The two stream frontal locations available for verification of 6 June (Table I) agree with the forecast locations within < 10 km, which is the limit of resolution for the location of the north wall of the front by interpolation, associated both with the AXBT estimate (sampling grid (~ 25 km)) and the model estimate (horizontal grid, 15 km).

4. CONCLUSIONS

We exercised the GULFCAST system of dynamical model, frontal segments in sea-surface temperature obtained from satellite IR, and dedicated, designed AXBT flights in the Gulf Stream Meander and Ring region from start-up on the 19 May until 6 June 1986. We carried out a series of 'nowcasts' and forecasts which, via data assimilation, improved to the point where verification flights agreed with a few days prediction within error bounds of resolution resulting from navigation, AXBT sampling and model resolution. This experiment together with similar results from four related experiments in the period November 1985 to June 1986 indicated (i) the applicability of the Harvard open-ocean quasi-geostrophic model to Gulf Stream and ring system forecasts, and (ii) the ability of the system to achieve accuracies that are useful practically when adequate in situ data are available for assimilation. This is valid for both periods of meander propagation and growth and for energetic synoptical–dynamical events. The data requirements are, of course, less in the former case.

The success of these experiments led to the establishment of an ongoing and continuous GULFCAST research–operational forecast system at Harvard in November of 1986. Weekly forecasts are carried out for 1 week ahead. The continued ability of the GULFCAST system to predict synoptical–dynamical events is demonstrated. GEOSAT altimetric data have been added to the observational network, and a surface boundary layer model is being attached to the quasi-geostrophic model (Walstad, 1987) to allow more accurate assimilation of satellite IR SST. A scheme for the continuous melding of observed frontal segments into ongoing dynamical model runs is

being developed in order to replace the less appropriate reinitializations that are presently used for assimilations.

ACKNOWLEDGMENTS

We acknowledge the help of Dr Arthur J. Mariano in providing selected relevant historical data for use during the May–June experiment at sea, of Mr Ralph Milliff for technical and logistical support, and Ms Marsha Glass Cormier for essential arrangements. This research was supported by the Office of Naval Research under Contract No. N00014-84-C-0461 for Ocean Dynamics and the analysis was partially supported by the Oceanographer of the Navy through NORDA (Contract No. N00014-86-K-6002).

REFERENCES

Carter, E.F. and Robinson, A.R., 1987. Analysis models for the estimation of oceanic fields. J. Atmos. Ocean. Techn., 4 (1): 49–74.

Ghil, M., 1988. Meteorological data assimilation for oceanographers. Dyn. Atmos. Oceans, submitted.

Glenn, S., Robinson, A.R. and Spall, M.A., 1987. Recent results from the Harvard Gulf Stream Forecasting Program. Oceanographic Monthly Summary, vii(4). NOAA, Washington, DC.

Mooers, C.M.K., Robinson, A.R. and Thompson, J.D. (Editors), 1987. Ocean Prediction Workshop 1986: A Status and Prospectus Report on the Scientific Basis and the Navy's Needs. Institute for Naval Oceanography, NSTL, MS., 486 pp.

Robinson, A.R., 1987. Predicting open ocean currents, fronts and eddies. In: J.C.J. Nihoul and B.M. Jamart (Editors), Three Dimensional Ocean Models of Marine and Estuarine Dynamics. Elsevier, Amsterdam, pp. 89–112.

Robinson, A.R. and Walstad, L.J., 1987. The Harvard open ocean model: calibration and application to dynamical process forecasting and data assimilation studies. J. Appl. Numer. Mathm., 3 (1–2): 89–131.

Robinson, A.R., Carton, J.A., Pinardi, N. and Mooers, C.N.K., 1986. Dynamical forecasting and dynamical interpolation: an experiment in the California current. J. Phys. Ocean., 16: 1561–1579.

Robinson, A.R., Spall, M.A., Leslie, W.G., Walstad, L.J. and McGillicuddy, D.J., 1987. Gulfcasting: dynamical forecast experiments for Gulf Stream rings and meanders November 1985–June 1986. Harvard University Reports in Meteorology and Oceanography, No. 22.

Robinson, A.R., Spall, M.A. and Pinardi, N., 1988. Gulf Stream simulations and the dynamics of ring and meander processes. J. Phys. Oceanogr., 18: 1811–1853.

Walstad, L.J., 1987. Modelling and forecasting deep ocean and near surface mesoscale eddies: hindcasting and forecasting with, and coupling a surface boundary layer model to, the Harvard quasi-geostrophic model. Ph.D. Thesis, Harvard University Reports in Meteorology and Oceanography, No. 23.

FORECASTING GULF STREAM MEANDERS AND RINGS

Allan R. Robinson
Scott M. Glenn
Michael A. Spall
Leonard J. Walstad
Geraldine M. Gardner
Wayne G. Leslie

Harvard University
Cambridge, MA

N00014-84-C-0476
N00014-86-K-6002

Reprinted from :

The Oceanography Report
EOS
Volume 70, No. 45
November 7, 1989

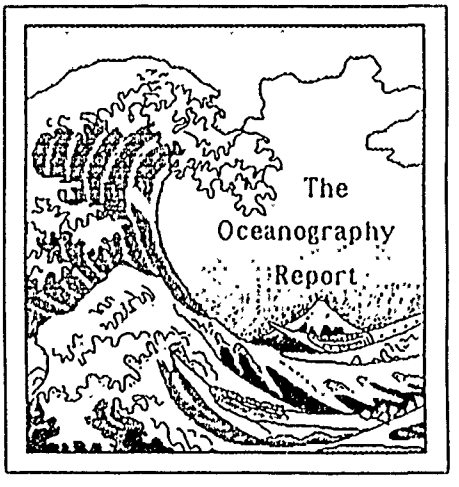

The Oceanography Report: *The focal point for physical, chemical, geological, and biological oceanographers.*

The Oceanography Report

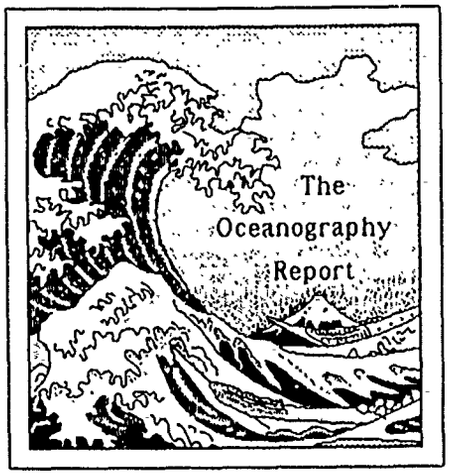

The Oceanography Report: *The focal point for physical, chemical, geological, and biological oceanographers.*

Editor: Robin D. Muench, SAIC, 13400B Northrup Way, Suite 36, Bellevue, WA 98005; GTE Mail: R.MUENCH/OCEAN.

Forecasting Gulf Stream Meanders and Rings

Allan R. Robinson, Scott M. Glenn, Michael A. Spall, Leonard J. Walstad, Geraldine M. Gardner, Wayne G. Leslie

Division of Applied Sciences, Harvard University, Cambridge, Mass.

The deep open ocean exhibits energetic space-time variability phenomena that are the counterpart of atmospheric weather systems. The internal weather of the sea occurs on the scale of the internal deformation radius (depth times the ratio of buoyancy to Coriolis frequencies), with features called "mesoscale" fronts and eddies, although the dynamical analogy is with the atmospheric synoptic scale [*Charney and Flierl*, 1980, Robinson, 1983]. Space scales range from tens to hundreds of kilometers and time scales from days to months, features extend from surface to bottom intensified in the upper ocean main thermocline.

Mesoscale effects include the intermittent energization of regions, the shifting of currents, the location of air-sea interaction events, the transport, entrapment and dispersion of such things as heat, chemicals, nutrients, larvae, and pollutants; and the alteration of sound propagation. Forecasting the internal weather of the sea is important scientifically and practically and is now feasible [*Mooers et al.*, 1987; *Robinson*, 1987] due to rapid, recent advances in physical oceanography and related technologies, especially satellites and computers. We have established a forecast system for the Gulf Stream Meander and Ring (GSM&R) region, called GULFCAST, that provides predictions one week ahead in real time and on an ongoing basis.

The GSM&R region and GULFCAST domain (~1000 × 2000 kms) are shown in Figure 1. Here the Gulf Stream flows as a well-defined free jet with a profile that varies little when viewed in coordinates tied to the instantaneous axis [*Watts*, 1983]. Warm core rings (eddies) trapped between the stream and the continental shelf translate generally southwestward; cold core rings, unconstrained, translate westward [*Richardson*, 1983].

The stream can grow and propagate waves and meanders, straighten out, perform contorted large-amplitude loops, and snap off warm and cold eddies. Rings can propagate in isolation, or interact with the stream and each other, singly or multiply. Grazing interactions with rings can result in rapid stream shifts in any direction, and reabsorption of a ring can distort the jet significantly and nonlocally. Associated with the downstream and swirl flow components of the stream and rings are strong cross-flow horizontal thermal fronts in the thermocline that usually extend to the sea surface (Figure 1D).

The Gulf Stream system is a feature of the general circulation and is energized remotely. Except for near-surface features and surface modification of deeper frontal signals, local atmospheric forcing is usually unimportant. The system evolves via internal dynamical processes, in a manner conceptually similar to atmospheric weather. The oceanic prediction problems differ dynamically for propagation regimes (meander growth and ring translation), and interaction regimes (rapid energetic synoptical-dynamical events, for example, ring birth and reabsorption).

The Forecast Scheme

GULFCAST is an implementation of the Ocean Descriptive Predictive System concept for field estimation initiated in the northwestern Atlantic Ocean [*Robinson and Leslie*, 1985] and developed in the California Current for real-time forecasting [*Rienecker and Mooers*, 1989]. A data assimilation scheme melds estimates from an ongoing observational network with the output of an oceanic dynamical model. Satellite observations provide coverage (mesoscale structure over a large region), and some essential in-situ observations provide critical subsurface information.

The dynamical model extrapolates surface observations downwards throughout the deep ocean, interpolates between sparse observations, and extrapolates forward in time (FORECASTS). The present best estimate from melded observations and model output is called a NOWCAST. The kinematical characteristics of the GSM&R region are used to exploit available surface data and decrease subsurface data requirements via Feature-Model Initialization of the dynamical model [*Robinson et al.*, 1988].

Observations position geographically the thermal fronts of the Gulf Stream and warm and cold rings. Then standard analytical structure models for the subsurface jet and ring profiles are located relative to the fronts. These feature models require only a few indices associated with maximum speeds, vertical shears, widths and radii of the jet and the ring vortices. The dynamical model first dynamically adjusts the features and initiates interactions, then dynamically interpolates the initially empty space between features while interactions develop, and finally the full dynamical system evolves with propagation and interaction events. These three phases overlap with evolution dominant in the thermocline a day or two after initialization.

The present dynamical Harvard open-ocean model that is used for operational forecasting is baroclinic and quasigeostrophic and is robust with respect to real data initializations [*Robinson and Walstad*, 1987]. Boundary conditions require specification of inflow (and vorticity) and outflow. To estimate future boundary conditions, simple propagation models for meanders and rings near boundaries are used, based on climatological or recent speeds. Either interaction events on the boundaries are avoided by domain shifting, or an auxiliary smaller domain forecast centered on the boundary longitude provides the larger region's boundary conditions. Also, an array of interior subdomain forecasts focussed on interaction events is performed to determine sensitivities to initial feature locations and to bracket expected developments [*Robinson et al.*, 1987; 1989].

The Harvard model has been calibrated for the GSM&R and shown capable of realistic evolution of thermal fronts for longer than two weeks, spanning several energetic synoptical-dynamical events [*Robinson et al.*, 1988]. Satellite observed infrared (IR) sea surface temperature (SST) signals can define thermocline fronts, but the domain is rarely cloud free. Overall, the jet and ring surface fronts are observable by IR about 50% of the time; any pass usually yields a few frontal segments separated by cloud covered regions.

The slow evolution in real time of internal oceanic weather favors the combination of frontal segments by assimilation. Forecasts were carried out on a regular basis at Harvard University for more than a two-year period including all of 1987 and 1988. In early 1988 sea surface height (SSH) measurements became available from the GEOSAT satellite's radar altimeter in near real time. GULFCASTS used GEOSAT data provided both by the Space Geophysics Group at Johns Hopkins University Applied Physics Laboratory (JHU/APL) in Laurel, Md., and the Remote Sensing Branch at Naval Ocean Research and Development Activity (NORDA) at Bay St. Louis, Miss. The satellite tracks spaced ~130 km apart repeat every 17 days in the GSM&R region where mesoscale frontal SSH signals are ~1 m. We avoided using a geoid by differencing signals along repeated tracks, although a synthetic geoid has now been formed with input from GULFCAST fields [*Porter et al.*, 1989]. Unambiguous interpretation of difference-signal shapes is made possible by a simulated estimate of the SSH difference from tracks across past and present GULFCASTS.

Occasional frontal crossings are valuable in the data assimilation context and incorporate immediately into the Feature-Model Initialization scheme. The in situ data base consisted of air-dropped expendable bathythermographs (AXBTs), air-dropped temperature probes to 300 m. GULFCAST used one dedicated flight per week of 30 AXBTs. The flight track was designed based on the existing GULFCAST to address critical problems and objectives, such as ambiguities in surface signals; the location of features without surface signals, such as cold rings covered with warm Sargasso water; and the accurate location and shapes of interacting features, such as a steep meander loop and a ring. The last objective is guided by subdomain sensitivity forecasts. The number of AXBTs required simply to map the GULFCAST domain would be an order of magnitude or two greater.

GULFCASTing

Figure 1 illustrates a GULFCAST. The nowcast of Figure 1A with IR, GEOSAT and AXBT data input, indicated on Figure 1B, initializes the model. The forecast field 7 days later is illustrated on Figure 1C and by sample vertical sections on Figure 1D. The new nowcast of Figure 1E is based on the forecast of Figure 1C melded with the new data of Figure 1F.

On March 2 the stream exhibits a low amplitude wave meander in the west, is absorbing a large warm ring at 65°W, has an intense long necked meander (60-62°W interacting with a small warm ring, and is flat to the east. The real time forecast indicated the complete coalescence of the large ring accompanied by western wave growth and propagation, the birth of a large new ring at 62°W with total absorption of the small warm eddy, and wave growth in the east. All of these energetic events are features of the verification nowcast of March 9.

Attribution and quantification of errors for the forecast scheme, which arise from data quality, quantity and treatment, model physics, numerics, and other factors, is essential but difficult. Issues include (i) the ability of the dynamical model to perform in the propagation regime, and, (ii) more demanding, to forecast through energetic synoptical-dynamical events, and (iii) the data required for assimilation to control the phase errors of forecasts.

During Phase 1 of GULFCAST from November 1985 to November 1986 five real time experiments established methodology, proved the concept, and indicated the ability of the dynamical model to perform successfully in the interaction regime. It was demonstrated also that when adequate AXBT data were available for assimilation, phase error could be controlled and the accuracy of a few days forecast of frontal locations maintained within about 10 km, the resolution limit imposed both by the AXBT sampling and model grids [*Robinson et al.*, 1989].

Phase 2 of GULFCAST (research-operational forecasting) began in November 1986 with regular real-time forecasts [*Glenn et al.*, 1987] and a data base of NOAA IR plus dedicated weekly AXBT flights designed for updating ambiguous regions and pinpointing intensive interactions. Phase 3 of GULFCAST (evaluation-operational forecasting) began in October 1987 and ended in January 1989. The data base included GEOSAT, NORDA IR and AXBTs with a sampling strategy that allotted half the 30 probes for verification.

The forecast system is currently undergoing evaluation via hindcast studies during data-rich periods, jointly with the Ocean Dynamics and Prediction Branch of NORDA. During 1987 and 1988 an average of four warm and four cold rings were present in the domain. Seventy-five synoptical-dynamical events (ring birth or absorption) were predicted and verified. Fourteen additional events forecast did not occur, and nine events occurred in nature but not the model. The dominant error source was inaccurately initialized meander shapes or ring locations due to sparse data.

Conclusion

GULFCASTING has demonstrated feasibility and usefulness for internal weather forecasting in the sea. The power of a systematic approach to the melding of remotely sensed and in situ observations through dynamical interpolation is essential. Improvements from an expanded data base (for example, drifters, continuous fields of SST), improved models (surface boundary layer, primitive equation physics) [*Walstad*, 1987; *Spall*, 1988; *Spall and Robinson*, 1989], and a continuous assimilation scheme are underway. NOWCAST and FORECAST fields are being used for realistic acoustical propagation computations [*Robinson*, 1987; *Lee et al.*, 1989], and a biological model is being coupled to the surface boundary layer.

The basis for construction of forecast schemes for other oceanic regions is clear, with important implications for marine science, technology and operations, and environmental management. Already ocean scientists have received and utilized real time GULFCASTS at sea to optimize sampling during SYNOP experiments (N. P. Fofonoff, personal communication, 1988). NOAA has found GULFCAST useful in preparation of its product [Clark, 1987]. The forecast scheme has been transitioned by NORDA to the Naval Oceanographic Office for operational forecasting and has been developed into their version known as NOGUFS (Navy Operational Gulf Stream Forecast).

Acknowledgments

We thank Marsha Glass Cormier for logistical support. This research was initiated with support from the Office of Naval Research and the Institute of Naval Oceanography and carried out with support by the Oceanographer of the Navy through NORDA.

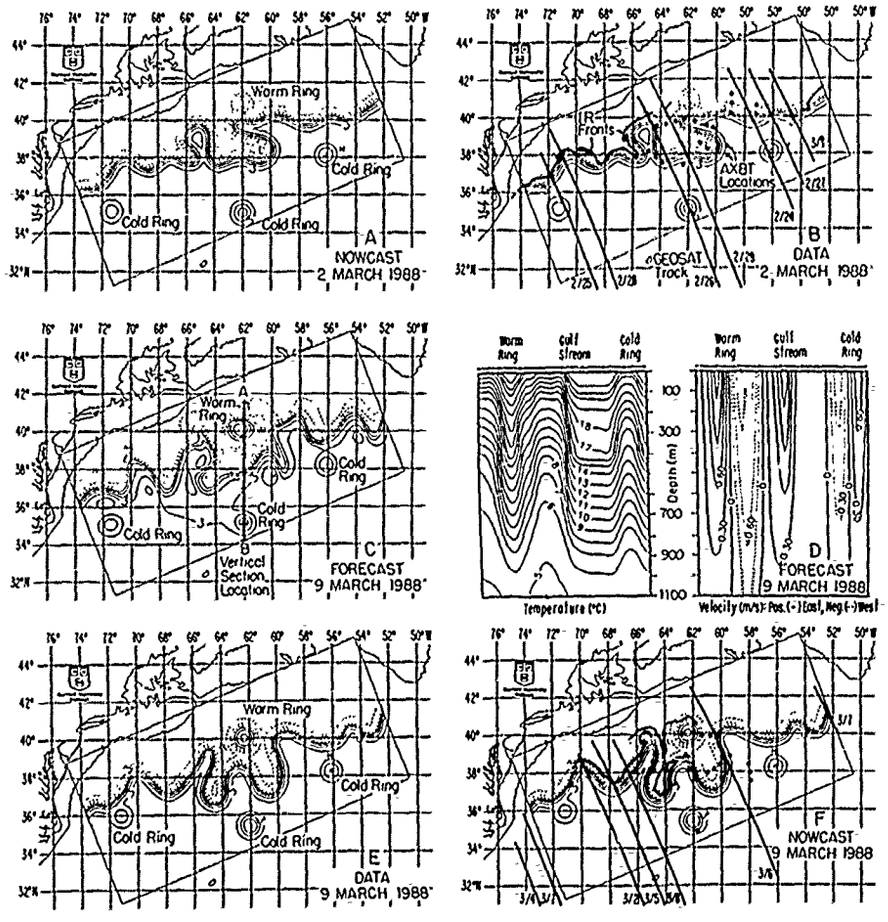

Fig. 1 GULFCAST Cycle: A, NOWCAST; B, input data; C, FORECAST; D, forecast vertical sections; E, new NOWCAST; F, new data.

References

Charney, J. G. and G. R. Flierl, Oceanic analogues of large-scale atmospheric motions, in *Evolution of Physical Oceanography*, edited by B. A. Warren and C. Wunsch, 504-548, MIT Press, Cambridge, Mass., 1980.

Clark, J., *Oceanographic Monthly Summary 7*, 12, 1987.

Glenn, S. M., A. R. Robinson, and M. A. Spall, Recent results from the Harvard Gulf Stream Forecast Program, *Oceanographic Monthly Summary 7*, 12, 1987.

Lee, D., G. Botseas, W. L. Siegmann, and A. R. Robinson, Numerical computations of acoustic propagation through three-dimensional ocean eddies, *Proceedings of the 12th IMACS World Congress*, July 19-22, 1988, Paris, France, Vol. II, 223-226, 1989.

Mooers, C. N. K., A. R. Robinson, and J. D. Thompson, editors, *A Status and Prospectus Report on the Scientific Basis and the Navy's Needs*, Ocean Prediction Workshop 1986, Cambridge, Mass., and NSTL, Miss., 1987.

Porter, D. L., A. R. Robinson, S. M. Glenn, and E. B. Dobson, The synthetic geoid and the estimation of mesoscale absolute topography from altimeter data, *Johns Hopkins University APL Technical Digest*, in press, 1989.

Richardson, P. L., Gulf Stream rings, in *Eddies in Marine Science*, edited by A. R. Robinson, 19-45, Springer-Verlag, New York, 1983.

Rienecker, M. M. and C. N. K. Mooers, The summary of the Optoma Program's mesoscale ocean prediction studies in the California Current system, in *Mesoscale-Synoptic Coherent Structures in Geophysical Turbulence*, edited by J. C. J. Nihoul and B. M. Jamart, 519-548, Elsevier Science Publishers, Amsterdam, Netherlands, 1989.

Robinson, A. R., Overview and summary of eddy science, in *Eddies in Marine Science*, edited by A. R. Robinson, 3-15, Springer-Verlag, New York, 1983.

Robinson, A. R., Predicting open ocean currents, fronts and eddies, in *Three-Dimensional Ocean Models of Marine and Estuarine Dynamics*, edited by J. C. J. Nihoul and B. M. Jamart, 89-112, Elsevier Science Publishers, Amsterdam, Netherlands, 1987.

Robinson, A. R., Dynamical forecasting of mesoscale fronts and eddies for accoustical applications, *Journal of Acoustical Society Supplement 1*, 82, 1987.

Robinson, A. R. and W. G. Leslie, Estimation and prediction of oceanic fields, *Progress in Oceanography 14*, 485, 1985.

Robinson, A. R., M. A. Spall, W. G. Leslie, L. J. Walstad, and D. J. McGillicuddy, GULFCASTING: Dynamical forecast experiments for Gulf Stream rings and meanders, November 1985-June 1986, *Harvard Open Ocean Model Reports 22*, Reports in Meteorology and Oceanography, Harvard University, Cambridge, Mass., 1987.

Robinson, A. R. and L. J. Walstad, The Harvard Open Ocean Model: calibration and application to dynamical process forecasting and data assimilation studies, *Applied Numerical Mathematics 3*, 89, 1987.

Robinson, A. R., M. A. Spall, and N. Pinardi, Gulf Stream simulations and the dynamics of ring and meander processes, *Journal of Physical Oceanography 18*, 1811, 1988.

Robinson, A. R., M. A. Spall, L. J. Walstad, and W. G. Leslie, Data assimilation and dynamical interpolation in GULFCASTING experiments, *Dynamics of Atmospheres and Oceans 13*, 301, 1989.

Spall, M. A., Regional ocean modelling: primitive equation and quasigeostrophic studies, *Harvard Open Ocean Model Reports 28*, Reports in Meteorology and Oceanography, Harvard University, Cambridge, Mass., 1988.

Spall, M. A. and A. R. Robinson, A new open ocean, hybrid coordinate primitive equation model, *Mathematics and Computers in Simulation*, in press, 1989.

Walstad, L. J., Modelling and forecasting deep ocean and near surface mesoscale eddies, hindcasting and forecasting with, and coupling a surface boundary layer model to, the Harvard Quasigeostrophic model, *Harvard Open Ocean Model Reports 23*, Reports in Meteorology and Oceanography, Harvard University, Cambridge, Mass., 1987.

Watts, D. R., Gulf Stream variability, in *Eddies in Marine Science*, edited by A. R. Robinson, 114-144, Springer-Verlag, New York, 1983.

Harvard University Gulfcast Verification Project

Working Paper Number 1

Verification Methodology and Implementation

Allan R. Robinson and Scott M. Glenn
Department of Earth Planetary Sciences
Harvard University
Cambridge, Massachusetts 02138

George W. Heburn and Robert C. Rhodes
Naval Ocean Research and Development Activity
NSTL, Mississippi 39529

March 16, 1988

1. Introduction

Harvard University and the Naval Ocean Research and Development Activity (NORDA) have begun a joint study to verify the Harvard Open Ocean Model in the Gulf Stream Meander and Ring Region. The first joint meeting of participants was held at NORDA on 19 January 1988 to discuss the verification project organization and scientific approach. This document is to serve as a summary of those discussions, and as an outline of our immediate tasks.

2. Personnel

The verification meeting was attended by the following personnel:

Harvard:	NORDA/NAVO:
Allan Robinson	George Heburn
Donald Dembo	Donna Blake
Scott Glenn	Michael Carron
Leonard Walstad	John Harding
	Jeff Hawkins
	Al Pressman
	Robert Rhodes

The following Verification Committee was instated at the meeting:

	Harvard:	NORDA:
Senior Scientist:	Allan Robinson	George Heburn
Lead Scientist:	Scott Glenn	George Heburn
Executive Scientist:	Scott Glenn	Robert Rhodes

The Harvard and NORDA Senior scientists, Prof. Allan Robinson and Dr. George Heburn are responsible for the overall conduct of the joint verification Study. The Lead Scientists, Dr. Scott Glenn and Dr. George Heburn, are responsible for the scientific execution of the verification Study. The Executive Scientists, Dr. Scott Glenn and Mr. Robert Rhodes, are responsible for the communication of the results between the Harvard and NORDA participants.

3. Harvard University Gulfcast Background

Dynamical ocean forecasts have been performed in the Gulf Stream Meander and Ring Region at Harvard over the last 2.5 years. The Gulf Stream Forecasts (Gulfcasts) were generated using the Quasi-Geostrophic (QG) Harvard Open Ocean Model. The QG forecast model is initialized using feature models developed for the Gulf Stream and the Warm and Cold Rings. The feature model initialization scheme defines the initial 3-dimensional velocity field based on estimates of the Gulf Stream and Ring locations and strengths. The feature locations and strengths are determined by updating the previous forecast using a combination of remote sensing and in situ data. The Gulfcasts performed during this time period can be divided into three phases.

Phase 1, the Research Phase, took place from November 1985 through November 1986. During this phase, the initial proof of concept forecasts were performed. This phase was highlighted by an at sea exercise during which Gulf Stream forecasts were generated in real time aboard ship in the North Atlantic. Phase 1 has been fully documented by Robinson et al. (1987).

Phase 2, the Research Operational Phase, took place from November 1986 through October 1987. One week Research Operational Forecasts were generated on a regular basis during this phase and were delivered each week to the Naval Eastern Oceanography Center (NEOC) at Norfolk, Virginia. Each week's forecast was generated by updating the previous week's forecast with frontal locations identified in available satellite infrared imagery (IR) and weekly dedicated air-deployable expendable bathythermograph (AXBT) survey flights. The satellite imagery was analyzed at NEOC and by the National Oceanographic and Atmospheric Administration (NOAA) and sent to Harvard in the form of frontal analysis charts. The AXBT flights were planned at Harvard for the sole purpose of updating forecasts, that is, the AXBT's were deployed in areas of ambiguity or in areas with poor data coverage.

Phase 3, the Evaluation Operational Phase, began in October 1987. In this ongoing phase, Harvard is continuing to generate one week forecasts, labeled Evaluation Operational Forecasts, which are submitted to NEOC each week. The quality and quantity of updating and verification data, however, has greatly improved during this phase. High resolution digital IR imagery and GEOSAT altimetry data are being sent to Harvard on a regular basis. The Harvard

designed AXBT flights have had their emphasis switched from obtaining only updating data to obtaining half updating and half verification data. The verification AXBTs are used to evaluate model performance and are not necessarily dropped in areas of ambiguity or poor data coverage. Harvard is using the IR, GEOSAT, and AXBT data to generate its own unclassified frontal analysis. Also during this phase, the Gulfcasting system will be transferred to NORDA in preparation for the transition to the operational Navy environment. This will soon make it possible to perform simultaneous hindcast and forecast model runs at Harvard and NORDA.

4. Harvard Verification Background

With model validation in mind, two forecast regimes that must be represented by the model physics were defined. The first is a propagation regime where the model must accurately predict: a) meander propagation, b) meander growth, and c) ring propagation. A second regime is the event regime characterized by energetic synoptic dynamical events that include: a) ring formation, b) ring absorbtion, c) ring-ring interactions, and d) ring-stream interactions. How well the forecasting system behaves in these regimes depends on the quality of the initialization/updating data. During the Phase 1 special interest Gulfcasts, such as the 1986 at sea exercise in which data assimilation was emphasized, it was demonstrated that with accurate initialization data, accurate forecasts with data assimilation could be achieved. The preliminary verification study conducted by Harvard during the Research Operational Phase also indicated that when good initialization/verification data was available, the forecast model does very well in both the propagation and event regimes. Specific results of the preliminary verification include:

A) During the Phase 1 at sea forecasting exercise, it was demonstrated that with data assimilation, the quantitative agreement between the forecasts and the verification data was within the navigational error of the data.

B) During the Phase 2 Research Operational Phase, it was found that Gulf Stream meander propagation and growth could be tuned to be in very good agreement with observations. It also was found that over many forecast periods, the rings propagate somewhat slowly. This does not affect our one week forecasts, since the one week propagation distance usually is small compared to the error in estimated ring center location. It simply means that the rings must be tracked over the long term so that their positions can be updated when necessary. This finding has prompted an ongoing study of ring propagation characteristics, and the optional inclusion of a background advective velocity in the model initialization code.

C) During Phase 2, it also was found that the forecast model's ability to predict major synoptic dynamical events was excellent. Given the IR and AXBT data, the prediction of major events, such as ring formations or absorptions, was demonstrated on a regular basis.

The successes noted in these preliminary evaluation studies have given us the confidence to proceed with the joint Harvard/NORDA evaluation phase of Gulfcasting.

5. Harvard/NORDA Verification Study Scientific Issues

Harvard and NORDA have recently begun the evaluation and transition phase of the Gulfcasting project, a joint effort in which we intend to validate the Gulf Stream forecasting model and transition the model into the operational Navy environment. The following summarizes the scientific issues raised during the January 19, 1988 verification meeting discussion of model validation in the Gulf Stream Meander and Ring Region.

The Harvard/NORDA joint model evaluation ideally should include the following items:

A) The systematic evaluation of existing examples. This will complete the Harvard preliminary verification study.

B) The performance of hindcasts during approximately 6 two-week periods for which accurate initialization/verification data is available. The hindcast data set will be assembled from available NORDA IR (April 1985 - present), NORDA GEOSAT Data, and AXBT survey data from NORDA (Regional Energetics Experiment (REX)), Harvard, the Fleet Numerical Oceanography Center (FNOC), and the National Oceanographic Data Center (NODC). The first objective of the hindcast approach will be to evaluate the model physics. This can be achieved by performing model forecasts from the "best" initialization data and statistically comparing the forecasts with other data available during the same periods. This should provide us information on how the model physics handles the different event regimes and also give us a controlled experiment representing the best-case scenario.

C) Other experiments will then be performed where we attempt to degrade the data quality to see what effect this will have on the model forecasts. One experiment will be to simulate a typical Gulfcast where only data that is normally available will be used for initialization. These experiments will give some idea about the error that can be expected due to the lack of data coverage. They will also give an idea of how much data is needed for a forecast that will be significantly better than persistence or climatology. These experiments can also be used to establish what kind of errors in data types we can accept and still have useful information for the forecasts.

D) The development of methods to carry out ongoing evaluations of the weekly operational forecasts.

E) The establishment of a new model initialization/verification data base for operational purposes. The present model data base includes satellite IR, GEOSAT altimetry, and weekly AXBT surveys. The AXBT surveys, which previously had been flown only for updating purposes, are now being flown half for verification data, half for updating data. Some of these AXBT surveys could be replaced with i) GEOSAT data for accurate Gulf Stream crossings and approximate ring locations, and ii) ARGOS buoys deployed in rings for accurate ring locations and swirl velocities.

Technical model validation issues to consider include error attribution, quality and quantity of available validation data, and specifying measures of accuracy. Can the errors be attributed to errors in initial conditions, boundary conditions or model physics? The preliminary validation study of Phase 2 results indicates that the dominant source of forecast error is due to incorrect model initializations based on low quality or insufficient data. The measures of accuracy should take into account the frontal structure of the features and the possibility of phase errors in space and time. Moreover, the error measures must be definitive, technically sound, and feasible considering the short time and limited resources available for verification.

Another issue discussed was the accuracy of initialization/verification data. It is necessary to establish the accuracy of the data since the model nowcasts and forecasts cannot be expected to be more accurate than the initialization or verification data itself. Knowing the data accuracy will help answer questions such as what level of forecast accuracy can be expected for a given initialization accuracy?

Validation criteria need to be defined and we must then determine the model performance level, relative to the criteria, necessary to justify operational deployment. The verification measures must be quantitative so that this model and new or improved models can be objectively compared to existing capabilities to judge their merit. As there is no present operational, dynamic forecast for the Gulf Stream region, the forecast must demonstrate a measurable and significant improvement over persistence and climatology. This demonstrated improvement would provide an important addition to Navy capabilities. Note that nowcasts may also improve with the inclusion of the forecast as first-guess information into the following week's analysis.

A final issue was the need to subjectively generate initialization and verification fields, along with the corresponding error fields. Unlike local area gridded XBT surveys, which can be objectively analyzed to produce initialization, verification, and error fields, the Gulf Stream Meander and Ring Region is too large of an area to cover with an XBT grid. Instead we must rely on a combination of remote sensing and in situ data. This data is patchy in space and time, is of varying quality, and must be subjectively analyzed to identify frontal locations. G[illegible] accuracy of the different data types and the data availability for [illegible] features, we can begin to construct subjective estimated error maps for initialization and verification. Data sources not having the required accuracy will be discarded. The REX AXBT data sets coupled with the Harvard AXBT surveys from the same time periods should be excellent for this study. Additional data, including available NORDA IR and NORDA GEOSAT data will be pooled with any data available from NAVOCEANO, FNOC, and NODC to form several time series for initializing and also verifying the hindcasts of the Gulfcast system.

6. Technical Approach

As stated earlier, the Harvard Gulfcast System is initialized using a "feature" model that uses only the Gulf Stream front and ring locations for initialization. Since the initialization is based on the location of the Gulf Stream front and rings and this is also the primary Navy interest for forecasts, the model performance should be based on how the forecast front and ring locations compare with the observed locations based on the best possible data. To do this we must define what is meant by frontal location and also what criteria will be used to specify the location and size of rings. Frontal and ring locations depend on the particular data source used to locate the front and it's associated errors. Consequently, one consistent method to locate the front based on all available data must be established.

A working definition for the Gulf Stream north wall was to be the location where the 15C isotherm crosses a depth of 200 meters. It was noted that the north wall location in satellite imagery has benn observed to differ by as much as 20 kilometers from this location. The ring frontal location was defined as the radius of maximum swirl velocity, since this is the location of the steepest sloping isotherms and the strongest front. It was noted that the radius of maximum velocity is well within the maximum radius of the rings as they are observed in satellite IR or GEOSAT data.

Once the criteria for locating the fronts and rings are established for the initialization and verification with associated data errors, statistics can be calculated to establish the skill of the model forecasts. Simple qualitative statistics can be useful in such a comparison. A yes/no criteria can be used

to determine whether an observed event actually occurred in the forecast. Beyond this, a determination of where or when the event occurred in the forecast and also the relative magnitude of the event can also be compared to observations.

Qualitative comparisons can be useful but quantitative comparisons must also be performed so that a measure of the skill of the forecast compared to persistence or climatology can be established. The position of the forecast and observed frontal locations can be overlayed and point by point statistical comparisons can be done. This will give quantitative information on the forecast accuracy of stream location. To compare the model Gulf Stream north wall with the typically fragmentary IR verification data, it was decided that the two frontal segments to be compared could be plotted and the area between the segments calculated. The area difference could then be divided by the verification segment length to give an average distance between model and data along the verification segment. Ring location can also be compared quantitatively using statistics on the centroid difference of ring locations from the forecast and from observed positions. The size of the rings can also be compared by drawing best fit circles through observed and forecast rings and comparing the radii.

Ring statistics of interest for verification include the ring center location and radius. It was noted that there is almost never enough AXBTs in a ring to accurately determine its center location or radius of maximum velocity, that the GEOSAT data can only locate the ring center in the along track direction once every 17 days and that the across track location is undetermined, and that even when the rings can be observed in the IR imagery, the radius is much larger than the radius to maximum velocity. ARGOS buoys deployed in rings will help eliminate these ambiguities in ring location and circulation parameters.

Both the qualitative and quantitative comparisons should be used for the hindcast model evaluations as well as for determining the quality of past Harvard forecasts and the on-going Harvard/NORDA forecasts.

7. Immediate Tasks

The following list of immediate tasks was developed:

A) Develop a summary of data availability and accuracy to serve as a guide for chossing quality initialization and verification data.

B) Choose 6 two-week time periods for the model hindcast evaluation. The time periods will be chosen based on the availability of quality initialization and verification data (Satellite IR, AXBT, and GEOSAT) during both propagation and dynamical event type regimes. Harvard, NORDA, FNOC, and NODC AXBT data will be summarized and pooled to identify time periods with significant AXBT coverage. These will be compared with the existing list of NORDA IR images to choose the hindcast time periods.

C) Develop the methodology for the qualitative construction of quantitative error maps for initialization and verification data.

D) Develop and implement the verification methodology so that it can be applied to the 6 hindcasts and to ongoing forecasts in real time. This includes computer codes that will calculate the average distance between frontal segments and will display error fields.

8. References

Robinson,A.R.,M.A.Spall,W.G.Leslie,L.J.Walstad,and D.J.McGillicuddy, "Gulfcasting: Dynamical Forecast Experiments for Gulf Stream Rings and Meanders,November 1985 - June 1986",Harvard Open Ocean Model Reports, Reports in Meteorology and Oceanography,Number 22,Harvard University,Division of Applied Sciences,Cambridge,Mass.,August,1987.

APPENDIX 2

HARVARD UNIVERSITY GULFCAST

OPERATIONAL FORECAST SUMMARY

26 NOVEMBER 1986 - 31 AUGUST 1988

HARVARD UNIVERSITY GULFCAST

RESEARCH OPERATIONAL FORECAST.

NEW DATA: IR.

Figure: Streamfunction at 100 m.

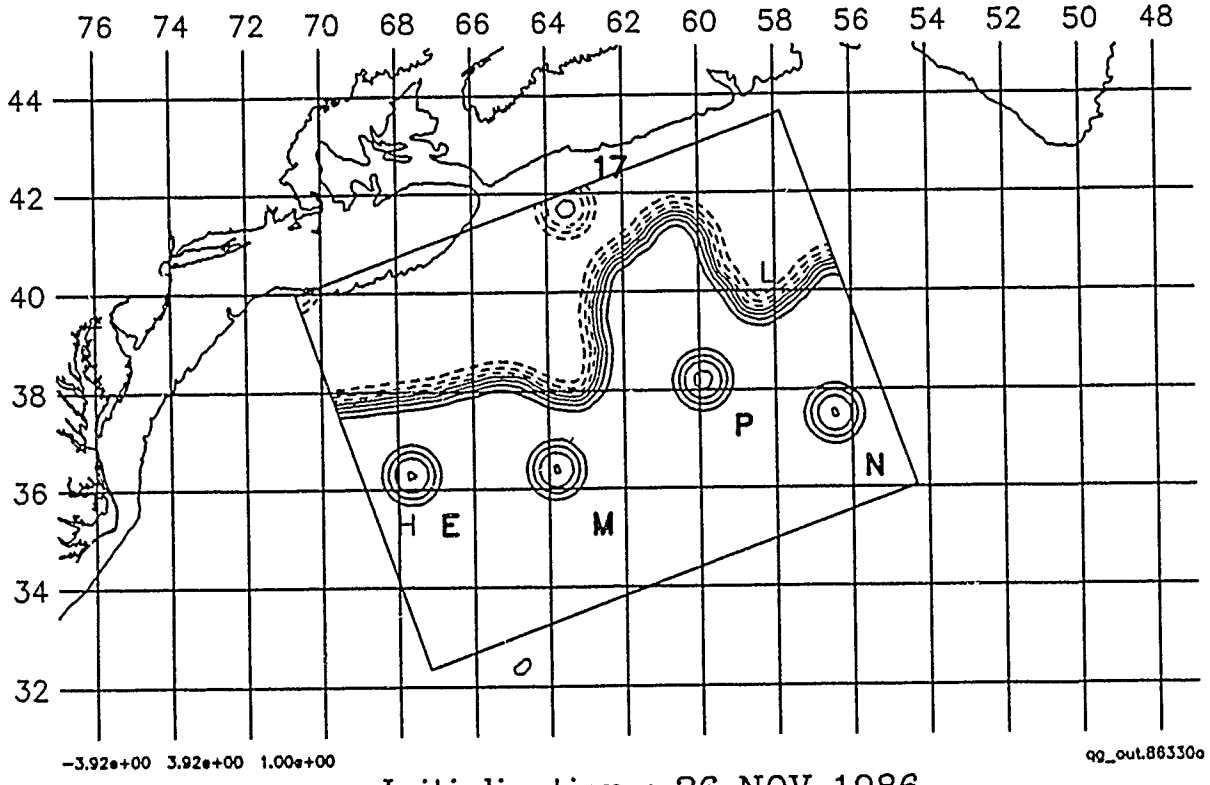

Initialization : 26 NOV 1986

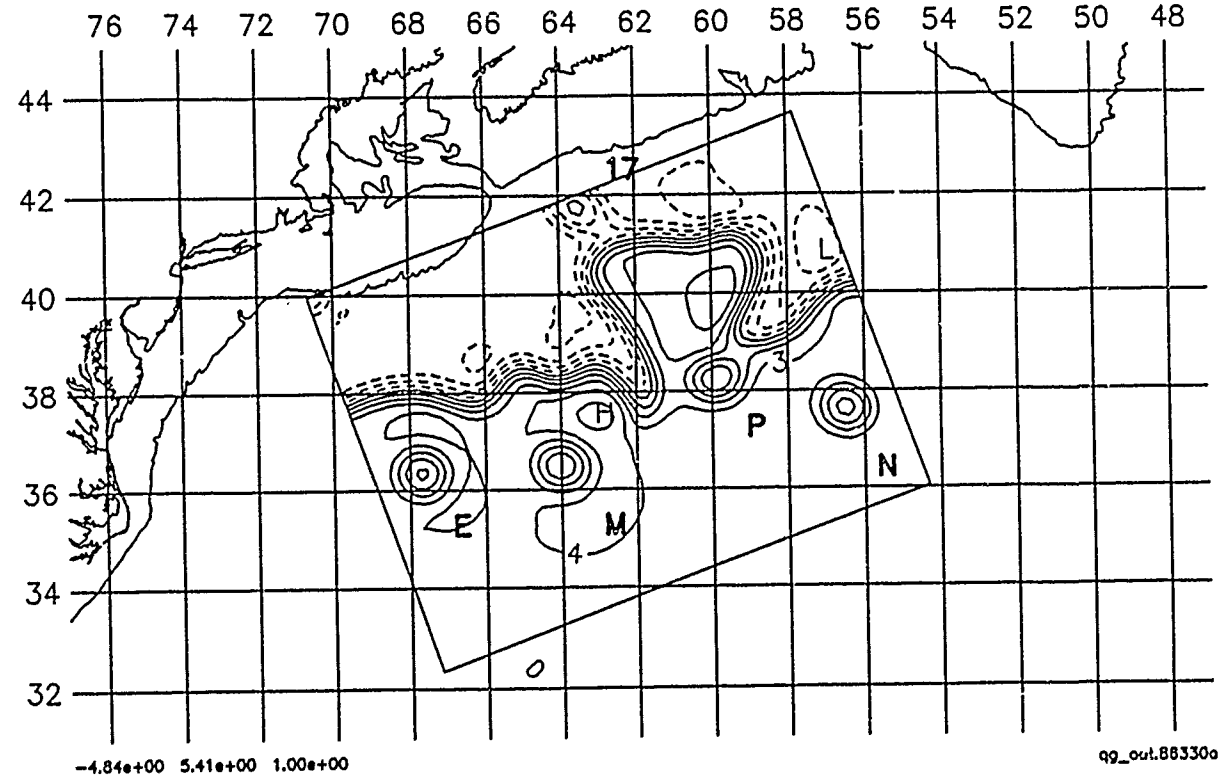

7 Day Forecast : 3 DEC 1986

HARVARD UNIVERSITY GULFCAST

RESEARCH OPERATIONAL FORECAST.

NEW DATA: IR.

Figure: Streamfunction at 100 m.

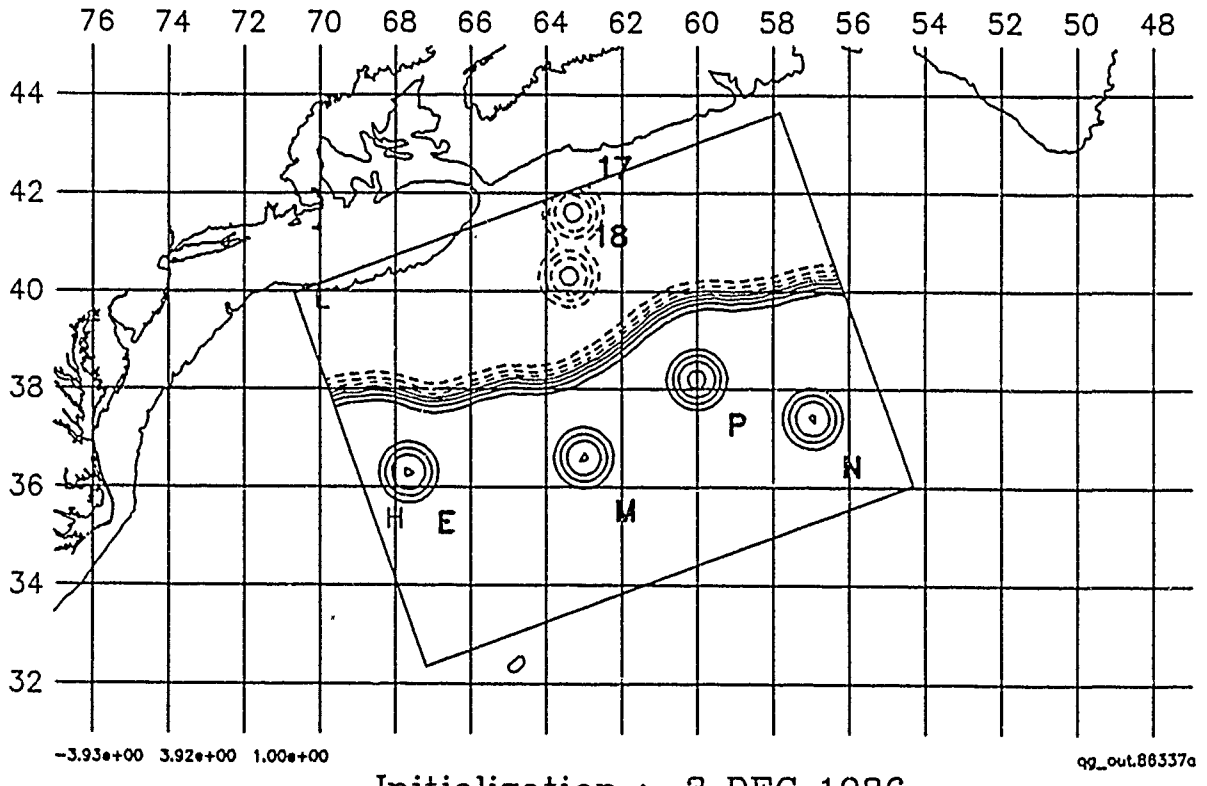

Initialization : 3 DEC 1986

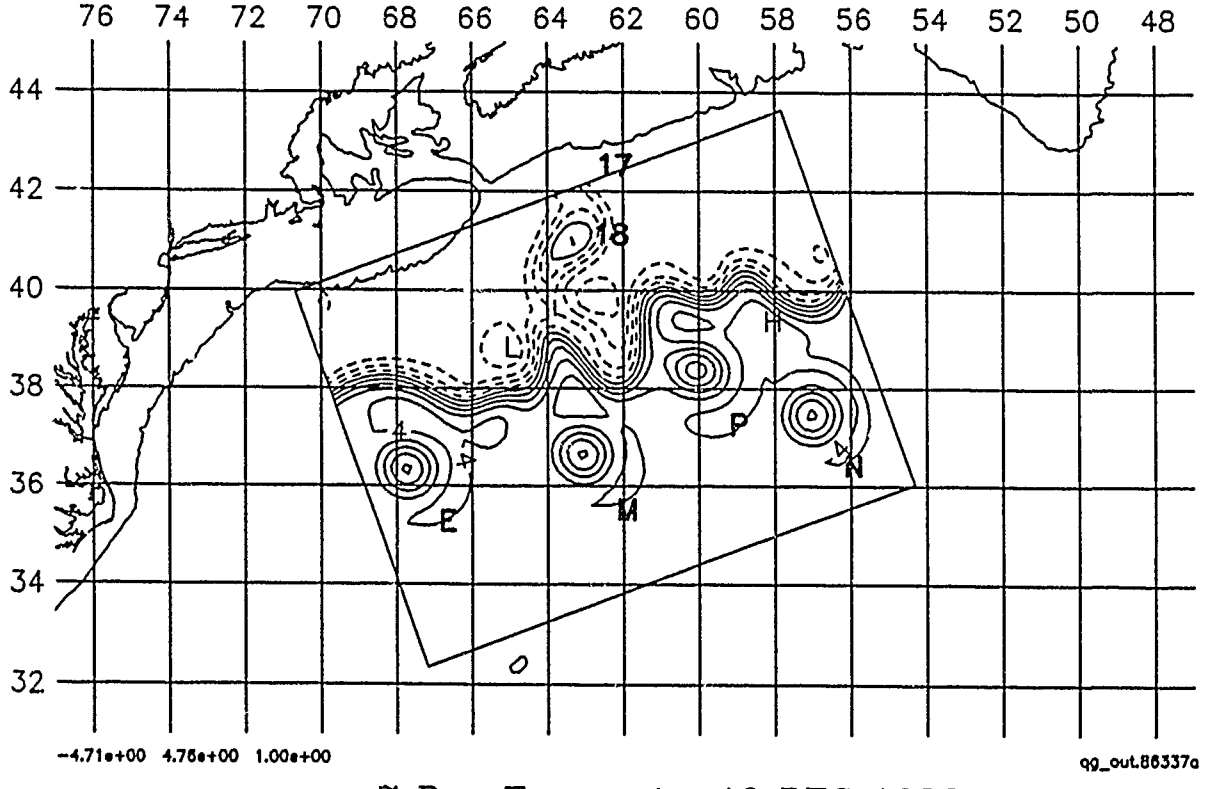

7 Day Forecast : 10 DEC 1986

HARVARD UNIVERSITY GULFCAST

RESEARCH OPERATIONAL FORECAST.

NEW DATA: IR, AXBT.

Figure: Streamfunction at 100 m.

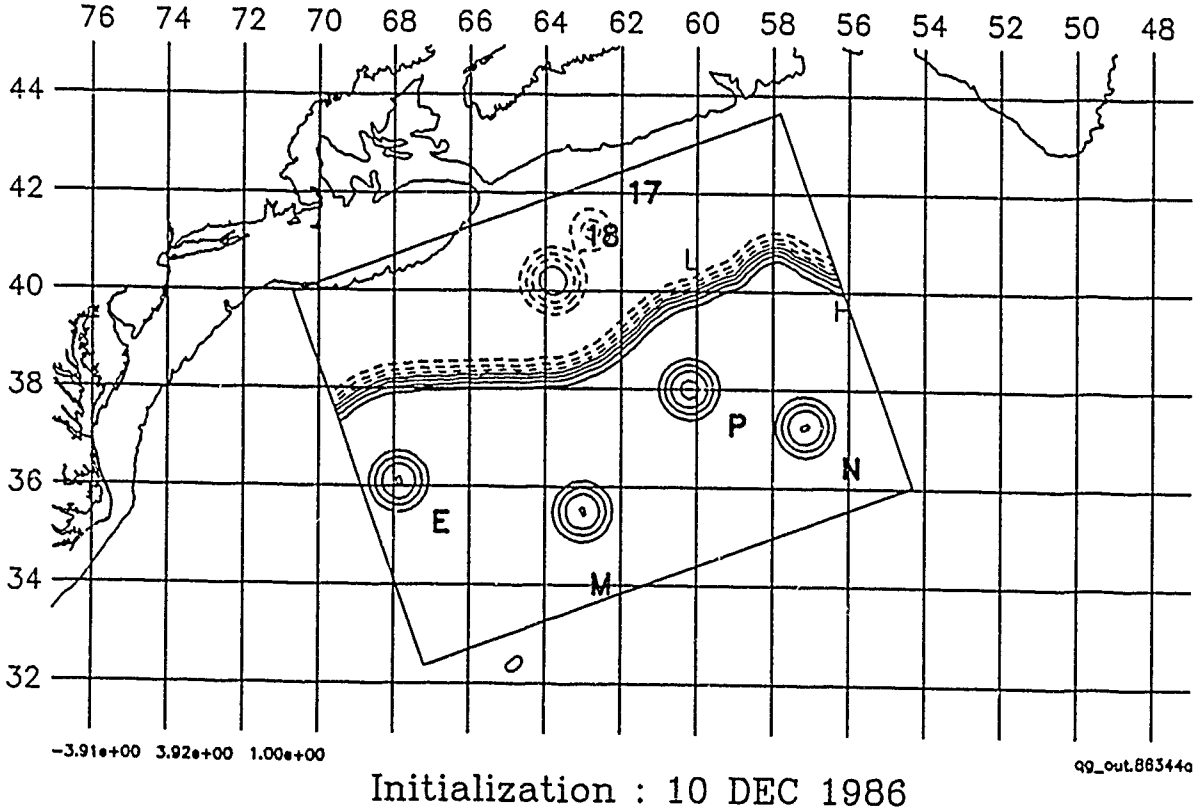

Initialization : 10 DEC 1986

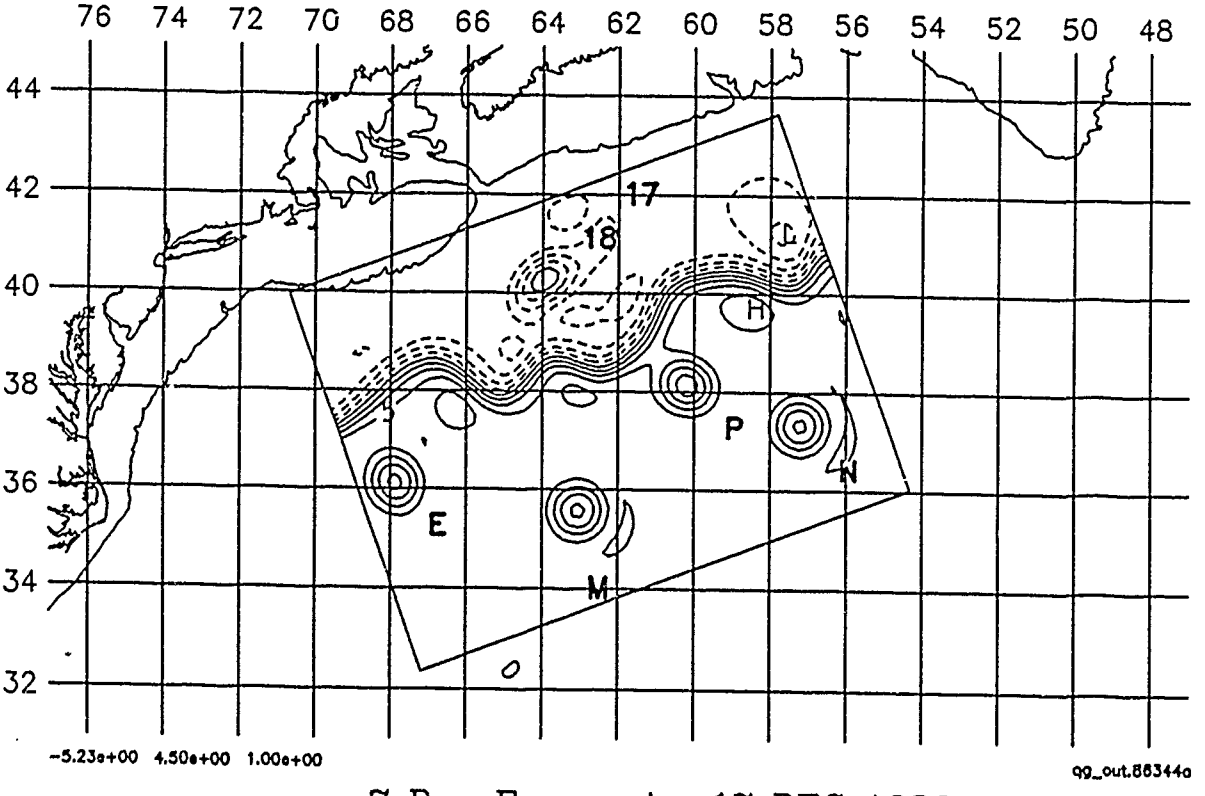

7 Day Forecast : 17 DEC 1986

HARVARD UNIVERSITY GULFCAST

RESEARCH OPERATIONAL FORECAST.

NEW DATA: IR, AXBT.

Figure: Streamfunction at 100 m.

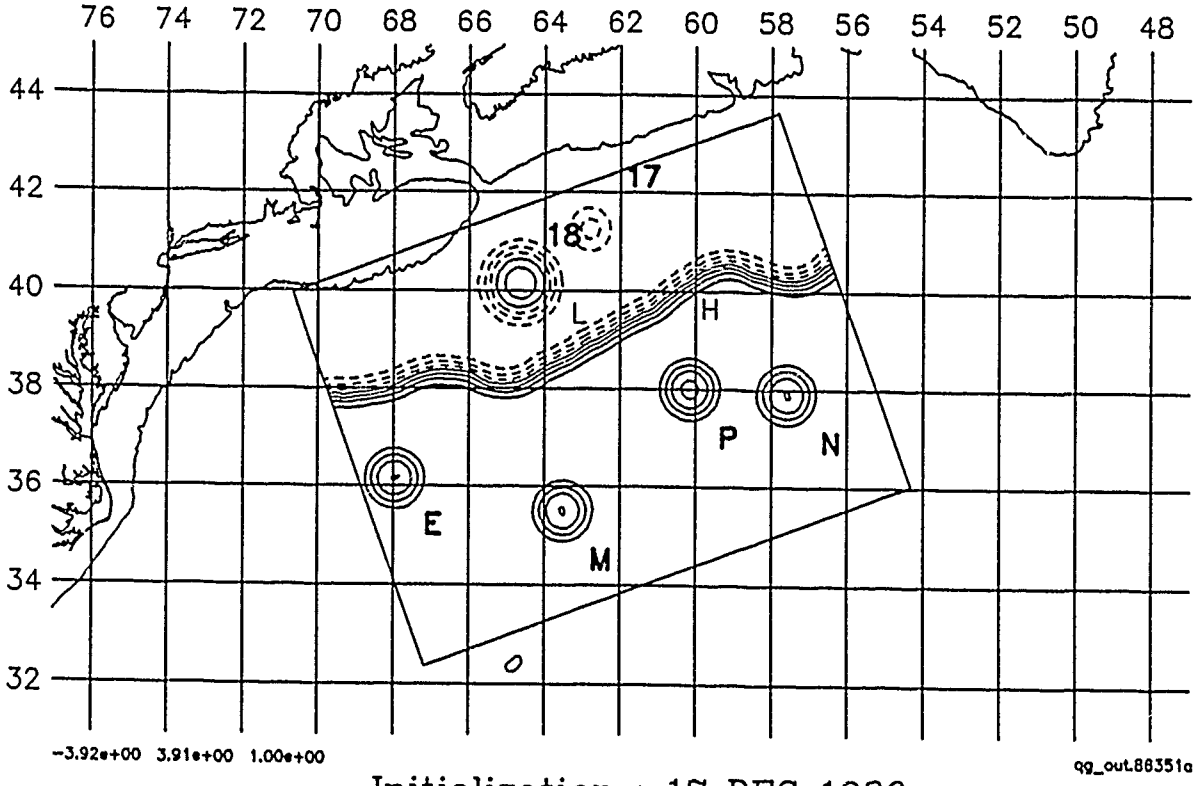

Initialization : 17 DEC 1986

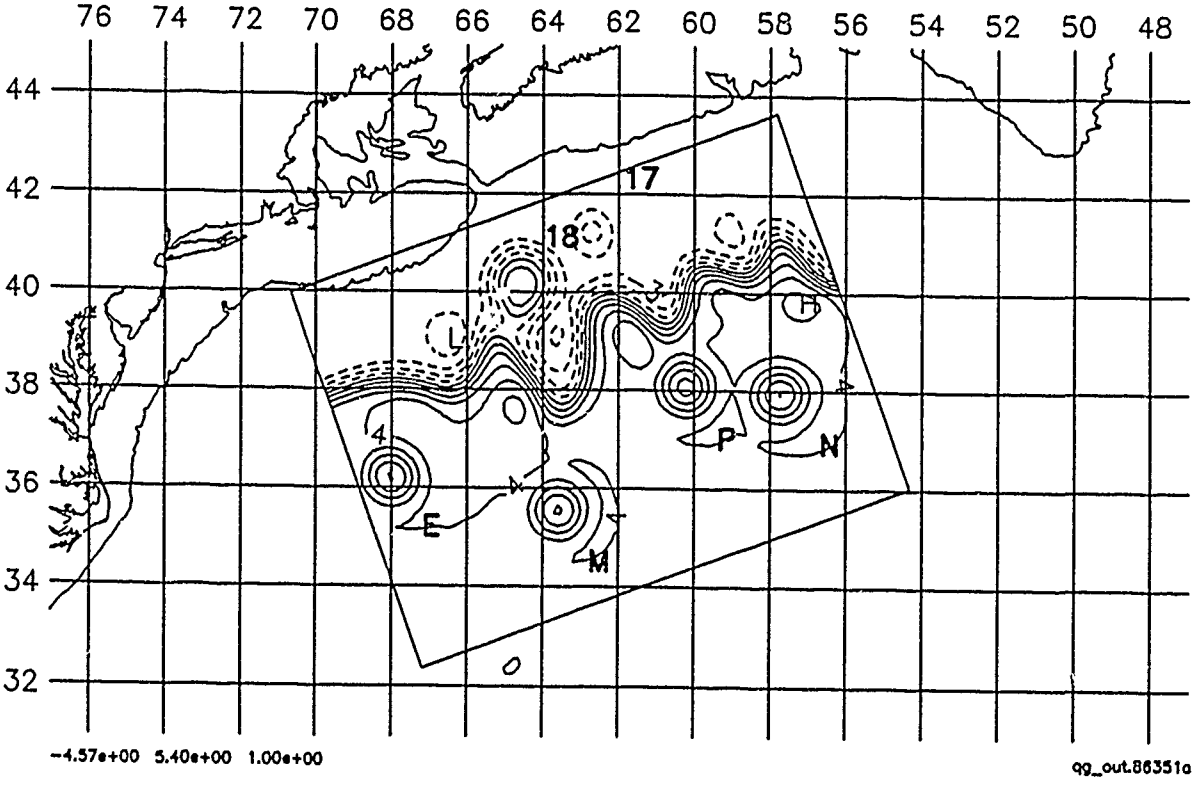

7 Day Forecast : 24 DEC 1986

HARVARD UNIVERSITY GULFCAST

RESEARCH OPERATIONAL FORECAST.

NEW DATA: IR, AXBT.

Figure: Streamfunction at 100 m.

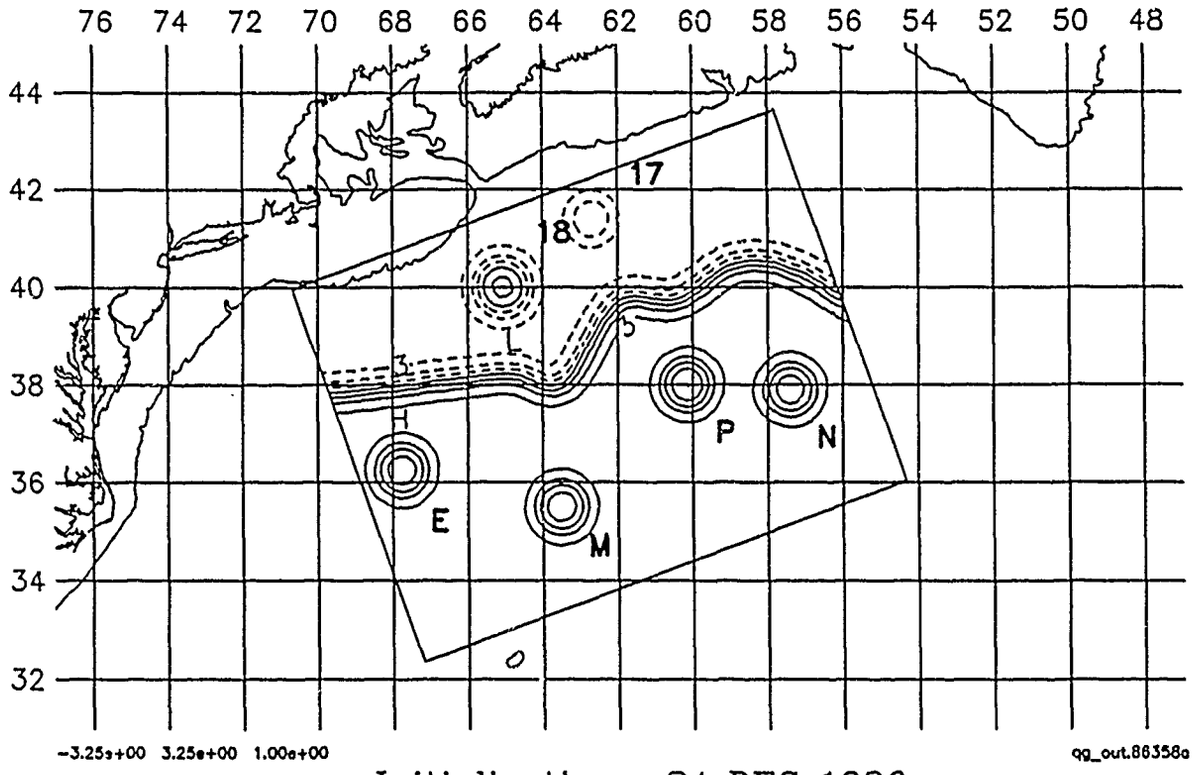

Initialization : 24 DEC 1986

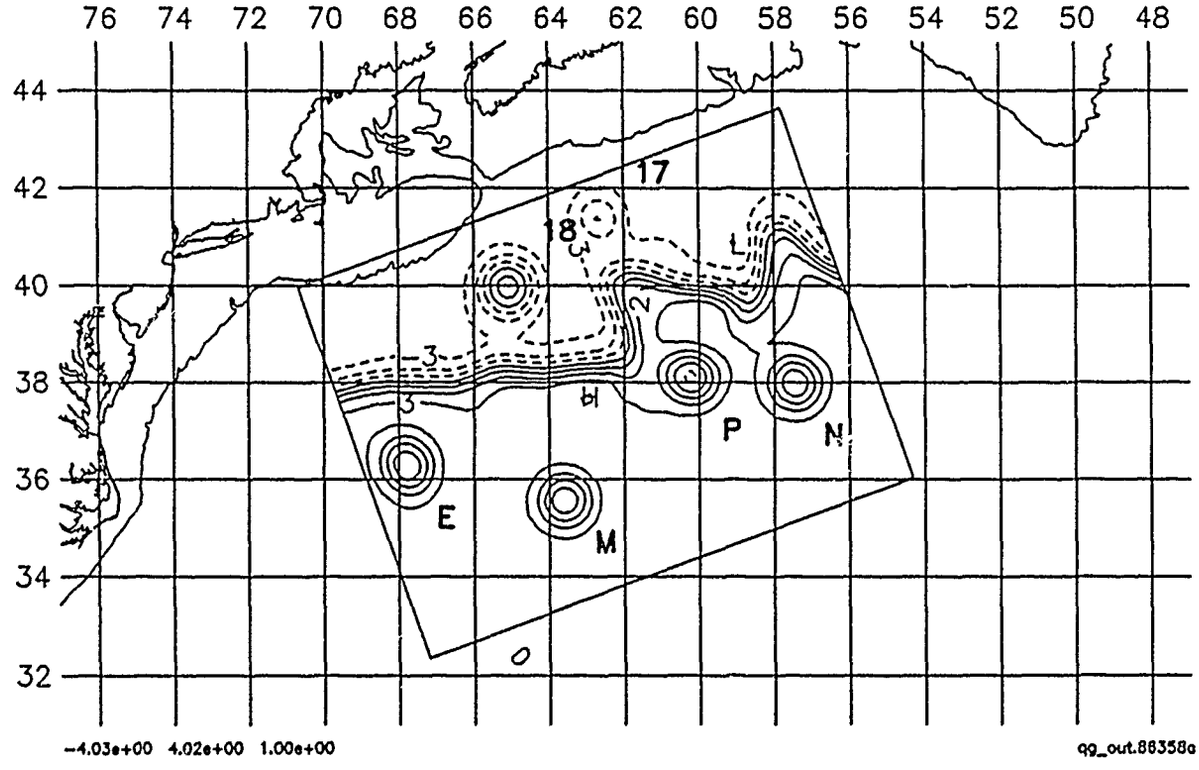

7 Day Forecast : 31 DEC 1986

HARVARD UNIVERSITY GULFCAST

RESEARCH OPERATIONAL FORECAST.

NEW DATA: IR, AXBT.

Figure: Streamfunction at 100 m.

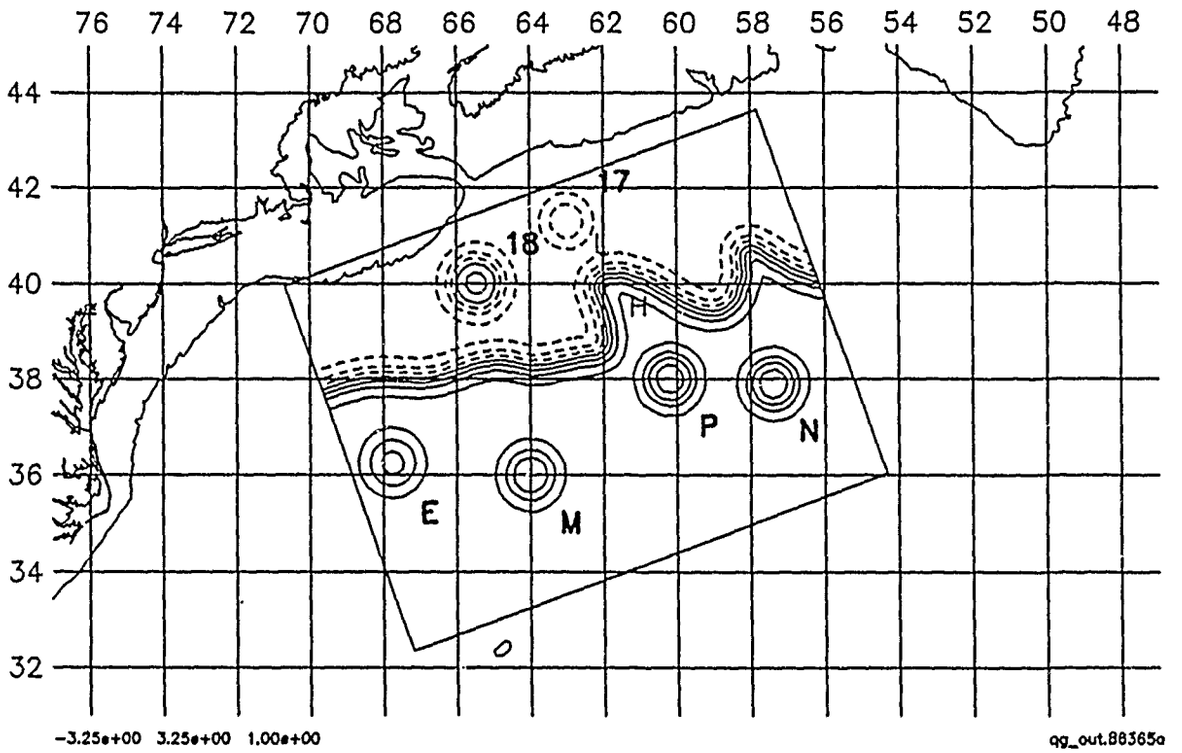

Initialization : 31 DEC 1986

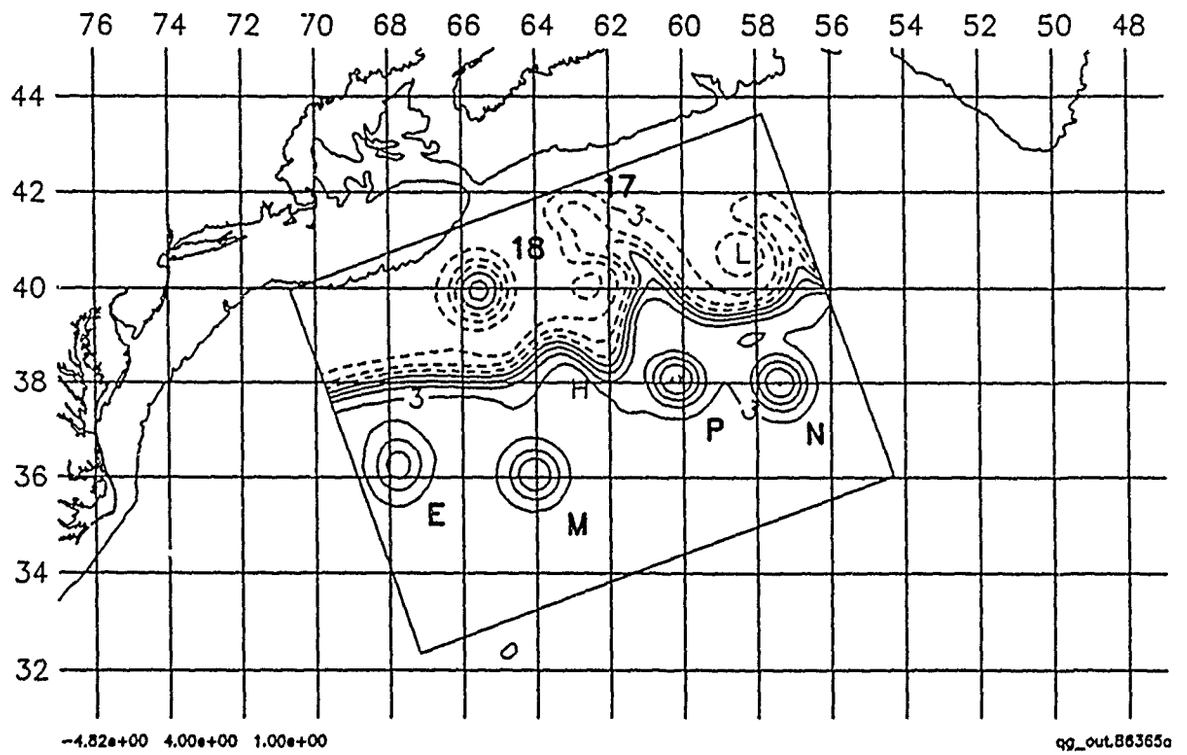

7 Day Forecast : 7 JAN 1987

HARVARD UNIVERSITY GULFCAST

RESEARCH OPERATIONAL FORECAST.

NEW DATA: IR, AXBT.

Figure: Streamfunction at 100 m.

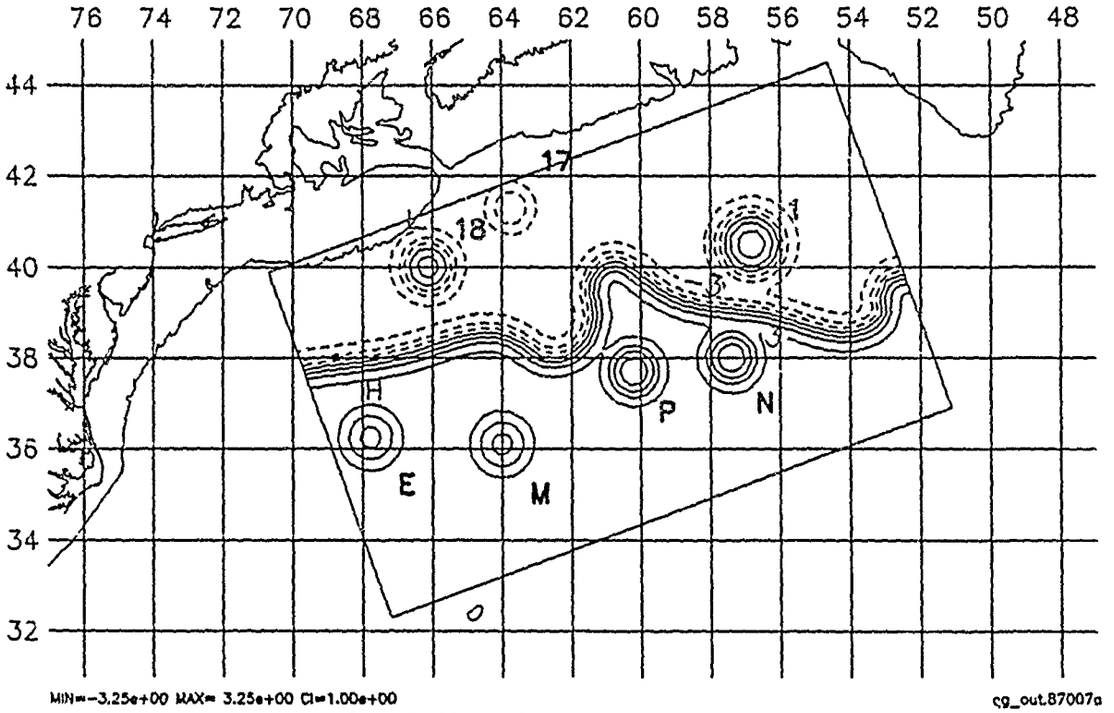

Initialization : 7 JAN 1987

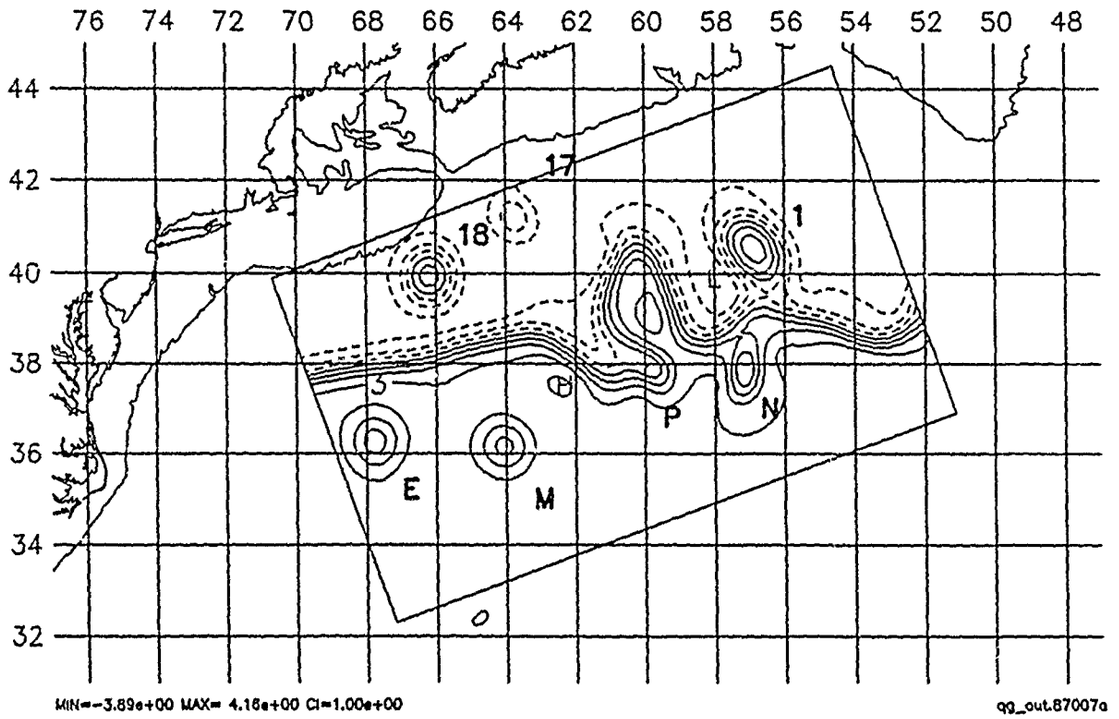

7 Day Forecast : 14 JAN 1987

HARVARD UNIVERSITY GULFCAST

RESEARCH OPERATIONAL FORECAST.

NEW DATA: IR, AXBT.

Figure: Streamfunction at 100 m.

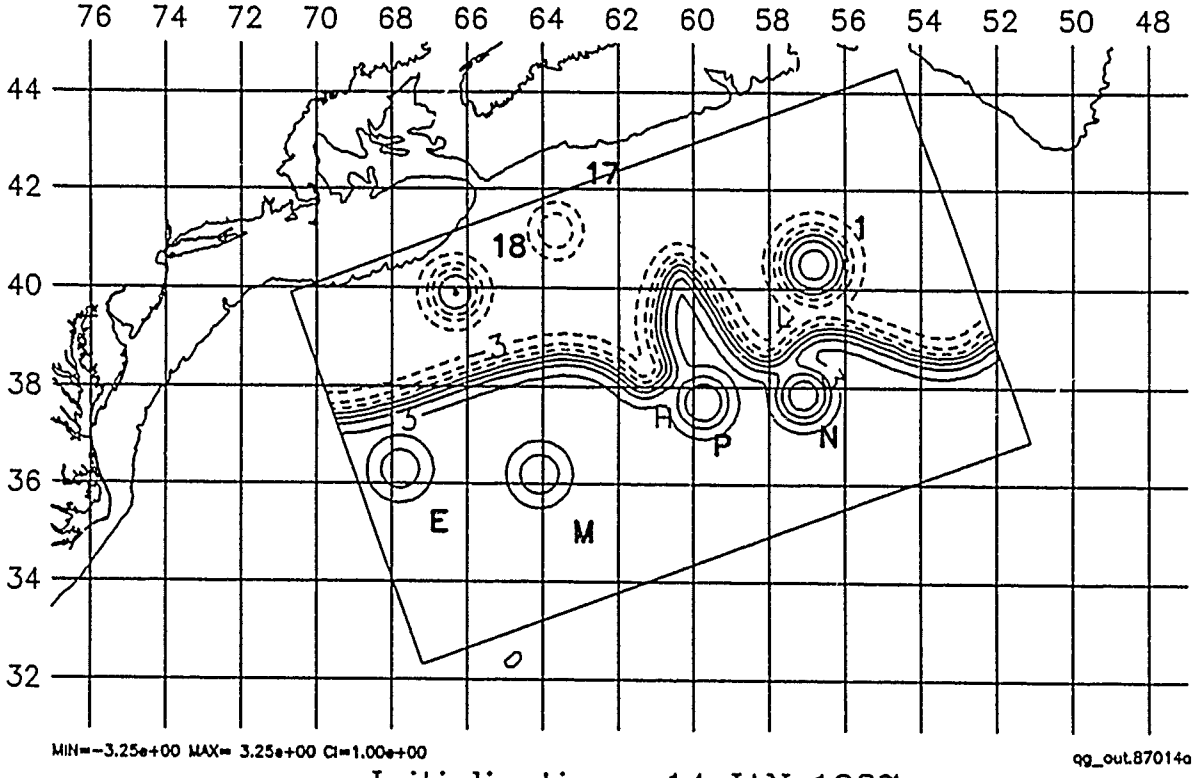

Initialization : 14 JAN 1987

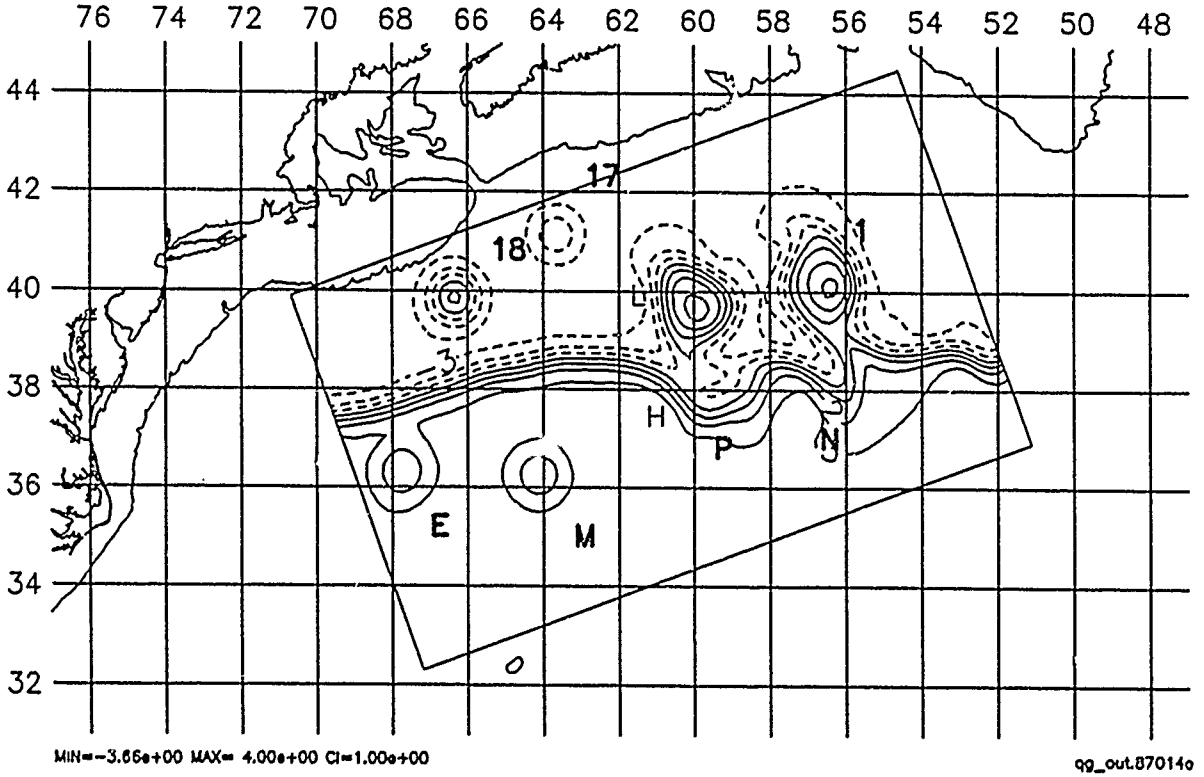

7 Day Forecast : 21 JAN 1987

HARVARD UNIVERSITY GULFCAST

RESEARCH OPERATIONAL FORECAST.

NEW DATA: IR.

Figure: Streamfunction at 100 m.

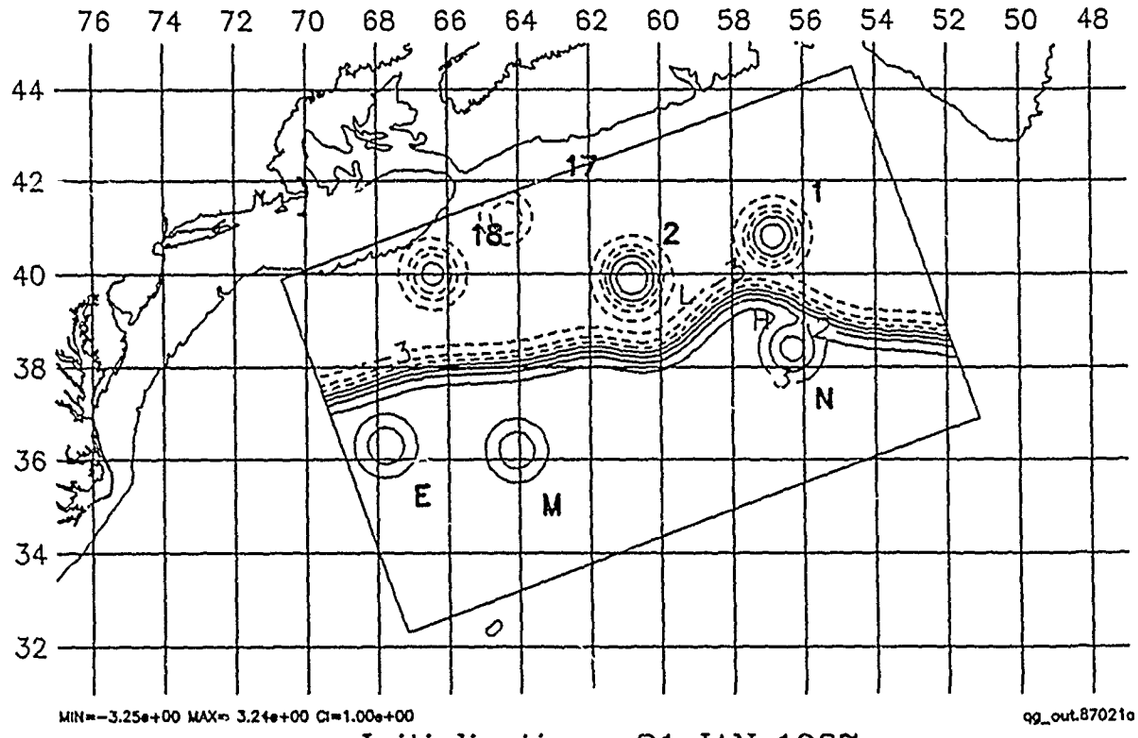

Initialization : 21 JAN 1987

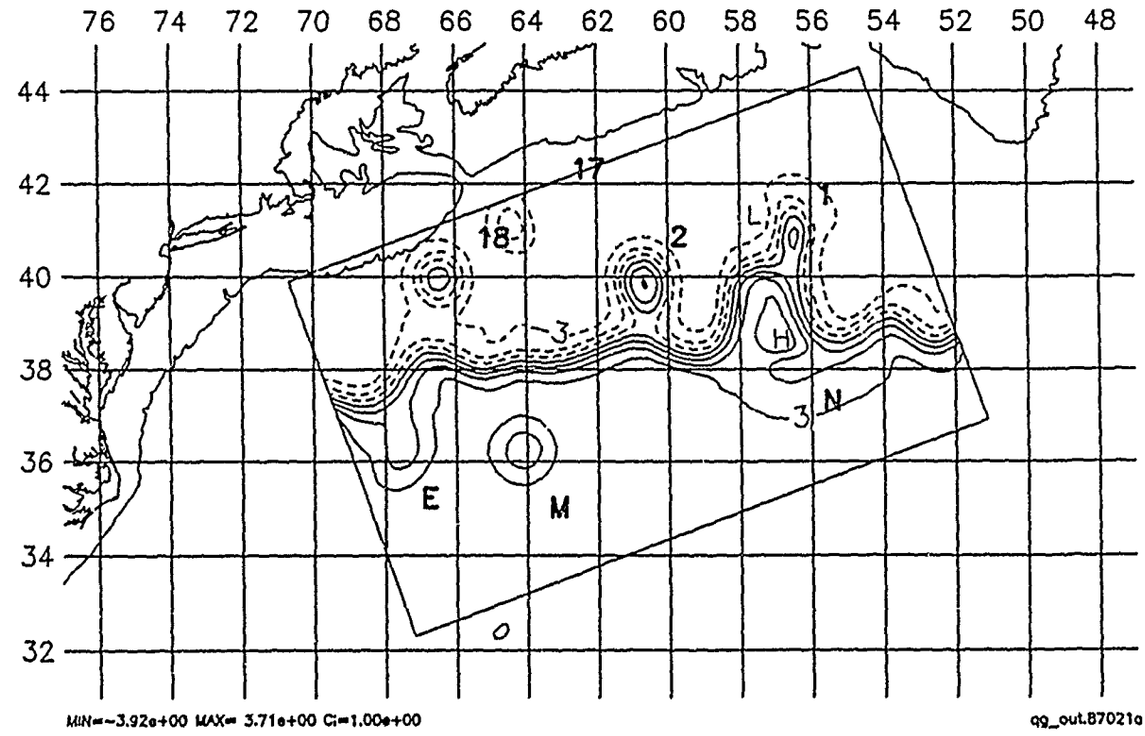

7 Day Forecast : 28 JAN 1987

HARVARD UNIVERSITY GULFCAST

RESEARCH OPERATIONAL FORECAST.

NEW DATA: IR, AXBT.

Figure: Streamfunction at 100 m.

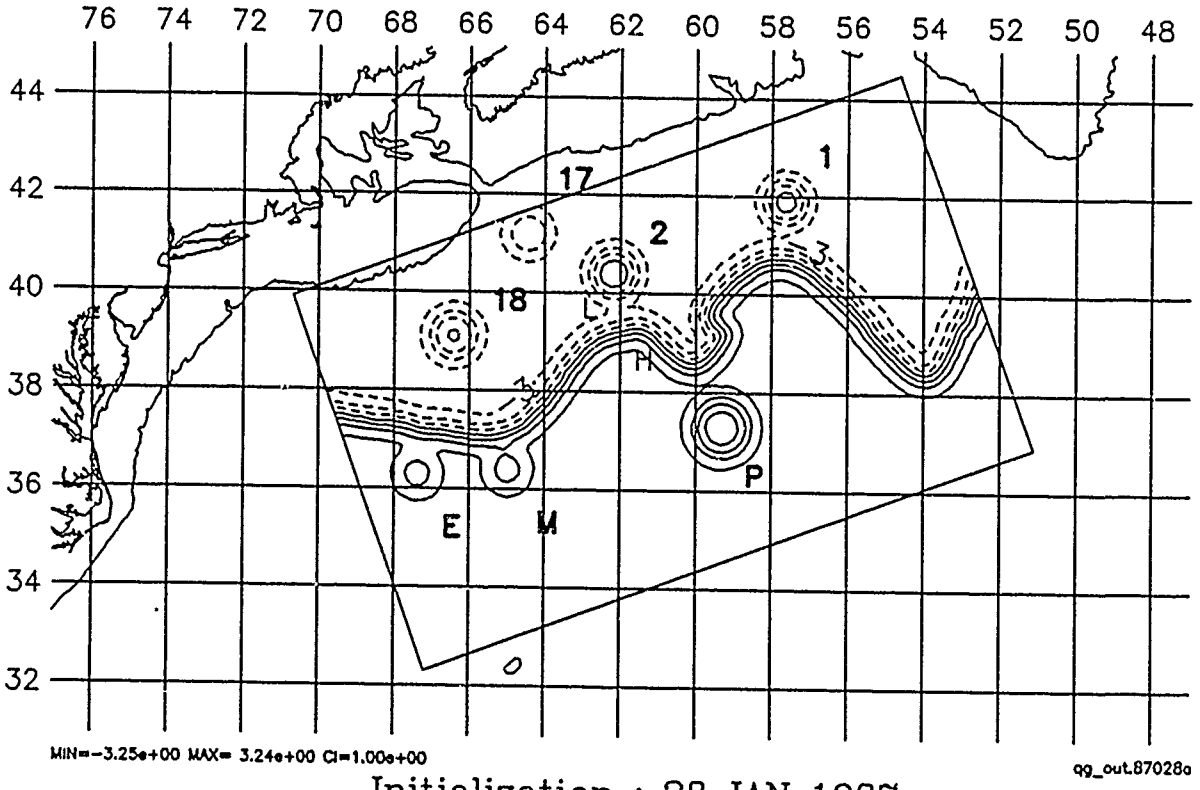

Initialization : 28 JAN 1987

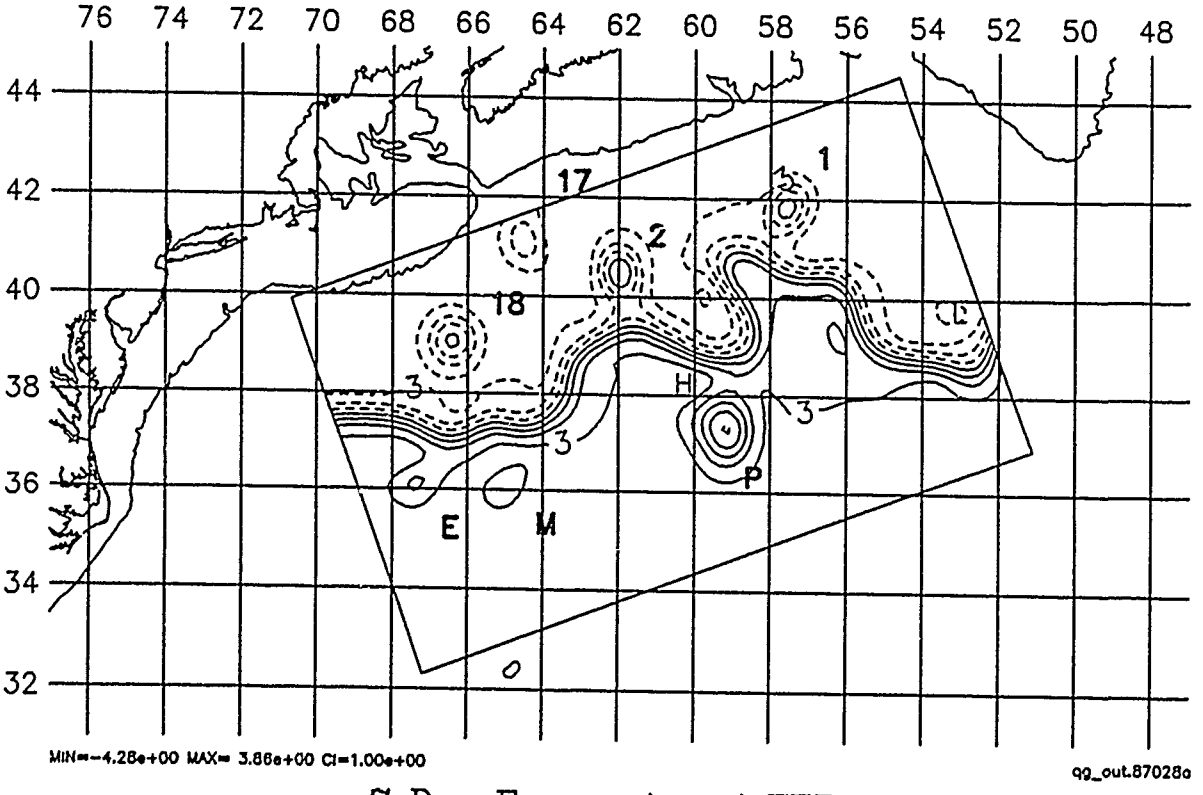

7 Day Forecast : 4 FEB 1987

HARVARD UNIVERSITY GULFCAST

VE RI TAS

RESEARCH OPERATIONAL FORECAST.

NEW DATA: IR.

Figure: Streamfunction at 100 m.

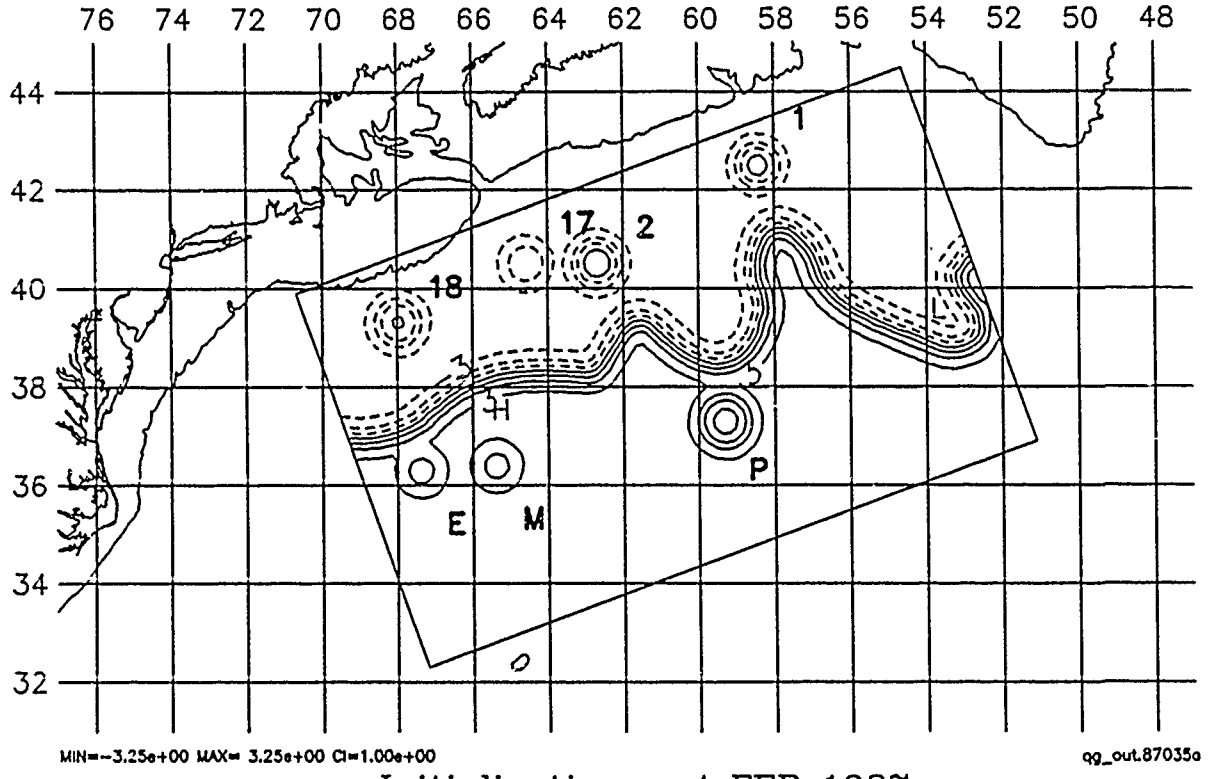

Initialization : 4 FEB 1987

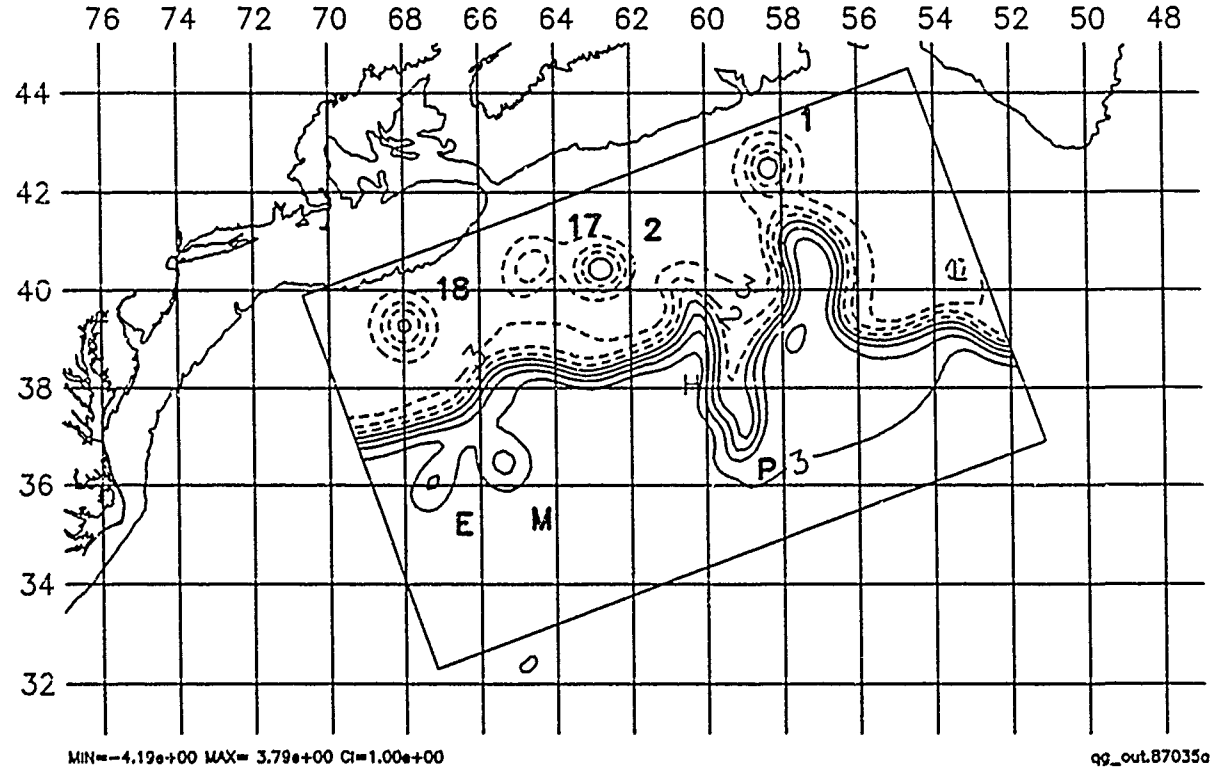

7 Day Forecast : 11 FEB 1987

HARVARD UNIVERSITY GULFCAST

RESEARCH OPERATIONAL FORECAST.

NEW DATA: IR, AXBT.

Figure: Streamfunction at 100 m.

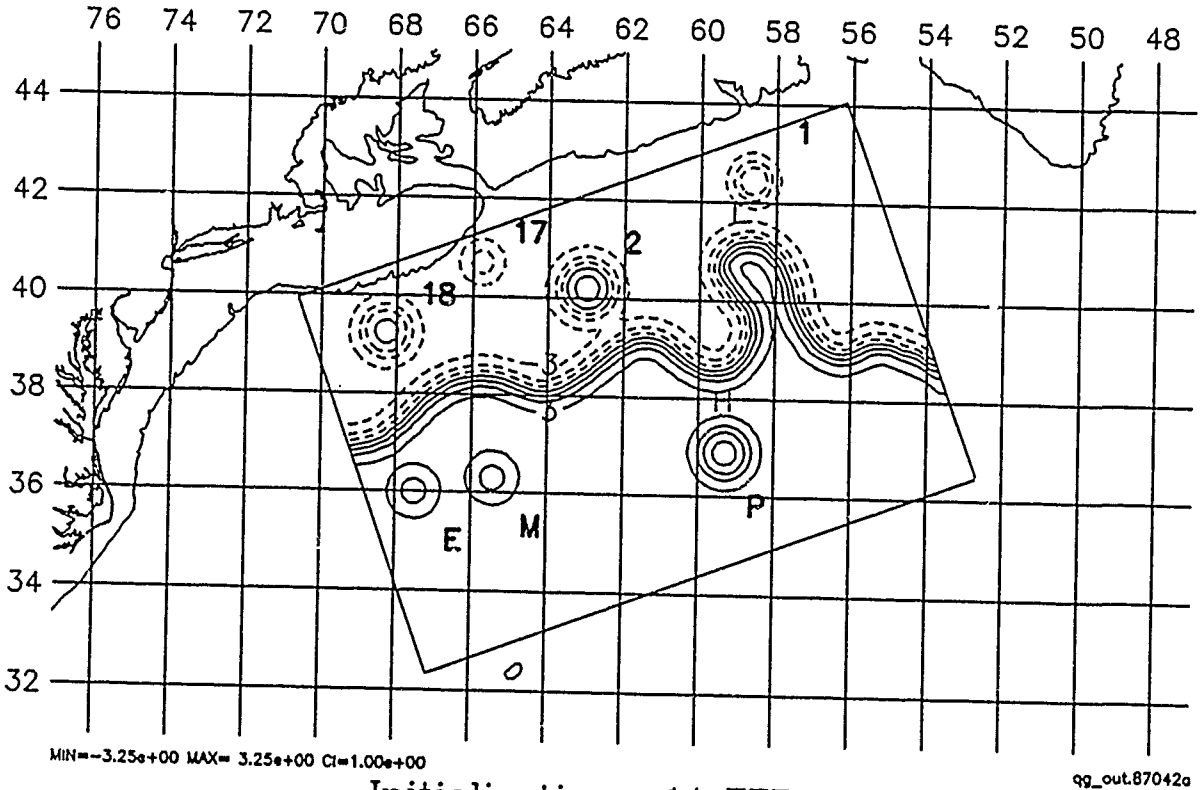

Initialization : 11 FEB 1987

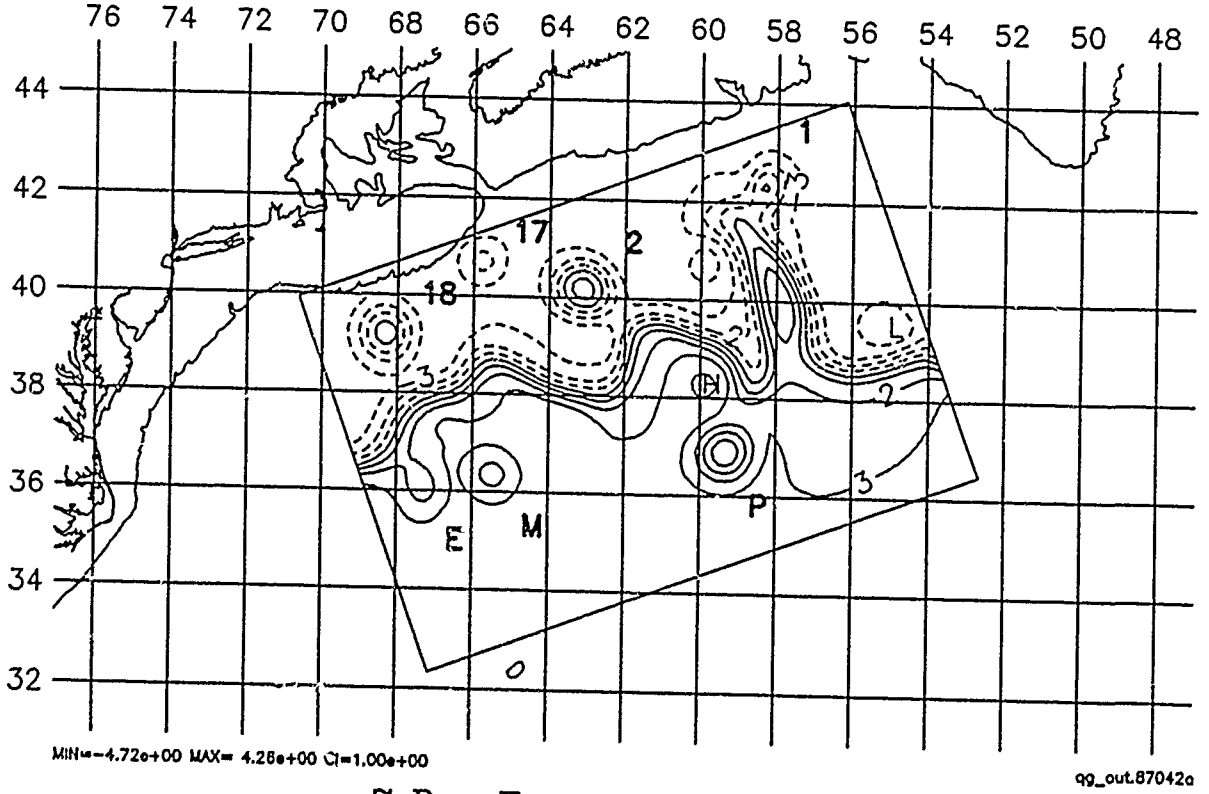

7 Day Forecast : 18 FEB 1987

HARVARD UNIVERSITY GULFCAST

RESEARCH OPERATIONAL FORECAST, H7 DOMAIN.
NEW DATA: IR (2/18), AXBT (2/18).
FIGURES: STREAMFUNCTION AT 100. M.

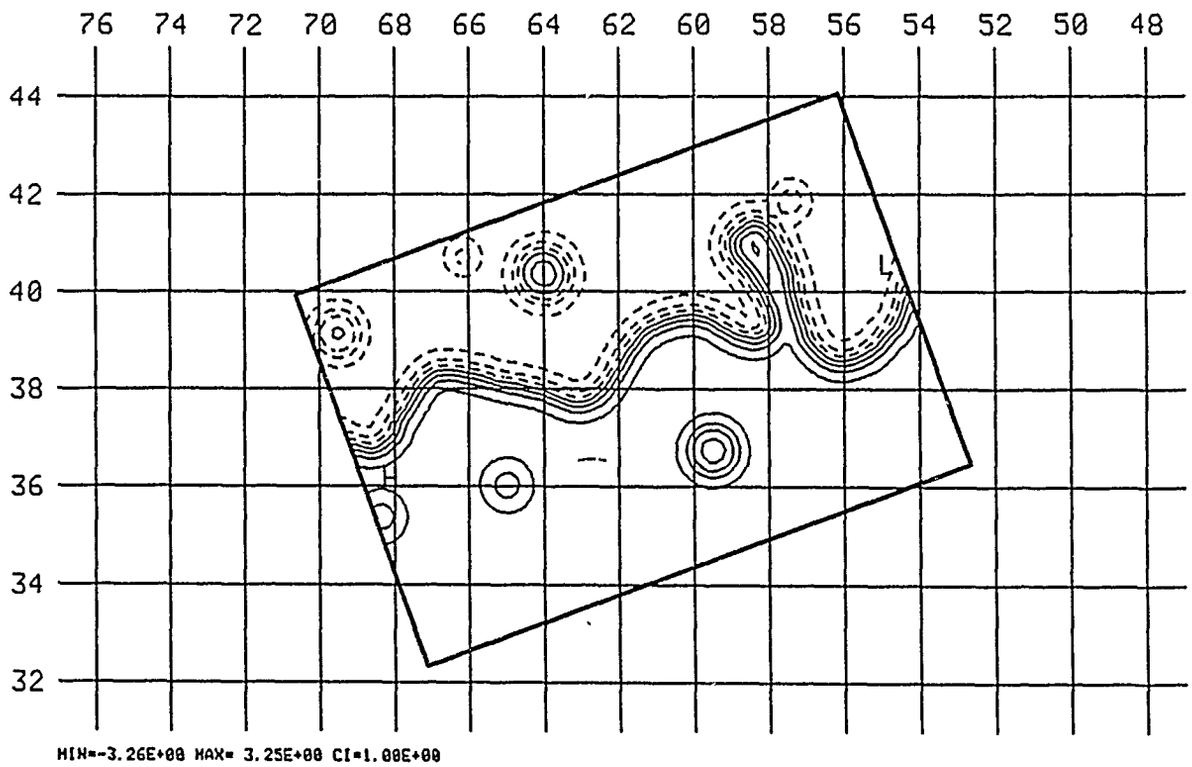

18 FEB 1987

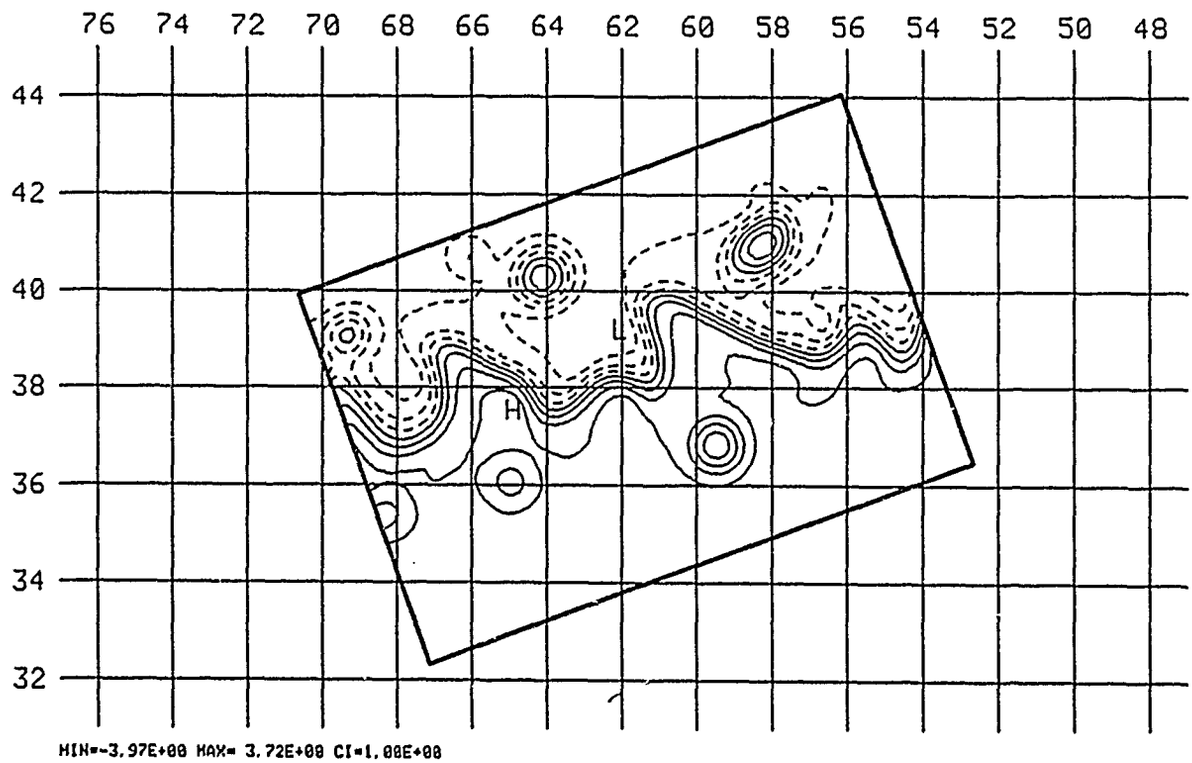

25 FEB 1987

HARVARD UNIVERSITY GULFCAST

RESEARCH OPERATIONAL FORECAST, H9 DOMAIN.
NEW DATA: IR (2/25).
FIGURES: STREAMFUNCTION AT 100. M.

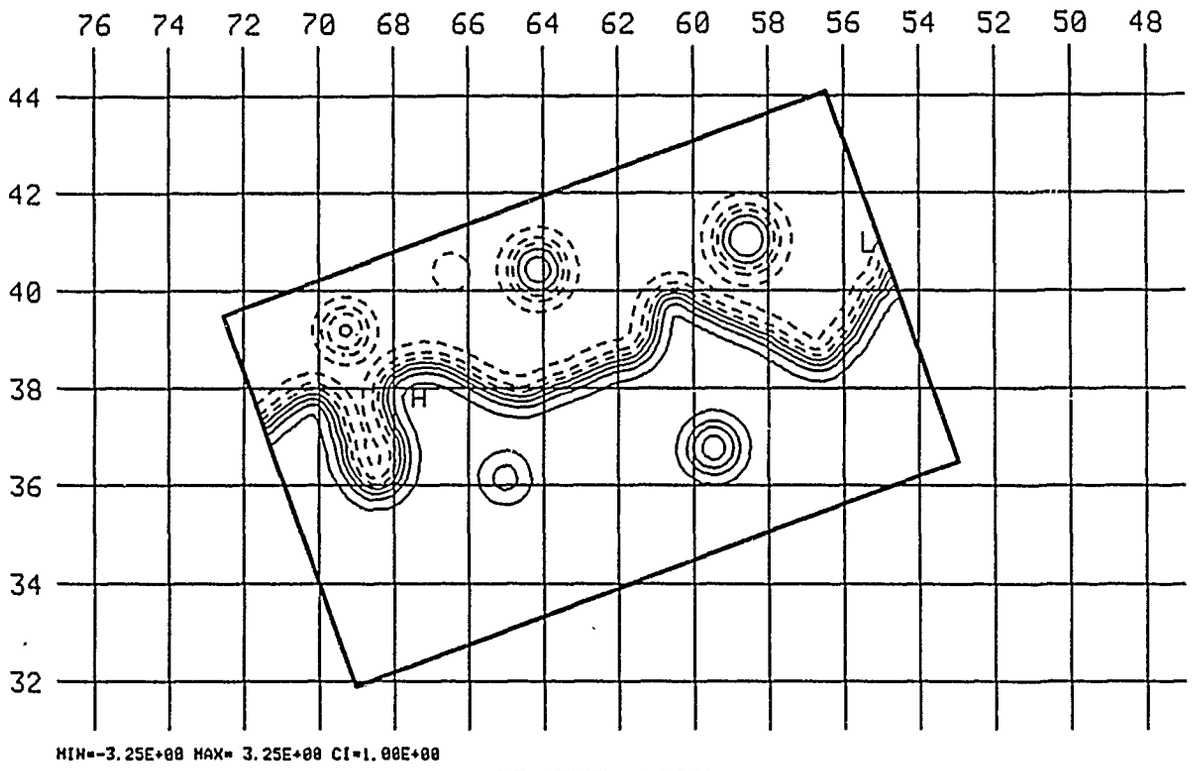

25 FEB 1987

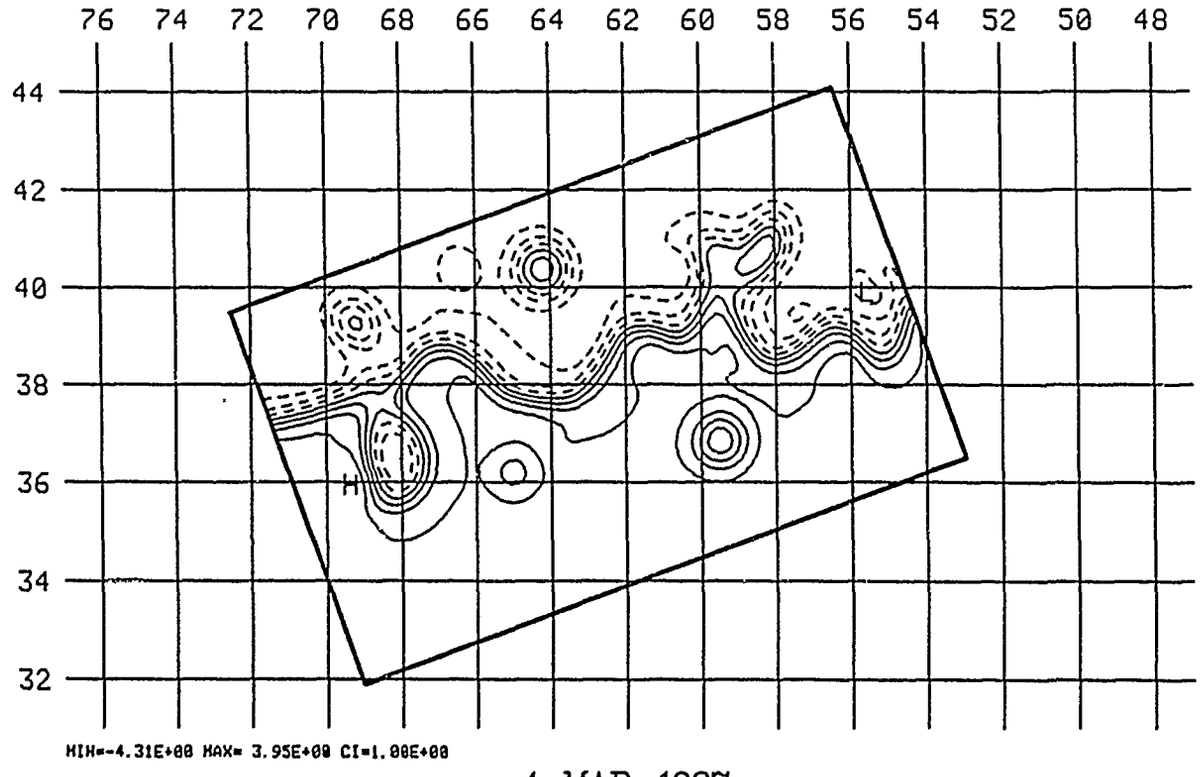

4 MAR 1987

HARVARD UNIVERSITY GULFCAST

RESEARCH OPERATIONAL FORECAST, H9 DOMAIN.
NEW DATA: IR (3/4).
FIGURES: STREAMFUNCTION AT 100. M.

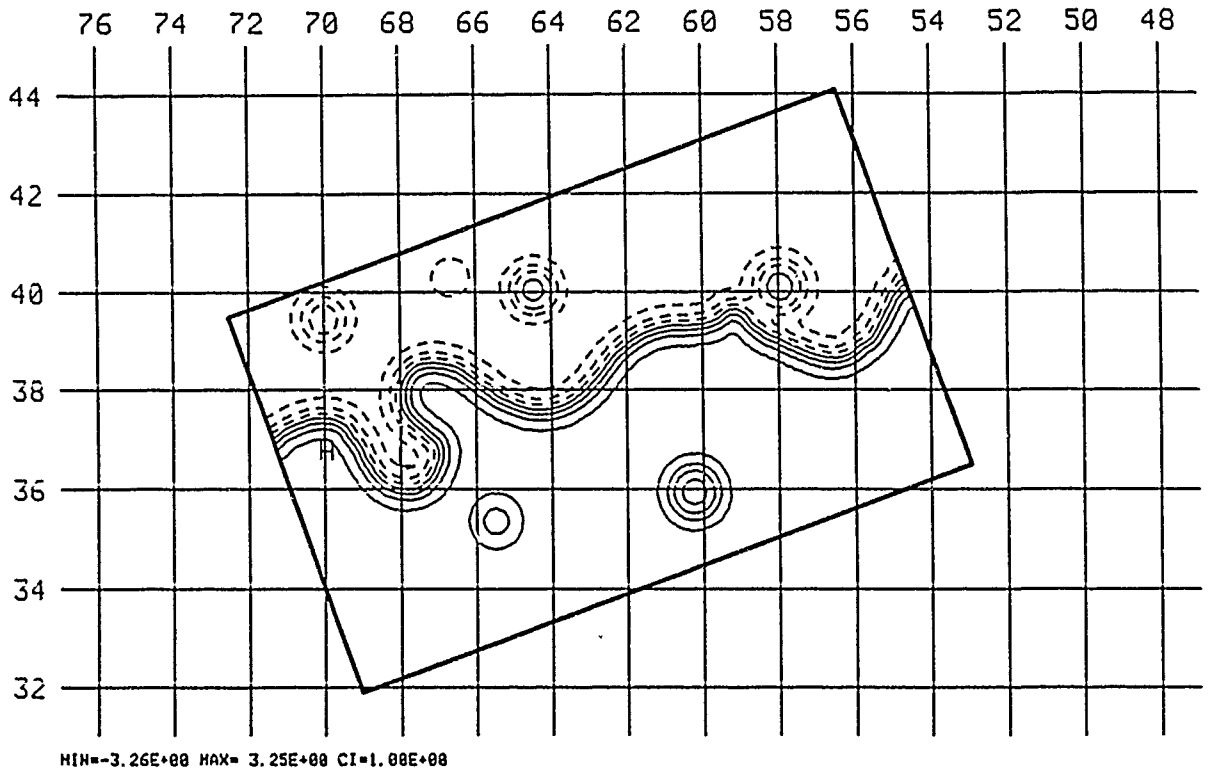

4 MAR 1987

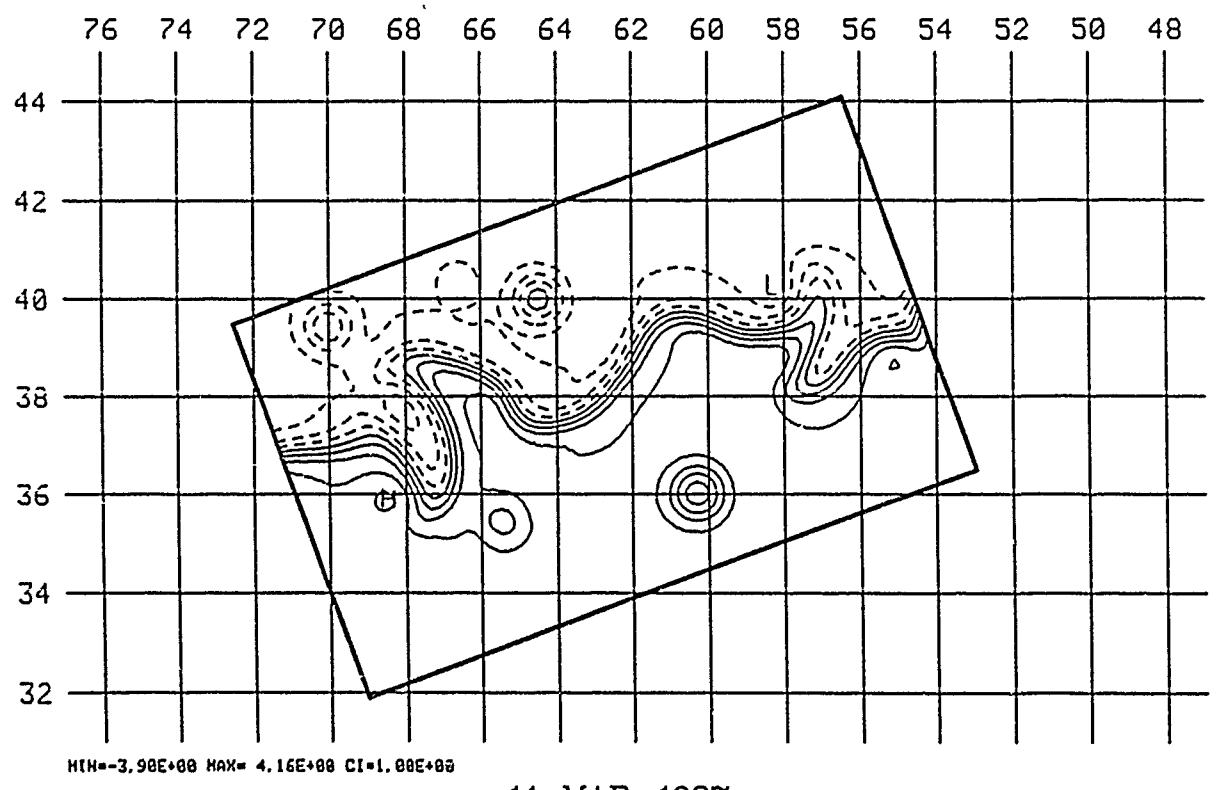

11 MAR 1987

HARVARD UNIVERSITY GULFCAST

RESEARCH OPERATIONAL FORECAST, H10 DOMAIN.
NEW DATA: IR (3/9), AXBT (3/11).
FIGURES: STREAMFUNCTION AT 100. M.

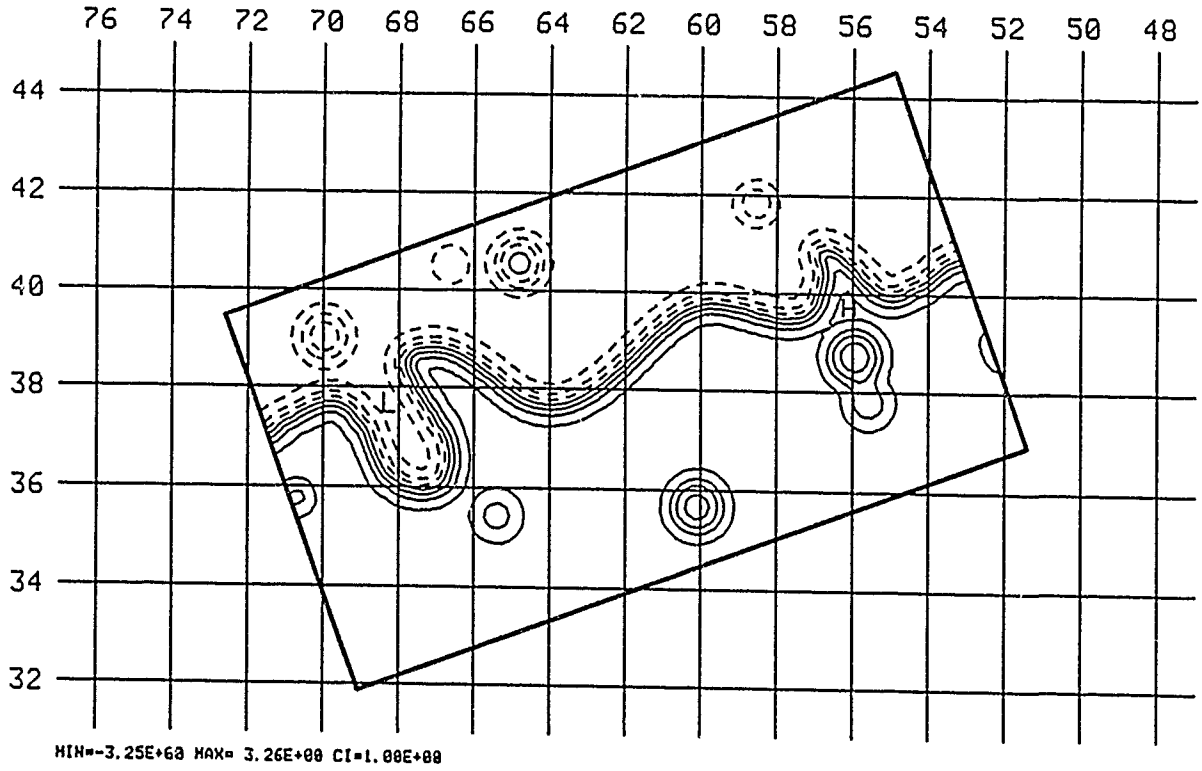

11 MAR 1987

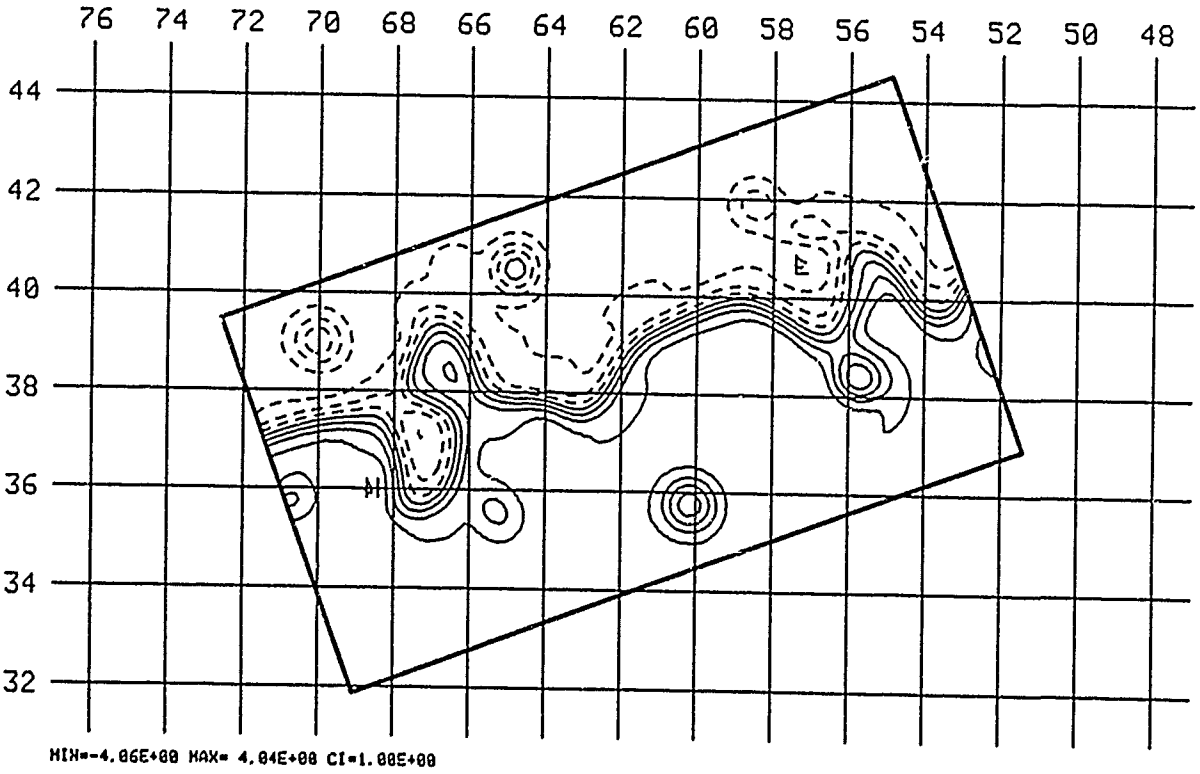

18 MAR 1987

HARVARD UNIVERSITY GULFCAST

RESEARCH OPERATIONAL FORECAST, H10 DOMAIN.
NEW DATA: IR (3/18).
FIGURES: STREAMFUNCTION AT 100. M.

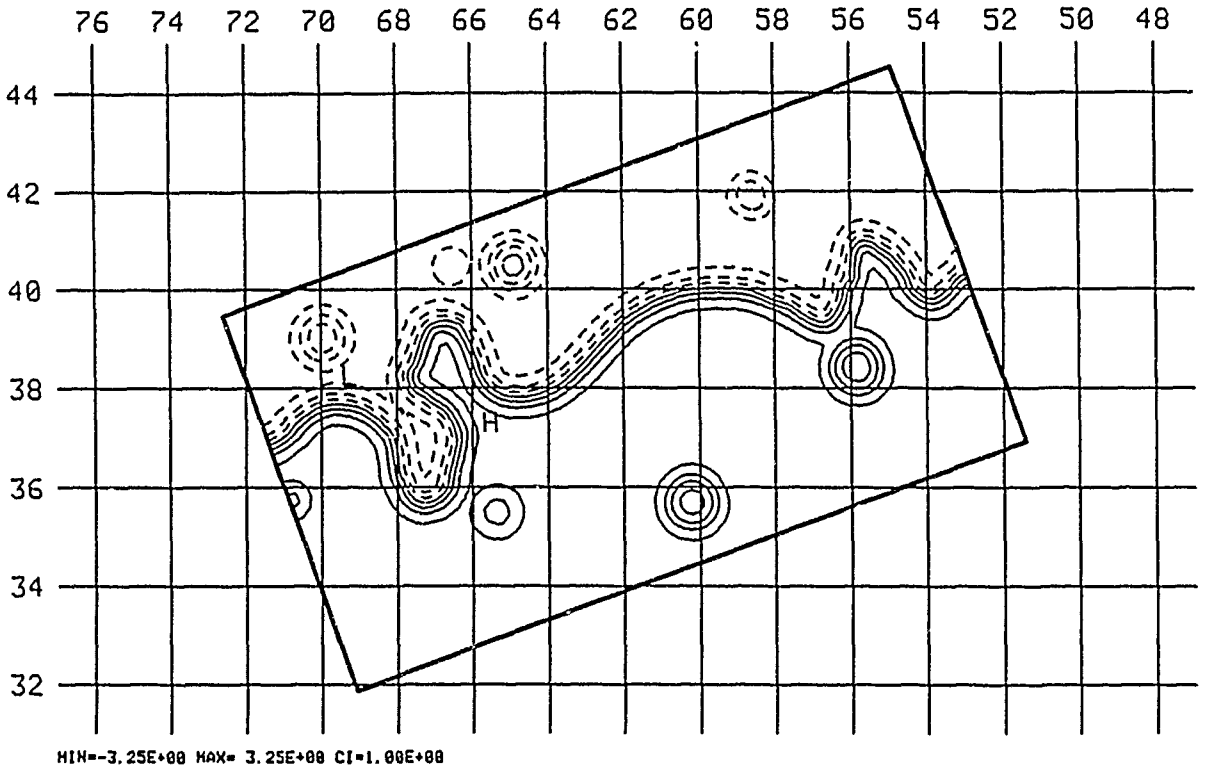

18 MAR 1987

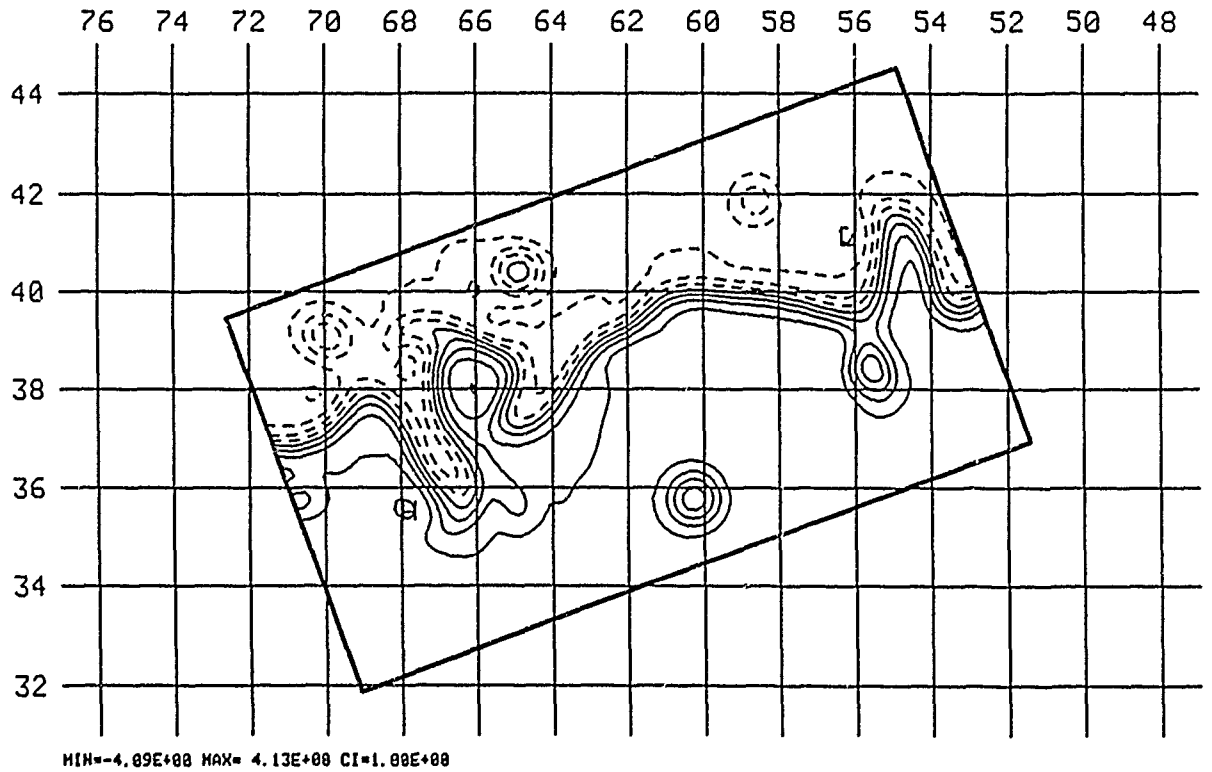

25 MAR 1987

HARVARD UNIVERSITY GULFCAST

RESEARCH OPERATIONAL FORECAST, H10 DOMAIN.
NEW DATA: IR (3/25).
FIGURES: STREAMFUNCTION AT 100. M.

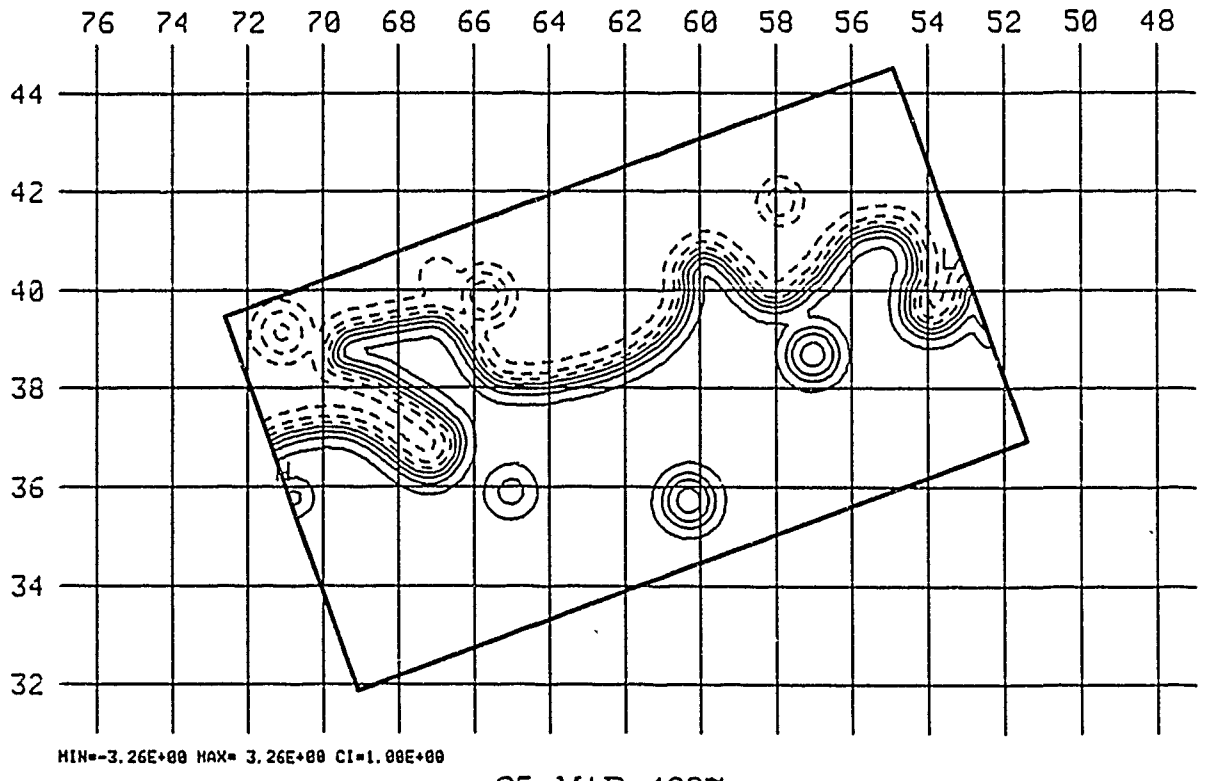

25 MAR 1987

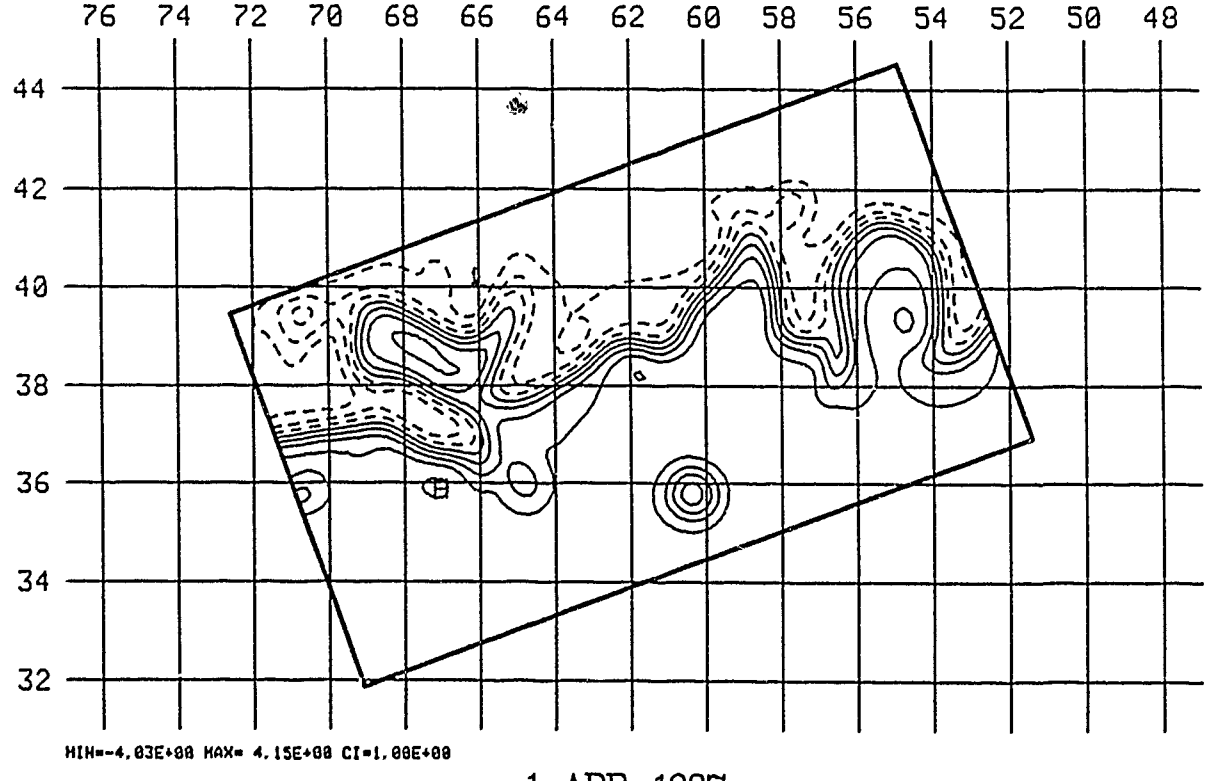

1 APR 1987

HARVARD UNIVERSITY GULFCAST

RESEARCH OPERATIONAL FORECAST, H10 DOMAIN.
NEW DATA: IR (4/1), AXBT(4/1) .
FIGURES: STREAMFUNCTION AT 100. M.

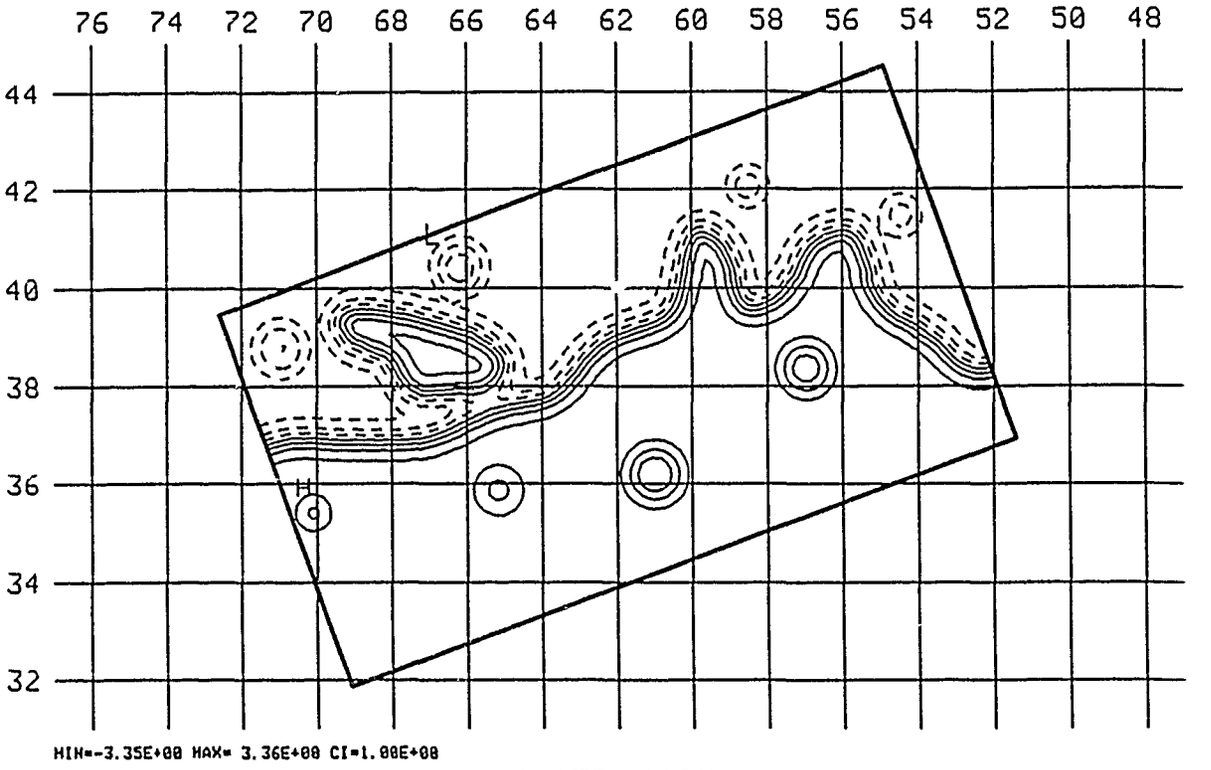

1 APR 1987

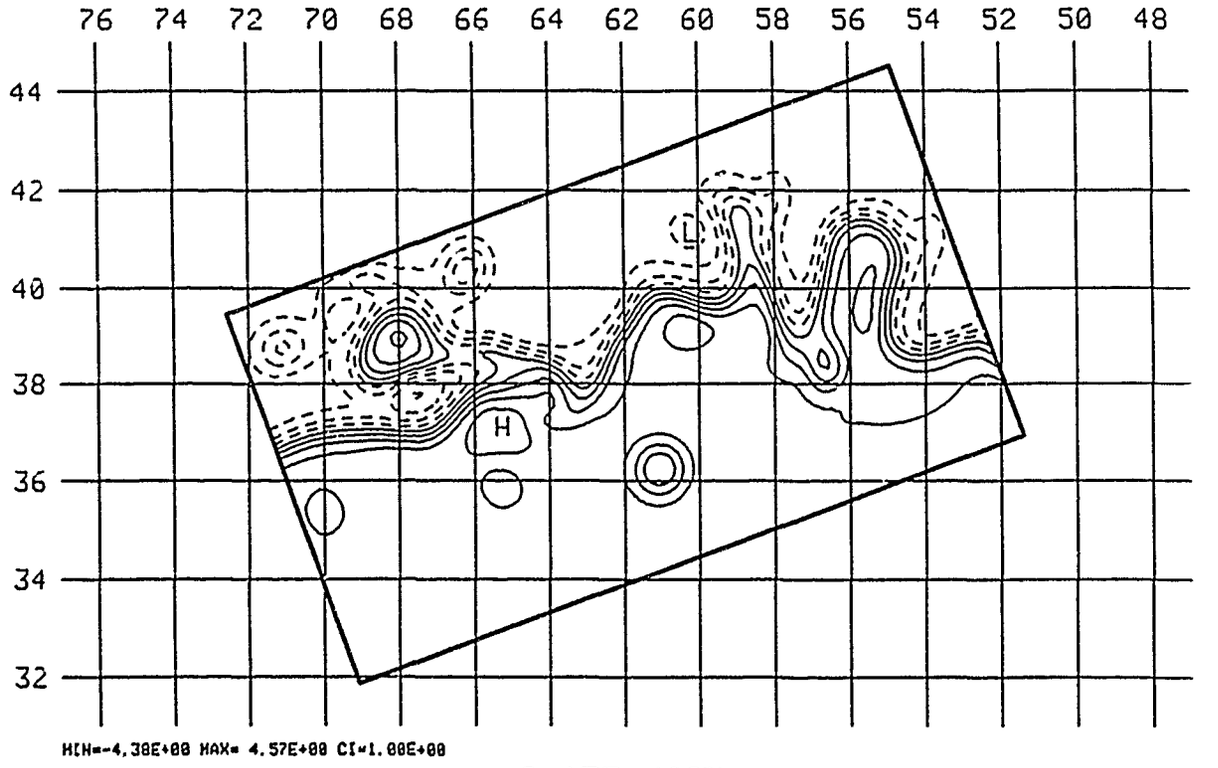

8 APR 1987

HARVARD UNIVERSITY GULFCAST

RESEARCH OPERATIONAL FORECAST, H10 DOMAIN.
NEW DATA: IR (4/8).
FIGURES: STREAMFUNCTION AT 100. M.

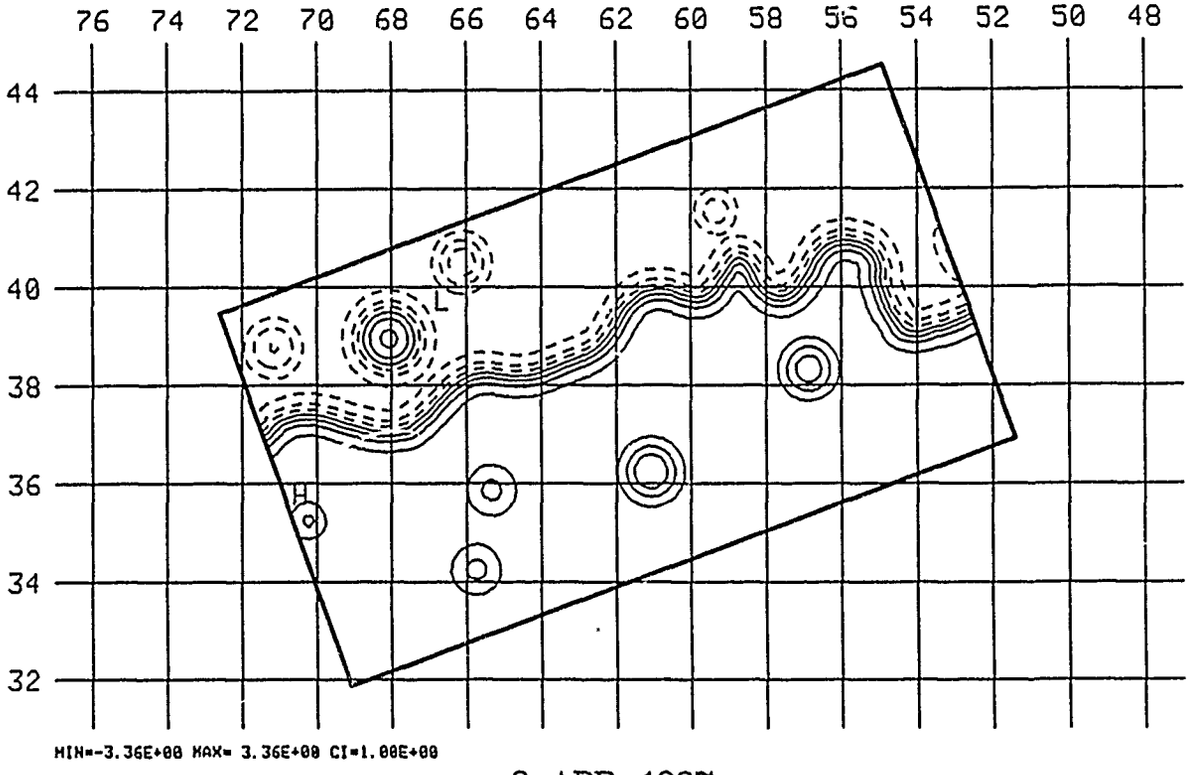

8 APR 1987

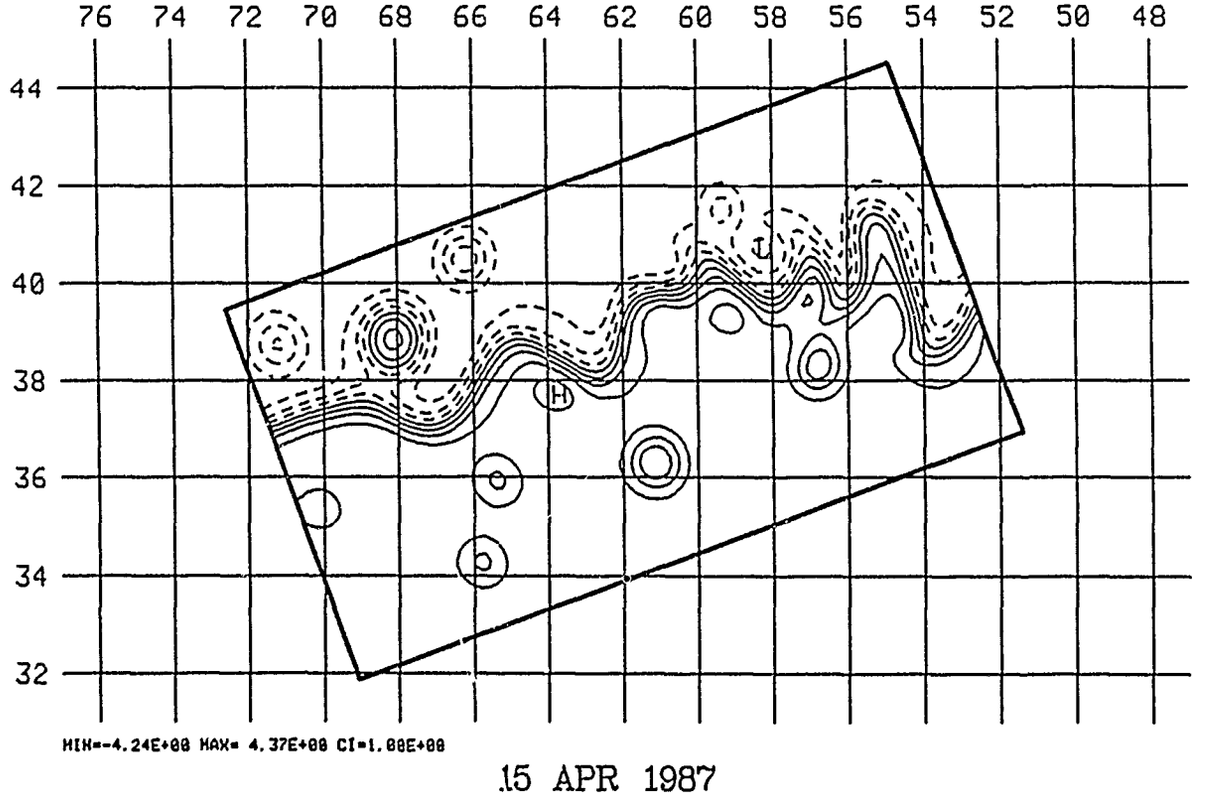

15 APR 1987

HARVARD UNIVERSITY GULFCAST

RESEARCH OPERATIONAL FORECAST, H10 DOMAIN.
NEW DATA: IR (4/13, 4/14, 4/15), XBT (4/15).
FIGURES: STREAMFUNCTION AT 100. M.

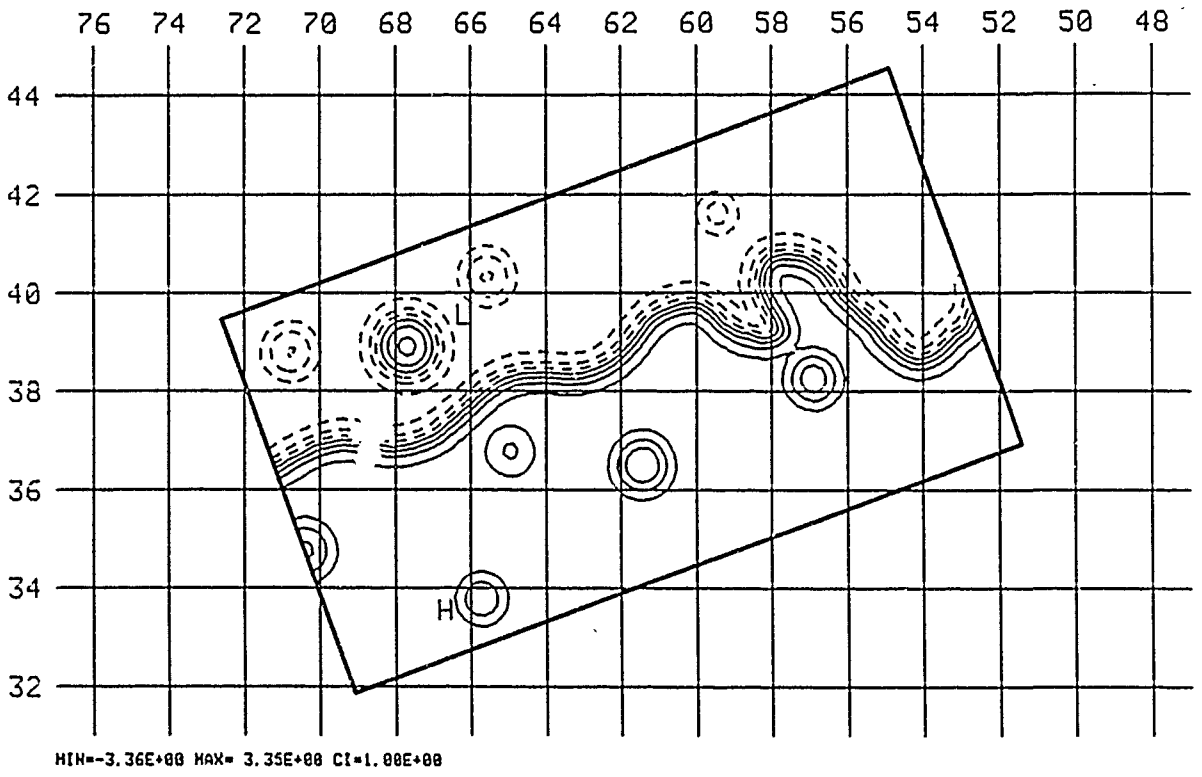

15 APR 1987

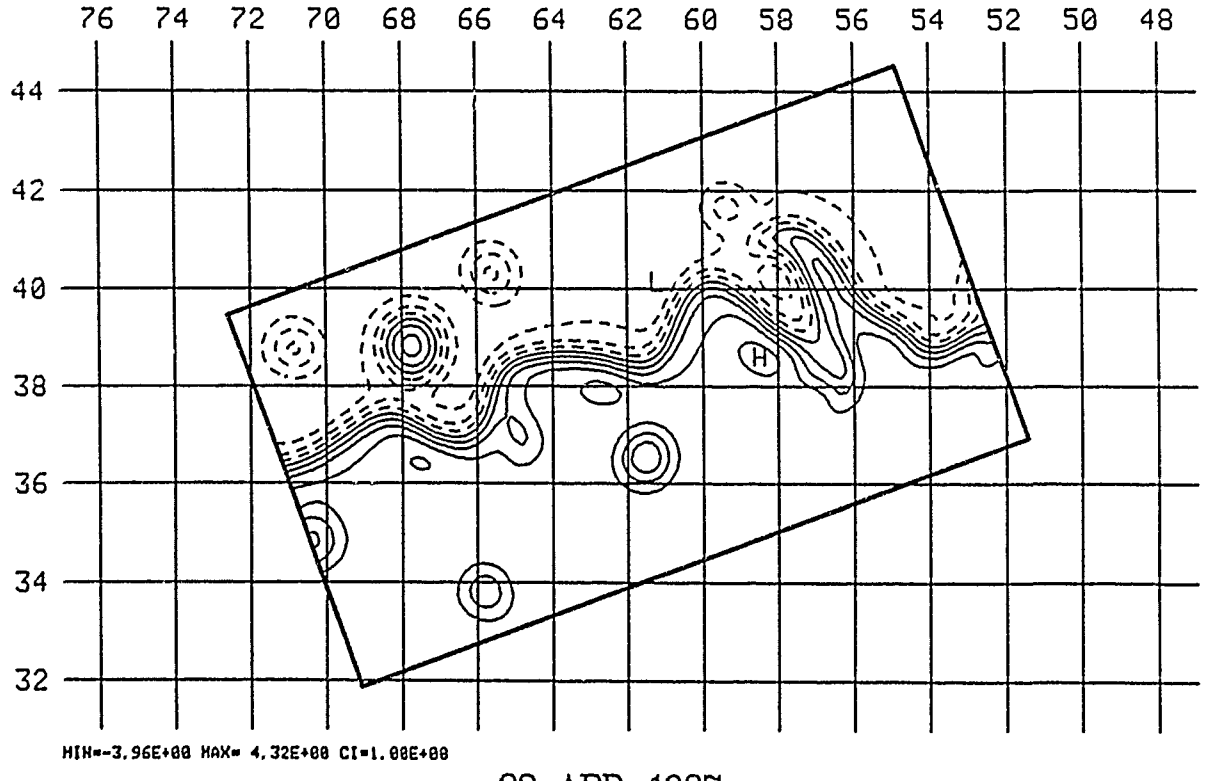

22 APR 1987

HARVARD UNIVERSITY GULFCAST

RESEARCH OPERATIONAL FORECAST, H10 DOMAIN.
NEW DATA: IR (4/20, 4/22), XBT(4/22).
FIGURES: STREAMFUNCTION AT 100. M.

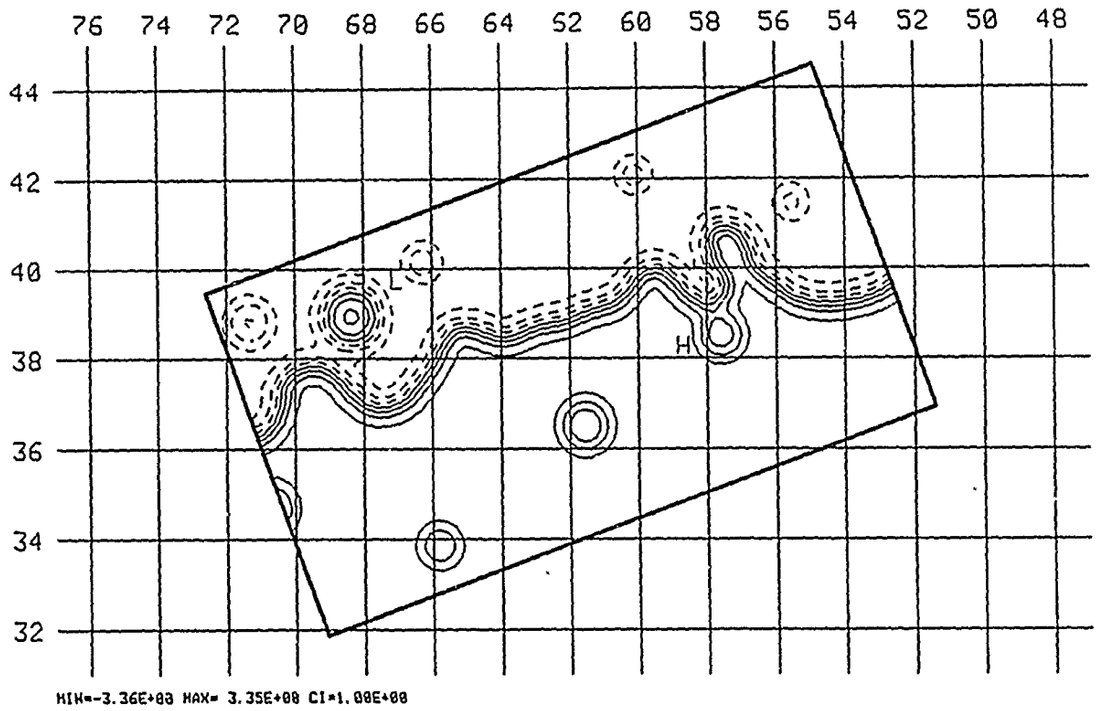

22 APR 1987

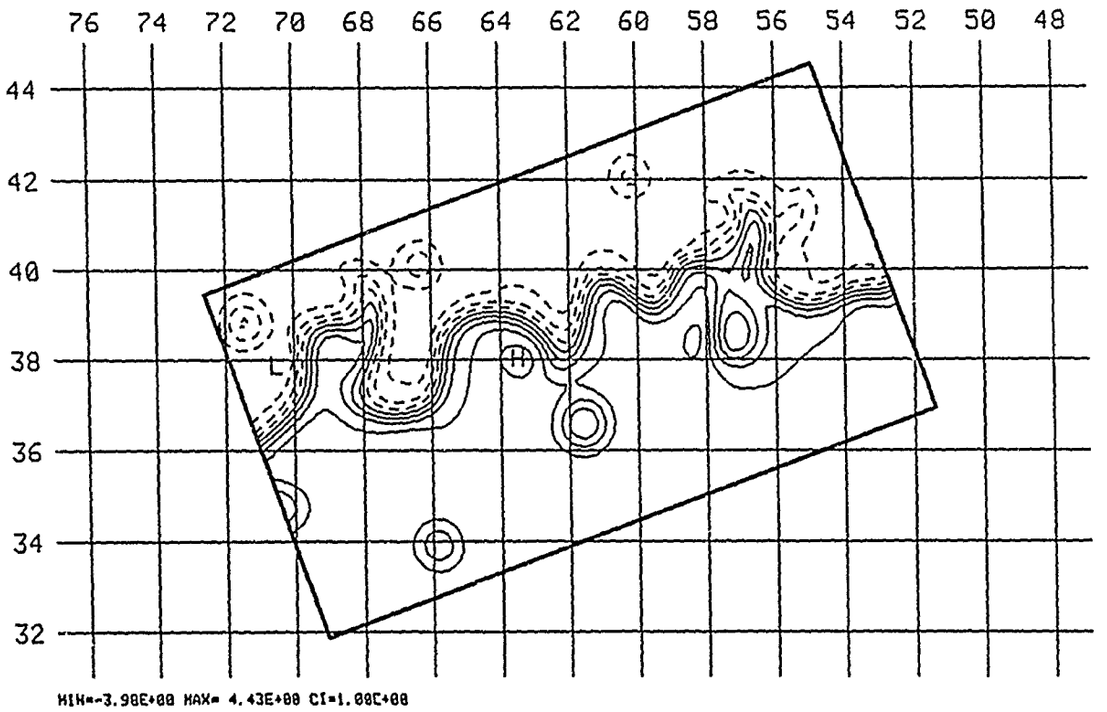

29 APR 1987

HARVARD UNIVERSITY GULFCAST

RESEARCH OPERATIONAL FORECAST, H10 DOMAIN.
NEW DATA: IR (4/29).
FIGURES: STREAMFUNCTION AT 100. M.

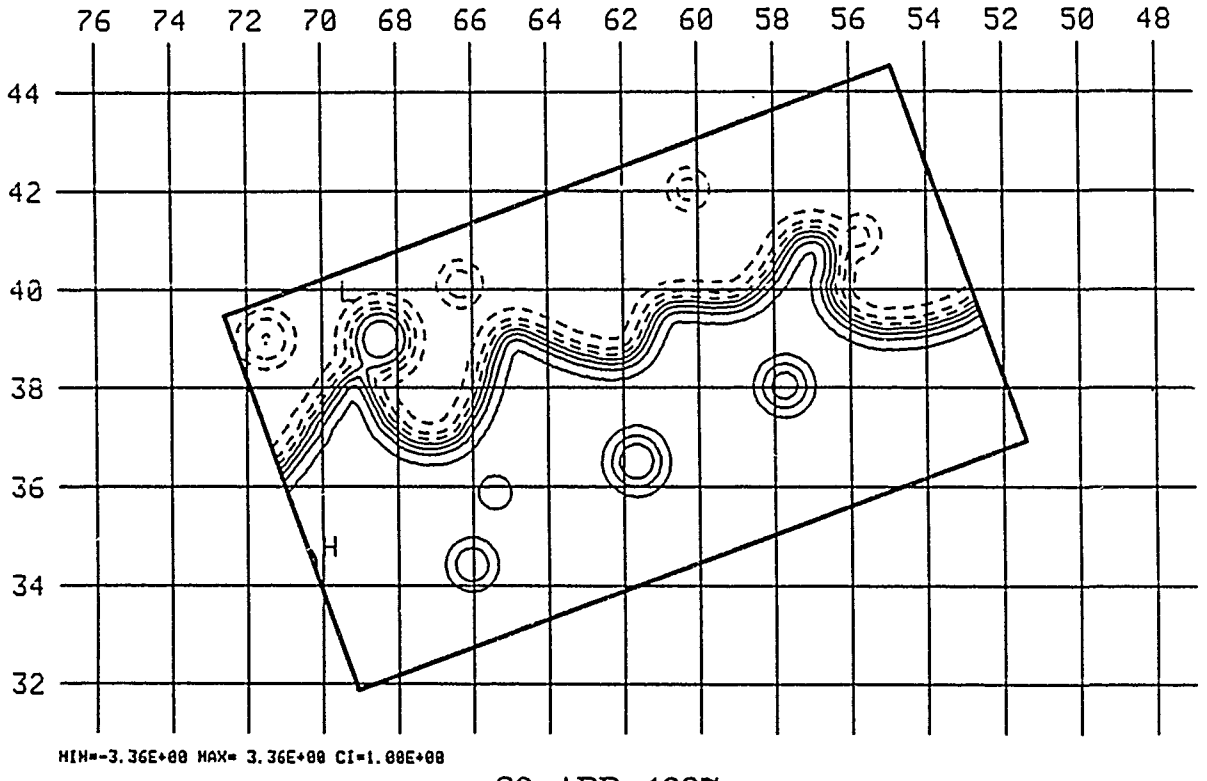

29 APR 1987

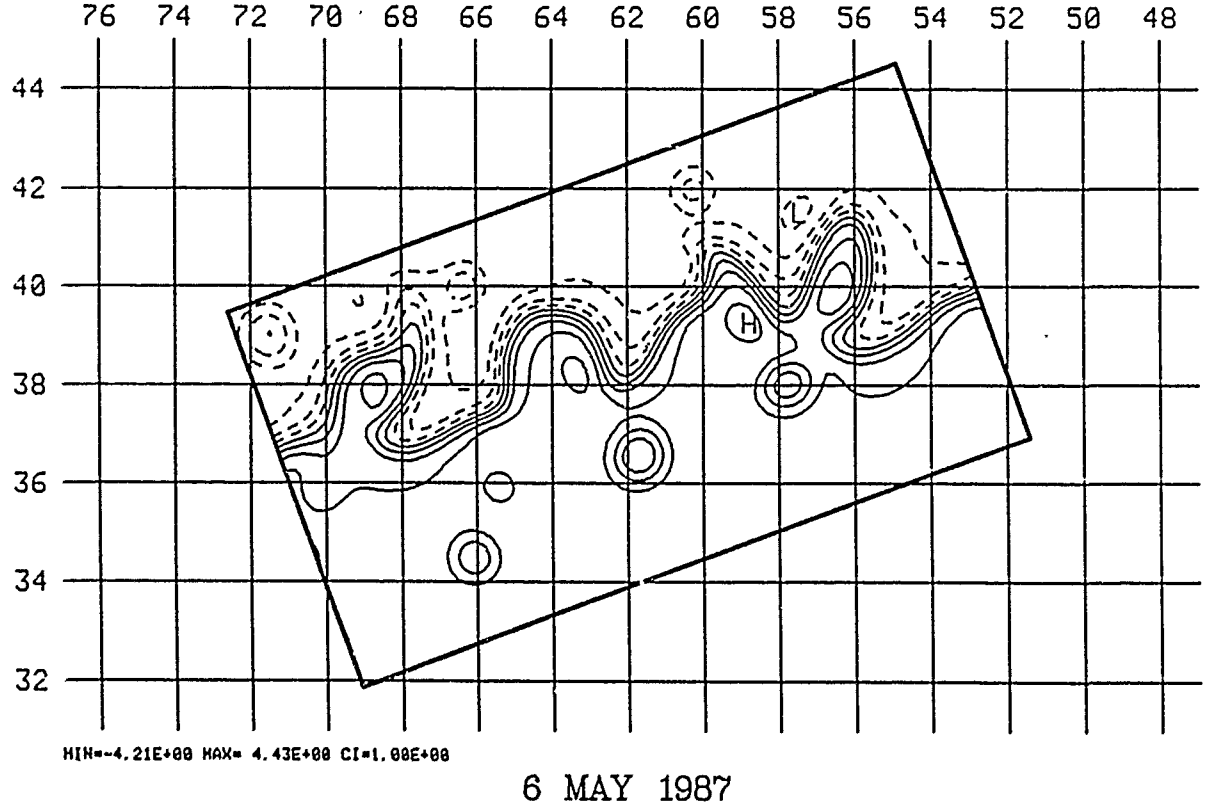

6 MAY 1987

HARVARD UNIVERSITY GULFCAST

RESEARCH OPERATIONAL FORECAST, H10 DOMAIN.
NEW DATA: IR (5/4, 5/6).
FIGURES: STREAMFUNCTION AT 100. M.

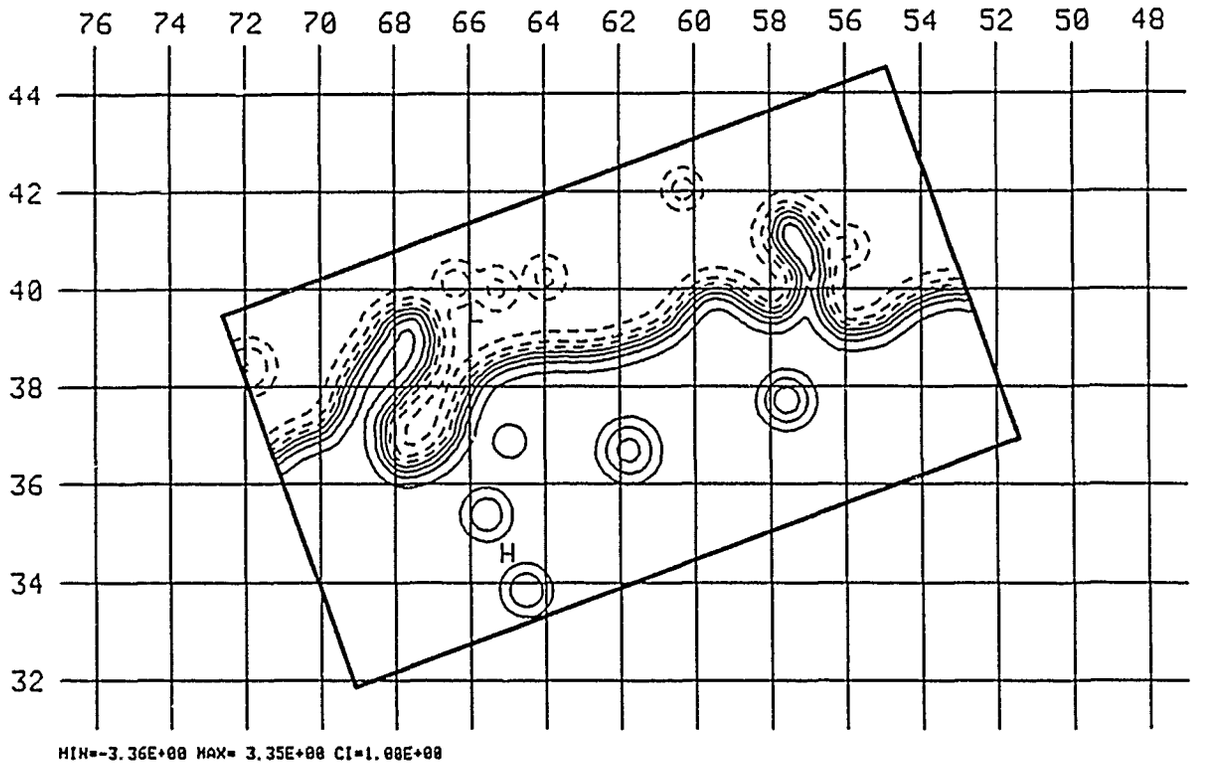

6 MAY 1987

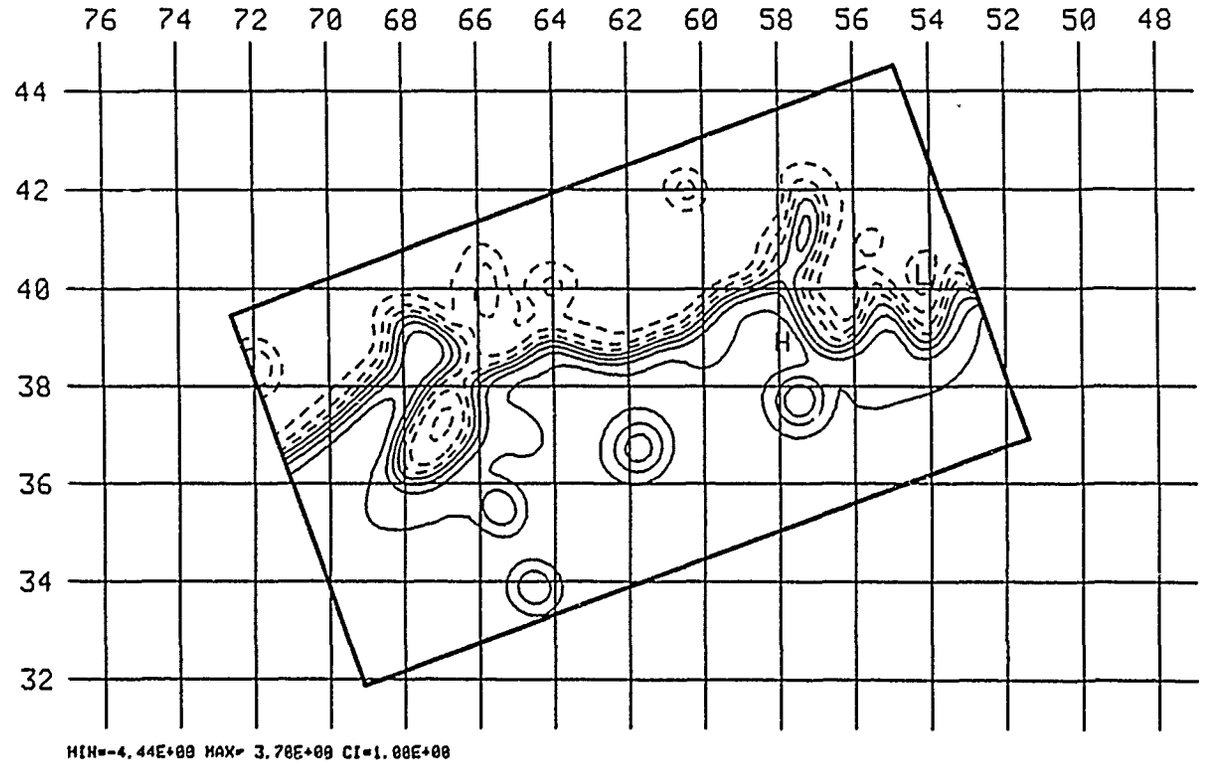

13 MAY 1987

HARVARD UNIVERSITY GULFCAST

RESEARCH OPERATIONAL FORECAST, H10 DOMAIN.
NEW DATA: IR (5/11).
Figures: Streamfunction at 100. m.

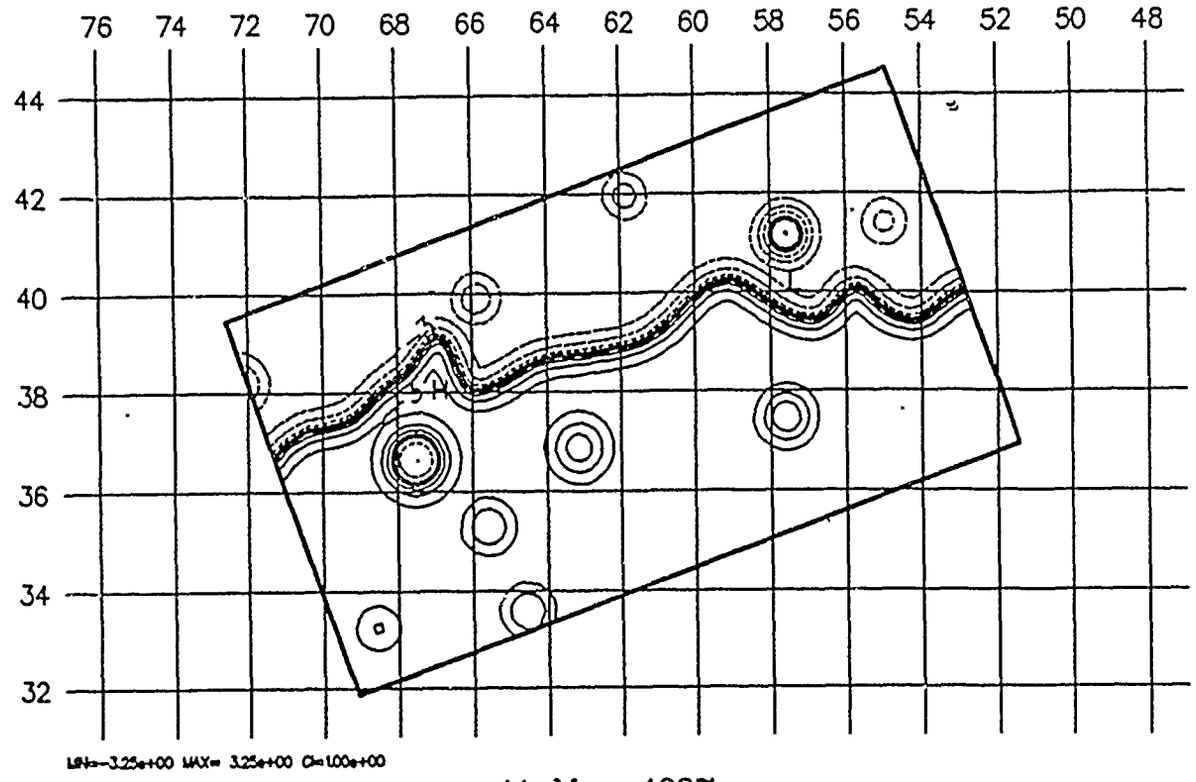

11 May 1987

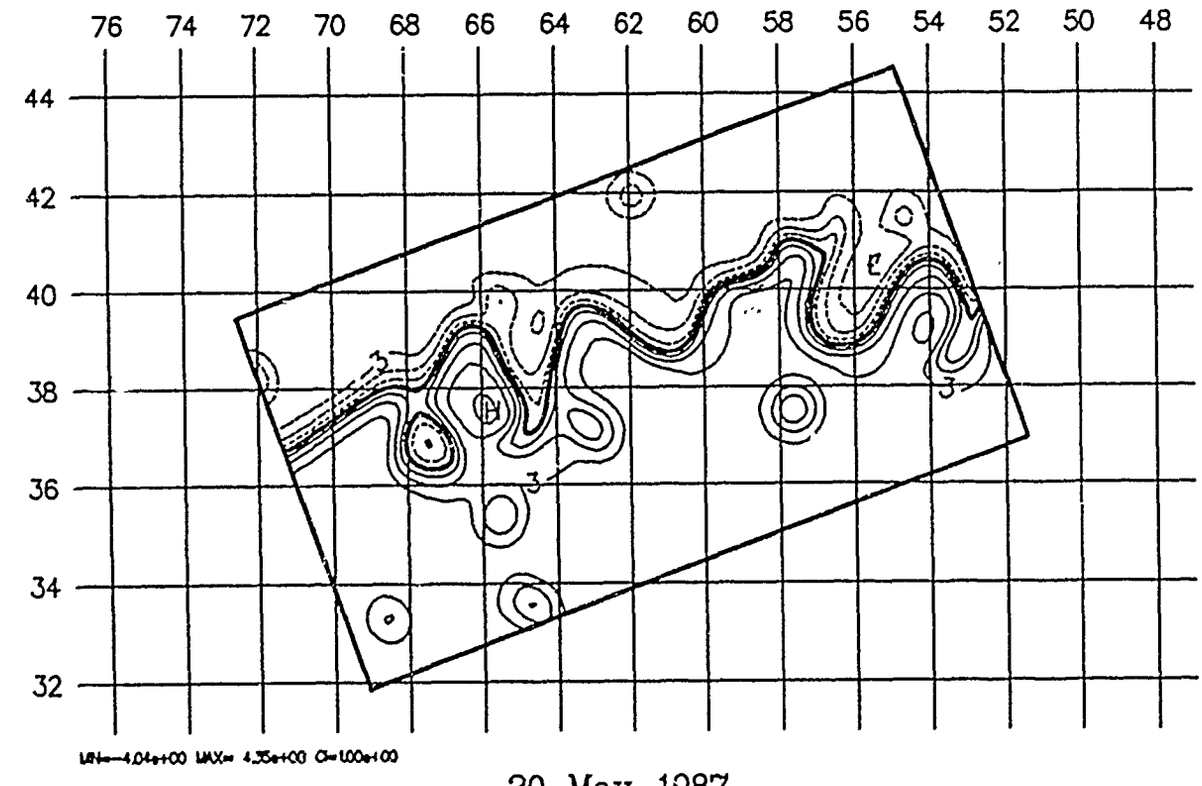

20 May 1987

HARVARD UNIVERSITY GULFCAST

RESEARCH OPERATIONAL FORECAST, H10 DOMAIN.
NEW DATA: IR (5/18,5/20).
Figures: Streamfunction at 100. m.

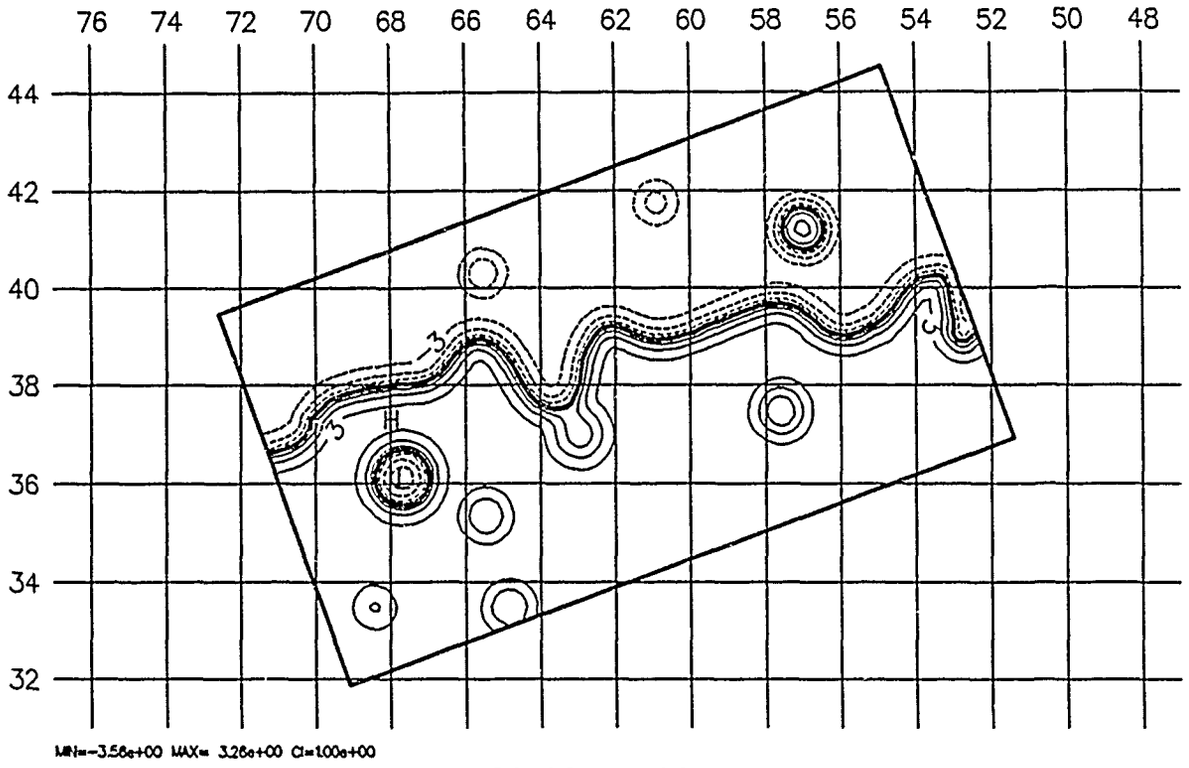

20 May 1987

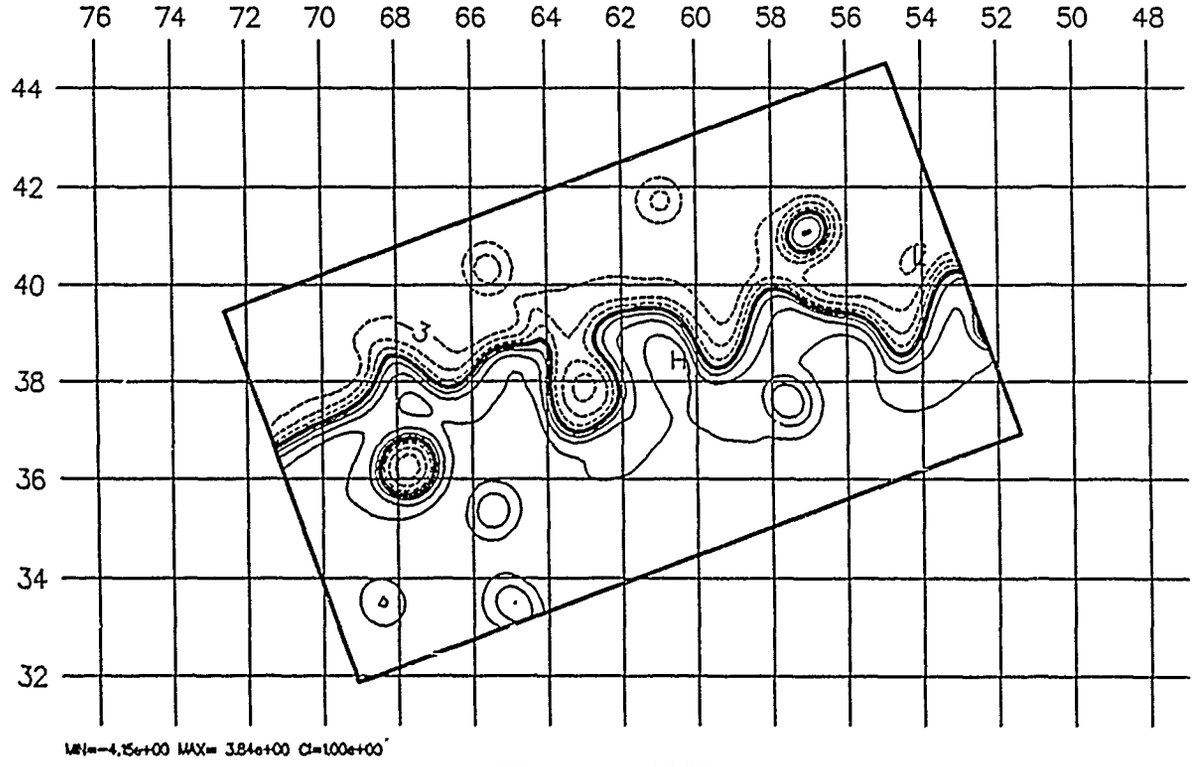

27 May 1987

HARVARD UNIVERSITY GULFCAST

RESEARCH OPERATIONAL FORECAST.

NEW DATA: IR (5/27).

Figures: Streamfunction at 100. m.

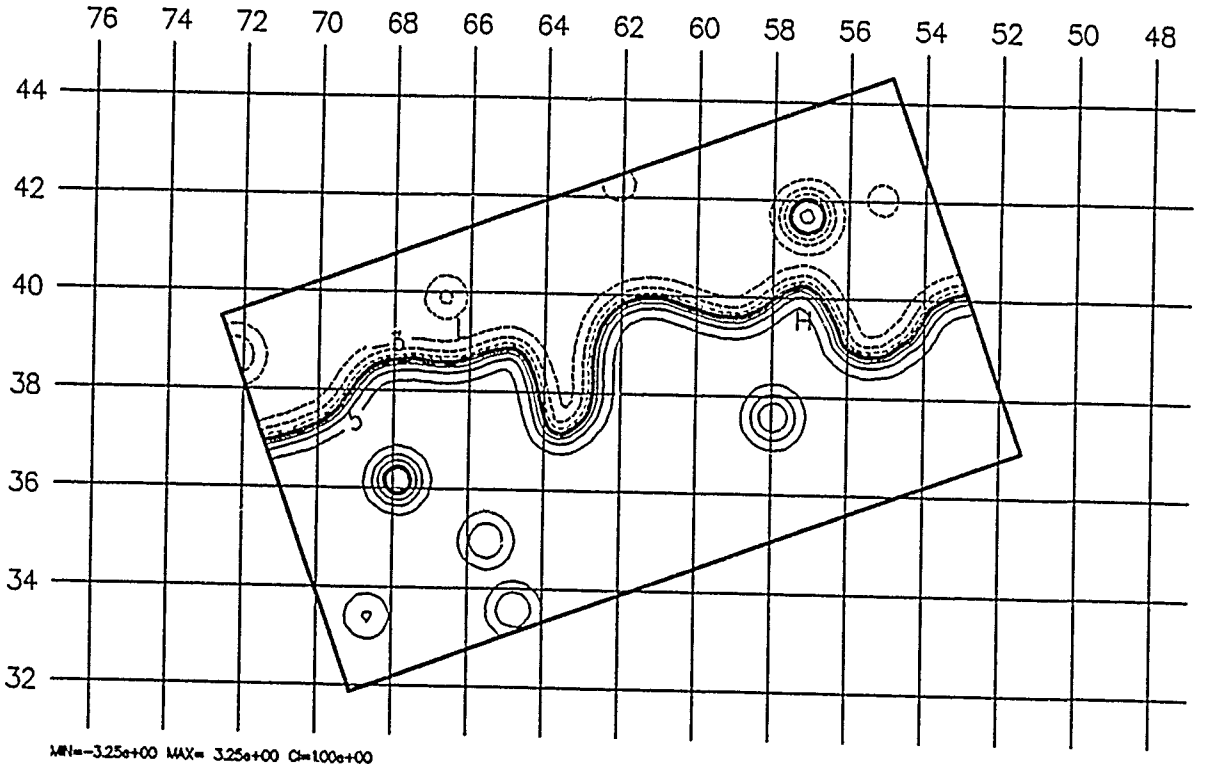

27 May 1987

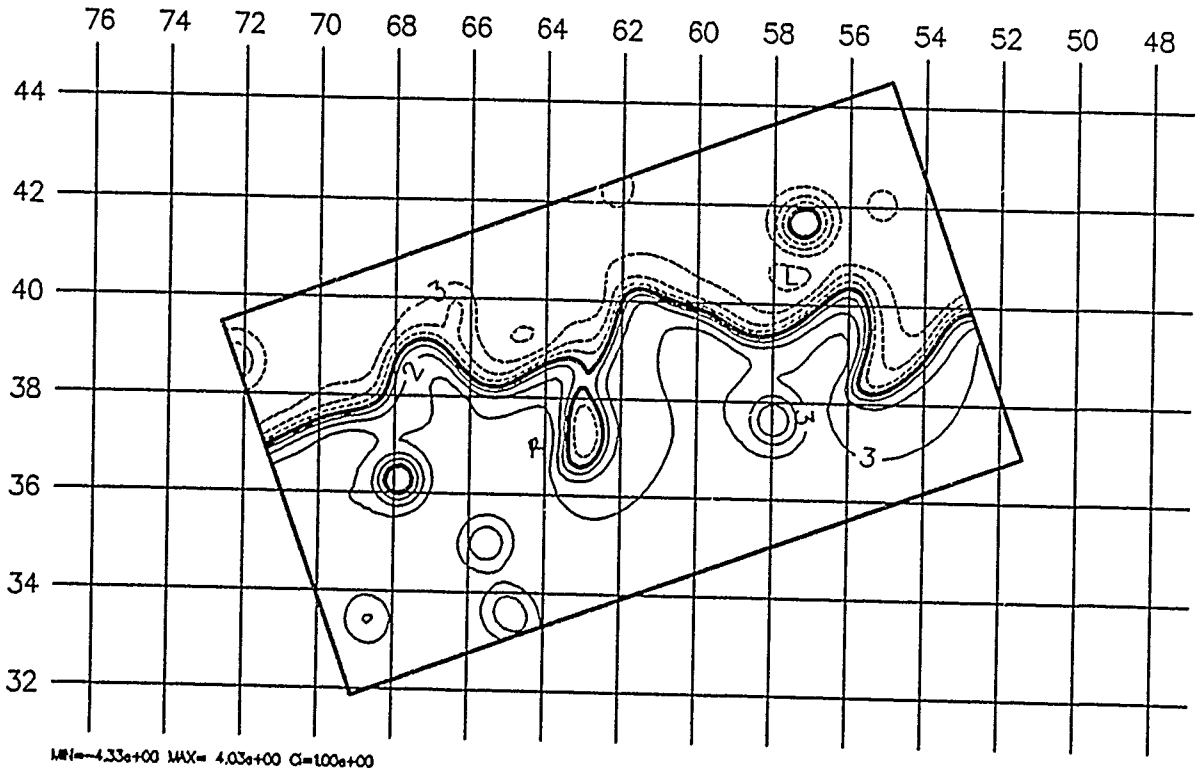

3 Jun 1987

HARVARD UNIVERSITY GULFCAST

RESEARCH OPERATIONAL FORECAST.
NEW DATA: IR (6/1, 6/3), AXBT (6/3).
Figures: Streamfunction at 100. m.

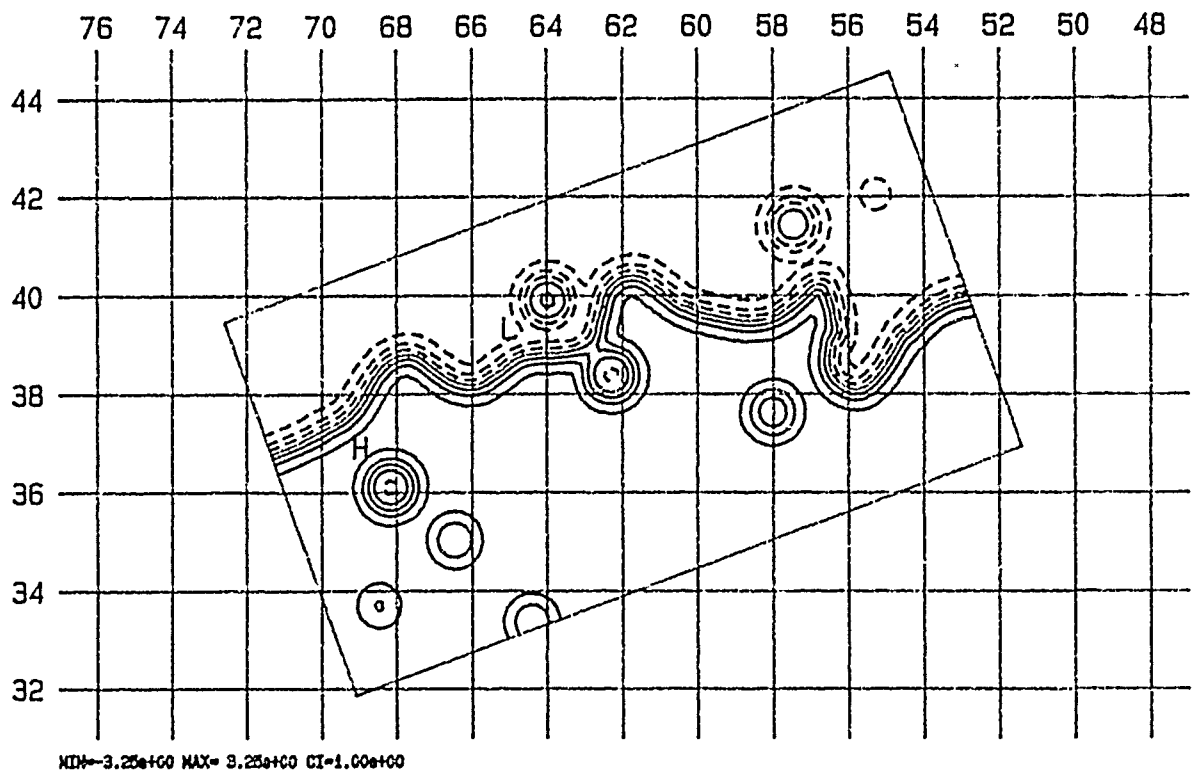

3 Jun 1987

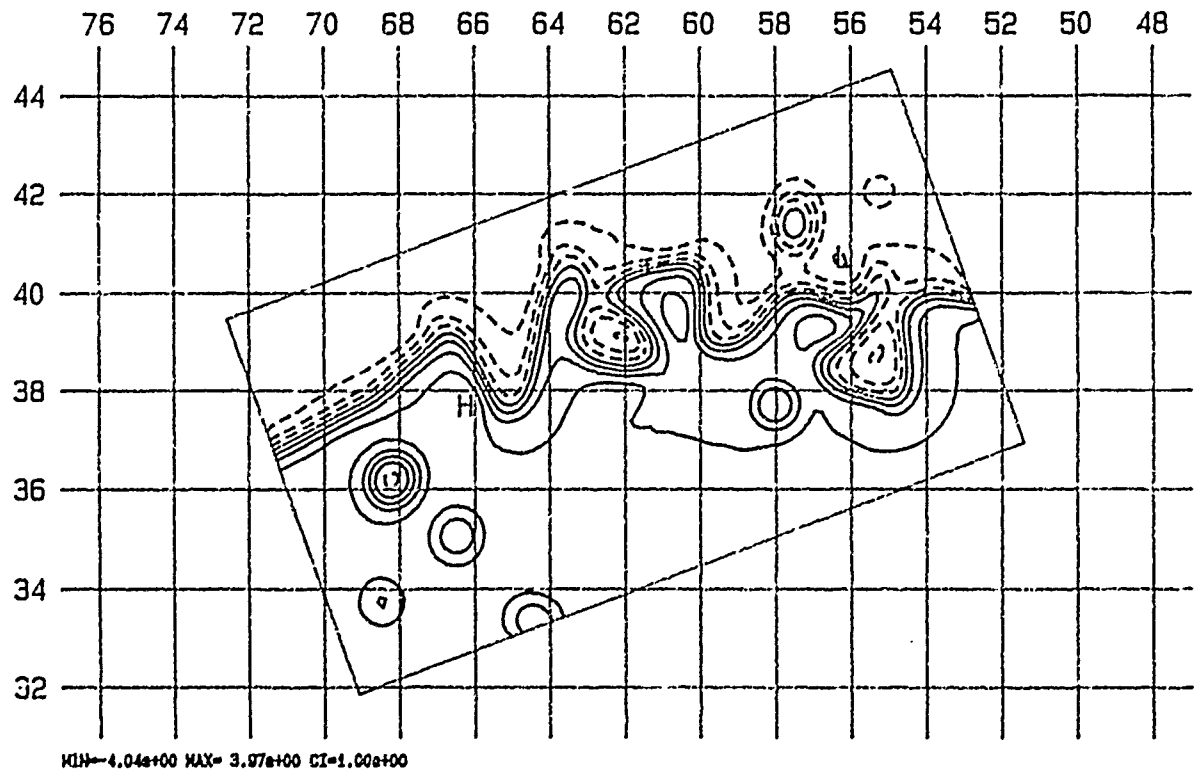

10 Jun 1987

HARVARD UNIVERSITY GULFCAST

RESEARCH OPERATIONAL FORECAST.
NEW DATA: IR (6/1, 6/3), AXBT(6/3).
Figures: Streamfunction at 100. m.

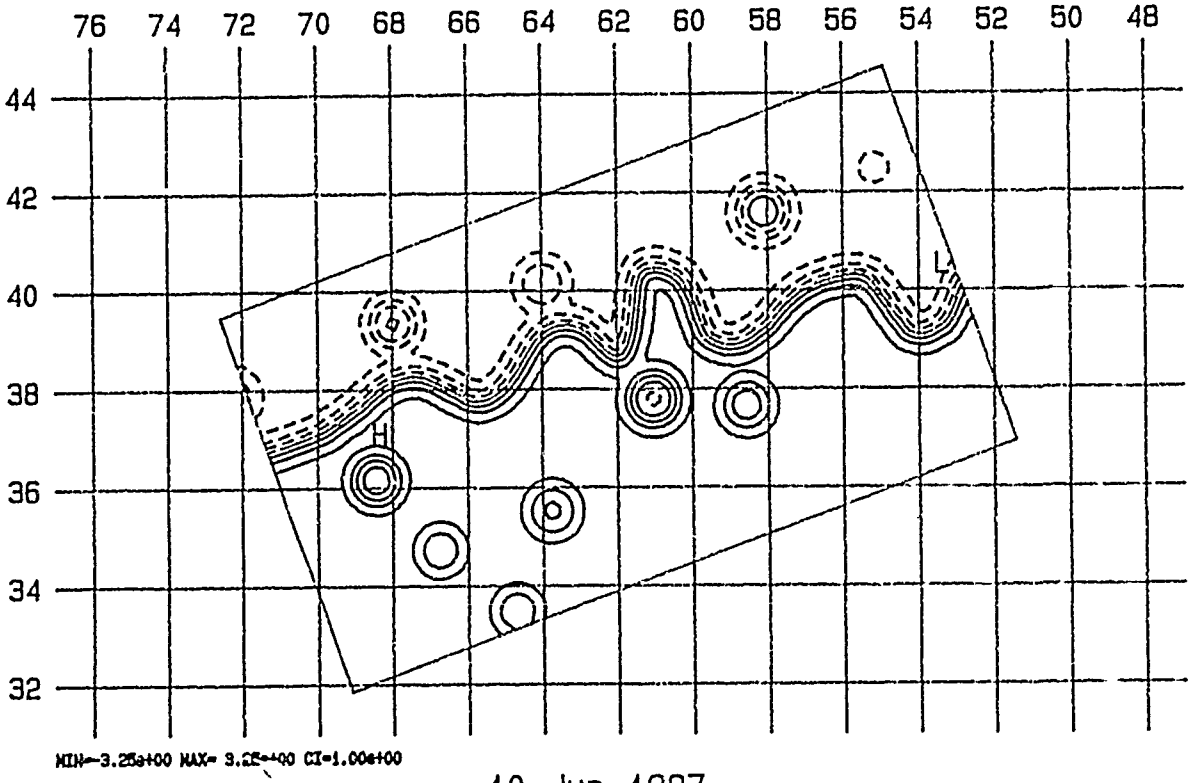

10 Jun 1987

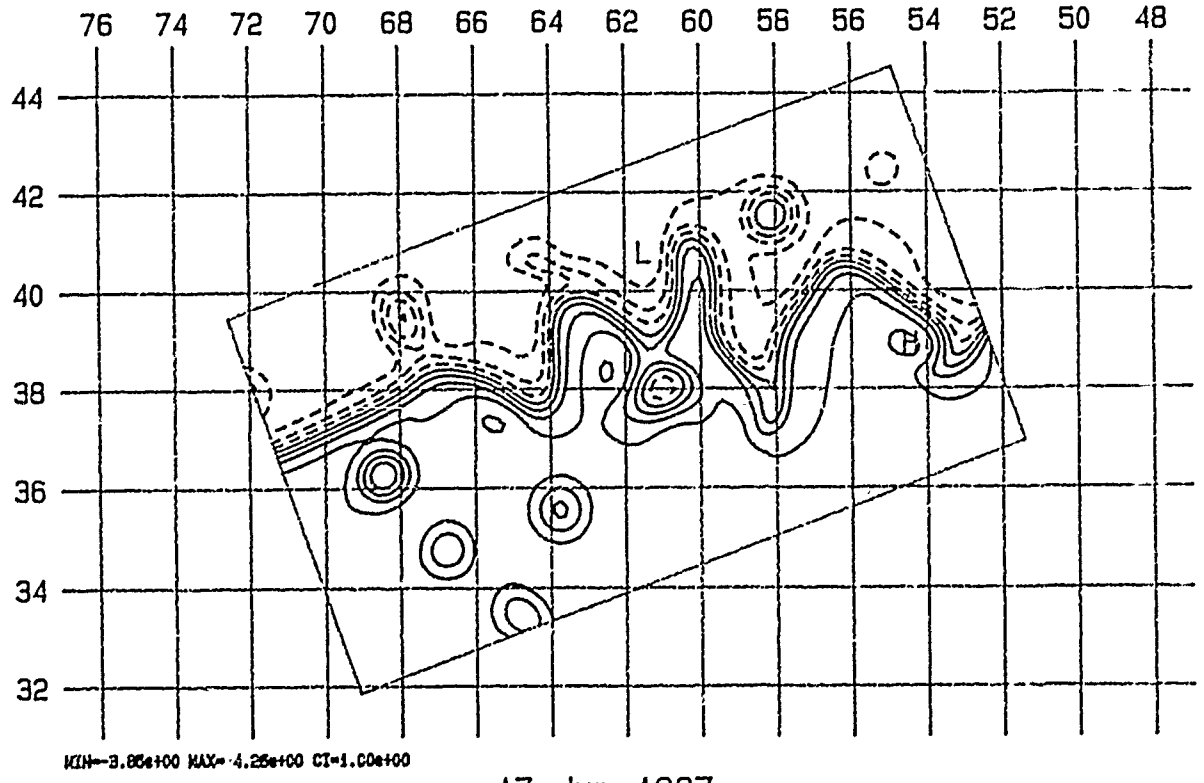

17 Jun 1987

HARVARD UNIVERSITY GULFCAST

RESEARCH OPERATIONAL FORECAST.
NEW DATA: IR (6/15, 6/17).
Figures: Streamfunction at 100. m.

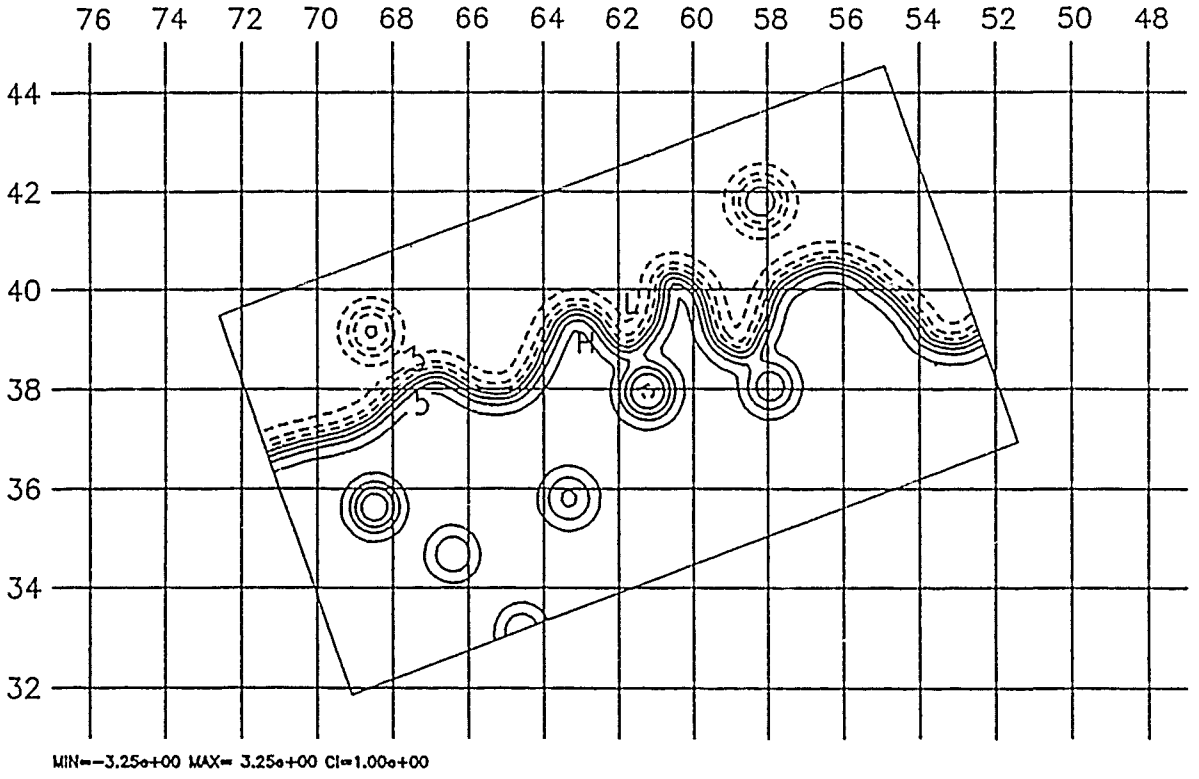

17 Jun 1987

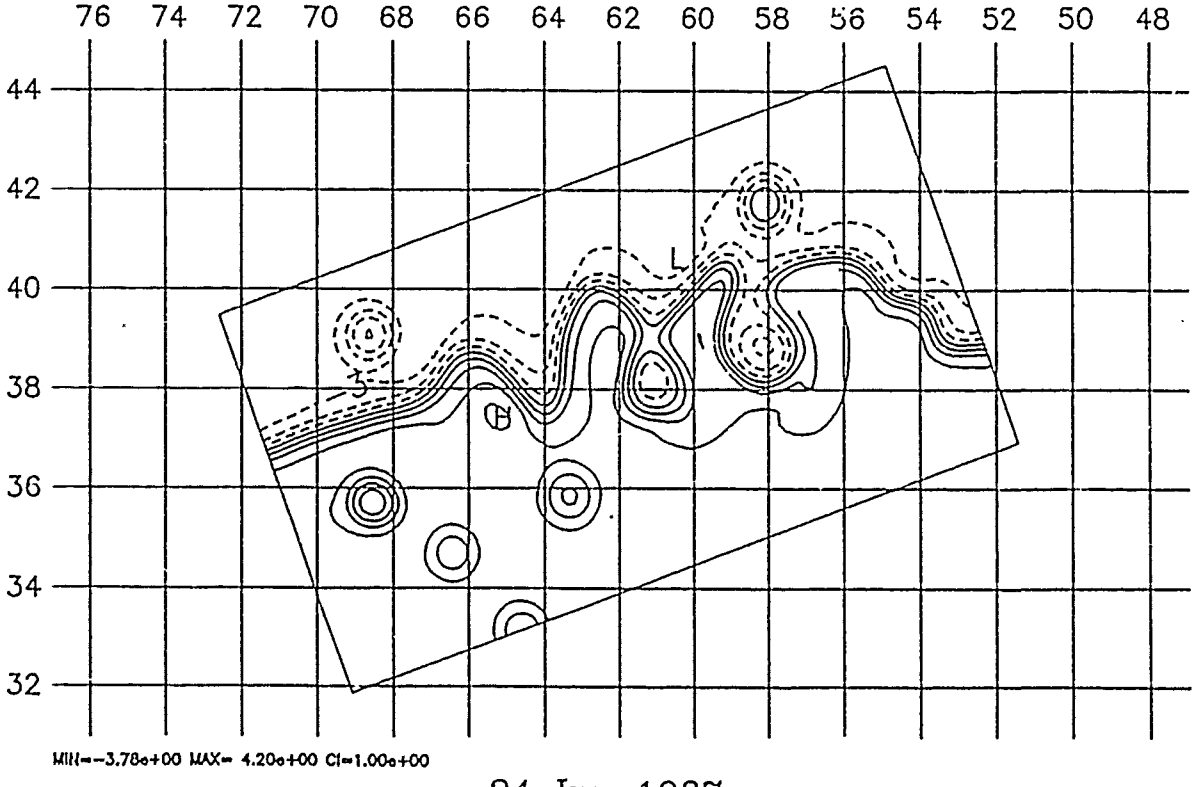

24 Jun 1987

HARVARD UNIVERSITY GULFCAST

RESEARCH OPERATIONAL FORECAST.
NEW DATA: IR (6/22, 6/24).
Figures: Streamfunction at 100. m.

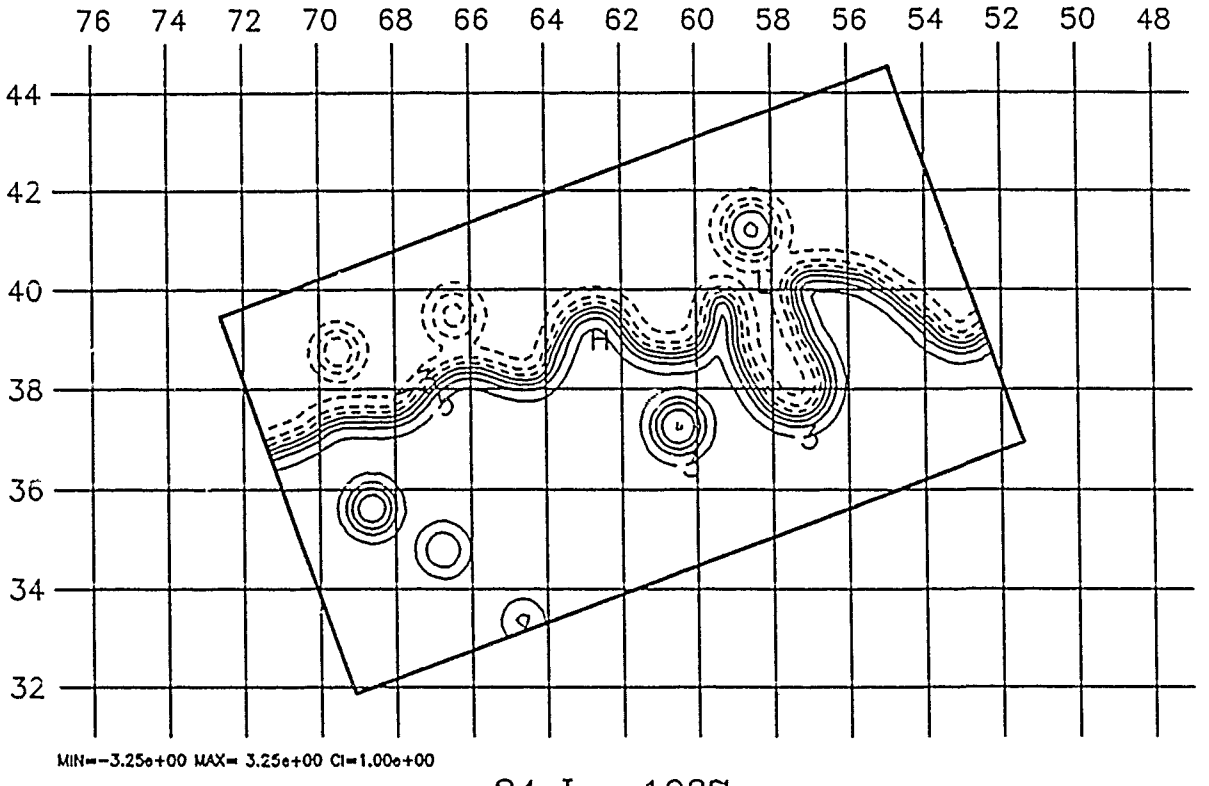

24 Jun 1987

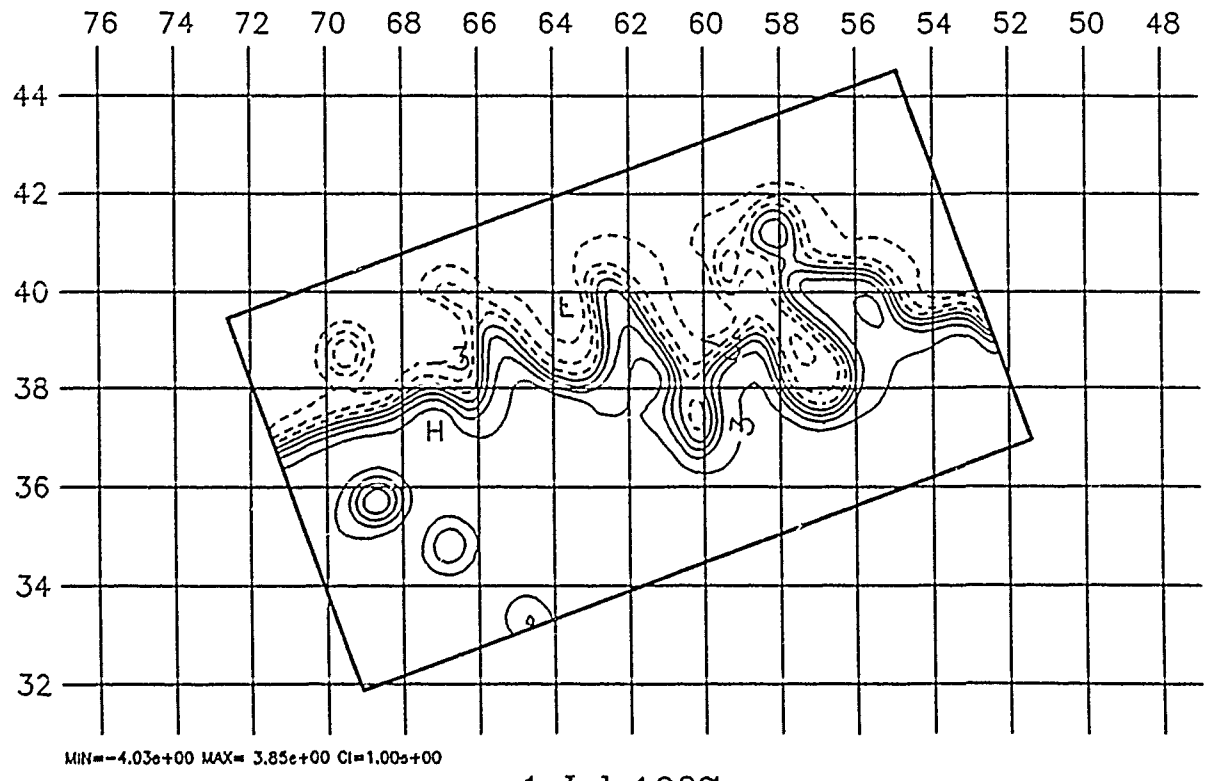

1 Jul 1987

HARVARD UNIVERSITY GULFCAST

RESEARCH OPERATIONAL FORECAST.
NEW DATA: IR (7/1), XBT(7/1).
Figures: Streamfunction at 100. m.

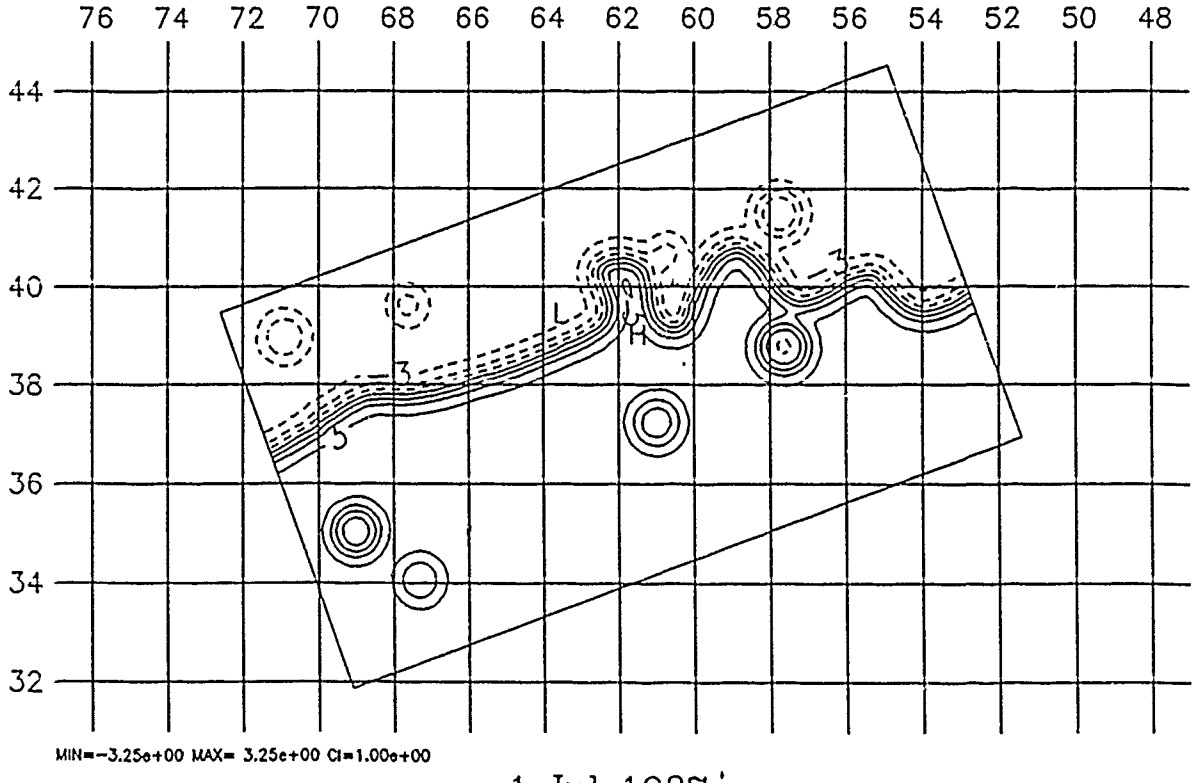

1 Jul 1987

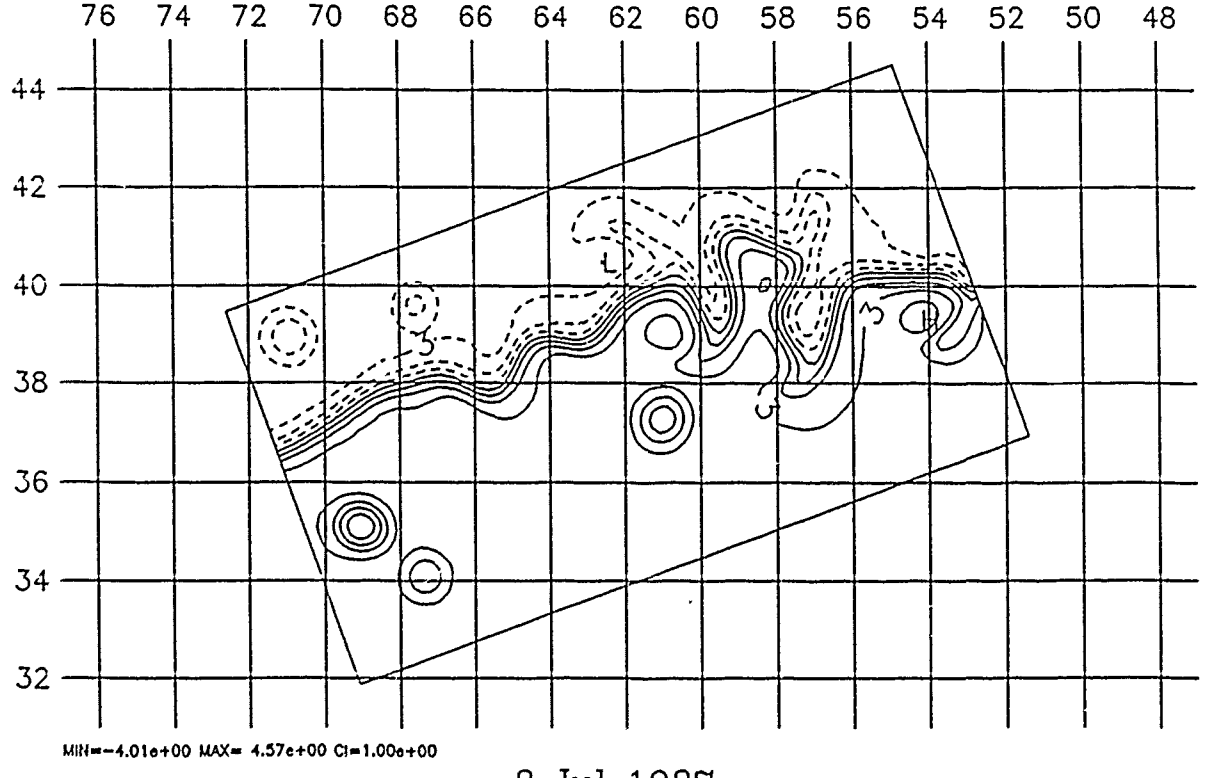

8 Jul 1987

HARVARD UNIVERSITY GULFCAST

RESEARCH OPERATIONAL FORECAST.
NEW DATA: IR (7/8).
Figures: Streamfunction at 100. m.

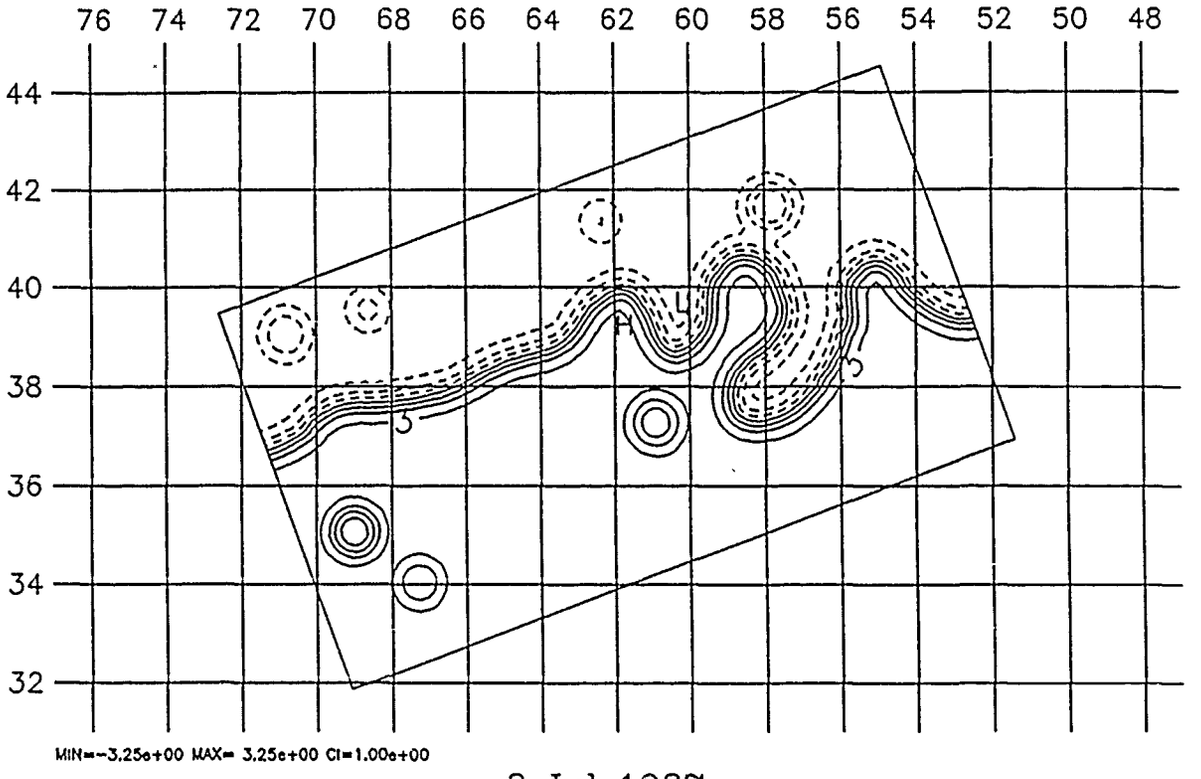

8 Jul 1987

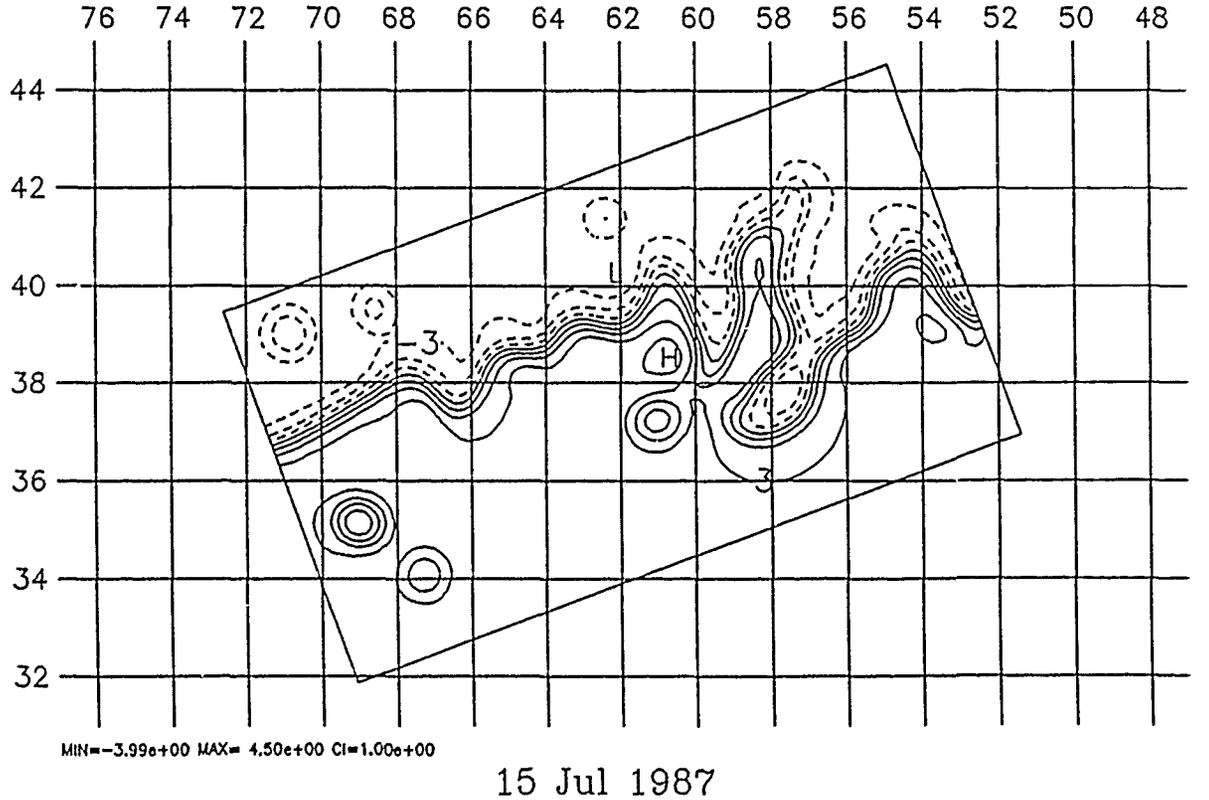

15 Jul 1987

HARVARD UNIVERSITY GULFCAST

RESEARCH OPERATIONAL FORECAST.
NEW DATA: IR (7/13, 7/15).
Figures: Streamfunction at 100. m.

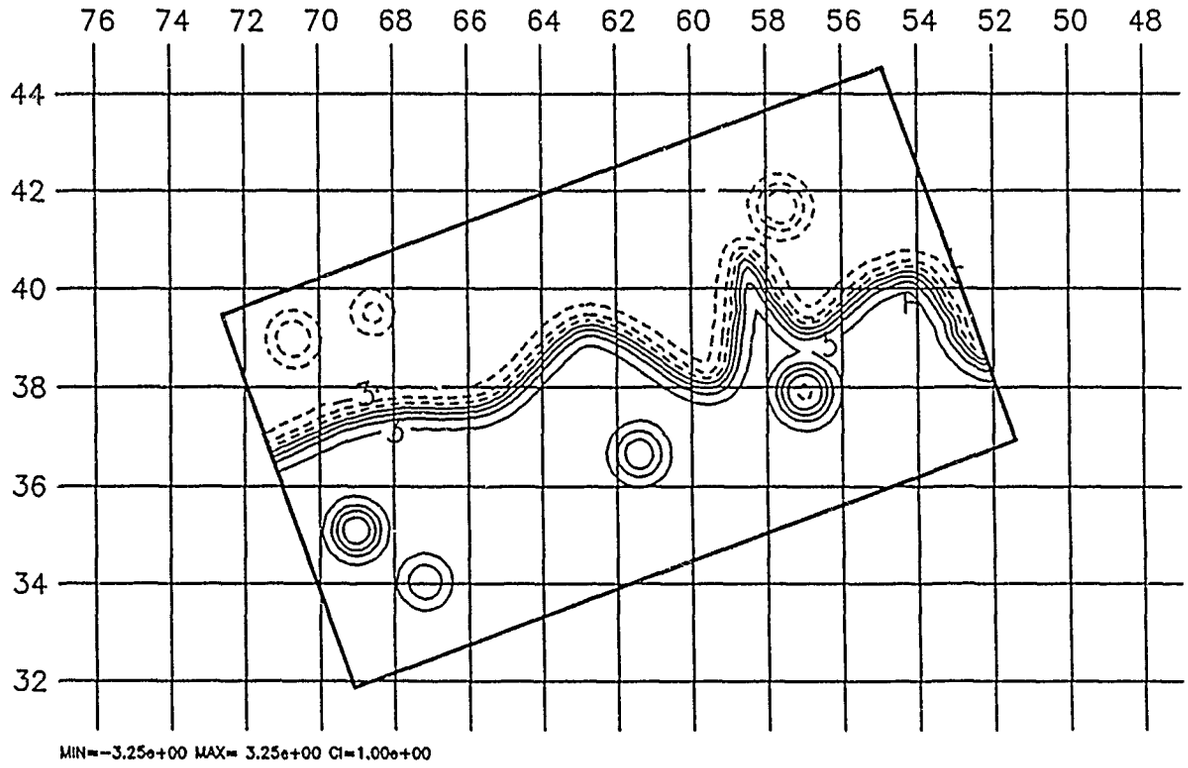

Initialization : 15 Jul 1987

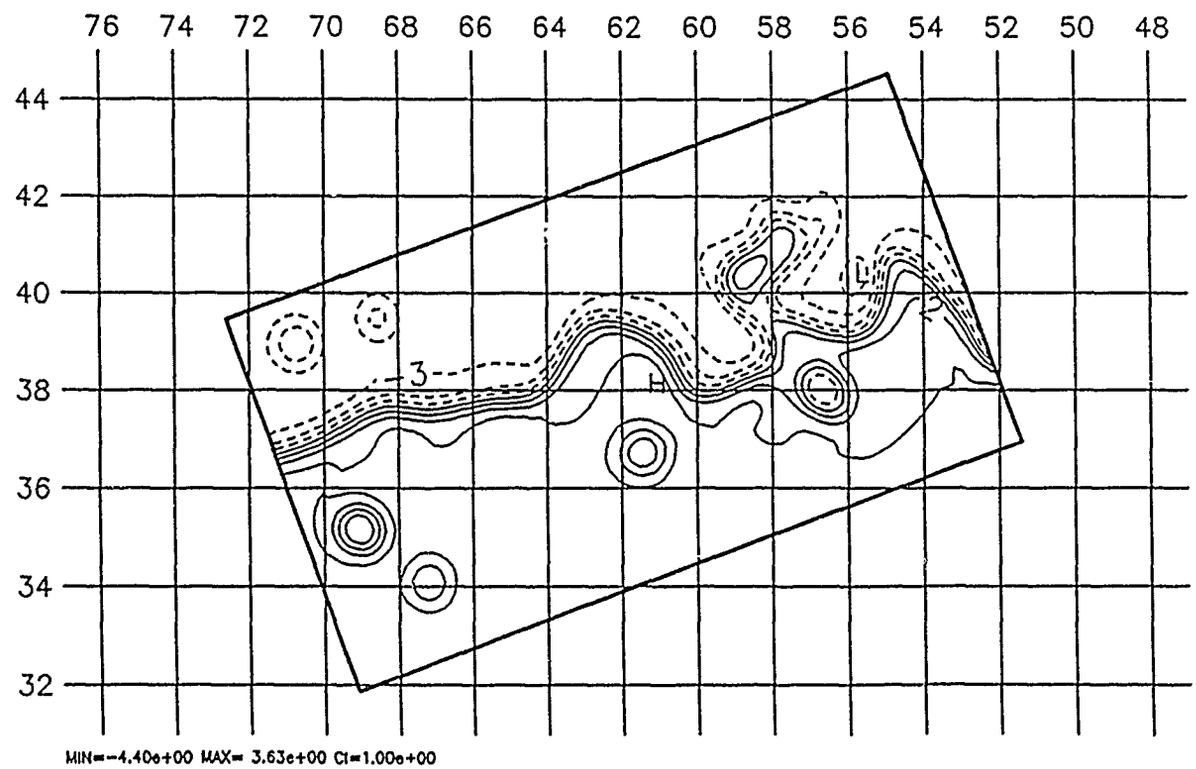

7 Day Forecast : 22 Jul 1987

HARVARD UNIVERSITY GULFCAST

RESEARCH OPERATIONAL FORECAST

NEW DATA: IR (7/20, 7/22)

Figures: Streamfunction at 100. m.

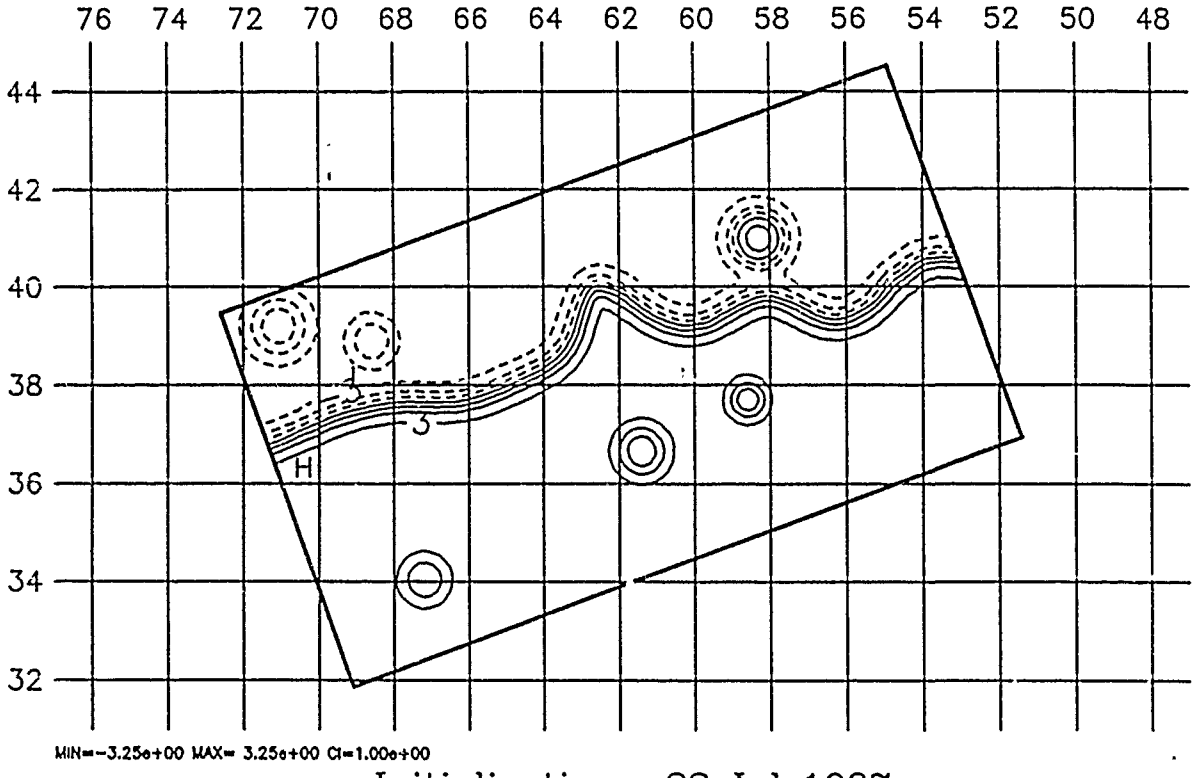

Initialization : 22 Jul 1987

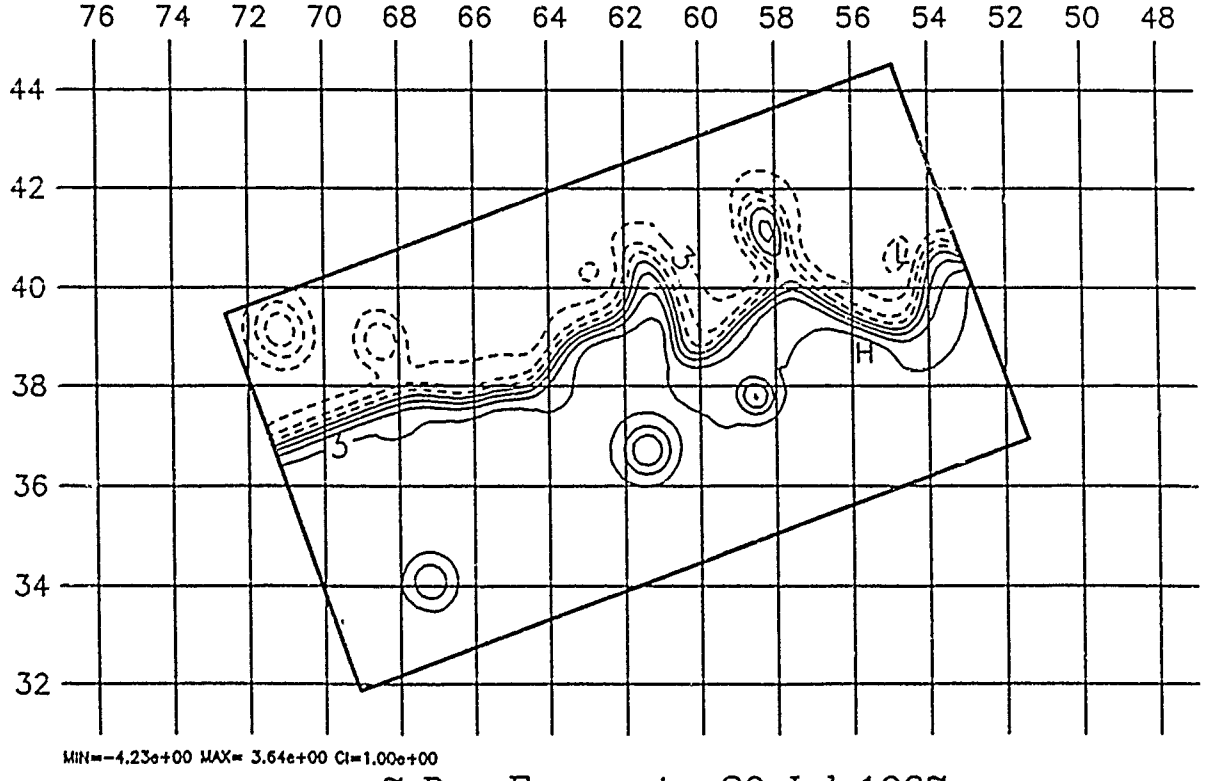

7 Day Forecast : 29 Jul 1987

HARVARD UNIVERSITY GULFCAST

RESEARCH OPERATIONAL FORECAST.
NEW DATA: IR (7/27).
Figures: Streamfunction at 100. m.

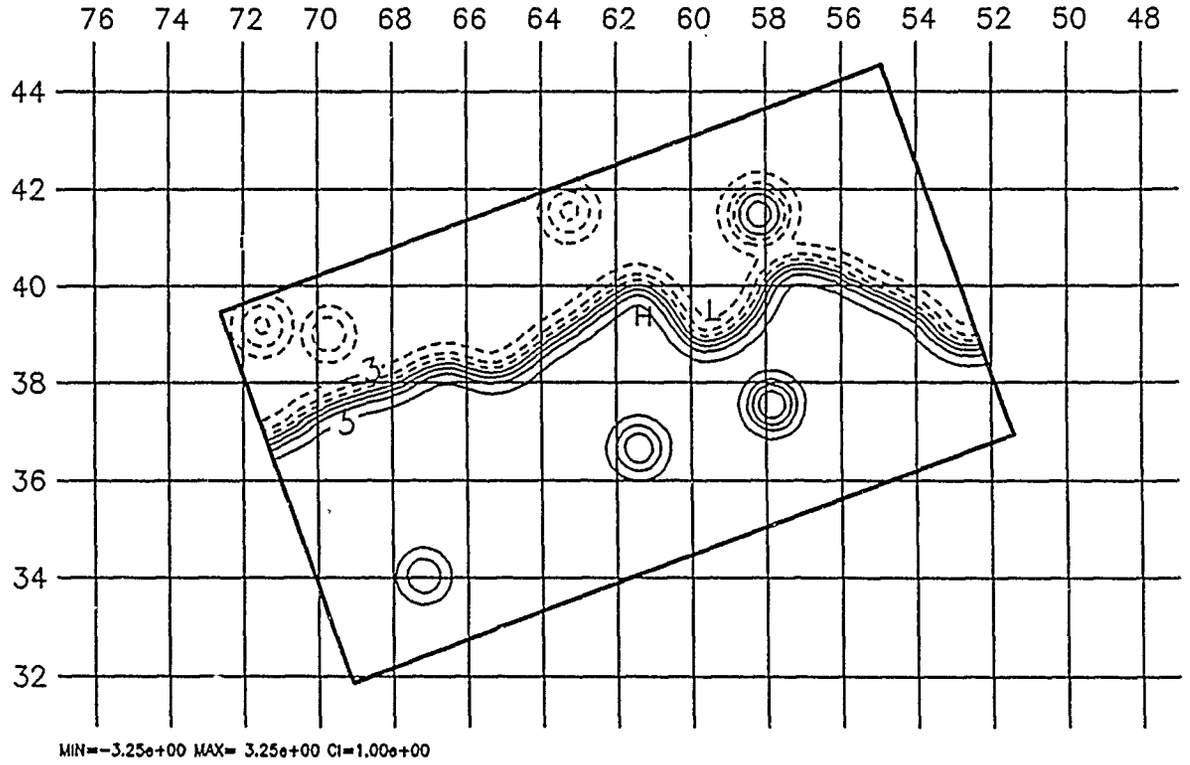

Initialization : 27 Jul 1987

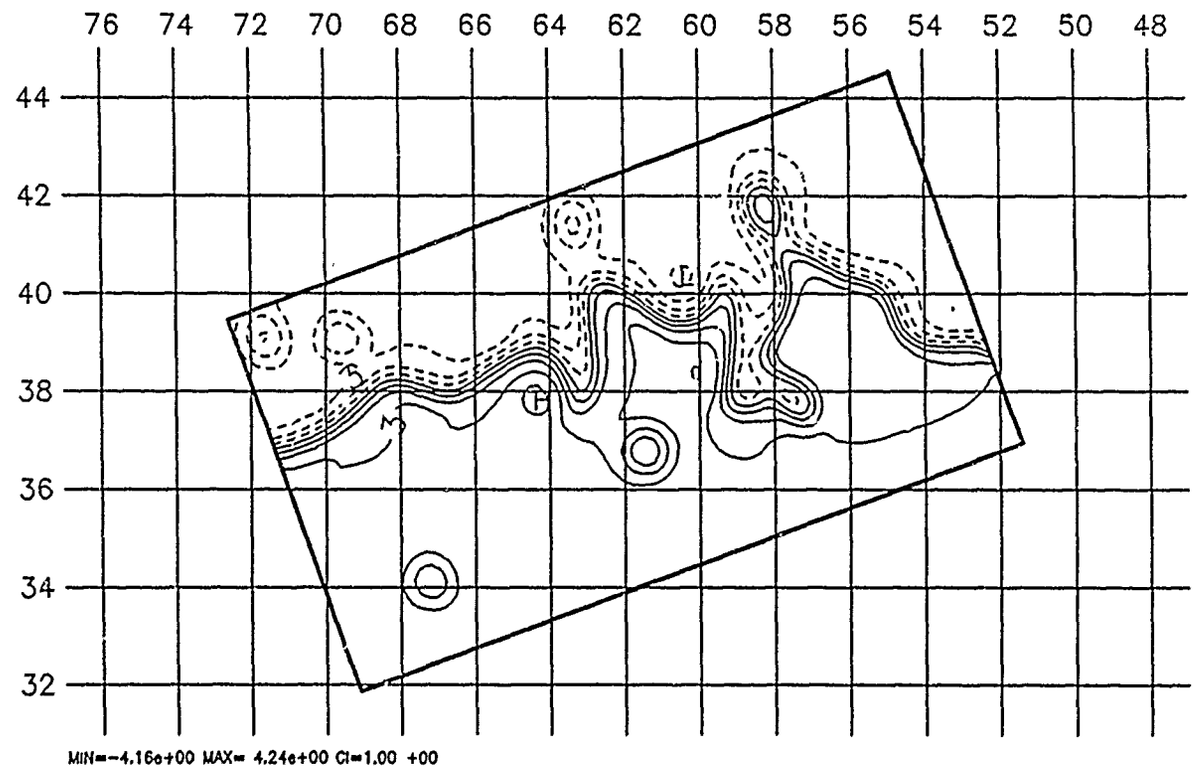

9 Day Forecast : 5 Aug 1987

HARVARD UNIVERSITY GULFCAST

RESEARCH OPERATIONAL FORECAST

NEW DATA: IR (8/3, 8/5)

Figures: Streamfunction at 100. m.

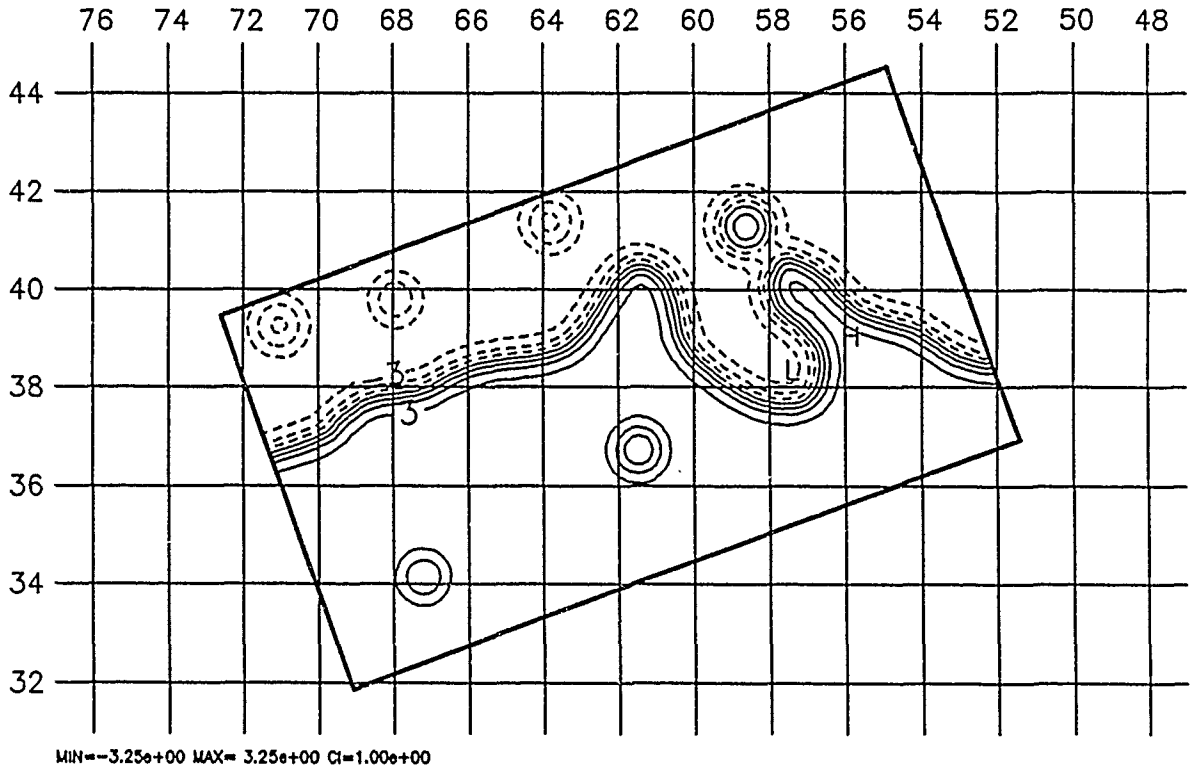

Initialization : 5 Aug 1987

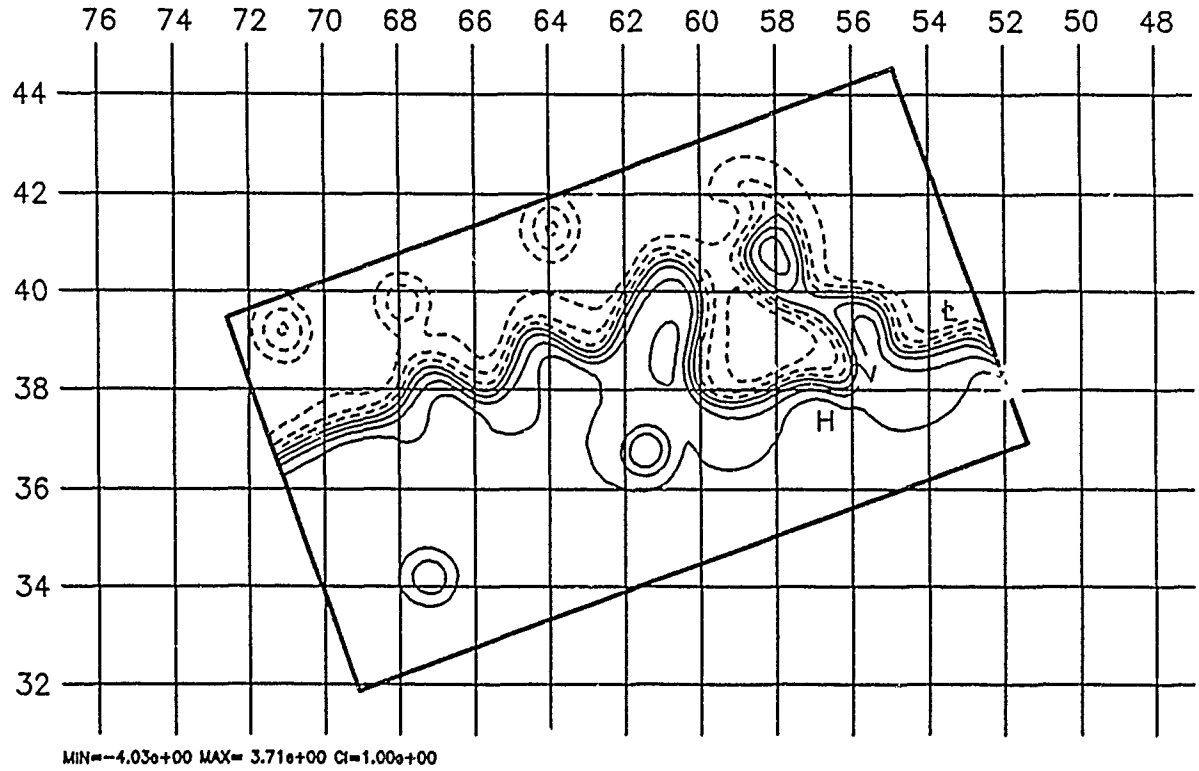

7 Day Forecast : 12 Aug 1987

HARVARD UNIVERSITY GULFCAST

RESEARCH OPERATIONAL FORECAST

NEW DATA: IR (8/10, 8/12)

Figures: Streamfunction at 100. m.

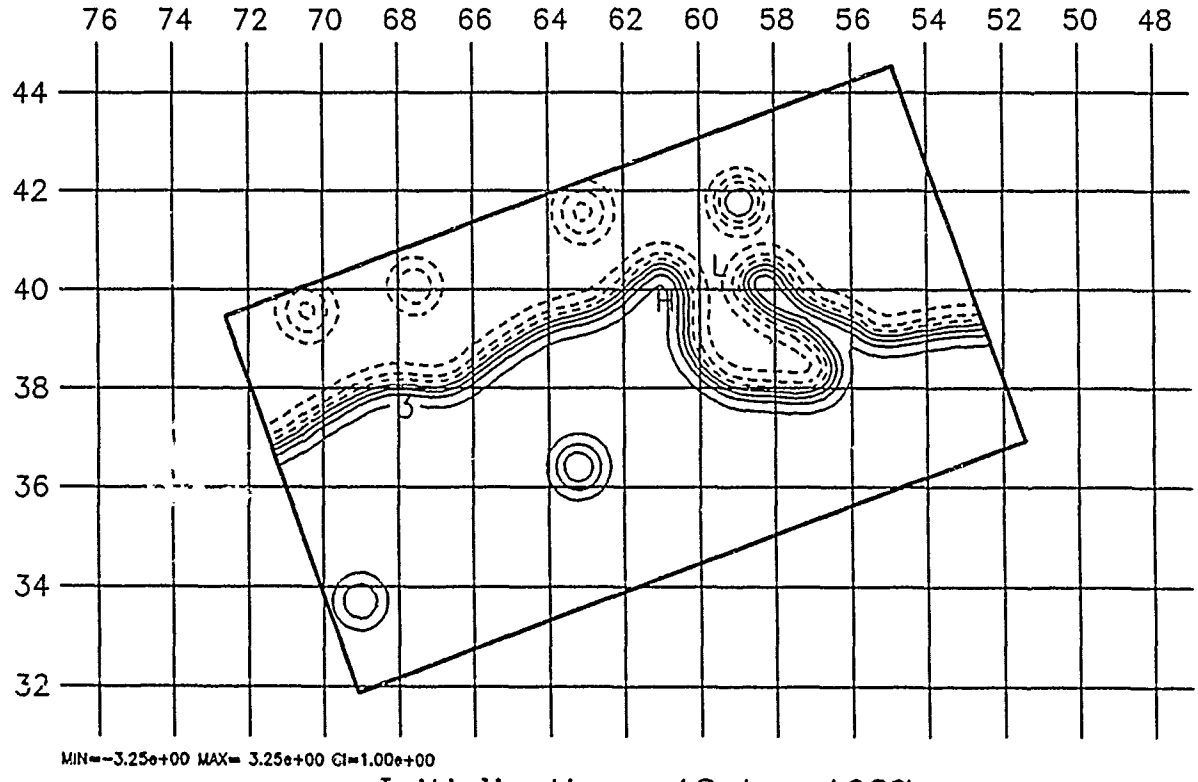

Initialization : 12 Aug 1987

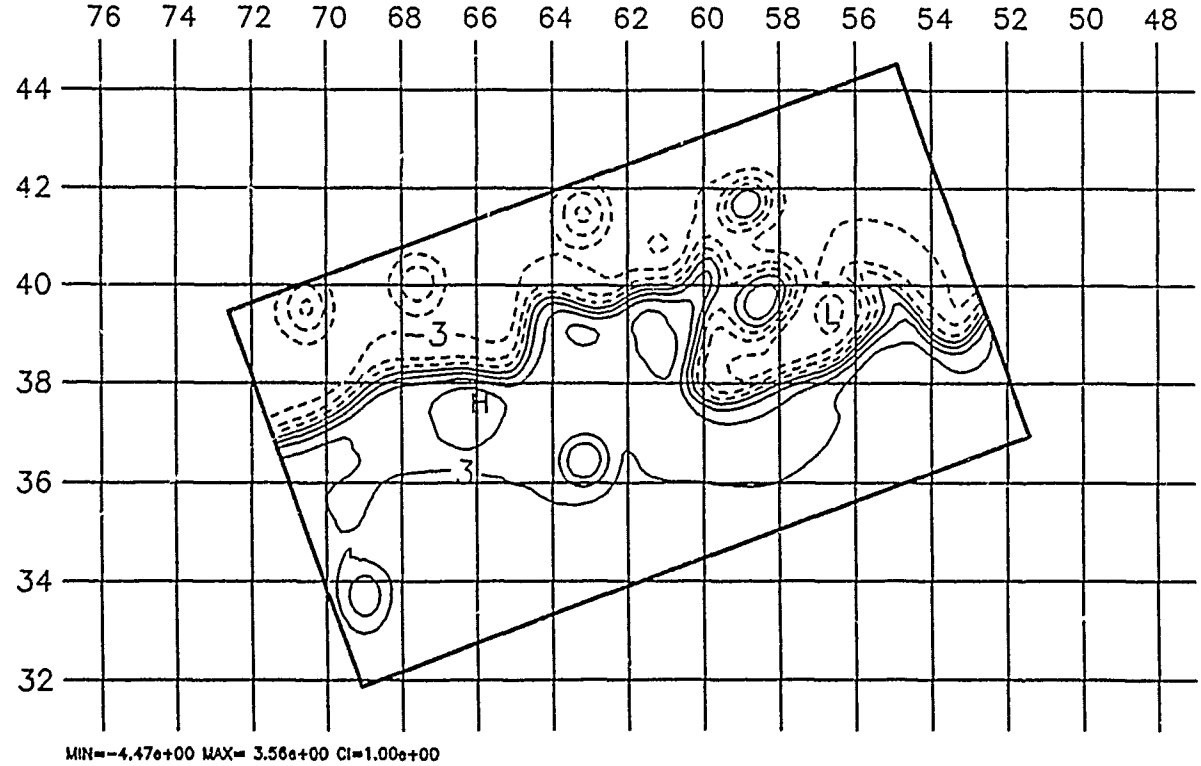

7 Day Forecast : 19 Aug 1987

HARVARD UNIVERSITY GULFCAST

RESEARCH OPERATIONAL FORECAST (OLD TOPOGRAPHY
NEW DATA: IR(8/17, 8/19), DIR(8/18), AXBT(8/20).
Figures: Streamfunction at 100. m.

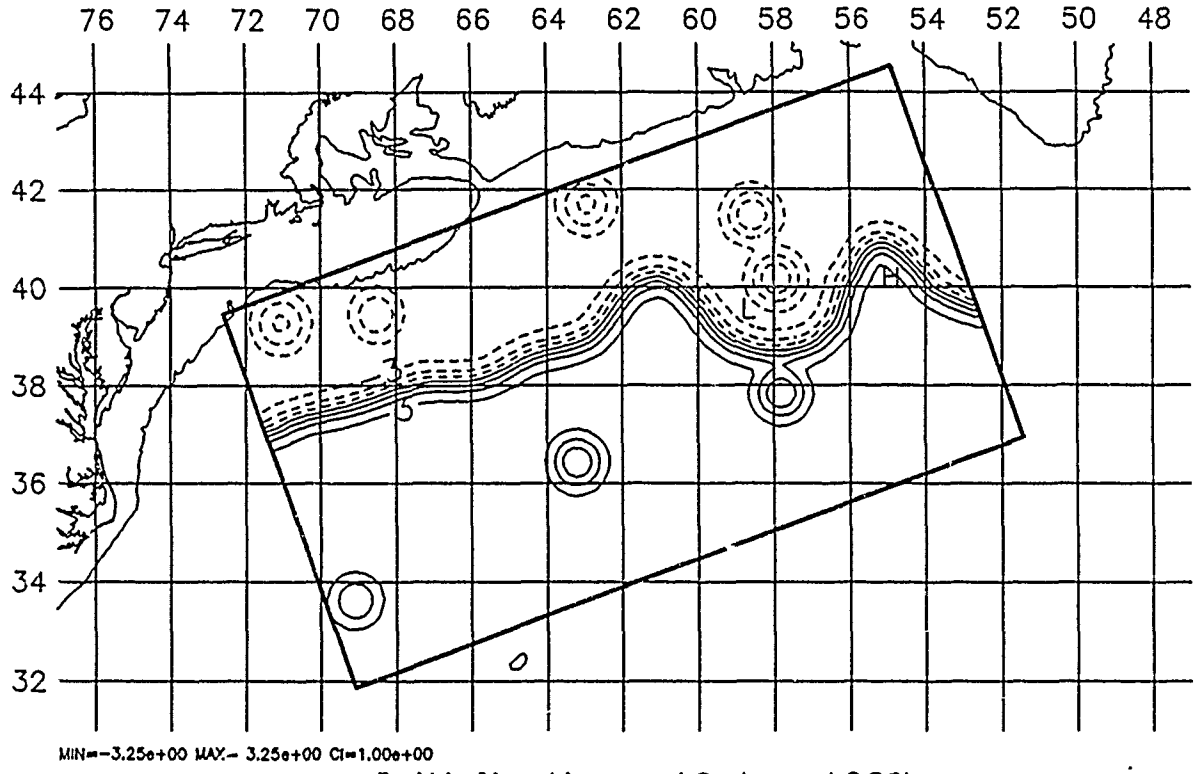

Initialization : 19 Aug 1987

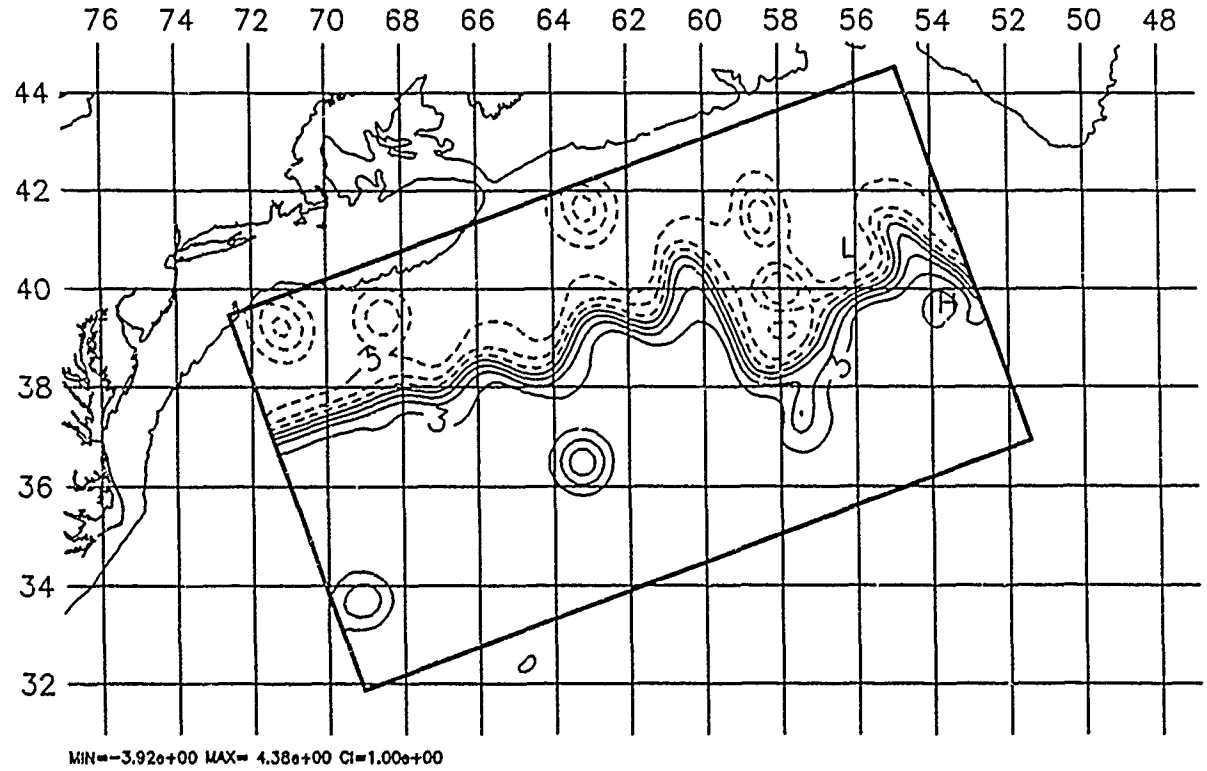

7 Day Forecast : 26 Aug 1987

HARVARD UNIVERSITY GULFCAST

RESEARCH OPERATIONAL FORECAST.

NEW DATA: IR(8/24, 8/26), DIR(8/21), XBT(8/26).

Figures: Streamfunction at 100. m.

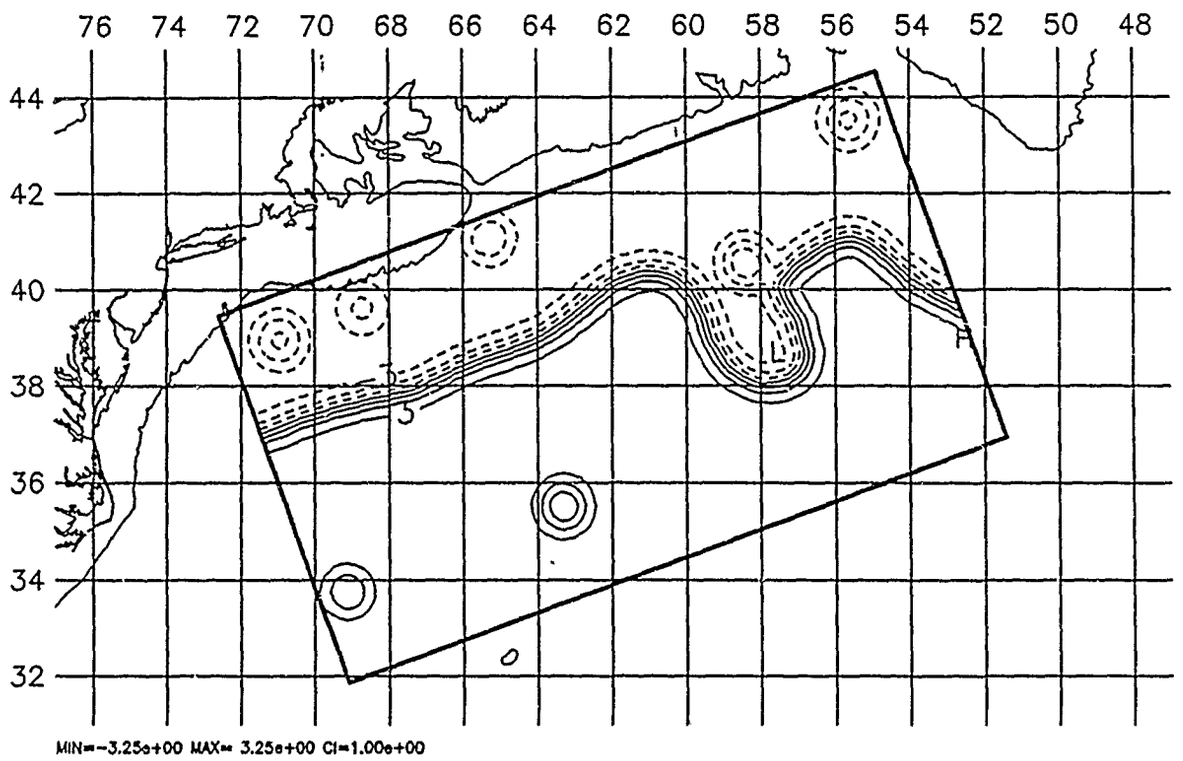

Initialization : 26 Aug 1987

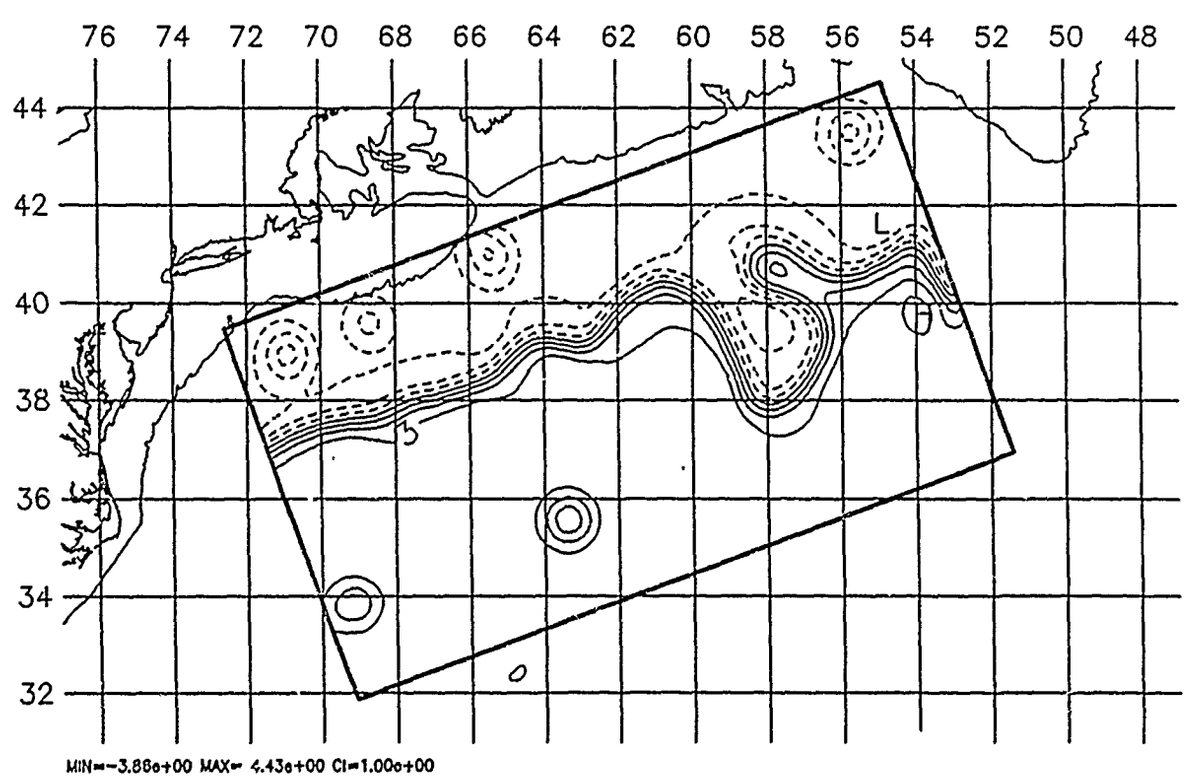

7 Day Forecast : 2 Sep 1987

HARVARD UNIVERSITY GULFCAST

RESEARCH OPERATIONAL FORECAST.
NEW DATA: IR(8/31,9/1,9/2), DIR(8/31).
Figures: Streamfunction at 100. m.

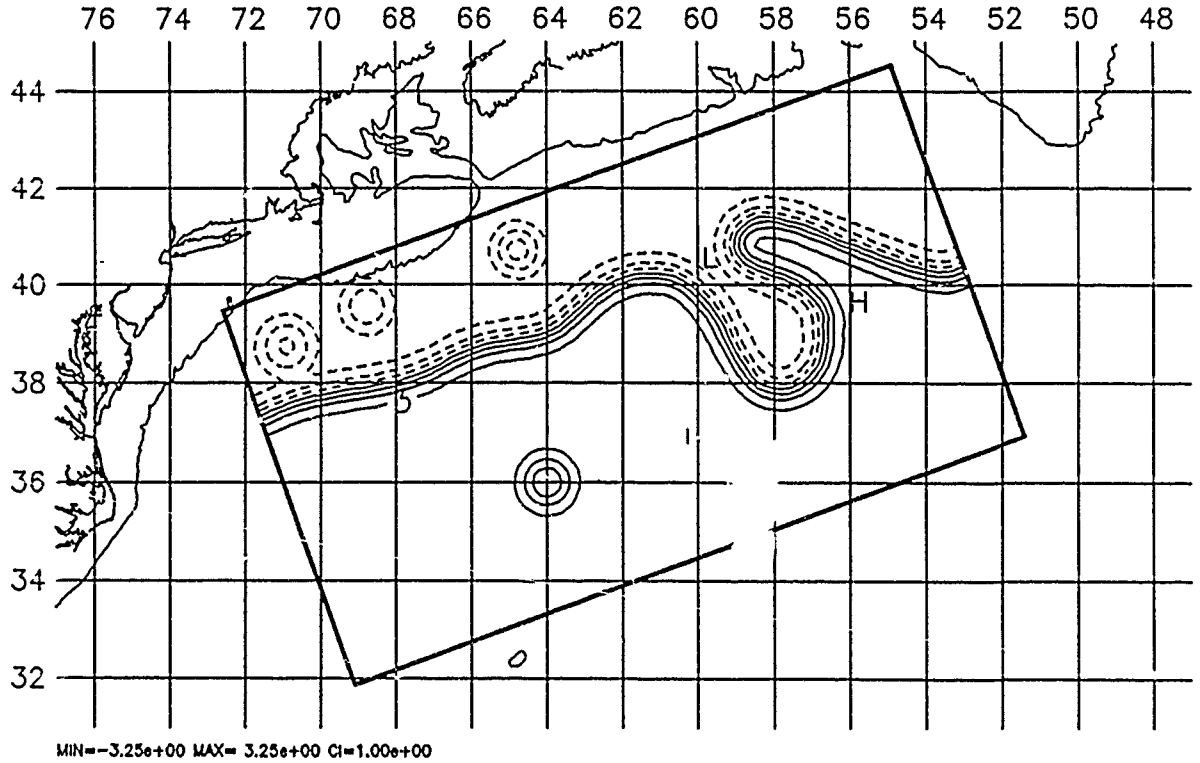

Initialization : 2 Sep 1987

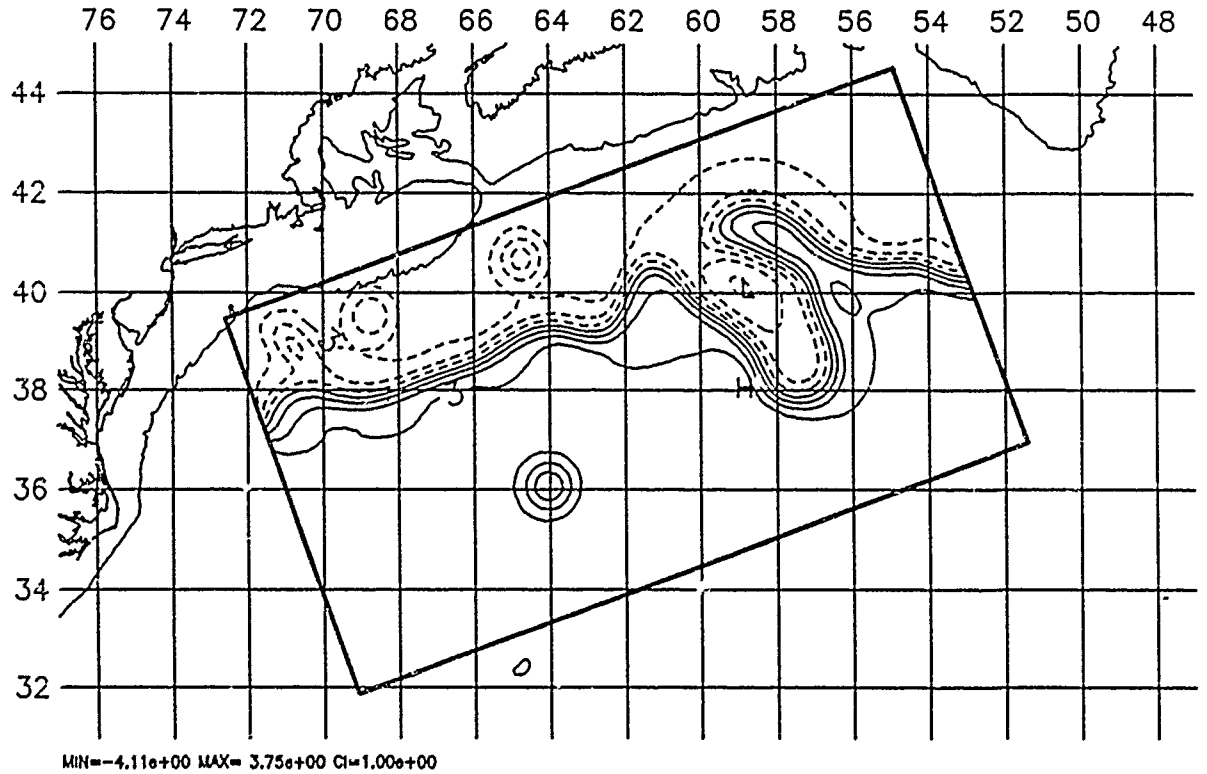

7 Day Forecast : 9 Sep 1987

HARVARD UNIVERSITY GULFCAST

RESEARCH OPERATIONAL FORECAST.
NEW DATA: IR(9/9), XBT(9/8).
Figures: Streamfunction at 100. m.

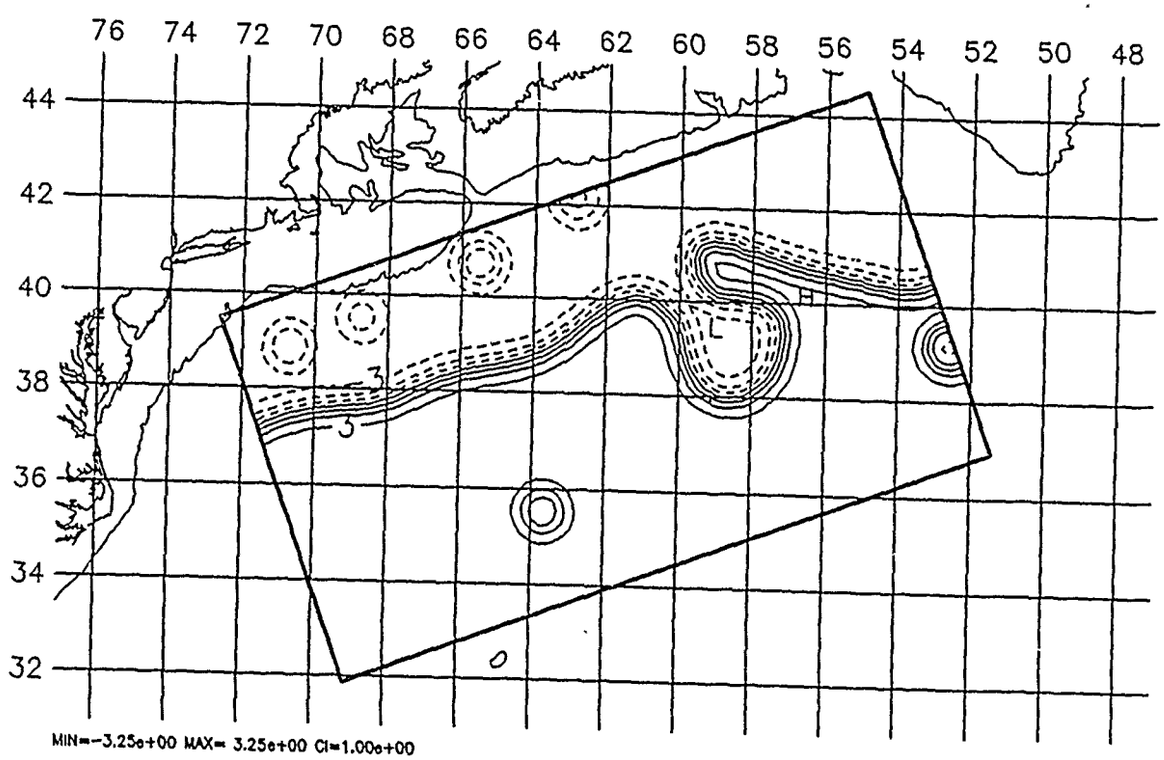

Initialization : 9 Sep 1987

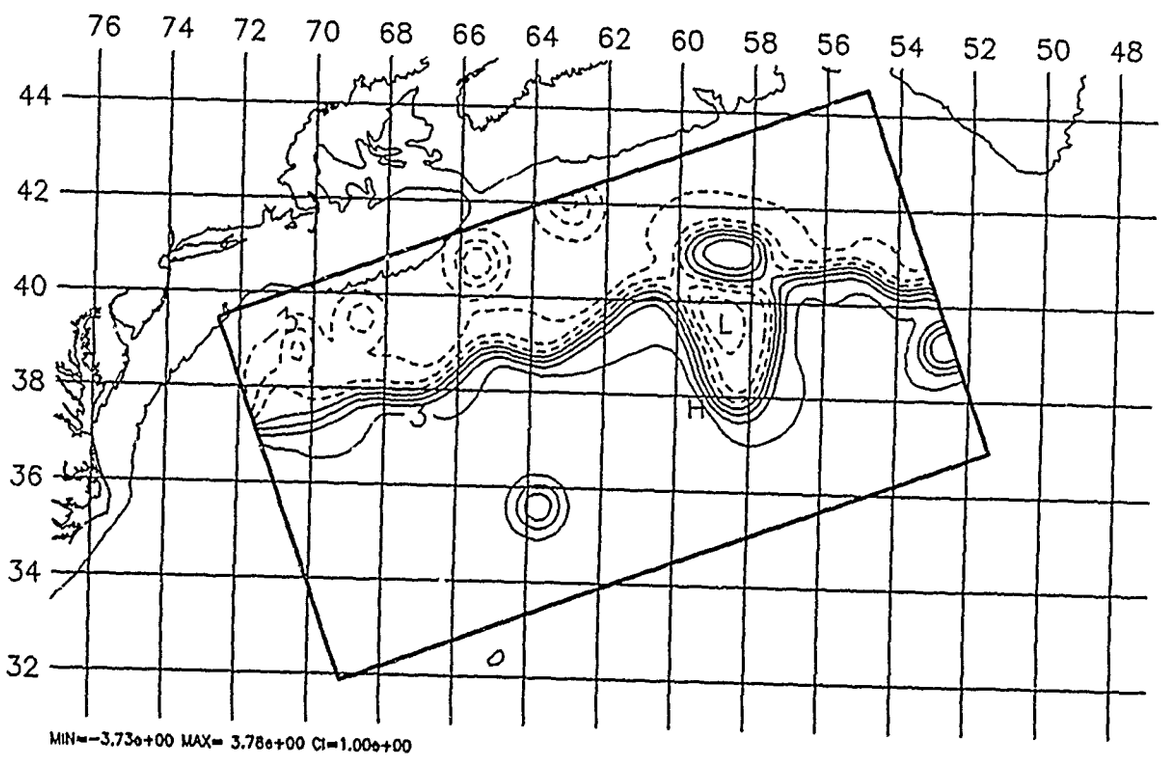

7 Day Forecast : 16 Sep 1987

HARVARD UNIVERSITY GULFCAST

RESEARCH OPERATIONAL FORECAST.
NEW DATA: IR(9/14,9/16).
Figures: Streamfunction at 100. m.

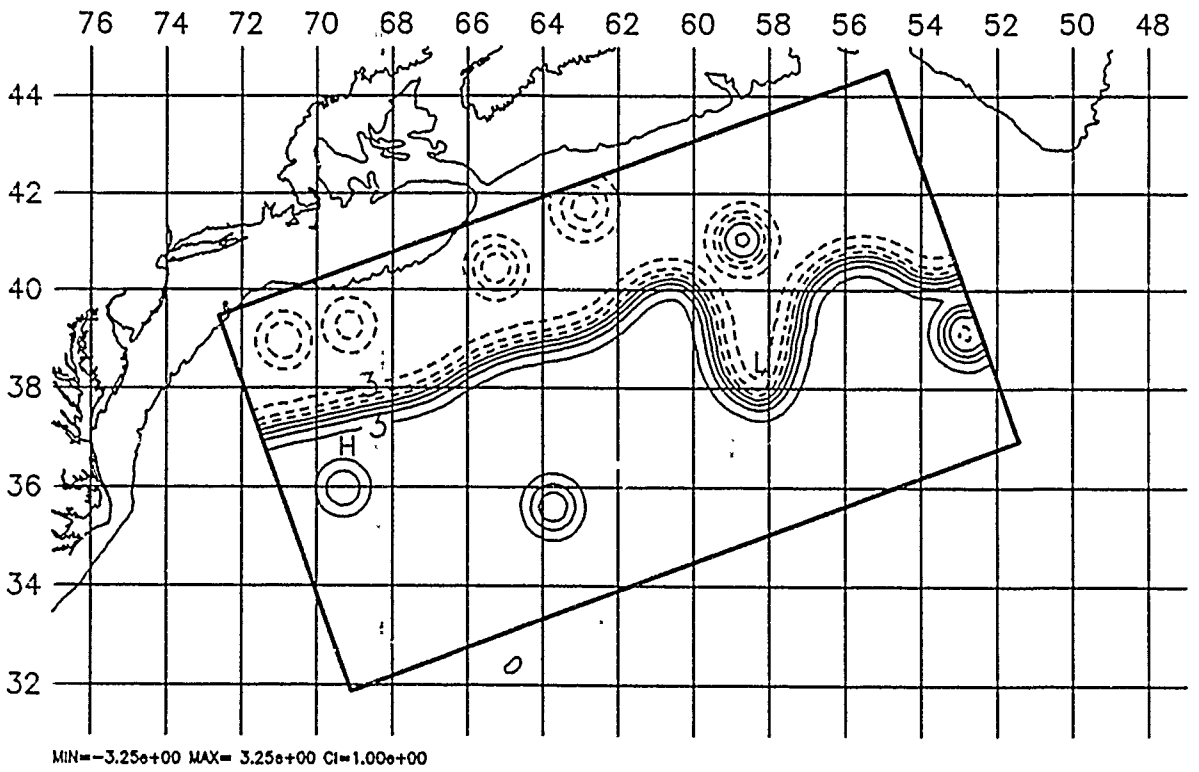

Initialization : 16 Sep 1987

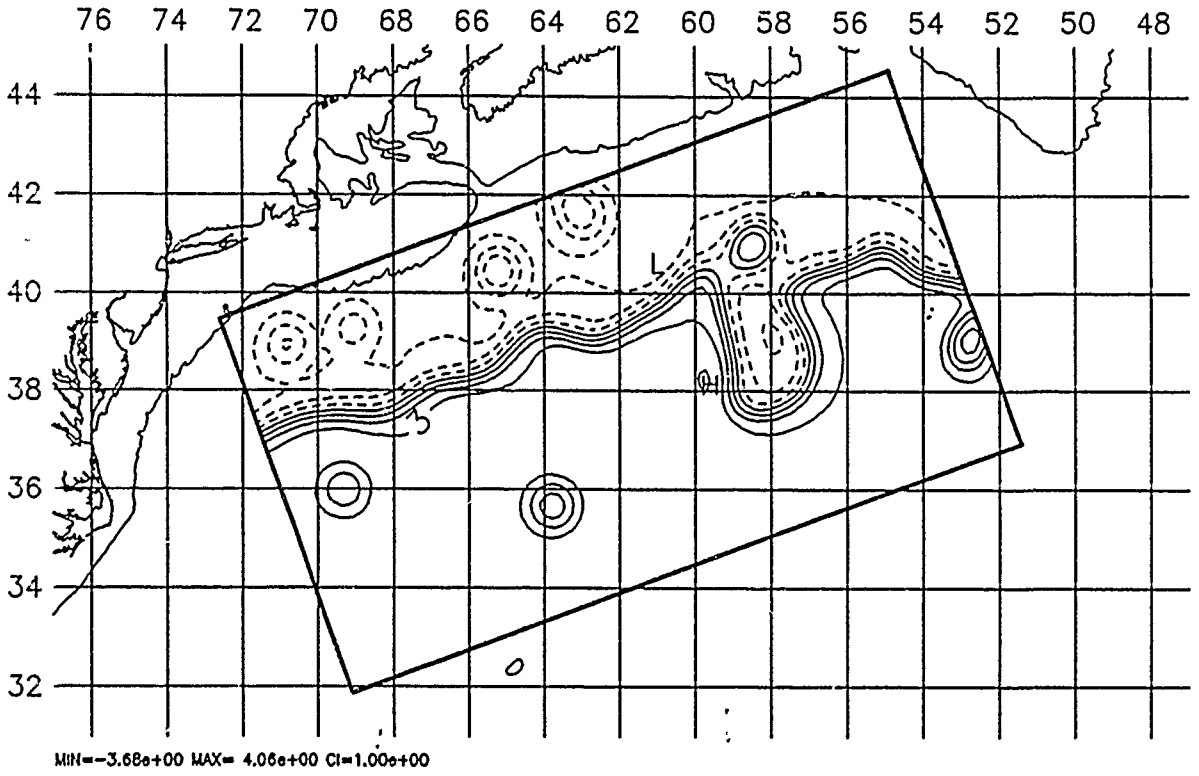

7 Day Forecast : 23 Sep 1987

HARVARD UNIVERSITY GULFCAST

RESEARCH OPERATIONAL FORECAST.

NEW DATA: IR(9/21,9/22,9/23),AXBT(9/23).

Figures: Streamfunction at 100. m.

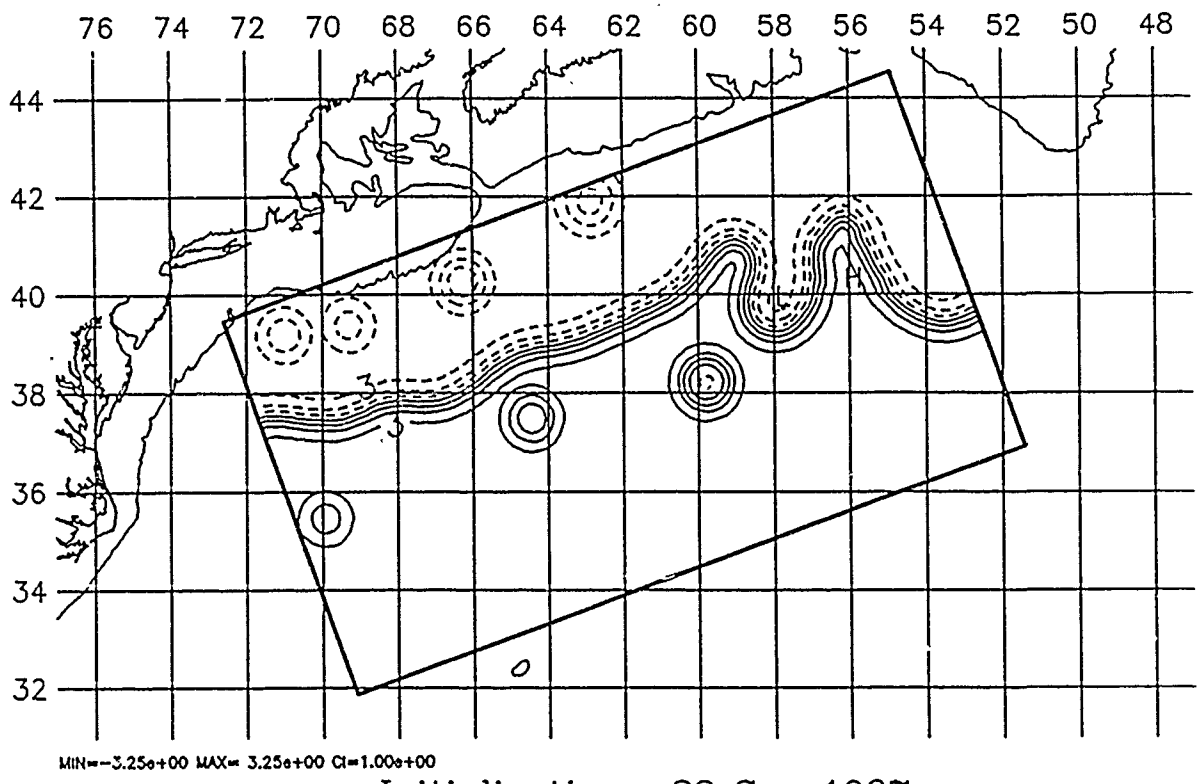

Initialization : 23 Sep 1987

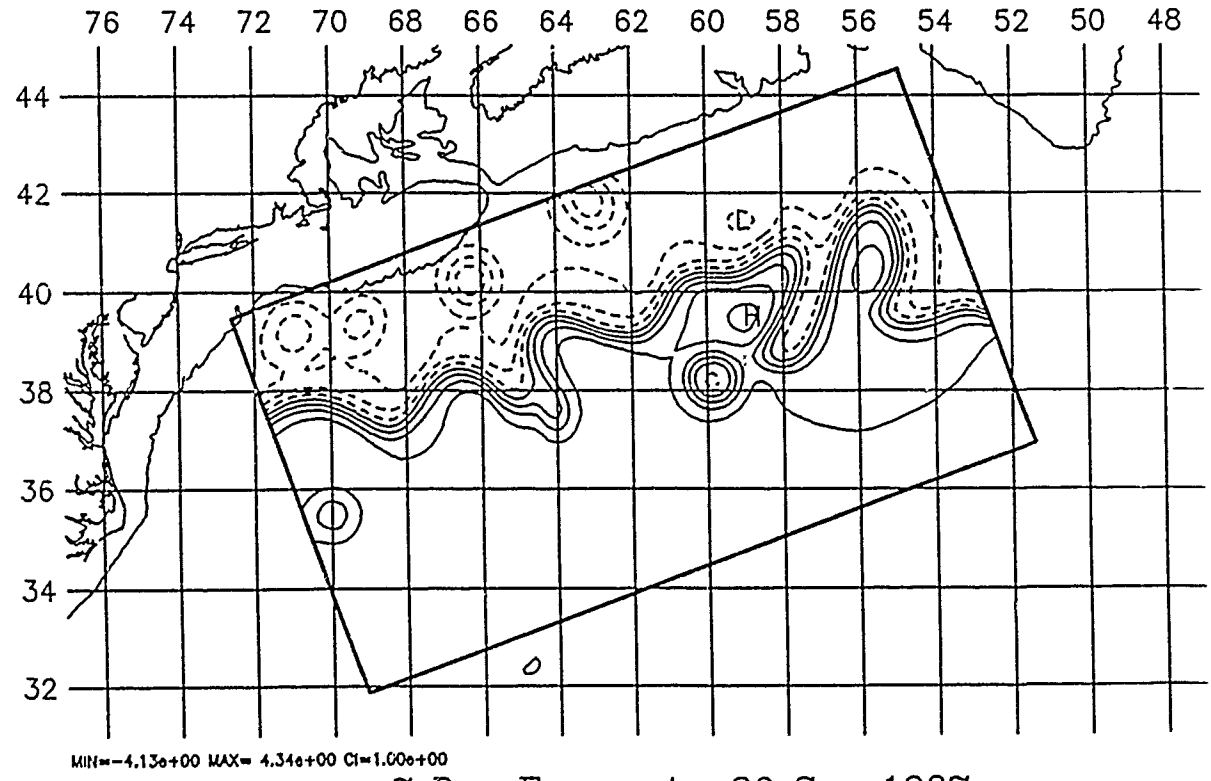

7 Day Forecast : 30 Sep 1987

HARVARD UNIVERSITY GULFCAST

RESEARCH OPERATIONAL FORECAST.

NEW DATA: IR(9/28,9/29,9/30).

Figures: Streamfunction at 100. m.

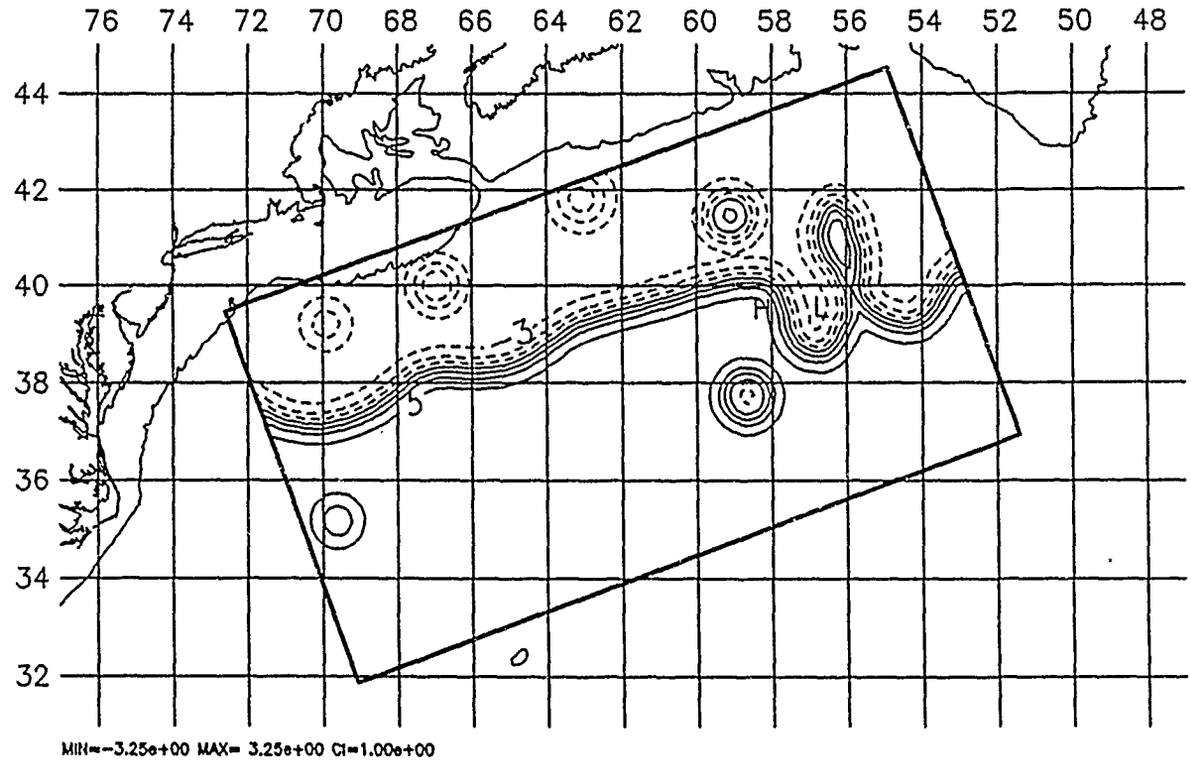

Initialization : 30 Sep 1987

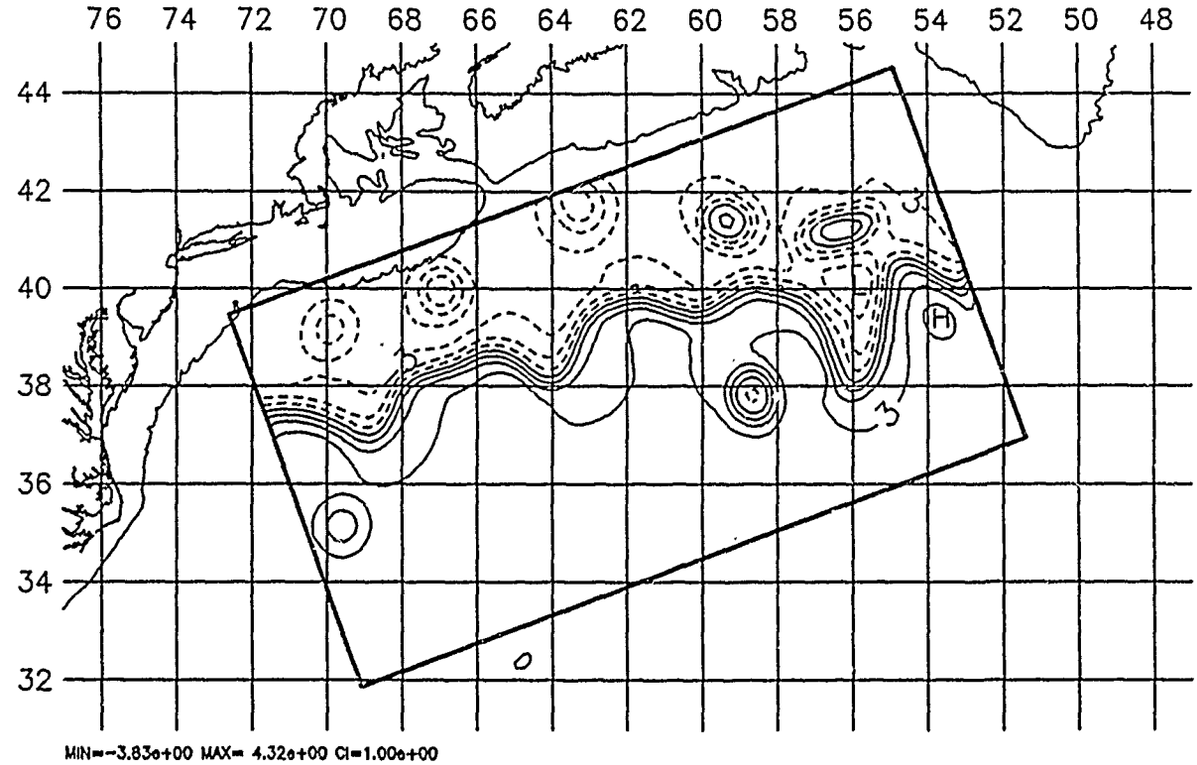

7 Day Forecast : 7 Oct 1987

HARVARD UNIVERSITY GULFCAST

OPERATIONAL EVALUATION FORECAST.

NEW DATA: IR, AXBT.

Figure: Streamfunction at 100 m.

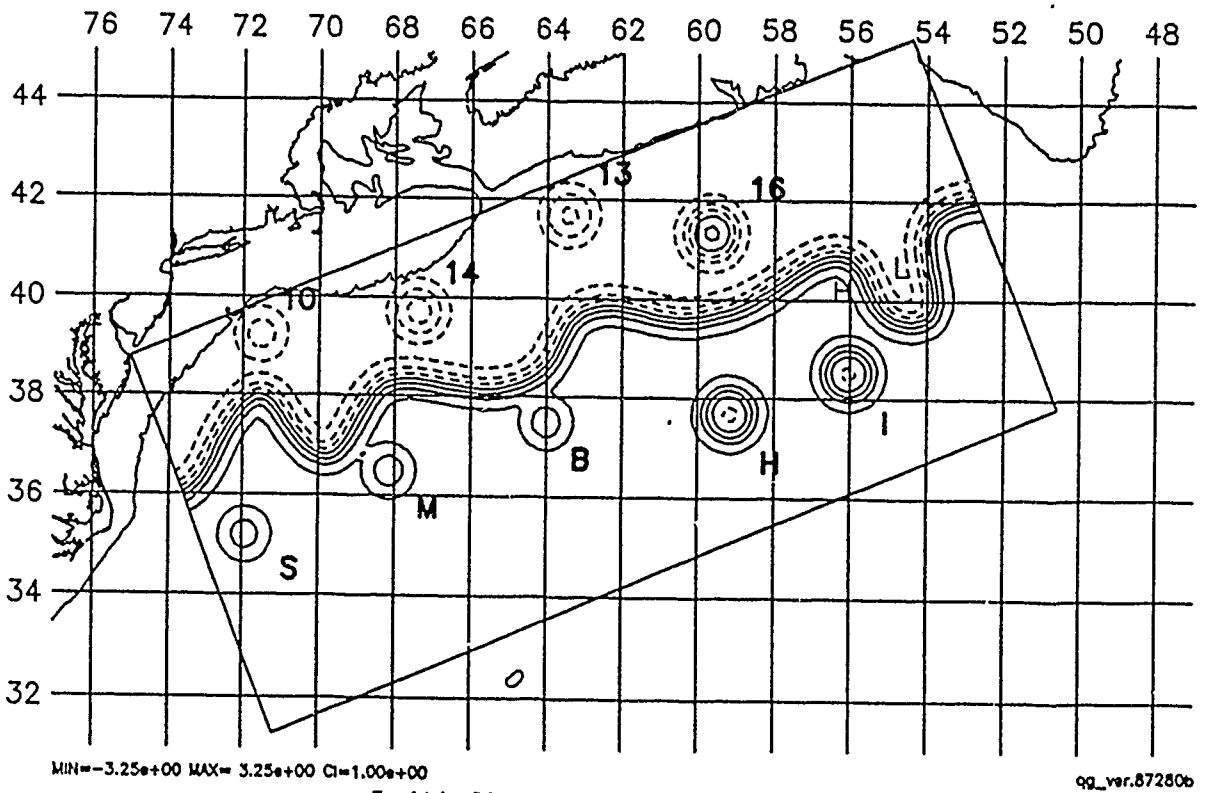

Initialization : 7 OCT 1987

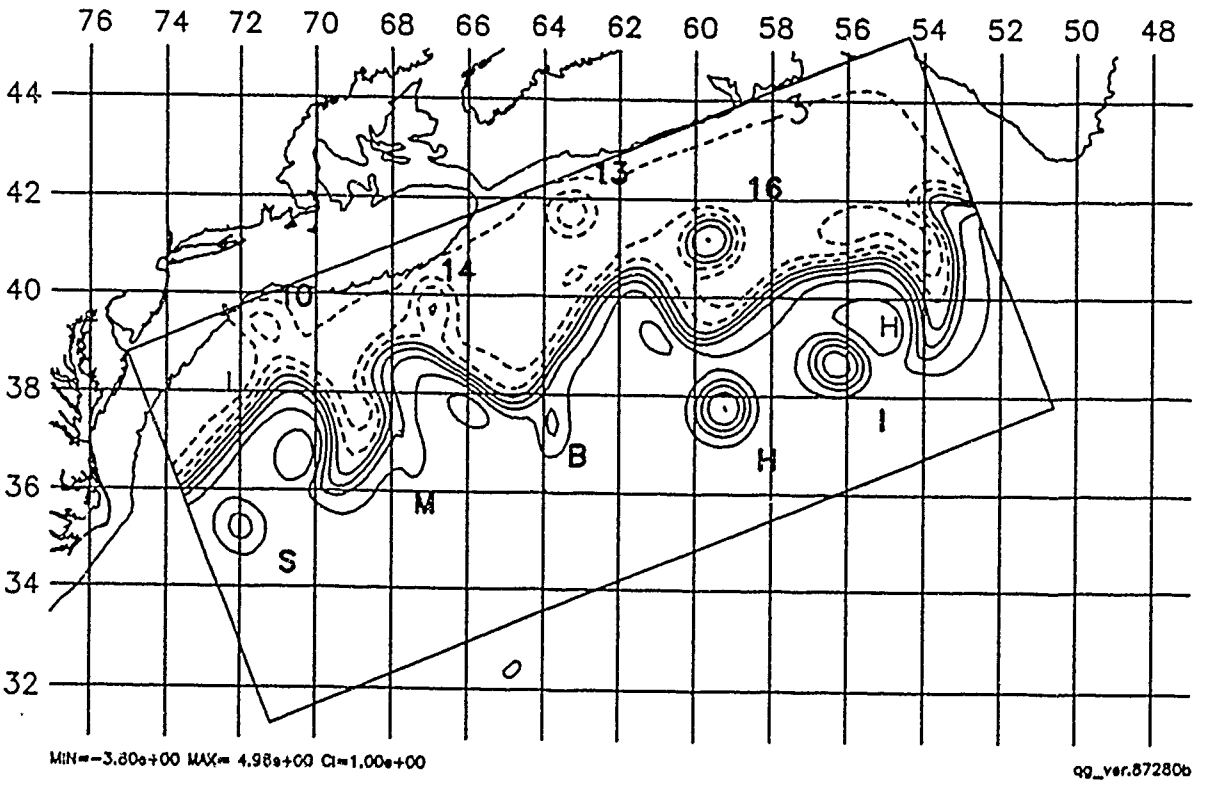

7 Day Forecast : 14 OCT 1987

HARVARD UNIVERSITY GULFCAST

OPERATIONAL EVALUATION FORECAST.

NEW DATA: IR.

Figure: Streamfunction at 100 m.

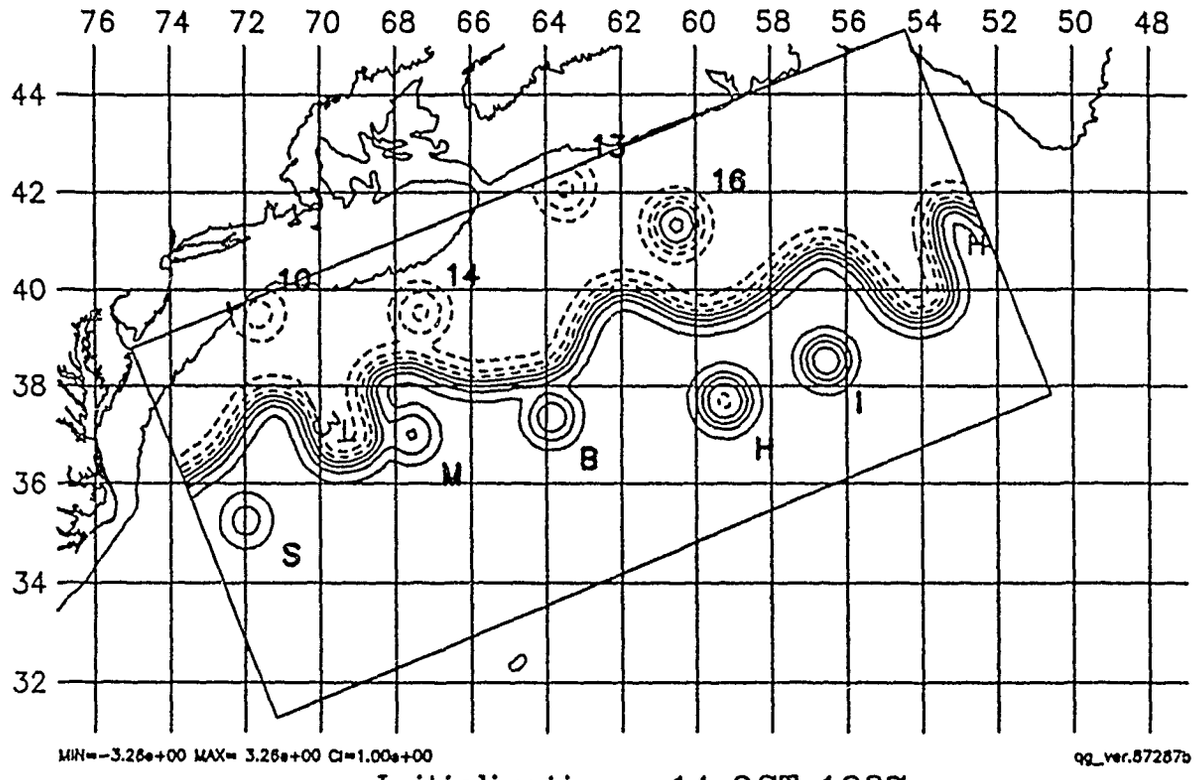

Initialization : 14 OCT 1987

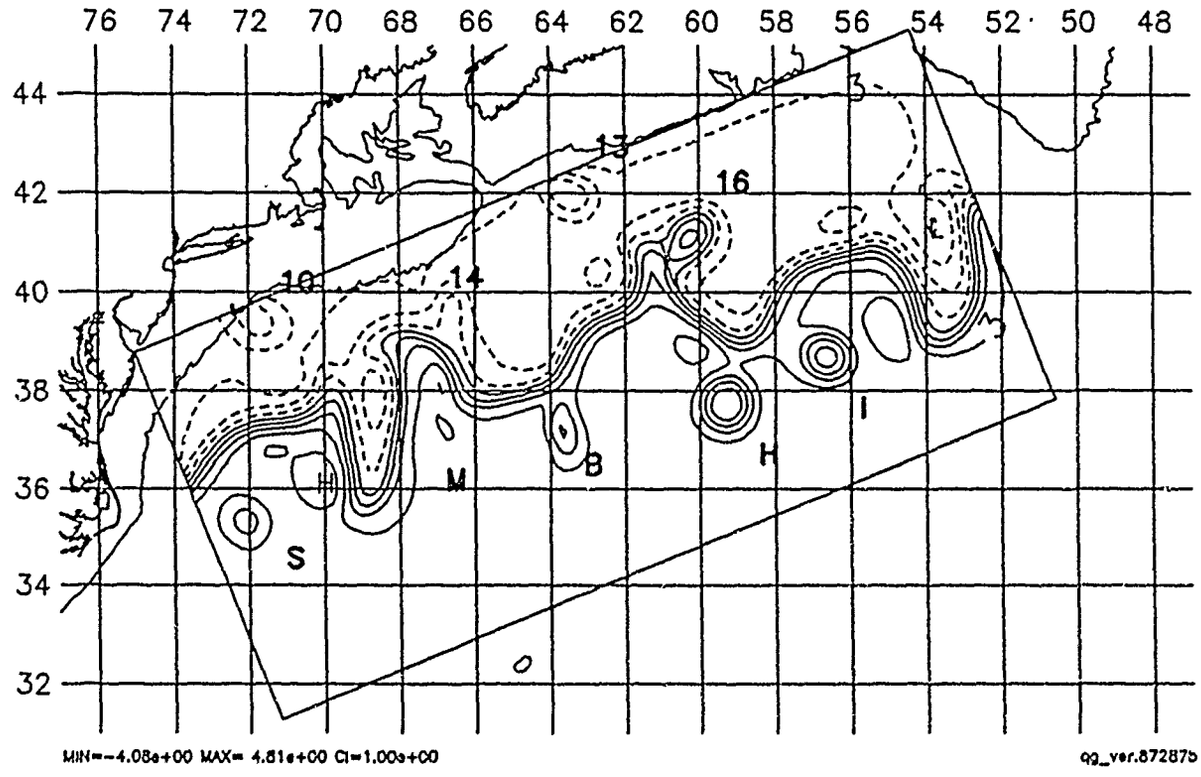

7 Day Forecast : 21 OCT 1987

VE RI TAS

HARVARD UNIVERSITY GULFCAST

OPERATIONAL EVALUATION FORECAST.

NEW DATA: IR, AXBT.

Figure: Streamfunction at 100 m.

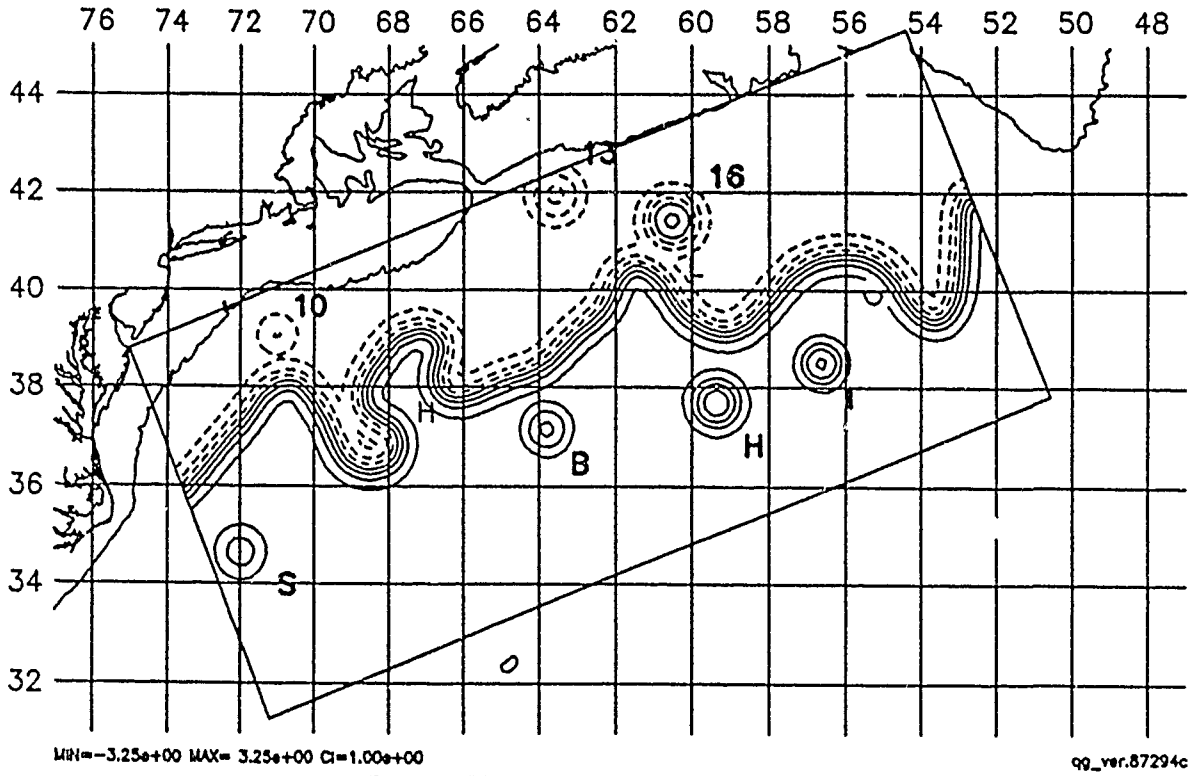

Initialization : 21 OCT 1987

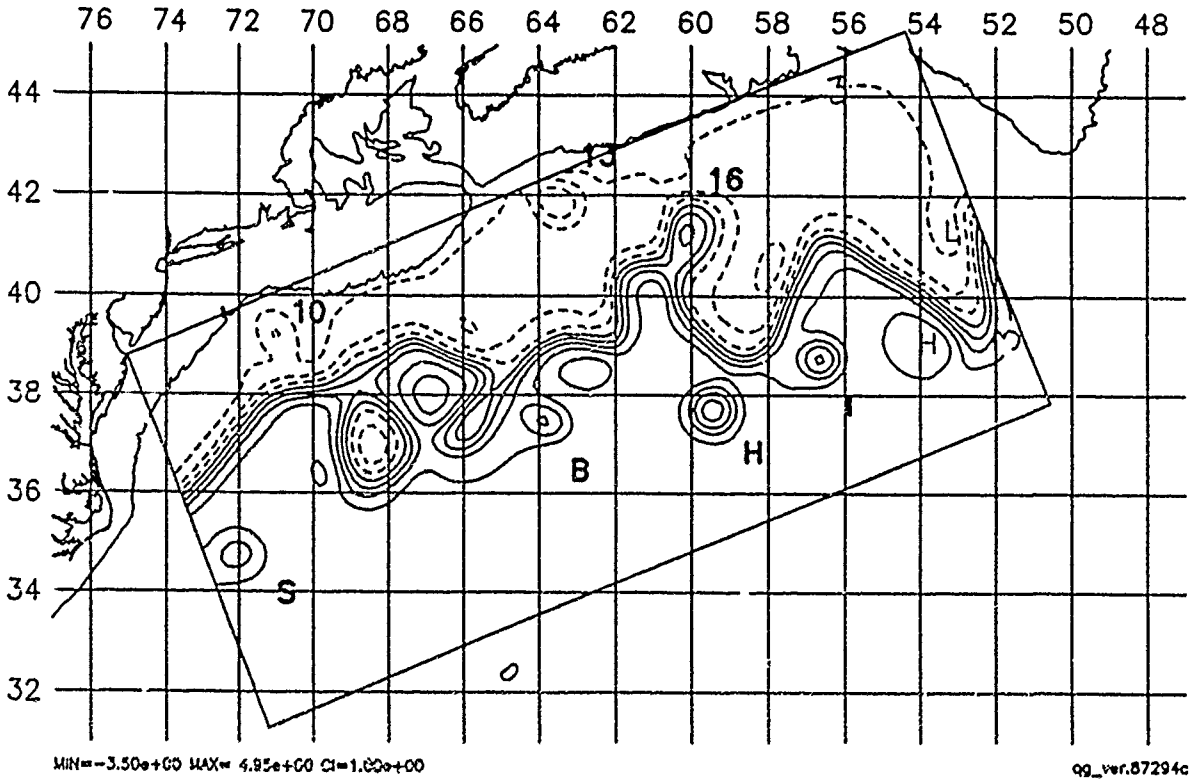

7 Day Forecast : 28 OCT 1987

HARVARD UNIVERSITY GULFCAST

OPERATIONAL EVALUATION FORECAST.

NEW DATA: IR.

Figure: Streamfunction at 100 m.

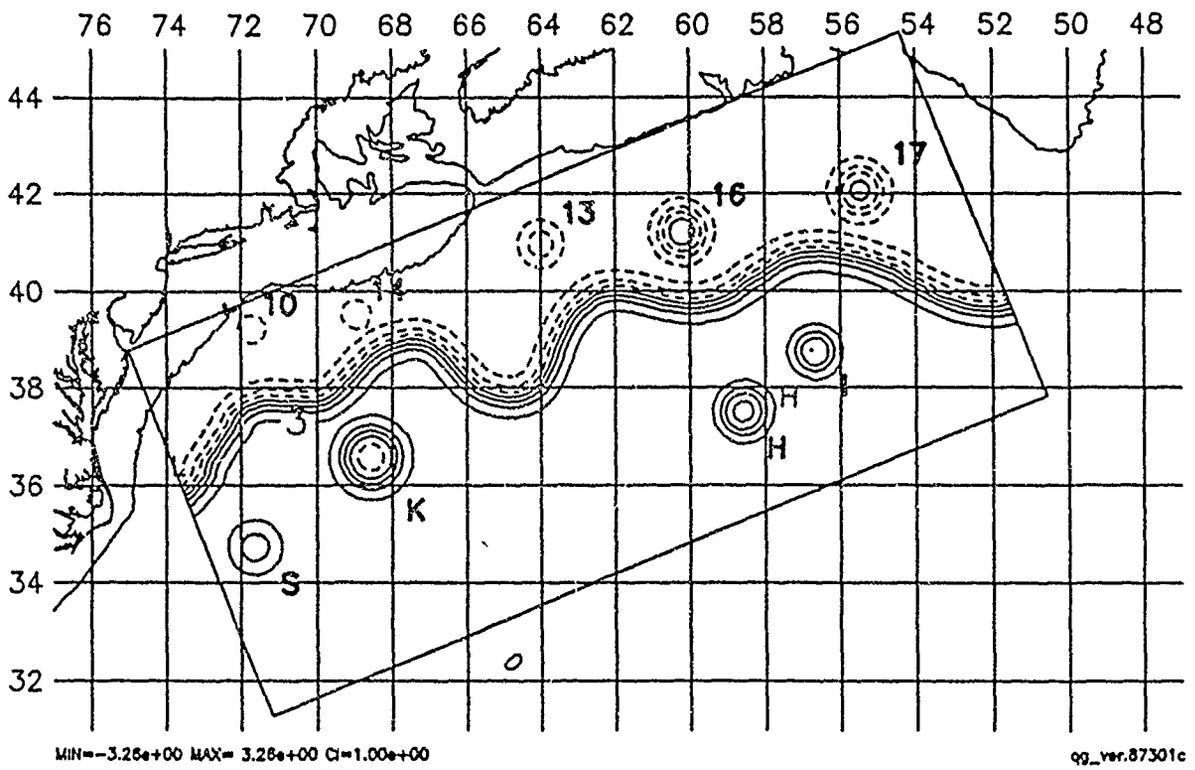

Initialization : 28 OCT 1987

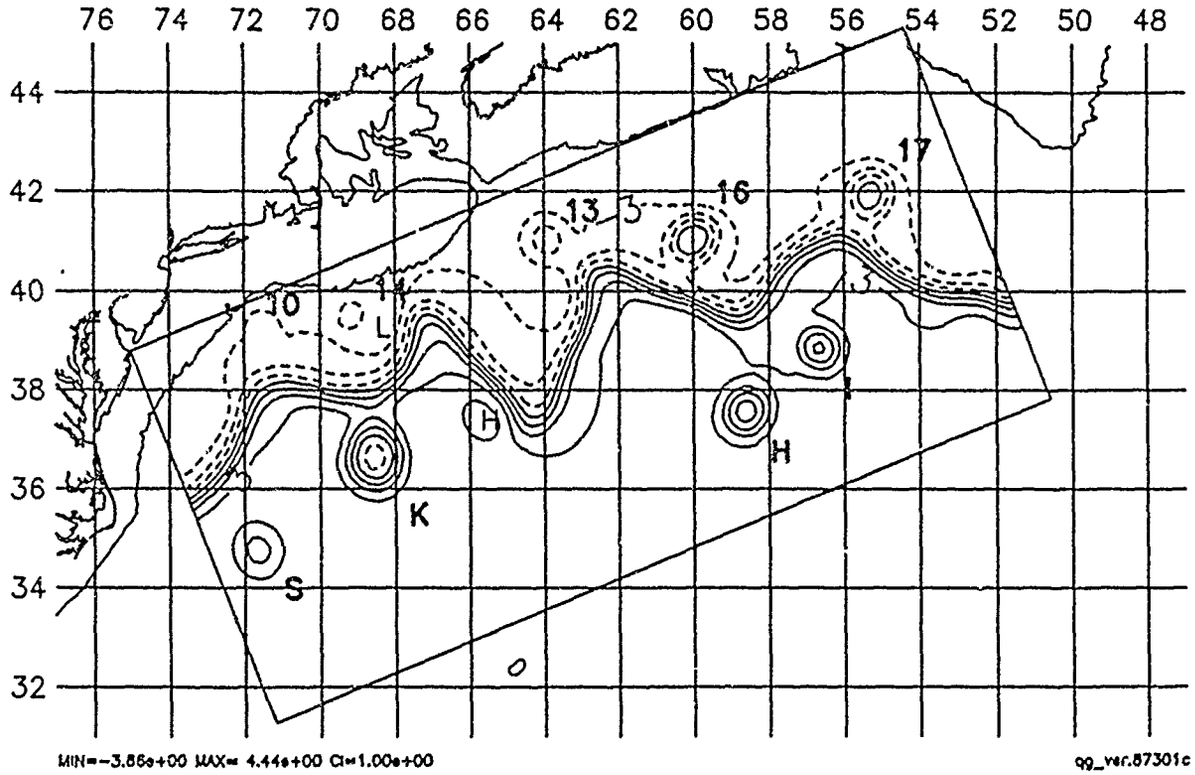

7 Day Forecast : 4 NOV 1987

HARVARD UNIVERSITY GULFCAST

OPERATIONAL EVALUATION FORECAST.

NEW DATA: IR, GEOSAT.

Figure: Streamfunction at 100 m.

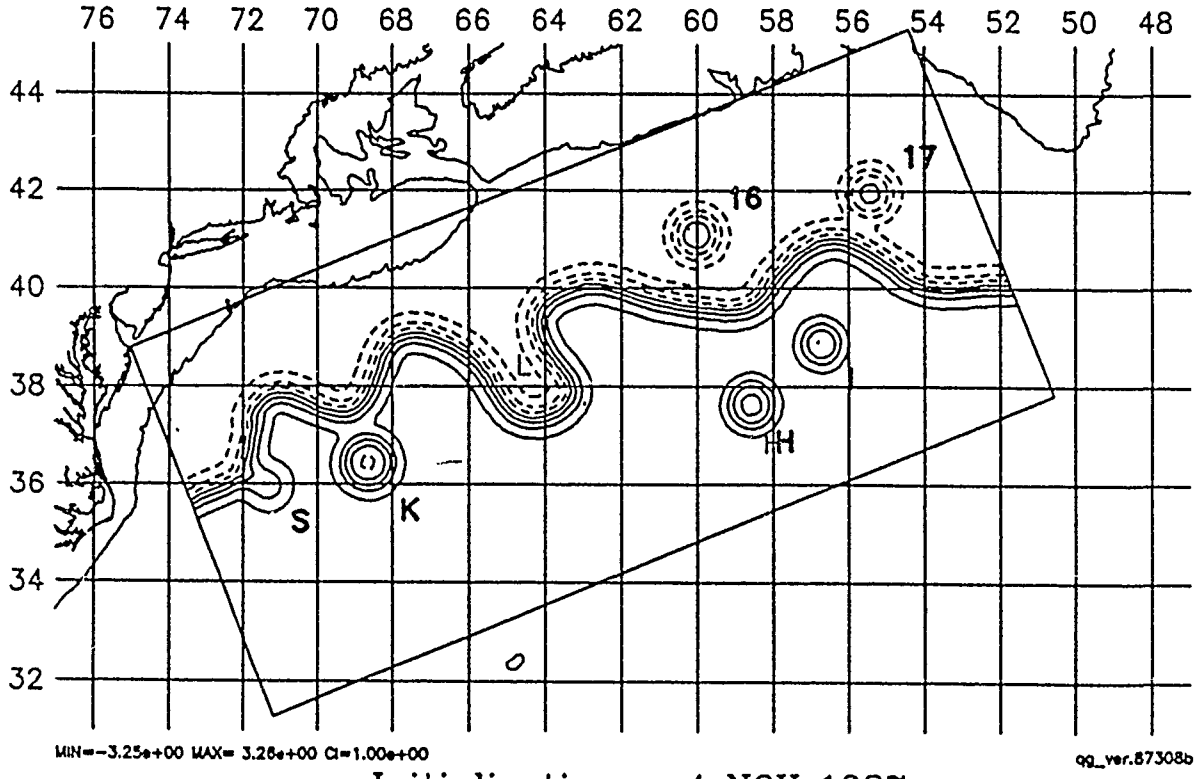

Initialization : 4 NOV 1987

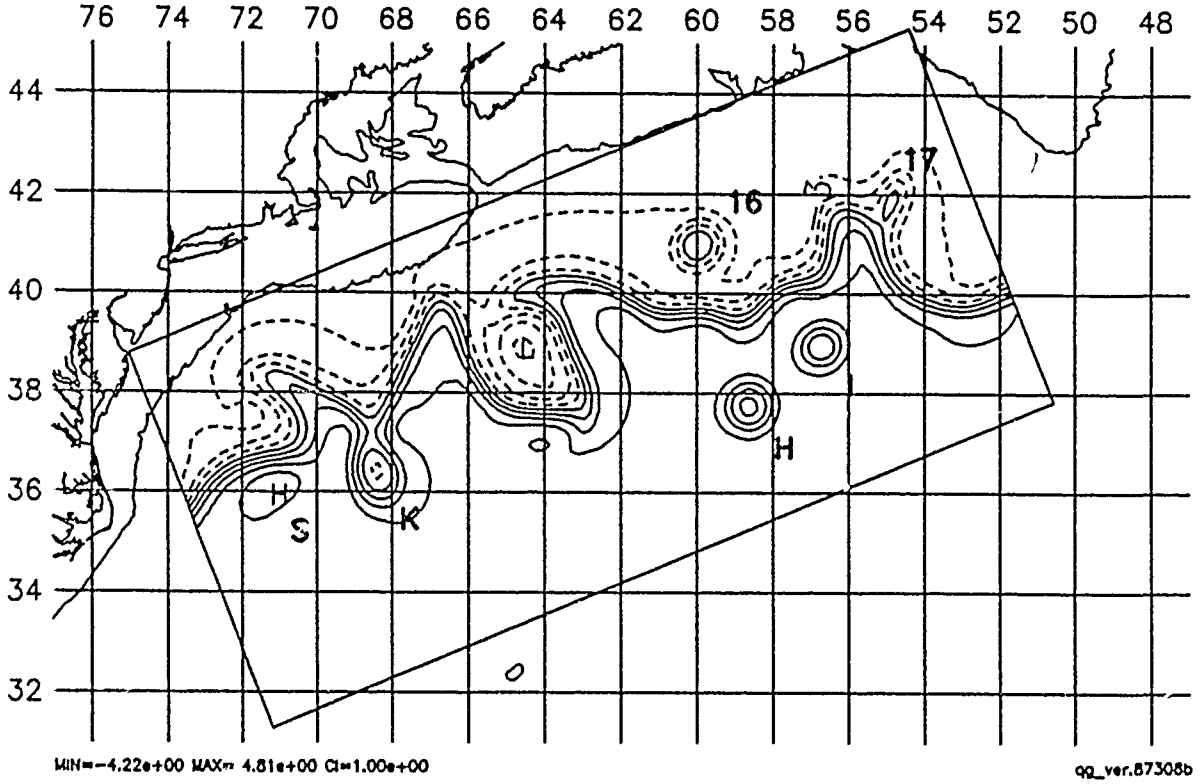

7 Day Forecast : 11 NOV 1987

HARVARD UNIVERSITY GULFCAST

OPERATIONAL EVALUATION FORECAST.

NEW DATA: IR, AXBT, GEOSAT.

Figure: Streamfunction at 100 m.

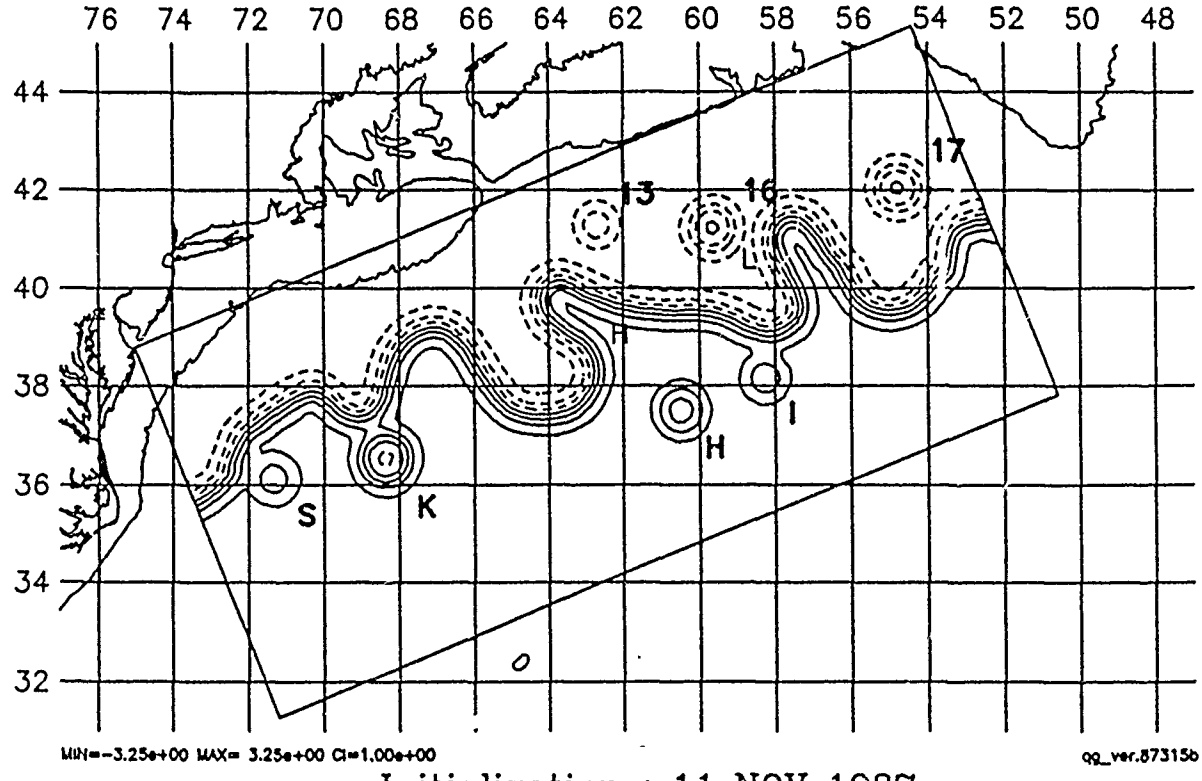

Initialization : 11 NOV 1987

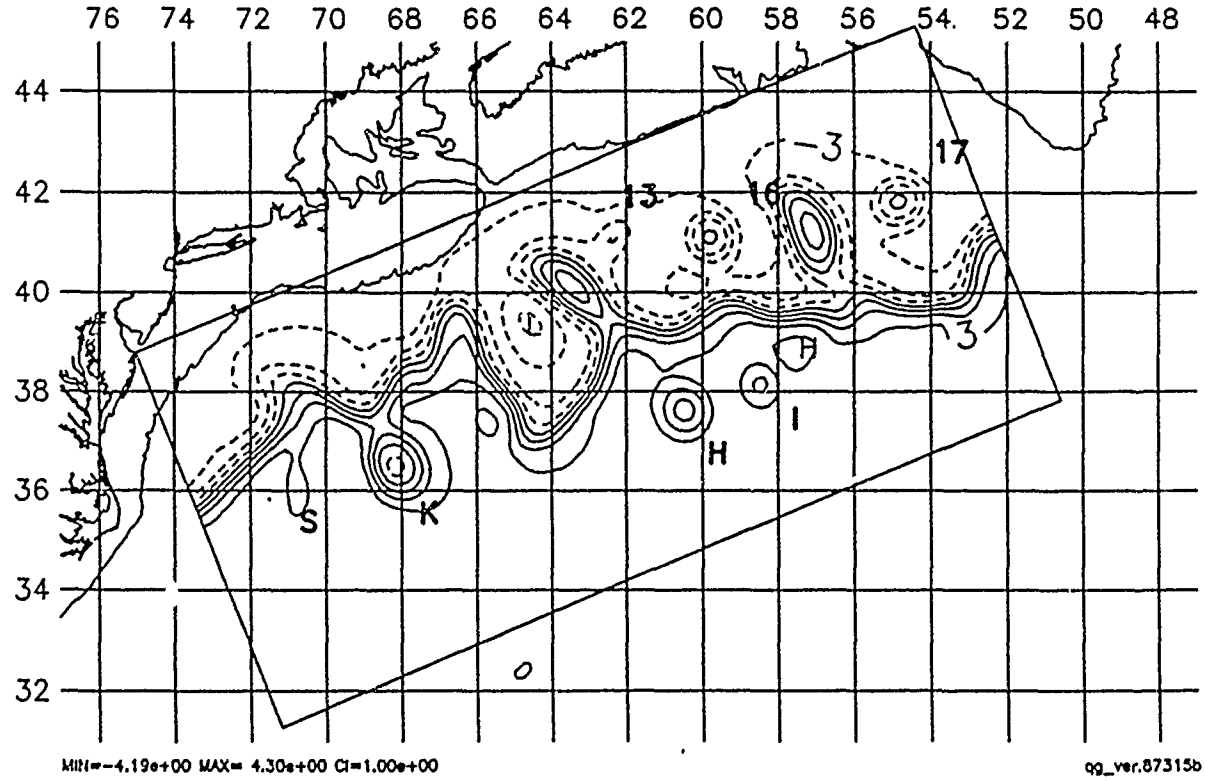

7 Day Forecast : 18 NOV 1987

HARVARD UNIVERSITY GULFCAST

OPERATIONAL EVALUATION FORECAST.

NEW DATA: IR.

Figure: Streamfunction at 100 m.

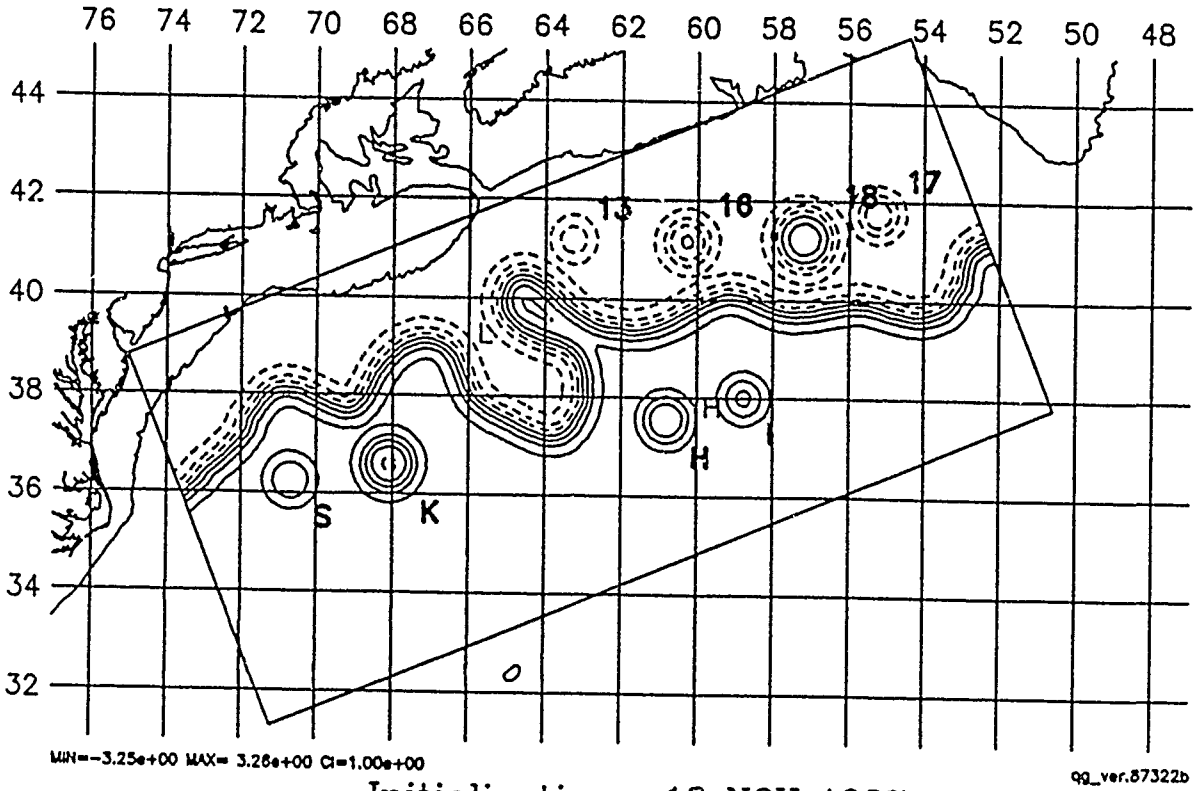

Initialization : 18 NOV 1987

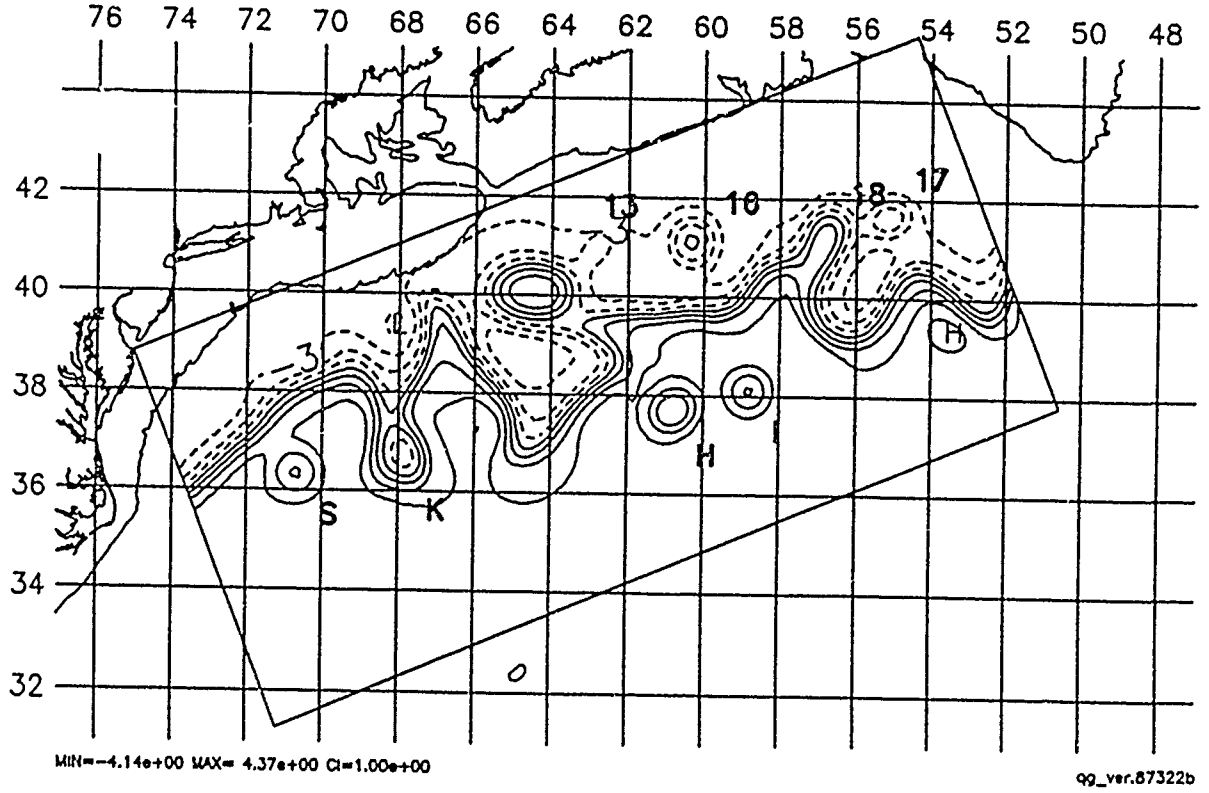

7 Day Forecast : 25 NOV 1987

HARVARD UNIVERSITY GULFCAST

OPERATIONAL EVALUATION FORECAST.

NEW DATA: IR.

Figure: Streamfunction at 100 m.

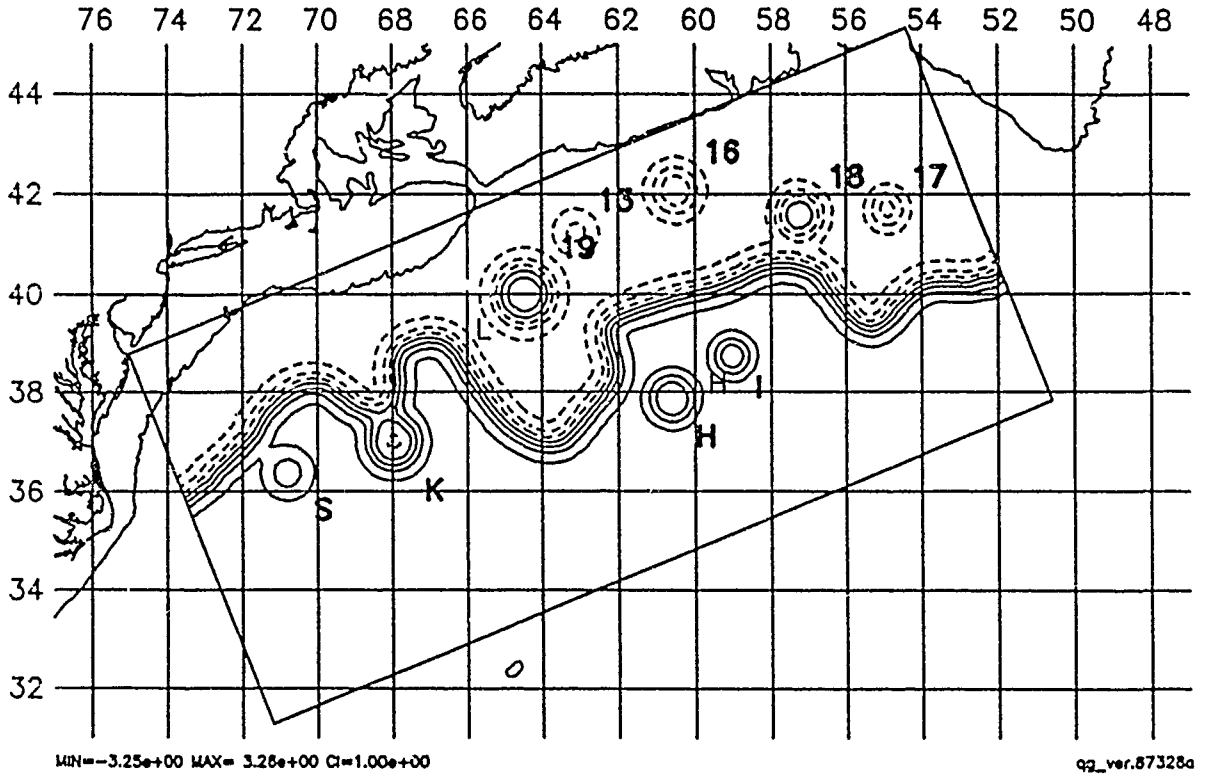

Initialization : 24 NOV 1987

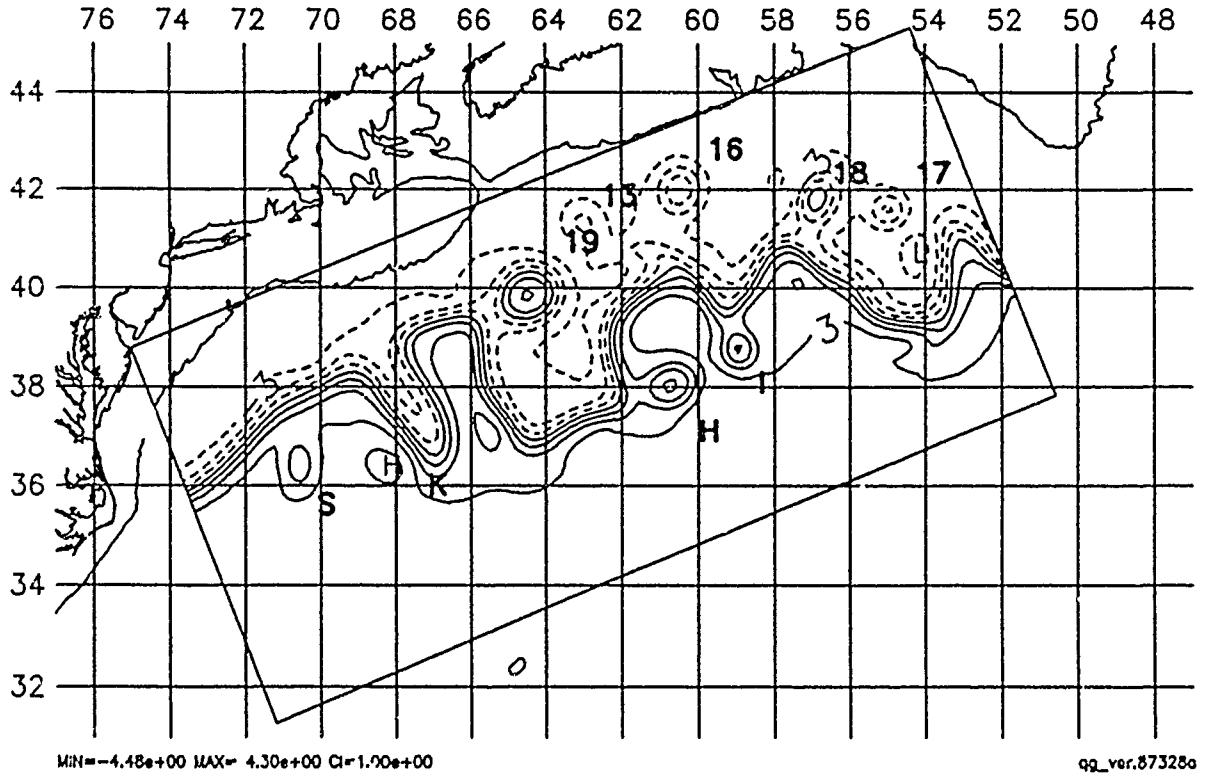

7 Day Forecast : 1 DEC 1987

VE RI TAS

HARVARD UNIVERSITY GULFCAST

OPERATIONAL EVALUATION FORECAST.

NEW DATA: IR.

Figure: Streamfunction at 100 m.

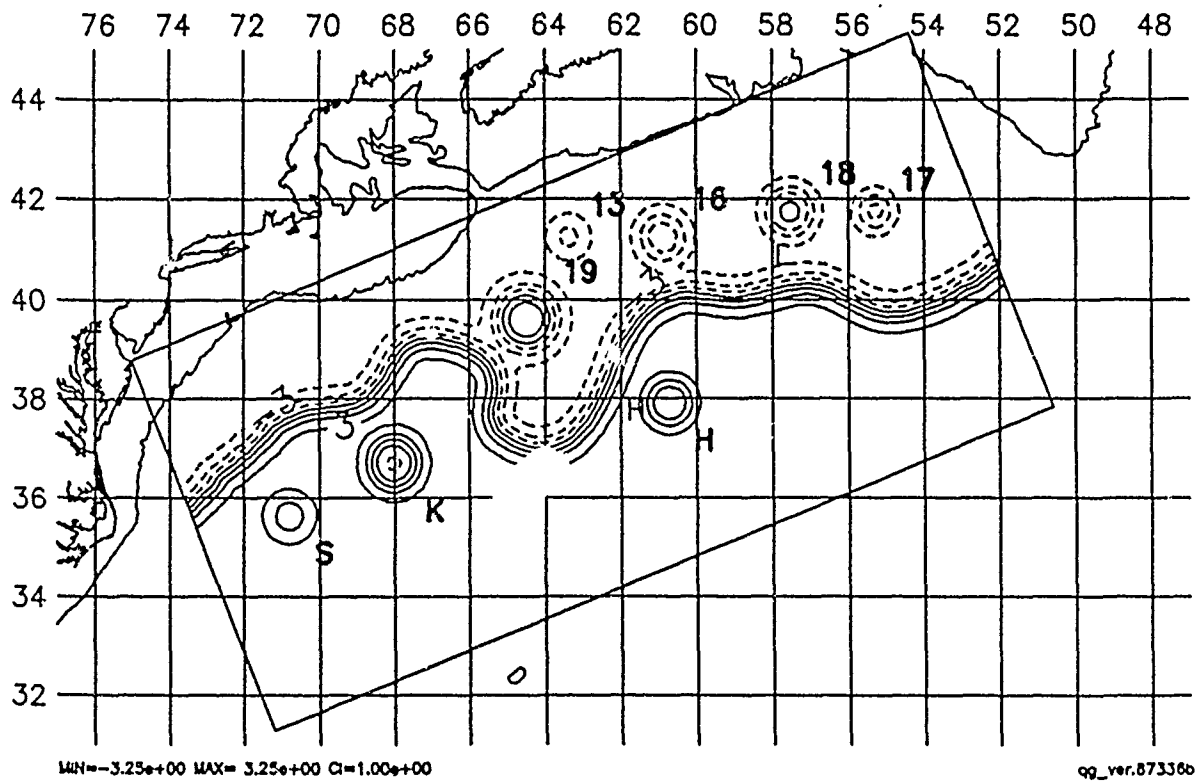

Initialization : 2 DEC 1987

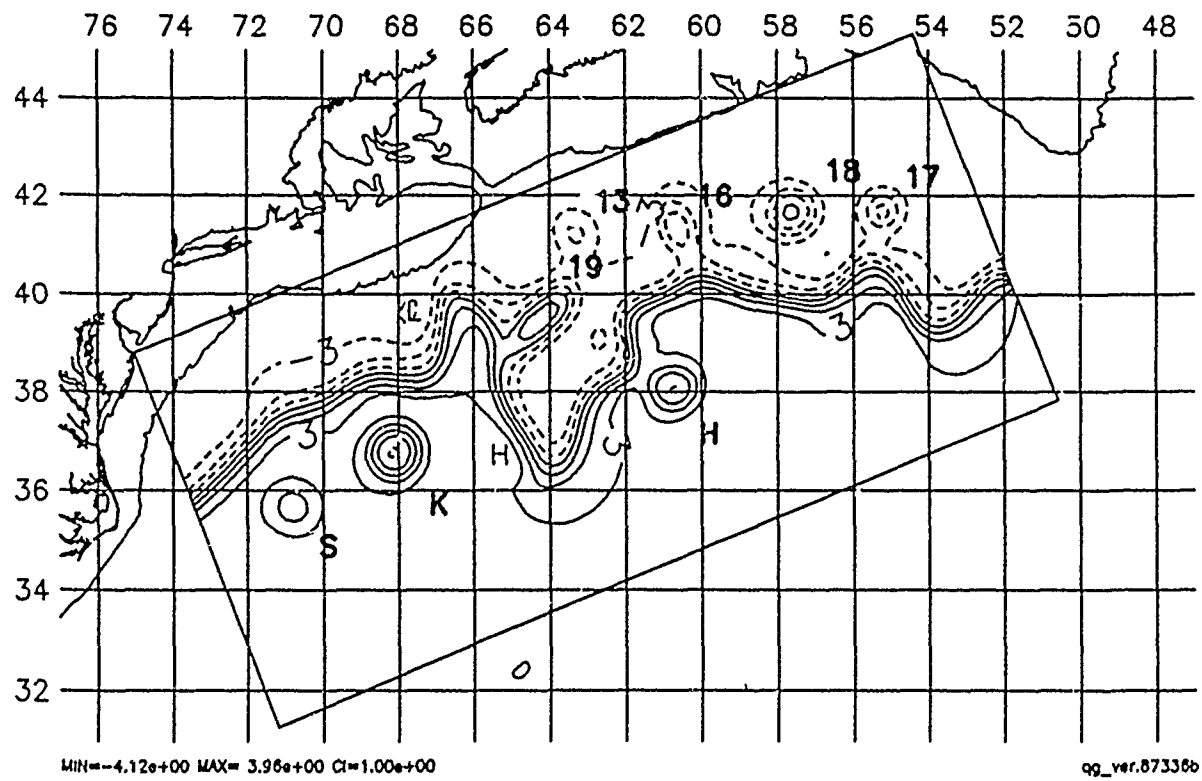

7 Day Forecast : 9 DEC 1987

HARVARD UNIVERSITY GULFCAST

OPERATIONAL EVALUATION FORECAST.

NEW DATA: IR, AXBT.

Figure: Streamfunction at 100 m.

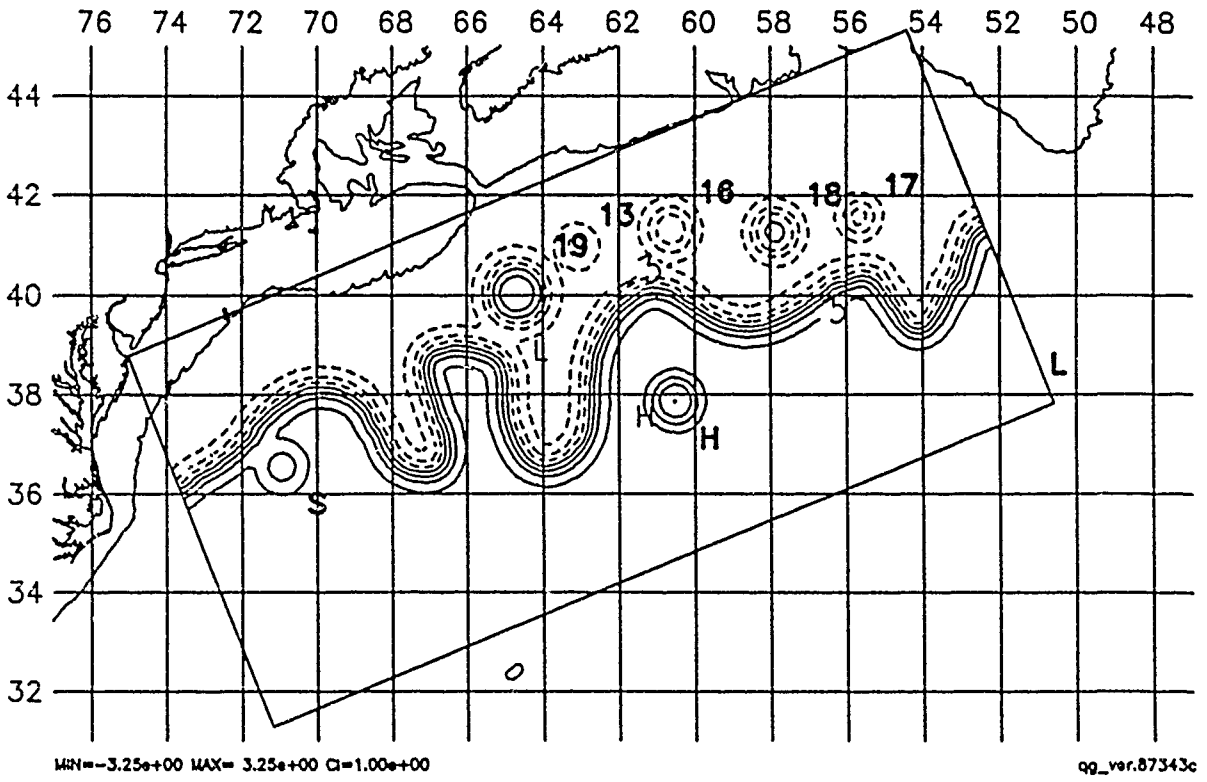

Initialization : 9 DEC 1987

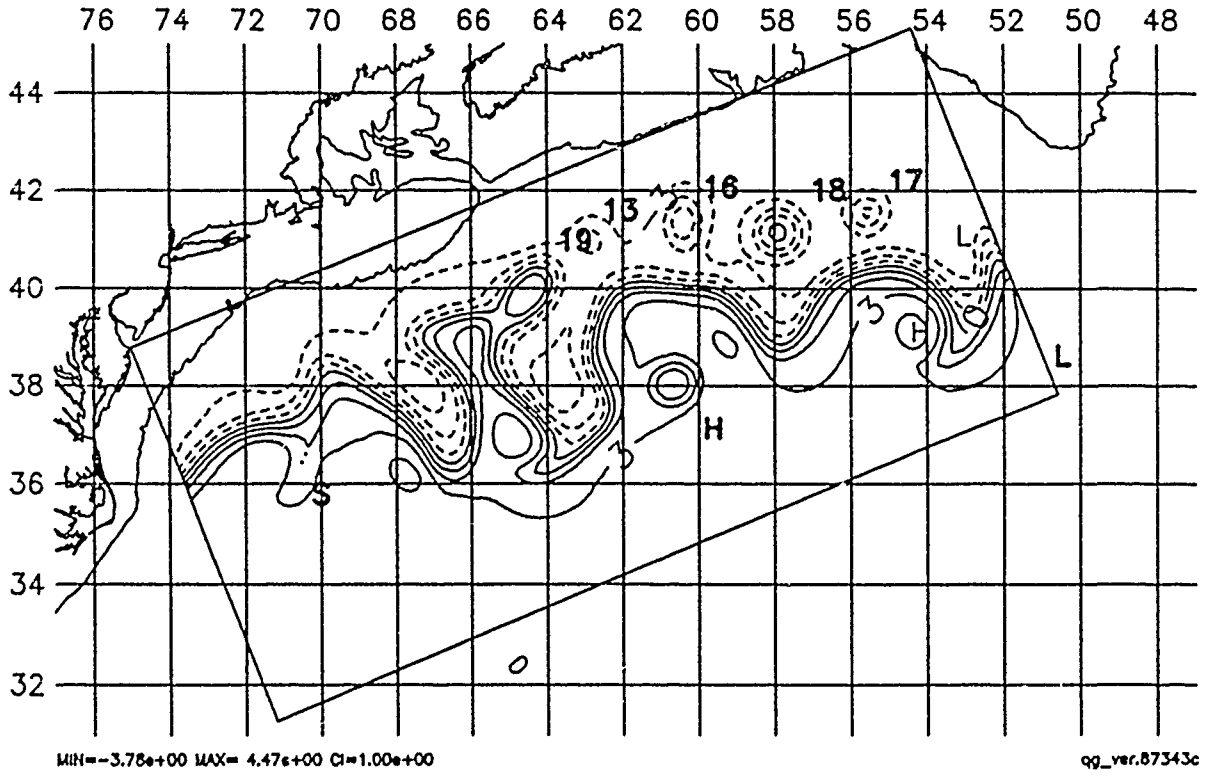

7 Day Forecast : 16 DEC 1987

VE RI TAS

HARVARD UNIVERSITY GULFCAST

OPERATIONAL EVALUATION FORECAST.

NEW DATA: IR.

Figure: Streamfunction at 100 m.

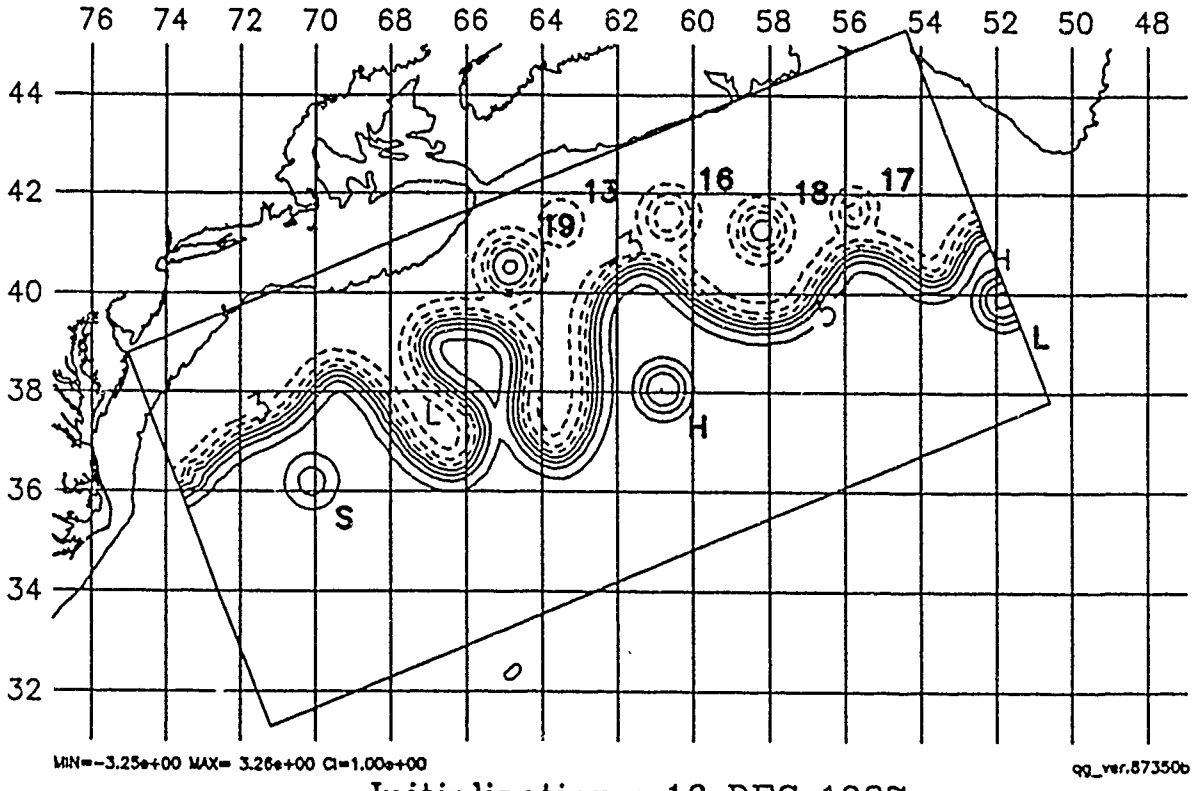

Initialization : 16 DEC 1987

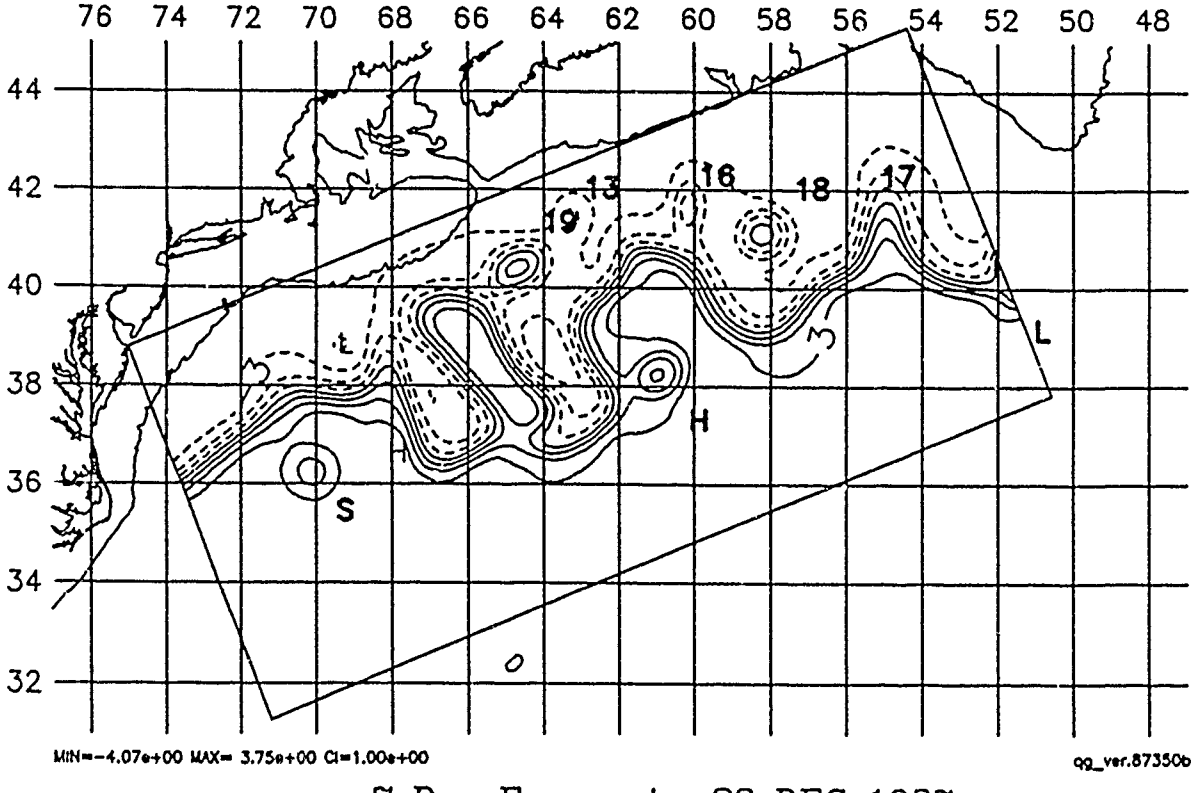

7 Day Forecast : 23 DEC 1987

HARVARD UNIVERSITY GULFCAST

OPERATIONAL EVALUATION FORECAST.

NEW DATA: IR.

Figure: Streamfunction at 100 m.

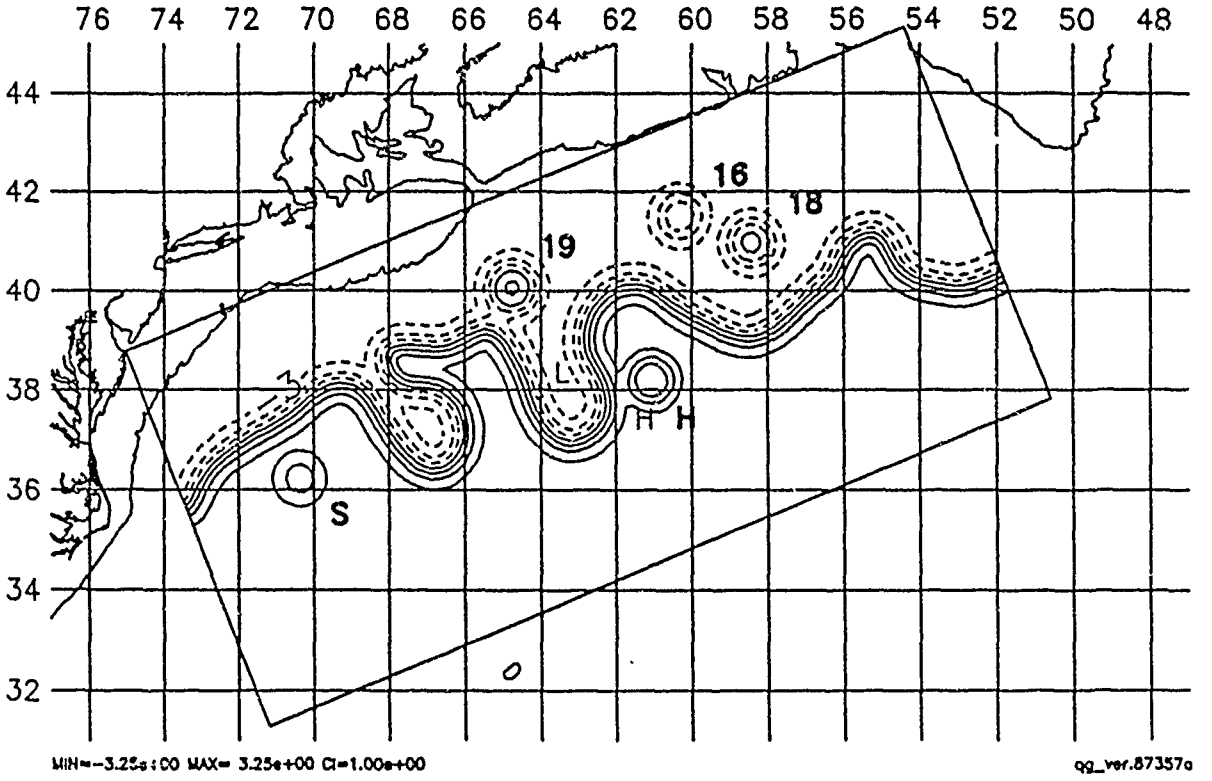

Initialization : 23 DEC 1987

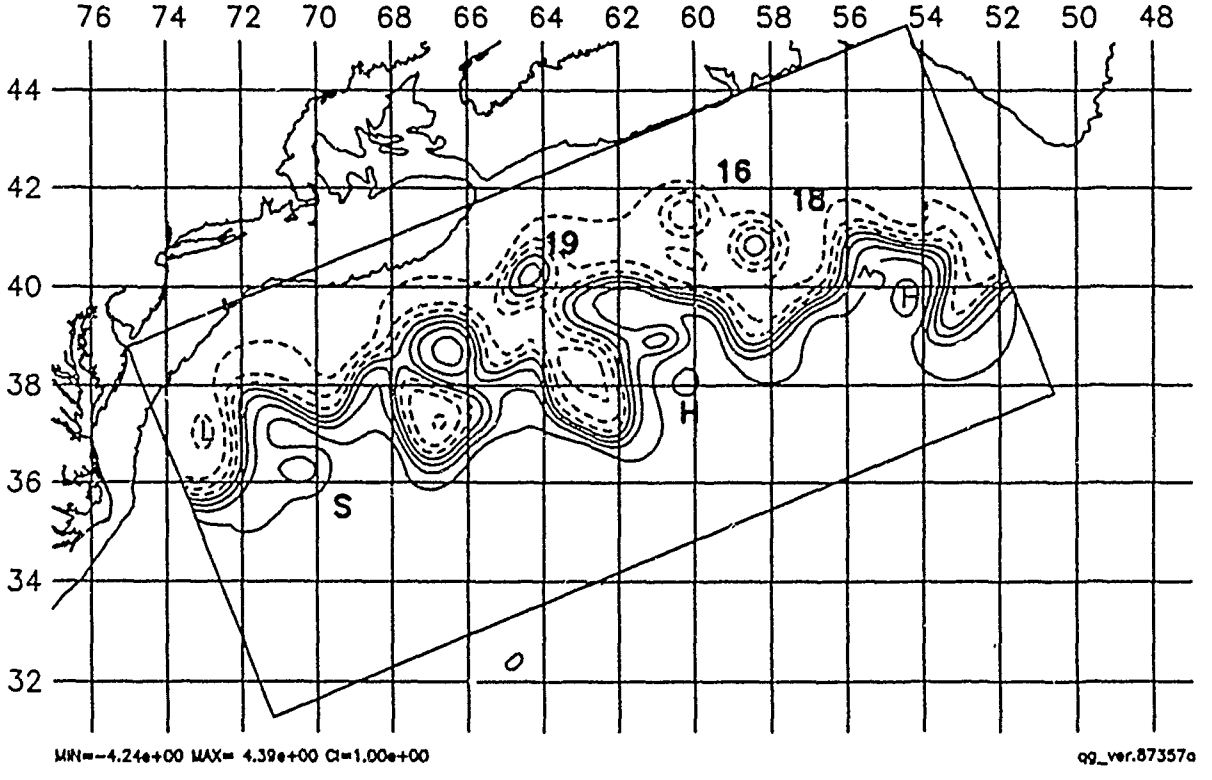

7 Day Forecast : 30 DEC 1987

HARVARD UNIVERSITY GULFCAST

OPERATIONAL EVALUATION FORECAST.

NEW DATA: IR.

Figure: Streamfunction at 100 m.

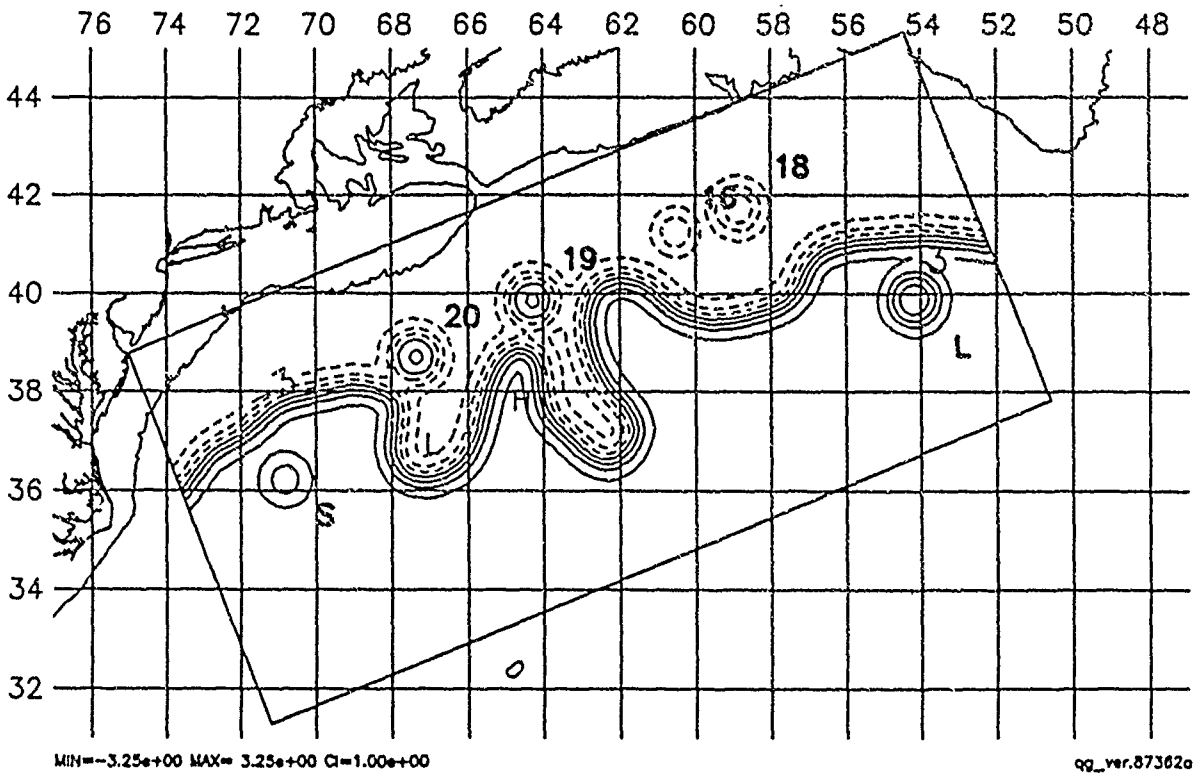

Initialization : 28 DEC 1987

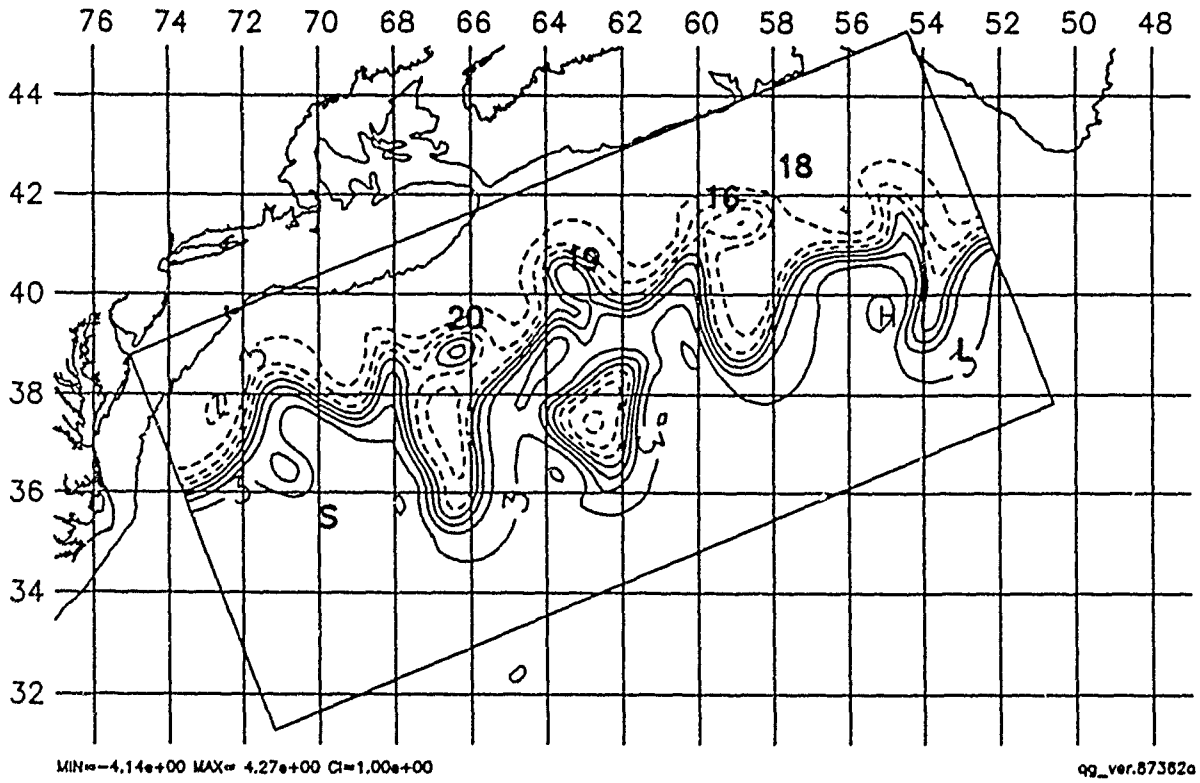

9 Day Forecast : 6 JAN 1988

HARVARD UNIVERSITY GULFCAST

OPERATIONAL EVALUATION FORECAST.

NEW DATA: IR, AXBT, ARGOS.

Figure: Streamfunction at 100 m.

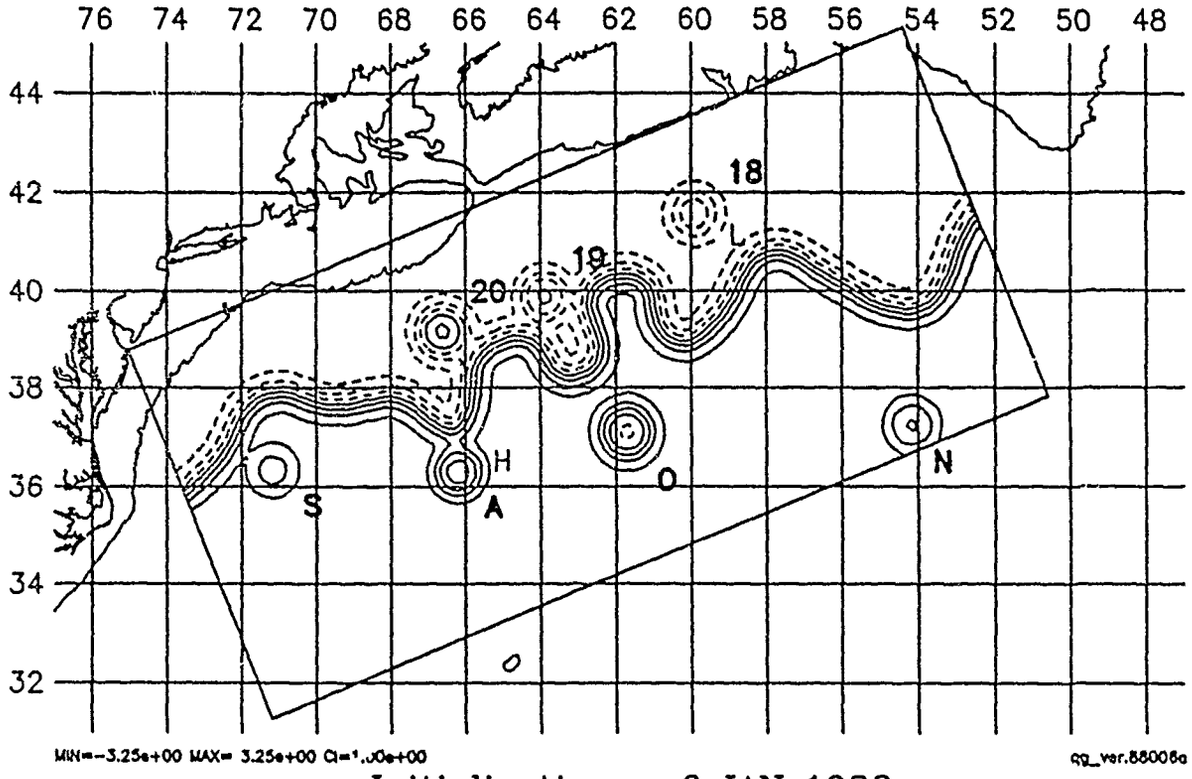

Initialization : 6 JAN 1988

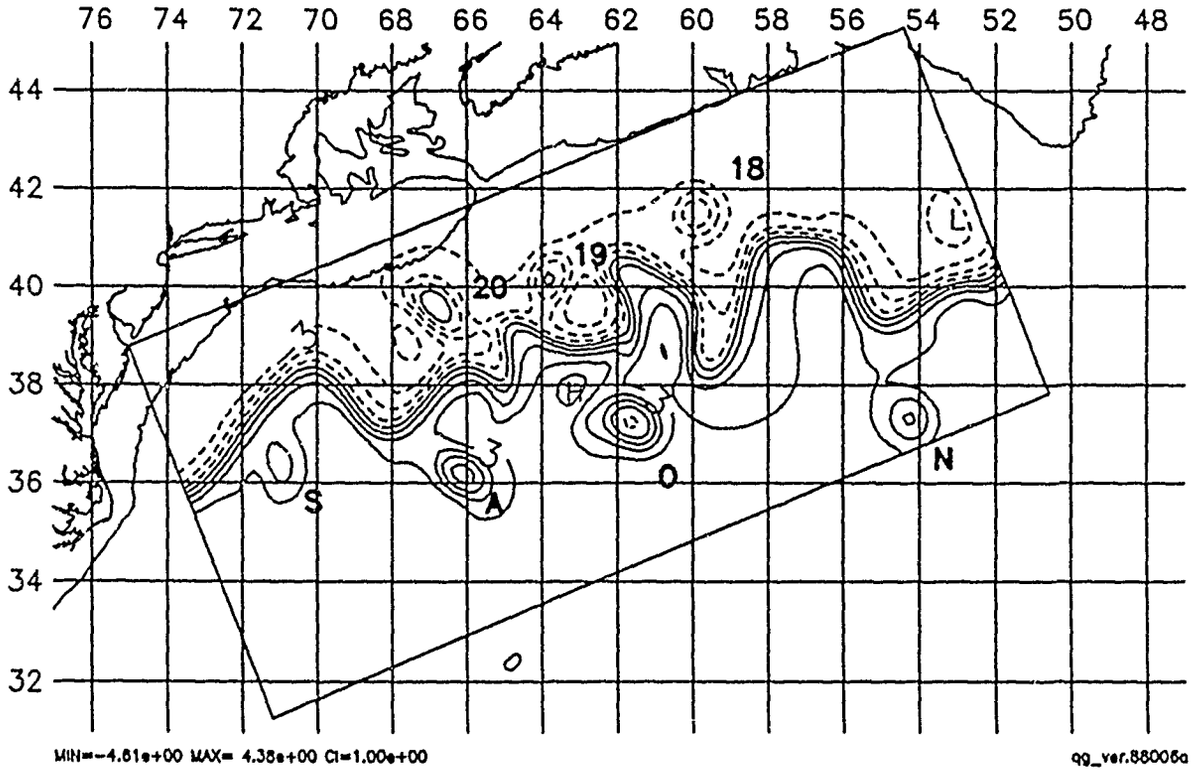

7 Day Forecast : 13 JAN 1988

HARVARD UNIVERSITY GULFCAST

OPERATIONAL EVALUATION FORECAST.

NEW DATA: IR, AXBT.

Figure: Streamfunction at 100 m.

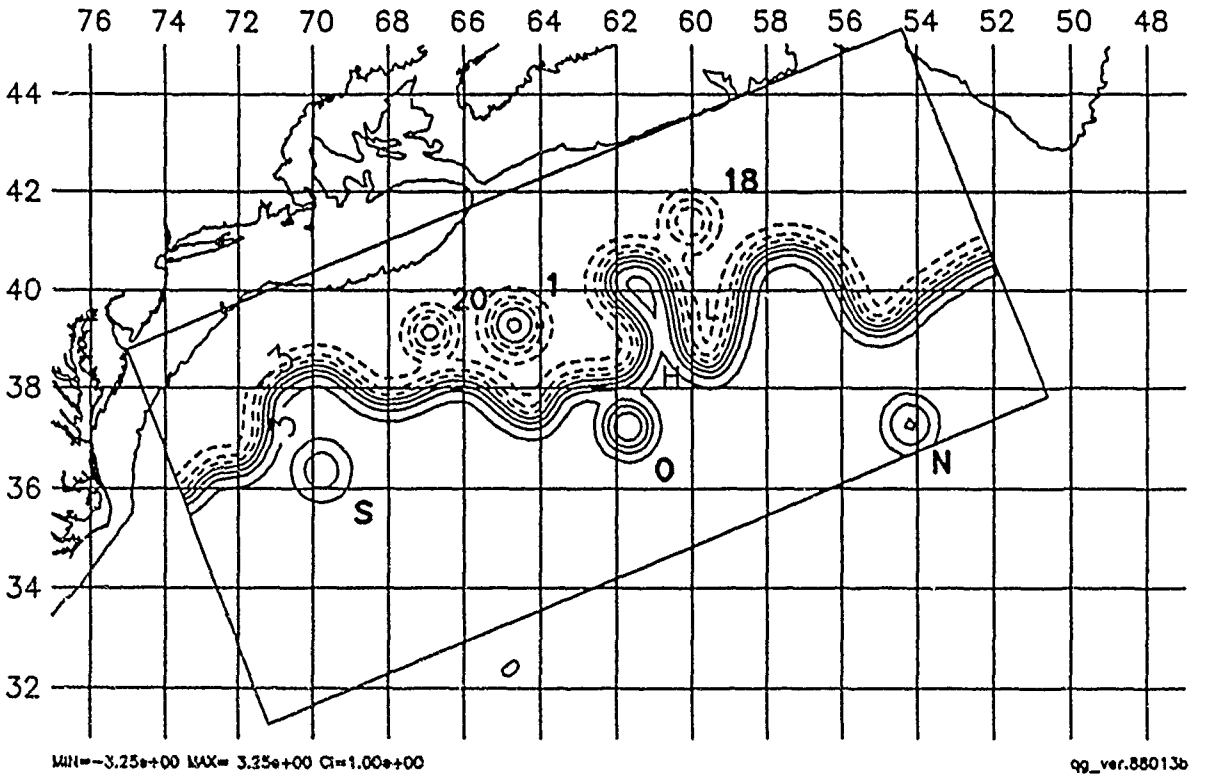

Initialization : 13 JAN 1988

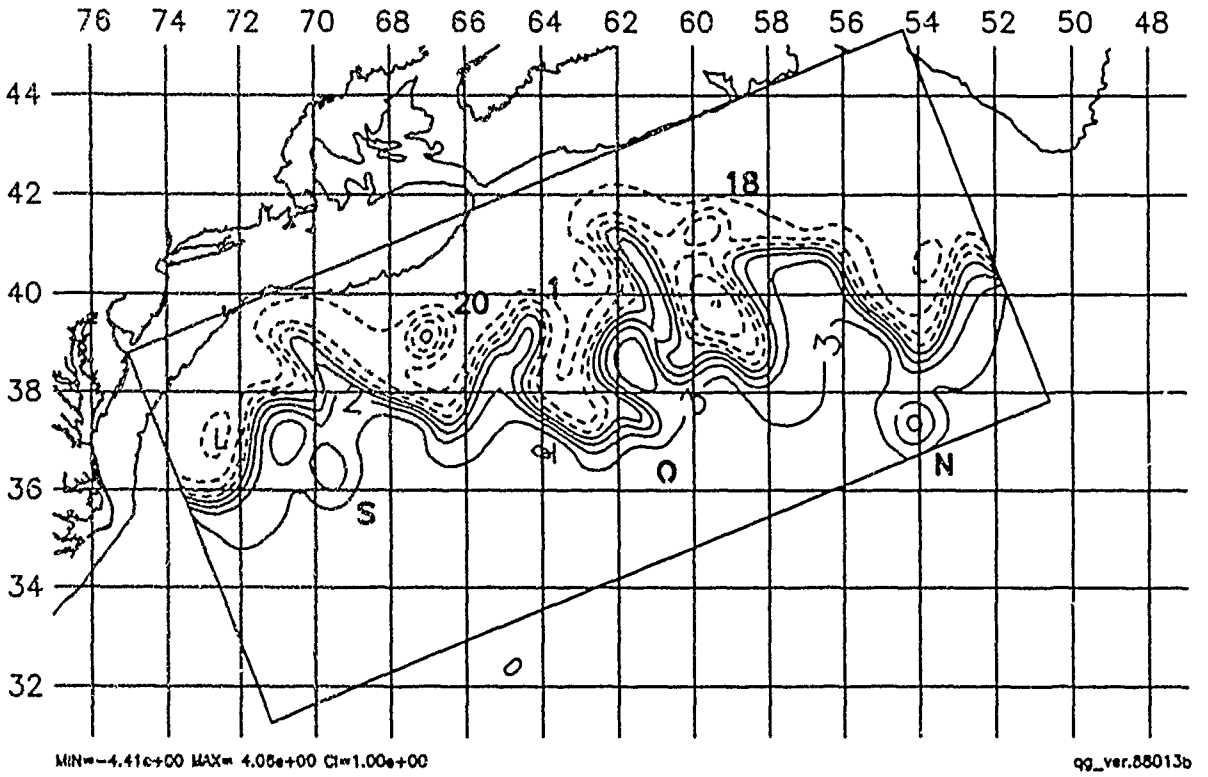

7 Day Forecast : 20 JAN 1988

HARVARD UNIVERSITY GULFCAST

OPERATIONAL EVALUATION FORECAST.

NEW DATA: IR.

Figure: Streamfunction at 100 m.

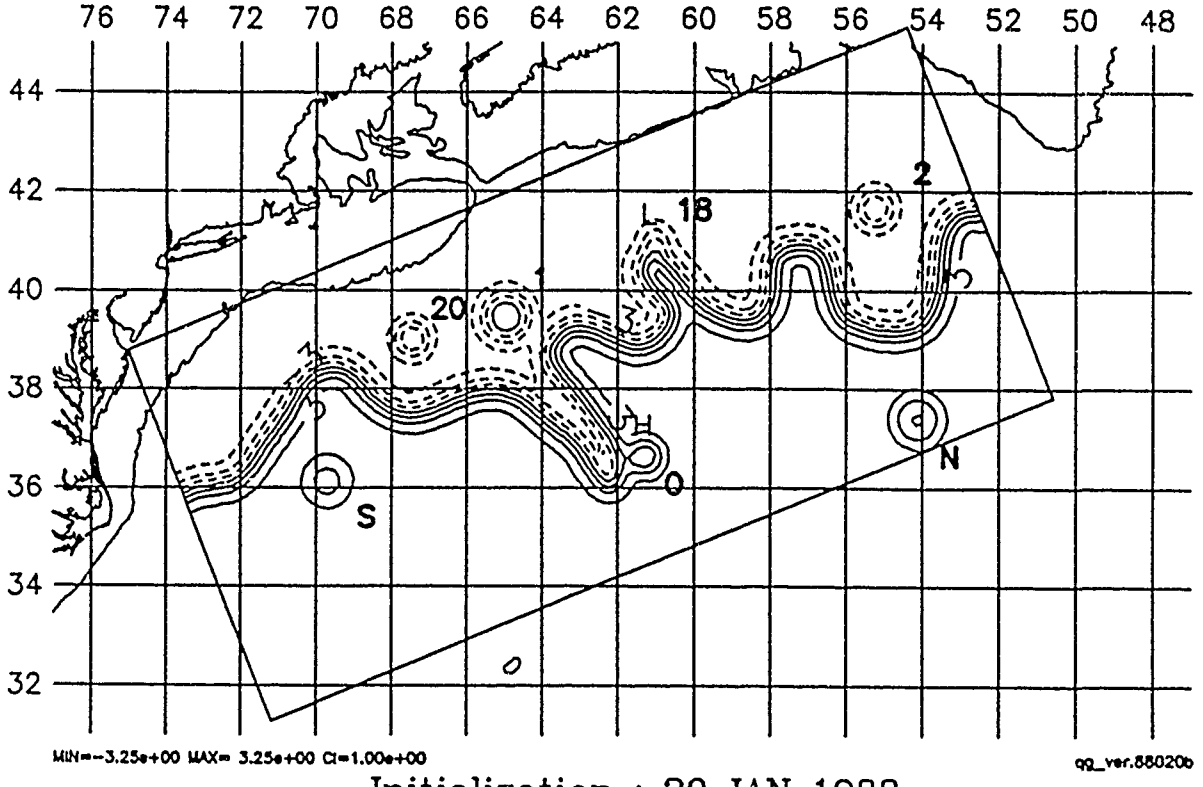

Initialization : 20 JAN 1988

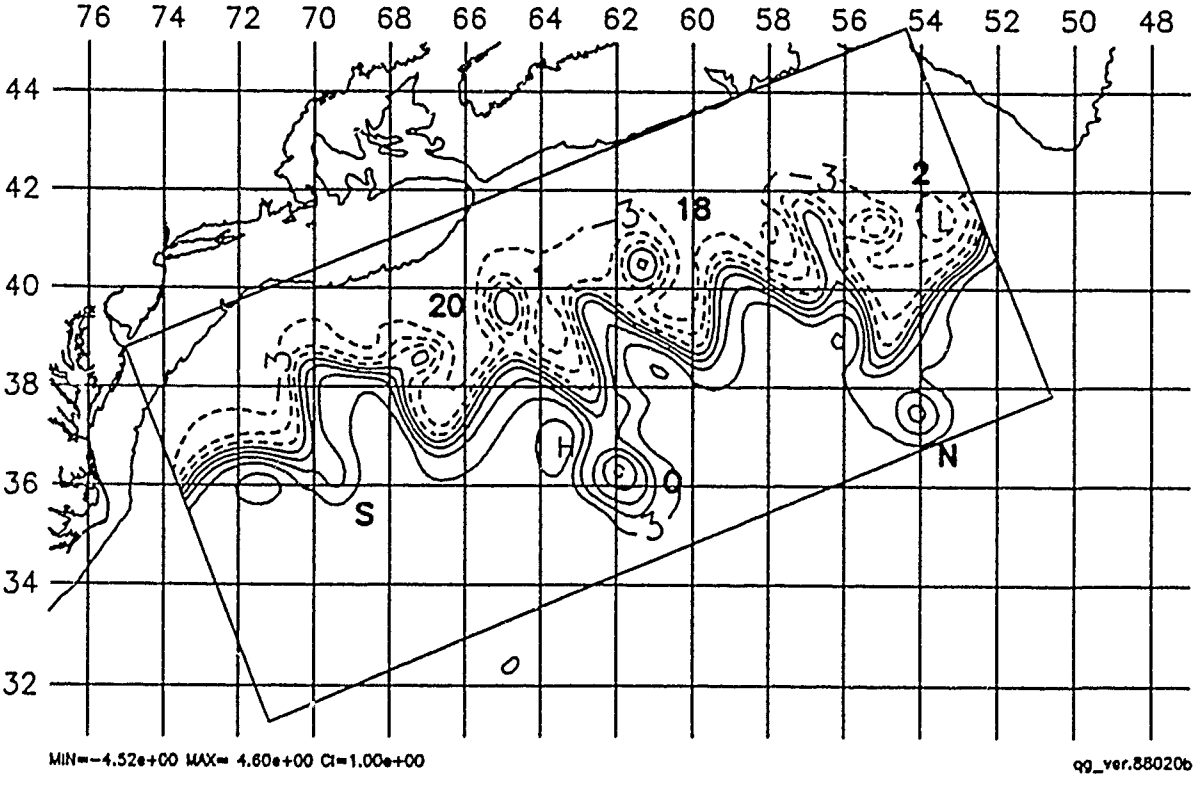

7 Day Forecast : 27 JAN 1988

HARVARD UNIVERSITY GULFCAST

OFERATIONAL EVALUATION FORECAST.

NEW DATA: IR, AXBT.

Figure: Streamfunction at 100 m.

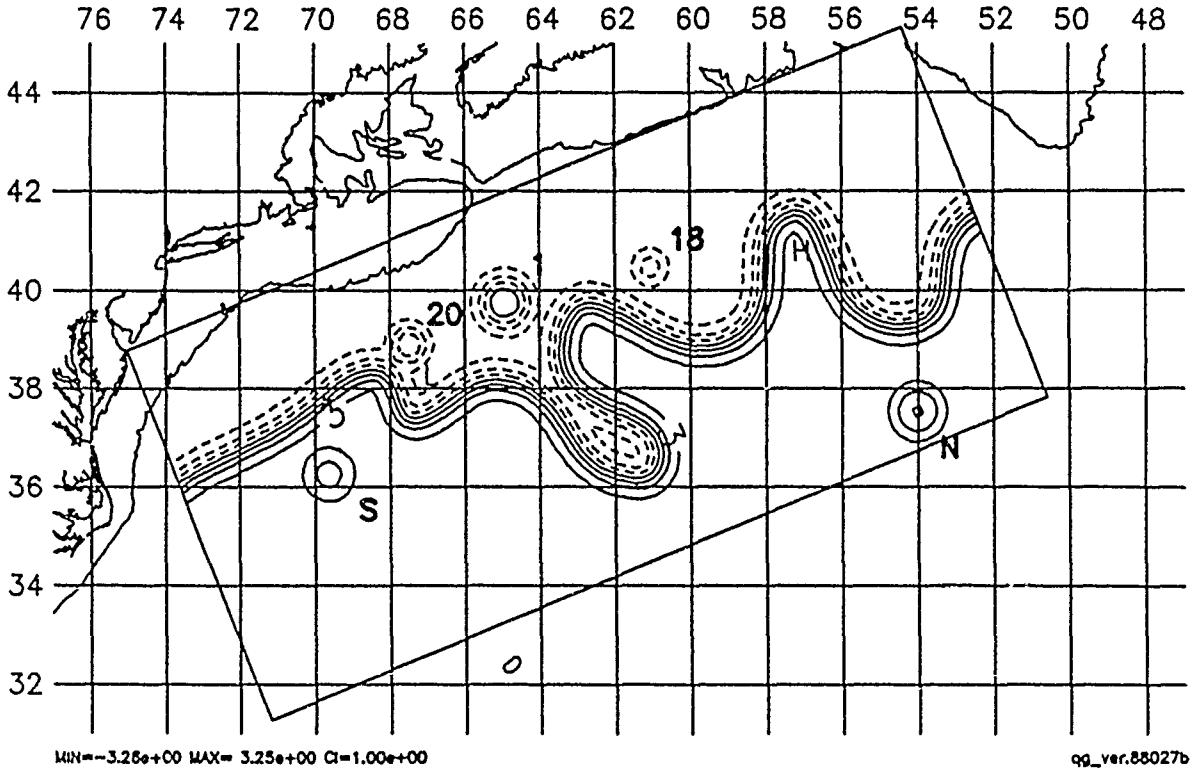

Initialization : 27 JAN 1988

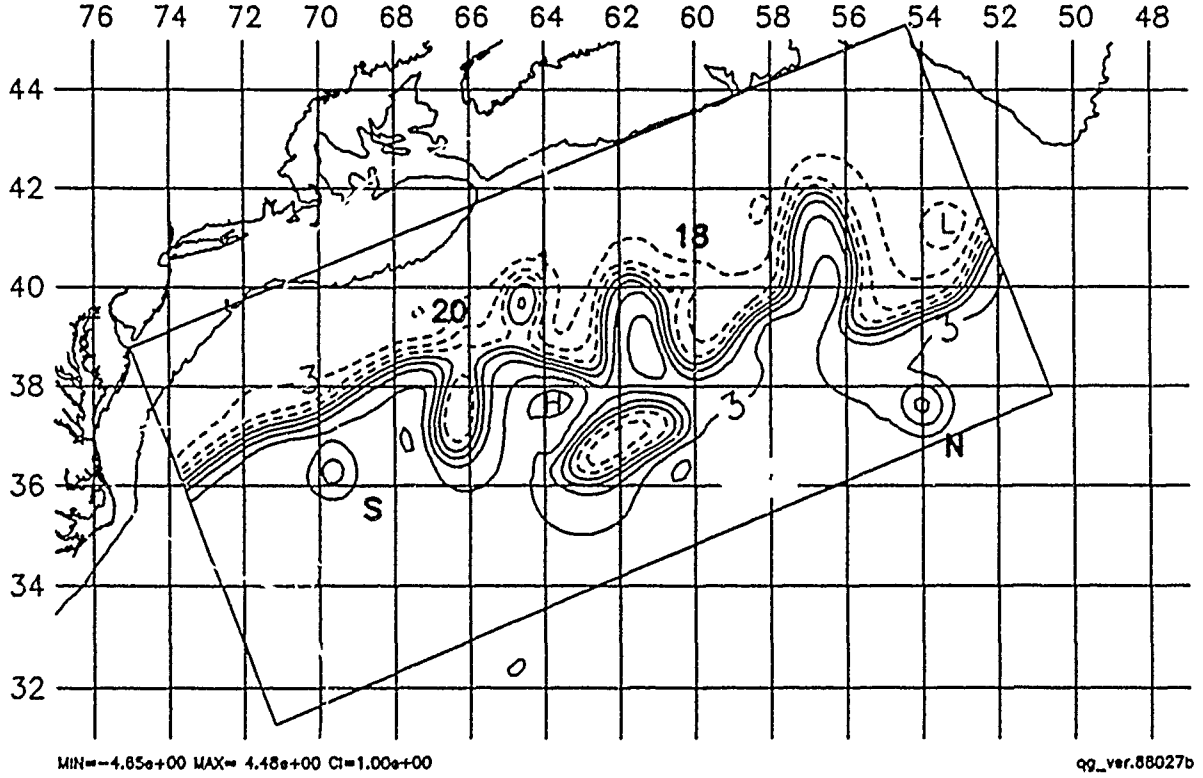

7 Day Forecast : 3 FEB 1988

HARVARD UNIVERSITY GULFCAST

OPERATIONAL EVALUATION FORECAST.

NEW DATA: IR, AXBT.

Figure: Streamfunction at 100 m.

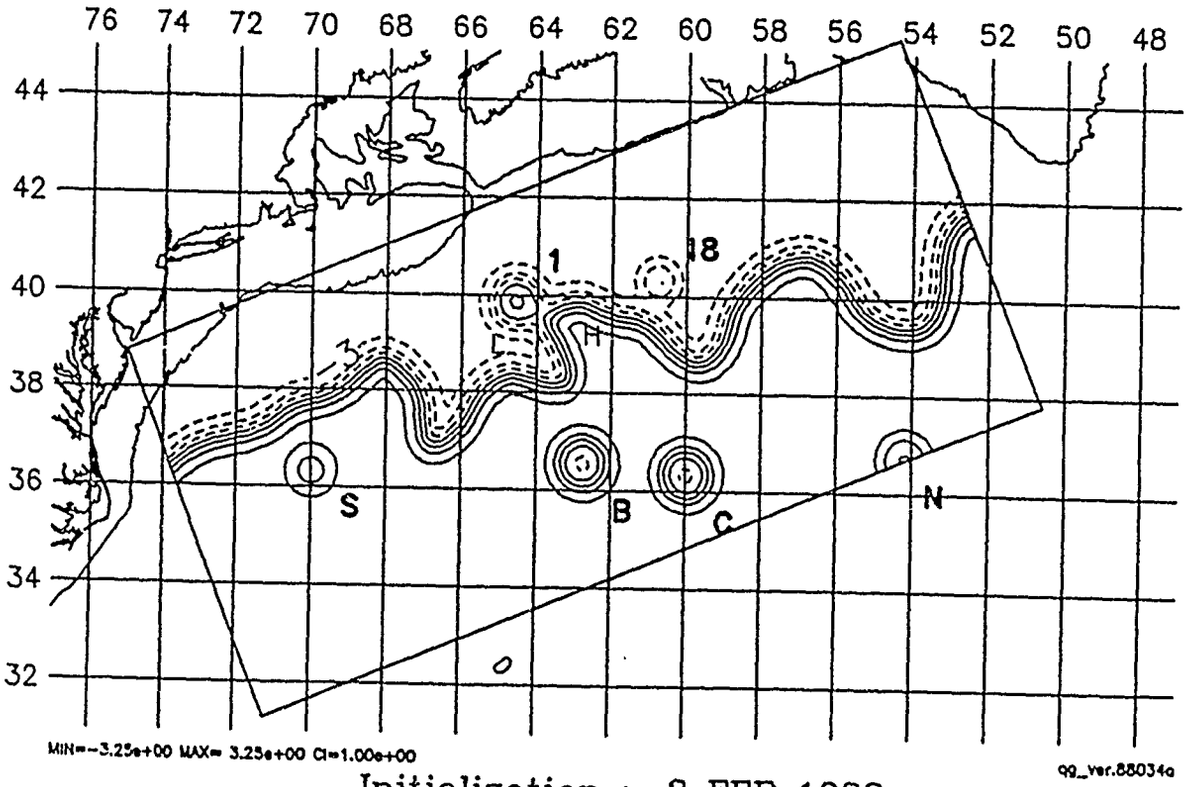

Initialization : 3 FEB 1988

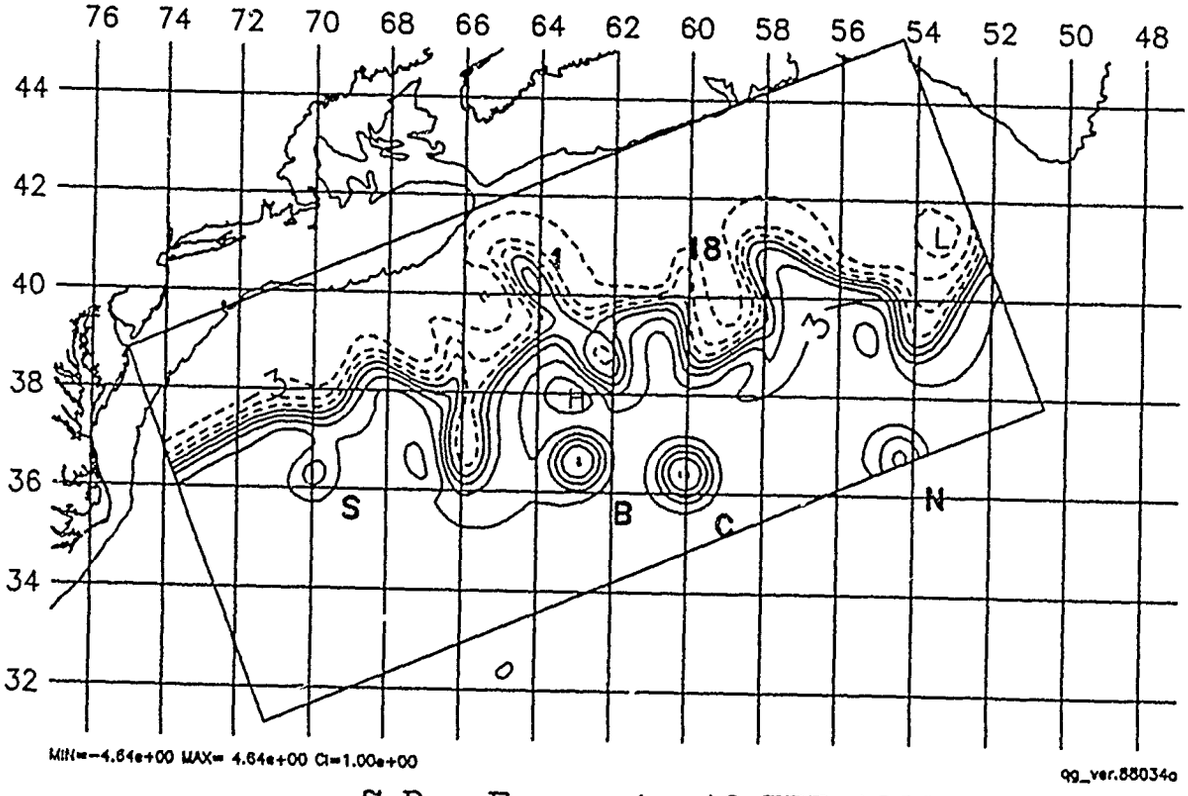

7 Day Forecast : 10 FEB 1988

HARVARD UNIVERSITY GULFCAST

OPERATIONAL EVALUATION FORECAST.

NEW DATA: IR, GEOSAT.

Figure: Streamfunction at 100 m.

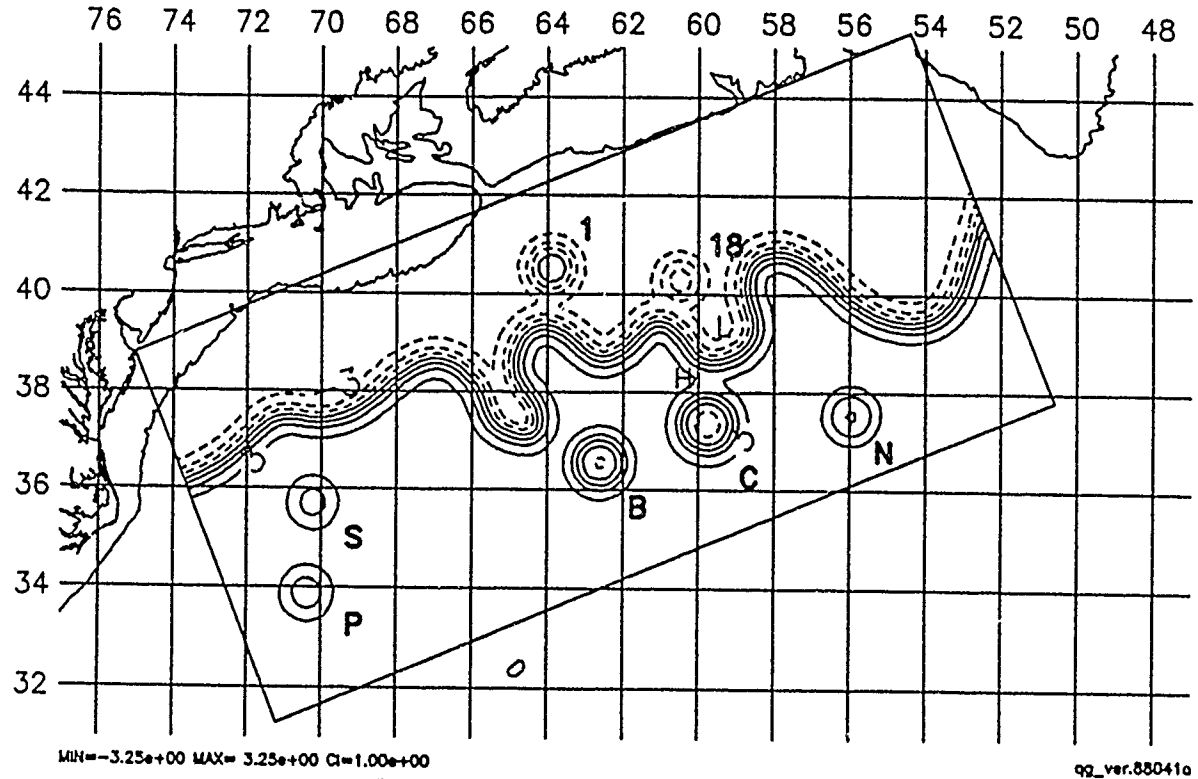

Initialization : 10 FEB 1988

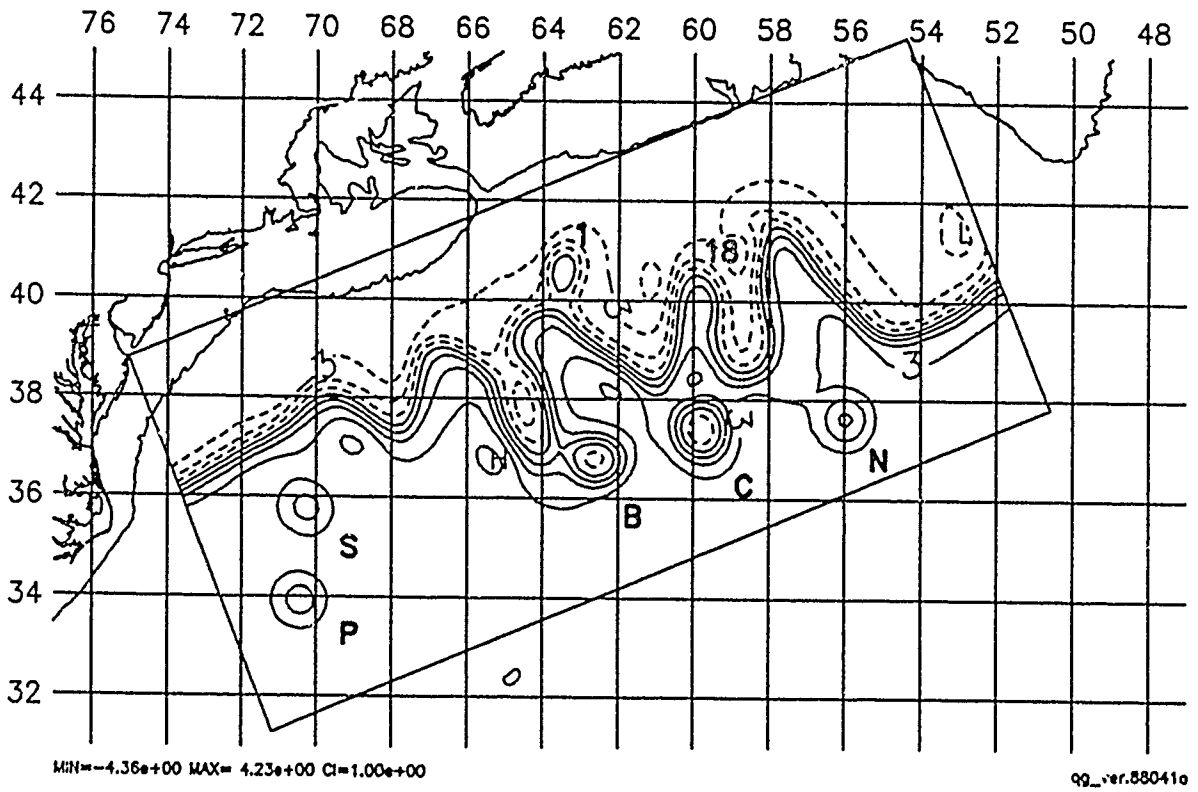

7 Day Forecast : 17 FEB 1988

HARVARD UNIVERSITY GULFCAST

OPERATIONAL EVALUATION FORECAST.

NEW DATA: IR, AXBT, GEOSAT.

Figure: Streamfunction at 100 m.

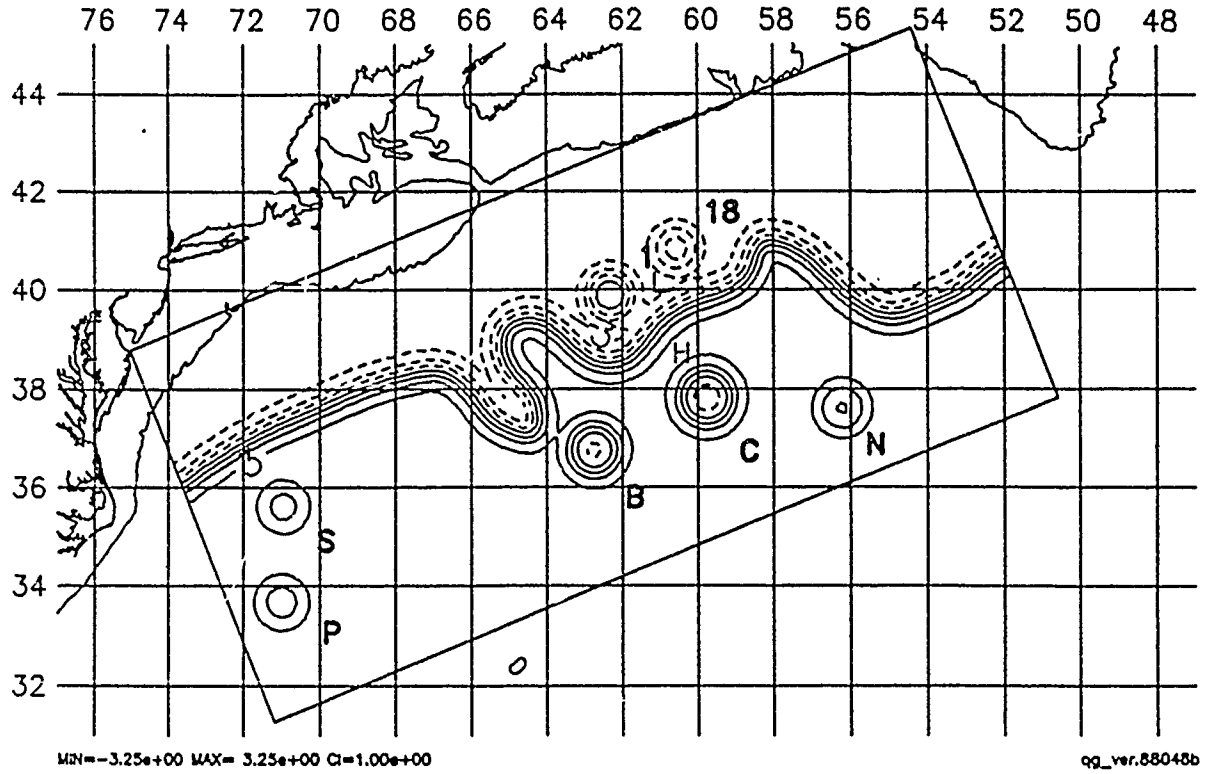

Initialization : 17 FEB 1988

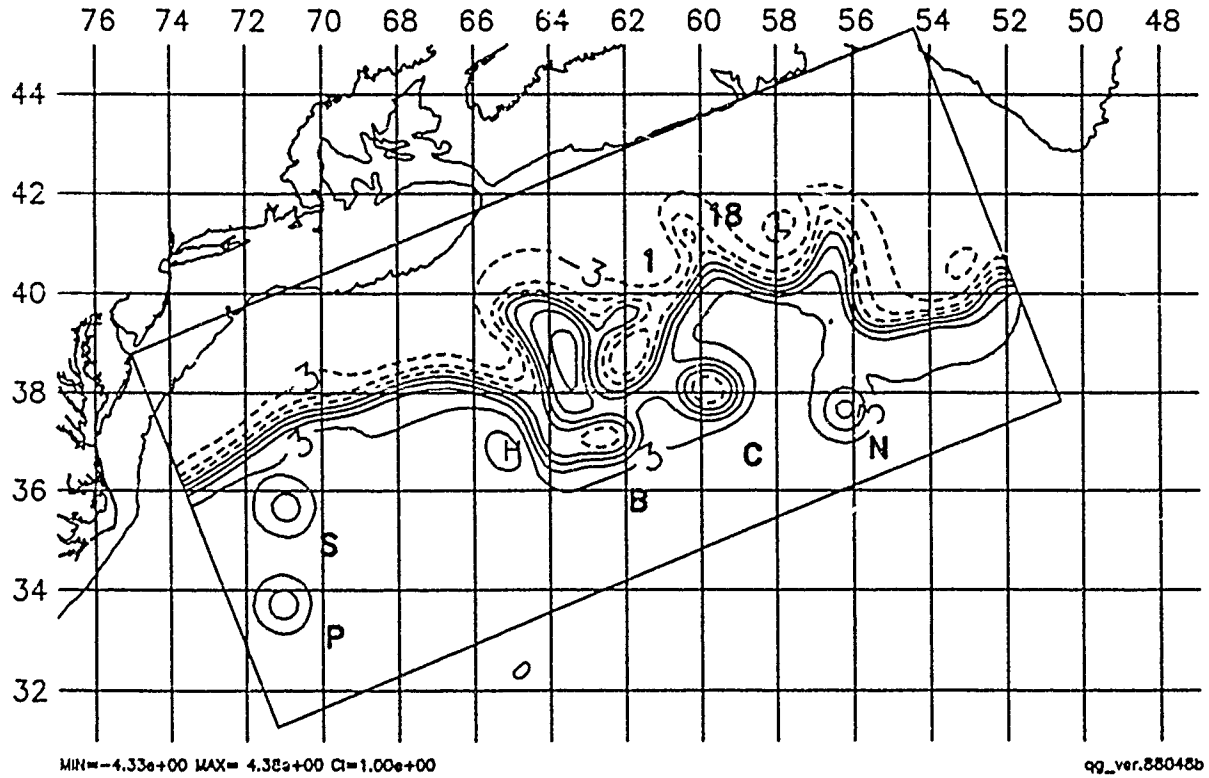

7 Day Forecast : 24 FEB 1988

HARVARD UNIVERSITY GULFCAST

OPERATIONAL EVALUATION FORECAST.

NEW DATA: IR, GEOSAT.

Figure: Streamfunction at 100 m.

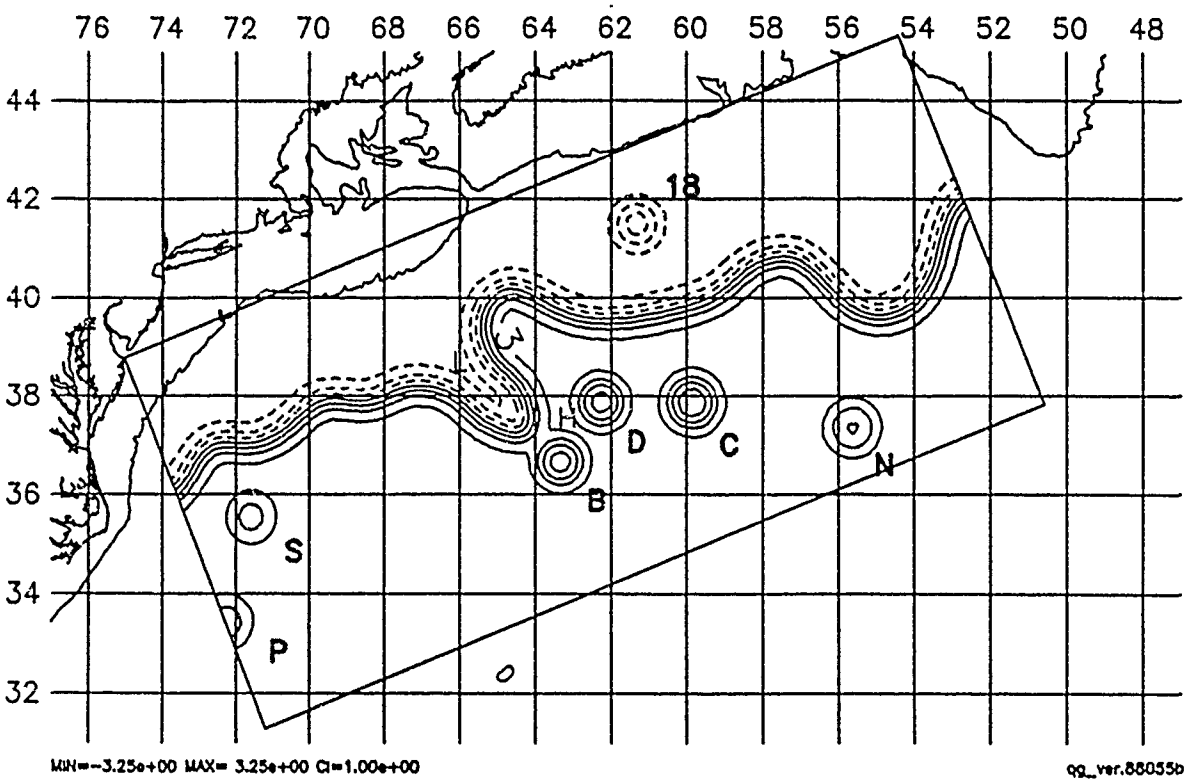

Initialization : 24 FEB 1988

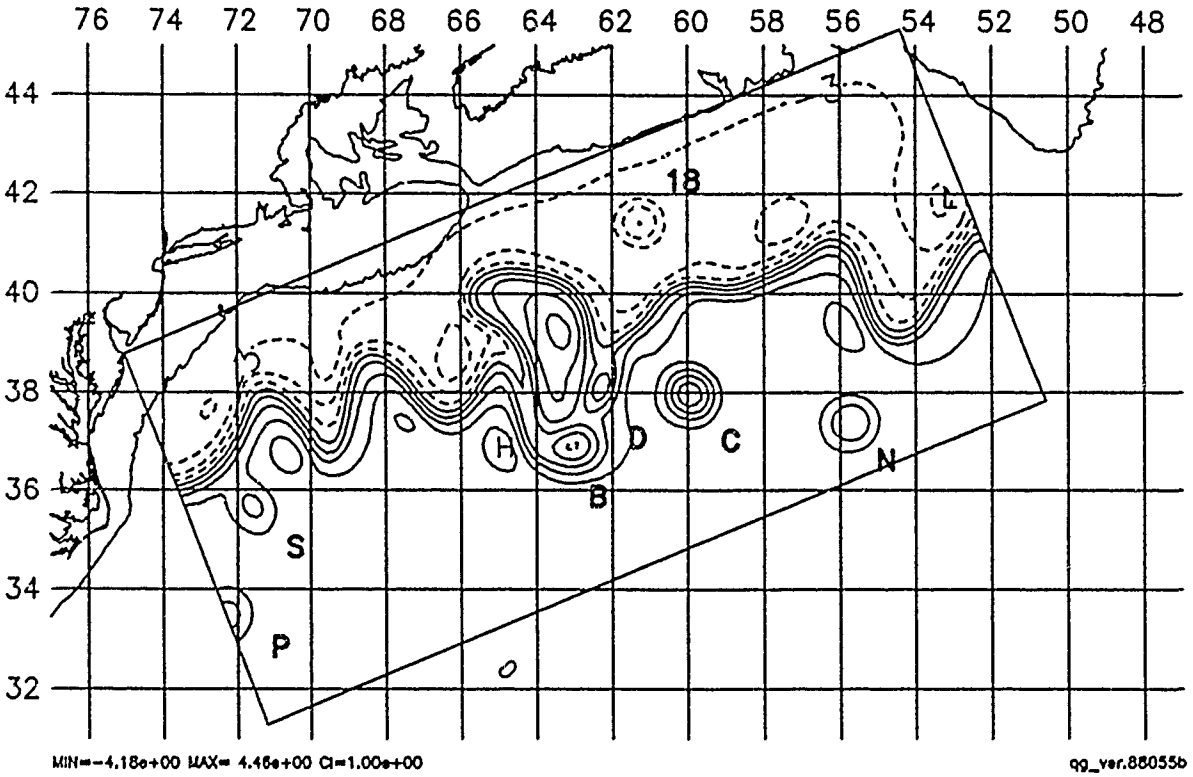

7 Day Forecast : 2 MAR 1988

HARVARD UNIVERSITY GULFCAST

OPERATIONAL EVALUATION FORECAST.

NEW DATA: IR, AXBT, GEOSAT.

Figure: Streamfunction at 100 m.

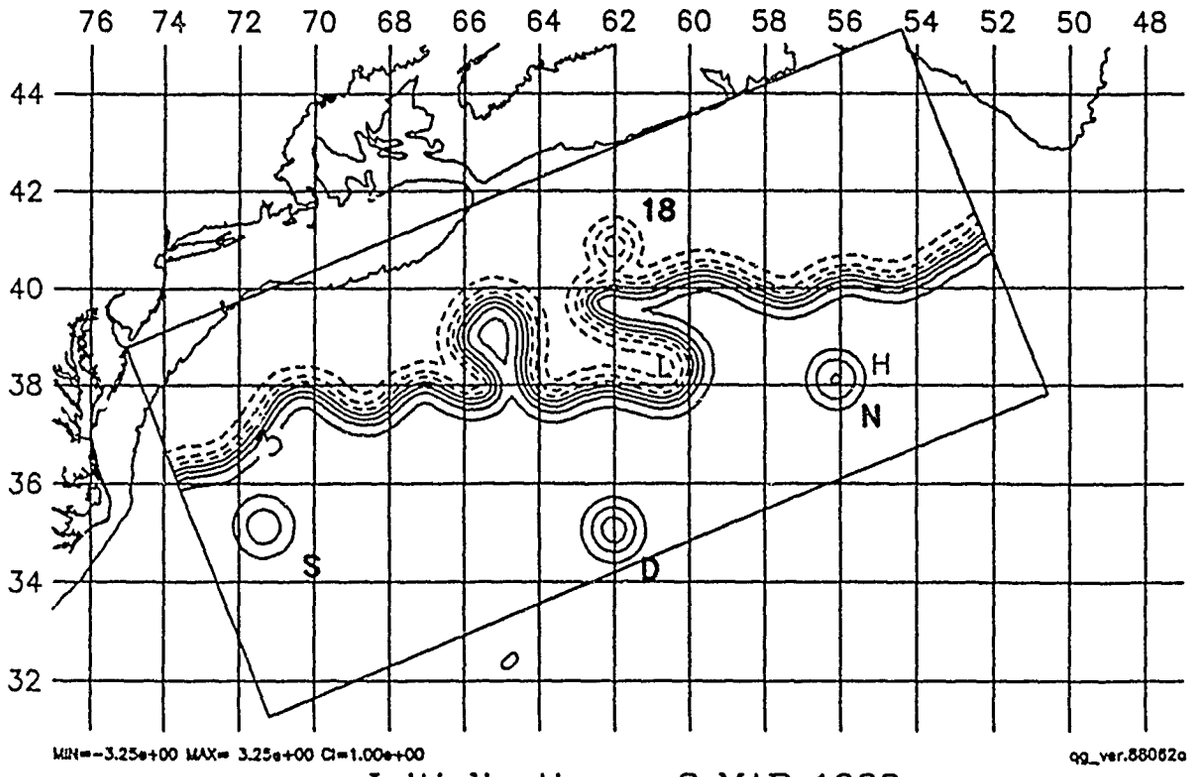

Initialization : 2 MAR 1988

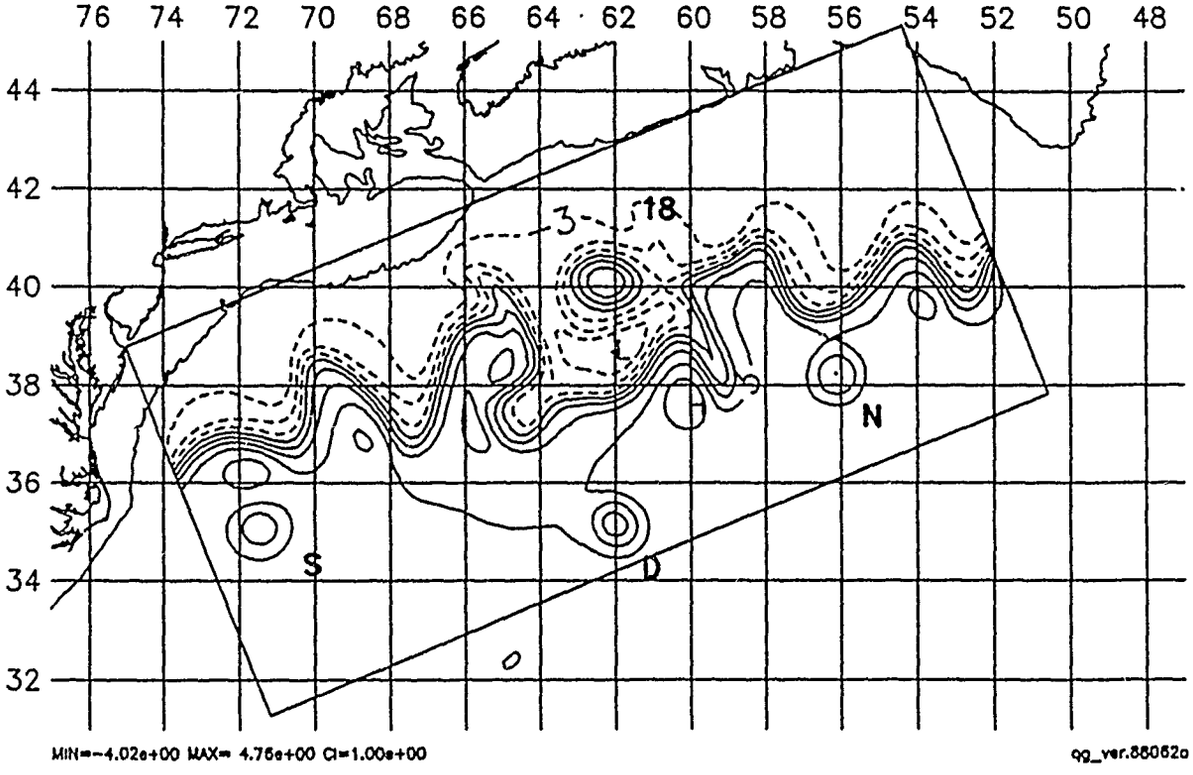

7 Day Forecast : 9 MAR 1988

HARVARD UNIVERSITY GULFCAST

OPERATIONAL EVALUATION FORECAST.

NEW DATA: IR, AXBT, GEOSAT.

Figure: Streamfunction at 100 m.

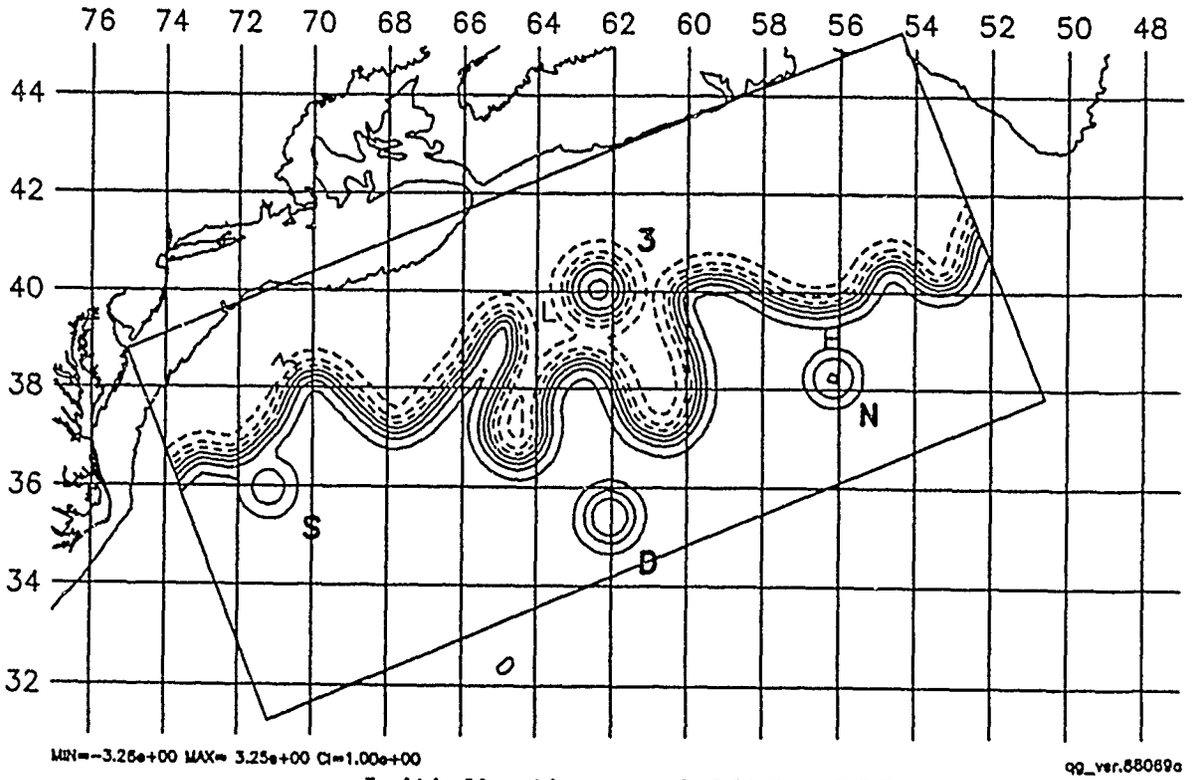

Initialization : 9 MAR 1988

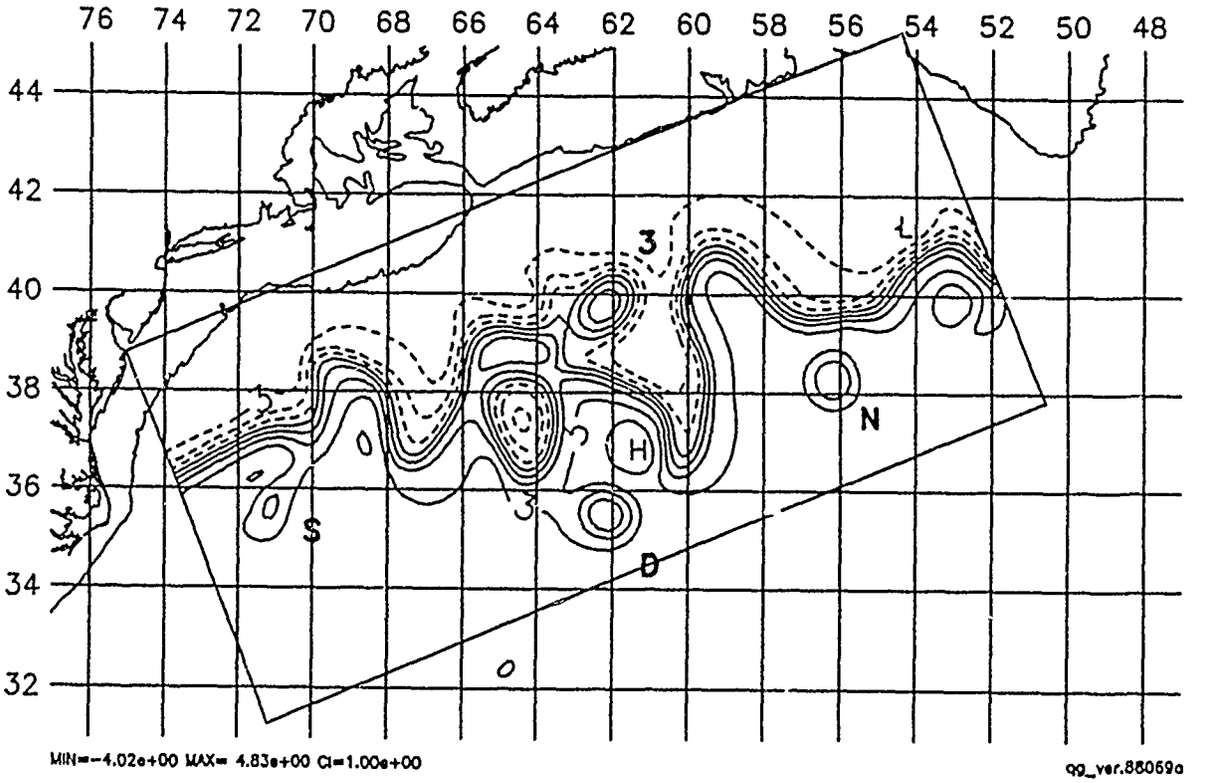

7 Day Forecast : 16 MAR 1988

HARVARD UNIVERSITY GULFCAST

OPERATIONAL EVALUATION FORECAST.

NEW DATA: IR, GEOSAT.

Figure: Streamfunction at 100 m.

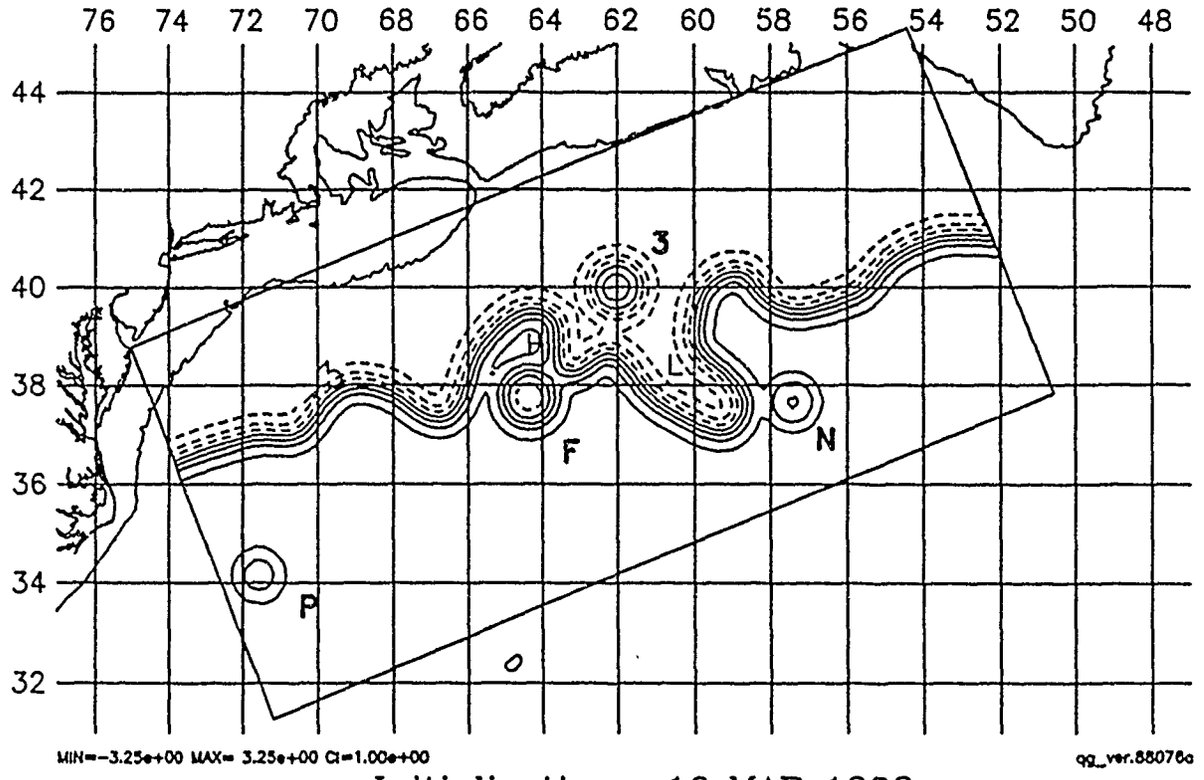

Initialization : 16 MAR 1988

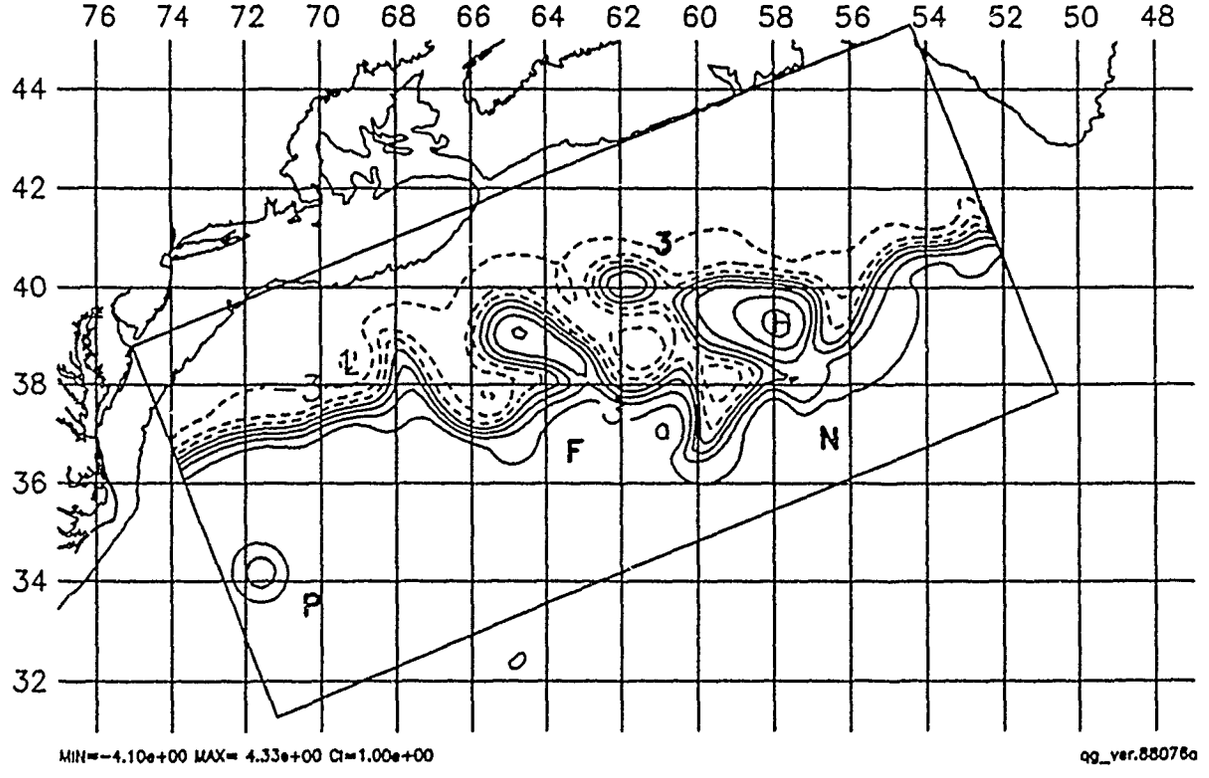

7 Day Forecast : 23 MAR 1988

HARVARD UNIVERSITY GULFCAST

OPERATIONAL EVALUATION FORECAST.

NEW DATA: IR, AXBT, GEOSAT.

Figure: Streamfunction at 100 m.

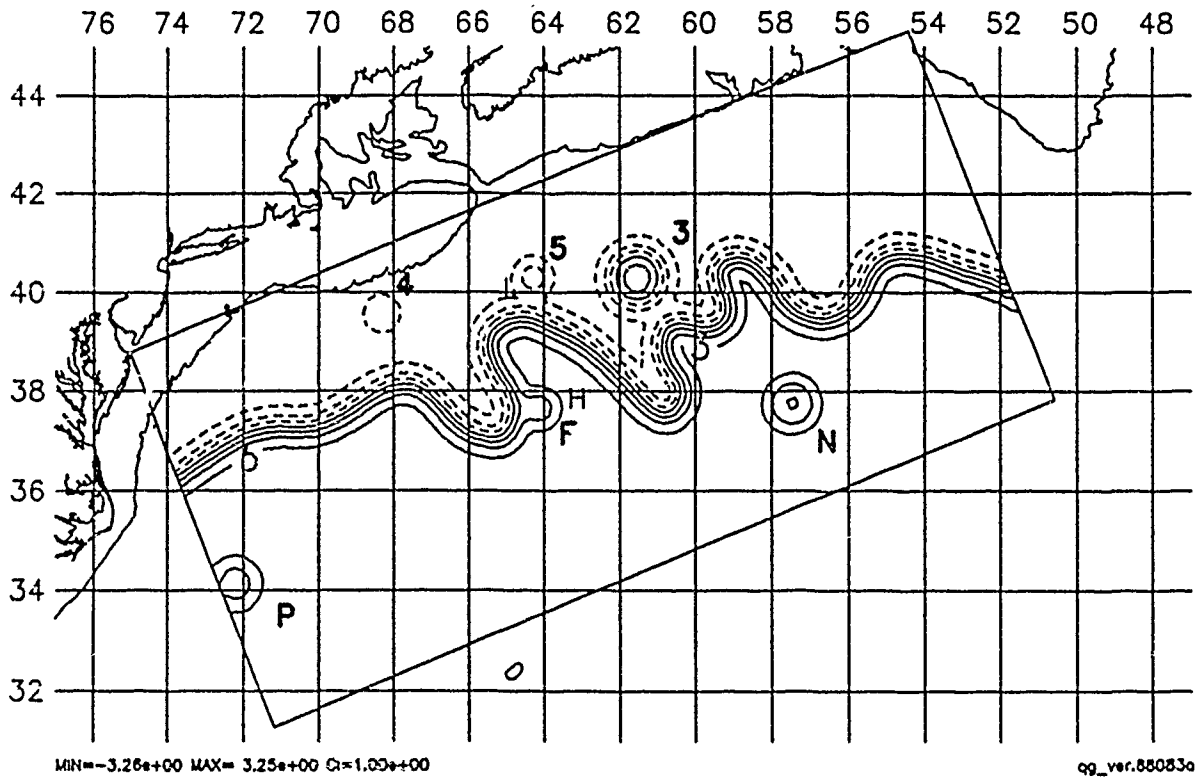

Initialization : 23 MAR 1988

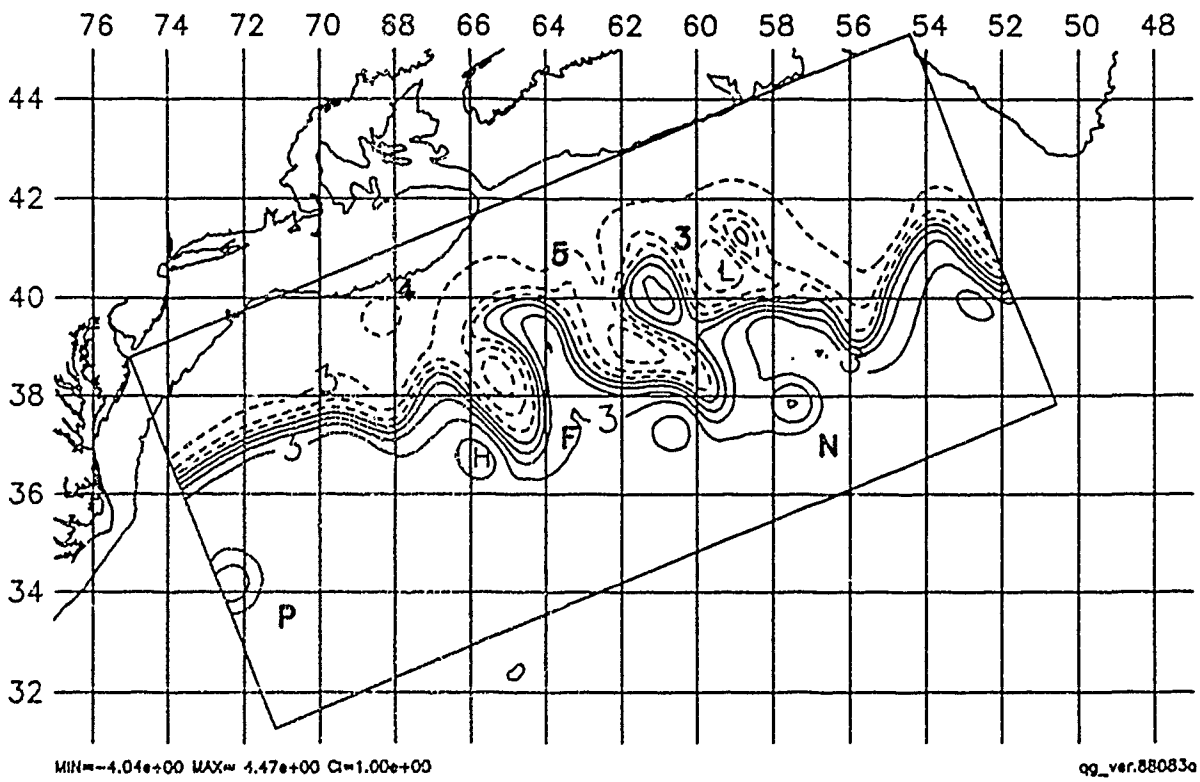

7 Day Forecast : 30 MAR 1988

HARVARD UNIVERSITY GULFCAST

OPERATIONAL EVALUATION FORECAST.

NEW DATA: IR, AXBT, GEOSAT.

Figure: Streamfunction at 100 m.

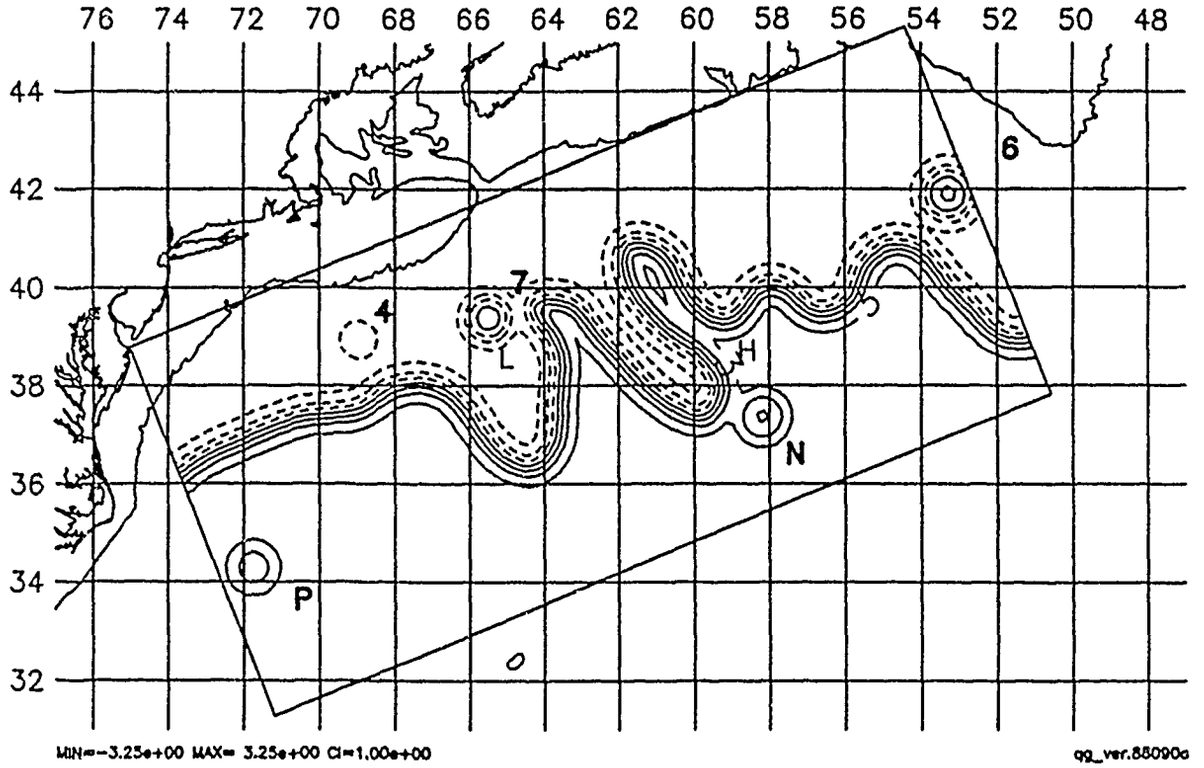

Initialization : 30 MAR 1988

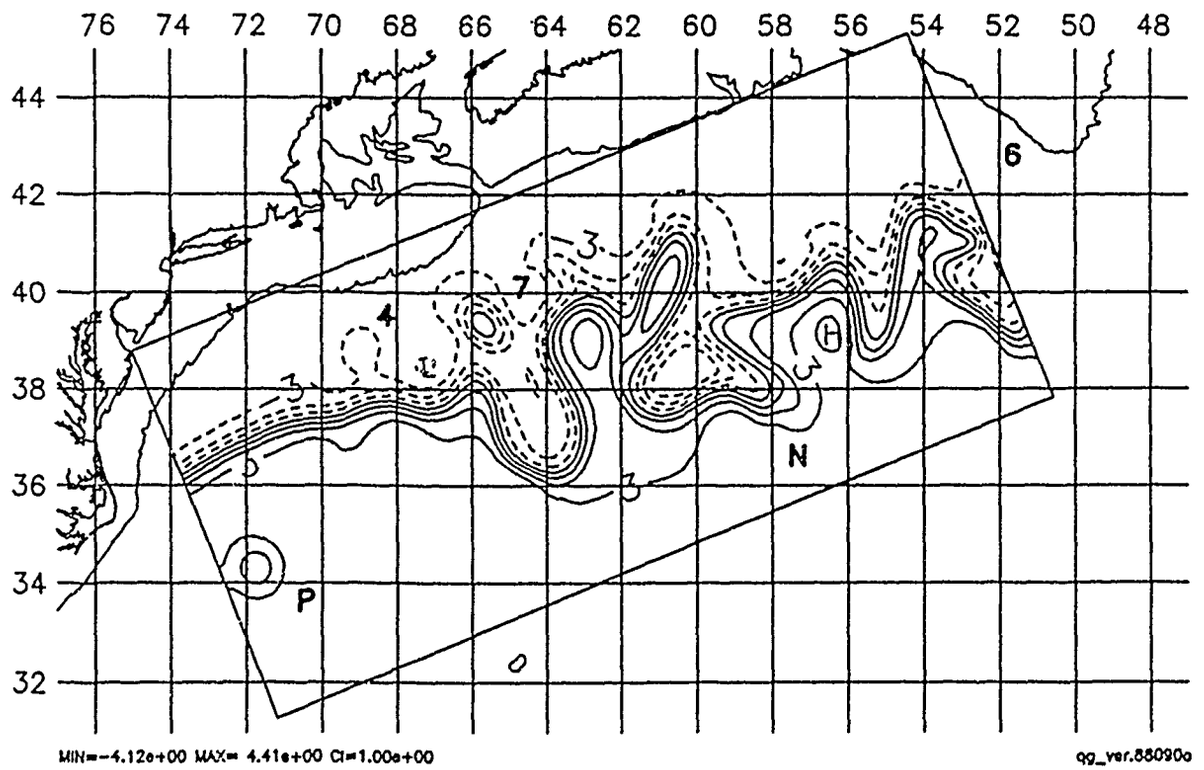

7 Day Forecast : 6 APR 1988

VE RI TAS

HARVARD UNIVERSITY GULFCAST

OPERATIONAL EVALUATION FORECAST.

NEW DATA: IR, GEOSAT.

Figure: Streamfunction at 100 m.

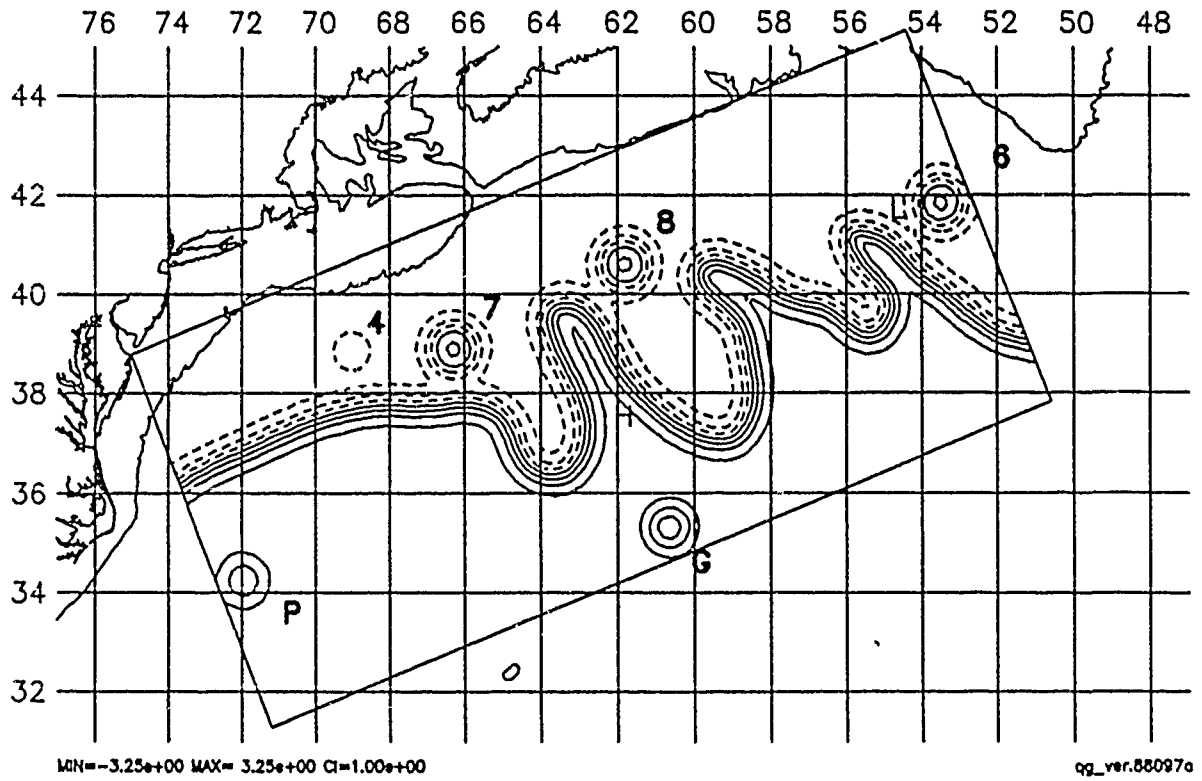

Initialization : 6 APR 1988

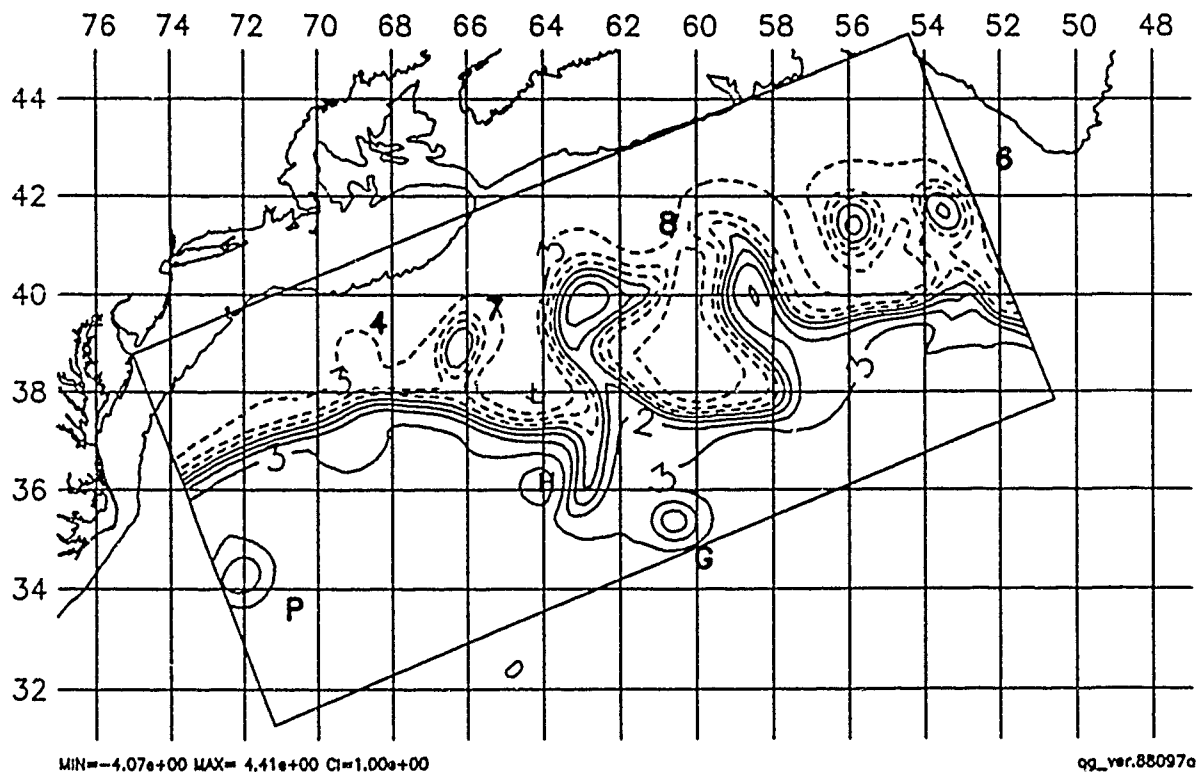

7 Day Forecast : 13 APR 1988

HARVARD UNIVERSITY GULFCAST

OPERATIONAL EVALUATION FORECAST.

NEW DATA: IR, AXBT, GEOSAT.

Figure: Streamfunction at 100 m.

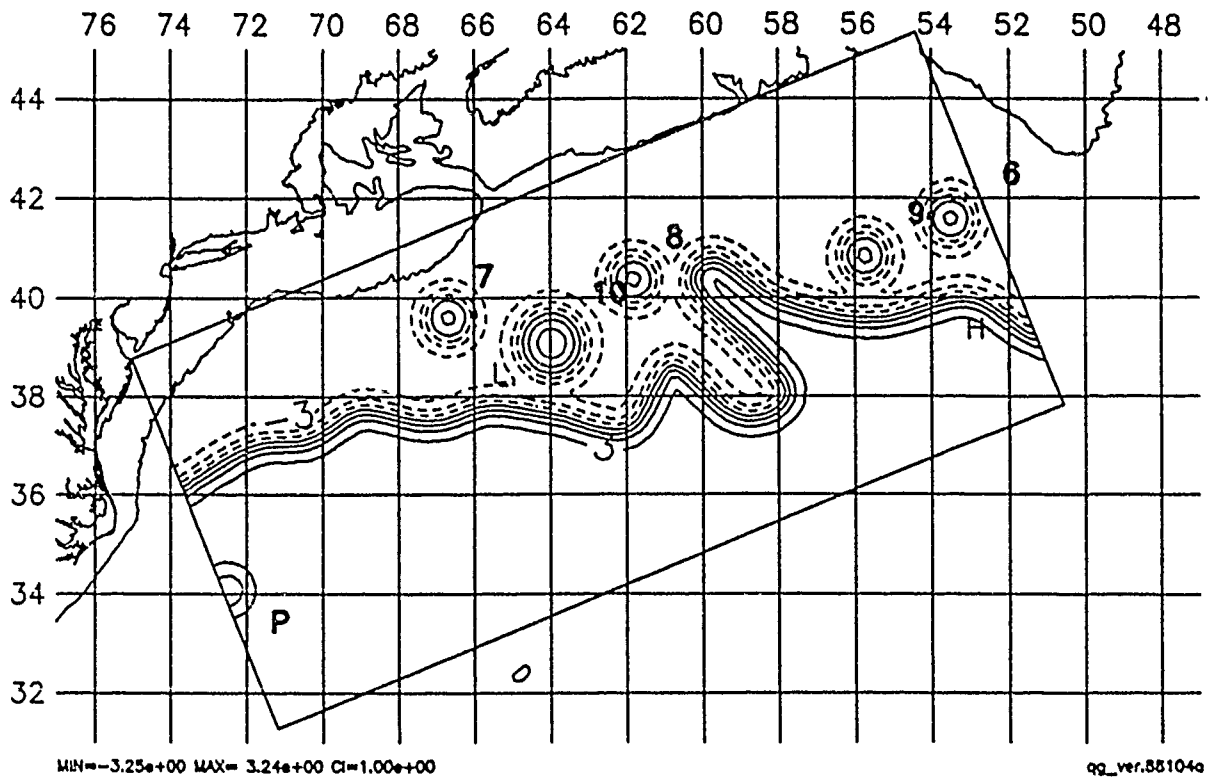

Initialization : 13 APR 1988

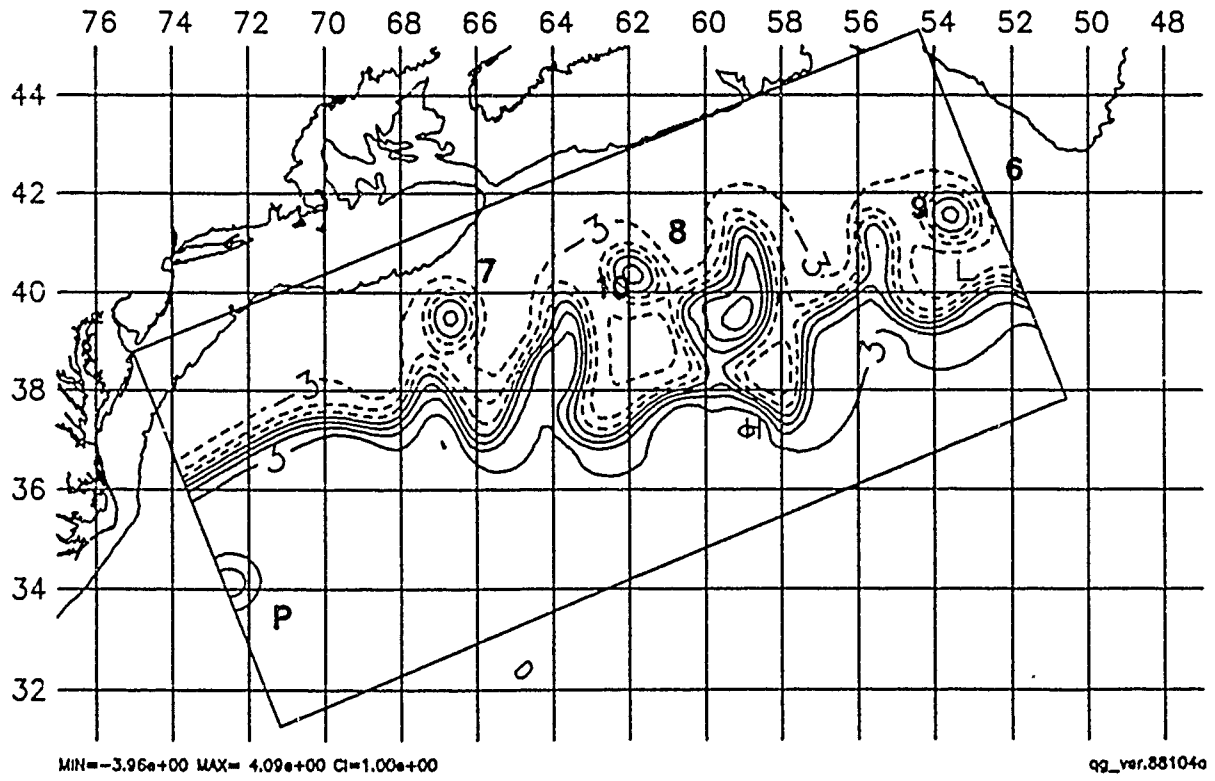

7 Day Forecast : 20 APR 1988

HARVARD UNIVERSITY GULFCAST

OPERATIONAL EVALUATION FORECAST.

NEW DATA: IR, GEOSAT.

Figure: Streamfunction at 100 m.

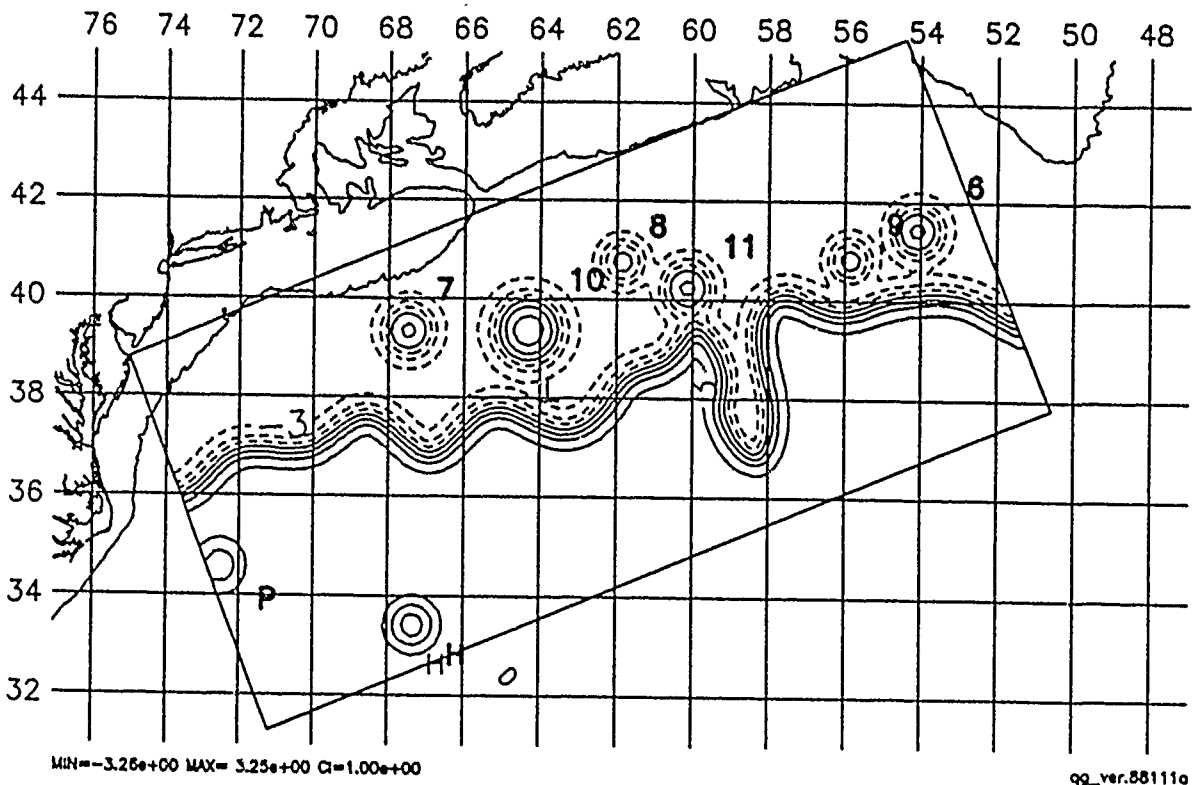

Initialization : 20 APR 1988

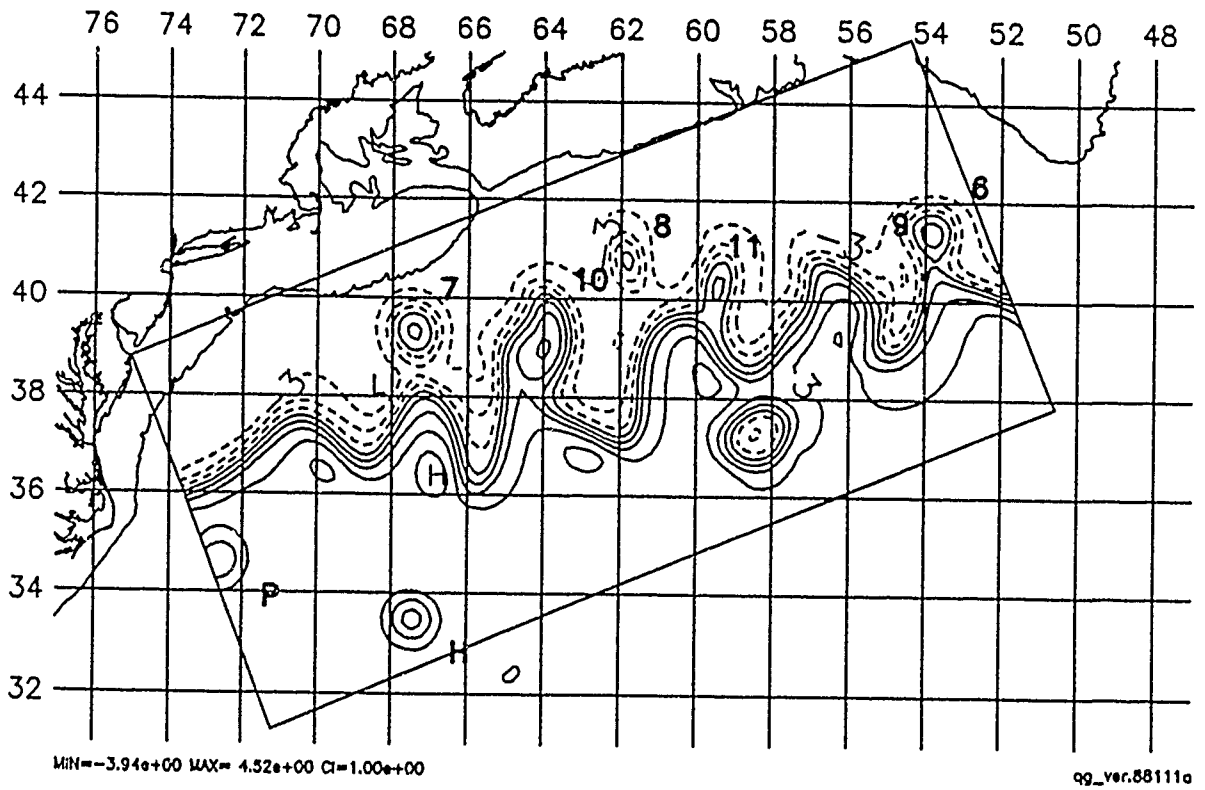

7 Day Forecast : 27 APR 1988

HARVARD UNIVERSITY GULFCAST

OPERATIONAL EVALUATION FORECAST.

NEW DATA: IR, GEOSAT.

Figure: Streamfunction at 100 m.

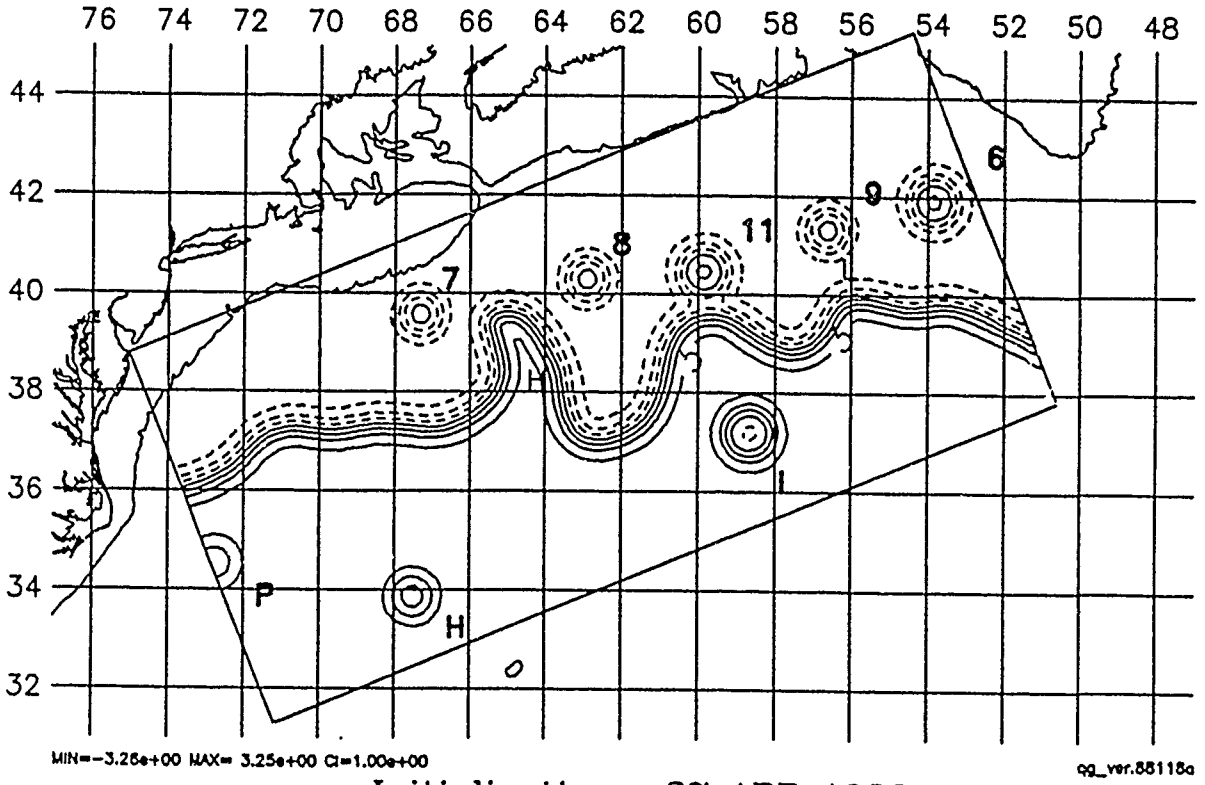

Initialization : 27 APR 1988

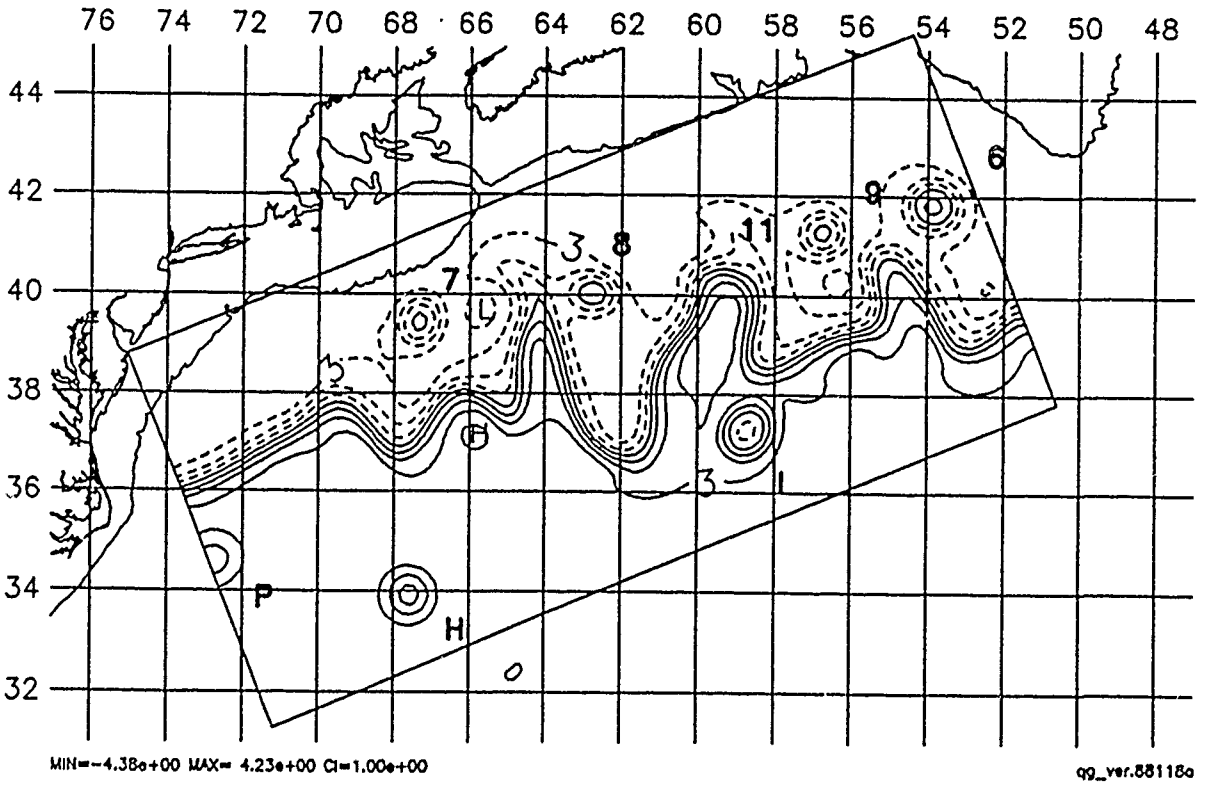

7 Day Forecast : 4 MAY 1988

HARVARD UNIVERSITY GULFCAST

OPERATIONAL EVALUATION FORECAST.

NEW DATA: IR, AXBT, GEOSAT.

Figure: Streamfunction at 100 m.

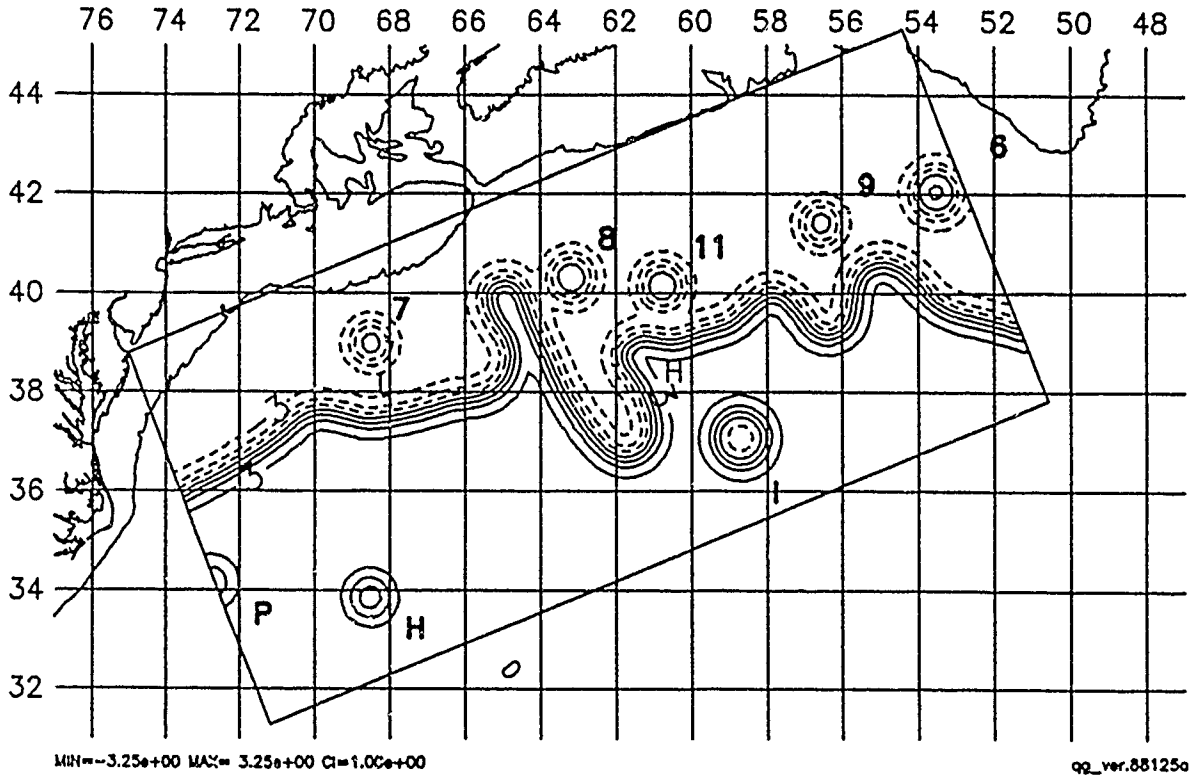

Initialization : 4 MAY 1988

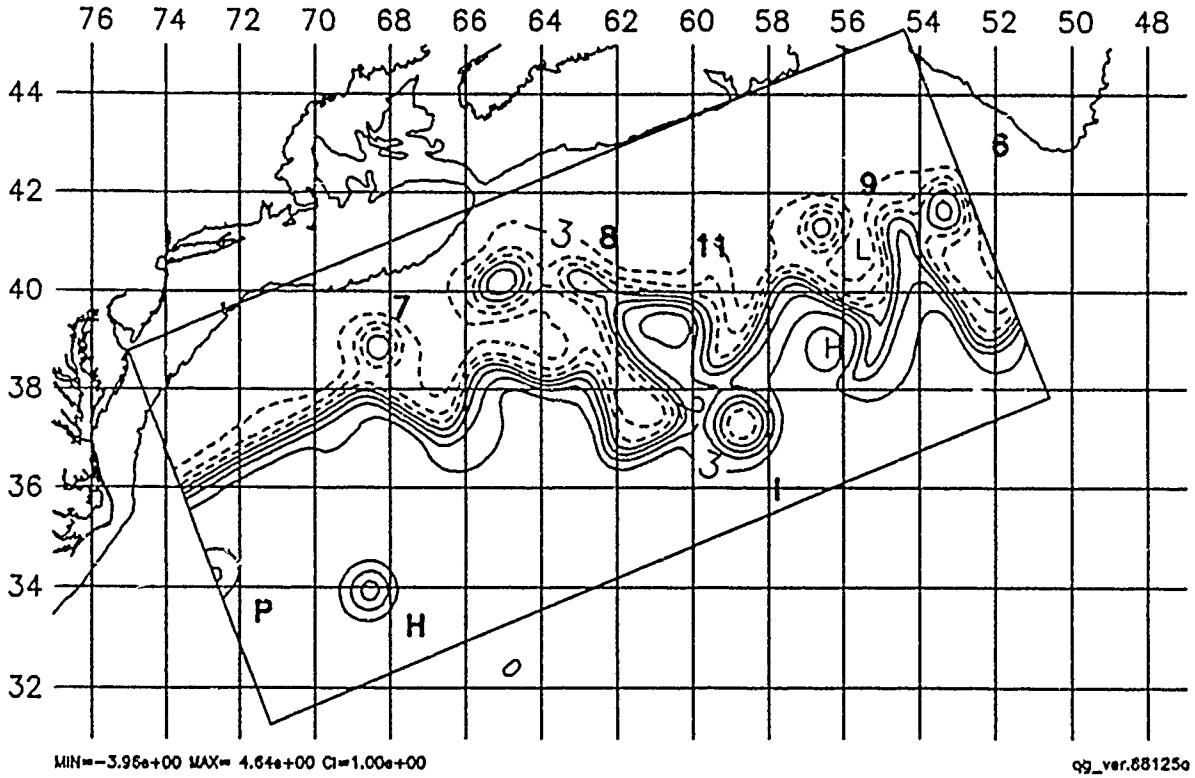

7 Day Forecast : 11 MAY 1988

HARVARD UNIVERSITY GULFCAST

OPERATIONAL EVALUATION FORECAST.

NEW DATA: IR, AXBT, GEOSAT.

Figure: Streamfunction at 100 m.

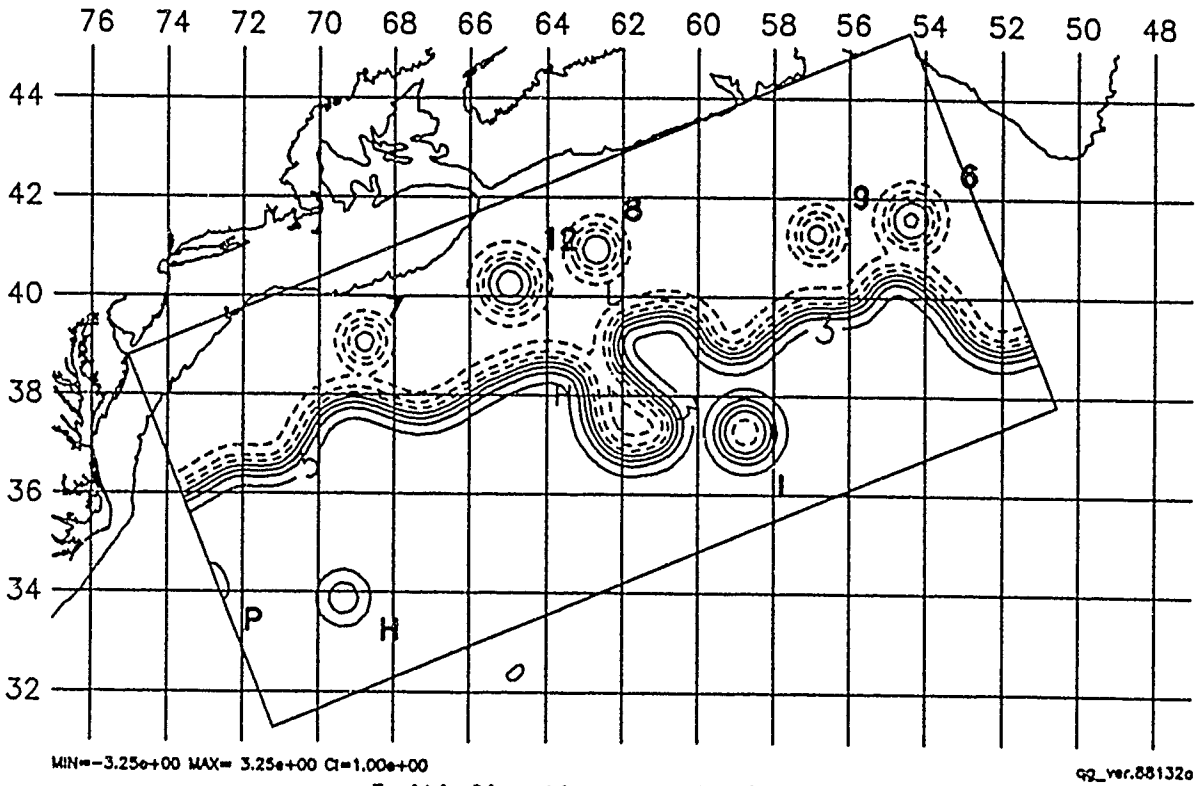

Initialization : 11 MAY 1988

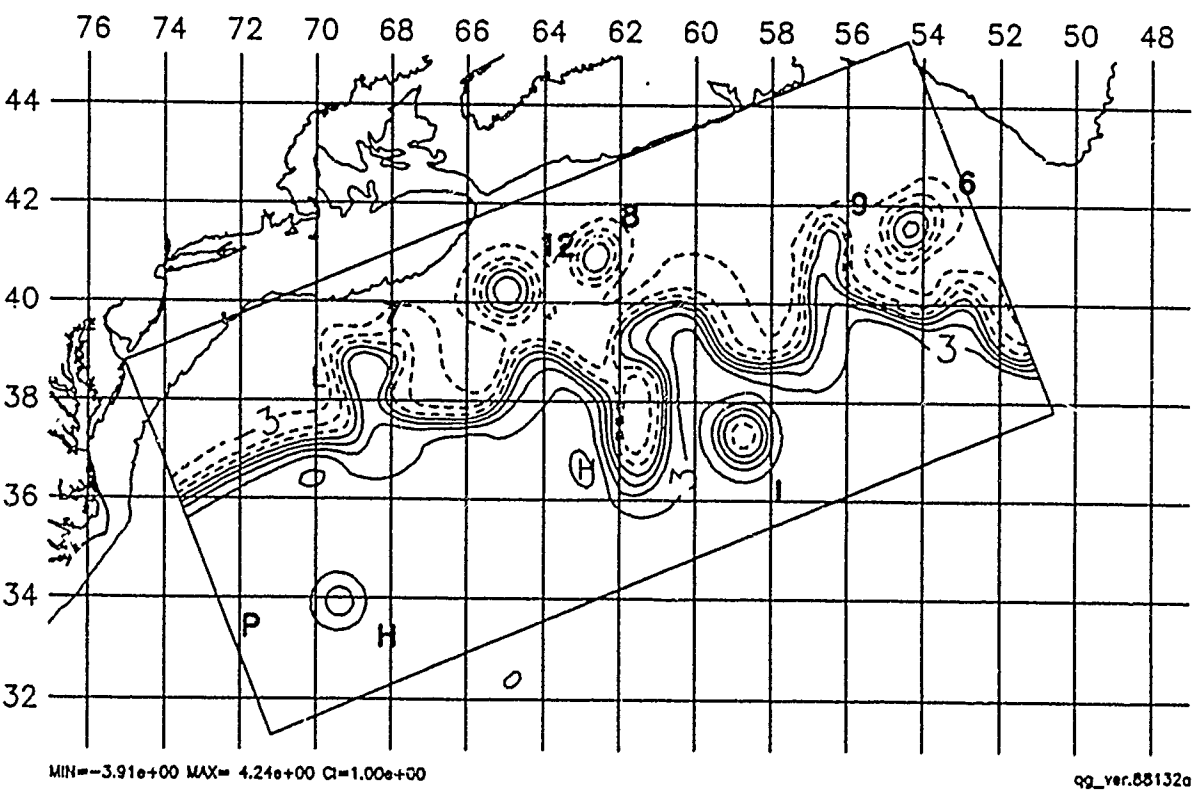

7 Day Forecast : 18 MAY 1988

HARVARD UNIVERSITY GULFCAST

OPERATIONAL EVALUATION FORECAST.

NEW DATA: IR, GEOSAT.

Figure: Streamfunction at 100 m.

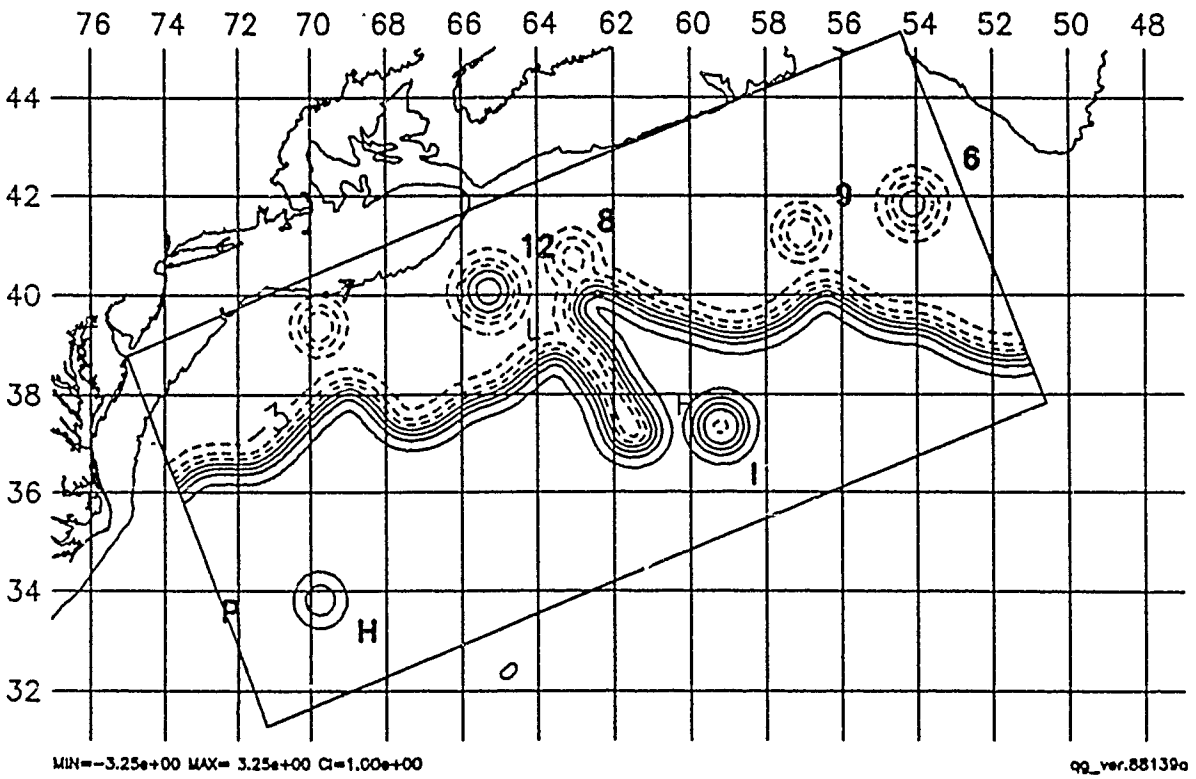

Initialization : 18 MAY 1988

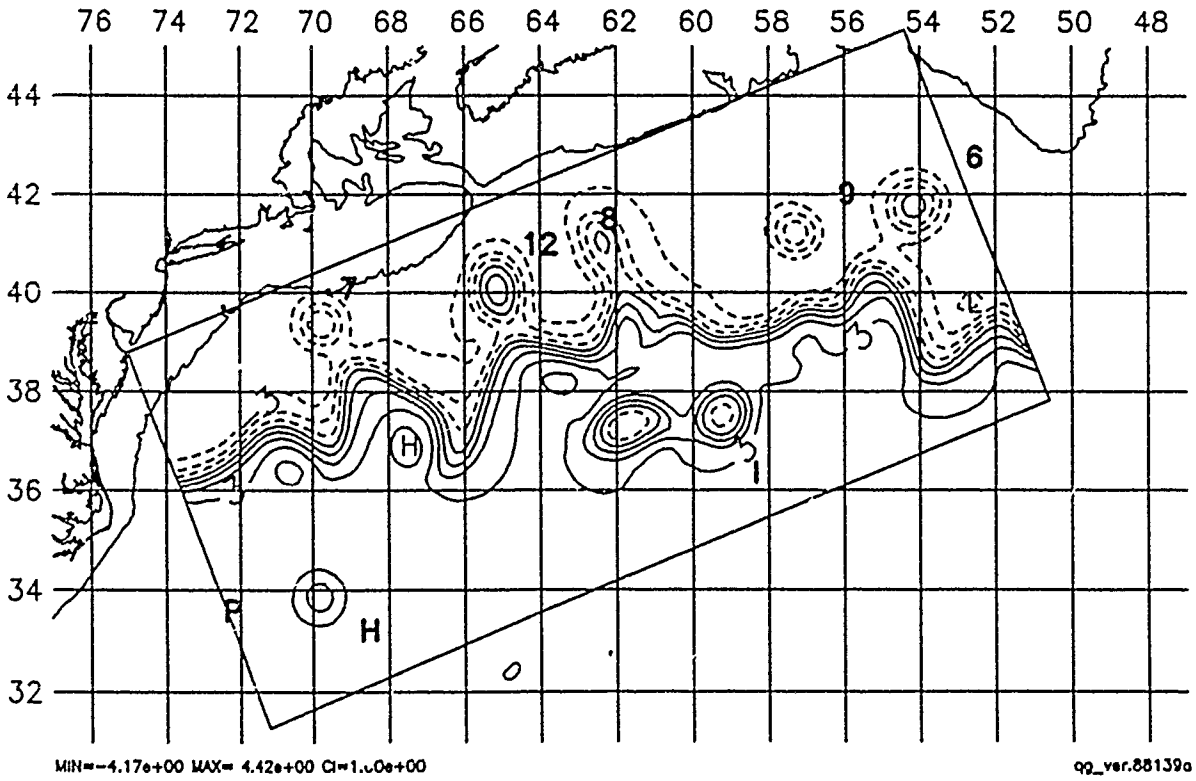

7 Day Forecast : 25 MAY 1988

HARVARD UNIVERSITY GULFCAST

OPERATIONAL EVALUATION FORECAST.

NEW DATA: IR, GEOSAT.

Figure: Streamfunction at 100 m.

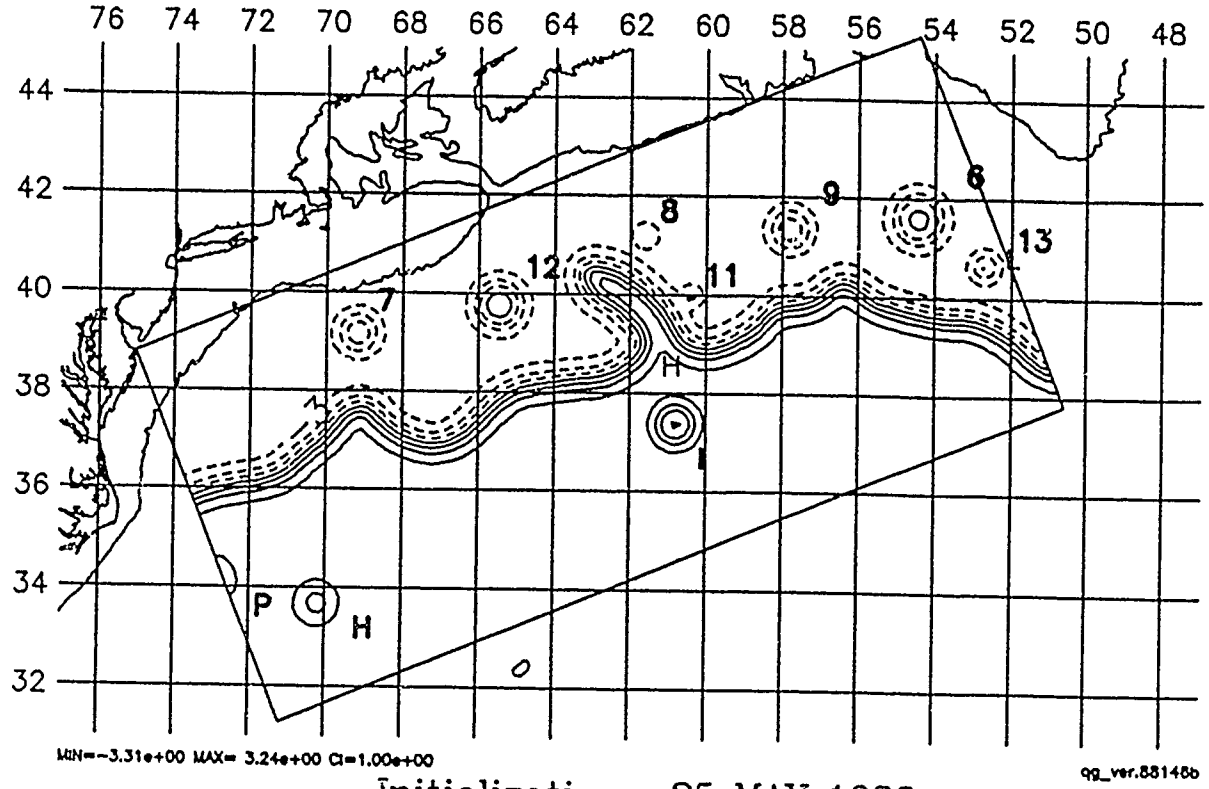

Initialization : 25 MAY 1988

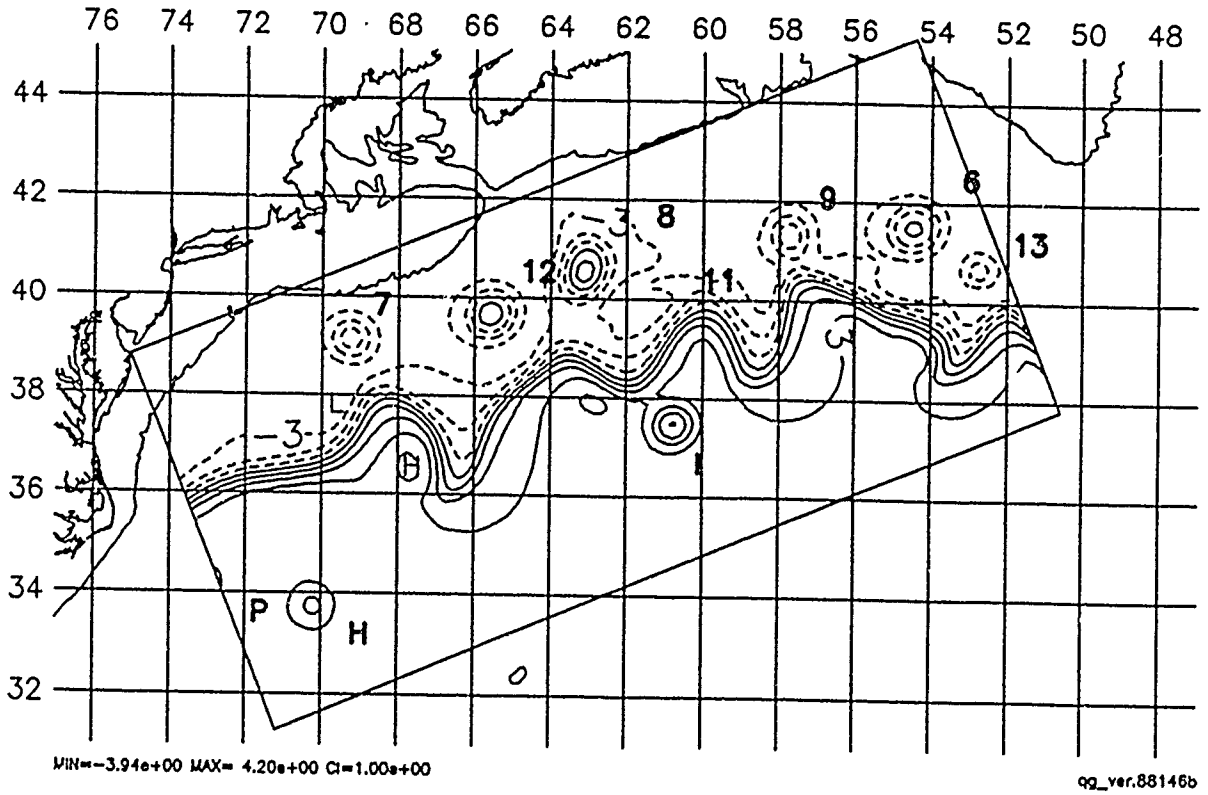

7 Day Forecast : 1 JUN 1988

HARVARD UNIVERSITY GULFCAST

OPERATIONAL EVALUATION FORECAST.

NEW DATA: IR, AXBT, GEOSAT.

Figure: Streamfunction at 100 m.

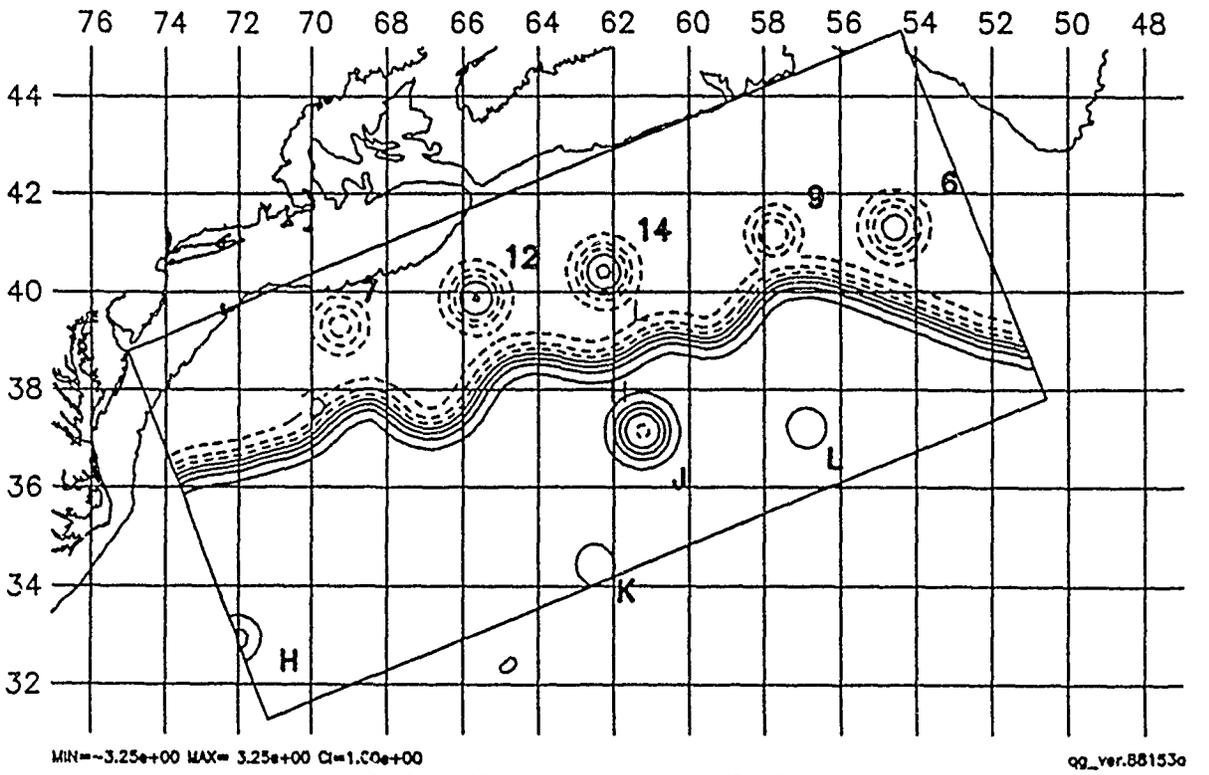

Initialization : 1 JUN 1988

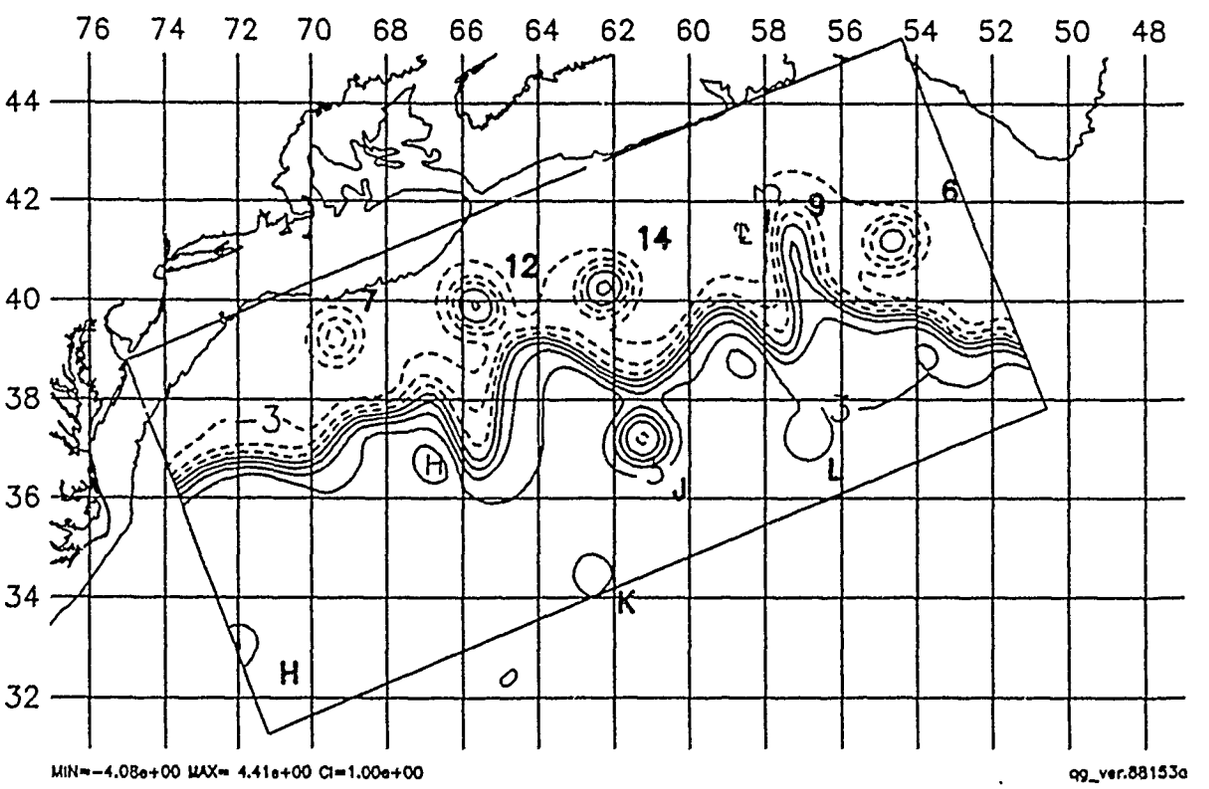

7 Day Forecast : 8 JUN 1988

HARVARD UNIVERSITY GULFCAST

OPERATIONAL EVALUATION FORECAST.

NEW DATA: IR, GEOSAT.

Figure: Streamfunction at 100 m.

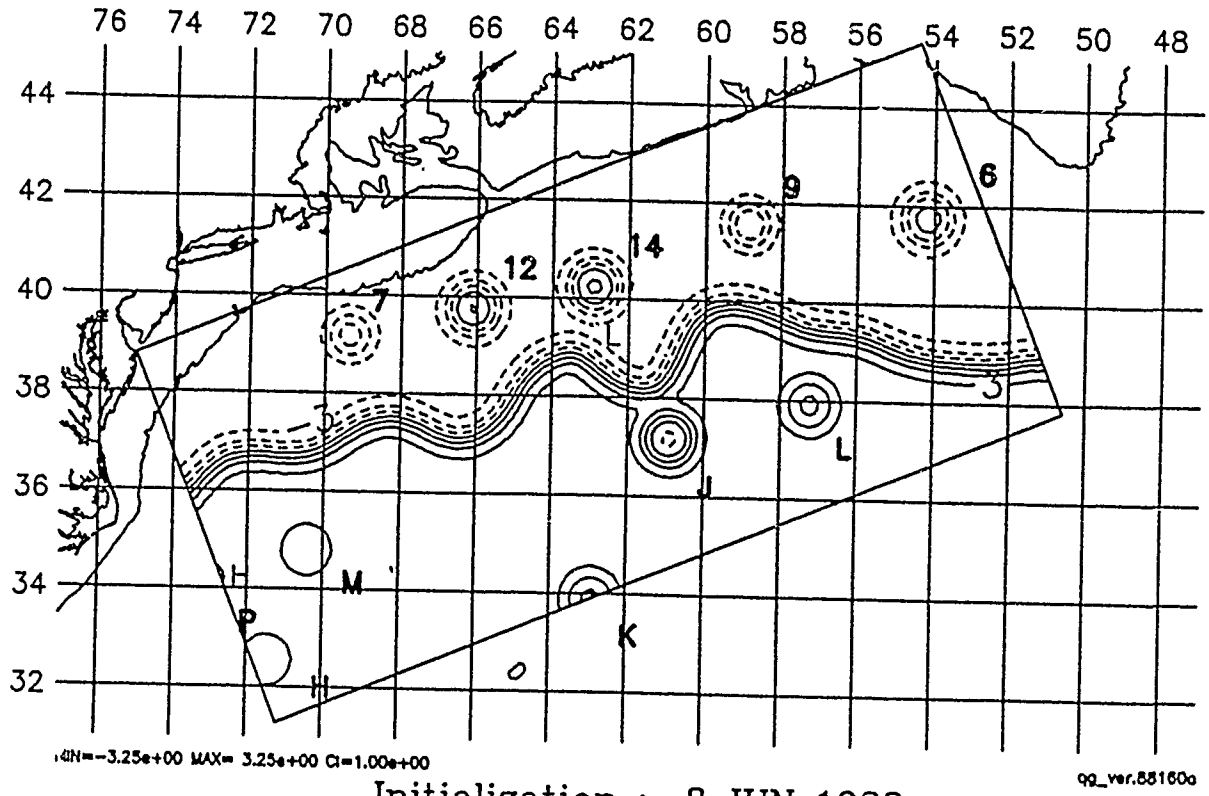

Initialization : 8 JUN 1988

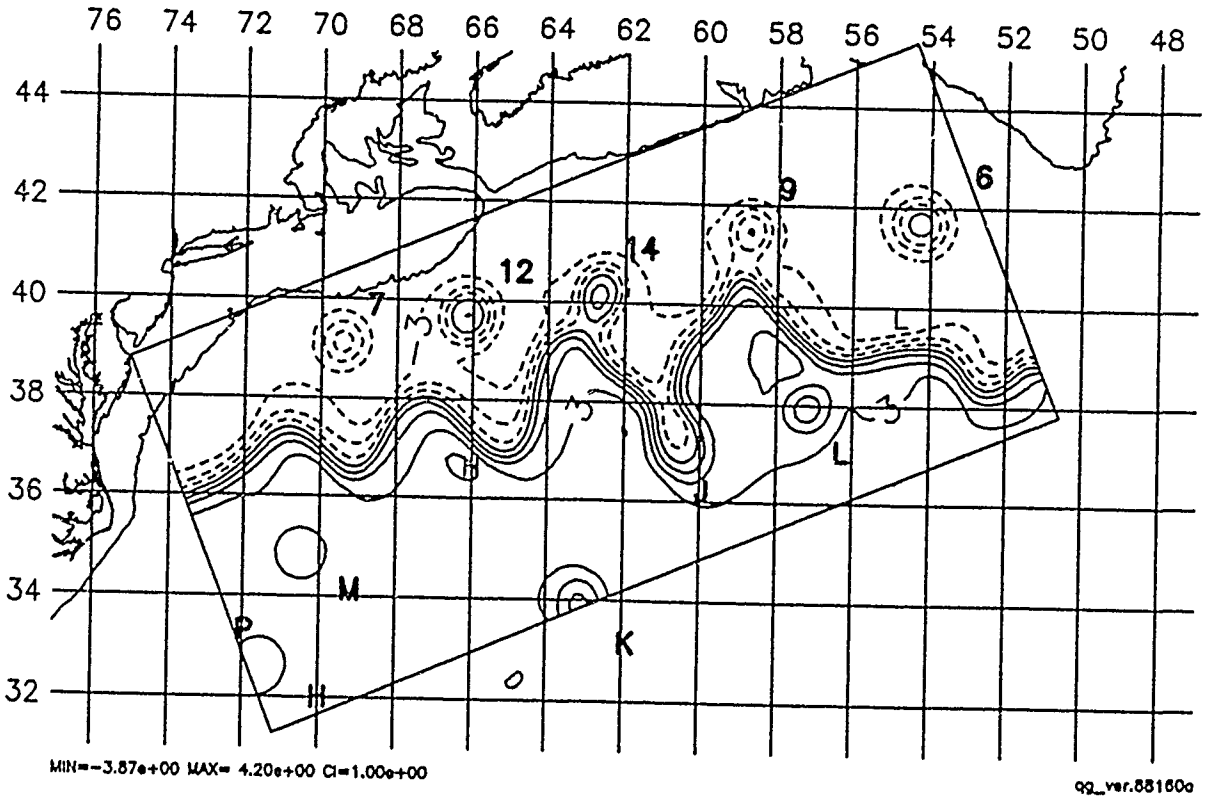

7 Day Forecast : 15 JUN 1988

HARVARD UNIVERSITY GULFCAST

OPERATIONAL EVALUATION FORECAST.

NEW DATA: IR, GEOSAT.

Figure: Streamfunction at 100 m.

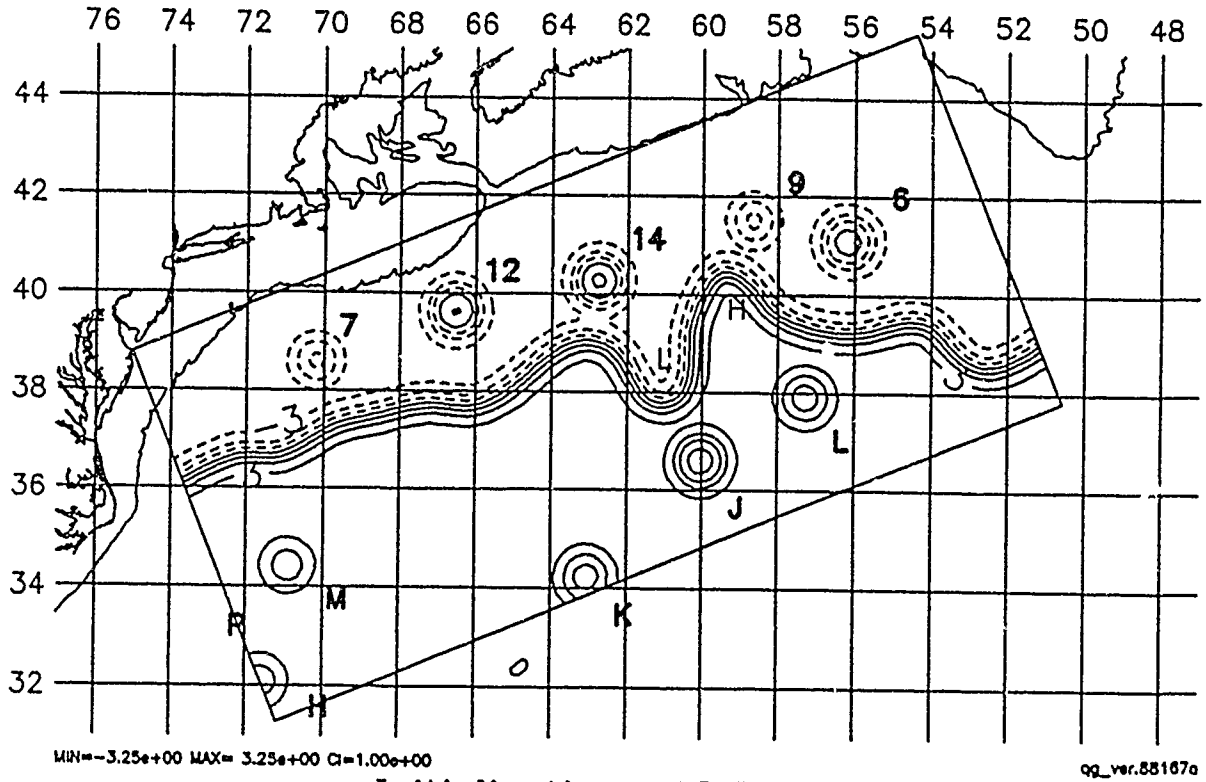

Initialization : 15 JUN 1988

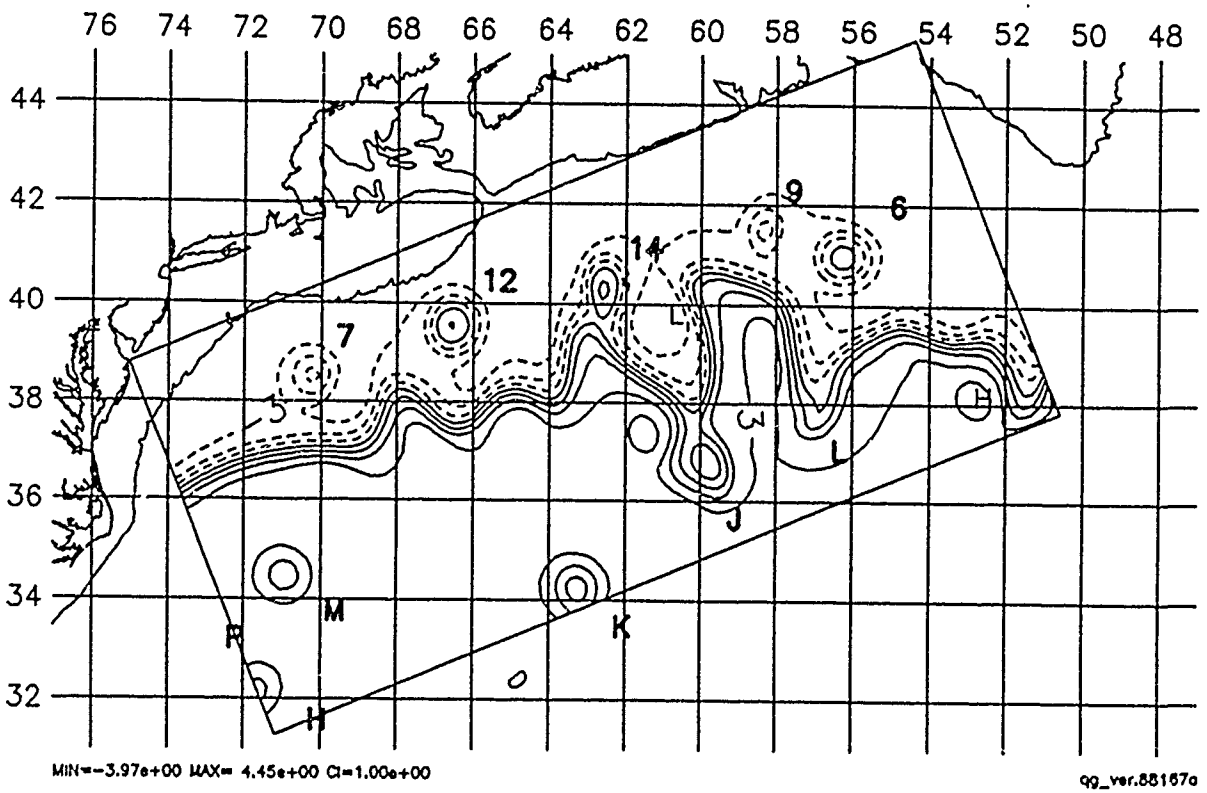

7 Day Forecast : 22 JUN 1988

HARVARD UNIVERSITY GULFCAST

OPERATIONAL EVALUATION FORECAST.

NEW DATA: IR, GEOSAT.

Figure: Streamfunction at 100 m.

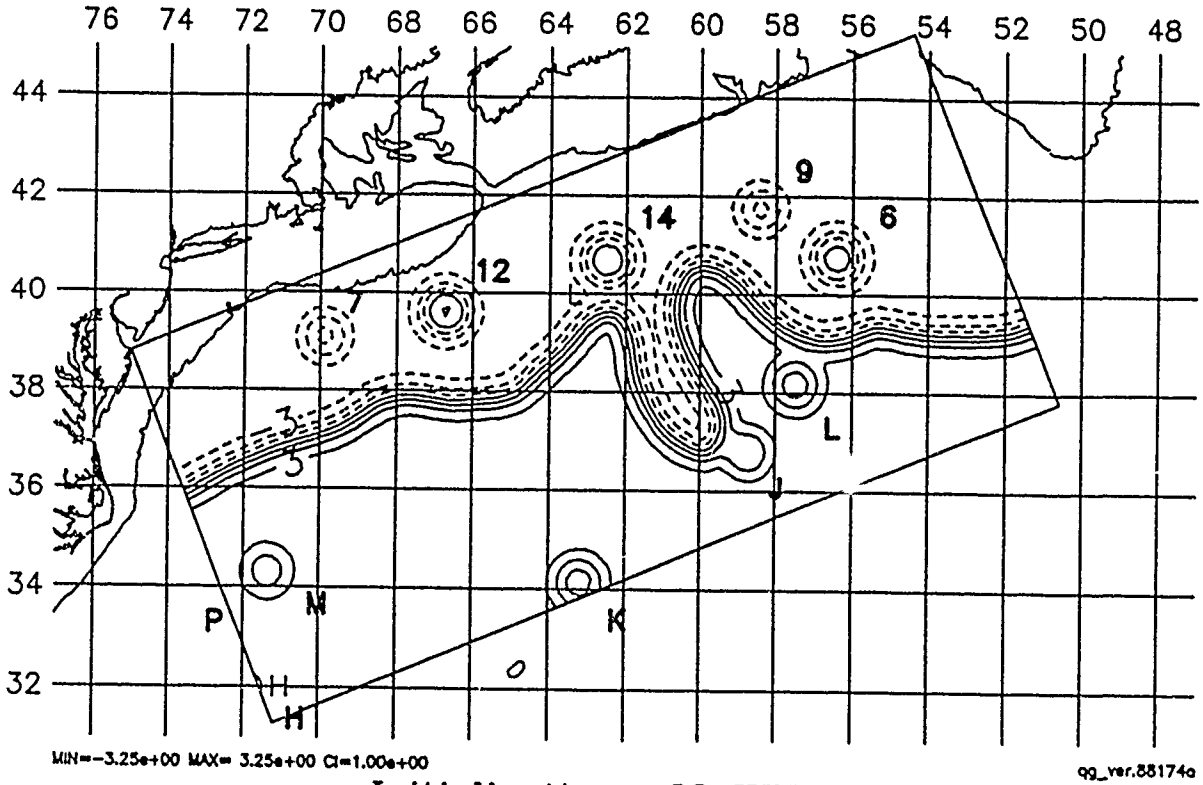

Initialization : 22 JUN 1988

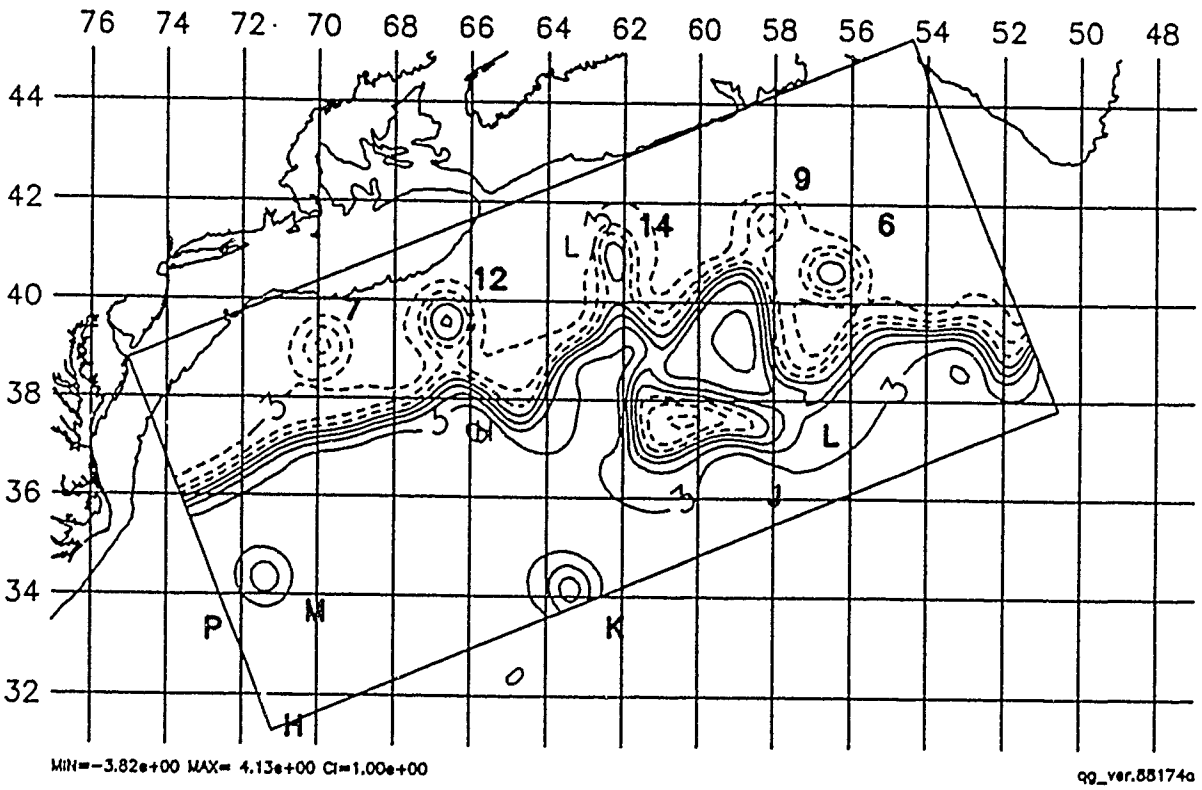

7 Day Forecast : 29 JUN 1988

HARVARD UNIVERSITY GULFCAST

OPERATIONAL EVALUATION FORECAST.

NEW DATA: IR, GEOSAT.

Figure: Streamfunction at 100 m.

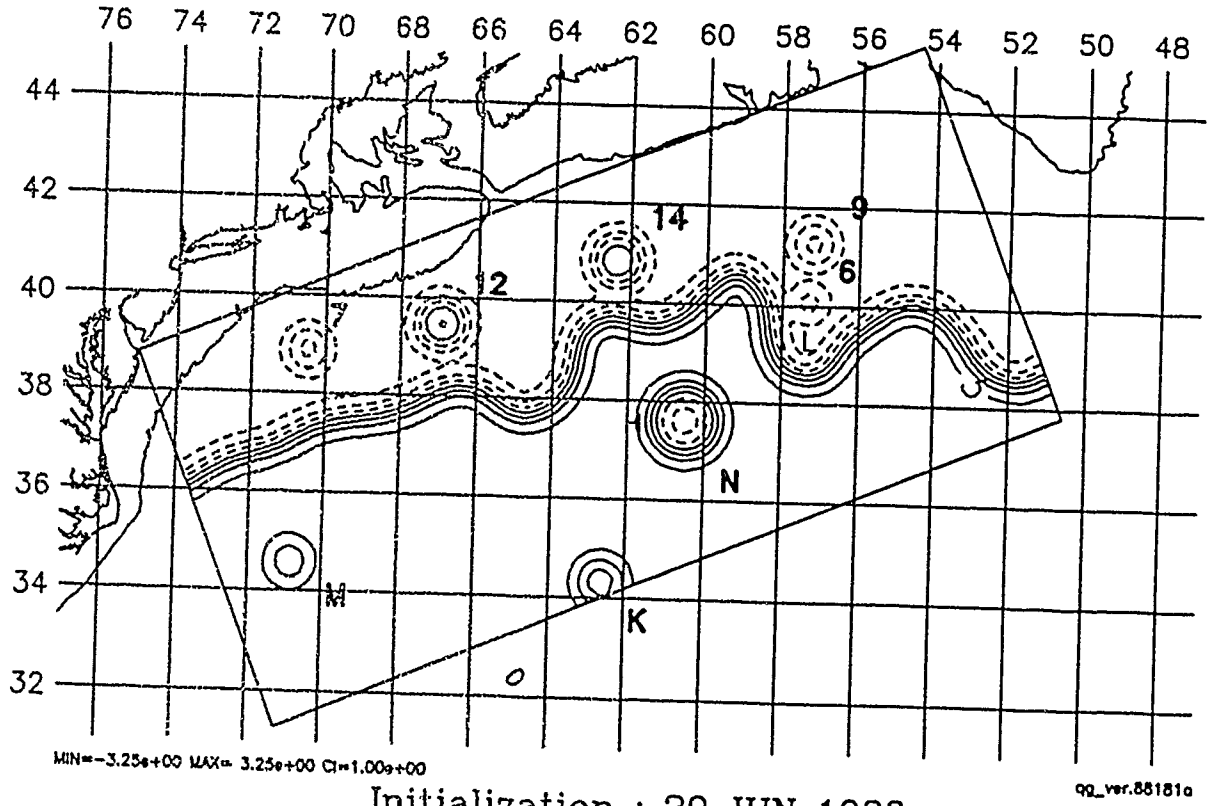

Initialization : 29 JUN 1988

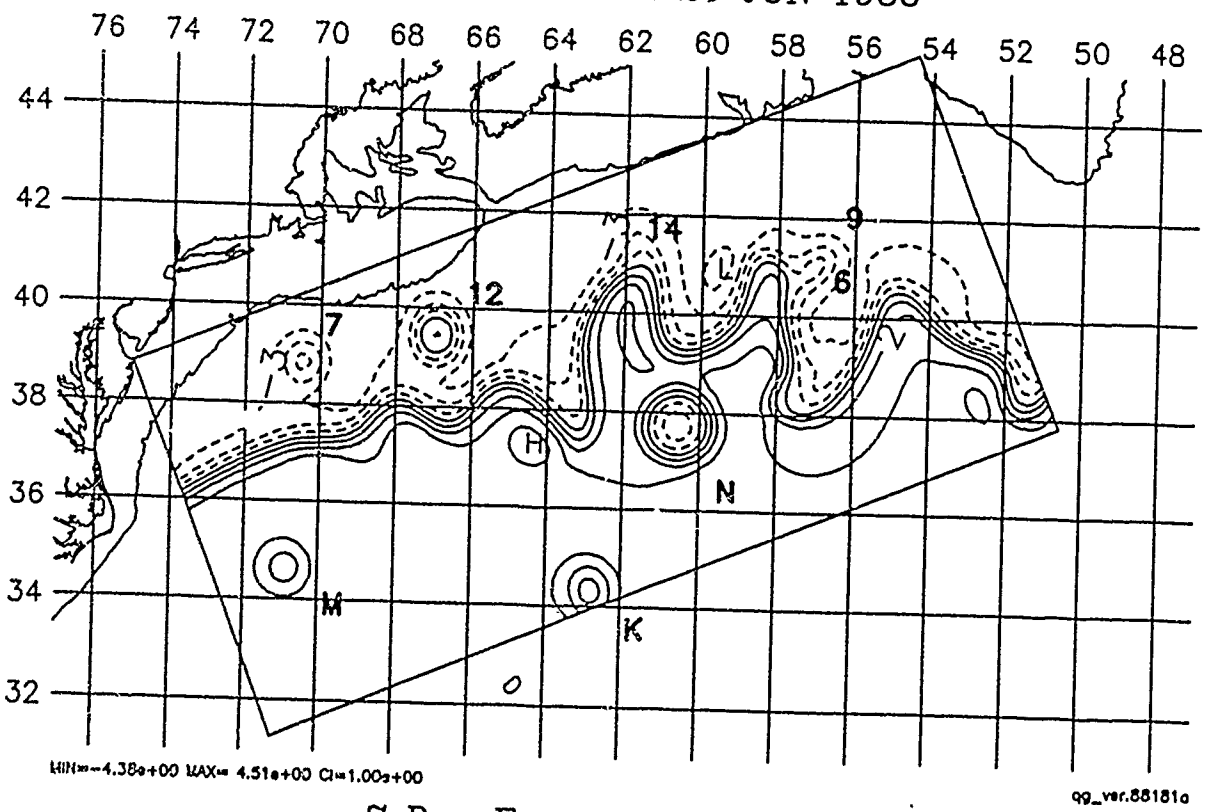

7 Day Forecast : 6 JUL 1988

HARVARD UNIVERSITY GULFCAST

OPERATIONAL EVALUATION FORECAST.

NEW DATA: IR, GEOSAT.

Figure: Streamfunction at 100 m.

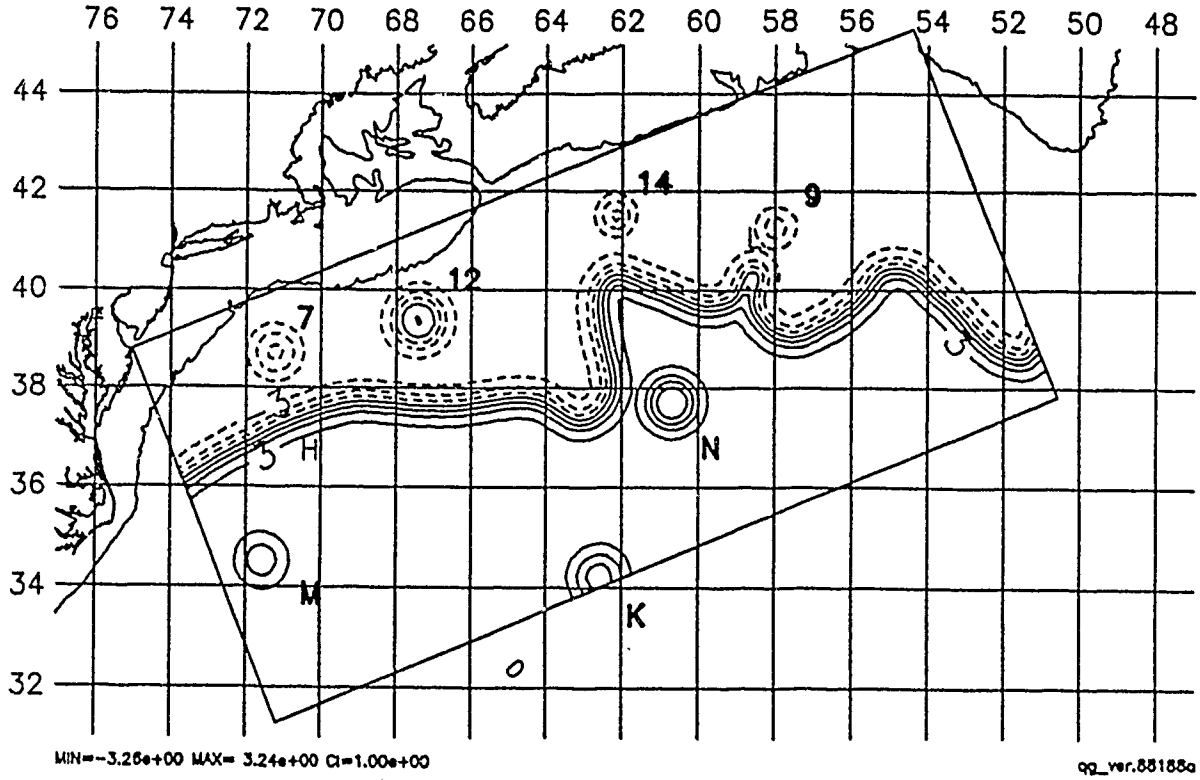

Initialization : 6 JUL 1988

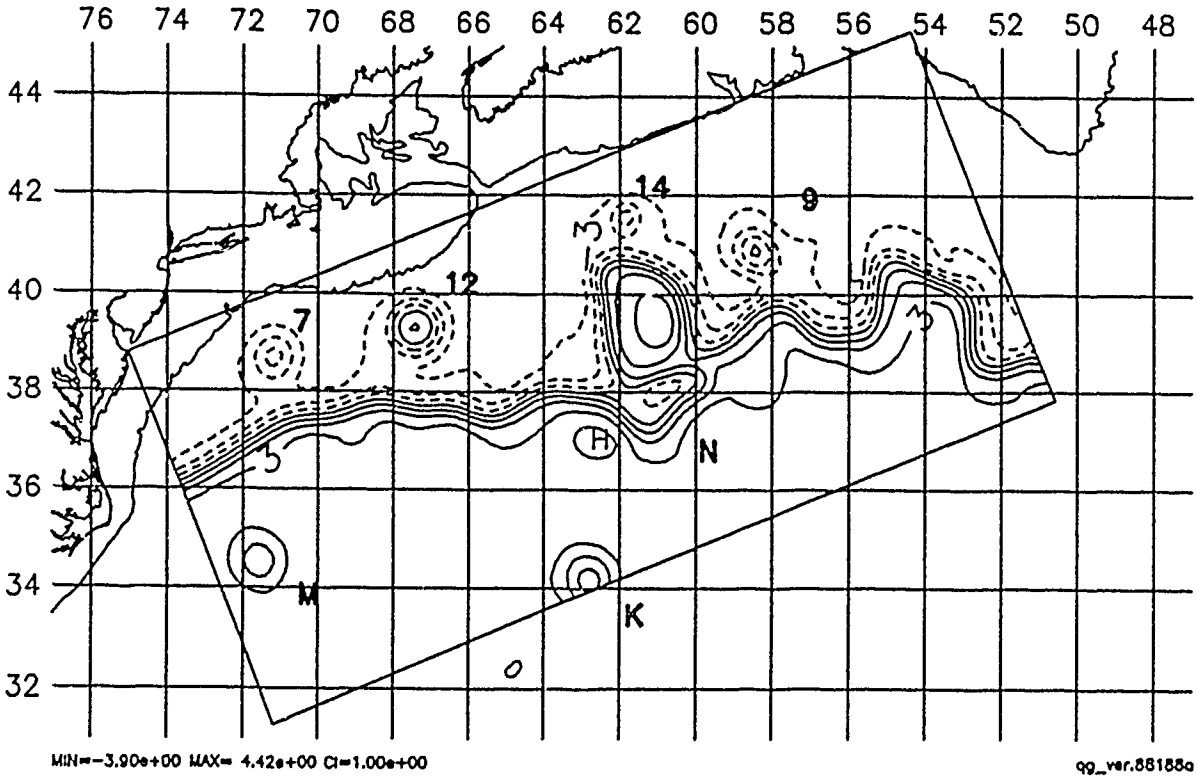

7 Day Forecast : 13 JUL 1988

HARVARD UNIVERSITY GULFCAST

OPERATIONAL EVALUATION FORECAST.

NEW DATA: IR, GEOSAT.

Figure: Streamfunction at 100 m.

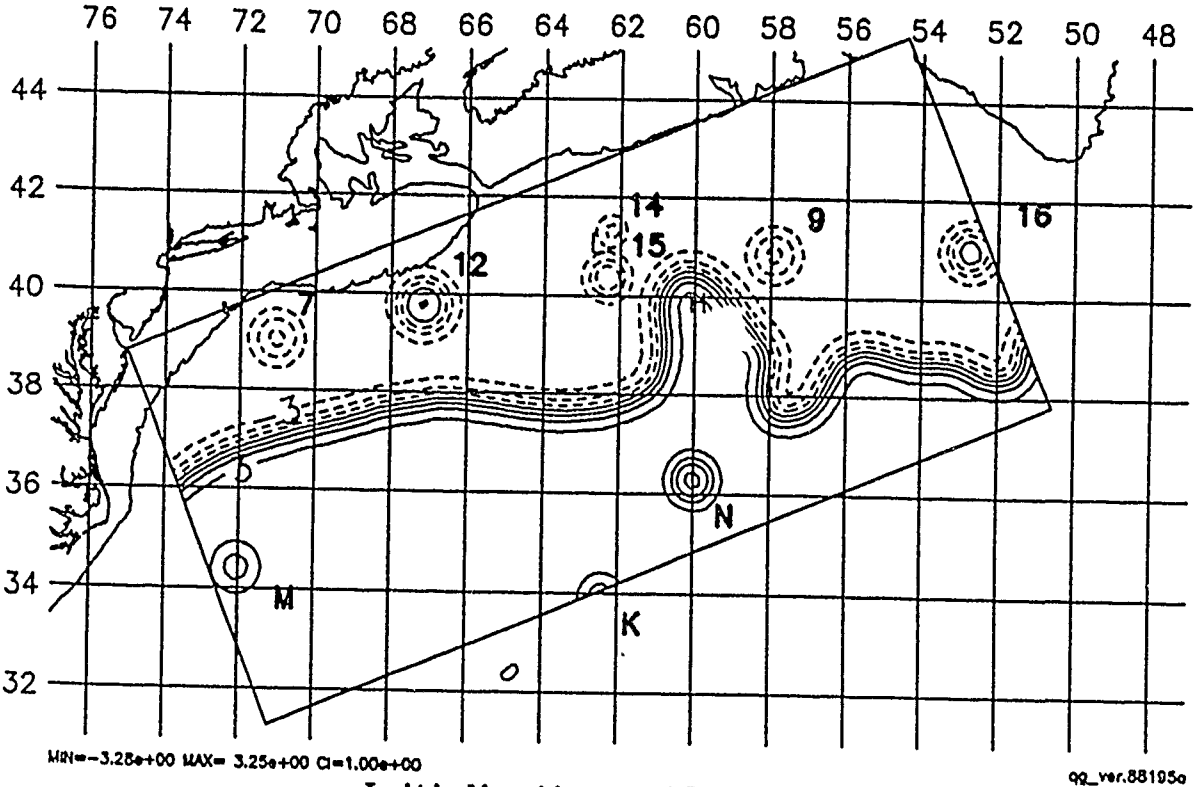

Initialization : 13 JUL 1988

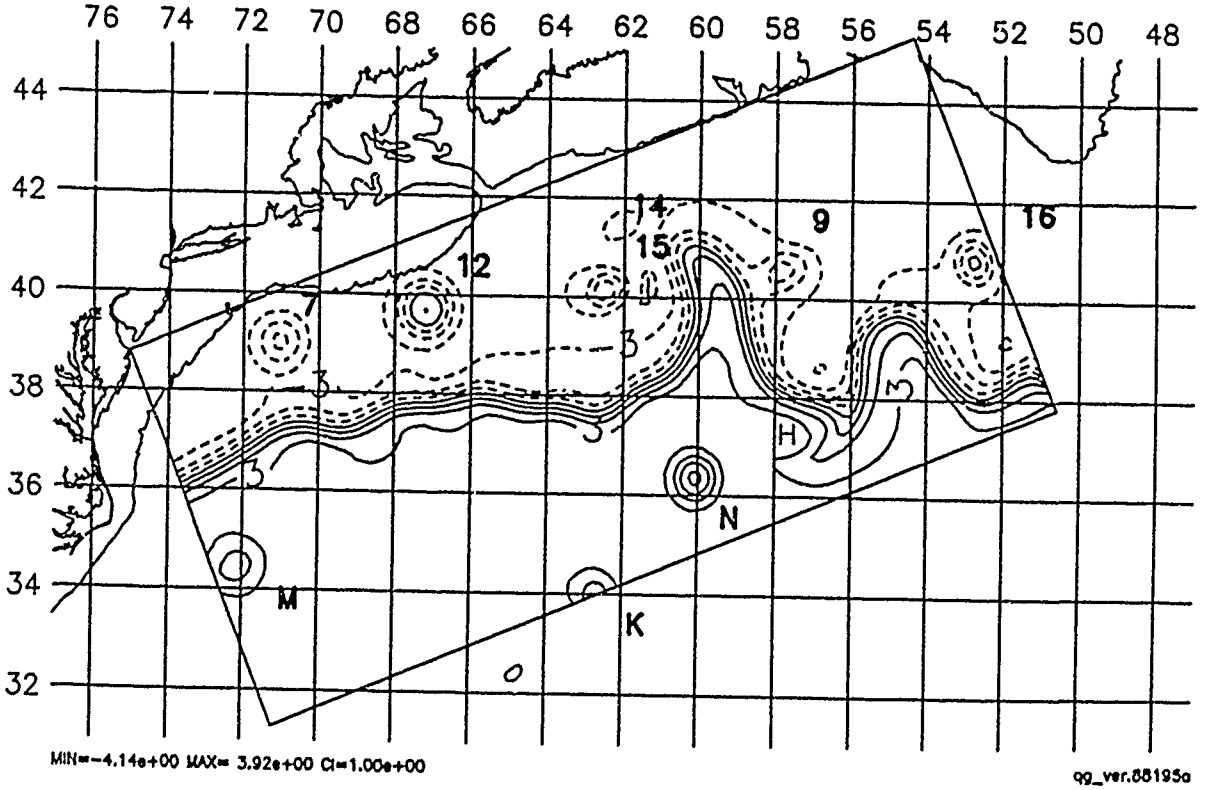

7 Day Forecast : 20 JUL 1988

HARVARD UNIVERSITY GULFCAST

OPERATIONAL EVALUATION FORECAST.

NEW DATA: IR, GEOSAT.

Figure: Streamfunction at 100 m.

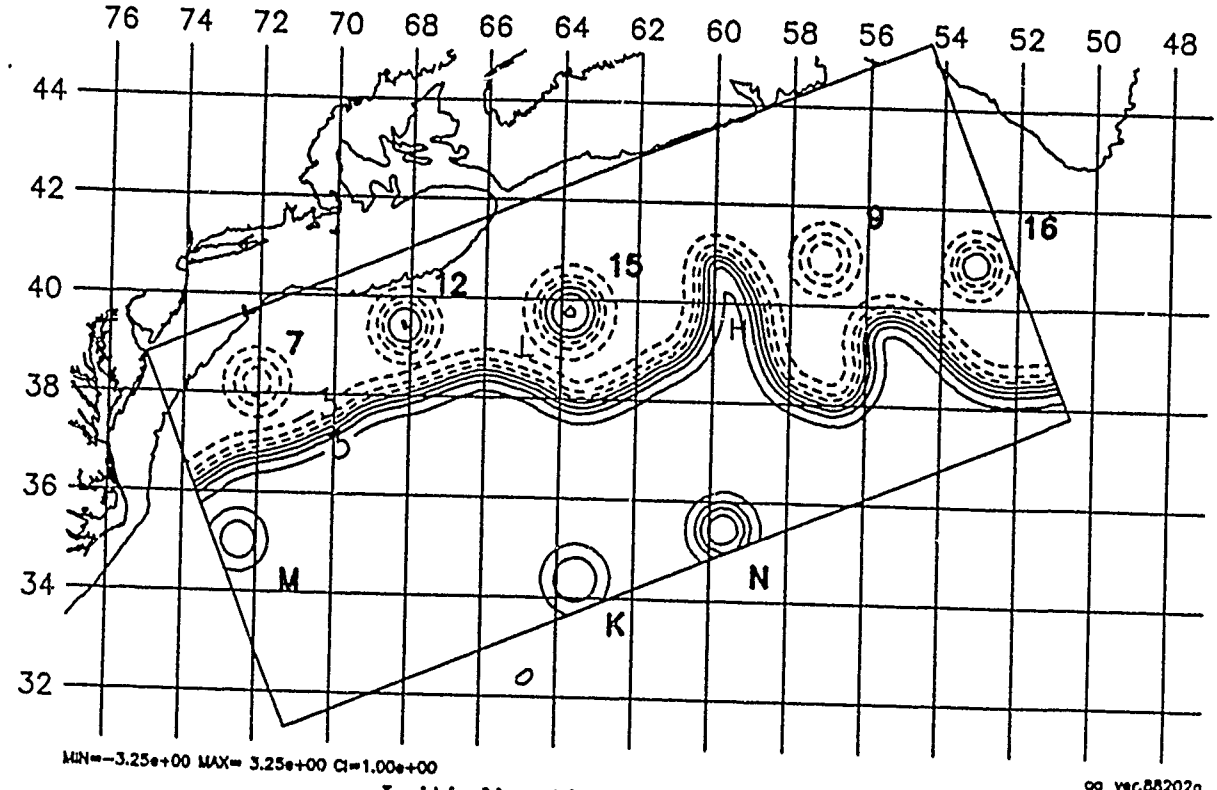

Initialization : 20 JUL 1988

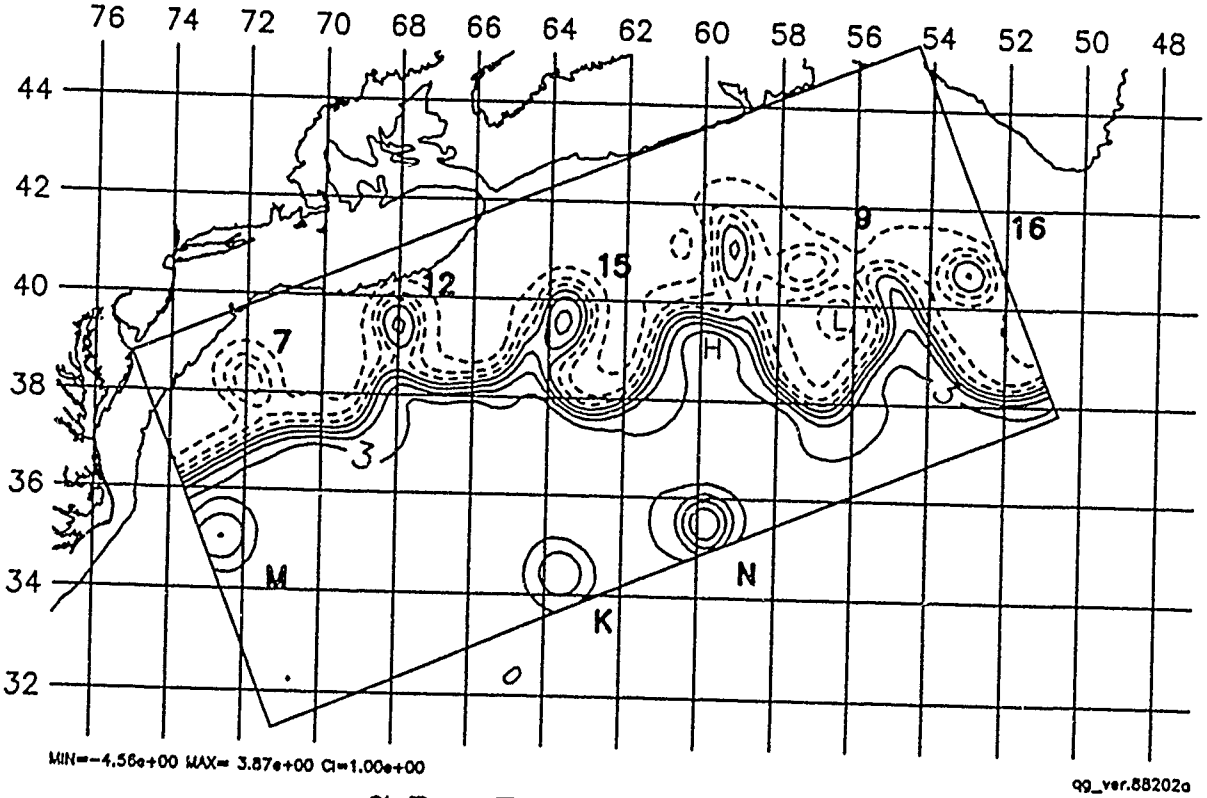

7 Day Forecast : 27 JUL 1988

HARVARD UNIVERSITY GULFCAST

OPERATIONAL EVALUATION FORECAST.

NEW DATA: IR, GEOSAT.

Figure: Streamfunction at 100 m.

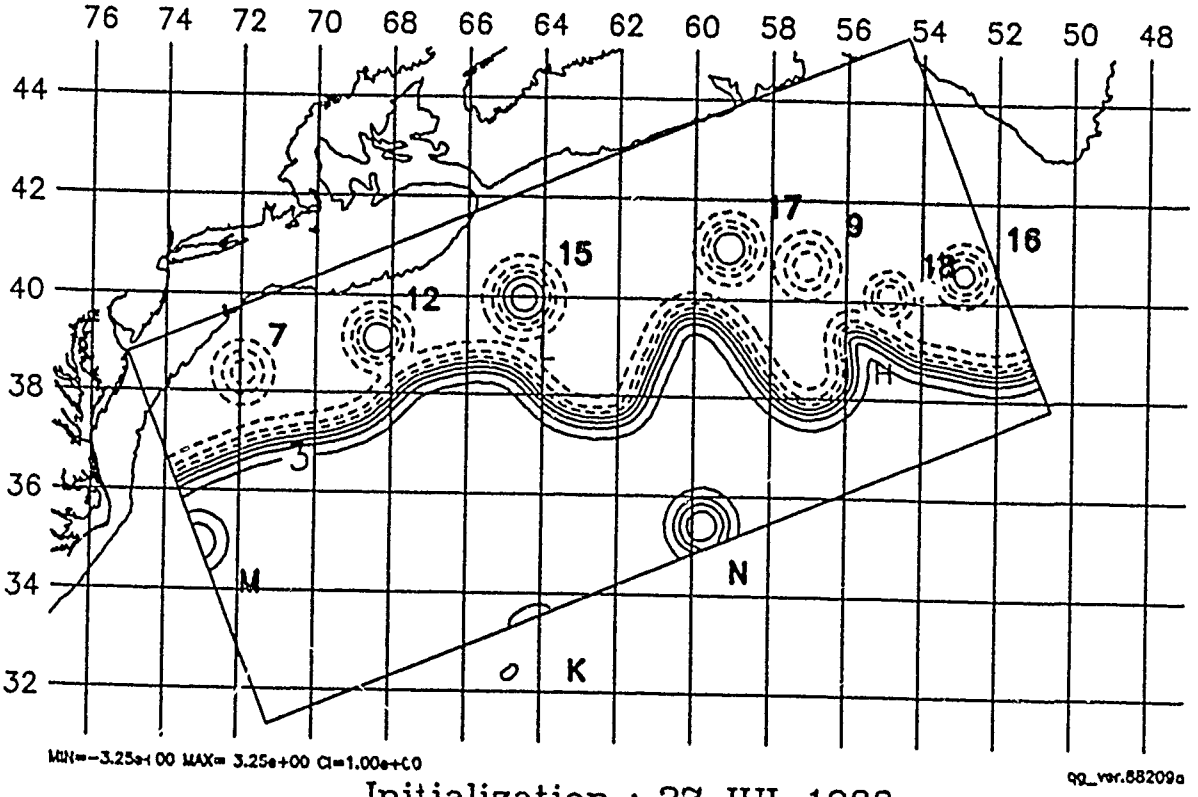

Initialization : 27 JUL 1988

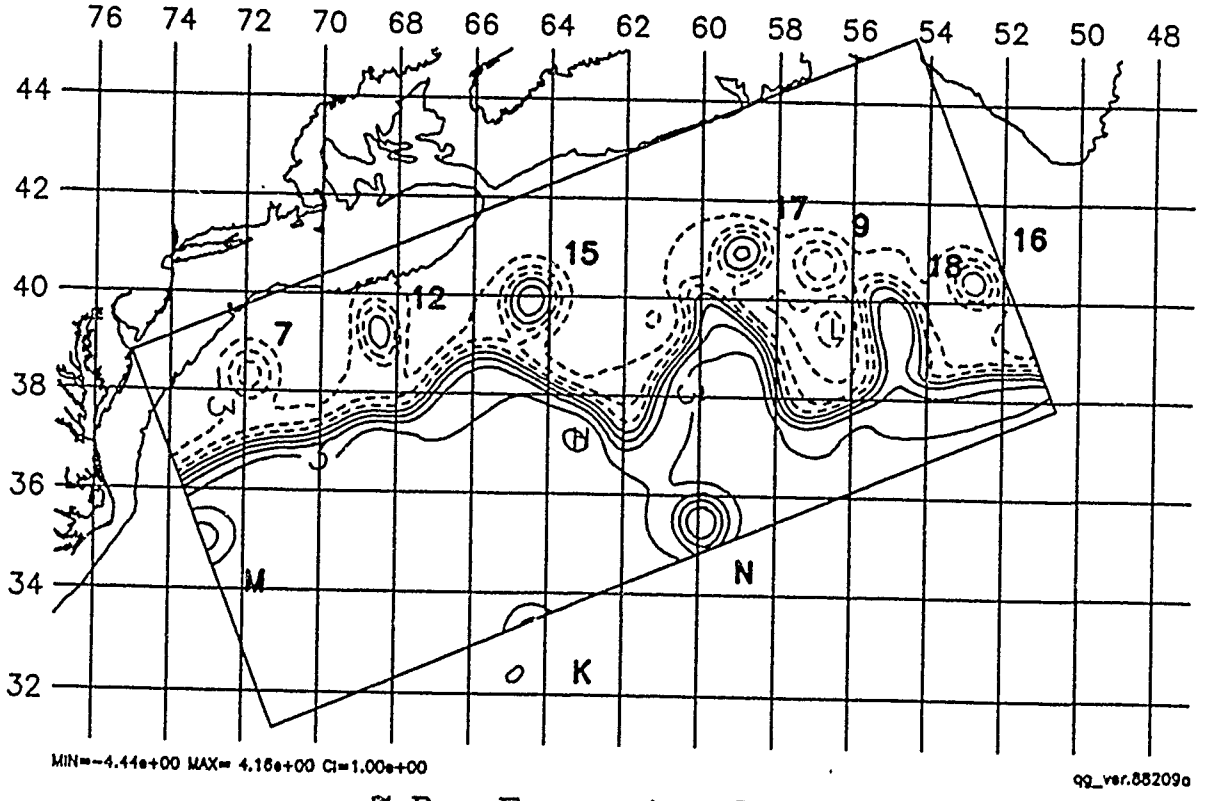

7 Day Forecast : 3 AUG 1988

HARVARD UNIVERSITY GULFCAST

OPERATIONAL EVALUATION FORECAST.

NEW DATA: IR, GEOSAT.

Figure: Streamfunction at 100 m.

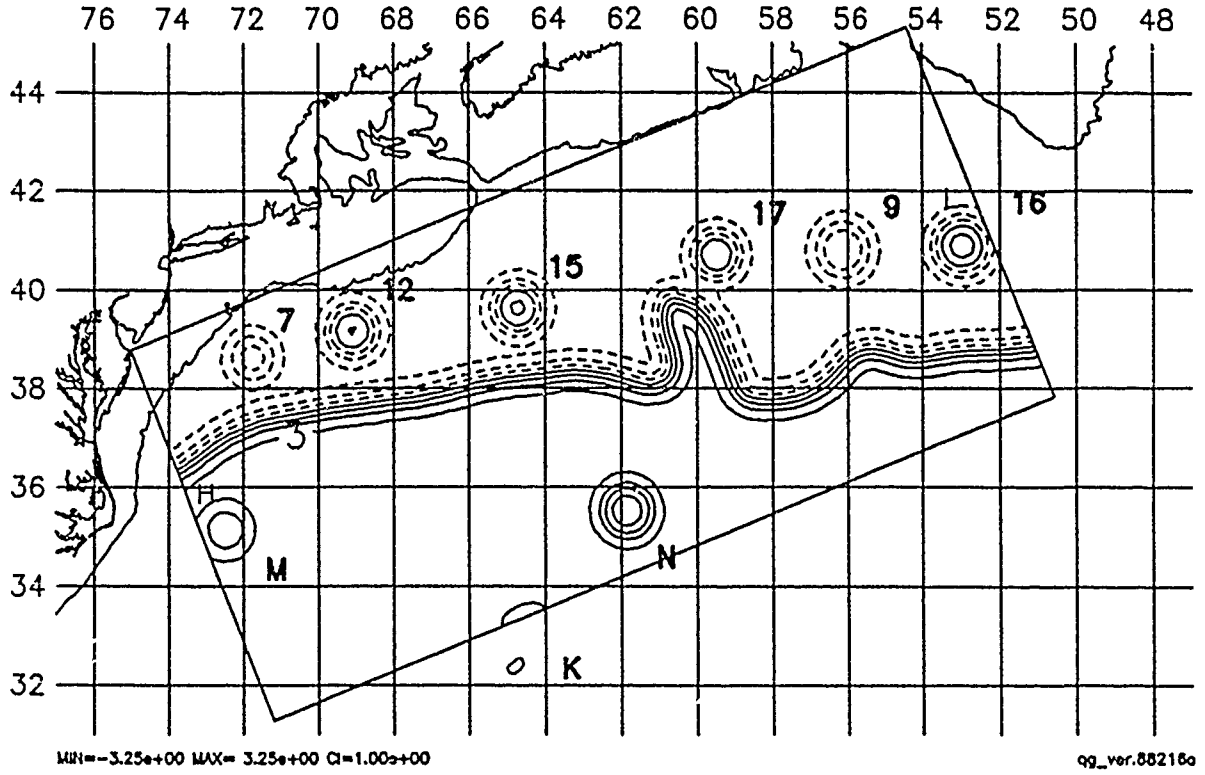

Initialization : 3 AUG 1988

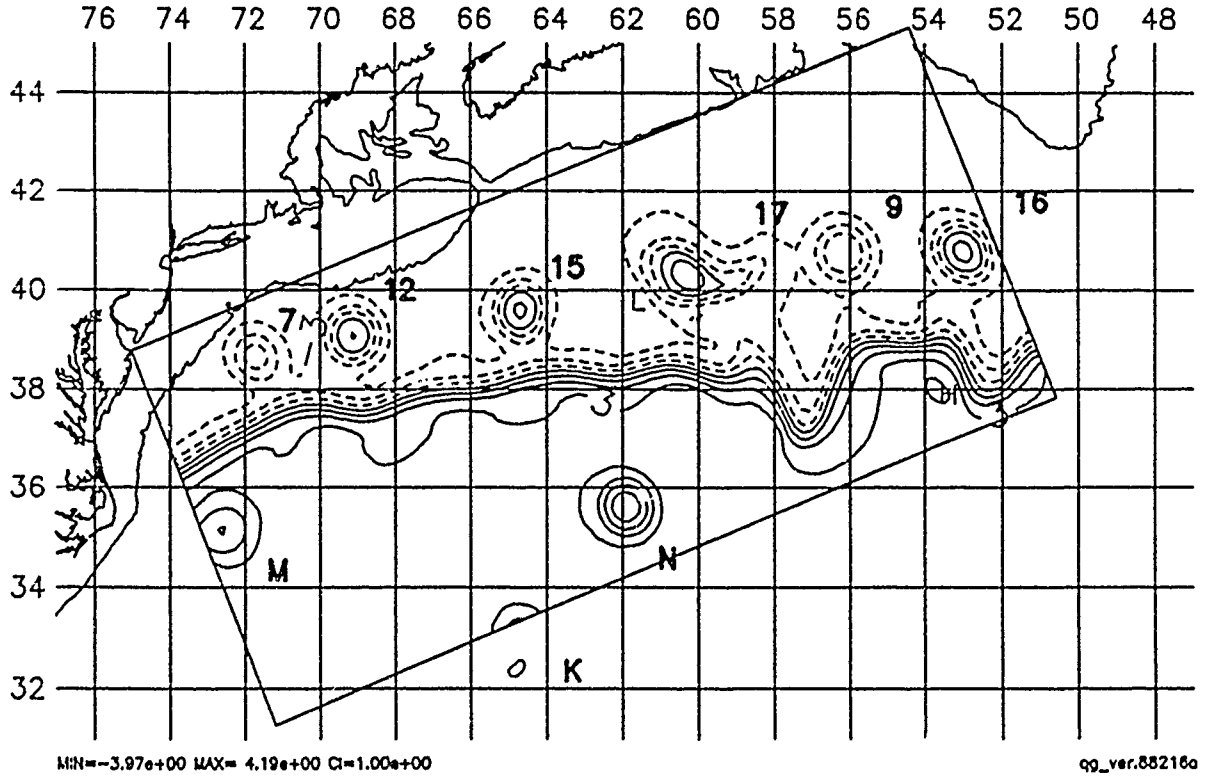

7 Day Forecast : 10 AUG 1988

HARVARD UNIVERSITY GULFCAST

OPERATIONAL EVALUATION FORECAST.

NEW DATA: IR, AXBT, GEOSAT.

Figure: Streamfunction at 100 m.

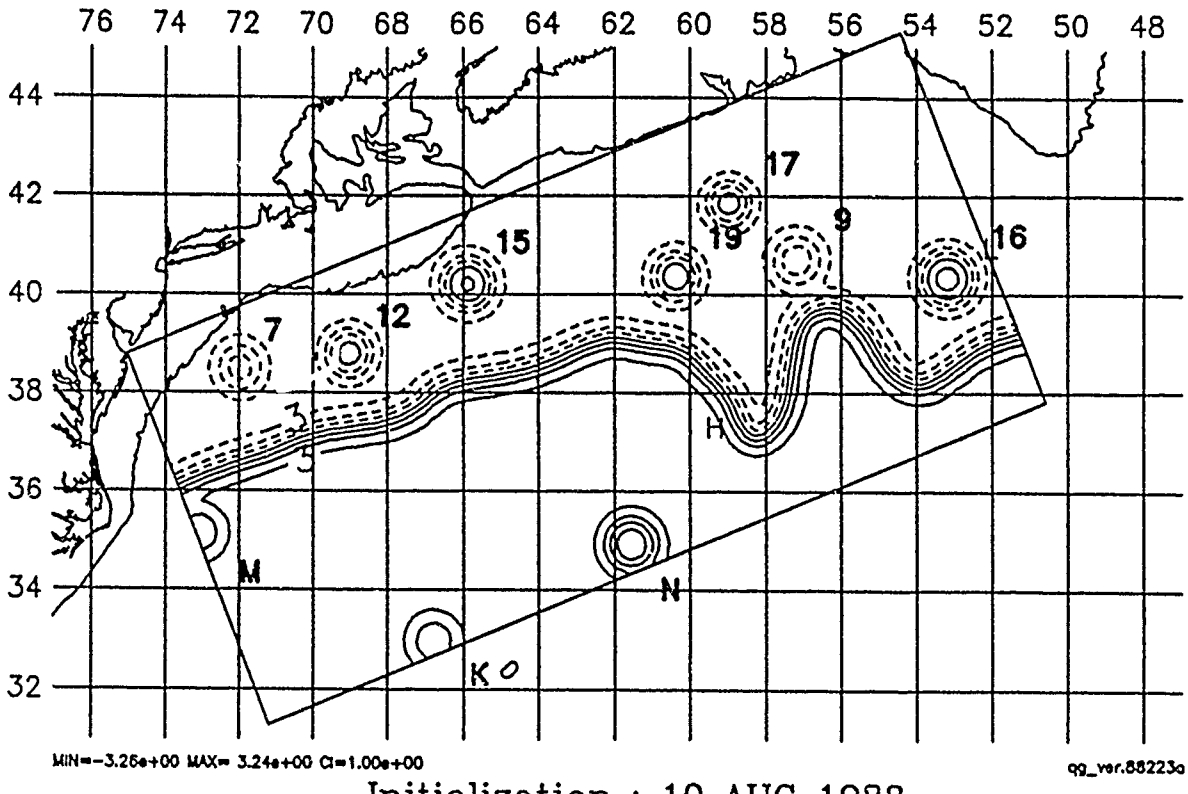

Initialization : 10 AUG 1988

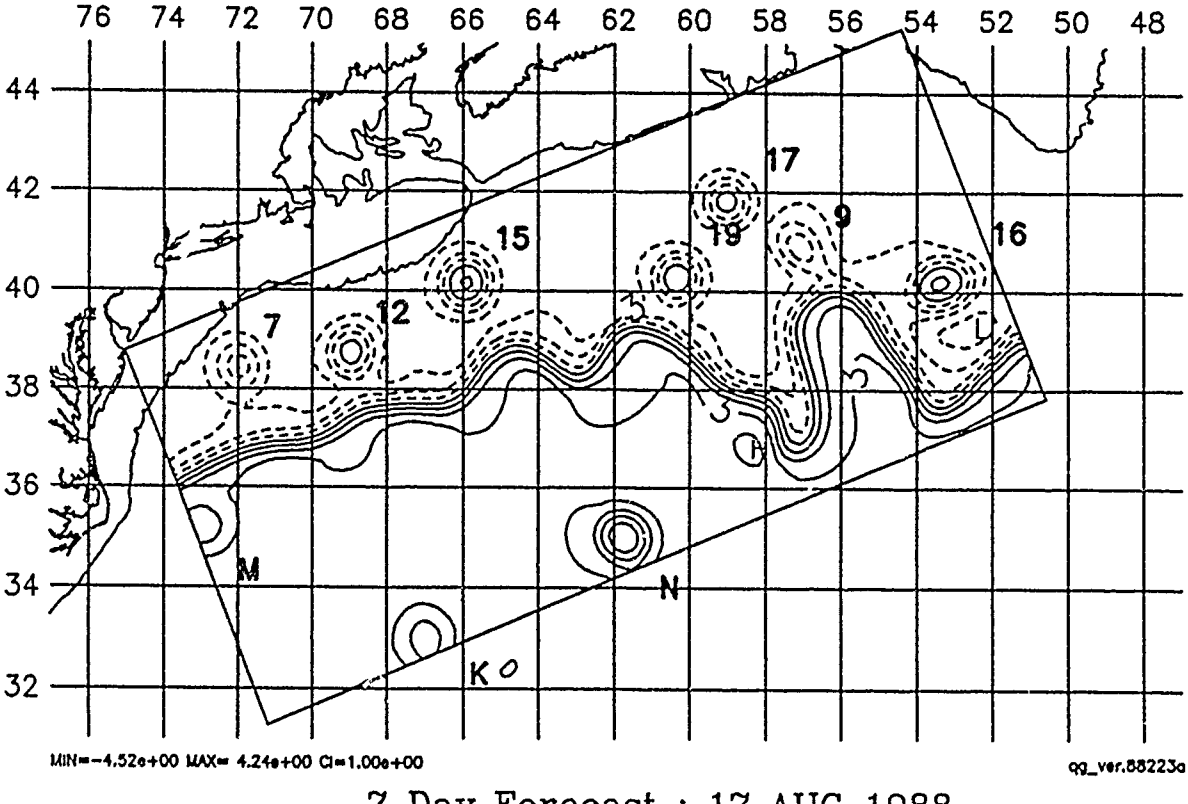

7 Day Forecast : 17 AUG 1988

HARVARD UNIVERSITY GULFCAST

OPERATIONAL EVALUATION FORECAST.

NEW DATA: IR, AXBT, GEOSAT.

Figure: Streamfunction at 100 m.

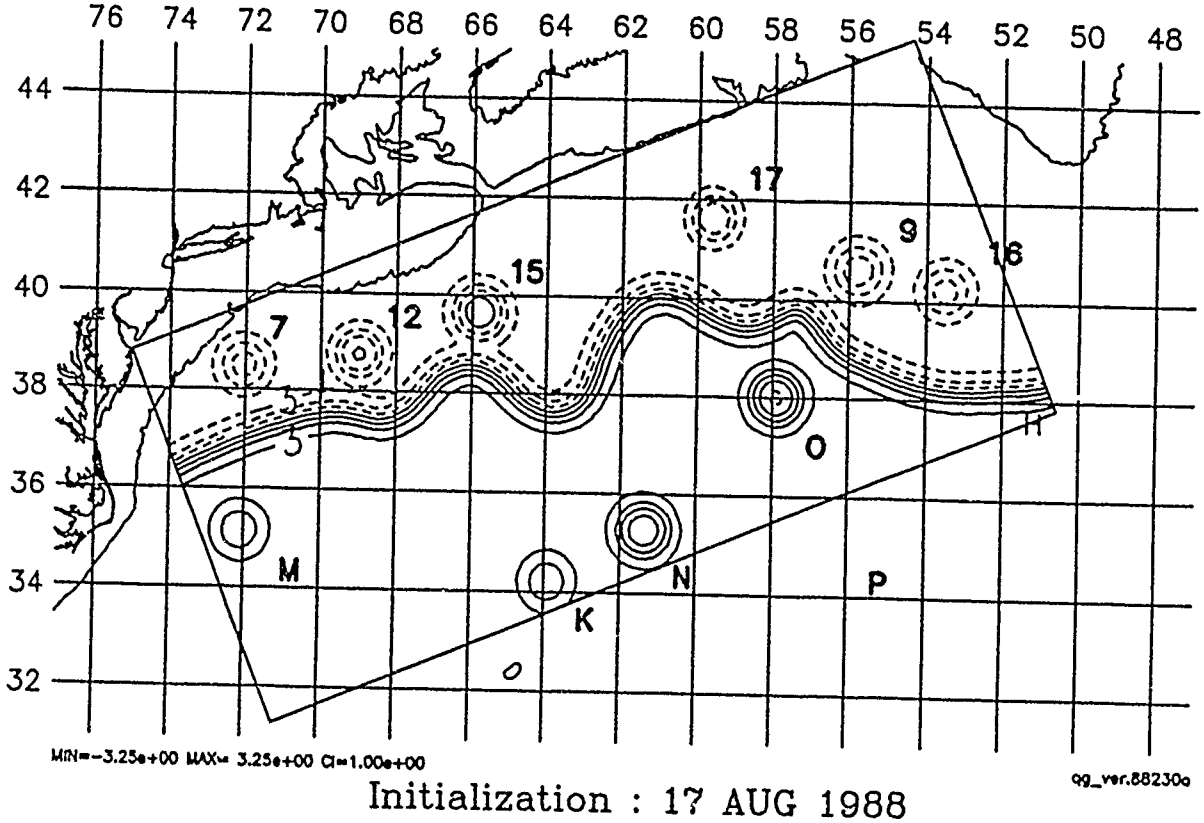

Initialization : 17 AUG 1988

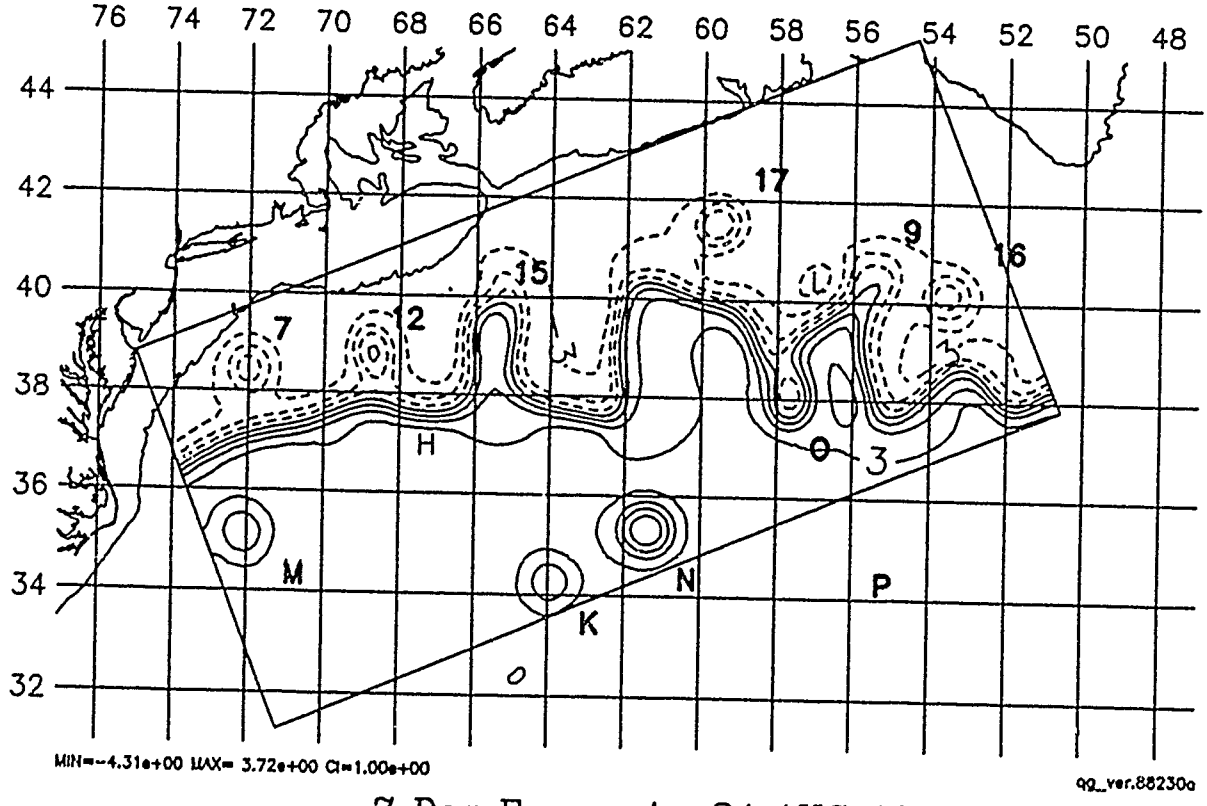

7 Day Forecast : 24 AUG 1988

HARVARD UNIVERSITY GULFCAST

OPERATIONAL EVALUATION FORECAST.

NEW DATA: IR, GEOSAT.

Figure: Streamfunction at 100 m.

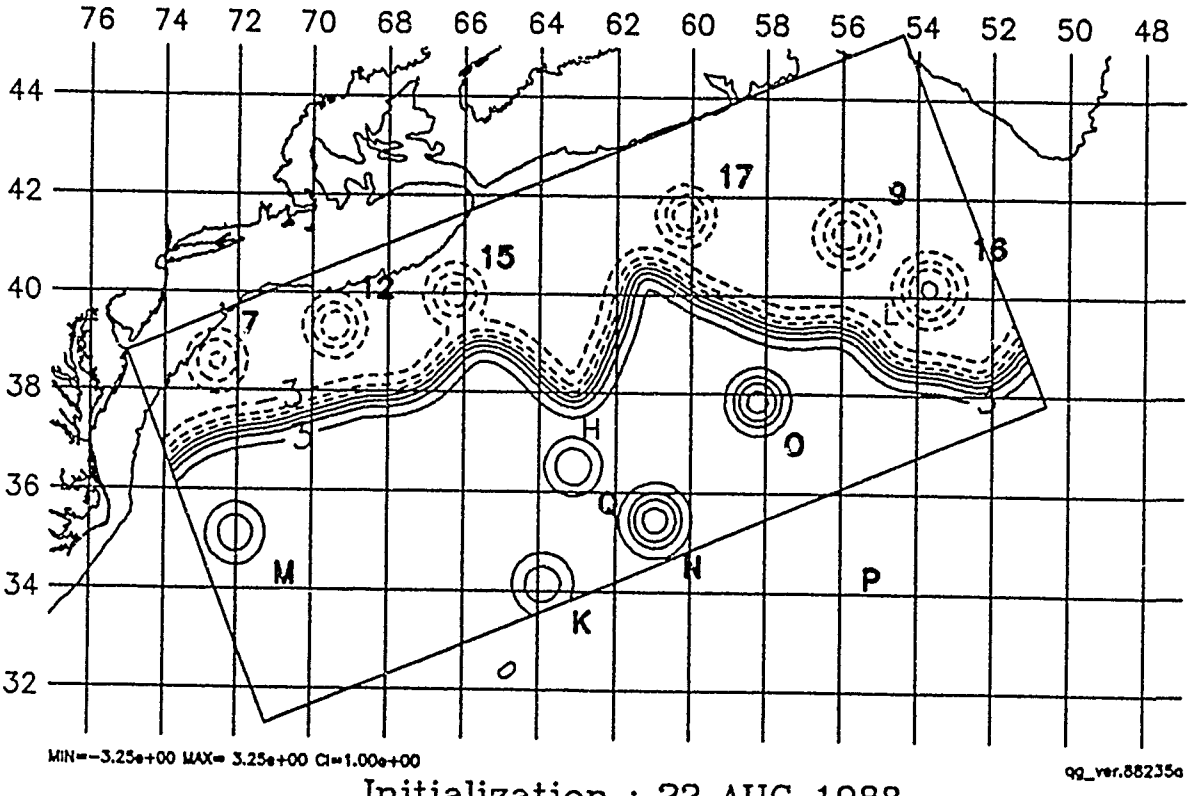

Initialization : 22 AUG 1988

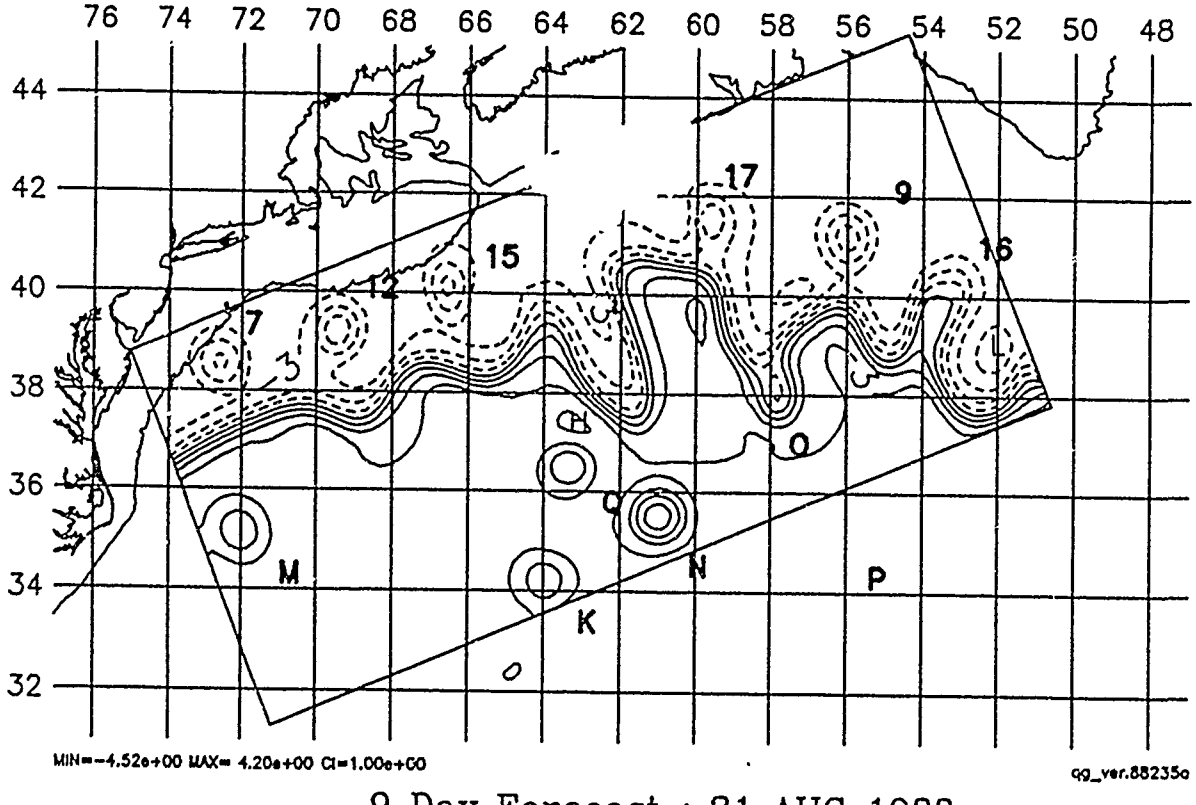

9 Day Forecast : 31 AUG 1988

HARVARD UNIVERSITY GULFCAST

OPERATIONAL EVALUATION FORECAST.

NEW DATA: IR, AXBT, GEOSAT.

Figure: Streamfunction at 100 m.

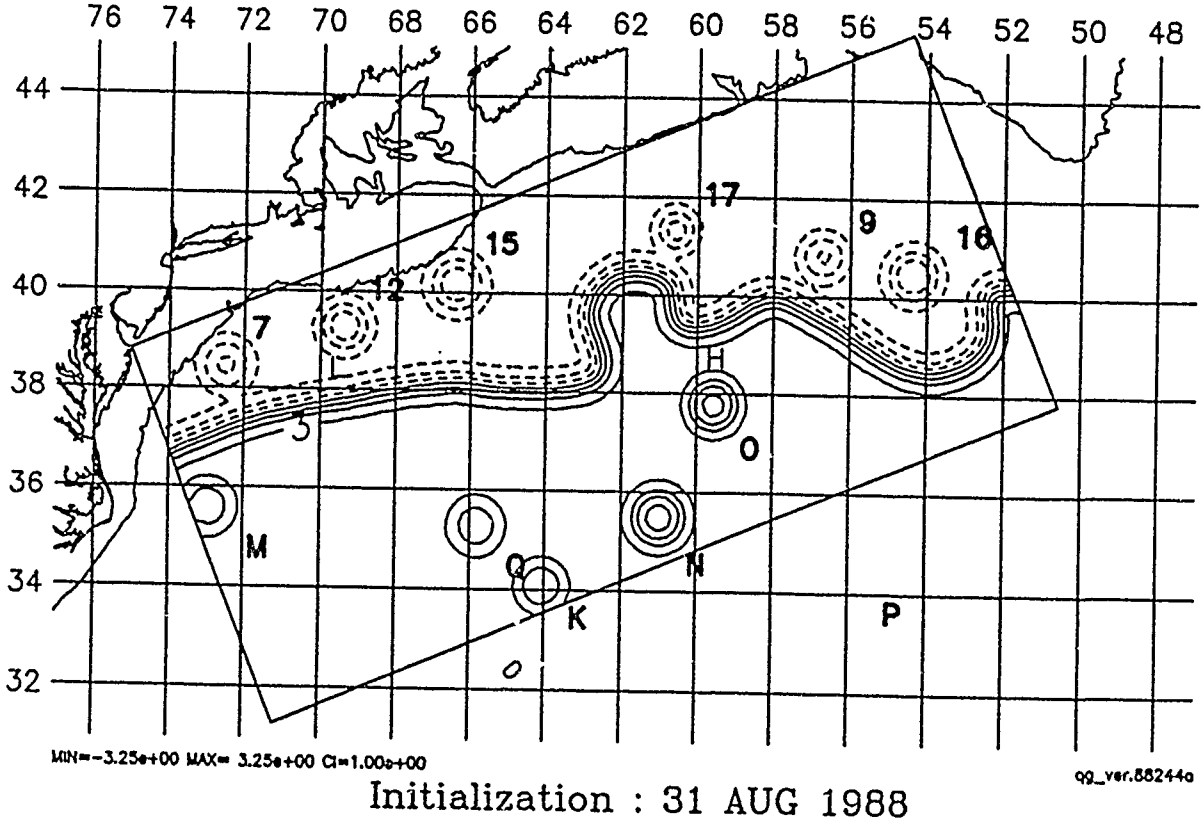

Initialization : 31 AUG 1988

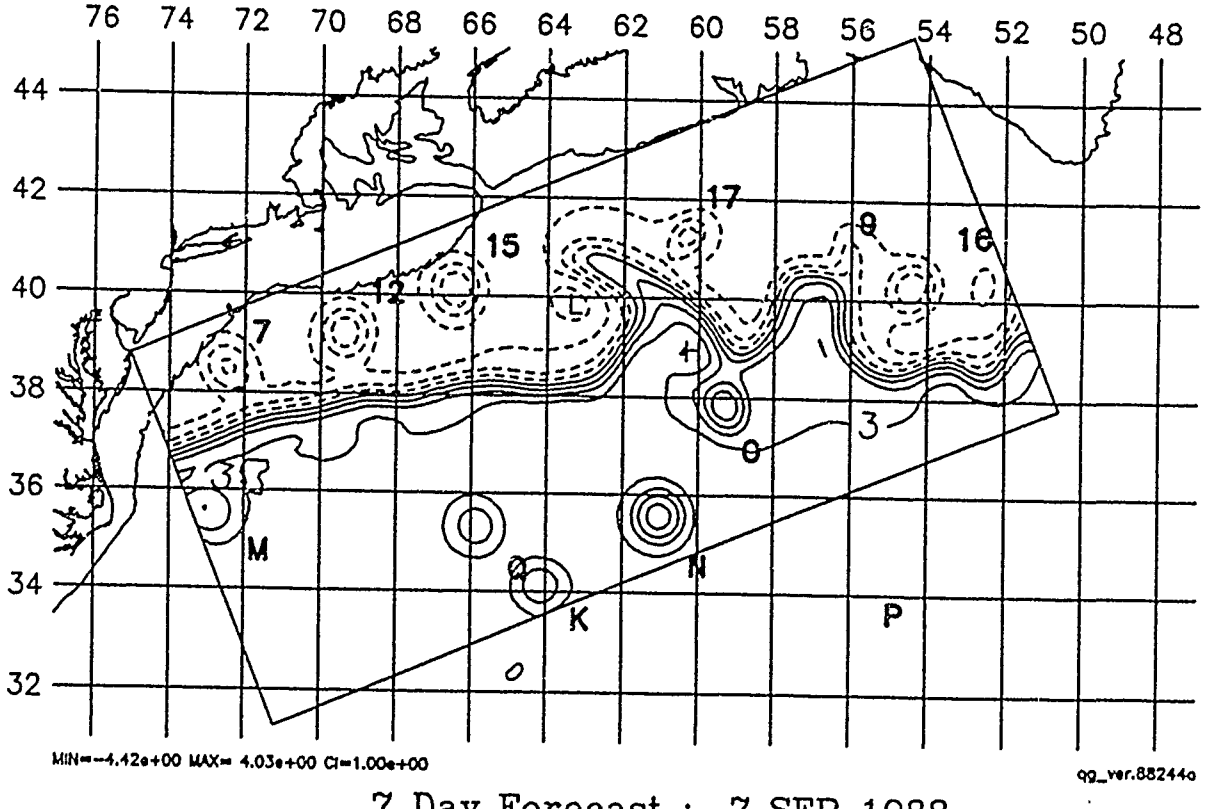

7 Day Forecast : 7 SEP 1988